2019年5月30日(木)

[E] 口頭発表 | セッション記号 P (宇宙惑星科学)：P-EM 太陽地球系科学・宇宙電磁気学・宇宙環境

9:00 ~ 10:30 | A03 東京ベイ幕張ホール

[P-EM09] Vertical coupling in the atmosphere and Ionosphere

コンビーナ:Liu Huixin(九州大学理学研究院地球惑星科学専攻 九州大学宙空環境研究センター)、Chang Loren(Institute of Space Science, National Central University)、大塚 雄一(名古屋大学宇宙地球環境研究所)、座長:Huixin Liu(Kyushu University, Japan)、Stan Solomon(National Center for Atmospheric Research, US)

9:00 ~ 9:20

[PEM09-11] Assimilation products of thermospheric and ionospheric measurements by the NASA Ionopsheric Connection Explorer

★Invited Papers

*Thomas J Immel[1]、Chihoko Cullens[1]、Yen-Jung Wu[1]、Gary Bust[2]、Jeffrey Forbes[3]、Scott L England[4] (1.University of California, Berkeley、2.Johns Hopkins University、3.University of Colorado、4.Virginia Tech)

9:20 ~ 9:35

[PEM09-12] petitSat - A 6U CubeSat to examine the link between MSTIDS and ionospheric plasma density enhancements

*Jeffrey Klenzing[1]、Ryan L Davidson[2]、Gregory D Earle[3]、Alexa J Halford[4]、Sarah L Jones[1]、Carlos Martinis[5]、Nikolaos Paschalidis[1]、Robert F Pfaff[1]、Jonathon M Smith[1,6] (1.NASA Goddard Space Flight Center, Greenbelt, MD, USA、2.Utah State University, Logan, UT, USA、3.Virginia Tech, Blacksburg, VA, USA、4.The Aerospace Corporation, Chantilly, VA, USA、5.Boston University, Boston, MA, USA、6.Catholic Universtiy of America, Washington, DC, USA)

9:35 ~ 9:55

[PEM09-13] A three-dimensional ionospheric electrodynamics model

★Invited Papers

*Astrid I Maute[1]、Arthur D Richmond[1] (1.High Altitude Observatory, National Center for Atmospheric Research, Boulder CO, USA.)

9:55 ~ 10:10

[PEM09-14] **Spatial Fluctuation of TEC Index: A new index of ionospheric irregularities**

*馬 冠一[1]、丸山 隆[2] (1.中国科学院国家天文台、2.国立研究開発法人情報通信研究機構)

10:10 ~ 10:25

[PEM09-15] Coupling of lower thermosphere planetary wave energy into the ionosphere

*Patrick J Espy[1,2]、Nora Stray[1,2,3]、Robert Hibbins[1,2] (1.Norwegian University of Science and Technology, Trondheim, Norway、2.Birkeland Centre for Space Science, Bergen, Norway、3.Teknova AS, Tordenskjolds Gate 9, 4612 Kristiansand, Norway)

[E] 口頭発表 | セッション記号 P (宇宙惑星科学)：P-EM 太陽地球系科学・宇宙電磁気学・宇宙環境

10:45 ~ 12:15 | A03 東京ベイ幕張ホール

[P-EM09] Vertical coupling in the atmosphere and Ionosphere

コンビーナ:Liu Huixin(九州大学理学研究院地球惑星科学専攻 九州大学宙空環境研究センター)、Chang Loren(Institute of Space Science, National Central University)、大塚 雄一(名古屋大学宇宙地球環境研究所)、座長:Jann-Yenq Liu(National Central University, Taiwan)、Loren Chang(National Central University, Taiwan)

10:45 ~ 11:00

[PEM09-16] Modulation of Lightning Occurrence by the Solar Wind

*Omar Angelo Nava[1]、Daniel Emmons[1]、Robert Loper[1] (1.Air Force Institute of Technology)

11:00 ~ 11:15

[PEM09-17] Long Term Mesopause Temperature Variations resolved by SD-WACCM, MSISE-00,TIMED SABER and Local Observations in Irkutsk (52.29o, 104.29o), Russia

*Yi Chung Chiu[1]、Loren Chang[1]、Yi Duann[1]、ALEXEI DMITRIEV[1]、Irina Medvedeva[2]、Konstantin Ratovsky[2]、Jia Yue[3] (1.Institute of Space Science, National Central University、2.Russian Academy of Sciences, Russian Federation、3.Hampton University, USA)

11:15 ~ 11:30

[PEM09-18] ISS-IMAP observation of the mesospheric disturbances generated by tropical cyclones

*齊藤 昭則[1]、坂野井 健[2]、Perwitasari Septi[4]、穂積 裕太[3]、岡田 凌太[1]、村上 涼[1] (1.京都大学大学院理学研究科地球物理学教室、2.東北大学大学院理学研究科惑星プラズマ・大気研究センター、3.電気通信大学、4.国立極地研究所宙空圏グループ)

11:30 ~ 11:45

[PEM09-19] A fast acoustic wave detected in GNSS total electron content after the foreshock of the 2011 Tohoku Earthquake

*柿並 義宏[1]、齊藤 大晶[2]、山本 哲生[3]、陳 佳宏[4]、山本 真行[2]、中島 健介[5]、劉 正彦[6] (1.北海道情報大学、2.高知工科大学、3.北海道大学、4.台湾国立成功大学、5.九州大学、6.台湾国立中央大学)

11:45 ~ 12:00

[PEM09-20] **Study of quiet-time high-latitude thermospheric winds using a Fabry-Perot interferometer at Tromsoe: Averages and exceptional events**

*徐 何秋岑[1]、塩川 和夫[1]、大山 伸一郎[1] (1.名古屋大学宇宙地球環境研究所)

12:00 ~ 12:15

[PEM09-21] **The longitudinal differences of lunar tidal characteristics between East Asian and American sectors during stratospheric sudden warming events: 2009-2018.**

*Jing Liu[1]、Donghe Zhang[1] (1.Peking University)

[E] 口頭発表 | セッション記号 P (宇宙惑星科学)：P-EM 太陽地球系科学・宇宙電磁気学・宇宙環境

9:00 ~ 10:30 | A04 東京ベイ幕張ホール

[P-EM11] Dynamics of Magnetosphere and Ionosphere

コンビーナ:中溝 葵(情報通信研究機構　電磁波研究所)、尾崎 光紀(金沢大学理工研究域電子情報学系)、藤本 晶子(九州工業大学)、堀 智昭(名古屋大学宇宙地球環境研究所)、座長:中野 慎也(情報・システム研究機構 統計数理研究所)、野和田 基晴(山東大学)

9:00 ~ 9:15

[PEM11-07] **Nightside Distorted Transpolar Arcs and Their Possible Formation Process Model**

*野和田 基晴[1]、　俊[1]、ヒューベルト ベノワ[2]、宗 秋 [3]、史 全岐[1]、王 永福[3]、周 煦之[3]、　宇[3] (1.山東大学 威海校 空間科学与物理学学院 空間科学研究院 空間天気物理与探計測研究中心 、2.リージュ大学 宇宙科学技術天文研究所、3.北京大学 地球与空間科学学院 空間物理与応用技術研究所)

9:15 ~ 9:30

[PEM11-08] Ionospheric Conductivity Dependence of the Subauroral Polarization Streams Observed by the SuperDARN HF Radars

張 玉テイ[1]、*西谷 望[1]、堀 智昭[1]、Simon Shepherd[2]、William Bristow[3] (1.名古屋大学宇宙地球環境研究所、2.ダートマス大学、3.アラスカ大学フェアバンクス校)

9:30 ~ 9:45

[PEM11-09] Ionospheric convection modeling based on convolution with a localized vector-valued basis function

*中野 慎也[1]、堀 智昭[2]、関 華奈子[3]、西谷 望[2] (1.統計数理研究所、2.名古屋大学宇宙地球環境研究所、3.東京大学大学院理学系研究科)

9:45 ~ 10:00

[PEM11-10] **Occurrence Statistics and Driving Mechanisms of Ionospheric ULF Waves Observed by SuperDARN Radars**

★Invited Papers

*Xueling Shi[1]、Joseph B. H. Baker[1]、John Michael Ruohoniemi[1]、Dong Lin[1]、Michael Hartinger[1,2] (1.Virginia Tech、2.Space Science Institute)

10:00 ~ 10:15

[PEM11-11] Magnetic Field Oscillations Observed by Swarm Satellites in the Nightside Upper Ionosphere During Low-latitude Pi2 Pulsations

*Khan-Hyuk Kim[1]、Jae-Hee Park[1] (1.School of Space Research, Kyung Hee Univ.)

10:15 ~ 10:30

[PEM11-12] Magnetospheric Multiscale observations of ULF waves and correlated low-energy ion monoenergetic acceleration

*Bin Li[1]、De-sheng Han[2]、Ze-jun Hu[1]、Jian-jun Liu[1]、Lei Dai[3] (1.Polar Research Institute of China、2.Tongji University、3.National Space Science Center, Chinese Academy of Sciences)

[E] 口頭発表 | セッション記号 P (宇宙惑星科学)：P-EM 太陽地球系科学・宇宙電磁気学・宇宙環境

10:45 ~ 12:15 | A04 東京ベイ幕張ホール

[P-EM11] Dynamics of Magnetosphere and Ionosphere

コンビーナ:中溝 葵(情報通信研究機構　電磁波研究所)、尾崎 光紀(金沢大学理工研究域電子情報学系)、藤本 晶子(九州工業大学)、堀 智昭(名古屋大学宇宙地球環境研究所)、座長:桂華 邦裕(東京大学大学院理学系研究科)、中野 慎也(情報・システム研究機構 統計数理研究所)、野和田 基晴(山東大学)

10:45 ~ 11:00

[PEM11-13] Statistical study on warm plasma in the magnetotail based on two-component fits of distribution functions

*桂華 邦裕[1]、浅見 隆太[1]、星野 真弘[1] (1.東京大学大学院理学系研究科地球惑星科学専攻)

11:00 ~ 11:15

[PEM11-14] Analysis on anisotropy variations for pitch angle distributions of electrons with various parameters at dipolarization sites in the inner plasma sheet

*Kaiti Wang[1]、Zhuo-Ren Lang[2]、Ching-Huei Lin[3]、Tohru Hada[4]、Toshi Nishimura[5] (1.Tamkang Univ.、2.National Cheng Kung Univ.、3.Chien-Hsin Univ. of Sci. & Tech.、4.Kyushu Univ.、5.Boston Univ.)

11:15 ~ 11:30

[PEM11-15] Study of slow-mode shock formation in the symmetric magnetic reconnection based on hybrid simulations

*Nehpreet Kaur Walia[1]、Kanako Seki[1]、Takanobu Amano[1] (1. Department of Earth & Planetary Science, Graduate School of Science, University of Tokyo)

11:30 ~ 11:45

[PEM11-16] Reconstruction of the electron diffusion region of magnetotail reconnection seen by the Magnetospheric Multiscale spacecraft

*長谷川 洋[1]、Richard Denton[2]、中村 るみ[3]、Kevin Genestreti[4]、中村 琢磨[3]、Joo Hwang[5]、Tai Phan[6]、Roy Torbert[4]、Jim Burch[5]、Barbara Giles[7]、Dan Gershman[7]、Chris Russell[8]、Bob Strangeway[8]、Per-Arne Lindqvist[9]、Yuri Khotyaintsev[10]、Robert Ergun[11]、北村 成寿[12]、斎藤 義文[1] (1.宇宙航空研究開発機構宇宙科学研究所、2.ダートマス大学、3.オーストリア宇宙科学研究所、4.ニューハンプシャー大学、5.サウスウェスト研究所、6.カリフォルニア大学バークレー校、7.NASAゴダード宇宙飛行センター、8.カリフォルニア大学ロサンゼルス校、9.スウェーデン王立工科大学、10.スウェーデン宇宙物理学研究所、11.コロラド大学、12.東京大学地球惑星科学専攻)

11:45 ~ 12:00

[PEM11-17] MMS observations of the dense high speed flow in the magnetotail

*Mingyu Wu[1]、Tielong Zhang[1] (1.Harbin Insitute of Technology, Shenzhen)

12:00 ~ 12:15

[PEM11-18] The spatio-temporal development of lightning-induced electron precipitation events

★Invited Papers

*Robert C Moore[1]、Dooyoung Kim[1] (1.University of Florida)

[E] 口頭発表 | セッション記号 P (宇宙惑星科学)：P-EM 太陽地球系科学・宇宙電磁気学・宇宙環境

13:45 ~ 15:15 | A04 東京ベイ幕張ホール

[P-EM11] Dynamics of Magnetosphere and Ionosphere

コンビーナ:中溝 葵(情報通信研究機構　電磁波研究所)、尾崎 光紀(金沢大学理工研究域電子情報学系)、藤本 晶子(九州工業大学)、堀 智昭(名古屋大学宇宙地球環境研究所)、座長:北村 成寿(東京大学大学院理学系研究科)、佐藤 由佳(日本工業大学)

13:45 ~ 14:00

[PEM11-19] サブストーム時におけるエネルギーの流れ、ダイナモ、沿磁力線電流

*海老原 祐輔[1]、田中 高史[2] (1.京都大学生存圏研究所、2.九州大学)

14:00 ~ 14:15

[PEM11-20] **Electron flux and field-aligned current associated with Pc5 auroral arc pulsations observed onboard THEMIS and DMSP satellites**

*佐藤 夏雄[1]、行松 彰[1,2]、田中 良昌[1,2]、堀 智昭[3]、門倉 昭[1,2]、櫻井 亨[4]、Desheng Han[5]、Yuzhang Ma[6]、Qinghe Zhang[6] (1.国立極地研究所、2.総研大、3.名古屋大学、4.東海大学、5.同済大学、6.山東大学)

14:15 ~ 14:30

[PEM11-21] Multiple spots of enhanced electron precipitation near the equatorward boundary of the cusp

*田口 聡[1]、小瀬 智史[1]、高須 浩平[1]、田中 杜雄[1]、細川 敬祐[2]、小川 泰信[3] (1.京都大学理学研究科地球惑星科学専攻地球物理学教室、2.電気通信大学情報理工学研究科、3.国立極地研究所)

14:30 ~ 14:45

[PEM11-22] Statistical study of auroral/resonant-scattering 427.8-nm emission observed at subauroral latitudes over 14 years

*塩川 和夫[1]、大塚 雄一[1]、Martin Connors[2] (1.名古屋大学宇宙地球環境研究所、2.アサバスカ大学)

14:45 ~ 15:00

[PEM11-23] 無人システムを利用したオーロラ現象の南極広域ネットワーク観測：共役点イベント解析（２）

*門倉 昭[1]、山岸 久雄[1]、岡田 雅樹[1]、小川 泰信[1]、田中 良昌[1]、片岡 龍峰[1]、内田 ヘルベルト陽仁[1]、大塚 雄一[2] (1.国立極地研究所、2.名古屋大学)

15:00 ~ 15:15

[PEM11-24] **Dawn-Dusk Asymmetry in Dayside and Nightside auroral Ovals: Surveys of auroral emissions based on the all-sky imagers in Arctic and Antarctic**

★Invited Papers

*Zejun Hu[1] (1.Polar Research Institute of China)

[E] 口頭発表 | セッション記号 P (宇宙惑星科学)：P-EM 太陽地球系科学・宇宙電磁気学・宇宙環境

15:30 ~ 17:00 | A04 東京ベイ幕張ホール

[P-EM11] Dynamics of Magnetosphere and Ionosphere

コンビーナ:中溝 葵(情報通信研究機構　電磁波研究所)、尾崎 光紀(金沢大学理工研究域電子情報学系)、藤本 晶子(九州工業大学)、堀 智昭(名古屋大学宇宙地球環境研究所)、座長:北村 成寿(東京大学大学院理学系研究科)、佐藤 由佳(日本工業大学)、西野 真木(名古屋大学宇宙地球環境研究所)

15:30 ~ 15:45

[PEM11-25] 静止軌道磁場の変化に伴う10MeVプロトンの異常増加

*小原 隆博[1] (1.東北大学　惑星プラズマ大気研究センター)

15:45 ~ 16:00

[PEM11-26] Solar-cycle variations of >30 keV proton flux enhancements under the inner radiation belt

*ALLA SUVOROVA[1] (1.National Central University)

16:00 ~ 16:15

[PEM11-27] Auroral Imaging with Commercial DSLR Cameras near Athabasca, Canada

*Martin G Connors[1,2]、Ian Schofield[1]、Mike Noble[2]、Alister Ling[2]、Ryuho Kataoka[3]、Ken Murata[4]、Kazunori Yamamoto[4] (1.Athabasca University、2.Edmonton Centre, Royal Astronomical Society of Canada、3.National Institute for Polar Research、4.National Institute for Communications Technology)

16:15 ~ 16:30

[PEM11-28] PARM: Investigation of precipitating high-energy electrons into the auroral ionosphere with sounding rockets

*浅村 和史[1]、三好 由純[2]、細川 敬祐[3]、三谷 烈史[1]、滑川 拓[1,5]、坂野井 健[4]、八木 直志[4]、吹澤 瑞貴[4]、石澤 元気[4]、笠原 慧[5]、菅生 真[5]、川島 桜也[5]、野村 麗子[6]、能勢 正仁[2]、寺本 万里子[2]、小川 泰信[7]、齊藤 慎司[2]、藤井 良一[8] (1.宇宙航空研究開発機構宇宙科学研究所、2.名古屋大学宇宙地球環境研究所、3.電気通信大学、4.東北大学、5.東京大学、6.自然科学研究機構国立天文台、7.情報・システム研究機構国立極地研究所、8.情報・システム研究機構)

16:30 ~ 16:45

[PEM11-30] Development of a miniaturized X-ray imager for GEOspace X-ray imager (GEO-X)

*石川 久美[1]、江副 祐一郎[2]、沼澤 正樹[2]、伊師 大貴[2]、藤谷 麻衣子[2]、大坪 亮太[2]、福島 碧都[2]、鈴木 光[2]、湯浅 辰哉[2]、中嶋 大[3]、平賀 純子[4]、三好 由純[5]、笠原 慧[6]、満田 和久[1] (1.宇宙航空研究開発機構/宇宙科学研究所、2.首都大学東京、3.関東学院大学、4.関西学院大学、5.名古屋大学、6.東京大学)

[E] 口頭発表 | セッション記号 P (宇宙惑星科学)：P-EM 太陽地球系科学・宇宙電磁気学・宇宙環境

9:00 ~ 10:30 | A01 東京ベイ幕張ホール

[P-EM15] 太陽地球系結合過程の研究基盤形成

コンビーナ:山本 衛(京都大学生存圏研究所)、小川 泰信(国立極地研究所)、野澤 悟徳(名古屋大学宇宙地球環境研究所)、吉川 顕正(九州大学大学院理学研究院地球惑星科学部門)、座長:山本 衛

9:00 ~ 9:15

[PEM15-01] Status of Equatorial MU Radar project in 2019

*山本 衛[1]、橋口 浩之[1]、横山 竜宏[1]、津田 敏隆[1] (1.京都大学生存圏研究所)

9:15 ~ 9:30

[PEM15-02] Recent Progress and Current Status of EISCAT_3D in 2018-2019

*宮岡 宏[1]、小川 泰信[1]、野澤 悟徳[2]、西村 耕司[1]、大山 伸一郎[2]、中村 卓司[1]、藤井 良一[2]、Heinselman Craig[3] (1.大学共同利用機関情報・システム研究機構国立極地研究所、2.名古屋大学宇宙地球環境研究所、3.EISCAT科学協会)

9:30 ~ 9:45

[PEM15-03] 超高層大気イメージングシステムとPWINGプロジェクトによる超高層大気・電磁気圏の地上多点観測網の現状

*塩川 和夫[1]、大塚 雄一[1]、PWING TEAM (1.名古屋大学宇宙地球環境研究所)

9:45 ~ 10:00

[PEM15-04] Development of MAGDAS project: Search for global electromagnetic coupling from polar to equatorial ionosphere

*吉川 顕正[1]、樺澤 大生[2]、魚住 禎司[3]、藤本 晶子[4]、阿部 修司[3] (1.九州大学大学院理学研究院地球惑星科学部門、2.九州大学大学院理学府地球惑星科学専攻、3.九州大学国際宇宙天気科学・教育センター、4.九州工業大学大学院情報工学研究院)

10:00 ~ 10:15

[PEM15-05] 太陽地球系結合研究推進のためのIUGONETデータ解析システム

*新堀 淳樹[1]、田中 良昌[2]、梅村 宜生[1]、阿部 修司[3]、能勢 正仁[1]、上野 悟[4] (1.名古屋大学宇宙地球環境研究所、2.国立極地研究所、3.九州大学 国際宇宙天気科学・教育センター、4.京都大学天文台)

10:15 ~ 10:30

[PEM15-06] 大型研究計画「太陽地球系結合過程の研究基盤形成」推進の議論（１）

*山本 衛[1] (1.京都大学生存圏研究所)

[E] 口頭発表 | セッション記号 P (宇宙惑星科学)：P-EM 太陽地球系科学・宇宙電磁気学・宇宙環境

10:45 ~ 12:15 | A01 東京ベイ幕張ホール

[P-EM15] 太陽地球系結合過程の研究基盤形成

コンビーナ:山本 衛(京都大学生存圏研究所)、小川 泰信(国立極地研究所)、野澤 悟徳(名古屋大学宇宙地球環境研究所)、吉川 顕正(九州大学大学院理学研究院地球惑星科学部門)、座長:野澤 悟徳

10:45 ~ 11:15

[PEM15-07] Numerical Experiments on Stratosphere-Troposphere Two-Way Dynamical Coupling in the Tropics through Organizations of Moist Convective Systems

★Invited Papers

*余田 成男[1]、Hai Bui[2]、畔野 貴弘[1] (1.京都大学大学院理学研究科地球惑星科学専攻、2.Geophysical Institute, University of Bergen)

11:15 ~ 11:30

[PEM15-08] 赤道プラズマバブル数値シミュレーションの発展と今後

*横山 竜宏[1] (1.京都大学)

11:30 ~ 11:45

[PEM15-09] Characteristics of CME- and CIR-driven ion upflows in the polar ionosphere

*小川 泰信[1]、関 華奈子[2]、桂華 邦裕[2]、海老原 祐輔[3] (1.国立極地研究所、2.東京大学理学研究科、3.京都大学生存圏研究所)

11:45 ~ 12:00

[PEM15-10] SuperDARN Hokkaido Pair of (HOP) radars and mid-latitude SuperDARN: today and future

*西谷 望[1] (1.名古屋大学宇宙地球環境研究所)

12:00 ~ 12:15

[PEM15-11] 南極昭和基地大型大気レーダー（39.6°E, 69.0°S）による適応的信号処理を用いた電離圏非干渉性散乱と沿磁力線不均一の同時観測

*橋本 大志[1]、齊藤 昭則[2]、西村 耕司[3]、堤 雅基[3]、佐藤 薫[4]、佐藤 亨[1] (1.京都大学大学院情報学研究科、2.京都大学大学院理学研究科、3.国立極地研究所、4.東京大学大学院理学研究科)

[E] 口頭発表 | セッション記号 P (宇宙惑星科学)：P-EM 太陽地球系科学・宇宙電磁気学・宇宙環境

13:45 ~ 15:15 | A01 東京ベイ幕張ホール

[P-EM15] 太陽地球系結合過程の研究基盤形成

コンビーナ:山本 衛(京都大学生存圏研究所)、小川 泰信(国立極地研究所)、野澤 悟徳(名古屋大学宇宙地球環境研究所)、吉川 顕正(九州大学大学院理学研究院地球惑星科学部門)、座長:小川 泰信

13:45 ~ 14:00

[PEM15-12] Mini/Micro Satellite Constelaltion for the study of LAI coupling

*小山 孝一郎[1,2,3] (1.国立成功プラズマ宇宙科学研究所　台湾、2.九州大学国際宇宙天気・教育センター、3.(株）アジア宇宙環境研究コンソーシアム)

14:00 ~ 14:15

[PEM15-13] Statistical study of daily and seasonal variation of the equatorial anomaly in Asia based on satellite-ground beacon experiment

*坂本 悠記[1]、山本 衛[1]、穂積 コンニャナット[2] (1.京都大学生存圏研究所、2.国立研究開発法人 情報通信研究機構)

14:15 ~ 14:30

[PEM15-14] Latest installation of FM-CW radar in Peru

*藤本 晶子[1]、池田 昭大[2]、吉川 顕正[3] (1.九州工業大学、2.鹿児島工業高等専門学校、3.九州大学)

14:30 ~ 14:45

[PEM15-15] Understanding the OH Meinel Band Emissions on the Terrestrial Planets

*Konstantinos S. Kalogerakis[1] (1.Center for Geospace Studies, SRI International, Menlo Park, California, U.S.A.)

14:45 ~ 15:00

[PEM15-16] Statistical study of Sporadic Sodium Layer (SSL) observed at Tromsø

*野澤 悟徳[1]、津田 卓雄[2]、斎藤 徳人[3]、高橋 透[4]、川原 琢也[5]、小川 泰信[4]、藤原 均[6]、和田 智之[3]、小川 洋平[1]、Hall Chris[7]、Brekke Asgeir[7] (1.名古屋大学宇宙地球環境研究所、2.電気通信大学情報理工学部、3.理化学研究所光量子工学研究センター、4.国立極地研究所、5.信州大学工学部、6.成蹊大学理工学部、7.UiTノルウェー北極大学)

15:00 ~ 15:15

[PEM15-17] 大型研究計画「太陽地球系結合過程の研究基盤形成」推進の議論（２）

*山本 衛[1] (1.京都大学生存圏研究所)

[E] 口頭発表 | セッション記号 A (大気水圏科学)：A-AS 大気科学・気象学・大気環境

9:00 ~ 10:30 | 104 1F

[A-AS02] 台風研究の新展開〜過去・現在・未来

コンビーナ:金田 幸恵(名古屋大学宇宙地球環境研究所)、和田 章義(気象研究所台風・災害気象研究部)、伊藤 耕介(琉球大学)、宮本 佳明(慶應義塾大学　環境情報学部)、座長:金田 幸恵(名古屋大学)、和田 章義(気象研究所)

9:00 ~ 9:15

[AAS02-01] A GRAPES-based mesoscale EPS for TC forecasting: configuration and performance

*Xubin Zhang[1] (1.Institute of Tropical and Marine Meteorology, CMA)

9:15 ~ 9:30

[AAS02-02] **Evaluation of operational Ensemble based Global Forecast System prediction for Tropical Cyclones over the North Indian Ocean**

*Medha Deshpande[1]、Radhika Kanase[1]、R P M Krishna[1]、Emmanuel Rongmie[1]、P Mukhopadhyay[1] (1.IITM, Pune, INDIA)

9:30 ~ 9:45

[AAS02-03] 270メンバーのアンサンブル実験から得られた急発達開始前の熱帯低気圧の構造変化

*宮本 佳明[1]、David Nolan[2] (1.慶應義塾大学　環境情報学部、2.Rosenstiel School of Marine and Atmospheric Science, University of Miami)

9:45 ~ 10:00

[AAS02-04] Potential impacts of tropical cyclone inner-core convective activity on the predictability of rapid intensification

*南出 将志[1]、Derek Posselt[1] (1.Jet Propulsion Laboratory, California Institute of Technology)

10:00 ~ 10:15

[AAS02-05] A link between high-speed solar wind streams and rapid intensification of tropical cyclones

*Paul Prikryl[1,2]、Lidia Nikitina[2]、Vojto Rušin[3] (1.Physics Department, University of New Brunswick, Fredericton, NB, Canada、2.Geomagnetic Laboratory, Natural Resources Canada, Ottawa, ON, Canada、3.Astronomical Institute, Slovak Academy of Sciences, Tatranská Lomnica, Slovak Republic)

10:15 ~ 10:30

[AAS02-06] Influence of Tropical Lower Stratospheric Cooling on Extreme Deep Convective Activity and Tropical Cyclones

*Kodera Kunihiko[1]、江口 菜穂[2]、Ueyama Rei[3]、Funatsu Beatriz[4]、Claud Chantal[5] (1.Meteorological Research Institute、2.Kyushu University、3.NASA Ames Research Center、4.Université de Nantes、5.Ecole Polytechnique)

[E] 口頭発表 | セッション記号 A (大気水圏科学)：A-AS 大気科学・気象学・大気環境

10:45 ~ 12:15 | 104 1F

[A-AS02] 台風研究の新展開〜過去・現在・未来

コンビーナ:金田 幸恵(名古屋大学宇宙地球環境研究所)、和田 章義(気象研究所台風・災害気象研究部)、伊藤 耕介(琉球大学)、宮本 佳明(慶應義塾大学　環境情報学部)、座長:宮本 佳明、伊藤 耕介(琉球大学)

10:45 ~ 11:15

[AAS02-07] A change in the inner-core structure of Typhoon Trami (2018) as observed through upper-tropospheric aircraft reconnaissance of T-PARCII

★Invited Papers

*山田 広幸[1]、坪木 和久[2]、篠田 太郎[2]、久保田 尚之[3]、高橋 幸弘[3]、長浜 則夫[4]、清水 健作[4]、大東 忠保[5]、伊藤 耕介[1]、山口 宗彦[6]、中澤 哲夫[6] (1.琉球大学、2.名古屋大学、3.北海道大学、4.明星電気、5.防災科学技術研究所、6.気象庁気象研究所)

11:15 ~ 11:30

[AAS02-08] **台風第21号の上陸に伴う内部構造の劇的変化及びメソ渦と突風の関係**

*嶋田 宇大[1]、小山 亮[1]、清水 慎吾[2] (1.気象庁気象研究所、2.防災科学技術研究所)

11:30 ~ 11:45

[AAS02-09] **Revisiting Asymmetric CAPE in Sheared Tropical Cyclones**

*Qingqing Li[1] (1.NUIST Nanjing University of Information Science and Technology)

11:45 ~ 12:00

[AAS02-10] **Observed rainfall asymmetry of tropical cyclone in the process of making landfall in Guangdong, South China**

*Guanhuan Wen[1] (1.Guangzhou Institute of Tropical and Marine Meteorology, China Meteorological Administation)

12:00 ~ 12:15

[AAS02-11] Volumetric Detection of Tornadic Vortices Associated with Typhoon Nanmadol (2017) Using PAWR and Deep Learning

*足立 透[1]、石津 尚喜[2]、楠 研一[1]、猪上 華子[1]、新井 健一郎[2]、藤原 忠誠[3]、鈴木 博人[3] (1.気象研究所、2.アルファ電子/気象研究所、3.東日本旅客鉄道)

[E] 口頭発表 | セッション記号 A (大気水圏科学)：A-AS 大気科学・気象学・大気環境

15:30 ~ 17:00 | 104 1F

[A-AS02] 台風研究の新展開〜過去・現在・未来

コンビーナ:金田 幸恵(名古屋大学宇宙地球環境研究所)、和田 章義(気象研究所台風・災害気象研究部)、伊藤 耕介(琉球大学)、宮本 佳明(慶應義塾大学　環境情報学部)、座長:金田 幸恵(名古屋大学)、宮本 佳明

15:30 ~ 15:45

[AAS02-12] Evaluation of the monthly Potential of the 2018 typhoon activity and the effect of the positive PMM and SST of the eastern northwestern Pacific

*石山 尊浩[1]、佐藤 正樹[1] (1.東京大学大気海洋研究所)

15:45 ~ 16:00

[AAS02-13] **Contributions of different time scale variations to tropical cyclogenesis over the western North Pacific**

*Xi Cao[1] (1. Institute of Atmospheric Physics, Chinese Academy of Sciences)

16:00 ~ 16:15

[AAS02-14] Binary interaction between TC Chanthu (2016) and a nearby cold low

*伊藤 耕介[1]、比嘉 未雅[1]、Chan Johnny[2] (1.琉球大学、2.City University of Hong Kong)

16:15 ~ 16:30

[AAS02-15] **Response of landfalling North Indian Ocean cyclonic disturbances to warming climate and associated environmental parameters**

*JAGABANDHU PANDA[1]、KASTURI SINGH[1] (1.Department of Earth and Atmospheric Sciences, National Institute of Technology Rourkela, India)

16:30 ~ 16:45

[AAS02-16] **Rainfall contribution of North Indian Ocean cyclonic disturbances over India in a warming climate**

*KASTURI SINGH[1]、JAGABANDHU PANDA[1] (1.Department of Earth and Atmospheric Sciences, National Institute of Technology Rourkela, India)

16:45 ~ 17:00

[AAS02-17] Analysis of typhoon tracks and associated precipitation amount over western Japan: A case study with Typhoon Nancy and Typhoon Jebi

*Sridhara Nayak[1]、Tetsuya Takemi[1] (1.Disaster Prevention Research Institute, Kyoto University)

[E] 口頭発表 | セッション記号 A (大気水圏科学)：A-OS 海洋科学・海洋環境

13:45 ~ 15:15 | 105 1F

[A-OS07] 季節内から十年規模の気候変動と予測可能性

コンビーナ:望月 崇(国立研究開発法人海洋研究開発機構)、V Ramaswamy(NOAA GFDL)、Doug Smith(Met Office)、森岡 優志(海洋研究開発機構)、座長:V Ramaswamy(NOAA GFDL)、望月 崇(海洋研究開発機構)

13:45 ~ 14:00

[AOS07-01] Seasonal Predictions of Tropical Cyclones in 2018 using GFDL and NICAM High-Resolution Global Models

★Invited Papers

*村上 裕之[1,2]、中野 満寿男[3]、V Ramaswamy[1]、Thomas Delworth[1]、Sarah Kapnick[1]、Rich Gudgel[1]、望月 崇[3]、土井 威志[3]、森岡 優志[3] (1.地球流体学研究所、2.大気研究大学連盟、3.海洋研究開発機構)

14:00 ~ 14:15

[AOS07-02] **Future change of tropical cyclone-induced waves in the Indian Ocean; An analysis based on super-high-resolution MRI-AGCM3.2 climate model**

*Bahareh Kamranzad[1,2]、Nobuhito Mori[1] (1.Disaster Prevention Research Institute, Kyoto University、2.Hakubi Center for Advanced Research, Kyoto University)

14:15 ~ 14:30

[AOS07-03] The ocean-coupled global cloud-resolving modeling era

★Invited Papers

*宮川 知己[1] (1.東京大学大気海洋研究所)

14:30 ~ 14:45

[AOS07-04] Westerly Wind Burst (WWB)/Easterly Wind Surge (EWS)-like stochastic forcing and the effects on ENSO prediction by the SINTEX-F system

*土井 威志[1]、Swadhin Behera[1]、山形 俊男[1] (1.JAMSTEC)

14:45 ~ 15:00

[AOS07-05] **The life-cycle of annual waves in the Pacific Ocean as identified by a seamless diagnosis for the energy flux**

*相木 秀則[1]、志村 貴寛[2] (1.名古屋大学宇宙地球環境研究所、2.名古屋大学大学院環境学研究科)

15:00 ~ 15:15

[AOS07-06] 気象研究所における弱結合同化システムの開発とその評価

★招待講演

*藤井 陽介[1]、小林 ちあき[1]、石橋 俊之[1]、高谷 祐平[1] (1.気象庁気象研究所)

[E] 口頭発表 | セッション記号 A (大気水圏科学)：A-OS 海洋科学・海洋環境

15:30 ~ 17:00 | 105 1F

[A-OS07] 季節内から十年規模の気候変動と予測可能性

コンビーナ:望月 崇(国立研究開発法人海洋研究開発機構)、V Ramaswamy(NOAA GFDL)、Doug Smith(Met Office)、森岡 優志(海洋研究開発機構)、座長:森岡 優志(海洋研究開発機構)、望月 崇(海洋研究開発機構)

15:30 ~ 15:45

[AOS07-07] Decadal variability and predictability of the North Atlantic Oscillation

★Invited Papers

*Rosemary Eade[1,2]、David Stephenson[2]、Doug Smith[1]、Adam Scaife[1,2]、Leon Hermanson[1]、Nick Dunstone[1] (1.Met Office Hadley Centre、2.University of Exeter)

15:45 ~ 16:00

[AOS07-08] Seasonal to multi-year climate predictability in a climate model MIROC6

*片岡 崇人[1]、建部 洋晶[1]、小山 博司[1]、望月 崇[1] (1.研究開発法人　海洋研究開発機構)

16:00 ~ 16:15

[AOS07-09] Identifying the early 2000s hiatus associated with internal climate variability

*Xin-Gang Dai[1]、Ping Wang[2] (1.Institute of Atmospheric Physics, Chinese Academy of Sciences、2.Chinese Academy of Meteorological Sciences)

16:15 ~ 16:30

[AOS07-10] Decadal Evolution of the Surface Energy Budget during the Fast Warming and Global Warming Hiatus Periods in the ERA-Interim

*XIAOMING HU[1] (1.Sun Yat-sen University)

16:30 ~ 16:45

[AOS07-11] The role of ocean variability for multi-year droughts in Australia

*Andrea Taschetto[1,2]、Alex Sen Gupta[1,2]、Caroline C Ummenhofer[3]、Matthew H England[1,2] (1.Climate Change Research Centre, University of New South Wales, Sydney, Australia、2.ARC Centre of Excellence for Climate Extremes, University of New South Wales, Sydney, Australia、3.Department of Physical Oceanography, Woods Hole Oceanographic Institution, Woods Hole, MA, USA)

16:45 ~ 17:00

[AOS07-12] Decadal variability and predictability in the Southern Ocean - implications for interpreting recent observed trends

★Invited Papers

*Liping Zhang[1,2]、Thomas L Delworth[2]、William Cooke[2,3]、Xiaosong Yang[2,3] (1.Princeton University、2.Geophysical Fluid Dynamics Laboratory、3.UCAR)

[E] 口頭発表 | セッション記号 A (大気水圏科学)：A-OS 海洋科学・海洋環境

9:00 ~ 10:30 | 105 1F

[A-OS10] Atlantic climate variability, and its global impacts and predictability

コンビーナ:Ingo Richter(JAMSTEC Japan Agency for Marine-Earth Science and Technology)、時長 宏樹(九州大学応用力学研究所)、Noel S Keenlyside(Geophysical Institute Bergen)、Carlos R Mechoso(University of California Los Angeles)、座長:時長 宏樹(京都大学白眉センター)、Ingo Richter

9:00 ~ 9:15

[AOS10-01] Atlantic impacts on the tropical Pacific climate in the 2000s

*望月 崇[1]、渡部 雅浩[2]、木本 昌秀[2] (1.国立研究開発法人海洋研究開発機構、2.東京大学大気海洋研究所)

9:15 ~ 9:30

[AOS10-02] Recent acceleration of Arabian Sea warming induced by the Atlantic-western Pacific trans-basin multidecadal variability

*Cheng Sun[1] (1.Beijing Normal University)

9:30 ~ 9:45

[AOS10-03] **Westward Wind Changes over the Tropical and Mid-latitude Pacific in the Past Three Decades Driven by the Inter-basin Teleconnections**

★Invited Papers

*Xichen Li[1] (1.Institute of Atmospheric Physics)

9:45 ~ 10:00

[AOS10-04] On the Usefulness of the Atlantic Multidecadal Oscillation Index for Identifying Origins of North Atlantic Sea Surface Temperature Variability

*Jing Sun[1,2]、Mojib Latif[1,3]、Wonsun Park[1]、Taewook Park[1,4] (1.GEOMAR Helmholtz Centre for Ocean Research Kiel、2.Ocean University of China、3.University of Kiel、4.Korea Polar Research Institute)

10:00 ~ 10:15

[AOS10-05] Atlantic Multidecadal SST Signal Modulated by the Low-Frequency Mixed Layer Depth Variability

*Ayako Yamamoto[1]、Hiroaki Tatebe[1]、Masami Nonaka[1] (1.Japan Agency for Marine-Earth Science and Technology)

10:15 ~ 10:30

[AOS10-06] A High-Resolution Future Wave Climate Projection for the Northwestern Atlantic

*Adrean Webb[1]、Tomoya Shimura[1]、Nobuhito Mori[1] (1.Kyoto University, Disaster Prevention Research Institute)

[E] 口頭発表 | セッション記号 A (大気水圏科学)：A-OS 海洋科学・海洋環境

10:45 ~ 12:15 | 105 1F

[A-OS10] Atlantic climate variability, and its global impacts and predictability

コンビーナ:Ingo Richter(JAMSTEC Japan Agency for Marine-Earth Science and Technology)、時長 宏樹(九州大学応用力学研究所)、Noel S Keenlyside(Geophysical Institute Bergen)、Carlos R Mechoso(University of California Los Angeles)、座長:Ingo Richter、時長 宏樹(京都大学白眉センター)

10:45 ~ 11:00

[AOS10-07] Tropical Atlantic Impact on ENSO predictability

★Invited Papers

*Belen Rodriguez-Fonseca[1,2]、Irene - Polo[1]、Elsa - Mohino[1]、Teresa - Losada[1]、Marta - Martin-Rey[5]、Roberto - Mechoso[3]、Noel - Keenlyside[4] (1.Department of Physics of the Earth and Astrophysics, UCM, Madrid, Spain、2.Institute of Geosciences, IGEO, UCM-CSIC, Madrid, Spain、3.Department of Atmospheric and Oceanic Sciences, UCLA, Los Angeles, USA、4.Geophysical Institute, University of Bergen, Norway、5.Instituto de Ciencias del Mar, Barcelona, Spain)

11:00 ~ 11:15

[AOS10-08] **Interannual variability of Antarctic Intermediate Water in the tropical North Atlantic**

*Yao Fu[1]、Chunzai Wang[1]、Peter Brandt[2,3]、Richard J. Greatbatch[2,3] (1.State Key Laboratory of Tropical Oceanography, South China Sea Institute of Oceanology, Chinese Academy of Sciences, Guangzhou, China、2.GEOMAR Helmholtz Centre for Ocean Research Kiel, Kiel, Germany 、3.Christian-Albrechts-Universität zu Kiel, Kiel, Germany)

11:15 ~ 11:30

[AOS10-09] **Understanding the mechanisms of the Atlantic meridional climate variability**

*Hyacinth C Nnamchi[1]、Riccardo Farneti[2]、Noel S Keenlyside[3]、Fred Fred Kucharski[2]、Mojib Latif[1] (1.GEOMAR Helmholtz Centre for Ocean Research Kiel, Kiel, Germany、2.Abdus Salam International Centre for Theoretical Physics, Trieste, Italy、3.Geophysical Institute, University of Bergen, and Bjerknes Centre for Climate Research, Bergen, Norway)

11:30 ~ 11:45

[AOS10-10] The corss-equatorical gradient variability: The role of heat, momentum, and freshwater flux

*片岡 崇人[1] (1.研究開発法人　海洋研究開発機構)

11:45 ~ 12:00

[AOS10-11] Generation mechanisms of the Benguela Nino with a focus on local amplification

*東塚 知己[1]、小林 諒[1] (1.東京大学大学院理学系研究科地球惑星科学専攻)

12:00 ~ 12:15

[AOS10-12] **Seasonal energy analysis for baroclinic waves in equatorial Atlantic through a diagnostic scheme for energy flux**

*Qingyang Song[1]、Hidenori AIKI[1] (1.Institute of space-earth environmental research, Nagoya University)

[E] 口頭発表 | セッション記号 A (大気水圏科学)：A-HW 水文・陸水・地下水学・水環境

9:00 ~ 10:30 | 201B 2F

[A-HW22] 流域の物質輸送と栄養塩循環ー源流域から沿岸海域までー

コンビーナ:小林 政広(国立研究開発法人森林研究・整備機構　森林総合研究所)、吉川 省子(農業・食品産業技術総合研究機構　農業環境変動研究センター)、安元 純(琉球大学　農学部　地域農業工学科)、Adina Paytan(University of California Santa Cruz)、座長:Adina Paytan(University of California, Santa Cruz)

9:00 ~ 9:15

[AHW22-06] 沿岸食物網における底生無脊椎動物群集の多様性と統合栄養位置（ITP）の関係：「栄養位置の多様性仮説」の検証

*奥田 昇[1]、苅部 甚一[2]、酒井 陽一郎[3]、武山 智博[4]、陀安 一郎[1]、由水 千景[1]、永田 俊[5] (1.総合地球環境学研究所、2.近畿大学、3.琵琶湖環境科学研究センター、4.岡山理科大学、5.東京大学)

9:15 ~ 9:30

[AHW22-07] The analysis of the community composition of riverine bacteria and microalgae in relation to nutrient status and diversity: the case in irrigation season in the Yasu River, Japan

*池谷 透[1]、石田 卓也[1]、上原 佳敏[1]、淺野 悟史[2]、陀安 一郎[1]、奥田 昇[1]、潮 雅之[3,4,5]、藤永 承平[4]、Chia-Ying Ko[6]、Elfritzson Peralta[7]、石川 尚人[8]、岩田 智也[9] (1.総合地球環境学研究所、2.滋賀県琵琶湖環境科学研究センター、3.京都大学白眉センター、4.京都大学生態学研究センター、5.さきがけ 科学技術振興機構、6.National Taiwan University、7.University of Santo Tomas、8.海洋研究開発機構生物地球化学研究分野、9.山梨大学生命環境学部)

9:30 ~ 9:45

[AHW22-08] **Multiple stressors and protection efforts in highly urbanized watersheds in the Philippines**

*Elfritzson M. Peralta[1,3]、Leocris S. Batucan Jr.[4,6]、Alexis E. Belen[2,3]、Irisse Bianca B. De Jesus[1,3]、Takuya Ishida[5]、Chia-Ying Ko[7]、Yuki Kobayashi[5]、Tohru Ikeya[5]、Yoshitoshi Uehara[5]、Tomoya Iwata[8]、Adelina S. Borja[9]、Jonathan Carlo A. Briones[1,2,3]、Francis S. Magbanua[4]、Rey Donne S. Papa[1,2,3]、Noboru Okuda[5] (1.Research Center for the Natural and Applied Sciences, University of Santo Tomas, PH、2.Department of Biological Sciences, University of Santo Tomas, PH、3.The Graduate School, University of Santo Tomas, PH、4.Institute of Biology, University of the Philippines Diliman, PH、5.Research Institute for Humanity and Nature, JP、6.Academia Sinica and Department of Life Science, National Taiwan Normal University, TW、7.Institute of Fisheries Science and Department of Life Science, National Taiwan University, TW、8.Faculty of Life and Environmental Sciences, University of Yamanashi, JP、9.Resource Management and Development Department, Laguna Lake Development Authority, PH)

9:45 ~ 10:00

[AHW22-09] ベトナム中部の野菜畑における浅層地下水のアンモニア態窒素汚染

★招待講演

*前田 守弘[1]、藤村 拓也[1]、Hoang Ngoc Tuong Van [2]、井上 大介[3]、近森 秀高[1]、兵藤 不二夫[1] (1.岡山大学、2.フエ大学、3.大阪大学)

10:00 ~ 10:15

[AHW22-10] Modelling nutrient and organic waste behaviour in a tropical wetland in Singapore under projected anthropogenic scenarios

*Swee Yang Edmund Low[1]、Dong Eon Kim[1]、Canh Tien Trinh Nguyen[1]、Yixiong Cai、Shie-Yui Liong[1] (1.National University of Singapore)

10:15 ~ 10:30

[AHW22-11] **Benthic macroinvertebrate assemblages and water quality reflect the impacts of land use and land cover in Marikina Watershed, Philippines**

*Julie - An N. Gregorio[1,2]、Elfritzson M. Peralta[3,5]、Irisse Bianca B. de Jesus[3,5]、Tohru Ikeya[6]、Jonathan Carlo A. Briones[3,4,5]、Rey Donne S. Papa[3,4,5]、Francis S. Magbanua[1]、Noboru Okuda[6] (1.Institute of Biology, University of the Philippines, Diliman, Quezon City, 1101 Philippines、2.Institute of Environmental Science and Meteorology, University of the Philippines, Diliman, Quezon City 1101 Philippines、3.Research Center for the Natural and Applied Sciences, University of Santo Tomas, España Boulevard, Manila, 1015, Philippines、4.Department of Biological Sciences, University of Santo Tomas, España Boulevard, Manila, 1015, Philippines、5.The Graduate School, University of Santo Tomas, España Boulevard, Manila, 1015, Philippines、6.Research Institute for Humanity and Nature, 457-4 Motoyama, Kamigamo, Kyoto, 603-8047, Japan)

[E] 口頭発表 | セッション記号 A (大気水圏科学)：A-HW 水文・陸水・地下水学・水環境

10:45 ~ 12:15 | 201B 2F

[A-HW22] 流域の物質輸送と栄養塩循環ー源流域から沿岸海域までー

コンビーナ:小林 政広(国立研究開発法人森林研究・整備機構　森林総合研究所)、吉川 省子(農業・食品産業技術総合研究機構　農業環境変動研究センター)、安元 純(琉球大学　農学部　地域農業工学科)、Adina Paytan(University of California Santa Cruz)、座長:安元 純(琉球大学　農学部　地域農業工学科)

10:45 ~ 11:00

[AHW22-12] **Characterization, distribution and degradation of environmental plastics in inland river system of Mongolia**

*Batdulam Battulga[1]、Masayuki Kawahigashi[1]、Bolormaa Oyuntsetseg[2] (1.Department of Geography, Tokyo Metropolitan University, Tokyo, 192-0397, Japan 、2.Department of Chemistry, National University of Mongolia, Ulaanbaatar, 210646, Mongolia)

11:00 ~ 11:15

[AHW22-13] Multi-site and multi-approach sediment transport modeling in tropical watersheds

★Invited Papers

*Assefa M Melesse[1]、Alemu Osore Aga[2]、Hagos Gebreselassie[2] (1.Florida International University、2.Addis Ababa University)

11:15 ~ 11:30

[AHW22-14] 流域土地利用モデルによるSS濃度係数の算出

*吉川 省子[1]、馬 東来[1,2]、齋藤 忠将[1,3]、松森 堅治[4]、伊藤 優子[5]、小林 政広[5] (1.農業・食品産業技術総合研究機構　農業環境変動研究センター、2.筑波大学大学院、3.茨城大学農学部、4.農業・食品産業技術総合研究機構　西日本農業研究センター、5.国立研究開発法人　森林研究・整備機構森林総合研究所)

11:30 ~ 11:45

[AHW22-15] Evaluation of long term variation in water balance and discharge of sediment and nitrogen in the urbanized catchment of Yamato River, using SWAT model

*王 崑陽[1,2]、清水 裕太[3]、小野寺 真一[1]、齋藤 光代[4]、友澤 裕介[1] (1.広島大学、2.首都師範大学、3.農研機構、4.岡山大学)

11:45 ~ 12:00

[AHW22-16] Causal correlation between water-use of the Tedori River and coastal erosion of Chirihama Nagisa Driveway, Ishikawa, Japan

*百瀬 年彦[1] (1.石川県立大学)

12:00 ~ 12:15

[AHW22-17] セレンガ河における元素動態への懸濁粒子の役割

★招待講演

*川東 正幸[1]、Orgilbold Myangan[2]、Bolormaa Oyuntsetseg[2] (1.首都大学東京、2.モンゴル国立大学)

[E] 口頭発表 | セッション記号 A (大気水圏科学)：A-HW 水文・陸水・地下水学・水環境

13:45 ~ 15:15 | 201B 2F

[A-HW22] 流域の物質輸送と栄養塩循環ー源流域から沿岸海域までー

コンビーナ:小林 政広(国立研究開発法人森林研究・整備機構　森林総合研究所)、吉川 省子(農業・食品産業技術総合研究機構　農業環境変動研究センター)、安元 純(琉球大学　農学部　地域農業工学科)、Adina Paytan(University of California Santa Cruz)、座長:吉川 省子(国立研究開発法人 農業・食品産業技術総合研究機構 農業環境変動研究センター)

13:45 ~ 14:00

[AHW22-18] Relationship between topographical characteristics in catchment area and dissolved iron concentration of river in permafrost area

*田代 悠人[1]、楊 宗興[1]、白岩 孝行[2]、大西 健夫[3] (1.東京農工大学、2.北海道大学、3.岐阜大学)

14:00 ~ 14:15

[AHW22-19] Water Source Zones and Hydrochemical Properties of Fluoride Water in Mt. Meru Watershed, Tanzania

*中屋 眞司[1]、高田 遼吾[1]、安元 純[2]、吉谷 純一[1]、ルゴディシャ イノセント[3]、ルインボ ズベリ[3]、コマケッチ ハンス[4]、モレル トーマス[5] (1.信州大学工学部水環境・土木工学科、2.琉球大学農学部地域農業工学科、3.ネルソンマンデラ科学技術大学、4.ネルソンマンデラ科学技術大学ワイズフューチャー、5.タンザニアさくら女子中学)

14:15 ~ 14:30

[AHW22-20] 水質総負荷量の計測システム開発とその適用例

★招待講演

*高瀬 恵次[1]、伊藤 優子[2] (1.石川県立大学、2.国立研究開発法人　森林総合研究所)

14:30 ~ 14:45

[AHW22-21] Water infiltration and uptake around a Japanese cypress growing on a flat upland

*小林 政広[1]、小野寺 真一[2]、伊藤 優子[1]、阪田 匡司[1] (1.国立研究開発法人森林研究・整備機構　森林総合研究所、2.広島大学大学院総合科学研究科)

14:45 ~ 15:00

[AHW22-22] Innovative Rainfall Simulator Design for Moving Storm Scenarios with Different Storm Patterns

*RAVI KUMAR MEENA[1]、SUMIT SEN[2] (1.M.Tech Student, Department of Hydrology, Indian Institute of Technology Roorkee, Roorkee, Uttarakhand, India、2. Associate Professor, Department of Hydrology, Indian Institute of Technology Roorkee, Roorkee, Uttarakhand, India)

[E] 口頭発表 | セッション記号 A (大気水圏科学)：A-GE 地質環境・土壌環境

9:00 ~ 10:30 | 301A 3F

[A-GE28] 地質媒体における物質移動，物質循環と環境評価

コンビーナ:小島 悠揮(岐阜大学工学部)、濱本 昌一郎(東京大学大学院農学生命科学研究科)、斎藤 広隆(東京農工大学大学院農学研究院)、森 也寸志(岡山大学大学院環境生命科学研究科)、座長:小島 悠揮(岐阜大学)、濱本 昌一郎(東京大学)、森 也寸志(岡山大学)、斎藤 広隆(東京農工大学)

9:00 ~ 9:25

[AGE28-01] **Humic substances in deep sedimentary groundwater**

★Invited Papers

*斉藤 拓巳[1] (1.東京大学大学院工学研究科)

9:25 ~ 9:40

[AGE28-02] Nano-Bubble Retention in Saturated Porous Media under Different Solution Chemistry

*濱本 昌一郎[1]、杉本 卓也[1]、竹村 貴人[2]、西村 拓[1]、Bradford Scott[3] (1.東京大学大学院農学生命科学研究科、2.日本大学文理学部、3.アメリカ農務省塩類研究所)

9:40 ~ 9:55

[AGE28-03] **Geochemical Investigation of Metals and Trace Elements around the Abandoned Cu – Ni Mine Site in Selibe Phikwe, Botswana**

*Fiona Segolame Motswaiso[1]、Kengo - Nakamura[1]、Noriaki - Watanabe[1]、Takeshi - Komai[1] (1.Tohoku Univeristy Graduate School of Environmental Studies)

9:55 ~ 10:10

[AGE28-04] Removal of Arsenic (III) From Aqueous Solution Using Pumice and Zeolite Supported Zero-Valent Iron Nanoparticle

*Shashi Ranjan[1]、Brijesh kumar yadav[1]、Himanshu Joshi[1] (1.Indian Institute of Technology Roorkee)

10:10 ~ 10:25

[AGE28-05] **Unsaturated Hydraulic Conductivity Estimation from Multi-step Centrifuge Outflow**

*Thanh Long Bui[1]、Yasushi Mori[1] (1.Graduate School of Environmental and Life Science, Okayama University)

[E] 口頭発表 | セッション記号 A (大気水圏科学)：A-GE 地質環境・土壌環境

10:45 ~ 12:15 | 301A 3F

[A-GE29] エネルギ・環境・水ネクサスと持続的発展

コンビーナ:張 銘(産業技術総合研究所地質調査総合センター地圏資源環境研究部門)、川本 健(埼玉大学大学院理工学研究科)、Jet-Chau Wen(National Yunlin University of Science and Technology)、? 永紅(天津師範大学)、座長:張 銘(産業技術総合研究所)、斎藤 広隆(東京農工大学)、郝 永紅(Tianjin Normal University)

10:50 ~ 11:05

[AGE29-01] Input-Output Analysis of Taiwan's Food-Energy-Water Risk

*CHU-CHUN YAO[1]、Gene Jiing-yun You[1] (1.National Taiwan University)

11:05 ~ 11:20

[AGE29-02] **Groundwater potential analysis using the multiple spatiotemporal remote sensing approach in fractured rock of mountainous region**

*Jung-Jun Lin[1,2]、Yuei-An Liou[1]、Chien-Chung Ke[2]、Su-Yun Chi[2]、Jia-Hung Liang[3] (1.National Central Univ.、2.Sinotech Engineering Consultants, Inc.、3.Ministry of Economic Affairs)

11:20 ~ 11:35

[AGE29-03] Estimating Soil Water Content with Color Calibration Method in the Image of Remote Sensing by Unmanned Aerial Vehicle

*Hong-Yi Li[1]、Hong-Ru Lin[1]、Jyun-Lin Chen[1]、Shao-Yang Huang[1]、Jet-Chau Wen[1] (1.National Yunlin University of Science and Technology)

11:35 ~ 11:50

[AGE29-04] **Characterizing Geotechnical Properties of Drinking Water Sludge Blended with Graded Crushed Clay Brick for Road Subgrade: Effects of Gradation and Mixing Proportion of Crushed Clay Brick on CBR and Water Permeability**

*Muhammad Rashid Iqbal[1]、Akihiro Matsuno[1]、Ken Kawamoto[1] (1.Graduate School of Science and Engineering, Saitama University)

11:50 ~ 12:05

[AGE29-05] Investigation and Evaluation of the Multiple-liquefaction Site at the Southern Taiwan

*Chih-Sheng KU[1] (1.I-Shou University)

[E] 口頭発表 | セッション記号 A (大気水圏科学)：A-GE 地質環境・土壌環境

13:45 ~ 15:15 | 301A 3F

[A-GE29] エネルギ・環境・水ネクサスと持続的発展

コンビーナ:張 銘(産業技術総合研究所地質調査総合センター地圏資源環境研究部門)、川本 健(埼玉大学大学院理工学研究科)、Jet-Chau Wen(National Yunlin University of Science and Technology)、? 永紅(天津師範大学)、座長:川本 健(埼玉大学)、温 志超(雲林科技大学)

13:50 ~ 14:05

[AGE29-06] Investigating the Reproducibility of Hydraulic Tomography Estimates with Time-Variable Boundary Conditions

*Jian-Dao Li[1]、Jyun-Lin Chen[1]、Hong-Ru Lin[1]、Shao-Yang Huang [1]、Tian-Chyi Jim Yeh[2]、Jet-Chau Wen[1] (1.National Yunlin University of Science and Technology、2.The University of Arizona)

14:05 ~ 14:20

[AGE29-07] **Applying river pollution index and QUAL2K model for water quality assessment and management in Ke-Ya river, Taiwan**

*Hong-Syuan Li[1]、Yu-Chih Lin[1] (1.Department of Environmental Engineering & Health, Yuanpei University of Medical Technology)

14:20 ~ 14:35

[AGE29-08] Environmental assessment at CDW disposal sites in Vietnam: Case study in Thanh Tri landfill, Hanoi

*Thanh Ha Ngo[1]、Akihiro Matsuno[1]、Ken Kawamoto[1] (1.Graduate School of Science and Engineering, Saitama University)

14:35 ~ 14:50

[AGE29-09] **Modeling Study on the Impacts of Groundwater Pumping to Regional Hydroclimatology in 37 World Major Aquifers**

*Pat J.-F. Yeh[1] (1.Monash University Malaysia)

14:50 ~ 15:05

[AGE29-10] CHRATERIZING BURIED WASTE COMPOSITION AT CONSTRUCTION AND DEMOLITION WASTE (CDW) DISPOSAL SITE IN VIETNAM: A CASE STUDY IN THANH TRI LANDFILL IN HANOI

*Tselmeg Aldarjav[1]、Akira Kato[1]、Akihiro Matsuno[1]、Ken Kawamoto[1,2] (1.Graduate School of Science and Engineering, Saitama University, Japan 、2.International Institute for Resilient Society, Saitama University, Japan)

[E] 口頭発表 | セッション記号 A (大気水圏科学)：A-CG 大気海洋・環境科学複合領域・一般

9:00 ~ 10:30 | 302 3F

[A-CG34] 衛星による地球環境観測

コンビーナ:沖 理子(宇宙航空研究開発機構)、本多 嘉明(千葉大学環境リモートセンシング研究センター)、高薮 縁(東京大学 大気海洋研究所)、松永 恒雄(国立環境研究所地球環境研究センター／衛星観測センター)、座長:鈴木 健太郎

9:00 ~ 9:15

[ACG34-07] GCOM-C「しきさい」による初年の観測について

★招待講演

*村上 浩[1]、堀 雅裕[1]、宮崎 理紗[1]、小林 利行[1]、永尾 隆[1]、緒方 一紀[1]、島田 利元[1]、高久 淳一[2] (1.宇宙航空研究開発機構地球観測研究センター、2.リモートセンシング技術センター)

9:15 ~ 9:30

[ACG34-08] Algorithm improvement for GCOM-C/SGLI Above Ground Biomass Standard product.

*梶原 康司[1]、本多 嘉明[1] (1.千葉大学)

9:30 ~ 9:45

[ACG34-09] Common retrieval of Atmospheric Aerosol Properties for geostationary and polar-orbital Satellite Imaging Sensors: Himawari8/AHI and GCOM-C/SGLI results

*吉田 真由美[1]、菊池 麻紀[1]、永尾 隆[1]、村上 浩[1]、弓本 桂也[2] (1.宇宙航空研究開発機構、2.九州大学)

9:45 ~ 10:00

[ACG34-10] Cloud optical properties from various ground and satellite instruments evaluated during an intensive campaign

*Alessandro Damiani[1]、Hitoshi Irie[1]、Takashi Horio[1]、Tamio Takamura[1]、Rei Kudo[2]、Pradeep Khatri[3]、Hironobu Iwabuchi[3]、Ryosuke Masuda[3]、Takashi M. Nagao[4] (1.CEReS, Chiba University、2.Meteorological Research Institute, Japan Meteorological Agency、3.Graduate School of Science, Tohoku University、4.Earth Observation Research Center, JAXA)

10:00 ~ 10:15

[ACG34-11] Issues in aerosol-cloud-climate interaction: Needs for future satellite mission

★Invited Papers

*鈴木 健太郎[1] (1.東京大学大気海洋研究所)

10:15 ~ 10:30

[ACG34-12] Impact of aerosol vertical profile and optical parameters on the accuracy of satellite AOD retrieval

*Jing Li[1]、Chong Li[1] (1.Peking University)

[E] 口頭発表 | セッション記号 A (大気水圏科学)：A-CG 大気海洋・環境科学複合領域・一般

10:45 ~ 12:15 | 302 3F

[A-CG34] 衛星による地球環境観測

コンビーナ:沖 理子(宇宙航空研究開発機構)、本多 嘉明(千葉大学環境リモートセンシング研究センター)、高薮 縁(東京大学 大気海洋研究所)、松永 恒雄(国立環境研究所地球環境研究センター／衛星観測センター)、座長:高橋 暢宏(名古屋大学宇宙地球環境研究所)

10:45 ~ 11:00

[ACG34-13] GPM/DPRの推定する雨滴粒径分布の統計的手法による検証

*高橋 暢宏[1] (1.名古屋大学　宇宙地球環境研究所)

11:00 ~ 11:15

[ACG34-14] Impact study of DPR SLH nudging method for data assimilation in the JMA Local NWP system

★Invited Papers

*幾田 泰酵[1] (1.気象庁)

11:15 ~ 11:30

[ACG34-15] Precipitation Extremes Monitoring using Global Satellite Mapping of Precipitation (GSMaP) Product

*久保田 拓志[1]、田島 知子[1]、沖 理子[1]、妻鹿 友昭[2]、牛尾 知雄[2] (1.宇宙航空研究開発機構　地球観測研究センター、2.首都大学東京　システムデザイン学部)

11:30 ~ 11:45

[ACG34-16] Estimation of cloud water content over land using satellite-based passive microwave observations with a coupled land and atmosphere assimilation method

*瀬戸 里枝[1]、鼎 信次郎[1] (1.東京工業大学)

11:45 ~ 12:00

[ACG34-17] Ensemble-Based Data Assimilation of GPM/DPR Reflectivity into the Nonhydrostatic Icosahedral Atmospheric Model NICAM

*小槻 峻司[1]、寺崎 康児[1]、三好 建正[1] (1.国立研究開発法人　理化学研究所　計算科学研究センター)

12:00 ~ 12:15

[ACG34-18] An ecohydrological land reanalysis by integrating simulation and satellite observations

*澤田 洋平[1]、仲江川 敏之[1]、岡本 幸三[1]、入口 武史[1]、藤井 秀幸[2] (1.気象庁気象研究所、2.宇宙航空研究開発機構)

[E] 口頭発表 | セッション記号 A (大気水圏科学)：A-CG 大気海洋・環境科学複合領域・一般

15:30 ~ 17:00 | 302 3F

[A-CG34] 衛星による地球環境観測

コンビーナ:沖 理子(宇宙航空研究開発機構)、本多 嘉明(千葉大学環境リモートセンシング研究センター)、高薮 縁(東京大学 大気海洋研究所)、松永 恒雄(国立環境研究所地球環境研究センター／衛星観測センター)、座長:松永 恒雄

15:30 ~ 15:45

[ACG34-19] How GOSAT has survived in-orbit anomalies and calibrated radiance spectra for 10 years.

★Invited Papers

*久世 暁彦[1]、hiroshi Suto[1]、Kei Shiomi[1]、菊地 信弘[1]、橋本 真喜子[1]、Fumie Kataoka[2] (1.宇宙航空研究開発機構、2.リモート・センシング技術センター)

15:45 ~ 16:00

[ACG34-20] Estimating regional anthropogenic methane emissions with GOSAT satellite retrievals and ground-based observations

*Shamil Maksyutov[1]、Aki Tsuruta[2]、Rajesh Janardanan[1]、Fenjuan Wang[1]、Akihiko Ito[1]、Motoki Sasakawa[1]、Toshinobu Machida[1]、Isamu Morino[1]、Yukio Yoshida[1]、Johannes Kaiser[3]、Greet Janssens-Maenhout[4]、Ed Dlugokencky[5]、Tsuneo Matsunaga[1] (1.National Institute for Environmental Studies、2.Finnish Meteorological Institute、3.Deutscher Wetterdienst、4.European Commission, Joint Research Centre 、5.National Oceanic and Atmospheric Administration, Global Monitoring Division)

16:00 ~ 16:15

[ACG34-21] The Status and the Future Plan of GOSAT-2 Level 2 and 4 Products

★Invited Papers

*松永 恒雄[1]、森野 勇[1]、吉田 幸生[1]、齊藤 誠[1]、野田 響[1]、大山 博史[1]、亀井 秋秀[1]、河添 史絵[1]、今須 良一[2]、中島 映至[4]、中島 孝[5]、齋藤 尚子[3]、橋本 真喜子[4] (1.国立環境研究所地球環境研究センター／衛星観測センター、2.東京大学、3.千葉大学、4.宇宙航空研究開発機構、5.東海大学)

16:15 ~ 16:30

[ACG34-22] 温室効果ガス観測技術衛星2号機搭載CAI-2による雲判別プロダクトの初期確認

*石原 吉明[1]、大石 優[2]、石田 春磨[3]、中島 孝[4] (1.国立環境研究所、2.農研機構、3.気象庁、4.東海大学)

16:30 ~ 16:45

[ACG34-23] **Drought monitoring and evaluation performance of temperature vegetation drought index (TVDI) over Eurasia**

*Fengmei Yao[1]、Siqi Shi[1]、Jiahua Zhang[2] (1.UCAS University of Chinese Academy of Sciences、2.Institute of Remote Sensing and Digital Earth, Chinese Academy of Sciences)

16:45 ~ 17:00

[ACG34-24] **IMPACT OF CHANGE IN LAND USE AND LAND COVER PATTERN ON LAND SURFACE TEMPERATURE AND THERMAL COMFORT USING MICRO-SCALE AREA MODEL: CASE STUDY OF AN EDUCATIONAL CAMPUS.**

*DILJIT KUMAR NAYAK[1]、MANJU MOHAN[1] (1.IIT DELHI)

[E] 口頭発表 | セッション記号 H (地球人間圏科学)：H-TT 計測技術・研究手法

13:45 ~ 15:15 | 301B 3F

[H-TT19] Geographic Information Systems and Cartography

コンビーナ:小口 高(東京大学空間情報科学研究センター)、村山 祐司(筑波大学大学院生命環境科学研究科地球環境科学専攻)、若林 芳樹(首都大学東京大学院都市環境科学研究科)、座長:村山 祐司、若林 芳樹

13:45 ~ 14:00

[HTT19-01] **A study on geographical changes in main roads and coastlines in the 200 years in Japan**

*岩井 優祈[1]、村山 祐司[1] (1.筑波大学大学院生命環境科学研究科地球環境科学専攻)

14:00 ~ 14:15

[HTT19-02] Comparative analysis of foreign tourists' spatial behavior in Tokyo using locational data from the photo-sharing service of Flickr

*Bochra Bettaieb[1]、Yoshiki Wakabayashi[1] (1.Tokyo Metropolitan University)

14:15 ~ 14:30

[HTT19-03] Neighborhood Walkability and its Potential Associations with Residents' Walking Habits

★Invited Papers

*山田 育穂[1]、眞田 佳市郎[2] (1.中央大学理工学部、2.中央大学理工学研究科)

14:30 ~ 14:45

[HTT19-04] **THE STUDY OF USING PARTICLE FILTER METHOD COMBINED INDOOR MAGNETIC MAP AND PEDESTRIAN DEAD RECKONING FOR INDOOR POSITIONING.**

*Yu-Chun Chen[1] (1.Department of Land Economics, National Chengchi University)

14:45 ~ 15:00

[HTT19-05] Assessing the Agriculture Sustainability based on Geospatial Technique in a Tropical Mountain Area : A Case Study in Kotmale Catchment in Sri Lanka.

*DM Sanjeewa Lasantha Bandara[1]、Takehiro Morimoto [2] (1.Division of Spatial Information Science, Graduate School of Life and Environmental Sciences, University of Tsukuba、2.Faculty of Life and Environmental Sciences, University of Tsukuba)

15:00 ~ 15:15

[HTT19-06] **Spatial Evaluation of Potential Tsunami Vertical Evacuation: A Case Study of the Western Coastal Belt in Sri Lanka**

*Ranagalage Mahinda Manjula[1]、Yuji Murayama[1] (1.Division of Spatial Science, Graduate School of Life and Environmental Sciences, University of Tsukuba, Japan)

[E] 口頭発表 | セッション記号 H (地球人間圏科学)：H-TT 計測技術・研究手法

15:30 ~ 17:00 | 301B 3F

[H-TT19] Geographic Information Systems and Cartography

コンビーナ:小口 高(東京大学空間情報科学研究センター)、村山 祐司(筑波大学大学院生命環境科学研究科地球環境科学専攻)、若林 芳樹(首都大学東京大学院都市環境科学研究科)、座長:小口 高、山田 育穂(中央大学)

15:30 ~ 15:45

[HTT19-07] A Framework for Assessing the Spatial Distribution of Vulnerability of Communities to Landslides in Tropical Mountainous Region: A Case study from Kegalle District – Sri Lanka.

★Invited Papers

*Nimala Chinthake Perera[1] (1.SANASA CAMPUS - SRI LANKA, IHRA - UNIVERSITY OF COLOMBO - SRI LANKA)

15:45 ~ 16:00

[HTT19-08] Applications of WebGIS to Educating Disaster Risk Reduction for Chinese and Japanese Students

*Jiali SONG[1]、Takashi Oguchi[2]、Hiroyuki Yamauchi[2]、Takuro Ogura[1] (1.Graduate School of Frontier Sciences, The University of Tokyo、2.Center for Spatial Information Science, The University of Tokyo)

16:00 ~ 16:15

[HTT19-09] Solar System Treks - GIS that provides interactive visualization and analysis for planetary science and exploration

★Invited Papers

*Emily Law[1]、Brian Hamilton Day[2] (1.NASA Jet Propulsion Laboratory、2.NASA Ames Research Center)

16:15 ~ 16:30

[HTT19-10] **Landslide Recognition using Remote Sensing Images and PCANet**

*魏 伊梅[1]、小口 高[1] (1.東京大学 新領域創成科学研究科)

16:30 ~ 16:45

[HTT19-11] Estimating the fractional vegetation cover using fixed-wing drone and multiple vegetation indices

★Invited Papers

*飯塚 浩太郎[1] (1.東京大学　空間情報科学研究センター)

16:45 ~ 17:00

[HTT19-12] スバールバル・ニーオーレスン地域における地形調査とマッピング手法の改善

*李 在庸[1]、小口 高[2] (1.東京大学大学院新領域創成科学研究科自然環境学専攻、2.東京大学空間情報科学研究センター)

[E] 口頭発表 | セッション記号 S (固体地球科学)：S-IT 地球内部科学・地球惑星テクトニクス

9:00 ~ 10:30 | A09 東京ベイ幕張ホール

[S-IT25] Planetary cores: Structure, formation, and evolution

コンビーナ:寺崎 英紀(大阪大学大学院理学研究科)、大谷 栄治(東北大学大学院理学研究科地学専攻)、William F McDonough(University of Maryland College Park)、George Helffrich(Earth-Life Science Institute, Tokyo Institute of Technology)、座長:George Helffrich(ELSI, Tokyo Institute of Technology)、寺崎 英紀

9:00 ~ 9:15

[SIT25-01] **High-pressure Equation of State of Schreibersite $Fe_{2.15}Ni_{0.85}P$: Implications for the Martian Core**

*Xuejing He[1]、Jiazeng Guo[2]、Xiang Wu[3]、Shengxuan Huang[1]、Fei Qin[1]、Xiangping Gu[4]、Shan Qin[1] (1.Peking Univ.、2.Nanyang Normal Univ.、3.China Univ. of Geosciences、4.Central South Univ.)

9:15 ~ 9:30

[SIT25-02] Bottom-up solidification versus top-down solidification of the liquid core of the relatively small planetary bodies

*浦川 啓[1]、寺崎 英紀[2] (1.岡山大学大学院自然科学研究科、2.大阪大学大学院理学研究科)

9:30 ~ 9:45

[SIT25-03] P-wave velocity of Fe_3S under high pressure and temperature

*鎌田 誠司[1,2]、寺崎 英紀[3]、福井 宏之[4,5]、坂巻 竜也[2]、内山 裕士[6]、筒井 智嗣[6]、大谷 栄治[2]、Baron Alfred[5] (1.東北大学学際科学フロンティア研究所、2.東北大学大学院理学研究科地学専攻、3.大阪大学大学院理学研究科宇宙地球科学専攻、4.兵庫県立大学物質理学研究科物質科学専攻、5.RIKEN、6.JASRI)

9:45 ~ 10:00

[SIT25-04] The sound velocity of liquid Fe-Ni-S-Si alloys under Mercury’s core condition

*山田 伊織[1]、寺崎 英紀[1]、神谷 朝香[1]、鶴岡 椋[1]、肥後 祐司[2]、町田 晃彦[3] (1.大阪大学大学院理学研究科、2.(財)高輝度光科学研究センター、3.量子科学技術研究開発機構)

10:00 ~ 10:15

[SIT25-05] レーザー衝撃実験によるFe-Si融体の重力不安定性成長のその場観察

*寺崎 英紀[1]、境家 達弘[1]、重森 啓介[2]、加藤 弘樹[2]、弘中 陽一郎[2]、近藤 忠[1] (1.大阪大学大学院理学研究科、2.大阪大学レーザー科学研究所)

[E] 口頭発表 | セッション記号 S (固体地球科学)：S-IT 地球内部科学・地球惑星テクトニクス

10:45 ~ 12:15 | A09 東京ベイ幕張ホール

[S-IT25] Planetary cores: Structure, formation, and evolution

コンビーナ:寺崎 英紀(大阪大学大学院理学研究科)、大谷 栄治(東北大学大学院理学研究科地学専攻)、William F McDonough(University of Maryland College Park)、George Helffrich(Earth-Life Science Institute, Tokyo Institute of Technology)、座長:William McDonough(University of Maryland / Tohoku University)、大谷 栄治(東北大学)

10:45 ~ 11:00

[SIT25-06] *P-V-T* equation-of-state of liquid Fe from *ab-initio* simulations to the TPa regime

*Gerd Steinle-Neumann[1]、Fabian Wagle[1] (1.Bayerisches Geoinstitut, University of Bayreuth, Germany)

11:00 ~ 11:15

[SIT25-07] ***Ab initio* study of Iron-Nickel alloys in Super-Earths cores**

*Francois Soubiran[1]、Razvan Caracas[1] (1.Ecole normale superieure de Lyon, Laboratoire de Géologie de Lyon, Université Lyon 1, CNRS UMR 5276, Lyon, France)

11:15 ~ 11:30

[SIT25-08] **Impurity effect on the iron's transport properties at Earth's core conditions: A key constraint for the evolution of the Earth's core**

*Youjun Zhang[1]、Mingqiang Hou[2]、Nilesh Salke[2]、Jung-Fu Lin[3] (1.Sichuan University、2.HPSTAR、3.University of Texas at Austin)

11:30 ~ 11:45

[SIT25-09] 214 GPaまでのFe-FeO系の共融点組成の決定

*岡 健太[1]、木所 佑斗、廣瀬 敬[1]、中島 陽一[2]、Guillaume Morard[3]、Guillaume Fiquet[3]、Nicolas Coudurier[3] (1.東京大学大学院理学系研究科地球惑星科学専攻、2.熊本大学大学院先導機構、3.ソルボンヌ大学)

11:45 ~ 12:00

[SIT25-10] B2 phase in the inner core: constraints from high pressure experiments

*Eiji Ohtani[1]、Daijo Ikuta[1]、Seiji Kamada[2]、Tatsuya Sakamaki[1]、Naohisa Hirao[3] (1.Department of Earth and Planetary Materials Science, Graduate School of Science, Tohoku University、2.Frontier Institute for Interdisciplinary Research, Tohoku University、3.SRring-8, Japan Synchrotron Research Institute)

[E] 口頭発表 | セッション記号 S (固体地球科学)：S-VC 火山学

9:00 ~ 10:30 | A07 東京ベイ幕張ホール

[S-VC34] Connecting magma dynamics in vent-conduit system with surface expression of volcanic eruption

コンビーナ:三輪 学央(防災科学技術研究所)、下司 信夫(産業技術総合研究所　活断層・火山研究部門)、座長:三輪 学央、Jacopo Taddeucci

9:00 ~ 9:15

[SVC34-01] An experimental basis for estimating particle properties following volcanic ash emissions

★Invited Papers

*Adrian Hornby[1]、Ulrich Kueppers[1]、Hanna Horsch[2]、Paul Ayris[1]、Nick Varley[3]、Daniele Andronico[4]、Boris Behncke[4]、Yan Lavallée[5]、Jackie E Kendrick[5]、James Utley[5]、Amy Hughes[5]、David Damby[6]、Benedikt Maurer[1]、Marlin Juchem[1]、Donald B Dingwell[1] (1.Ludwig-Maximilians-Universität München, DE、2.Hazen Research, Golden, USA、3.University of Colima, MX、4.INGV Catania, IT、5.University of Liverpool, UK、6.USGS Cascades Volcano Observatory, USA)

9:15 ~ 9:30

[SVC34-02] **Vapor transport in shallow intruded magmas: insights from diktytaxitic texture**

*櫻井 亮輔[1]、中村 美千彦[2]、奥村 聡[2]、無盡 真弓[2]、中谷 貴之[2] (1.東北大学理学部地球惑星物質科学科、2.東北大学大学院理学研究科地学専攻地球惑星物質科学講座)

9:30 ~ 9:45

[SVC34-03] First observation of nanolites and ultrananolites in alkaline volcanic glasses (Eifel, Germany)

*Marija Putak Juricek[1]、Michihiko Nakamura[2]、Mayumi Mujin[2]、Hans-Ulrich Schmincke[3]、Mari Sumita[3]、Nobuyoshi Miyajima[1] (1.BGI、2.Tohoku Univ.、3.GEOMAR)

9:45 ~ 10:00

[SVC34-04] Textural Study of Pumice Clasts from The Youngest Toba Tuff Eruption

*Gabriela Nogo Retnaningtyas Bunga Naen[1]、Atsushi Toramaru[1]、Tomoharu Miyamoto[1]、Haryo Edi Wibowo[2] (1.Department Earth and Planetary Sciences, Graduate School of Sciences, Kyushu University, Nishiku, 744, Motooka, Fukuoka, 819-0395, Japan、2.Geological Engineering Department, Universitas Gadjah Mada, 55284, Yogyakarta, Indonesia)

10:00 ~ 10:15

[SVC34-05] **Oomurodashi volcano: Past effusive and phreatomagmatic activity revealed by submarine and subaerial deposits**

*Iona McIntosh[1]、Kenichiro Tani[2]、Alexander Nichols[3]、Qing Chang[1]、Jun-Ichi Kimura[1] (1.Japan Agency for Marine-Earth Science and Technology, Yokosuka、2.National Museum of Nature and Science, Tsukuba、3.University of Canterbury, Christchurch, New Zealand)

10:15 ~ 10:30

[SVC34-06] Mechanism of volatile transport from mafic to silicic magma upon mixing

*吉村 俊平[1]、松本 亜希子[1]、中川 光弘[1] (1.北海道大学・地球惑星科学)

[E] 口頭発表 | セッション記号 S (固体地球科学)：S-VC 火山学

10:45 ~ 12:15 | A07 東京ベイ幕張ホール

[S-VC34] Connecting magma dynamics in vent-conduit system with surface expression of volcanic eruption

コンビーナ:三輪 学央(防災科学技術研究所)、下司 信夫(産業技術総合研究所　活断層・火山研究部門)、座長:下司 信夫(産総研　活断層・火山研究部門)、Adrian Hornby(Ludwig-Maximilians-University Munich)

10:45 ~ 11:00

[SVC34-07] The in-flight grain size distribution of lapilli and bombs from Strombolian explosions

*Jacopo Taddeucci[1]、Piergiorgio Scarlato[1]、Elisabetta Del Bello[1]、Tullio Ricci[1]、Ulrich Kueppers[2]、Bruce Houghton[3] (1.Istituto Nazionale di Geofisica e Vulcanologia, Rome, Italy、2.Department of Earth and Environmental Sciences. Ludwig-Maximilians-Universität (LMU). Munich, Germany、3.Department of Earth Sciences, University of Hawai‘i at Mānoa, Honolulu, USA)

11:00 ~ 11:15

[SVC34-08] **Pyrrotite oxidation as a proxy for air entrainment in eruption columns**

*松本 恵子[1]、中村 美千彦[2] (1.産業技術総合研究所地質調査総合センター、2.東北大学大学院理学研究科)

11:15 ~ 11:30

[SVC34-09] **Thermal signals in volcano monitoring: combining MODIS-MIROVA data with ground-based measurements at Aso Volcano, Japan**

*Corrado CIGOLINI[1]、Akihiko Yokoo[2]、Diego Coppola[1]、Marco Laiolo[1] (1.Department of Earth Sciences, University of Torino, Italy、2.Aso Volcanological Laboratory, Institute for Geothermal Sciences, Kyoto University, Japan)

11:30 ~ 11:45

[SVC34-10] Magma transfer processes in the NE Japan arc: insights from crustal ambient noise tomography combined with volcanic eruption records

*Georg F Zellmer[1]、Kai-Xun Chen[2]、Yuancheng Gung[2]、Ban-Yuan Kuo[3]、Takeyoshi Yoshida[4] (1.Massey University, Palmerston North, New Zealand、2.National Taiwan University, Taipei, Taiwan、3.Academia Sinica, Taipei, Taiwan、4.Tohoku University, Sendai, Japan)

11:45 ~ 12:00

[SVC34-11] **STRATIGRAPHY RENEWAL, MAGMA CHAMBER STRATIFICATION, AND CONDUIT PROCESS OF THE 1815 TAMBORA CALDERA FORMING ERUPTION**

*Indranova Suhendro[1]、Atsushi Toramaru[1]、Yasuo Miyabuchi[2]、Tomoharu Miyamoto[1] (1.Department of Earth and Planetary Sciences, Graduate School of Sciences, Kyushu University, Japan、2.Faculty of Advanced Science and Technology, Kumamoto University, Kurokami 2-40-1, Chuo-ku, Kumamoto 860-8555, Japan)

[E] 口頭発表 | セッション記号 S (固体地球科学)：S-CG 固体地球科学複合領域・一般

9:00 ~ 10:30 | コンベンションホールA 2F

[S-CG48] Science of slow earthquakes: Toward unified understandings of whole earthquake process

コンビーナ:井出 哲(東京大学大学院理学系研究科地球惑星科学専攻)、廣瀬 仁(神戸大学都市安全研究センター)、氏家 恒太郎(筑波大学生命環境系)、波多野 恭弘(東京大学地震研究所)、座長:望月 公廣(東京大学地震研究所)、新井 隆太

9:00 ~ 9:15

[SCG48-17] Three-dimensional seismic structure of the shallow plate boundary in the northern Hikurangi margin from NZ3D OBS data

*新井 隆太[1]、小平 秀一[1]、Kellett Richard[2]、Stucker Valerie[2]、Bassett Dan[2]、Henrys Stuart[2]、尾鼻 浩一郎[1]、Bangs Nathan[3]、Barker Dan[2]、Bell Rebecca[4]、望月 公廣[5]、藤江 剛[1]、三浦 誠一[1]、Fry Bill[2]、NZ3D team (1.国立研究開発法人海洋研究開発機構、2.GNS Science、3.University of Texas Institute for Geophysics、4.Imperial College London、5.東京大学地震研究所)

9:15 ~ 9:45

[SCG48-18] **Using earthquake focal mechanisms to investigate slow slip driving forces in the northern Hikurangi**

★Invited Papers

*Emily Warren-Smith[1]、Bill Fry[1]、Laura Wallace[1] (1.GNS Science)

9:45 ~ 10:00

[SCG48-19] 広帯域レシーバ関数が示す南海トラフ沈み込み帯スロー地震発生域の地震学的構造変化

*佐脇 泰典[1]、伊藤 喜宏[2]、太田 和晃[2]、澁谷 拓郎[2]、岩田 知孝[2] (1.京都大学大学院理学研究科、2.京都大学防災研究所)

10:00 ~ 10:15

[SCG48-20] Slip tendency maps for compressional and extensional stress states on a shallow decollement in Nankai Trough

*橋本 善孝[1]、佐藤 茂行[1]、グレゴリー ムーア[2]、木下 正高[3]、木村 学[4]、宮川 歩夢[5]、白石 和也[6]、山田 泰広[6] (1.高知大学、2.ハワイ大学、3.東京大学、4.東京海洋大学、5.産業技術総合研究所、6.海洋研究開発機構)

10:15 ~ 10:30

[SCG48-21] Permeability and its anisotropy on creeping Chihshang Fault, Taiwan

*Tyas Dwi Aprilniadi[1]、Wen-Jie Wu[1]、Li-Wei Kuo[1]、Jian-Cheng Lee[2]、Jia-Jyun Dong[3] (1.Department of Earth Sciences, National Central University、2.Institute of Earth Sciences, Academia Sinica、3.Graduate Institute of Applied Geology, National Central University)

[E] 口頭発表 | セッション記号 S (固体地球科学)：S-CG 固体地球科学複合領域・一般

10:45 ~ 12:15 | コンベンションホールA 2F

[S-CG48] Science of slow earthquakes: Toward unified understandings of whole earthquake process

コンビーナ:井出 哲(東京大学大学院理学系研究科地球惑星科学専攻)、廣瀬 仁(神戸大学都市安全研究センター)、氏家 恒太郎(筑波大学生命環境系)、波多野 恭弘(東京大学地震研究所)、座長:氏家 恒太郎(筑波大学生命環境系)、ウォリス サイモン(Nagoya University)

10:45 ~ 11:00

[SCG48-22] Short fluid infiltration events in the low permeable metamorphic rocks triggered by crustal fracturing at amphibolite–granulite facies conditions

*Diana Mindaleva[1]、Masaoki Uno[1]、Fumiko Higashino[1]、Atsushi Okamoto[1]、Noriyoshi Tsuchiya[1] (1.Graduate school of environmental studies, Tohoku University)

11:00 ~ 11:15

[SCG48-23] Generation of high fluid pressure at the base of the shallow mantle wedge—evidence from serpentinite of the Sanbagawa belt, SW Japan

*ウォリス サイモン[1]、纐纈 佑衣[2]、横田 麻莉[1,2] (1.東京大学、2.名古屋大学)

11:15 ~ 11:30

[SCG48-24] **Overpressured subduction plate boundary caused by infiltration of mantle-derived fluids: Evidence from helium isotope analysis on veins in subduction mélange**

*西山 直毅[1]、氏家 恒太郎[1]、角野 浩史[2] (1.筑波大学　生命環境系、2.東京大学)

11:30 ~ 11:45

[SCG48-25] **Geological and rheological conditions of subduction plate boundary between the seismogenic zone and the ETS zone in warm-slab environments**

*氏家 恒太郎[1]、野呂 和也[1]、重松 紀生[2]、Fagereng Ake[3]、西山 直毅[1]、Tulley Christopher[3]、増山 春菜[1]、森 康[4] (1.筑波大学生命環境系、2.産業技術総合研究所活断層・火山研究部門、3.カーディフ大学、4.北九州市立自然史・歴史博物館)

11:45 ~ 12:00

[SCG48-26] Temperature variation in tectonic mélanges of the Shimanto Belt, SW Japan

*Tsai-Wei Chen[1]、Donald M Fisher[1]、Andrew J Smye[1]、Yoshitaka Hashimoto[2] (1.Penn State Univ.、2.Kochi Univ.)

12:00 ~ 12:15

[SCG48-27] Frictional properties of opal gouge at low-temperature hydrothermal conditions and their implications for seismogenic faulting along subduction-zone megathrusts

*金川 久一[1]、中西 智哉[2]、桑名 盛人[3]、澤井 みち代[1]、廣瀬 丈洋[4] (1.千葉大学理学研究院、2.千葉大学大学院融合理工学府、3.千葉大学理学部、4.海洋研究開発機構高知コア研究所)

[E] 口頭発表 | セッション記号 S (固体地球科学)：S-CG 固体地球科学複合領域・一般

13:45 ~ 15:15 | コンベンションホールA 2F

[S-CG48] Science of slow earthquakes: Toward unified understandings of whole earthquake process

コンビーナ:井出 哲(東京大学大学院理学系研究科地球惑星科学専攻)、廣瀬 仁(神戸大学都市安全研究センター)、氏家 恒太郎(筑波大学生命環境系)、波多野 恭弘(東京大学地震研究所)、座長:波多野 恭弘、鈴木 岳人

13:45 ~ 14:00

[SCG48-28] **Rate and State Dependent Friction Law and Static Friction Force**

*松川 宏[1] (1.青山学院大学)

14:00 ~ 14:30

[SCG48-29] **Stable sliding, slow and silent slip events and laboratory earthquakes across the brittle ductile transition**

★Invited Papers

*Alexandre Schubnel[1]、Aubry Jérôme[1]、François Passelègue[2] (1.Laboratoire de Géologie, ENS, PARIS, France、2.EPFL, Switzerland)

14:30 ~ 14:45

[SCG48-30] Dramatic velocity weakening of dry quartz friction at relatively slow slip velocities

*堤 昭人[1]、飯田 大貴[2]、 尾上 裕子[1] (1.京都大学大学院理学研究科、2.地熱エンジニアリング（株）)

14:45 ~ 15:00

[SCG48-31] ゲルの摩擦実験における微動とゆっくりすべりを伴う破壊核形成過程

*山口 哲生[1] (1.九州大学)

15:00 ~ 15:15

[SCG48-32] 多孔質媒質中の乱流におけるk-εモデルの解軌道

*鈴木 岳人[1] (1.青山学院大学理工学部物理・数理学科)

[E] 口頭発表 | セッション記号 S (固体地球科学)：S-CG 固体地球科学複合領域・一般

15:30 ~ 17:00 | コンベンションホールA 2F

[S-CG48] Science of slow earthquakes: Toward unified understandings of whole earthquake process

コンビーナ:井出 哲(東京大学大学院理学系研究科地球惑星科学専攻)、廣瀬 仁(神戸大学都市安全研究センター)、氏家 恒太郎(筑波大学生命環境系)、波多野 恭弘(東京大学地震研究所)、座長:麻生 尚文、波多野 恭弘

15:30 ~ 16:00

[SCG48-33] **Modelling precursory seismicity in the laboratory using a roughness derived rate and state friction model**

★Invited Papers

*Paul A Selvadurai[1]、Percy Galvez[2]、Stefan Wiemer[1]、P. Martin Mai[2] (1.Swiss Seismological service, ETH Zurich, Switzerland、2.King Abdullah University of Science and Technology, Thuwal, Saudi Arabia)

16:00 ~ 16:15

[SCG48-34] Exponential dependence on perturbation stress of earthquake nucleation

*齋藤 拓也[1]、波多野 恭弘[1] (1.東京大学)

16:15 ~ 16:30

[SCG48-35] Stochastic modeling of slow earthquakes comparable to observations

*麻生 尚文[1]、安藤 亮輔[2]、井出 哲[2] (1.東京工業大学、2.東京大学)

16:30 ~ 16:45

[SCG48-36] Migration of aqueous fluid near the subducting plate interface

*森重 学[1] (1.国立研究開発法人海洋研究開発機構)

16:45 ~ 17:00

[SCG48-37] EnKF estimation of frictional properties and slip evolution on a LSSE fault and the changing slip deficit rate on a megathrust fault

*平原 和朗[1,2] (1.香川大学四国危機管理教育・研究・地域連携推進機構、2.理化学研究所　AIPセンター)

[E] 口頭発表 | セッション記号 S (固体地球科学)：S-CG 固体地球科学複合領域・一般

9:00 ~ 10:30 | A02 東京ベイ幕張ホール

[S-CG50] Intraslab and intraplate earthquakes

コンビーナ:北 佐枝子(建築研究所)、大内 智博(愛媛大学地球深部ダイナミクス研究センター)、Marcel Thielmann(Bavarian Geoinstitute, University of Bayreuth)、奥脇 亮(産業技術総合研究所 地質調査総合センター 活断層・火山研究部門)、座長:北 佐枝子(建築研究所)、大内 智博(愛媛大学地球深部ダイナミクス研究センター)、Marcel Thielmann(University of Bayreuth)、奥脇 亮(筑波大学)、Thomas Ferrand(UC San Diego)

9:00 ~ 9:15

[SCG50-01] On a reversely-dipping low-velocity layer in the Tohoku-slab beneath the forearc: unbending induced fluid pathway?

★招待講演
発表キャンセル

*川勝 均[1]、Kim HyeJeong[1] (1.東京大学地震研究所)

9:15 ~ 9:30

[SCG50-02] Evidence for transient fluid pathways in the mantle of the subducting Nazca slab from seismological observations and modeling of the Poisson's ratio

★Invited Papers

*Wasja Bloch[1,2]、Timm John[2]、Jörn Kummerow[2]、Bernd Schurr[1]、Pablo Salazar[3,4]、Serge A. Shapiro[2] (1.GeoForschungszentrum GFZ, Potsdam, Germany、2.Freie Universität Berlin, Germany、3.Universidád Católica del Norte, Antofagasta, Chile、4.National Research Center for Integrated Natural Disasters Management (CIGIDEN), Santiago, Chile)

9:30 ~ 9:45

[SCG50-03] Numerical simulation of water transportation along subducting slabs and implications for intraslab earthquakes

★Invited Papers

*中尾 篤史[1]、岩森 光[1,2,3]、中久喜 伴益[4]、鈴木 雄治郎[1]、中川 貴司[5]、中村 仁美[2,3,6,7] (1.東京大学地震研究所、2.海洋研究開発機構地球内部物質循環研究分野、3.東京工業大学理学院、4.広島大学大学院理学研究科、5.Department of Earth Sciences, The University of Hong Kong、6.産業技術総合研究所地質調査総合センター、7.千葉工業大学次世代海洋資源研究センター)

9:45 ~ 10:00

[SCG50-04] Subduction of serpentinized fracture zone and intraslab earthquakes in southern Mexico

★Invited Papers

*Marina Manea[1,2] (1.Computational Geodynamics Laboratory, Geosciences Center, National Autonomous University of Mexico、2.Institute of Astronomy, Romanian Academy)

10:00 ~ 10:15

[SCG50-05] Reaction-induced embrittlement of the lower continental crust

*Alexandre Schubnel[1]、Sarah Incel[2]、Julien Gasc[1]、Nadège Hilairet[5]、Yanbin Wang[3]、Feng Shi[3]、Loic Labrousse[4] (1.Laboratoire de Géologie, ENS、2.University of Oslo、3.GCECARS, University of Chicago、4.ISTEP, Sorbonne Université、5.UMET, Université de Lille)

10:15 ~ 10:30

[SCG50-06] **Transformation-induced, melt-enhanced faulting in orthoenstatite: implications for global intermediate-depth earthquakes**

Feng Shi[1]、Jianguo Wen[2]、Tony Yu[1]、Lupei Zhu[3]、*Yanbin Wang[1] (1.Center for Advanced Radiation Sources, University of Chicago, Chicago, IL, USA、2.Center for Nanoscale Materials, Argonne National Laboratory, Argonne, IL, USA、3.Department of Earth & Atmospheric Sciences, Saint Louis University, St. Louis, MO, USA)

[E] 口頭発表 | セッション記号 S (固体地球科学)：S-CG 固体地球科学複合領域・一般

10:45 ~ 12:15 | A02 東京ベイ幕張ホール

[S-CG50] Intraslab and intraplate earthquakes

コンビーナ:北 佐枝子(建築研究所)、大内 智博(愛媛大学地球深部ダイナミクス研究センター)、Marcel Thielmann(Bavarian Geoinstitute, University of Bayreuth)、奥脇 亮(産業技術総合研究所 地質調査総合センター 活断層・火山研究部門)、座長:北 佐枝子(建築研究所)、大内 智博(愛媛大学地球深部ダイナミクス研究センター)、Marcel Thielmann(University of Bayreuth)、奥脇 亮(筑波大学)、Thomas Ferrand(UC San Diego)

10:45 ~ 11:00

[SCG50-07] The Isolated M7.9 Deep Earthquake of 30 May 2015 Under the Present Bonin Wadati-Benioff Zone: Evidence from the New ISC-EHB Earthquake Catalogue (1930-2015) and CMT Focal Mechanisms

*Kirby Stephen[1]、Engdahl E.[2]、Okal Emile[3] (1.United States Geological Survey, Menlo Park、2.University of Colorado、3.Northwestern University)

11:00 ~ 11:15

[SCG50-08] What Can M_W –4 Lab-Quakes Teach Us About Deep-Focus Earthquakes?

★Invited Papers

*Julien Gasc[1]、Julien Fauconnier[1]、Clémence Daigre[1]、Arefeh Moarefvand[1]、Damien Deldicque[1]、Blandine Gardonio[1]、Alexandre Schubnel[1]、Pamela Burnley[2] (1.Laboratoire de Géologie, ENS-CNRS, Paris, FRANCE、2.University of Nevada Las Vegas, Las Vegas, USA)

11:15 ~ 11:30

[SCG50-09] Deep intraslab earthquake rupture due to grain size assisted thermal runaway

*Marcel Thielmann[1]、Thibault Duretz[2] (1.Bavarian Geoinstitute, University of Bayreuth, Germany、2.Université de Rennes, Rennes, France)

11:30 ~ 11:45

[SCG50-10] 2012年宮城沖プレート内ダブレット地震の震源断層モデルから検討した日本海溝近傍における海洋プレート内レオロジー

*久保田 達矢[1]、日野 亮太[2]、鈴木 秀市[2] (1.国立研究開発法人防災科学技術研究所、2.東北大学大学院理学研究科)

11:45 ~ 12:00

[SCG50-11] Source-rupture process of the intraplate earthquake; its diversity related to the fault geometry and damaged fault zone

*奥脇 亮[1]、八木 勇治[1] (1.筑波大学大学院生命環境科学研究科)

12:00 ~ 12:15

[SCG50-12] **Aftershocks of the NEXT Cascadia Intraslab Earthquake**

*Paul Bodin[1,2] (1.University of Washington Seattle、2.Pacific Northwest Seismic Network)

[E] 口頭発表 | セッション記号 S (固体地球科学)：S-CG 固体地球科学複合領域・一般

13:45 ~ 15:15 | A11 東京ベイ幕張ホール

[S-CG51] Role of volatiles on Earth and planetary dynamics

コンビーナ:石井 貴之(バイロイト大学バイエルン地球科学研究所)、大谷 栄治(東北大学大学院理学研究科地学専攻)、中村 美千彦(東北大学大学院理学研究科地学専攻地球惑星物質科学講座)、Mysen Bjorn(Geophysical Laboratory, Carnegie Inst. Washington)、座長:中村 美千彦、大谷 栄治(東北大学)

13:45 ~ 14:00

[SCG51-01] Constraining the degassing rate of the mantle since 3 Ga using the deficit of xenon-129 in the ancient atmosphere

★Invited Papers

*Bernard Marty[1]、David Bekaert[1]、Michael Broadley[1] (1.Centre de Recherches Pétrographiques et Géochimiques/ CNRS - Universite de Lorraine France)

14:00 ~ 14:15

[SCG51-02] **Investigating volatile cycles in the terrestrial mantle by incorporating He and Ar isotopes into geodynamical models of mantle convection**

★Invited Papers

*Rosie Ellen Jones[1]、Peter van Keken[2]、Jonathan M Tucker[2]、Chris J Ballentine[1] (1.Department of Earth Sciences, University of Oxford, Oxford, UK、2.Department of Terrestrial Magnetism, Carnegie Institution of Washington, Washington, USA)

14:15 ~ 14:30

[SCG51-03] Fluid circulation in the forearc mantle wedge inferred from the dihedral angle in an olivine-H_2O-NaCl system

*Yongsheng HUANG[1]、Takayuki Nakatani[1]、Michihiko Nakamura[1]、Catherine McCammon[2] (1.Graduate School of Science, Tohoku University、2.Byerisches Geoinstitut, University of Bayreuth)

14:30 ~ 14:45

[SCG51-04] The oxygen fugacity of serpentinites: implications for subduction zone redox evolution

*Lisa Eberhard[1]、Dan Frost[1]、Catherine McCammon[1] (1.BGI)

14:45 ~ 15:00

[SCG51-05] Experimental study of the effect of composition on water solubility in natural silicate melts

*山下 茂[1] (1.岡山大学惑星物質研究所)

15:00 ~ 15:15

[SCG51-06] Deep mantle volatile cycle and plate tectonics: Impact to the climate evolution

*中川 貴司[1]、門屋 辰太郎[2]、田近 英一[3] (1.香港大学、2.ワシントン大学、3.東京大学)

[E] 口頭発表 | セッション記号 S (固体地球科学)：S-CG 固体地球科学複合領域・一般

15:30 ~ 17:00 | A11 東京ベイ幕張ホール

[S-CG51] Role of volatiles on Earth and planetary dynamics

コンビーナ:石井 貴之(バイロイト大学バイエルン地球科学研究所)、大谷 栄治(東北大学大学院理学研究科地学専攻)、中村 美千彦(東北大学大学院理学研究科地学専攻地球惑星物質科学講座)、Mysen Bjorn(Geophysical Laboratory, Carnegie Inst. Washington)、座長:石井 貴之(バイロイト大学バイエルン地球科学研究所)、Bjorn Mysen(Carnegie Institution of Washington)

15:30 ~ 15:45

[SCG51-07] The nature of water induced small degree melts in the deep mantle

★Invited Papers

*Daniel James Frost[1]、Pierre Condamine[3]、 Davide Novella[2]、Rong Huang[1] (1.University of Bayreuth、2.University of Cambridge、3.Université de Lorraine)

15:45 ~ 16:00

[SCG51-08] **Phase separation of hydrous Vesuvius melt: vesicle nucleation or spinodal decomposition?**

★Invited Papers

*Anja Allabar[1]、Marcus Nowak[1] (1.University of Tuebingen)

16:00 ~ 16:15

[SCG51-09] Role of water on dynamics in the lower mantle and core-mantle boundary regions

*Eiji Ohtani[1]、Takayuki Ishii[2]、Liang Yuan[1]、Daijo Ikuta[1]、Tomoo Katsura[2]、Dan Frost[2] (1.Department of Earth and Planetary Materials Science, Graduate School of Science, Tohoku University、2.Bavarian Research Institute, University of Bayreuth)

16:15 ~ 16:30

[SCG51-10] Stability of Fe-bearing hydrous phases and element partitioning in the system MgO-Al_2O_3-Fe_2O_3-SiO_2-H_2O in Earth's lowermost mantle

*Hongsheng Yuan[1]、Li Zhang[1]、Eiji Ohtani[2]、Yue Meng[3]、Eran Greenberg[4]、Vitali B. Prakapenka [4] (1.Center for High Pressure Science and Technology Advanced Research、2.Department of Earth Science, Graduate School of Science, Tohoku University、3.HPCAT, X-Ray Science Division, Argonne National Laboratory、4.Center for Advanced Radiation Sources, University of Chicago)

16:30 ~ 16:45

[SCG51-11] **Laboratory Micro-Seismicity during Serpentinite Deformation as a Potential Analogue for Lower Wadati-Benioff Plane Seismicity**

*Julien Gasc[1,3]、Nadège Hilairet[2]、Tony Yu[3]、Yanbin Wang[3]、Thomas P. Ferrand[1]、Alexandre Schubnel[1] (1.Laboratoire de Géologie, CNRS - ENS, Paris, FRANCE、2.Unité Matériaux et Transformations, CNRS - Lille University, Villeneuve d'Ascq, FRANCE、3.GeoSoilEnviro-CARS, University of Chicago, Argonne IL, USA)

16:45 ~ 17:00

[SCG51-12] Water transport and mixing in the whole-mantle scale convection

*金子 岳郎[1]、中久喜 伴益[1]、亀山 真典[2]、岩森 光[3] (1.広島大学大学院理学研究科地球惑星システム学専攻、2.愛媛大学地球深部ダイナミクス研究センター、3.東京大学地震研究所)

[E] 口頭発表 | セッション記号 M (領域外・複数領域)：M-IS ジョイント

13:45 ~ 15:15 | 304 3F

[M-IS03] アジア・モンスーンの進化と変動，新生代全球気候変化におけるモンスーンの位置づけ

コンビーナ:山本 正伸(北海道大学大学院地球環境科学研究院)、多田 隆治(東京大学大学院理学系研究科地球惑星科学専攻)、座長:山本 正伸(北海道大学)、入野 智久、久保田 好美(国立科学博物館)、多田 隆治(東京大学)

13:45 ~ 14:00

[MIS03-01] **Reconstruction of Indian summer monsoon variability during the last 1,460,000 years**

*山本 正伸[1]、クレメンス スティーブ[2] (1.北海道大学大学院地球環境科学研究院、2.ブラウン大学地球環境惑星科学科)

14:00 ~ 14:20

[MIS03-02] Pleistocene Seawater $\delta^{18}O$ reconstructions from the Indian and East Asian Monsoon Regions

★Invited Papers

*Steven C Clemens[1]、Masanobu Yamamoto[2] (1.Brown University、2.Hokkaido University)

14:20 ~ 14:40

[MIS03-03] The Monsoon Erosion Pump

★Invited Papers

Cancelled

*Liviu Giosan[1] (1.Woods Hole Oceanographic Institution)

14:40 ~ 15:00

[MIS03-04] East Asian winter monsoon intensity in the Pleistocene based on seasonal land snail shell stable isotope ratios

★Invited Papers

*David L Dettman[1,3]、Xin Wang[2]、Mi Wang[2]、Junhui Zhang[2] (1.University of Arizona, Geosciences Dept., Environmental Isotope Lab.、2.Lanzhou University, Key Laboratory of Western China's Environmental Systems, College of Earth and Environmental Sciences、3.Shimane University, Estuary Research Center)

15:00 ~ 15:15

[MIS03-05] Reconstruction of ventilation history of the Japan Sea based on physical properties data collected during IODP Exp. 346

*入野 智久[1]、Liviu Giosan[2]、多田 隆治[3]、池原 研[4] (1.北海道大学　大学院地球環境科学研究院、2.Woods Hole Oceanographic Institution、3.東京大学大学院　理学系研究科、4.産業技術総合研究所　地質情報部門)

[E] 口頭発表 | セッション記号 M (領域外・複数領域)：M-IS ジョイント

15:30 ~ 17:00 | 304 3F

[M-IS03] アジア・モンスーンの進化と変動，新生代全球気候変化におけるモンスーンの位置づけ

コンビーナ:山本 正伸(北海道大学大学院地球環境科学研究院)、多田 隆治(東京大学大学院理学系研究科地球惑星科学専攻)、座長:多田 隆治(東京大学)、久保田 好美(国立科学博物館)、山本 正伸(北海道大学)

15:30 ~ 15:45

[MIS03-06] The spatial-temporal patterns of Indian monsoonal variations during the past 80 kyr recorded in NGHP-02 Hole 19B, western Bay of Bengal: Implications from chemical and mineral properties

*太田 雄貴[1,2,3,4]、川幡 穂高[4]、黒田 潤一郎[4,3]、鈴木 淳[2]、荒岡 大輔[2]、山口 飛鳥[4]、阿部 彩子[4] (1.東京大学大学院理学系研究科地球惑星科学専攻、2.産業技術総合研究所、3.海洋開発研究機構、4.東京大学大気海洋研究所)

15:45 ~ 16:05

[MIS03-07] **400,000 years millennial scale temperature and rainfall in East Asia deduced from paired Mg/Ca and oxygen isotope of planktic foraminifera from the East China Sea**

★Invited Papers

*久保田 好美[1]、Steven Clemens[2]、Kyung-Eun Lee[3]、Ann Holbourn[4]、脇坂 恵都子[5]、堀川 恵司[5]、多田 隆治[6]、木元 克典[7] (1.国立科学博物館、2.ブラウン大学、3.韓国海洋大学、4.クリスチャンアルブレヒト大学、5.富山大学、6.東京大学、7.海洋研究開発機構)

16:05 ~ 16:20

[MIS03-08] 日本海堆積物に記録された東アジアモンスーン千年スケール変動の開始と時代変化：新しいデータによる新しい解釈

*多田 隆治[1]、入野 智久[2]、関 有沙[3]、村山 雅史[4]、三武 司[1]、池田 昌之[5] (1.東京大学大学院理学系研究科地球惑星科学専攻、2.北海道大学大学院地球環境科学研究院、3.信州大学理学部、4.高知大学農林海洋科学部海洋資源科学科、5.静岡大学)

16:20 ~ 16:40

[MIS03-09] Interhemispheric linkages of Australian and Asian monsoons on a warmer-than-modern Earth

★Invited Papers

*Ann E Holbourn[1]、Wolfgang Kuhnt[1]、Janika Joehnck[1]、Sebastian Beil[1]、Julia Luebbers[1]、Kenji Marc Raymond Matsuzaki[2]、Yair Rosenthal[3]、Denise Kulhanek[4]、IODP Expedition 363 Scientists (1.University of Kiel、2.University of Tokyo、3.Rutgers University、4.Texas A&M University)

16:40 ~ 17:00

[MIS03-10] **Miocene evolution of the Asian Monsoon from climate and productivity proxies in the Bay of Bengal and South China Sea**

★Invited Papers

*Wolfgang Kuhnt[1]、Julia Luebbers[1]、Ann Holbourn[1]、Karlos GD Kochhann[2]、Steven C Clemens[3]、Clara T Bolton[4]、Yoichi Usui[5] (1.University of Kiel、2.UNISINOS University、3.Brown University、4.Aix-Marseille Université、5.Japan Agency for Marine-Earth Science and Technology)

[E] 口頭発表 | セッション記号 M (領域外・複数領域)：M-IS ジョイント

13:45 ~ 15:15 | A02 東京ベイ幕張ホール

[M-IS04] Interdisciplinary studies on pre-earthquake processes

コンビーナ:服部 克巳(千葉大学大学院理学研究科)、劉 正彦(国立中央大学太空科学研究所)、Ouzounov Dimitar(Center of Excellence in Earth Systems Modeling & Observations (CEESMO) , Schmid College of Science & Technology Chapman University, Orange, California, USA)、Qinghua Huang(Peking University)、座長:Jann-Yenq Liu(National Central University, Taiwan)、長尾 年恭

13:45 ~ 14:00

[MIS04-01] Application of blind source separation method in seismo-magnetic data analysis

★Invited Papers

*Peng Han[1]、Yi Zhong[1]、Yuanyuan Zhou[1]、Yonghui Ma[2]、Chengliang Xie[3]、Katsumi Hattori[4]、Chie Yoshino[4] (1.Southern University of Science and Technology, Shenzhen, China、2.Harbin Institute of Technology (Shenzhen), Shenzhen 518055, China、3.China University of Geosciences (Beijing), Beijing, 100083, China、4.Chiba University, Chiba, Japan)

14:00 ~ 14:15

[MIS04-02] 房総旭観測点近傍の地震活動と地中ラドン濃度変動

*小島 春奈[1]、服部 克巳[2]、吉野 千恵[2]、下 道國[3]、小西 敏春[4]、古屋 隆一[5] (1.千葉大学大学院融合理工学府地球環境科学専攻地球科学コース、2.千葉大学大学院理学研究院、3.藤田保健衛生大学、4.応用光研株式会社、5.コムシステム株式会社)

14:15 ~ 14:30

[MIS04-03] Geochemical evidence for the occurrence of 2018 Hualien earthquake triggered by earlier earthquake swarm

*Ching-Chou Fu[1]、Lou-Chuang Lee[1]、Cheng-Horng Lin[1]、Vivek Walia[2]、Dimitar Ouzounov[3] (1.Institute of Earth Sciences, Academia Sinica、2.National Center for Research on Earthquake Engineering, NARL, Taiwan、3.Chapman University, One University Drive, Orange, CA, USA)

14:30 ~ 14:45

[MIS04-04] b値の時間変化及び統計的評価

*謝 蔚云[1]、服部 克巳[1]、韓 鵬[2] (1.千葉大学、2.中国南方科技大学)

14:45 ~ 15:00

[MIS04-05] The S-K characteristics of the borehole areal strains associated with the Ms 8.0 Wenchuan and Ms 7.0 Lushan earthquakes

★Invited Papers

*Kaiguang Zhu [1]、Zining Yu[1]、Chenquan Chi[1]、Mengxuan Fan[1]、Kaiyan Lii[1] (1.Jilin University)

15:00 ~ 15:15

[MIS04-06] The Relationship between Earthquakes and Lightning Events of the globe during 2009-2017

*Ching-Chung Cheng[1]、JANN-YENQ Liu[1,2,3] (1.Graduate Institute of Space Science, National Central University, TAIWAN、2.Center for Astronautical Physics and Engineering, National Central University, TAIWAN、3.Center for Space and Remote Sensing Research, National Central University, TAIWAN)

[E] 口頭発表 | セッション記号 M (領域外・複数領域)：M-IS ジョイント

15:30 ~ 17:00 | A02 東京ベイ幕張ホール

[M-IS04] Interdisciplinary studies on pre-earthquake processes

コンビーナ:服部 克巳(千葉大学大学院理学研究科)、劉 正彦(国立中央大学太空科学研究所)、Ouzounov Dimitar(Center of Excellence in Earth Systems Modeling & Observations (CEESMO) , Schmid College of Science & Technology Chapman University, Orange, California, USA)、Qinghua Huang(Peking University)、座長:Peng Han、服部 克巳

15:30 ~ 15:45

[MIS04-07] 3D-Tomography of the Ionospheric Anomalies Preceding the 2011 Tohoku-Oki (M_W9.0) Earthquake

*Ihsan Naufal Muafiry[1,2]、Kosuke Heki[1] (1.Hokkaido University, Japan、2.Universitas Esa Unggul, Indonesia)

15:45 ~ 16:00

[MIS04-08] Statistical Analysis of Pre-seismic Ionospheric Electron Density Anomalies and Investigation of Precursor

*齊藤 央[1]、吉野 千恵[1]、服部 克巳[1] (1.千葉大学)

16:00 ~ 16:15

[MIS04-09] Spatial clustering of pre-earthquake anomalies as an indicator of the preparation/activation zone

*Dimitar Ouzounov[1]、Sergey Pulinets[2]、Tiger Liu[3]、Katsumi Hattori[4] (1.Center of Excellence in Earth Systems Modeling & Observations (CEESMO) , Schmid College of Science & Technology Chapman University, Orange, California, USA、2.Space Research Institute, RAS, Moscow, Russia、3.National Central University, Taoyuan City, Taiwan、4. Chiba University, Chiba, Japan)

16:15 ~ 16:30

[MIS04-10] **Application of the ionospheric parameters on the seismic research**- -Seismic-ionospheric effect detected from China Seismo-Electromagnetic Satellite

★Invited Papers

*Rui Song[1]、Hattori Katsumi[2]、Xuemin Zhang[3] (1.Graduate School of Science and Engeering, Chiba University、2.Graduate School of Science, Chiba University、3.Institute of Earthquake Science, China Earthquake Administration)

16:30 ~ 16:45

[MIS04-11] ROC curve analyses on the ionospheric TEC of M>=6.0 earthquakes in Japan during 1998-2015

★Invited Papers

*JANN-YENQ Liu[1]、Yuh-Ing Chen[2]、Pei-Jung Lee[1] (1.Center for Astronautical Physics and Engineering; Graduate Institute of Space Science, National Central University, Taiwan、2.Graduate Institute of Statistics, National Central University, Taiwan)

16:45 ~ 17:00

[MIS04-12] FORMOSAT-5/AIP observes seismo-ionospheric precursors

*JANN-YENQ Liu[1]、Chi-Kuang Chao[1] (1.Center for Astronautical Physics and Engineering; and Graduate Institute of Space Science, National Central University, TAIWAN)

[E] 口頭発表 | セッション記号 M (領域外・複数領域)：M-IS ジョイント

13:45 ~ 15:15 | 202 2F

[M-IS06] ジオパーク、ジオサイト、石造文化財の保存修復：風化プロセスとダメージアセスメント

コンビーナ:小口 千明(埼玉大学大学院理工学研究科)、藁谷 哲也(日本大学大学院理工学研究科)、目代 邦康(東北学院大学)、Magdalini Theodoridou(School of Engineering, Cardiff University)、座長:藁谷 哲也(日本大学大学院　理工学研究科)、目代 邦康(ジャパンジオサービス)

13:45 ~ 14:00

[MIS06-01] 自然災害発生時におけるジオサイトの保全についてのジオパークの対応

*目代 邦康[1]、長谷川 修一[2] (1.日本ジオサービス株式会社、2.香川大学)

14:00 ~ 14:15

[MIS06-02] Physical and mechanical properties for damage assesment of Taya Cave rocks, central Japan

*小口 千明[1]、秋元 友理奈[2]、田村 裕彦[3]、坂根 海征[1] (1.埼玉大学大学院理工学研究科、2.埼玉大学工学部、3.田谷の洞窟保存実行委員会)

14:15 ~ 14:30

[MIS06-03] **多分野統合共同調査から地域づくりへ展開させる地下文化財「田谷の洞窟」保存活動の実践的試行**

★招待講演

*田村 裕彦[1,2]、小口 千明[4]、早川 裕弋[5,2]、小倉 拓郎[2]、緒方 啓介[6]、守田 正志[3] (1.田谷の洞窟保存実行委員会、2.東京大学空間情報科学研究センター、3.横浜国立大学大学院都市イノベーション学府・研究院、4.埼玉大学理工学研究科 環境科学・社会基盤部門、5.北海道大学大学院地球環境科学研究院、6.鶴見大学文学部文化財学科)

14:30 ~ 14:45

[MIS06-04] **Italian underground cultural heritage: from monitoring to enhancement**

★Invited Papers

*Mario Parise[1]、Tiziana Vitolo[2]、Roberta Varriale[2] (1.Univ. Aldo Moro, Dept. Earth and Environmental Sciences, Bari, Italy、2.CNR-ISSM, Italy)

14:45 ~ 15:00

[MIS06-05] アンコール遺跡を構成する砂岩ブロックの日射による風化の可能性

*藁谷 哲也[1] (1.日本大学大学院理工学研究科)

15:00 ~ 15:15

[MIS06-06] **Durability evaluation of pyroclastic rocks used in the historical built environment of Hungary**

*Luigi Germinario[1,2]、Ákos Török[1] (1.Budapest University of Technology and Economics, Hungary、2.Saitama University, Japan)

[E] 口頭発表 | セッション記号 M (領域外・複数領域)：M-IS ジョイント

9:00 ~ 10:30 | 201A 2F

[M-IS07] アストロバイオロジー

コンビーナ:薮田 ひかる(広島大学大学院理学研究科地球惑星システム学専攻)、杉田 精司(東京大学大学院理学系研究科地球惑星科学専攻)、深川 美里(国立天文台)、藤島 皓介(東京工業大学地球生命研究所)、座長:薮田 ひかる(広島大学大学院 理学研究科)、杉田 精司(東京大学大学院 理学系研究科)、深川 美里(名古屋大学大学院 理学研究科)、藤島 皓介(ELSI 地球生命研究所)

9:00 ~ 9:20

[MIS07-06] How to find and characterize nearby habitable exoplanets

★Invited Papers

*成田 憲保[1] (1.アストロバイオロジーセンター)

9:20 ~ 9:40

[MIS07-07] **Organic Matter Preserved in Mudstones of a 3-Billion-Year-Old Lake Deposit in Gale Crater, Mars**

★Invited Papers

*Jennifer L Eigenbrode[1]、Roger E Summons[2]、Andrew Steele[3]、Caroline Freissinet[4]、Maëva Millan[5]、Rafael Navarro-González[6]、Paul Mahaffy[1] (1.NASA Goddard Space Flight Center、2.Massachusetts Institute of Technology、3.Carnegie Institution of Washington、4.Institut Pierre Simon Laplace, CNRS、5.Georgetown University、6.Universidad Nacional Autónoma de México)

9:40 ~ 9:55

[MIS07-08] **The third year sample return of Tanpopo: Capture and Exposure Experiment of Micrometeorite and Microbes on Exposure Facility of International Space Station**

*山岸 明彦[1]、Hashimoto Hirofumi[2]、Yano Hajime[2]、Yokobori Shin-ichi[3]、Kobayashi Kensei[4]、Mita Hajime[5]、Yabuta Hikaru[6]、Higashide Masumi[7]、Tabata Makoto[8]、Kawai Hideyuki[8]、Imai Eiichi[9] (1.Tokyo University of Pharmacy and Life Science, Department of Molecular Biology、2.ISAS/JAXA, Sagamihara, Japan、3.Tokyo University of Pharmacy and Life Science, Tokyo, Japan、4.Yokohama National University, Yokohama, Japan、5.Fukuoka Institute of Technology, Fukuoka, Japan、6.Hiroshima University, Hirosima, Japan、7.Japan Aerospace Exploration Agency (JAXA), Tokyo, Japan、8.Chiba University, Chiba, Japan、9.Nagaoka University of Technology, Nagaoka, Japan)

9:55 ~ 10:10

[MIS07-09] 低温度周りに適応可能な光合成色素の理論的探索：中心金属による物理化学的特性の調整

*小松 勇[1,2]、滝澤 謙二[1,3] (1.アストロバイオロジーセンター 、2.国立天文台、3.基礎生物学研究所)

10:10 ~ 10:25

[MIS07-10] 地球類似惑星の気候安定性とハビタビリティにおける炭化水素エアロゾルの影響

*渡辺 泰士[1]、田近 英一[1]、尾崎 和海[2]、洪 鵬[3] (1.東京大学、2.東邦大学、3.千葉工業大学)

[E] 口頭発表 | セッション記号 M (領域外・複数領域)：M-IS ジョイント

10:45 ~ 12:15 | 201A 2F

[M-IS07] アストロバイオロジー

コンビーナ:薮田 ひかる(広島大学大学院理学研究科地球惑星システム学専攻)、杉田 精司(東京大学大学院理学系研究科地球惑星科学専攻)、深川 美里(国立天文台)、藤島 皓介(東京工業大学地球生命研究所)、座長:藤島 皓介(ELSI 地球生命研究所)、深川 美里(名古屋大学大学院 理学研究科)、杉田 精司(東京大学大学院 理学系研究科)、薮田 ひかる(広島大学大学院 理学研究科)

10:45 ~ 11:05

[MIS07-11] the emergence of iron-sulfur protometabolism

★Invited Papers

*Sheref Mansy[1] (1.University of Trento)

11:05 ~ 11:25

[MIS07-12] Life-water-mineral interactions and their products

★Invited Papers

*白石 史人[1] (1.広島大学)

11:25 ~ 11:40

[MIS07-13] How much can we learn about ancient cells from sequence analysis? New metrics on an old problem.

*Shawn E McGlynn[1]、Sarah J Berkemer[2,3] (1.Earth-Life Science Institute, Tokyo Institute of Technology、2.Bioinformatics Group, Department of Computer Science, Interdisciplinary Center for Bioinformatics, University of Leipzig、3.Max Planck Institute for Mathematics in the Sciences, Leipzig, Germany)

11:40 ~ 11:55

[MIS07-14] Scientific significance of searching living cells on Mars surface by Life Detection Microscope (LDM)

*吉村 義隆[1]、山岸 明彦[2]、佐藤 毅彦[3]、宮川 厚夫[2]、今井 栄一[4]、佐々木 聰[5]、小林 憲正[6]、癸生川 陽子[6]、岡田 朋華[6]、塩谷 圭吾[3]、薮田 ひかる[7]、長沼 毅[7]、三田 肇[8]、藤田 和央[3]、臼井 寛裕[3] (1.玉川大学農学部、2.東京薬科大学、3.宇宙航空研究開発機構、4.長岡技術科学大学、5.東京工科大学、6.横浜国立大学、7.広島大学、8.福岡工業大学)

11:55 ~ 12:10

[MIS07-15] Civilization-bearing planets in the Milky-Way Galaxy; 50 necessary conditions must be satisfied in order

*丸山 茂徳[1] (1.東京工業大学地球生命研究所)

[E] 口頭発表 | セッション記号 M (領域外・複数領域)：M-AG 応用地球科学

13:45 ~ 15:15 | 302 3F

[M-AG38] Satellite Land Physical Processes Monitoring at Medium/High/Very High Resolution

コンビーナ:Jean-Claude Roger(University of Maryland College Park)、Shinichi Sobue(Japan Aerospace Exploration Agency)、Eric Vermote(NASA Goddard Space Flight Center)、座長:Jean-Claude Roger、Eric Vermote

13:50 ~ 14:05

[MAG38-01] 15-years of LSA-SAF/Eumetsat satellite-derived albedo products: method for retrieval validation, and recent advances using neural networks during spectral integration

*Florian Pinault[1]、Dominique Carrer[1]、Xavier Ceamanos[1]、Gabriel Lellouch[1]、Catherine Meurey[1]、Suman Moparthy[1]、Chloé Vincent[1]、Sandra Coelho[2]、Isabel Trigo[2] (1.Météo France, CNRM-GAME, UMR3589, Toulouse, France、2.IPMA, Lisbon, Portugal)

14:05 ~ 14:20

[MAG38-02] **Toward a Consistent Land Long Term Climate Data Records from Large Field of View Polar Orbiting Earth Observation Satellites**

*Eric Vermote[1]、Jean-Claude Roger[1,2]、Belen Franch[1,2]、Christopher Justice[2]、Ivan Csiszar[3]、Sadashiva Devadiga[1]、Edward Masuoka[1] (1.NASA Goddard Space Flight Center、2.University of Maryland, Dept. of Geographical Sciences、3.NOAA/NESDIS/STAR)

14:20 ~ 14:35

[MAG38-03] **LaSRC Cloud Detection Algorithm for Landsat 8 and Sentinel-2 Data**

*Sergii Skakun[1]、Eric Vermote[2]、Jean-Claude Roger[1] (1.University of Maryland College Park、2.NASA Goddard Space Flight Center)

14:35 ~ 14:50

[MAG38-04] **Aerosol models for the validation of Surface Reflectances for MODIS, VIIRS, Landsat-8, Sentinel-2 from LaSRC**

*Jean-Claude Roger[1,2]、Eric Vermote[2]、Sergii Skakun[1,2]、Belen Franch[1,2]、Georgia Doxani[4]、William Rountree[1,2]、Ferran Gascon[4]、chris justice[1]、oleg dubovik[3]、Brent holben[2] (1.University of Maryland, College Park, USA、2.NASA Goddard Space flight Center, Greenbelt, USA、3.LOA, University of Lille, Villeneuve d'Ascq, France、4.ESA, Frascati, Italy)

14:50 ~ 15:05

[MAG38-05] Quantity and spatial distribution of aboveground biomass carbon in Colombia’s forest

*Pedro Rodriguez-Veiga[1,2]、Adriana Paola Barbosa-Herrera[3]、Edersson Cabrera[3]、Gustavo Galindo[3]、Valentin Louis[1]、Pilar Lozano[3]、Pacheco-Pascagaza Ana Maria[1]、Indira Pachon-Cendales[3]、Salinas Nelso Ricardo[3]、Heiko Balzter[1,2] (1.Centre for Landscape and Climate Research, University of Leicester, Leicester, UK、2.NERC National Centre for Earth Observation (NCEO), Leicester, UK、3.Institute of Hydrology, Meteorology and Environmental Studies (IDEAM), Bogota, Colombia)

[E] 口頭発表 | セッション記号 M (領域外・複数領域)：M-AG 応用地球科学

15:30 ~ 17:00 | 201B 2F

[M-AG38] Satellite Land Physical Processes Monitoring at Medium/High/Very High Resolution

コンビーナ:Jean-Claude Roger(University of Maryland College Park)、Shinichi Sobue(Japan Aerospace Exploration Agency)、Eric Vermote(NASA Goddard Space Flight Center)、座長:Sergii Skakun(University of Mrayland, USA)、Eric Vermote

15:35 ~ 15:50

[MAG38-06] Introduction of GCOM-C/SGLI Leaf Area Index & Fraction of Absorbed Photosynthetically Active Radiation products

*小林 利行[1]、本多 嘉明[2]、小野 祐作[2]、小林 秀樹[3]、Wei Yang[2]、永井 信[3]、秋津 朋子[4]、奈佐原 顕郎[4]、宮崎 理紗[1]、堀 雅裕[1]、村上 浩[1] (1.国立研究開発法人　宇宙航空研究開発機構、2.千葉大学環境リモートセンシング研究センター、3.国立研究開発法人　海洋研究開発機構、4.筑波大学)

15:50 ~ 16:05

[MAG38-07] **35-years of Land Surface Albedo and 15-years of Down-Welling Short-Wave Radiation Retrievals from Satellites through the EUMETSAT/LSA-SAF and ECMWF/C3S projects**

*Dominique Carrer[1]、Florian Pinault[1]、Iskander Benhadj[2]、Xavier Ceamanos[1]、Sandra Coelho[3]、Gabriel Lellouch[1]、Catherine Meurey[1]、Suman Moparthy[1]、Else Swinnen[2]、Chloé Vincent[1]、Isabel Trigo[3] (1.Meteo France, CNRM, France、2.VITO, Belgium、3.IPMA, Portugal)

16:05 ~ 16:20

[MAG38-08] **Integrating the satellite-based biophysical model and environmental zonation scheme to estimate rice yield gap in Northeast China**

*Jiahua Zhang[1,3]、Jingwen Wang[1,2,3] (1.Institute of Remote Sensing and Digital Earth, Chinese Academy of Sciences、2.University of Chinese Academy of Sciences、3.Aerospace Information Research Institute, Chinese Academy of Sciences)

16:20 ~ 16:35

[MAG38-09] Landsat-based Phenological Classification Mapping in Japan

*堤田 成政[1]、永井 信[2]、Pedro Rodriguez-Veiga[3,4,1]、三浦 知昭[5] (1.京都大学大学院地球環境学堂、2.海洋研究開発機構 地球環境観測研究センター、3.Centre for Landscape and Climate Research, University of Leicester、4. National Centre for Earth Observation, University of Leicester、5.Department of Natural Resources and Environmental Management University of Hawaii at Manoa)

16:35 ~ 16:50

[MAG38-10] **Incorporating satellite-retrieved canopy nitrogen content into the biophysical process model for estimating crop yield and N fertilizer recommendation**

*Jingwen Wang[1,2,3]、Jiahua Zhang[1,3] (1.Institute of Remote Sensing and Digital Earth, Chinese Academy of Sciences、2.University of Chinese Academy of Sciences、3.Aerospace Information Research Institute, Chinese Academy of Sciences)

[E] 口頭発表 | セッション記号 M (領域外・複数領域)：M-AG 応用地球科学

9:00 ~ 10:30 | 202 2F

[M-AG40] CTBT IMS Technologies for Detecting Nuclear Explosion and Their Applications to Earth Science

コンビーナ:Nurcan Meral　Ozel(Comprehensive Nuclear-Test-Ban Treaty Organization)、松本 浩幸(国立研究開発法人海洋研究開発機構)、直井 洋介(国立研究開発法人日本原子力研究開発機構)、座長:Nurcan Meral Özel(Comprehensive Nuclear-Test-Ban Treaty Organization)、松本 浩幸(海洋研究開発機構)、鎌谷 紀子(東京大学地震研究所)

9:00 ~ 9:15

[MAG40-01] Japanese Contributions and Collaborations for IMS Technologies and the Verification Regime

*Nurcan Meral Ozel[1]、David Jepsen[1]、Naoko Nakashima[1]、Hideaki Komiyama[1]、Hiroyuki Matsumoto[1,2] (1.Comprehensive Nuclear-Test-Ban Treaty Organization (CTBTO)、2.Japan Agency for Marine-Earth Science and Technology (JAMSTEC))

9:15 ~ 9:30

[MAG40-02] 日本における地震波による核実験探知の研究

★招待講演

*鎌谷 紀子[1] (1.東京大学地震研究所)

9:30 ~ 9:45

[MAG40-03] Waveform Analysis on Induced Earthquakes after the 2017 Nuclear Test and Detected Mining Events in DPRK

*本橋 昌志[1]、藤井 孝成[1]、乙津 孝之[1] (1.一般財団法人日本気象協会)

9:45 ~ 10:00

[MAG40-04] Submarine volcanoes and where to find them: Harnessing IMS hydroacoustic data

★Invited Papers

*Dirk Metz[1] (1.Japan Agency for Marine-Earth Science and Technology)

10:00 ~ 10:15

[MAG40-05] **CTBT検証技術における希ガス監視の重要性と高崎放射性核種監視観測所での観測結果**

*山本 洋一[1]、木島 佑一[1]、冨田 豊[1] (1.国立研究開発法人日本原子力研究開発機構)

10:15 ~ 10:30

[MAG40-06] 日本で検出された放射性キセノンに関するATM解析結果

*木島 佑一[1]、山本 洋一[1]、冨田 豊[1] (1.国立研究開発法人　日本原子力研究開発機構)

[E] 口頭発表 | セッション記号 P (宇宙惑星科学)：P-EM 太陽地球系科学・宇宙電磁気学・宇宙環境

2019年5月30日(木) 9:00 ~ 10:30 | A03 東京ベイ幕張ホール

[P-EM09] Vertical coupling in the atmosphere and Ionosphere

コンビーナ:Liu Huixin(九州大学理学研究院地球惑星科学専攻 九州大学宙空環境研究センター)、Chang Loren(Institute of Space Science, National Central University)、大塚 雄一(名古屋大学宇宙地球環境研究所)、座長:Huixin Liu(Kyushu University, Japan)、Stan Solomon(National Center for Atmospheric Research, US)

Vertical coupling mechanisms throughout the whole atmosphere are critical to understanding the near Earth space environment, as well as its sensitivity to the solar, geomagnetic, and atmospheric drivers. This international session focuses on physical/chemical processes occurring in the mesosphere, thermosphere, and ionosphere (MTI). Both quiet and disturbed states in response to lower atmospheric forcing or solar forcing are important for understanding the MTI system and its coupling to other regions. We invite presentations of observations and observational concepts with ground-based and/or space-borne instruments, theoretical studies, numerical simulations, and development of data analysis systems for various kinds of temporal and spatial variations in atmosphere-ionosphere coupled system.

9:00 ~ 9:20

[PEM09-11] Assimilation products of thermospheric and ionospheric measurements by the NASA Ionopsheric Connection Explorer

★Invited Papers

*Thomas J Immel[1]、Chihoko Cullens[1]、Yen-Jung Wu[1]、Gary Bust[2]、Jeffrey Forbes[3]、Scott L England[4] (1.University of California, Berkeley、2.Johns Hopkins University、3.University of Colorado、4.Virginia Tech)

9:20 ~ 9:35

[PEM09-12] petitSat - A 6U CubeSat to examine the link between MSTIDS and ionospheric plasma density enhancements

*Jeffrey Klenzing[1]、Ryan L Davidson[2]、Gregory D Earle[3]、Alexa J Halford[4]、Sarah L Jones[1]、Carlos Martinis[5]、Nikolaos Paschalidis[1]、Robert F Pfaff[1]、Jonathon M Smith[1,6] (1.NASA Goddard Space Flight Center, Greenbelt, MD, USA、2.Utah State University, Logan, UT, USA、3.Virginia Tech, Blacksburg, VA, USA、4.The Aerospace Corporation, Chantilly, VA, USA、5.Boston University, Boston, MA, USA、6.Catholic Universtiy of America, Washington, DC, USA)

9:35 ~ 9:55

[PEM09-13] A three-dimensional ionospheric electrodynamics model

★Invited Papers

*Astrid I Maute[1]、Arthur D Richmond[1] (1.High Altitude Observatory, National Center for Atmospheric Research, Boulder CO, USA.)

9:55 ~ 10:10

[PEM09-14] Spatial Fluctuation of TEC Index: A new index of ionospheric irregularities

*馬 冠一[1]、丸山 隆[2] (1.中国科学院国家天文台、2.国立研究開発法人情報通信研究機構)

10:10 ~ 10:25

[PEM09-15] Coupling of lower thermosphere planetary wave energy into the ionosphere

*Patrick J Espy[1,2]、Nora Stray[1,2,3]、Robert Hibbins[1,2] (1.Norwegian University of Science and Technology, Trondheim, Norway、2.Birkeland Centre for Space Science, Bergen, Norway、3.Teknova AS, Tordenskjolds Gate 9, 4612 Kristiansand, Norway)

10:25 ~ 10:30

Discussion

Assimilation products of thermospheric and ionospheric measurements by the NASA Ionopsheric Connection Explorer

*Thomas J Immel[1], Chihoko Cullens[1], Yen-Jung Wu[1], Gary Bust[2], Jeffrey Forbes[3], Scott L England[4]

1. University of California, Berkeley, 2. Johns Hopkins University, 3. University of Colorado, 4. Virginia Tech

ICON is an orbiting NASA observatory built to simultaneously observe the characteristics of the ionosphere and thermosphere in order to understand the connection between conditions in space and energy sources in the atmosphere below. Ready for launch in 2019 into a 27 degree inclination, 575 km altitude orbit, it will provide neutral wind, density and temperature products as well as in-situ and remotely-sensed ionospheric densities. These products will inform the conditions of two models that assimilate the data in different ways, and be available on the ICON website. The first is the TIEGCM, where assimilation is accomplished through modification of the winds and temperatures at the lower boundary as prescribed by observations . The second is the IDA4D model, that through a Gauss-Markhov scheme modifies a background ionosphere with actual observations that include many different sources including ICON. Given the expected sampling and data uncertainties from ICON, the expected performance of these models is reported. ICON expects a launch in 2019.

Keywords: ionosphere , thermosphere, atmospheric tides

©2019. Japan Geoscience Union. All Right Reserved.



©2019. Japan Geoscience Union. All Right Reserved.

petitSat - A 6U CubeSat to examine the link between MSTIDS and ionospheric plasma density enhancements

*Jeffrey Klenzing[1], Ryan L Davidson[2], Gregory D Earle[3], Alexa J Halford[4], Sarah L Jones[1], Carlos Martinis[5], Nikolaos Paschalidis[1], Robert F Pfaff[1], Jonathon M Smith[1,6]

1. NASA Goddard Space Flight Center, Greenbelt, MD, USA, 2. Utah State University, Logan, UT, USA, 3. Virginia Tech, Blacksburg, VA, USA, 4. The Aerospace Corporation, Chantilly, VA, USA, 5. Boston University, Boston, MA, USA, 6. Catholic Universtiy of America, Washington, DC, USA

The mid- and low-latitude ionosphere is home to a variety of plasma density irregularities, including depletions (bubbles), enhancements (blobs), and small-scale scintillation, which result in the distortion of radio wave propagation. Recent observations from the C/NOFS satellite suggest that multiple mechanisms are responsible for forming plasma density enhancements, with wave action in the thermosphere as a significant driver of the enhanced densities. Indeed, statistical analysis of enhancements observed from satellites resembles the statistics of Medium-Scale Traveling Ionosphere Disturbances (MSTIDs) with respect to seasonal variability and solar activity. In order to investigate the link between these two phenomena, both in-situ data of the plasma enhancement and remote data of the MSTID at the magnetic footpoint are required. petitSat is a CubeSat mission designed to provide in situ measurements of the plasma density, 3D ion drift, as well as ion and neutral composition. The instrument suite includes a combined retarding potential analyzer and cross-track drift meter and an ion neutral mass spectrometer. This instrument suite will provide comprehensive information about the fluctuations in plasma, as well as changes in the neutral profile. petitSat will launch into a 51 deg inclination orbit at 400 km (consistent with an International Space Station deployment), allowing for numerous conjunctions with the Boston University All-Sky Imager network and GPS receivers from the International Global Navigation Satellite Systems (GNSS) Service (IGS) network over the mission lifetime.

Keywords: Ionosphere, CubeSat, MSTIDs

©2019. Japan Geoscience Union. All Right Reserved.

A three-dimensional ionospheric electrodynamics model

*Astrid I Maute[1], Arthur D Richmond[1]

1. High Altitude Observatory, National Center for Atmospheric Research, Boulder CO, USA.

Ionospheric electric fields and currents are driven by collisional interaction between thermospheric winds and ions, by magnetospherically driven convection and field-aligned currents at high latitudes, by gravitational and pressure-gradient forces on the ionospheric plasma, and by weak currents from the lower atmosphere. The electrodynamics of the ionospheric E and F regions are strongly coupled. For time scales longer than a few minutes the electric field is electrostatic. The electric potential is nearly constant along geomagnetic-field lines, and can be represented in two dimensions in a coordinate system aligned with the magnetic field. The current density, however, varies in all three dimensions. Knowing the ionospheric current flow in three dimension is important for determining the magnetic perturbations at Low Earth Orbit (LEO) satellite height.

We are developing a model of ionospheric electrodynamics that takes into account all of the sources and calculates the three-dimensional structure of currents and their associated magnetic perturbation fields. This model will be used to simulate ionospheric drifts, currents, and ground and LEO geomagnetic perturbations. In this presentation we discuss the modeling principles and present results relevant to the electrodynamics of the middle and low latitude ionosphere, including the effects of coupling with F-region electrodynamics and the expected observable effects at low Earth orbit satellites.

Keywords: Ionospheric electrodynamics, ionospheric current, magnetic perturbations

©2019. Japan Geoscience Union. All Right Reserved.

Spatial Fluctuation of TEC Index: A new index of ionospheric irregularities

*馬 冠一[1]、丸山 隆[2]
*Guanyi Ma[1], Takashi Maruyama[2]

1. 中国科学院国家天文台、2. 国立研究開発法人情報通信研究機構
1. National Astronomical Observatories, Chinese Academy of Sciences, 2. National Institute of Information and Communications Technology

This study presents a new spatial fluctuation of total electron content (TEC) index (SFTI) to identify and analyze ionospheric irregularities. SFTI is defined as the dispersion of vertical TEC (VTEC) within a specific area at a given time. With the data from the Global Navigation Satellite System (GNSS) Earth Observation Network of Japan (GEONET), the size of the specific area for SFTI calculation can be chosen as 0.8˚× 0.8˚ in longitude and latitude. An SFTI map generated by sliding window shows the spatial variation of the ionospheric irregularities in two dimensions. It can be used to obtain the size, shape, orientation and intensity distribution of the irregularity structures. With a series of SFTI maps, we analyzed three strong irregularity events on 12 February 2000, 20 March 2001 and 10 November 2004. The irregularities are found to consist of branching structures, which are anisotropic and elongate along longitudinal direction when first seen at low latitudes. The structures can drift and eventually move perpendicular to their orientations. It is concluded that SFTI will provide an unprecedented view of irregularity development and help to understand the process of irregularity generation.

キーワード：ionospheric irregularities、GNSS observation、SFTI
Keywords: ionospheric irregularities, GNSS observation, SFTI

©2019. Japan Geoscience Union. All Right Reserved.

Coupling of lower thermosphere planetary wave energy into the ionosphere

*Patrick J Espy[1,2], Nora Stray[1,2,3], Robert Hibbins[1,2]

1. Norwegian University of Science and Technology, Trondheim, Norway, 2. Birkeland Centre for Space Science, Bergen, Norway, 3. Teknova AS, Tordenskjolds Gate 9, 4612 Kristiansand, Norway

Neutral atmosphere winds derived from meteor trail drifts observed by a longitudinal chain of Super Dual Auroral Radar Network (SuperDARN) radars have characterized planetary waves with wavenumber 1 and 2 in the lower thermosphere near 95 km. The simultaneous wind observations at stations between 50° and 66° N removes the temporal-spatial aliasing associated with satellite observations and shows the continuous evolution of the planetary waves near the turbopause. A similar technique has been applied to a longitudinal chain of ionosondes in the same latitude band, and the same wavenumber components were observed in f_oF2. An analysis of the two signals shows them to be highly correlated, with the ionospheric waves lagging behind those in the lower thermosphere. We will describe the technique to extract the waves and compare it with other observations. We will also show the relationship of the ionospheric waves with magnetic and solar activity, and describe a process, commensurate with our measurements, by which planetary wave signals near the turbopause can be transmitted into the ionospheric electron density.

Keywords: dynamics, turbopause, ionosphere

©2019. Japan Geoscience Union. All Right Reserved.

[E] 口頭発表 | セッション記号 P (宇宙惑星科学)：P-EM 太陽地球系科学・宇宙電磁気学・宇宙環境

2019年5月30日(木) 10:45 ~ 12:15 | A03 東京ベイ幕張ホール

[P-EM09] Vertical coupling in the atmosphere and Ionosphere

コンビーナ:Liu Huixin(九州大学理学研究院地球惑星科学専攻 九州大学宙空環境研究センター)、Chang Loren(Institute of Space Science, National Central University)、大塚 雄一(名古屋大学宇宙地球環境研究所)、座長:Jann-Yenq Liu(National Central University, Taiwan)、Loren Chang(National Central University, Taiwan)

Vertical coupling mechanisms throughout the whole atmosphere are critical to understanding the near Earth space environment, as well as its sensitivity to the solar, geomagnetic, and atmospheric drivers. This international session focuses on physical/chemical processes occurring in the mesosphere, thermosphere, and ionosphere (MTI). Both quiet and disturbed states in response to lower atmospheric forcing or solar forcing are important for understanding the MTI system and its coupling to other regions. We invite presentations of observations and observational concepts with ground-based and/or space-borne instruments, theoretical studies, numerical simulations, and development of data analysis systems for various kinds of temporal and spatial variations in atmosphere-ionosphere coupled system.

10:45 ~ 11:00

[PEM09-16] Modulation of Lightning Occurrence by the Solar Wind

*Omar Angelo Nava[1]、Daniel Emmons[1]、Robert Loper[1] (1.Air Force Institute of Technology)

11:00 ~ 11:15

[PEM09-17] Long Term Mesopause Temperature Variations resolved by SD-WACCM, MSISE-00,TIMED SABER and Local Observations in Irkutsk (52.29o, 104.29o), Russia

*Yi Chung Chiu[1]、Loren Chang[1]、Yi Duann[1]、ALEXEI DMITRIEV[1]、Irina Medvedeva[2]、Konstantin Ratovsky[2]、Jia Yue[3] (1.Institute of Space Science, National Central University、2.Russian Academy of Sciences, Russian Federation、3.Hampton University, USA)

11:15 ~ 11:30

[PEM09-18] ISS-IMAP observation of the mesospheric disturbances generated by tropical cyclones

*齊藤 昭則[1]、坂野井 健[2]、Perwitasari Septi[4]、穂積 裕太[3]、岡田 凌太[1]、村上 涼[1] (1.京都大学大学院理学研究科地球物理学教室、2.東北大学大学院理学研究科惑星プラズマ・大気研究センター、3.電気通信大学、4.国立極地研究所宙空圏グループ)

11:30 ~ 11:45

[PEM09-19] A fast acoustic wave detected in GNSS total electron content after the foreshock of the 2011 Tohoku Earthquake

*柿並 義宏[1]、齊藤 大晶[2]、山本 哲生[3]、陳 佳宏[4]、山本 真行[2]、中島 健介[5]、劉 正彦[6] (1.北海道情報大学、2.高知工科大学、3.北海道大学、4.台湾国立成功大学、5.九州大学、6.台湾国立中央大学)

11:45 ~ 12:00

[PEM09-20] **Study of quiet-time high-latitude thermospheric winds using a Fabry-Perot interferometer at Tromsoe: Averages and exceptional events**

*徐 何秋岑[1]、塩川 和夫[1]、大山 伸一郎[1] (1.名古屋大学宇宙地球環境研究所)

12:00 ~ 12:15

[PEM09-21] **The longitudinal differences of lunar tidal characteristics between East Asian and American sectors during stratospheric sudden warming events: 2009-2018.**

*Jing Liu[1]、Donghe Zhang[1] (1.Peking University)

Modulation of Lightning Occurrence by the Solar Wind

*Omar Angelo Nava[1], Daniel Emmons[1], Robert Loper[1]

1. Air Force Institute of Technology

The connection between terrestrial and space weather phenomena is an emerging field of study with implications for different aspects of operational weather forecasting. This study investigates the influence of solar wind events on the frequency of lightning occurrence over North America. Empirical mode decomposition (EMD) is applied to National Lightning Detection Network (NLDN) data from 1996 to 2012 and correlated against various solar wind parameters. EMD performs operations that partition the lightning time series data into modes or Intrinsic Mode Functions (IMFs). Using composite analysis, we identified an IMF that corresponds to a 27-day co-rotating interaction region (CIR) that results in a statistically significant decrease in thunderstorm occurrence across the entire NLDN for approximately three to nine days. This finding is consistent with previous studies indicating that faster solar wind speeds are correlated with a decrease in galactic cosmic ray (GCR) flux and a reduction in lightning reports. However, the analysis also highlighted a latitudinal stratification in the thunderstorm response. In the mid-latitudes (30-38 deg N), faster solar wind speeds initially increased the number of lightning occurrences before decreasing significantly over the next 14 days. In the upper mid-latitudes (38-46 deg N), the response was reversed with an increase in thunderstorm events followed by a significant decrease. Additional “lightning response reversals” are noted at even higher latitudes. It is hypothesized that solar energetic particles associated with the CIRs are able to penetrate to tropospheric altitudes and increase lightning rates at higher latitudes, while at lower latitudes, the solar wind modulated GCR flux drives the decrease in lightning occurrence. Overall, understanding the electrodynamic connection between the lower and upper atmospheres has important implications for both space physics and atmospheric science communities.

Keywords: Lightning, Solar Wind, Empirical Mode Decomposition, National Lightning Detection Network

©2019. Japan Geoscience Union. All Right Reserved.

Long Term Mesopause Temperature Variations resolved by SD-WACCM, MSISE-00,TIMED SABER and Local Observations in Irkutsk (52.29o, 104.29o), Russia

*Yi Chung Chiu[1], Loren Chang[1], Yi Duann[1], ALEXEI DMITRIEV[1], Irina Medvedeva[2], Konstantin Ratovsky[2], Jia Yue[3]

1. Institute of Space Science, National Central University, 2. Russian Academy of Sciences, Russian Federation, 3. Hampton University, USA

Measurements of mesopause temperature are quite challenging and must rely on remote sensing methods. As part of the Taiwan-Russia joint research cooperation program, we carry out an analysis comparing mesopause temperature measurements made by the Irkutsk spectrophotometer between 2008 - 2018 and those resolved by the SD-WACCM data assimilation model, the empirical MSISE-00 model, and TIMED SABER satellite measurements. Spectral decomposition is performed on the datasets to determine the differences between the different observed and modelled seasonal and inter-annual variability, as well as to resolve long term trends.

Keywords: Mesopause, Temperature variability

©2019. Japan Geoscience Union. All Right Reserved.

ISS-IMAP observation of the mesospheric disturbances generated by tropical cyclones

*齊藤 昭則[1]、坂野井 健[2]、Perwitasari Septi[4]、穂積 裕太[3]、岡田 凌太[1]、村上 涼[1]
*Akinori Saito[1], Takeshi Sakanoi[2], Septi Perwitasari[4], Yuta Hozumi[3], Ryota Okada[1], Ryo Murakami[1]

1. 京都大学大学院理学研究科地球物理学教室、2. 東北大学大学院理学研究科惑星プラズマ・大気研究センター、3. 電気通信大学、4. 国立極地研究所宙空圏グループ
1. Department of Geophysics, Graduate School of Science, Kyoto University, 2. Planetary Plasma and Atmospheric Research Center, Graduate School of Science, Tohoku University, 3. University of Electro-Communications, 4. Space and Upper Atmospheric Sciences Group, National Institute of Polar Research

Troposphere was investigated to elucidate the vertical atmospheric coupling process using the global observational data from the International Space Station (ISS). The vertical coupling between the lower and the upper atmospheres has been revealed to be significant to control the dynamics and disturbances in the upper atmosphere by recent studies. The phenomena generated by the vertical coupling processes have been detected with various observational instruments, and studied with numerical simulations. TC, such as typhoon, hurricane and cyclone, is regarded as one of the intense sources in the Troposphere to affect the Mesosphere, the Thermosphere and the Ionosphere. There is a plenty of studies that reports the observation of the upper atmospheric disturbances associating with TC using ground-based instruments, such as HF doppler radars, IS radars, GNSS receiver arrays, and optical imagers. Because the ground-based observation cannot track the movement of TC, and TC is much active over the ocean, the observational opportunity is limited for the ground-based instruments. ISS-Ionosphere, Mesosphere, upper Atmosphere, and Plasmasphere (ISS-IMAP) mapping mission made a global observation of the airglow in the mesosphere and the ionosphere for three years. The data set of visible-light and infrared spectrum imager (VISI) of ISS-IMAP is idealistic to investigate the effect of TC on the Mesosphere and the Ionosphere. Mesospheric disturbances were detected by the airglow from the molecular oxygen in 762nm of wavelength, and the ionospheric disturbances were detected by the airglow from the atomic oxygen in 630nm of wavelength. In its three years observation, the number of TC that ISS-IMAP/VISI made the conjugate observation was 171. It was found that more than 20% of TC was associated with the mesospheric disturbances that seems to be generated by TC. The duration of these disturbances was one or two days in spite of the lifetime of TC is longer than a week. The relationship among TC, the mesospheric and the ionospheric disturbances will be discussed in the presentation.

キーワード：ISS-IMAP、台風、大気光、中間圏、電離圏
Keywords: ISS-IMAP, Tropical cyclone, airglow, Mesosphere, Ionosphere

©2019. Japan Geoscience Union. All Right Reserved.

A fast acoustic wave detected in GNSS total electron content after the foreshock of the 2011 Tohoku Earthquake

*柿並 義宏[1]、齊藤 大晶[2]、山本 哲生[3]、陳 佳宏[4]、山本 真行[2]、中島 健介[5]、劉 正彦[6]
*Yoshihiro Kakinami[1], Hiroaki Saito[2], Tetsuo Yamamoto[3], Chia-Hung Chen[4], Masa-yuki Yamamoto[2], Kensuke Nakajima[5], JANN-YENQ Liu[6]

1. 北海道情報大学、2. 高知工科大学、3. 北海道大学、4. 台湾国立成功大学、5. 九州大学、6. 台湾国立中央大学
1. Hokkaido Information University, 2. Kochi University of Technology, 3. Hokkaido University, 4. National Cheng Kung University, 5. Kyushu University, 6. National Central University

Acoustic waves are often emitted from large earthquakes, reach the thermosphere and disturb the ionosphere. The disturbances are observed by using of GNSS total electron content (TEC). After the foreshock of the 2011 Tohoku Earthquake, which occurred on 9 March 2011, traveling ionospheric disturbance induced by tsunami was detected. When vertical propagation of acoustic wave from the tsunami source area is assumed, the onset points of co-seismic ionospheric disturbance (CID) must coincide. However, the onset points of the co- CID were detected at different locations in different satellite data assuming that the altitude of CID were the same (ex. at 300 km). Furthermore, we found the onset times were different in the different satellite data. The results suggest that the altitudes of CID are different and timings of observation are also different in the different satellite data. By changing the altitudes of CID, we found coinciding onset point. Once the coinciding onset point is found in the different data sets, the altitudes of the CID are also estimated because the sub-ionospheric point is a function of the altitude of observation. The CID altitude were found at 155.4 and 234.9 km. Considering the time difference of the onset time (399.9 s to the altitude of 155.4 km and 476.1 s to 234.9 km), the acoustic wave velocity is estimated to be 1.04 km/s which is 1.4 times higher than the velocity calculated using the empirical model NRLMSISE-00. The fast acoustic wave would arise from temperature elevated by the limited degrees of freedom of motion of atmospheric molecules, and dissipation of the acoustic wave. Especially, the neutral temperature with heating by the dissipation of the acoustic wave would increase by a factor of 3 for acoustic waves with 0.1 Hz and a pressure at sea level of ~2 Pa, which is on the order of the pressure of the acoustic wave emitted from the sea surface during the observed event. The elevated temperature explains the fast acoustic wave.

キーワード：速い音波、2011年東北地震前震、地震後電離圏擾乱、GNSS全電子数、電離圏擾乱の高度推定、熱圏の加熱
Keywords: fast acoustic wave, the foreshock of the 2011 Tohoku Earthquake, co-seismic ionospheric disturbance , GNSS total electron content, altitude estimation of ionospheric disturbance , heating of the thermosphere

©2019. Japan Geoscience Union. All Right Reserved.

Study of quiet-time high-latitude thermospheric winds using a Fabry-Perot interferometer at Tromsoe: Averages and exceptional events

*徐 何秋岑[1]、塩川 和夫[1]、大山 伸一郎[1]
*Heqiucen XU[1], Kazuo Shiokawa[1], Shin-ichiro Oyama[1]

1. 名古屋大学宇宙地球環境研究所
1. Institute for Space-Earth Environmental Research, Nagoya University

In the previous reports, we studied the dependences of average winds on Kp and F10.7 indices by using a Fabry-Perot interferometer (FPI) at Tromsoe, Norway. In this study, we have further focused on the winds during both globally (Kp < 1+) and locally quiet times in order to provide a baseline wind without magnetic disturbances at latitude of Tromsoe. The wind variations were measured from the Doppler shift of both red-line (630.0 nm, altitudes: 200-300 km, upper thermosphere) and green-line (557.7 nm, altitudes: 90-100 km, mesopause region) emissions with a time resolution of ~13 min. The wind data were collected from 2009 to 2015. In the upper thermosphere, the quiet-time average zonal wind shows westward acceleration at pre-midnight side at ~21-24 LT, while the meridional wind has a minimum around the midnight. In the mesopause region, the average wind tends to show a westward and eastward flow at dusk and dawn side, respectively. By applying sinusoidal regression to the mesospheric average zonal wind, we found that the semidiurnal component has a dominant amplitude of 12.1 m/s. During quiet time, we also found a few exceptional events of more than 100 m/s westward at dusk side in the upper thermosphere. We speculate these exceptional westward winds are related to local plasma convection under quiet time or substorm activities occurred at some other latitudes/local times.

キーワード：熱圏、ファブリ・ペロー干渉計
Keywords: Thermosphere, Fabry-Perot interferometer

©2019. Japan Geoscience Union. All Right Reserved.

The longitudinal differences of lunar tidal characteristics between East Asian and American sectors during stratospheric sudden warming events: 2009-2018.

*Jing Liu[1], Donghe Zhang[1]

1. Peking University

With data of total electron content (TEC), equatorial electrojet (EEJ), stratospheric temperature and wind field, variations of the low-latitudinal ionosphere in East Asian and American sectors were investigated during stratospheric sudden warming events from 2009-2018. The lunar tidal amplitudes (M2) were derived with the least-square method. Then their features were compared separately during outstanding major events, moderate major events, minor events, and a non-SSW winter. Brief results are listed as follows: (1) In the American sector, the M2 tides appeared to be dominant over solar tides in all major events since distinct time-shifted semi-diurnal patterns could always be detected during those periods. (2) In the East Asian sector, the M2 characteristics were less clear, and sometimes even hard to identify, which means the relative strengths of lunar and solar tides are more complex in this sector. (3) The M2 amplitudes in TEC tend to be larger in the American sector than in East Asian sector during the same event. (4) The longitudinal differences tend to be lessened in minor SSWs compared to major SSWs. (5) During the non-SSW winter, lunitidal features could still be detected in both sectors. Similar results can be found in previous works for different kinds of parameters. Such longitudinal differences were attributed to combined effects of the geomagnetic field configuration, the latitudinal dependence of lunar and solar tides, the changes of atmospheric circulation, and the coupling process from the lower-atmosphere to the F region ionosphere.

Keywords: Stratospheric Sudden Warming, Low-latitudinal Ionosphere, Longitudinal Differences, Lunitidal Characteristics

©2019. Japan Geoscience Union. All Right Reserved.

[E] 口頭発表 | セッション記号 P (宇宙惑星科学)：P-EM 太陽地球系科学・宇宙電磁気学・宇宙環境

2019年5月30日(木) 9:00 ~ 10:30 | A04 東京ベイ幕張ホール

[P-EM11] Dynamics of Magnetosphere and Ionosphere

コンビーナ:中溝 葵(情報通信研究機構　電磁波研究所)、尾崎 光紀(金沢大学理工研究域電子情報学系)、藤本 晶子(九州工業大学)、堀 智昭(名古屋大学宇宙地球環境研究所)、座長:中野 慎也(情報・システム研究機構 統計数理研究所)、野和田 基晴(山東大学)

This session provides an opportunity to present recent results from satellite and ground-based observations and theoretical and simulation studies on the magnetosphere, ionosphere, and their coupling processes. We invite talks and posters discussing various phenomena related to the magnetosphere-ionosphere system: solar wind-magnetosphere interaction, magnetosphere-ionosphere convection, field-aligned current, magnetic storms/substorms, neutral-plasma interaction, ionospheric ion inflow and outflow, aurora phenomena, and so forth. Discussions on planetary and satellite ionosphere and magnetospheres, future missions and instrument developments are also welcome.

9:00 ~ 9:15

[PEM11-07] **Nightside Distorted Transpolar Arcs and Their Possible Formation Process Model**

*野和田 基晴[1]、　俊[1]、ヒューベルト ベノワ[2]、宗 秋 [3]、史 全岐[1]、王 永福[3]、周 煦之[3]、　宇[3] (1.山東大学 威海校 空間科学与物理学学院 空間科学研究院 空間天気物理与探計測研究中心 、2.リージュ大学 宇宙科学技術天文研究所、3.北京大学 地球与空間科学学院 空間物理与応用技術研究所)

9:15 ~ 9:30

[PEM11-08] Ionospheric Conductivity Dependence of the Subauroral Polarization Streams Observed by the SuperDARN HF Radars

張 玉テイ[1]、*西谷 望[1]、堀 智昭[1]、Simon Shepherd[2]、William Bristow[3] (1.名古屋大学宇宙地球環境研究所、2.ダートマス大学、3.アラスカ大学フェアバンクス校)

9:30 ~ 9:45

[PEM11-09] Ionospheric convection modeling based on convolution with a localized vector-valued basis function

*中野 慎也[1]、堀 智昭[2]、関 華奈子[3]、西谷 望[2] (1.統計数理研究所、2.名古屋大学宇宙地球環境研究所、3.東京大学大学院理学系研究科)

9:45 ~ 10:00

[PEM11-10] **Occurrence Statistics and Driving Mechanisms of Ionospheric ULF Waves Observed by SuperDARN Radars**

★Invited Papers

*Xueling Shi[1]、Joseph B. H. Baker[1]、John Michael Ruohoniemi[1]、Dong Lin[1]、Michael Hartinger[1,2] (1.Virginia Tech、2.Space Science Institute)

10:00 ~ 10:15

[PEM11-11] Magnetic Field Oscillations Observed by Swarm Satellites in the Nightside Upper Ionosphere During Low-latitude Pi2 Pulsations

*Khan-Hyuk Kim[1]、Jae-Hee Park[1] (1.School of Space Research, Kyung Hee Univ.)

10:15 ~ 10:30

[PEM11-12] Magnetospheric Multiscale observations of ULF waves and correlated low-energy ion monoenergetic acceleration

*Bin Li[1]、De-sheng Han[2]、Ze-jun Hu[1]、Jian-jun Liu[1]、Lei Dai[3] (1.Polar Research Institute of China、2.Tongji University、3.National Space Science Center, Chinese Academy of Sciences)

Nightside Distorted Transpolar Arcs and Their Possible Formation Process Model

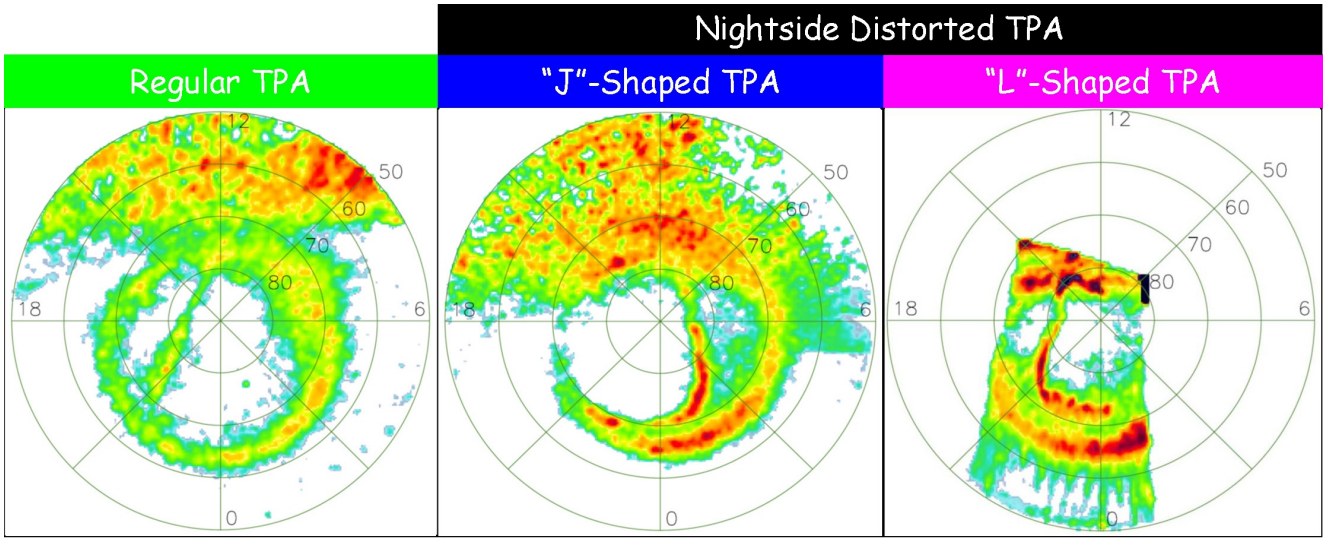
*野和田 基晴[1]、 俊[1]、ヒューベルト ベノワ[2]、宗 秋[3]、史 全岐[1]、王 永福[3]、周 煦之[3]、 宇[3]
*Nowada Motoharu[1], Jun Yang[1], Benoit Hubert[2], Qiu-Gang Zong[3], Quan-Qi Shi[1], Yong-Fu Wang[3], Xu-Zhi Zhou[3], Zhao Hua-Yu[3]

1. 山東大学 威海校 空間科学与物理学学院 空間科学研究院 空間天気物理与探計測研究中心 、2. リージュ大学 宇宙科学技術天文研究所、3. 北京大学 地球与空間科学学院 空間物理与応用技術研究所
1. Shandong University at Weihai, 2. Université de Liège, 3. Peking University

Transpolar Arc (TPA) is an important auroral phenomenon when considering how the energy stored in magnetotail is transported to ionosphere via magnetic reconnection under the northward interplanetary magnetic field. Magnetotail reconnection is considered to play a crucial role in TPA formation. Reconnection X-points are expected to retreat tailward as TPA grows from nightside auroral oval to the dayside. Usually, they straightforwardly retreat tailward, and reconnection-formed TPA morphology is straight-bar shape. However, we wonder how the TPA shape would be expected when traces of the tailward X-point retreats were not straightforward. The Wideband Imaging Camera (WIC), which is a part of Far Ultraviolet (FUV) instrument, onboard the Imager for Magnetopause-to-Aurora Global Exploration (IMAGE) satellite detected an interesting type of TPAs, which are identified as “nightside distorted TPAs”. Their main bar-shaped parts were located at the dawn or dusk sides, and the nightside ends of them got distorted toward pre- or post-midnight sectors. Because these TPAs look like the shape of an alphabetical letter of “J” or “L”, we distinguished the nightside distorted TPAs from “J”- and “L”-shaped TPAs. We followed the time sequence of the evolutions of several nightside distorted TPAs with the IMAGE FUV-WIC imager data. In most cases, the “J” and “L”-shaped TPAs started to grow from the nightside main auroral oval, and protruded to the dayside auroral oval via the experience of distortion, suggesting that magnetotail magnetic reconnection was closely be related with the formation of the nightside distorted TPAs. In this study, we have proposed a model to explain the nightside distorted TPA formation, in order to discuss that TPAs with their nightside ends distorted toward pre- or post-midnight were formed through how physical process. Furthermore, we have tried to verify whether or not our model proposed is appropriate to adequately explain formation process of nightside distorted TPA based on the global MHD simulation using the BATS-R-US codes.

キーワード：夜側に歪みを持つトランスポーラーアーク: “J”- and “L” 型トランスポーラーアーク、夜側磁気圏磁気リコネクション、リコネクションポイントの磁気圏尾部への直線的或いは歪曲的後退、動的平衡状態、磁気圏対流
Keywords: Nightside distorted transpolar arc: “J”- and “L”-shaped TPAs, Nightside magnetic reconnection, Straightforward or wry tailward retreats of X-points , State of dynamic equilibrium, Magnetospheric convection

©2019. Japan Geoscience Union. All Right Reserved.



©2019. Japan Geoscience Union. All Right Reserved.

Ionospheric Conductivity Dependence of the Subauroral Polarization Streams Observed by the SuperDARN HF Radars

張 玉テイ[1]、*西谷 望[1]、堀 智昭[1]、Simon Shepherd[2]、William Bristow[3]
Yuting Zhang[1], *Nozomu Nishitani[1], Tomoaki Hori[1], Simon G. Shepherd[2], William A. Bristow[3]

1. 名古屋大学宇宙地球環境研究所、2. ダートマス大学、3. アラスカ大学フェアバンクス校
1. Institute for Space-Earth Environmental Research, Nagoya University, 2. Thayer School of Engineering, Dartmouth College, 3. University of Alaska Fairbanks

We investigate the characteristics of the subauroral polarization stream (SAPS), with a main focus on the solar zenith angle (SZA) dependence using the Super Dual Auroral Radar Network (SuperDARN) HF radars and NOAA POES spacecraft data. In this study, we used 3 SuperDARN radars (HOK / CVE / ADW), and checked data from 2008 to 2017 and found 124 SAPS events where the line-of-sight velocity is larger than 150m/s, magnetic local time is 13 to 19 hours and the flow regions are identified to be equatorward of the auroral precipitation region. For each event, we examined the SZA using the geographic latitude, longitude and the UT span of SAPS. We found that the results of CVE radar are different from the result of HOK and ADW radar, the SAPS observed by CVE radar can happen in high conductivity occasion when both hemispheres are illuminated. However, we found that these illuminated SAPS could only occur under geomagnetically disturbed condition and mostly in spring and fall. In addition, when the geomagnetic activity is low, SAPS tends to appear when the minimum threshold of illuminated ionospheric altitude is 130 km or more, which is near and slightly above the altitude of the peak of Pedersen conductivity. These results suggest that the generation mechanism of SAPS is affected by both geomagnetic activity and the Pedersen conductivity. Results of detailed discussion will be presented.

キーワード：SuperDARN北海道-陸別第一レーダー、太陽天頂角、サブオーロラ帯高速プラズマ流(SAPS)、電離圏-磁気圏結合、Pedersen電気伝導度
Keywords: SuperDARN Hokkaido East radar, solar zenith angle, sub-auroral polarization stream (SAPS), magnetosphere-ionosphere coupling, Pedersen conductivity

©2019. Japan Geoscience Union. All Right Reserved.

Ionospheric convection modeling based on convolution with a localized vector-valued basis function

*中野 慎也[1]、堀 智昭[2]、関 華奈子[3]、西谷 望[2]
*Shin ya Nakano[1], Tomoaki Hori[2], Kanako Seki[3], Nozomu Nishitani[2]

1. 統計数理研究所、2. 名古屋大学宇宙地球環境研究所、3. 東京大学大学院理学系研究科
1. The Institute of Statistical Mathematics, 2. Institute for Space-Earth Environmental Research, Nagoya University, 3. Graduate School of Science, University of Tokyo

Divergence free assumption is useful for modeling the flow velocity distribution in the ionosphere where plasma velocity can be assumed to be orthogonal to a potential electric field. If the divergence of two-dimensional plasma velocity is assumed to be zero, we can consider a stream function yielding the plasma velocity distribution. In order to estimate the two-dimensional flow velocity distribution in the ionosphere, we propose a framework which expresses the stream function by a convolution with a spherical Gaussian function. From this spherical Gaussian function, we can obtain a localized vector-valued basis function for flow velocity distribution satisfying the divergence-free condition. Accordingly, flow velocity distribution can be represented by a convolution with the vector-valued basis functions. We combine this model with a state space model and estimate a temporal evolution using the Kalman filter algorithm. Hyperparameters of the model are determined by maximizing marginal likelihood.

The proposed framework is applied for estimating the two-dimensional ionospheric convection pattern from the Super Dual Auroral Radar Network (SuperDARN) data. Although there are some wide gaps in the spatial coverage of the SuperDARN radar network for ionospheric observation, the use of the localized basis function enhances the robustness of the estimate. This basis function also enables us to evaluate the uncertainty of the estimate which would be helpful for incorporating other observations. Some results of the analysis of the SuperDARN data will be demonstrated.

キーワード：電離圏対流、SuperDARN、球面ガウス関数
Keywords: ionospheric convection, SuperDARN, spherical Gaussian function

©2019. Japan Geoscience Union. All Right Reserved.

Occurrence Statistics and Driving Mechanisms of Ionospheric ULF Waves Observed by SuperDARN Radars

*Xueling Shi[1], Joseph B. H. Baker[1], John Michael Ruohoniemi[1], Dong Lin[1], Michael Hartinger[1,2]

1. Virginia Tech, 2. Space Science Institute

Ultra-low frequency (ULF; 1 mHz - 5 Hz) waves are known to play an important role in the transfer of energy from the solar wind to Earth's magnetosphere and ionosphere. The Super Dual Auroral Radar Network (SuperDARN) is an international network consisting of 35 low-power high frequency coherent scatter radars at middle to polar latitudes that look into Earth's upper atmosphere and ionosphere. In this study, we use Doppler velocity measurements obtained by the SuperDARN radars and coordinated spacecraft observations to investigate the occurrence statistics and driving mechanisms of ionospheric ULF waves. Pc3-5 band (1.7-40.0 mHz) ULF waves were surveyed using high time resolution radar data from 2010 to 2016. Specifically, we have investigated the wave spatial occurrence, frequency characteristics, seasonal factors, and dependence on solar wind and geomagnetic conditions. We note two particular findings: (i) an internal wave-particle interaction source is responsible for Pc4 waves at high latitudes in the duskside ionosphere; and, (ii) a source associated with the magnetotail dynamics during active geomagnetic times is suggested for Pc3-4/Pi2 waves at midlatitudes in the nightside ionosphere. A few interesting ULF wave events will be further analyzed for their driving mechanisms via coordinated observations from spacecraft. Collectively, these research findings provide better constraints on where and when ionospheric ULF waves occur and how they might affect magnetospheric and ionospheric dynamics.

Keywords: ULF Waves, SuperDARN, Ionosphere

©2019. Japan Geoscience Union. All Right Reserved.

Magnetic Field Oscillations Observed by Swarm Satellites in the Nightside Upper Ionosphere During Low-latitude Pi2 Pulsations

*Khan-Hyuk Kim[1], Jae-Hee Park[1]

1. School of Space Research, Kyung Hee Univ.

Pi2-associated geomagnetic oscillations in the nighside upper ionosphere are studied using magnetic field data acquired by low-Earth orbiting multispacecraft Swarm and at the low-latitude Bohyun (BOH) station located at magnetic shell of L = 1.3 on 22 October 2014. Four Pi2 events were identified from the BOH data near midnight (MLT = 1.5) while Swarm A, B, and C spacecraft were orbiting on the nightside (MLT = 21-22) upper ionosphere from 70˚ to --60˚ in magnetic latitude (MLAT) at 450-500 km altitudes. It is found that the horizontal H component of BOH data is well correlated with the radial (B_x) and compressional (B_z) components of ionospheric magnetic fields when Swarm spacecraft were at |MLAT| < 30˚. Both B_x and B_z components exhibit in phase or out of phase with the BOH H oscillations depending on the location of the spacecraft (i.e., in the Northern Hemisphere or in the Southern Hemisphere). This indicates that Pi2-associated magnetic oscillation in the ionosphere is the consequence of field line displacement that is symmetric or odd mode about the magnetic equator. We also find that stationary magnetic field perturbation, which is similar to Pi2 oscillation but not associated Pi2 signals, in the upper ionosphere near magnetic equator. A statistical analysis for the global distribution of static/spatial magnetic field perturbations using low-latitude Pi2 oscillation as a reference is a subject of future work.

Keywords: Pi2 pulsation

©2019. Japan Geoscience Union. All Right Reserved.

Magnetospheric Multiscale observations of ULF waves and correlated low-energy ion monoenergetic acceleration

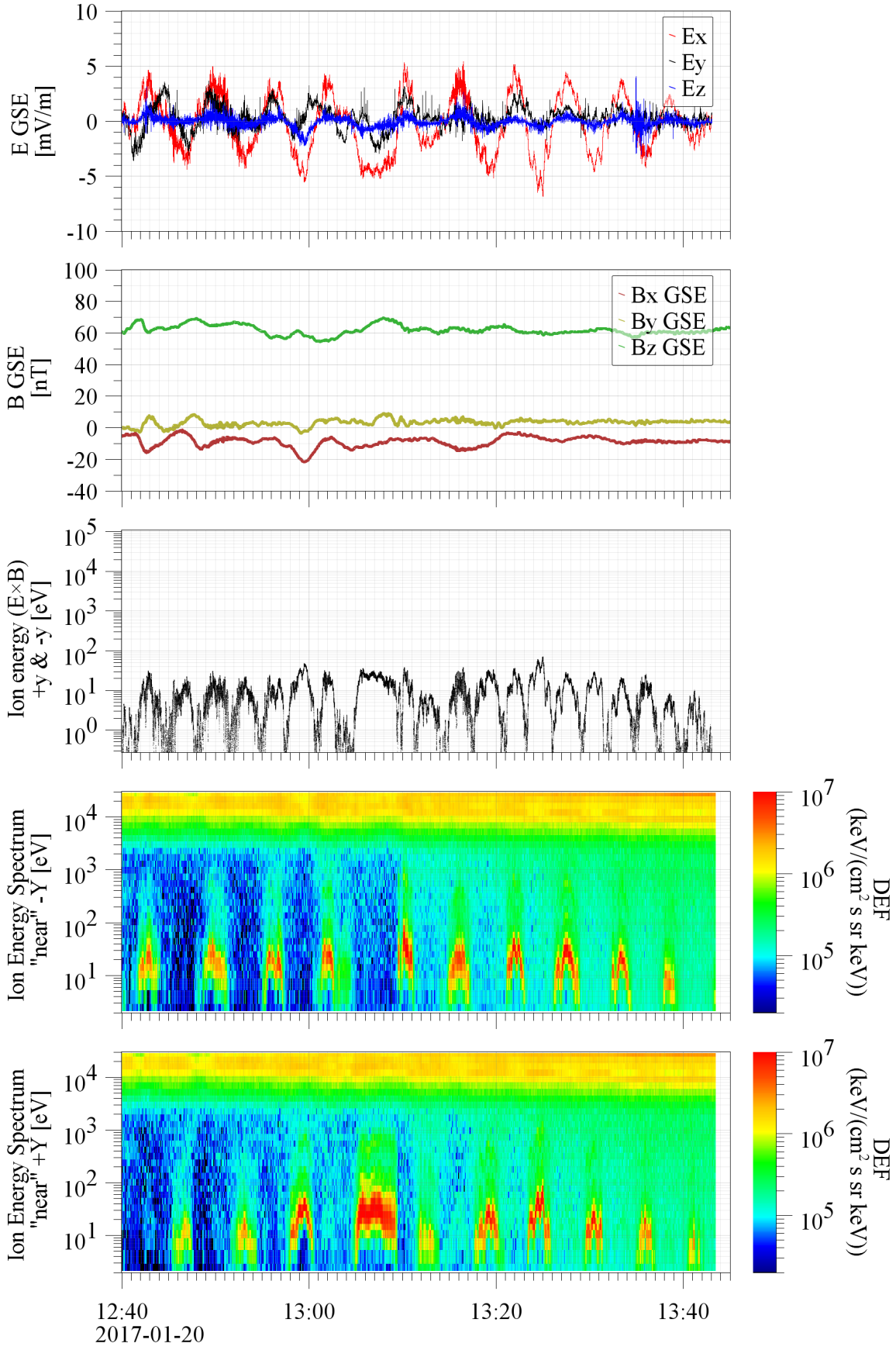
*Bin Li[1], De-sheng Han[2], Ze-jun Hu[1], Jian-jun Liu[1], Lei Dai[3]

1. Polar Research Institute of China, 2. Tongji University, 3. National Space Science Center, Chinese Academy of Sciences

Low-energy ions of ionospheric origin with energies below tens of eV dominate most of the volume and mass of the terrestrial magnetosphere. However, sunlit spacecraft often become positively charged to several tens of volts, which prevents low-energy ions from reaching the particle detectors on the spacecraft. Magnetospheric multiscale spacecraft (MMS) observations show that ultralow-frequency (ULF) waves drive low-energy ions to drift in the E×B direction with a drift velocity equal to $V_{E\times B}$, and low-energy ions were accelerated to a higher energy level to reach the detection range of the MMS/Fast Plasma Investigation (FPI). The maximum ion flux energy level detected by MMS1 DIS agreed perfectly with the theoretical calculation of H^+ ion E×B drift energy. The density of ions in the energy range below 2 eV was between 1 cm^{-3} and 3 cm^{-3} in the magnetosphere subsolar region in this event.

Keywords: low-energy ion monoenergetic acceleration, ultralow-frequency wave, E×B drift

©2019. Japan Geoscience Union. All Right Reserved.



©2019. Japan Geoscience Union. All Right Reserved.

[E] 口頭発表 | セッション記号 P (宇宙惑星科学)：P-EM 太陽地球系科学・宇宙電磁気学・宇宙環境

2019年5月30日(木) 10:45 ~ 12:15 | A04 東京ベイ幕張ホール

[P-EM11] Dynamics of Magnetosphere and Ionosphere

コンビーナ:中溝 葵(情報通信研究機構　電磁波研究所)、尾崎 光紀(金沢大学理工研究域電子情報学系)、藤本 晶子(九州工業大学)、堀 智昭(名古屋大学宇宙地球環境研究所)、座長:桂華 邦裕(東京大学大学院理学系研究科)、中野 慎也(情報・システム研究機構 統計数理研究所)、野和田 基晴(山東大学)

This session provides an opportunity to present recent results from satellite and ground-based observations and theoretical and simulation studies on the magnetosphere, ionosphere, and their coupling processes. We invite talks and posters discussing various phenomena related to the magnetosphere-ionosphere system: solar wind-magnetosphere interaction, magnetosphere-ionosphere convection, field-aligned current, magnetic storms/substorms, neutral-plasma interaction, ionospheric ion inflow and outflow, aurora phenomena, and so forth. Discussions on planetary and satellite ionosphere and magnetospheres, future missions and instrument developments are also welcome.

10:45 ~ 11:00

[PEM11-13] Statistical study on warm plasma in the magnetotail based on two-component fits of distribution functions

*桂華 邦裕[1]、浅見 隆太[1]、星野 真弘[1] (1.東京大学大学院理学系研究科地球惑星科学専攻)

11:00 ~ 11:15

[PEM11-14] Analysis on anisotropy variations for pitch angle distributions of electrons with various parameters at dipolarization sites in the inner plasma sheet

*Kaiti Wang[1]、Zhuo-Ren Lang[2]、Ching-Huei Lin[3]、Tohru Hada[4]、Toshi Nishimura[5] (1.Tamkang Univ.、2.National Cheng Kung Univ.、3.Chien-Hsin Univ. of Sci. & Tech.、4.Kyushu Univ.、5.Boston Univ.)

11:15 ~ 11:30

[PEM11-15] Study of slow-mode shock formation in the symmetric magnetic reconnection based on hybrid simulations

*Nehpreet Kaur Walia[1]、Kanako Seki[1]、Takanobu Amano[1] (1. Department of Earth & Planetary Science, Graduate School of Science, University of Tokyo)

11:30 ~ 11:45

[PEM11-16] Reconstruction of the electron diffusion region of magnetotail reconnection seen by the Magnetospheric Multiscale spacecraft

*長谷川 洋[1]、Richard Denton[2]、中村 るみ[3]、Kevin Genestreti[4]、中村 琢磨[3]、Joo Hwang[5]、Tai Phan[6]、Roy Torbert[4]、Jim Burch[5]、Barbara Giles[7]、Dan Gershman[7]、Chris Russell[8]、Bob Strangeway[8]、Per-Arne Lindqvist[9]、Yuri Khotyaintsev[10]、Robert Ergun[11]、北村 成寿[12]、斎藤 義文[1] (1.宇宙航空研究開発機構宇宙科学研究所、2.ダートマス大学、3.オーストリア宇宙科学研究所、4.ニューハンプシャー大学、5.サウスウェスト研究所、6.カリフォルニア大学バークレー校、7.NASAゴダード宇宙飛行センター、8.カリフォルニア大学ロサンゼルス校、9.スウェーデン王立工科大学、10.スウェーデン宇宙物理学研究所、11.コロラド大学、12.東京大学地球惑星科学専攻)

11:45 ~ 12:00

[PEM11-17] MMS observations of the dense high speed flow in the magnetotail

*Mingyu Wu[1]、Tielong Zhang[1] (1.Harbin Insitute of Technology, Shenzhen)

12:00 ~ 12:15

[PEM11-18] The spatio-temporal development of lightning-induced electron precipitation events

★Invited Papers

*Robert C Moore[1]、Dooyoung Kim[1] (1.University of Florida)

Statistical study on warm plasma in the magnetotail based on two-component fits of distribution functions

*桂華 邦裕[1]、浅見 隆太[1]、星野 真弘[1]
*Kunihiro Keika[1], Ryuta Asami[1], Masahiro Hoshino[1]

1. 東京大学大学院理学系研究科地球惑星科学専攻
1. Department of Earth and Planetary Science, Graduate School of Science, The University of Tokyo

A large number of observations reported two distinct plasma populations with different temperatures in the Earth's magnetotail: 1-10 keV for the hotter component and <1 keV for the colder. It is well accepted that plasma of solar wind origin can enter into the magnetosphere due to tailward convection of magnetic field lines that were reconnected at the dayside magnetopause, or due to instabilities or waves that develop on the dawn and dusk flanks. Cold plasma of ionospheric origin can be also transported into the plasma sheet predominantly along the field lines. Such cold plasma can be then heated/accelerated to 1 keV or higher. The dominant transport region(s) and heating mechanism(s) are, however, not well understood. This study investigates global characteristics of warm (10-1000 eV) plasma populations observed in the magnetotail in order to better understand transport regions of solar wind and ionospheric plasma.

We use data from plasma observations made by the Hot Plasma Composition Analyzer (HPCA) on board the Magnetospheric Multiscale (MMS) spacecraft. HPCA measures ions with energies of a few eV to ~40 keV with the determination of ion mass. We perform a one-component Maxwellian fit and a two-component Maxwellian fit to a distribution function of the omni-directional proton flux during intervals of slow flow speed (<~70 km/s). The best fit provides density and temperature of one-component Maxwellian plasma or density and temperature for each component of two-component Maxwellian plasma. This study is focused most on the colder (hotter) component of the two-component plasma, which we term a cold (normal) population. We apply this analysis and categorization to HPCA proton data obtained for a period of May 1 to August 31 of Year 2017. MMS dwelled in the magnetotail for the period, and HPCA data are available in the regions of 6 Re < r < 24 Re.

We examine dependence of density and temperature on plasma beta, which is the ratio of plasma thermal pressure to the magnetic pressure and thus represents the distance from the current sheet. The normal population shows clear positive correlations of density and temperature to plasma beta. This indicates adiabatic heating of lobe plasma transported toward the central plasma sheet. The cold population, on the other hand, does not show clear correlations. It is separated into three different types. Type 1 is characterized by positive correlations of density to plasma beta, similar to the normal population. Density is between 0.01 and 0.1 cm^{-3} at a beta range of 0.001 to 0.01, and increases to ~1 cm^{-3} at beta of >0.1. We confirm that the relation between density and temperature is well explained by adiabatic heating with the specific heat ratio of 5/3. Type 2 is seen only in the high beta (>0.1) regions, with density of ~0.01 cm^{-3}. Type 3 can be identified by a different relation between density and beta; density is between 0.01 and 1.0 with the highest occurrence frequency at 0.1 cm^{-3}, and temperature is a few 10s to 100s eV. Spatial distributions of each type show that Types 1 and 2 are observed at the radial distance of >10 Re. Type 1 shows no clear dawn-dusk asymmetry of occurrence frequency or average temperature, while Type 2 is more frequently observed on the dusk and dawn sides than around midnight. Type 3 occupies the region closer to 10 Re and is also observed at the radial distance of 10-20 Re with lower occurrence.

©2019. Japan Geoscience Union. All Right Reserved.

We interpret that Type 1 is dominated by plasma of solar wind origin transported over the polar regions, through the lobe toward the plasma sheet. Type 2 is likely solar wind plasma that enters through the flank magnetopauses. Type 3 is of ionospheric origin, presumably from nightside auroral regions. We suggest that the north-south component of magnetospheric convection over the polar cap becomes dominant at the radial distance of 10 Re or further. Instabilities or waves that allow solar wind plasma to enter the plasma sheet are likely to sufficiently develop on the night side (i.e., $X < 0$).

キーワード：太陽風プラズマ流入、電離圏プラズマ供給、プラズマ混合、磁気圏低温プラズマ
Keywords: Entry of solar wind plasma, Supply of ionospheric plasma , plasma mixing, magnetospheric cold plasma

©2019. Japan Geoscience Union. All Right Reserved.

Analysis on anisotropy variations for pitch angle distributions of electrons with various parameters at dipolarization sites in the inner plasma sheet

*Kaiti Wang[1], Zhuo-Ren Lang[2], Ching-Huei Lin[3], Tohru Hada[4], Toshi Nishimura[5]

1. Tamkang Univ., 2. National Cheng Kung Univ., 3. Chien-Hsin Univ. of Sci. & Tech., 4. Kyushu Univ., 5. Boston Univ.

During geomagnetic activities, dipolarization of geomagnetic fields can been found to occur at tailside. In this study, we investigate variations in anisotropies of pitch angle distributions for electrons at 63 observed dipolarization sites around distance of 10 R_E (Earth radii) near the magnetic equator in the inner plasma sheet when auroral electrojet AL index decreases. Observational data from 2008 to 2011 for electrons below ~26 keV from the instrument ESA (ElectroStatic Analyzer) onboard of THEMIS mission are adopted. Followed from our previous presentation in which the dependence of these variations on field line lengths (FLL) was focused on [*Wang et al.*, 2018], we present new analysis results concentrating on the dependence of the changes as well as the rates of changes in FLL, magnetic field strengths, and dipolarization angles, during a dipolarizaion period. Comparisons between the anisotropy variations in pitch angle distributions of electrons and the associated bounce time of electrons, event dipolarization time, and measured environmental electric fields will also be presented and discussed.

References

Wang, K., Z. R. Lang, C. H. Lin, T. Hada, A. B. C. Chen, Y. Nishimura (2018). On the field line length dependence of variations in anisotropies for pitch angle distributions of keV electrons at dipolarization sites in the tailside. PEM16-25, JpGU Meeting 2018, Chiba, Japan.

Keywords: dipolarization, anisotropy of pitch angle distributions of electrons , observations of THEMIS mission

©2019. Japan Geoscience Union. All Right Reserved.

Study of slow-mode shock formation in the symmetric magnetic reconnection based on hybrid simulations

*Nehpreet Kaur Walia[1], Kanako Seki[1], Takanobu Amano[1]

1. Department of Earth & Planetary Science, Graduate School of Science, University of Tokyo

Fast magnetic reconnection is achieved in the Petschek' s reconnection theory [1964] via a pair of slow-mode shocks on each side of the diffusion region. The occurrence of these slow-mode shocks has been established in MHD regime by the various MHD and Hall-MHD simulation studies [e.g., e.g., Hoshino and Nishida, 1983; Biernat et al., 1989; Lin and Lee, 1993; Hau and Wang, 2016]. However, in the kinetic regime, their existence is still debated. Some of the hybrid and PIC simulations studies of magnetic reconnection region show slow-shock like structures, where either all the Rankine-Hugoniot (RH) or the Mach number conditions are not satisfied [e.g., Krauss-Varban and Omidi, 1995; Lottermoser et al. 1998; Higashimori and Hoshino, 2012], while some show the presence of Petschek like slow-mode shocks [e.g., Lin and Swift, 1996; Liu et al. 2012; Innocenti et al., 2015]. With satellite observations, the presence of slow-mode shocks have been confirmed for both asymmetric dayside magnetopause reconnection [Walia et al., 2018 and Sonnerup at al., 2016] and symmetric magnetotail reconnection [e.g. Feldman et al., 1987; Saito et al., 1995; Eriksson et al., 2004]. Walia et al. [2018] and Saito et al. [1995] reported that the detection probability of slow-mode shocks at around 20% and 10% in the dayside magnetopause and the magnetotail, respectively. One of the reasons for low detection probability of slow-mode shocks can be that the non-slow mode shock crossings used in the observational studies are very close to the X-point, and hence the slow-mode structure has not developed fully. The error in the determination of the shock normal direction and the shock frame of reference can be another reason for lack of observations of slow-mode shocks. In situ measurements via the use of the satellite data, can help us to look into the detailed structure of a magnetic reconnection crossing, but if one wants to look at the whole structure of magnetic reconnection region, simulation studies are needed. Especially, if one wants to look into the transition from the kinetic scales to MHD scales to find out how the structure of reconnection region changes and slow-mode shocks or other discontinuities form and develop.

In the present study we use 2D hybrid simulations for symmetric magnetic reconnection with isotropic temperature to investigate the formation of slow-mode shocks. The presence of slow-shocks in the magnetic reconnection region is established by checking the satisfaction of the RH conditions and specific conditions of Mach numbers, normal angles etc. [e.g., Seon et al., 1995, 1996]. We check the set of 12 slow-mode shock conditions and use the 30% satisfaction criteria [e.g., Walia et al., 2018; Eriksson et al., 2004] at all distances from the X-point to study the formation of slow-mode shocks from the ion inertial length scales to MHD scale. We found that the Petschek like slow-mode shocks can be identified as close as ~10 λ_i (λ_i = ion inertial length) to the X-point. Below, 10 λi slow-mode shocks are not fully developed, and rather slow shock-like structure is present. Also, it is found that the slow-mode shock identification is sensitive to the slow-shock normal determination. We will also report the differences in the satisfaction of various conditions (e.g., RH conditions, Mach numbers) and the characteristics of the ion distribution functions between the regions with slow-mode shocks and slow shock-like structures.

Keywords: Magnetic reconnection, Slow-mode shocks

©2019. Japan Geoscience Union. All Right Reserved.

Reconstruction of the electron diffusion region of magnetotail reconnection seen by the Magnetospheric Multiscale spacecraft

*長谷川 洋[1]、Richard Denton[2]、中村 るみ[3]、Kevin Genestreti[4]、中村 琢磨[3]、Joo Hwang[5]、Tai Phan[6]、Roy Torbert[4]、Jim Burch[5]、Barbara Giles[7]、Dan Gershman[7]、Chris Russell[8]、Bob Strangeway[8]、Per-Arne Lindqvist[9]、Yuri Khotyaintsev[10]、Robert Ergun[11]、北村 成寿[12]、斎藤 義文[1]

*Hiroshi Hasegawa[1], Richard E. Denton[2], Rumi Nakamura[3], Kevin J. Genestreti[4], Takuma Nakamura[3], Kyoung Joo Hwang[5], Tai D. Phan[6], Roy B. Torbert[4], Jim L. Burch[5], Barbara L. Giles[7], Dan J. Gershman[7], Chris T. Russell[8], Bob J. Strangeway[8], Per Arne Lindqvist[9], Yuri V. Khotyaintsev[10], Robert E. Ergun[11], Naritoshi Kitamura[12], Yoshifumi Saito[1]

1. 宇宙航空研究開発機構宇宙科学研究所、2. ダートマス大学、3. オーストリア宇宙科学研究所、4. ニューハンプシャー大学、5. サウスウェスト研究所、6. カリフォルニア大学バークレー校、7. NASAゴダード宇宙飛行センター、8. カリフォルニア大学ロサンゼルス校、9. スウェーデン王立工科大学、10. スウェーデン宇宙物理学研究所、11. コロラド大学、12. 東京大学地球惑星科学専攻

1. Institute of Space and Astronautical Science, Japan Aerospace Exploration Agency, 2. Dartmouth College, 3. Space Research Institute, Austrian Academy of Science, 4. University of New Hampshire, 5. Southwest Research Institute, 6. University of California Berkeley, 7. NASA Goddard Space Flight Center, 8. University of California Los Angeles, 9. Royal Institute of Technology, 10. Swedish Institute of Space Physics, 11. University of Colorado, 12. University of Tokyo

Magnetic reconnection is a fundamental plasma process that controls transfer of solar wind energy and mass to planetary magnetospheres and causes explosive energy release associated with solar flares and sudden auroral brightening. NASA's Magnetospheric Multiscale (MMS) mission, which consists of four identical spacecraft launched in March 2015, aims at elucidating how magnetic reconnection works with unprecedented high temporal and spatial resolution measurements of charged particles and electromagnetic fields in space. MMS has been observing Earth's magnetotail since May 2017, and encountered the central region of magnetic reconnection, called the electron diffusion region (EDR), on 11 July 2017 (Torbert et al., Science, 2018). We present results from the reconstruction of the electron diffusion region (EDR) observed in this event. The conditions were suited for the reconstruction technique, developed by Sonnerup et al. (JGR, 2016), that produces magnetic field and electron streamline maps based on a two-dimensional (2-D), time independent, inertia-less form of electron magnetohydrodynamic equation, assuming an approximately symmetric current sheet and negligible guide magnetic field. Our reconstruction results (Hasegawa et al., JGR, 2019) indicate that although the X point was not captured inside its tetrahedron, MMS approached the X point as close as one electron inertial length ~27 km. The opening angle of the recovered separatrix field line, combined with theory, suggests that the dimensionless reconnection rate was 0.17, which is consistent with the measured reconnection electric field 2–4 mV/m. The stagnation point of the reconstructed electron flow is shifted earthward of the X point by ~90 km, one possible interpretation of which is discussed. The energy conversion rate **j'E'** in the electron frame tends to be higher near the stagnation point, consistent with earlier observations and simulations, and is not correlated with the amplitude of broadband electrostatic waves observed in the upper-hybrid frequency range. The latter suggests that the waves did not contribute to energy dissipation in this particular EDR.

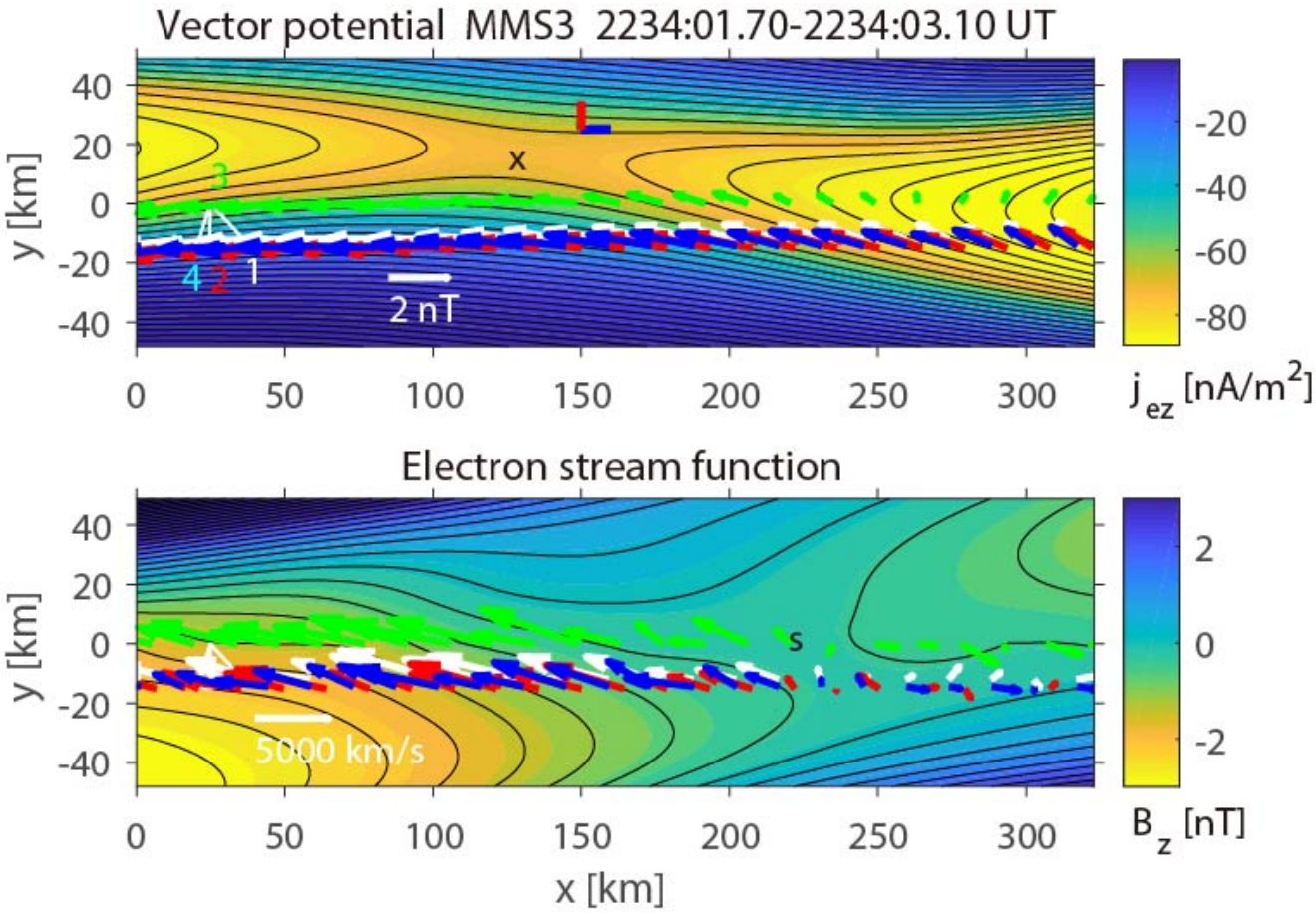
References:

Hasegawa, H., Denton, R. E., Nakamura, R., Genestreti, K. J., Nakamura, T. K. M., Hwang, K.-J., et al.,

©2019. Japan Geoscience Union. All Right Reserved.

Reconstruction of the electron diffusion region of magnetotail reconnection seen by the MMS spacecraft on 11 July 2017. Journal of Geophysical Research: Space Physics, 124. https://doi.org/10.1029/2018JA026051, 2019.
Sonnerup, B. U. O., H. Hasegawa, R. E. Denton, and T. K. M. Nakamura, Reconstruction of the electron diffusion region, J. Geophys. Res. Space Physics, 121, 4279-4290, doi:10.1002/2016JA022430, 2016.
Torbert, R. B., J. L. Burch, T. D. Phan, ... Y. Saito, Electron-scale dynamics of the diffusion region during symmetric magnetic reconnection in space, Science, doi:10.1126/science.aat2998, 2018.

キーワード：磁気リコネクション、磁気圏尾部、電子拡散領域
Keywords: magnetic reconnection, magnetotail, electron diffusion region



©2019. Japan Geoscience Union. All Right Reserved.

MMS observations of the dense high speed flow in the magnetotail

*Mingyu Wu[1], Tielong Zhang[1]

1. Harbin Insitute of Technology, Shenzhen

With the MMS observations in the magnetotail, we report a earthward, dense, high speed, bulk flow event. In this event, two dense high speed flows (DHSF) are observed. Compared with the plasma sheet, DHSF contains much denser and colder plasma. Ion density of DHSF is about 8 times higher to plasma sheet density, while temperature of DHSF is several times lower to plasma sheet plasma. Due to the high density, DHSF can transport mass more effective than normal bursty bulk flows. Such DHSF can be generated by Magnetic reconnection, but the generation mechanism is still unclear.

Keywords: High-density bulk flow, Plasma sheet, Magnetic reconnection

©2019. Japan Geoscience Union. All Right Reserved.

The spatio-temporal development of lightning-induced electron precipitation events

*Robert C Moore[1], Dooyoung Kim[1]

1. University of Florida

Lightning-induced electron precipitation (LEP) events occur when the electromagnetic energy radiated by lightning couples to the magnetosphere and scatters ¬stably trapped radiation belt electrons. A portion of these scattered electrons in turn precipitate into the underlying ionosphere, producing electron density disturbances in the D-region ionosphere which can be detected by VLF remote sensing. When LEP events are observed nearly simultaneously at both the northern and southern ends of a field line, the LEP event is known as a conjugate LEP event. In this paper, an array of VLF receivers in the northern hemisphere is used to measure the spatial-temporal development of the LEP-related ionization patch produced within the D-region ionosphere. During one interesting event, LEP-associated VLF signal perturbations were observed at three receiver sites in the northern hemisphere (Florida, North Carolina, and Connecticut) and at one receiver in the conjugate hemisphere (Palmer Station, Antarctica). The LEP-related disturbance is observed to move poleward with time, consistent with many past observations. A second interesting event indicates the detection of an eastward expansion (with time) of the LEP-related disturbance, however. Together, these observations indicate that previous large-scale statistics compiled for conjugate LEP events may be seriously impacted by the spatio-temporal development of the LEP-associated ionospheric disturbances in the two hemispheres. Perhaps equally importantly, these observations indicate that VLF remote sensing can be used to measure the temporal and spatial development of energetic electron precipitation from the Earth's radiation belts.

Keywords: Lightning-induced electron precipitation, Radiation belts, Ionosphere

©2019. Japan Geoscience Union. All Right Reserved.

[E] 口頭発表 | セッション記号 P (宇宙惑星科学)：P-EM 太陽地球系科学・宇宙電磁気学・宇宙環境

2019年5月30日(木) 13:45 ~ 15:15 | A04 東京ベイ幕張ホール

[P-EM11] Dynamics of Magnetosphere and Ionosphere

コンビーナ:中溝 葵(情報通信研究機構　電磁波研究所)、尾崎 光紀(金沢大学理工研究域電子情報学系)、藤本 晶子(九州工業大学)、堀 智昭(名古屋大学宇宙地球環境研究所)、座長:北村 成寿(東京大学大学院理学系研究科)、佐藤 由佳(日本工業大学)

This session provides an opportunity to present recent results from satellite and ground-based observations and theoretical and simulation studies on the magnetosphere, ionosphere, and their coupling processes. We invite talks and posters discussing various phenomena related to the magnetosphere-ionosphere system: solar wind-magnetosphere interaction, magnetosphere-ionosphere convection, field-aligned current, magnetic storms/substorms, neutral-plasma interaction, ionospheric ion inflow and outflow, aurora phenomena, and so forth. Discussions on planetary and satellite ionosphere and magnetospheres, future missions and instrument developments are also welcome.

13:45 ~ 14:00

[PEM11-19] サブストーム時におけるエネルギーの流れ、ダイナモ、沿磁力線電流

*海老原 祐輔[1]、田中 高史[2] (1.京都大学生存圏研究所、2.九州大学)

14:00 ~ 14:15

[PEM11-20] **Electron flux and field-aligned current associated with Pc5 auroral arc pulsations observed onboard THEMIS and DMSP satellites**

*佐藤 夏雄[1]、行松 彰[1,2]、田中 良昌[1,2]、堀 智昭[3]、門倉 昭[1,2]、櫻井 亨[4]、Desheng Han[5]、Yuzhang Ma[6]、Qinghe Zhang[6] (1.国立極地研究所、2.総研大、3.名古屋大学、4.東海大学、5.同済大学、6.山東大学)

14:15 ~ 14:30

[PEM11-21] Multiple spots of enhanced electron precipitation near the equatorward boundary of the cusp

*田口 聡[1]、小瀬 智史[1]、高須 浩平[1]、田中 杜雄[1]、細川 敬祐[2]、小川 泰信[3] (1.京都大学理学研究科地球惑星科学専攻地球物理学教室、2.電気通信大学情報理工学研究科、3.国立極地研究所)

14:30 ~ 14:45

[PEM11-22] Statistical study of auroral/resonant-scattering 427.8-nm emission observed at subauroral latitudes over 14 years

*塩川 和夫[1]、大塚 雄一[1]、Martin Connors[2] (1.名古屋大学宇宙地球環境研究所、2.アサバスカ大学)

14:45 ~ 15:00

[PEM11-23] 無人システムを利用したオーロラ現象の南極広域ネットワーク観測：共役点イベント解析（２）

*門倉 昭[1]、山岸 久雄[1]、岡田 雅樹[1]、小川 泰信[1]、田中 良昌[1]、片岡 龍峰[1]、内田 ヘルベルト陽仁[1]、大塚 雄一[2] (1.国立極地研究所、2.名古屋大学)

15:00 ~ 15:15

[PEM11-24] **Dawn-Dusk Asymmetry in Dayside and Nightside auroral Ovals: Surveys of auroral emissions based on the all-sky imagers in Arctic and Antarctic**

★Invited Papers

*Zejun Hu[1] (1.Polar Research Institute of China)

サブストーム時におけるエネルギーの流れ、ダイナモ、沿磁力線電流
Energy flow, dynamo and field-aligned current during a substorm

*海老原 祐輔[1]、田中 高史[2]
*Yusuke Ebihara[1], Takashi Tanaka[2]

1. 京都大学生存圏研究所、2. 九州大学
1. Research Institute for Sustainable Humanosphere, Kyoto University, 2. Kyushu University

A substorm is one of the most severe disturbances that occur in the magnetosphere. Extremely bright aurora is a great manifestation of the substorm. Since the bright aurora is caused by precipitating electrons, the bright aurora is closely associated with the upward field-aligned currents (FACs). Simultaneously, a large amount of energy, of the order of 10^{11} watts, is consumed in the auroral ionosphere due to Joule dissipation during the substorm. The dissipating energy is brought by the FACs that are rapidly intensified. Thus, the formation of the FACs is a key to understand the substorm. The generation of the FACs is accompanied with conversion of energy (dynamo). The energy comes from the solar wind. The purpose of this study is to provide a unified view of a substorm in terms of the energy flow, energy conversion (dynamo) and field-aligned current on the basis of a global magnetohydrodynamics (MHD) simulation. The recent global MHD simulation tells us that, at least, some dynamo regions appear one by one in association with the substorm. The first dynamo region is found in the bow shock where the solar wind kinetic energy is converted to the magnetic energy and the internal energy. However, the role of the bow shock dynamo is suggested to be minor. The second dynamo region is found in the lobe region when the interplanetary magnetic field (IMF) is northward. A complicated structure of the plasma pressure in the lobe gives rise to the generation of FACs that could manifest high-latitude auroral arcs during the growth phase. The third dynamo region appears in the mantle region when IMF is southward. The internal energy is converted to the magnetic energy by way of the kinetic energy in the mantle dynamo. Simultaneously, a large-scale FACs (known as Region 1 FACs) are generated in association with the mantle dynamo, which is probably responsible to the formation of a quiet auroral arc during growth phase. The fourth dynamo appears in the near-Earth magnetosphere on the nightside as a consequence of the formation of the near-Earth neutral line. The magnetic energy (coming from the lobe region) is converted to the internal energy, followed by the kinetic energy and the magnetic energy. The near-Earth dynamo is associated with the onset of the sudden intensification of the upward FACs that are related to the initiation of the auroral breakup. The fifth dynamo is located near the leading/trailing edges of the bright auroral surge where charge separation takes place due to the gradient of the ionospheric Hall conductivity. A localized upward FAC is generated, which probably manifests the bright auroral surge traveling westward. It is concluded that the evolution of the substorm can be understood to the evolution of the dynamo regions in the magnetosphere and the ionosphere.

キーワード：サブストーム、エネルギー変換、電磁流体シミュレーション
Keywords: Substorm, Energy conversion, MHD simulation

©2019. Japan Geoscience Union. All Right Reserved.

Electron flux and field-aligned current associated with Pc5 auroral arc pulsations observed onboard THEMIS and DMSP satellites

*佐藤 夏雄[1]、行松 彰[1,2]、田中 良昌[1,2]、堀 智昭[3]、門倉 昭[1,2]、櫻井 亨[4]、Desheng Han[5]、Yuzhang Ma[6]、Qinghe Zhang[6]
*Natsuo Sato[1], Akira S Yukimatu[1,2], Yoshimasa Tanaka[1,2], Tomoaki Hori[3], Akira Kadokura[1,2], Tohru Sakurai[4], Desheng Han[5], Yuzhang Ma[6], Qinghe Zhang[6]

1. 国立極地研究所、2. 総研大、3. 名古屋大学、4. 東海大学、5. 同済大学、6. 山東大学
1. National Institute of Polar Research, 2. SOKENDAI, 3. Nagoya University, 4. Tokai University, 5. Tongji University, 6. Shandong University

Pc5 poleward moving auroral arc (PMAA) pulsations observed on the ground in the post-midnight sector exhibit east-west-aligned auroral arcs elongated ~ 1000-3000 km and behave poleward moving form with a recurrence period of ~ 2-10 minutes (Pc5 range). They appear just poleward side of common type pulsating auroras. We examined the space-ground coordinated observations with the THEMIS-A, D, and E spacecraft whose footprints were located near the PMAA observed with the all-sky imager on the ground. The latitudinal wave amplitudes and phase structures are consistent with the field-line resonance (FLR) model, while the period of oscillation was longer at the higher latitude side (not a monochromatic wave). The electron flux in the higher energy range of ~ 2–20 keV showed decreasing modulation in conjunction with the FLR oscillations. The intensity of the electric field and the velocity showed a spatial gradient that suggests the existence of a field-aligned current flow around the region of the satellites. The period of FLR oscillations in the magnetosphere was ~ 15–25% longer than that of the auroral pulsations in the ionosphere, and the enhancement of FLR oscillations was ~ 3–4 minutes ahead of the auroral pulsations. These signals imply that the FLR oscillations could not directly enhance the luminosity oscillation but needed some other process that could enhance the luminosity pulsation. We will examine the mechanism of how to produce the field-aligned electric field in association with the PMAA. In this study we focus on the characteristics of the electron flux variations observed onboard the THEMIS and DMSP satellites. The THEMIS satellites were located near the equatorial plane in the magnetosphere, and the DMSP satellites traversed in the ionosphere and crossed over the field of view of all-sky imager at observatories in Canada and Alaska and Syowa Station in Antarctica. It is found that the DMSP satellites observed the precipitating electron flux that behaved the feature of field-aligned acceleration and also observed the field-aligned currents when the DMSP satellite crossed the region of the PMAA.

キーワード：オーロラアーク脈動、Pc5脈動、脈動オーロラ、磁力線共鳴、THEMIS衛星、DMSP衛星
Keywords: auroral arc pulsation, Pc 5 pulsation, pulsating aurora, field-line resonance, THEMIS spacecraft, DMSP satellite

©2019. Japan Geoscience Union. All Right Reserved.

Multiple spots of enhanced electron precipitation near the equatorward boundary of the cusp

*田口 聡[1]、小瀬 智史[1]、高須 浩平[1]、田中 杜雄[1]、細川 敬祐[2]、小川 泰信[3]
*Satoshi Taguchi[1], Satoshi Kose[1], Kohei Takasu[1], Morio Tanaka[1], Keisuke Hosokawa[2], Yasunobu Ogawa[3]

1. 京都大学理学研究科地球惑星科学専攻地球物理学教室、2. 電気通信大学情報理工学研究科、3. 国立極地研究所
1. Department of Geophysics, Graduate School of Science, Kyoto University, 2. Department of Communication Engineering and Informatics, University of Electro-Communications, 3. National Institute of Polar Research

Localized enhancements of electron precipitation near the equatorward boundary of the cusp is thought to be caused by enhanced fluxes of soft magnetosheath electrons in the flux tube immediately after localized intermitted reconnection on the dayside magnetopause. A recent study based on an all-sky imager has reported an event which shows that enhanced electron precipitation appears in two separate locations along the equatorward boundary of the cusp, and that the distance between them is approximately 0.2 MLT. In this study we have examined if there is any characteristic scale in the distance between neighboring electron precipitation spots near the equatorward of the cusp to understand the characteristics of the occurrence point of intermittent reconnection. We analyzed 630-nm aurora data from an all-sky imager at Longyearbyen, Svalbard, and electron precipitation and field-aligned current data from DMSP spacecraft, which flied in the field-of-view of the auroral imager. A simultaneous observation event shows that six enhanced electron precipitation regions, each of which is accompanied with an upward/downward pair of mesoscale field-aligned currents, were observed along the pass of the DMSP satellite, and that all of those enhanced electron precipitation regions were also identified as auroral spots in the 630-nm auroral image data. By examining auroral image data obtained before the simultaneous observation event, we traced back to the initial brightening for each auroral spot. The result of analysis has shown that the longitudinal distance between the neighboring spots near the equatorward boundary of the cusp lies between 0.15 and 0.4 MLT. The statistical analysis with data obtained for longer period of time on the same day has also shown a similar tendency. We discuss why localized intermittent reconnection tends to occur in such locations.

キーワード：カスプ、オーロラ、電子降下、リコネクション
Keywords: cusp, aurora, electron precipitation, reconnection

©2019. Japan Geoscience Union. All Right Reserved.

Statistical study of auroral/resonant-scattering 427.8-nm emission observed at subauroral latitudes over 14 years

*塩川 和夫[1]、大塚 雄一[1]、Martin Connors[2]
*Kazuo Shiokawa[1], Yuichi Otsuka[1], Martin Connors[2]

1. 名古屋大学宇宙地球環境研究所、2. アサバスカ大学
1. Institute for Space-Earth Environmental Research, Nagoya University, 2. Athabasca University

Auroral emission at 427.8-nm from N_2^+ ions is caused by precipitation of energetic electrons, or by resonant scattering of sunlight at high altitudes by N_2^+ ions. The latter often causes impressive purple aurora at high altitudes. However, statistical characteristics of auroral 427.8-nm emission have not well been understood. In this paper we report occurrence characteristics of high 427.8-nm emission intensities (more than 100 R) at subauroral latitudes, based on measurements by a filter-tilting photometer over 14 years (2005-2018) at Athabasca, Canada (magnetic latitude: ~62^o). We divided the dataset into the elevation angles (θ s) of the sun more than and less than -24^o (shadow height of sunlight: 600 km) to separate the 427.8-nm emissions caused by resonant scattering of sunlight and those excited by auroral electrons, respectively. The occurrence rate of 427.8-nm emissions of more than 100 R is 10.6 % and 7.65 % for θ s more than and less than -24^o, respectively. The occurrence rate is high in the post-midnight sector, and increases with increasing geomagnetic activity, solar-wind speed, and density. The occurrence rate is highest in summer. A high occurrence rate was also observed in 2015-2018, from the maximum to the declining phase of the 11-year solar activity. Superposed epoch analysis indicates that the 427.8-nm emission exceeds 100 R when solar wind speed increases and solar wind density concurrently decreases, suggesting that the solar wind structures typically observed at the arrival of corotating interaction regions (CIR) can be responsible for the high 427.8-nm emission.

キーワード：427.8 nm発光、太陽光の共鳴散乱、紫のオーロラ
Keywords: 427.8 nm emission, resonant scattering of sunlight, purple aurora

©2019. Japan Geoscience Union. All Right Reserved.

無人システムを利用したオーロラ現象の南極広域ネットワーク観測：共役点イベント解析（２）

Antarctic large area network observation of auroral phenomena using unmanned system: Conjugate auroral event studies (2)

*門倉 昭[1]、山岸 久雄[1]、岡田 雅樹[1]、小川 泰信[1]、田中 良昌[1]、片岡 龍峰[1]、内田 ヘルベルト陽仁[1]、大塚 雄一[2]
*Akira Kadokura[1], Hisao Yamagishi[1], Masaki Okada[1], Yasunobu Ogawa[1], Yoshimasa Tanaka[1], Ryuho Kataoka[1], Herbert Akihito Uchida[1], Yuichi Otsuka[2]

1. 国立極地研究所、2. 名古屋大学
1. National Institute of Polar Research, 2. Nagoya University

2017年9月28日に、南極昭和基地とアイスランドとの間で同時観測された共役点オーロライベントの解析結果について紹介する。この時、南極側では、昭和基地から東に約500km離れた沿岸域のアムンゼン湾に設置されている「無人オーロラ観測装置（UAO：Unmanned Auroral Observation system）」によっても、全天オーロライメージャのデータが取得されており、従来よりもより広い経度範囲でのオーロラ活動の共役性の議論を行う。

キーワード：オーロラ、共役点観測、サブストーム
Keywords: aurora, conjugate observation, substorm

©2019. Japan Geoscience Union. All Right Reserved.

Dawn-Dusk Asymmetry in Dayside and Nightside auroral Ovals: Surveys of auroral emissions based on the all-sky imagers in Arctic and Antarctic

*Zejun Hu[1]

1. Polar Research Institute of China

The synoptic distributions of dayside aurora in the Northern and Southern Hemispheres, acquired from all-sky imagers at Yellow River Station in Arctic and South Pole Station in Antarctica, respectively, present the same two-peak structure, namely, the prenoon 09:00 MLT and postnoon 14:00-15:00 MLT peaks. The auroral intensity presents a hemispheric asymmetry, i.e., the postnoon intensity is less than the prenoon intensity in the Southern Hemisphere but more in the Northern Hemisphere. The hemispheric asymmetry is not changed with the change of IMF’ s polarity, although 1) the negative (positive) IMF By favors the postnoon 557.7/630.0-nm auroral emissions, and the positive (negative) By favor to the excitation of 630.0-nm auroral on prenoon oval in the Northern (Southern) Hemisphere; 2) the 630.0-nm auroral intensity in dayside oval increases dramatically during the negative IMF Bz. We suggested that 1) the two-peak structure in the dayside oval are predominantly related with the prenoon/postnoon antiparallel reconnection in high-latitude magnetopause produced to the prenoon and postnoon peaks; 2) the IMF By should modulate the dayside aurora through the inter-hemispheric current, which is produced by a north-south oriented electric field , and changing the distribution of midday R0-R1 current; 3) the opposite prenoon-postnoon asymmetries of dayside auroral distributions in the two hemispheres are the combined effect of the prenoon-postnoon variations of the magnetosheath density and the variation of the local ionospheric conductivity in the two ground-based observatories.

The synoptic distributions of nightside aurora in the Northern Hemisphere, acquired from all-sky imagers at China-Iceland joint Aurora Observatory (CIAO) in Iceland, present that there are different characteristics on 427.8, 557.7, and 630.0 nm: 1) There is a two-peak structure on 427.8 and 557.7 nm, namely the pre-midnight 20:00- 21:00 MLT and post-midnight 04:00 peaks. For 427.8-nm auroral emission, the intensity of two peaks are same. For 557.7-nm emission, the maximal intensity is at peak 21:00 MLT. 2) There is only on peak on 630.0 nm, namely the pre-midnight 20:00-21:00 MLT. The dawn-dusk asymmetry in the nightside auroral oval should be related with the asymmetries of field-aligned currents and plasma waves in magnetosphere.

Keywords: dawn-dusk asymmetry, dayside & nightside auroral oval, particle precipitation, auroral morphology

©2019. Japan Geoscience Union. All Right Reserved.

[E] 口頭発表 | セッション記号 P (宇宙惑星科学)：P-EM 太陽地球系科学・宇宙電磁気学・宇宙環境

2019年5月30日(木) 15:30 ~ 17:00 | A04 東京ベイ幕張ホール

[P-EM11] Dynamics of Magnetosphere and Ionosphere

コンビーナ:中溝 葵(情報通信研究機構　電磁波研究所)、尾崎 光紀(金沢大学理工研究域電子情報学系)、藤本 晶子(九州工業大学)、堀 智昭(名古屋大学宇宙地球環境研究所)、座長:北村 成寿(東京大学大学院理学系研究科)、佐藤 由佳(日本工業大学)、西野 真木(名古屋大学宇宙地球環境研究所)

This session provides an opportunity to present recent results from satellite and ground-based observations and theoretical and simulation studies on the magnetosphere, ionosphere, and their coupling processes. We invite talks and posters discussing various phenomena related to the magnetosphere-ionosphere system: solar wind-magnetosphere interaction, magnetosphere-ionosphere convection, field-aligned current, magnetic storms/substorms, neutral-plasma interaction, ionospheric ion inflow and outflow, aurora phenomena, and so forth. Discussions on planetary and satellite ionosphere and magnetospheres, future missions and instrument developments are also welcome.

15:30 ~ 15:45

[PEM11-25] 静止軌道磁場の変化に伴う10MeVプロトンの異常増加

*小原 隆博[1] (1.東北大学　惑星プラズマ大気研究センター)

15:45 ~ 16:00

[PEM11-26] Solar-cycle variations of >30 keV proton flux enhancements under the inner radiation belt

*ALLA SUVOROVA[1] (1.National Central University)

16:00 ~ 16:15

[PEM11-27] Auroral Imaging with Commercial DSLR Cameras near Athabasca, Canada

*Martin G Connors[1,2]、Ian Schofield[1]、Mike Noble[2]、Alister Ling[2]、Ryuho Kataoka[3]、Ken Murata[4]、Kazunori Yamamoto[4] (1.Athabasca University、2.Edmonton Centre, Royal Astronomical Society of Canada、3.National Institute for Polar Research、4.National Institute for Communications Technology)

16:15 ~ 16:30

[PEM11-28] PARM: Investigation of precipitating high-energy electrons into the auroral ionosphere with sounding rockets

*浅村 和史[1]、三好 由純[2]、細川 敬祐[3]、三谷 烈史[1]、滑川 拓[1,5]、坂野井 健[4]、八木 直志[4]、吹澤 瑞貴[4]、石澤 元気[4]、笠原 慧[5]、菅生 真[5]、川島 桜也[5]、野村 麗子[6]、能勢 正仁[2]、寺本 万里子[2]、小川 泰信[7]、齊藤 慎司[2]、藤井 良一[8] (1.宇宙航空研究開発機構宇宙科学研究所、2.名古屋大学宇宙地球環境研究所、3.電気通信大学、4.東北大学、5.東京大学、6.自然科学研究機構国立天文台、7.情報・システム研究機構国立極地研究所、8.情報・システム研究機構)

16:30 ~ 16:45

[PEM11-30] Development of a miniaturized X-ray imager for GEOspace X-ray imager (GEO-X)

*石川 久美[1]、江副 祐一郎[2]、沼澤 正樹[2]、伊師 大貴[2]、藤谷 麻衣子[2]、大坪 亮太[2]、福島 碧都[2]、鈴木 光[2]、湯浅 辰哉[2]、中嶋 大[3]、平賀 純子[4]、三好 由純[5]、笠原 慧[6]、満田 和久[1] (1.宇宙航空研究開発機構/宇宙科学研究所、2.首都大学東京、3.関東学院大学、4.関西学院大学、5.名古屋大学、6.東京大学)

16:45 ~ 17:00

Discussion

静止軌道磁場の変化に伴う10MeVプロトンの異常増加
Enhancement of 10MeV protons associated with a change of magnetic field configuration at geosynchronous orbit

*小原 隆博[1]
*Takahiro Obara[1]

1. 東北大学　惑星プラズマ大気研究センター
1. Planetary Plasma and Atmospheric Research Center,Tohoku University

静止軌道での磁場の引き伸ばし（thinning）に伴い、10MeVプロトンのフラックスが急激に増加した例が見つかった。磁気圏外・太陽風中では、対応する10MeVプロトンの増大が見られなかった事から、10MeVプロトンの増加は, 磁気圏が関与した事になる。10MeVプロトンを観測したGOES13/15衛星の地方時は20時で、プロトンの増加は、磁場引き伸ばし(thinning)の開始から始まった。同じくGOES衛星で計測している2MeV電子のフラックスは、磁場引き伸ばし(thinning)の開始で減少し、その後の双極子化(dipolarization) で増加したが、10MeVプロトンは、双極子化(dipolarization)では減少せずにフラックスを維持した。GOES13/15衛星位置での10MeVプロトン増加に先立つこと3時間前、太陽風衝撃波が地球磁気圏に到達した。この時、GOES衛星は6.5MeVのプロトンの増加を観測した。6.5 MeV プロトンは、磁気圏境界面で、太陽風衝撃波によって生成されたと考えられる(Shimazu and Tanaka, 2005)。10MeVプロトンも衝撃波の到来によって生成され、磁気圏内に侵入したと考えられるが、エネルギーが大きい事から,静止軌道位置には達せずに周辺に存在していた。そして、磁場の引き伸ばし(thinning）が起きたことによって、10MeVプロトンが静止軌道位置まで到達したと思われる。本イベントは、衝撃波によって生成された1~10MeVのエネルギーを持ったプロトンが、磁気圏の形状の変化によって、静止軌道位置で観測されるタイミングに時間差を生じた点で興味深いので、更に、同様の例を集めている。

キーワード：静止軌道、10MeVプロトン増加、磁場の変化
Keywords: Geosynchronous orbit, Enhancement of 10MeV protons , Magnetic field change

©2019. Japan Geoscience Union. All Right Reserved.

Solar-cycle variations of >30 keV proton flux enhancements under the inner radiation belt

*ALLA SUVOROVA[1]

1. National Central University

Upper atmosphere is continually affected by intense fluxes of energetic electrons and protons penetrating from the magnetosphere to low altitudes. The energetic particles ionize and excite neutral species altering local characteristics of the ionosphere. Continuous monitoring of energetic particles at low heights of ~850 km with the MEPED instrument onboard the NOAA/POES satellites allows studying of particle flux variations with geomagnetic activity and solar cycle. The instrument measures precipitating/trapped electrons and protons in the wide energy range. In the previous study, we revealed enhancements of electrons with energies 30 - 300 keV at low latitudes in a so-called forbidden zone. It was established that the electrons were injected from the inner radiation belt probably due to a mechanism of fast radial transport in the crossed electric and magnetic fields. In the current work, we study fluxes of >30 keV protons in the forbidden zone. We distinguish two types of proton enhancements, which have different spatial-temporal characteristics. One type of proton enhancements occurs due to the charge-exchange mechanism of the ring current and is always observed during magnetic storms. Another type is due to injections from the inner radiation belt. The last enhancements are similar to the electron enhancements. Results of long-term analysis of proton injections will be presented.

Keywords: magnetosphere-ionosphere, energetic protons, low latitudes, solar cycle

©2019. Japan Geoscience Union. All Right Reserved.

Auroral Imaging with Commercial DSLR Cameras near Athabasca, Canada

*Martin G Connors[1,2], Ian Schofield[1], Mike Noble[2], Alister Ling[2], Ryuho Kataoka[3], Ken Murata[4], Kazunori Yamamoto[4]

1. Athabasca University, 2. Edmonton Centre, Royal Astronomical Society of Canada, 3. National Institute for Polar Research, 4. National Institute for Communications Technology

Commercial DSLR Cameras have permitted a revolution in auroral imaging, due to their digital nature, low cost, high sensitivity, and other advantages. Athabasca University Geophysical Observatory is in the subauroral zone, but due to the high altitude of auroras, usually has optical auroral activity visible on its northern horizon. We have operated mostly northward-pointing DSLR cameras, either with a field of view of about 50 degrees, or nearly allsky coverage. Since the “allsky” cameras we have used in fact do not cover the whole sky, we have tilted them northward to cover that horizon preferentially. We have livestreamed images to http://autumn.athabascau.ca/auroracamhd.htm. Ironically, the northward orientation of cameras at the observatory has precluded us capturing images of the newly-recognized STEVE phenomenon, which is normally located south of our location. However, STEVE events found on auroral imaging campaigns in the Edmonton area can often be identified on EMCCD images from our Keo Scientific intensified allsky camera. Then we can combine the images, showing for example, that STEVE is roughly 200 km above the surface. The auroral imaging campaigns have used three fullframe DSLRs to produce partial sky images that are then stitched together using software to produce approximately 10k-pixel color auroral movies, suited for use with modem planetarium projector systems as impressive high resolution sky shows. Most recently we have used a Sony Alpha 7000 camera, taking advantage of the fiber optic internet link to the Athabasca site, to make livecasting of auroras to Japan possible. Since reliability of cameras with moving parts has been a problem, we hope that the direct imaging Sony Alpha camera will be more reliable than the “reflex” cameras previously used. To get around the problem of moving parts wearing out under the very high frame rate, we also tested inexpensive CMOS-type sensors controlled by single-board computers, and sending a digital image stream, but so far with different, but still present, reliability problems. Another issue faced is that in continuous operation, a large amount of data is produced due to the high pixel count of the cameras. We will discuss technical issues and challenges, but also show some results of DSLR operation over the years, including auroral movies and high resolution still frames.

Keywords: aurora, imaging, STEVE

©2019. Japan Geoscience Union. All Right Reserved.

[E] 口頭発表 | セッション記号 P (宇宙惑星科学) | P-EM 太陽地球系科学・宇宙電磁気学・宇宙環境

[P-EM11] Dynamics of Magnetosphere and Ionosphere

コンビーナ:中溝 葵(情報通信研究機構　電磁波研究所)、尾崎 光紀(金沢大学理工研究域電子情報学系)、藤本 晶子(九州工業大学)、堀 智昭(名古屋大学宇宙地球環境研究所)、座長:北村 成寿(東京大学大学院理学系研究科)、佐藤 由佳(日本工業大学)、西野 真木(名古屋大学宇宙地球環境研究所)

2019年5月30日(木) 15:30 〜 17:00 A04 (東京ベイ幕張ホール)

This session provides an opportunity to present recent results from satellite and ground-based observations and theoretical and simulation studies on the magnetosphere, ionosphere, and their coupling processes. We invite talks and posters discussing various phenomena related to the magnetosphere-ionosphere system: solar wind-magnetosphere interaction, magnetosphere-ionosphere convection, field-aligned current, magnetic storms/substorms, neutral-plasma interaction, ionospheric ion inflow and outflow, aurora phenomena, and so forth. Discussions on planetary and satellite ionosphere and magnetospheres, future missions and instrument developments are also welcome.

16:15 〜 16:30

[PEM11-28]PARM: Investigation of precipitating high-energy electrons into the auroral ionosphere with sounding rockets

*浅村 和史[1]、三好 由純[2]、細川 敬祐[3]、三谷 烈史[1]、滑川 拓[1,5]、坂野井 健[4]、八木 直志[4]、吹澤 瑞貴[4]、石澤 元気[4]、笠原 慧[5]、菅生 真[5]、川島 桜也[5]、野村 麗子[6]、能勢 正仁[2]、寺本 万里子[2]、小川 泰信[7]、齊藤 慎司[2]、藤井 良一[8]

(1.宇宙航空研究開発機構宇宙科学研究所、2.名古屋大学宇宙地球環境研究所、3.電気通信大学、4.東北大学、5.東京大学、6.自然科学研究機構国立天文台、7.情報・システム研究機構国立極地研究所、8.情報・システム研究機構)

キーワード：高エネルギー電子降り込み、観測ロケット、脈動オーロラ

Bursty precipitations of high-energy electrons into the polar ionopshere have been observed by low-altitude satellite, for example, SAMPEX and FIREBIRD II. These precipitations, called microburst, may contribute to the loss of the terrestrial radiation belt through the collisional energy loss with the dense, cold atmospheric particles. Recent numerical simulations successfully reproduce these microburst precipitations with a few Hz modulations by taking into account the pitch angle scattering with the whistler chorus elements at off-equator regions in the inner magnetosphere. Therefore, one can expect that the miscroburst precipitations have properties depending on auroral activities especially the pulsating auroras. In order to investigate the mechanisms of the microburst precipitations by in-situ observations, we are developing two instrument packages: PARM (Pulsating AuRora and Microbursts; already developed) and PARM-2 (being developed), both of which are designed suitable for sounding rocket experiments. PARM consists of four sensors; HEP (high-energy electron energy spectrometer), MED (medium-energy electron detector), AIC (auroral camera), and AFG (ASIC-based fluxgate magnetometer). PARM was onboard the NASA's RockSat-XN sounding rocket, and launched from Andoya, Norway at 09:13UT, Jan 13, 2019. On the other hand, PARM-2 is under development. It consists of HEP, two AICs, and MIM (magneto-impedance magnetometer). PARM-2 is to be onboard the NASA's LAMP sounding rocket which will fly from Poker Flat, Alaska in the period between the end of 2019 and the beginning of 2020.

We will present the overview of PARM missions including the initial results of RockSat-XN/PARM with ground-based observations and preparation status of LAMP/PARM-2.

©日本地球惑星科学連合

Development of a miniaturized X-ray imager for GEOspace X-ray imager (GEO-X)

*石川 久美[1]、江副 祐一郎[2]、沼澤 正樹[2]、伊師 大貴[2]、藤谷 麻衣子[2]、大坪 亮太[2]、福島 碧都[2]、鈴木 光[2]、湯浅 辰哉[2]、中嶋 大[3]、平賀 純子[4]、三好 由純[5]、笠原 慧[6]、満田 和久[1]
*Kumi Ishikawa[1], Yuichiro Ezoe[2], Masaki Numazawa[2], Daiki Ishi[2], Maiko Fujitani[2], Ryota Otsubo[2], Aoto Fukushima[2], Hikari Suzuki[2], Tatsuya Yuasa[2], Hiroshi Nakajima[3], Junko Hiraga[4], Yoshizumi Miyoshi[5], Satoshi Kasahara[6], Kazuhisa Mitsuda[1]

1. 宇宙航空研究開発機構/宇宙科学研究所、2. 首都大学東京、3. 関東学院大学、4. 関西学院大学、5. 名古屋大学、6. 東京大学
1. Japan Aerospace Exploration Agency/Institute of Space and Astronautical Science , 2. Tokyo Metropolitan University, 3. Kanto Gakuin University, 4. Kwansei Gakuin University, 5. Nagoya University, 6. The university of Tokyo

A reduction in weight of instrument, especially optics, is a key technique for explorers or small satellite missions. GEO-X (GEOspace X-ray imager) is a Japanese small satellite mission for X-ray observations of the dayside boundaries of the Earth’ s magnetosphere. An instrument is composed of a X-ray telescope
and a radio hard semiconductor pixel detector. Conventional X-ray optics have a trend that optics with better angular resolution have larger ratio of the weight to effective area. Therefore, it is difficult to utilize them for the X-ray planetary mission which has a severe weight limit. Micro pore optics are being developed based on a concept of a miniature optics. An original micro pore optics based on Si micromachining technologies will be used. A CMOS image sensor and a DEPFET (DEPleted P-Channle FET) are candidates for the X-ray detector. These new type semiconductor detectors are radiation hard and have optical light resistance, which are crucial in GEO-X to observe magnetosheaths and cusps near the dayside of the Earth. We report a summary of the instrument design and development for GEO-X.

キーワード：X線、磁気圏
Keywords: X-ray, magnetosphere

©2019. Japan Geoscience Union. All Right Reserved.

[E] 口頭発表 | セッション記号 P (宇宙惑星科学)：P-EM 太陽地球系科学・宇宙電磁気学・宇宙環境

2019年5月30日(木) 9:00 ~ 10:30 | A01 東京ベイ幕張ホール

[P-EM15] 太陽地球系結合過程の研究基盤形成

コンビーナ:山本 衛(京都大学生存圏研究所)、小川 泰信(国立極地研究所)、野澤 悟徳(名古屋大学宇宙地球環境研究所)、吉川 顕正(九州大学大学院理学研究院地球惑星科学部門)、座長:山本 衛

地球には太陽から膨大なエネルギーと物質の流入がある。地球の環境はそれらの入出力のバランスの上に成り立っており、地球大気におけるエネルギーと物質の循環の理解が重要である。本セッションは、日本学術会議マスタープラン2011/2014/2017で継続的に重点大型研究計画とされ、2020年度に向けても提案準備中である研究プロジェクト「太陽地球系結合過程の研究基盤形成」に関する議論を目的として、国際セッションとして提案する。研究プロジェクトに関連する設備とネットワークとしては、赤道大気の全域を観測する赤道MUレーダーと極域の磁気圏ー電離圏結合過程の詳細な観測を主とするEISCAT_3Dレーダー、赤道から極域までをグローバルにつなぐ地上観測網と観測データ網が含まれている。本セッションでは、研究プロジェクトの内容と進捗状況を報告すると共に、国内外の関連研究者から幅広い話題を集約することで、研究の動向と方向性について議論を深める。大型大気レーダー、非干渉散乱レーダー、観測ネットワーク、衛星観測、モデル研究等を用いた多様な研究やプロジェクトとの連携が重要であり、多くの論文の参加を求める。

9:00 ~ 9:15

[PEM15-01] Status of Equatorial MU Radar project in 2019

*山本 衛[1]、橋口 浩之[1]、横山 竜宏[1]、津田 敏隆[1] (1.京都大学生存圏研究所)

9:15 ~ 9:30

[PEM15-02] Recent Progress and Current Status of EISCAT_3D in 2018-2019

*宮岡 宏[1]、小川 泰信[1]、野澤 悟徳[2]、西村 耕司[1]、大山 伸一郎[2]、中村 卓司[1]、藤井 良一[2]、Heinselman Craig[3] (1.大学共同利用機関情報・システム研究機構国立極地研究所、2.名古屋大学宇宙地球環境研究所、3.EISCAT科学協会)

9:30 ~ 9:45

[PEM15-03] 超高層大気イメージングシステムとPWINGプロジェクトによる超高層大気・電磁気圏の地上多点観測網の現状

*塩川 和夫[1]、大塚 雄一[1]、PWING TEAM (1.名古屋大学宇宙地球環境研究所)

9:45 ~ 10:00

[PEM15-04] Development of MAGDAS project: Search for global electromagnetic coupling from polar to equatorial ionosphere

*吉川 顕正[1]、樺澤 大生[2]、魚住 禎司[3]、藤本 晶子[4]、阿部 修司[3] (1.九州大学大学院理学研究院地球惑星科学部門、2.九州大学大学院理学府地球惑星科学専攻、3.九州大学国際宇宙天気科学・教育センター、4.九州工業大学大学院情報工学研究院)

10:00 ~ 10:15

[PEM15-05] 太陽地球系結合研究推進のためのIUGONETデータ解析システム

*新堀 淳樹[1]、田中 良昌[2]、梅村 宜生[1]、阿部 修司[3]、能勢 正仁[1]、上野 悟[4] (1.名古屋大学宇宙地球環境研究所、2.国立極地研究所、3.九州大学 国際宇宙天気科学・教育センター、4.京都大学天文台)

10:15 ~ 10:30

[PEM15-06] 大型研究計画「太陽地球系結合過程の研究基盤形成」推進の議論（１）

*山本 衛[1] (1.京都大学生存圏研究所)

Status of Equatorial MU Radar project in 2019

*山本 衛[1]、橋口 浩之[1]、横山 竜宏[1]、津田 敏隆[1]
*Mamoru Yamamoto[1], Hiroyuki Hashiguchi[1], Tatsuhiro Yokoyama[1], Toshitaka Tsuda[1]

1. 京都大学生存圏研究所
1. Research Institute for Sustainable Humanosphere, Kyoto University

Research Institute for Sustainable Humanosphere, Kyoto University (RISH) has been studying the atmosphere and ionosphere by using radars. The first big facility was the MU (Middle and Upper atmosphere) radar installed in Shiga, Japan in 1984. This is one of the most powerful and multi-functional radar, and is successful of revealing importance of atmospheric waves for the dynamical vertical coupling processes. The next big radar was the Equatorial Atmosphere Radar (EAR) installed at Kototabang, West Sumatra, Indonesia in 2001. The EAR was operated under close collaboration with LAPAN (Indonesia National Institute for Aeronautics and Space), and conducted the long-term continuous observations of the equatorial atmosphere/ionosphere. The EAR, however, had a limited sensitivity to the MU radar as the total output power is just 1/10 to the MU radar. Our new project is to establish "Equatorial MU (EMU) Radar" just next to the EAR site in Indonesia. The EMU will have an active phased array antenna with the 163 m diameter and 1055 cross-element Yagis. Total output power of the EMU will be more than 500 kW. The EMU is the "MU radar class" facility, and can detect turbulent echoes from the mesosphere (60-80 km). In the ionosphere incoherent-scatter observations of plasma density, drift, and temperature would be possible. Multi-channel receivers will realizes radar-imaging observations. Preparation for the EMU progress in many aspect including site survey for the construction, discussion with local government, etc. In March 2019, RISH and LAPAN have 1st Internal School on Equatorial Atmosphere (ISQUAR) 2019 with more than 100 participants at Bandung, Indonesia. ISQUAR aims to promote interesting studies of the equatorial atmosphere and use of the atmospheric radar including the EMU. The EMU is one of the key element in the project "Study of coupling processes in the solar-terrestrial system" that is one of the important project in the Master Plan 2014 and 2017 of the Science Council of Japan (SCJ). We continue proposing the project to the SCJ Masterplan 2020.

キーワード：大気レーダー、赤道大気、 低緯度電離圏
Keywords: Atmospheric radar, Equatorial atmosphere, Low-latitude ionosphere

©2019. Japan Geoscience Union. All Right Reserved.

Recent Progress and Current Status of EISCAT_3D in 2018-2019

*宮岡 宏[1]、小川 泰信[1]、野澤 悟徳[2]、西村 耕司[1]、大山 伸一郎[2]、中村 卓司[1]、藤井 良一[2]、Heinselman Craig[3]
*Hiroshi Miyaoka[1], Yasunobu Ogawa[1], Satonori Nozawa[2], Koji Nishimura[1], Shin-ichiro Oyama[2], Takuji Nakamura[1], Ryoichi Fujii[2], Craig James Heinselman[3]

1. 大学共同利用機関情報・システム研究機構国立極地研究所、2. 名古屋大学宇宙地球環境研究所、3. EISCAT科学協会
1. National Institute of Polar Research, 2. Institute for Space-Earth Environmental Research, Nagoya University, 3. European Incoherent Scatter Scientific Association

The European Incoherent Scatter(EISCAT) Scientific Association with associate members from Sweden, Norway, Finland, UK, China and Japan, has officially started the construction of the 1st stage of EISCAT_3D from September 2017 toward its completion by the end of 2021, including the commissioning of the radar system. EISCAT 3D is the major upgrade of the existing EISCAT mainland radars, with a multi-static phased array system composed of one central active (transmit-receive) site and 4 receive-only sites to provide us 50-100 times higher temporal resolution than the present system. The construction of EISCAT 3D is planned to implement by 4-staged approach, starting from the core site with half transmitting power about 5MW at Skibotn (Norway) and 2 receiving sites at Kaiseniemi (Sweden) and Karesuvanto (Finland) at the 1st stage. As for site preparation, geotechnical surveys have been completed at three sites, and ground cleaning with trenching for power lines and optical fiber cables have almost finished at the core site, Skibotn. All site buildings are scheduled to be built in 2019 to start installation of the radar system from 2020.

Through the international tendering process led by the EISCAT headquarter, antenna units with housing containers, first stage receiver units, sub-array transmitter units and pulse and steering control units have been completed and contracted providers have just started their preparation for productions to meet the EISCAT_3D implementation plan for sub-systems in 2020.

National Institute of Polar Research has been pursuing the opportunity to contribute in-kind to the construction of EISCAT_3D by supplying radar transmitter units in cooperation with the EISCAT Headquarters and ISEE/Nagoya University. The EISCAT_3D program in Japan was successfully granted as as one of high-priority programs of the Master Plan 2014/2017 and the Roadmap 2014 program, as a core facility of ’Study of Coupling Processes in the Solar-Terrestrial System’ (PI: Prof. Toshitaka Tsuda, ROIS/Kyoto Univ.). Supported by these positive evaluations, high energy-efficient transmitter power amplifiers (SSPAs) has been developed and produced for the engineering verification test at the EISCAT Tromso site with partial fundings for development since 2016.
In this paper, we will overview the recent progress and current status of the project including our strategy for the transmitter units as our national contribution to the EISCAT_3D project.

キーワード：非干渉散乱レーダー、宇宙天気、北極、マスタープラン
Keywords: incoherent scatter radar, space weather, arctic, master plan

©2019. Japan Geoscience Union. All Right Reserved.

超高層大気イメージングシステムとPWINGプロジェクトによる超高層大気・電磁気圏の地上多点観測網の現状

Current status of the ground-based multi-point network observation of the upper atmosphere, ionosphere, and magnetosphere by the PWING Project and the Optical Mesosphere Thermosphere Imagers (OMTIs)

*塩川 和夫[1]、大塚 雄一[1]、PWING TEAM
*Kazuo Shiokawa[1], Yuichi Otsuka[1], PWING Team

1. 名古屋大学宇宙地球環境研究所
1. Institute for Space-Earth Environmental Research, Nagoya University

The Optical Mesosphere Thermosphere Imagers (OMTIs) consist of ~20 all-sky cooled-CCD imagers, 5 Fabry-Perot interferometers, 3 airglow temperature photometers, and 3 meridian-scanning photometers. They measure two-dimensional airglow images in the mesopause region and in the thermosphere, wind and temperatures in the lower thermosphere, and airglow rotational temperatures in the mesopause region. Details of the OMTIs project can be seen at http://stdb2.isee.nagoya-u.ac.jp/omti/. The PWING stands for "study of dynamical variation of Particles and Waves in the INner magnetosphere using Ground-based network observations." The PWING project started on April 2016 as a 5-year project of the Grant-in-Aid for Specially Promoted Research of the Japan Society for the Promotion of Science (JSPS) (16H06286). The PWING project deploy OMTIs all-sky cooled-CCD airglow imagers, 64-Hz sampled induction magnetometers, 40-kHz VLF receivers, and 64-Hz riometers at 8 stations at magnetic latitudes of ~60 degree around the north-pole to cover longitudinal variation of aurora and electromagnetic disturbances in the inner magnetosphere. Details of the PWING project can be seen at http://www.isee.nagoya-u.ac.jp/dimr/PWING/PWING_web_e.htm. These PWING and OMTIs instruments are in automatic operation at various locations from high to equatorial latitudes in Canada, US (Alaska), Russia, Norway, Finland, Iceland, Japan, Thailand, Indonesia, Nigeria, and Australia. In the presentation, we introduce current status and some recent results obtained by these multi-instrument ground networks around the world.

PWING Team: http://www.isee.nagoya-u.ac.jp/dimr/PWING/en/

キーワード：超高層大気イメージングシステム、PWINGプロジェクト、超高層大気、電磁気圏
Keywords: Optical Mesosphere Thermosphere Imagers (OMTIs) , PWING Project, upper atmosphere , ionosphere and magnetosphere

©2019. Japan Geoscience Union. All Right Reserved.

Development of MAGDAS project: Search for global electromagnetic coupling from polar to equatorial ionosphere

*吉川 顕正[1]、樺澤 大生[2]、魚住 禎司[3]、藤本 晶子[4]、阿部 修司[3]
*Akimasa Yoshikawa[1], Taisei Kabasawa[2], Teiji Uozumi[3], Akiko Fujimoto[4], Shuji Abe[3]

1. 九州大学大学院理学研究院地球惑星科学部門、2. 九州大学大学院理学府地球惑星科学専攻、3. 九州大学国際宇宙天気科学・教育センター、4. 九州工業大学大学院情報工学研究院
1. Department of Earth and Planetary Sciences, Kyushu University, 2. Graduate school of Sciences, Kyushu Univerity, 3. International center for Space weather science and education, Kyushu University, 4. Kyushu Institute of Technology

The equatorial ionosphere is a final destination of electromagnetic energy brought about by energy incidence to the polar ionosphere. Distribution of geomagnetic disturbance accompanying such a coupling phenomenon shows strong asymmetry. Such an aspect suggests that the magnetosphere-ionosphere form a unique transmission and / or propagation system depending on each event.
The MAGDAS project investigates such a global electromagnetic coupling system by combining global geomagnetic field network observation with electric field observation using ionosonde installed at low and dip-equator region.
Recently, by using 250Hz sampling and 10Hz averaged MAGDAS 9 magnetometer data, we found that when the auroral substorm were enhanced during geomagnetic storm, together with enhancement of Pc1 wave at the polar region, the global Pc2 type disturbances (period range from 5 to 20 sec) can be captured from polar to equatorial region. In this talk, we will present recent update of MAGDAS project and of which scientific results.

キーワード：全球電磁結合、Pc2脈動、磁気圏電離圏結合
Keywords: global electromagnetic coupling, Pc2 pulsation, Magnetosphere-ionosphere Coupling

©2019. Japan Geoscience Union. All Right Reserved.

太陽地球系結合研究推進のためのIUGONETデータ解析システム
IUGONET data analysis system for a study of coupling processes in the solar-terrestrial system

*新堀 淳樹[1]、田中 良昌[2]、梅村 宜生[1]、阿部 修司[3]、能勢 正仁[1]、上野 悟[4]
*Atsuki Shinbori[1], Yoshimasa Tanaka[2], Norio Umemura[1], Shuji Abe[3], Masahito Nose[1], Satoru UeNo[4]

1. 名古屋大学宇宙地球環境研究所、2. 国立極地研究所、3. 九州大学 国際宇宙天気科学・教育センター、4. 京都大学天文台
1. Institute for Space-Earth Environment Research (ISEE), Nagoya University, 2. National institute of Polar Research, 3. International Center for Space Weather Science and Education Kyushu University, 4. Observatory, Kyoto University

The earth’ s atmosphere in a height range of more than 80 km is called the upper atmosphere, and the atmospheric layer is influenced by both the solar activity and the atmospheric waves propagating from the lower atmosphere. Therefore, in order to understand the physical mechanism of the short-term and long-term variations in the upper atmosphere, we need to perform an integrated analysis of various kinds of ground-based and satellite observation data taken by different instruments. Since these observation data were separately being managed by each institute, it was difficult for users to effectively find and analyze them for promotion of an interdisciplinary study. In order to solve this problem, the Inter-university Upper atmosphere Global Observation NETwork (IUGONET) project has been initiated in 2009, consisting of five institutes (Tohoku University, National Institute of Polar Research, Nagoya University, Kyoto University, and Kyushu University). In this project, we have added data information (metadata) for various kinds of ground-based observation data in the solar-terrestrial physics and built a practical database (IUGONET Type-A) to share them on the Internet. We have also developed an integrated data analysis tool (IUGONET Data Analysis Software: UDAS) written in an Interactive Data Language (IDL). This analysis tool is a plugin software for Space Physics Environment Data Analysis Software (SPEDAS) to analyze and visualize various kinds of ground-based and satellite observation data. In the IUGONET Type-A, users can easily learn characteristics of observation data through the quick look images/plots and how to use several basic commands to visualize the data. Recently, we developed a UDAS EGG (UDAS Easy Guide to Generate your load routines) to provide users with the templates for IDL procedures that can load their own data in CSV and CDF format into SPEDAS/IDL. In order to enhance an international use of these IUGONET products and to promote an interdisciplinary study of coupling processes on the sun-earth system, we have held tutorial seminars and workshops several times in Japan and foreign countries (India, Indonesia, Nigeria, Malaysia etc.). As a result, many scientific papers [e.g., Dao et al., 2017; Batubara et al., 2018; Koushik et al., 2018] and Master/Doctor theses become published by preparing an analysis environment, and the IUGONET products effectively works as an international platform. This fact suggests that the IUGONET project is in the position enough to serve the subjects of a large research project: Study of coupling processes in the solar-terrestrial system (Master Plan 2014/2017, Load Map 2014) through a collaboration with other ground-based and satellite observation plans and international programs as already planned by Master Plan 2014/2017. Judging from the above situations, the IUGONET project has a potential possibility to extend human development and strong international cooperation to a whole equatorial region (South America, Africa) in addition to India and Indonesia in future. Therefore, it can be concluded that the IUGONET activity effectively promotes the equatorial and polar atmospheric observations, international collaboration and data science (data assimilation), which are three main subjects of Master Plan (2014/2017).

©2019. Japan Geoscience Union. All Right Reserved.

Reference:

Batubara. M, et al., Long-term distribution of meteors in a solar cycle period observed by VHF meteor radars at near-equatorial latitudes, J. Geophysical Res., doi:10.1029/2018JA025906, 2018.

Koushik, N., et al., Response of equatorial and low latitude mesosphere lower thermospheric dynamics to the northern hemispheric sudden stratospheric warming events, JAtmos.Solar-Terr. Phys., 169, 66-77, doi:10.1016/j.jastp.2018.01.021, 2018.
Dao, T., et al., Coordinated observations of postmidnight irregularities and thermospheric neutral winds and temperatures at low latitudes, J. Geophys. Res. Space Physics, 122, 7, 7504-7518, doi:10.1002/2017JA024048, 2017.

キーワード：IUGONET、太陽地球系結合研究、国際協力、データベース、解析ツール(SPEDAS/UDAS)、赤道大気
Keywords: IUGONET, Study of coupling process in the solar-terrestrial system, International collaboration, Database, Analysis tool (SPEDAS/UDAS), Equatorial atmosphere

©2019. Japan Geoscience Union. All Right Reserved.

大型研究計画「太陽地球系結合過程の研究基盤形成」推進の議論（１）
Discussion on large-scale research project "Study of coupling processes in solar-terrestrial system" (1)

*山本 衛[1]
*Mamoru Yamamoto[1]

1. 京都大学生存圏研究所
1. Research Institute for Sustainable Humanosphere, Kyoto University

大型研究計画「太陽地球系結合過程の研究基盤形成」は、マスタープラン2014と2017において重点大型研究計画に認められた。現在、マスタープラン2020への継続提案のための準備を進めている。本国際セッションにおいて、研究計画の推進に関する議論を実施するため、議論のための時間を申請する。

©2019. Japan Geoscience Union. All Right Reserved.

[E] 口頭発表 | セッション記号 P (宇宙惑星科学)：P-EM 太陽地球系科学・宇宙電磁気学・宇宙環境

2019年5月30日(木) 10:45 ~ 12:15 | A01 東京ベイ幕張ホール

[P-EM15] 太陽地球系結合過程の研究基盤形成

コンビーナ:山本 衛(京都大学生存圏研究所)、小川 泰信(国立極地研究所)、野澤 悟徳(名古屋大学宇宙地球環境研究所)、吉川 顕正(九州大学大学院理学研究院地球惑星科学部門)、座長:野澤 悟徳

地球には太陽から膨大なエネルギーと物質の流入がある。地球の環境はそれらの入出力のバランスの上に成り立っており、地球大気におけるエネルギーと物質の循環の理解が重要である。本セッションは、日本学術会議マスタープラン2011/2014/2017で継続的に重点大型研究計画とされ、2020年度に向けても提案準備中である研究プロジェクト「太陽地球系結合過程の研究基盤形成」に関する議論を目的として、国際セッションとして提案する。研究プロジェクトに関連する設備とネットワークとしては、赤道大気の全域を観測する赤道MUレーダーと極域の磁気圏－電離圏結合過程の詳細な観測を主とするEISCAT_3Dレーダー、赤道から極域までをグローバルにつなぐ地上観測網と観測データ網が含まれている。本セッションでは、研究プロジェクトの内容と進捗状況を報告すると共に、国内外の関連研究者から幅広い話題を集約することで、研究の動向と方向性について議論を深める。大型大気レーダー、非干渉散乱レーダー、観測ネットワーク、衛星観測、モデル研究等を用いた多様な研究やプロジェクトとの連携が重要であり、多くの論文の参加を求める。

10:45 ~ 11:15

[PEM15-07] Numerical Experiments on Stratosphere-Troposphere Two-Way Dynamical Coupling in the Tropics through Organizations of Moist Convective Systems

★Invited Papers

*余田 成男[1]、Hai Bui[2]、畔野 貴弘[1] (1.京都大学大学院理学研究科地球惑星科学専攻、2.Geophysical Institute, University of Bergen)

11:15 ~ 11:30

[PEM15-08] 赤道プラズマバブル数値シミュレーションの発展と今後

*横山 竜宏[1] (1.京都大学)

11:30 ~ 11:45

[PEM15-09] Characteristics of CME- and CIR-driven ion upflows in the polar ionosphere

*小川 泰信[1]、関 華奈子[2]、桂華 邦裕[2]、海老原 祐輔[3] (1.国立極地研究所、2.東京大学理学研究科、3.京都大学生存圏研究所)

11:45 ~ 12:00

[PEM15-10] SuperDARN Hokkaido Pair of (HOP) radars and mid-latitude SuperDARN: today and future

*西谷 望[1] (1.名古屋大学宇宙地球環境研究所)

12:00 ~ 12:15

[PEM15-11] 南極昭和基地大型大気レーダー（39.6°E, 69.0°S）による適応的信号処理を用いた電離圏非干渉性散乱と沿磁力線不均一の同時観測

*橋本 大志[1]、齊藤 昭則[2]、西村 耕司[3]、堤 雅基[3]、佐藤 薫[4]、佐藤 亨[1] (1.京都大学大学院情報学研究科、2.京都大学大学院理学研究科、3.国立極地研究所、4.東京大学大学院理学研究科)

Numerical Experiments on Stratosphere-Troposphere Two-Way Dynamical Coupling in the Tropics through Organizations of Moist Convective Systems

*余田 成男[1]、Hai Bui[2]、畔野 貴弘[1]
*Shigeo Yoden[1], Hai Bui[2], Takahiro Banno[1]

1. 京都大学大学院理学研究科地球惑星科学専攻、2. Geophysical Institute, University of Bergen
1. Division of Earth and Planetary Sciences, Graduate School of Science, Kyoto University, 2. Geophysical Institute, University of Bergen

Recently, we started a new international research activity on Stratospheric And Tropospheric Influences on Tropical Convective Systems (SATIO-TCS) under WCRP/SPARC. It focuses on stratosphere-troposphere (S-T) two-way dynamical coupling in the tropics, where moist convection and its large-scale organization in the troposphere could be influenced by the stratospheric variations, such as stratospheric sudden warming events, the equatorial quasi-biennial oscillation (QBO), or anthropogenic cooling trend in the lower stratosphere, as revealed by some observational studies. For example, Nishimoto and Yoden (2017) made a statistical analysis on the influence of QBO on the Madden-Julian oscillation (MJO) during boreal winter in neutral ENSO periods from 1979 to 2013, and showed that the composite OLR anomaly for a particular MJO phase over the Maritime Continent has a larger negative value and slower eastward propagation with a prolonged period of active convection in the easterly phase of QBO than in the westerly phase.

The tropical dynamics is largely different from the counterpart in the extratropics where dry quasi-geostrophic dynamics prevail. Multi-scale dynamics of moist convection and its organizations are likely to play a vital role in determining the tropospheric response to the stratospheric variations, but numerical model studies from such viewpoint are still limited. Thus, we had performed a series of numerical experiments on radiative-moist convective quasi-equilibrium states in a highly-idealized two-dimensional regional model of an S-T coupled system with explicit moist convection under a periodic lateral boundary condition without Coriolis effects, in which self-sustained oscillations dynamically analogous to the QBO were obtained (Yoden et al. 2014). Modulation of moist convective systems is associated with the QBO-like oscillation of the mean zonal wind, as alternative appearance of squall-line- or back-building-type precipitation patterns, and vertical momentum transports associated with slant-wise moist convection and convectively generated gravity waves are periodically modulated in the oscillation (Nishimoto et al. 2016). Downward influence of the QBO-like oscillation on organized moist convective systems was further investigated in a series of experiments that control the vertical shear of the mean zonal wind with a nudging term (Bui et al. 2017).

Recently, we have performed numerical experiments in a three-dimensional minimal model framework that produces a QBO-like oscillation in a radiative-moist convective quasi-equilibrium state. The computational domain is rectangular (640 km x 160 km, 5 km grid size; Bui et al., 2019), or square (100 km x 100 km, 1 km grid size), without Coriolis effects under doubly periodic boundary conditions. In these experiments, an oscillation with a period of about 300 days emerges in the stratosphere, both in the domain-averaged zonal wind and meridional wind. Synchronization of the zonal and meridional winds is characterized as an anti-clockwise rotation of a skewed spiral feature with height in the horizontal wind hodograph. The QBO-like wind oscillation penetrates into the troposphere with large reduction of

©2019. Japan Geoscience Union. All Right Reserved.

oscillation amplitude, and influences tropospheric temperature anomalies and precipitation with an irregular period of about 100 days. Heavy precipitation is associated with positive temperature anomalies. The simulation reveals three types of precipitation patterns; fast-moving back-building- and squall-line-type patterns, and isolated quasi-stationary type clusters, which is newly identified in this three-dimensional model. The zonal-height cross sections of the meridionally averaged clouds and relative humidity for this pattern show clear-sky areas with low humidity without shallow clouds, whereas shallow clouds exist over the entire domain including non-precipitating areas with high humidity for the fast-moving two patterns. Intermittent self-organization of convective systems into quasi-stationary type and transition back to the fast-moving back-building- or squall-line-type patterns are fundamental characteristics of self-aggregation in the three-dimensional model.

References

Bui, H.-H., E. Nishimoto, and S. Yoden, 2017: *J. Atmos. Sci.*, 74, 3635–3655.

Bui H., S. Yoden, and E. Nishimoto, 2019: *SOLA*, **15**, 59–62.

Nishimoto, E., and S. Yoden, 2017: *J. Atmos. Sci.*, **74**, 1105–1125.

Nishimoto, E., S. Yoden, and H.-H. Bui, 2016: *J. Atmos. Sci.*, **73**, 2935–2957.

Yoden, S., H.-H. Bui, and E. Nishimoto, 2014: *SOLA*, **10**, 112–116.

キーワード：成層圏-対流圏力学結合、湿潤対流システム、熱帯気象学
Keywords: Stratosphere-Troposphere Dynamical Coupling, Moist Convective Systems, Tropical Meteorology

©2019. Japan Geoscience Union. All Right Reserved.

赤道プラズマバブル数値シミュレーションの発展と今後
Future development of numerical simualtion of equatorial plasma bubbles

*横山 竜宏[1]
*Tatsuhiro Yokoyama[1]

1. 京都大学
1. Kyoto University

Equatorial plasma bubbles (EPBs) have been a longstanding and increasingly important subject because they cause severe scintillations in radio waves from Global Navigation Satellite System satellites. The phenomenon was found in the 1930s as irregular ionosonde observations and was termed equatorial spread F (ESF). ESF is interpreted as plasma density irregularities associated with EPBs that have nonlinearly evolved into the topside ionosphere. Since late 1970s, numerical simulations have been powerful tools to study the fully nonlinear evolution of EPBs, which cannot be wholly understood from theoretical predictions. The most recent model, High-Resolution Bubble (HIRB) model, could reproduce very turbulent structures inside EPBs such as bufurcation, zonal asymmetry, and two-component power law spectral characteristics. Future directions toward scintillation evaluation and forecasting are discussed.

キーワード：赤道プラズマバブル、シミュレーション、電離圏
Keywords: equatorial plasma bubble, simulation, ionosphere

©2019. Japan Geoscience Union. All Right Reserved.

Characteristics of CME- and CIR-driven ion upflows in the polar ionosphere

*小川 泰信[1]、関 華奈子[2]、桂華 邦裕[2]、海老原 祐輔[3]
*Yasunobu Ogawa[1], Kanako Seki[2], Kunihiro Keika[2], Yusuke Ebihara[3]

1. 国立極地研究所、2. 東京大学理学研究科、3. 京都大学生存圏研究所
1. National Institute of Polar Research, 2. School of Science, the University of Tokyo, 3. Research Institute for Sustainable Humanosphere, Kyoto University

We investigated how velocity and flux of ionospheric ion upflows vary during magnetic storms driven by corotating interaction regions (CIRs) and coronal mass ejections (CMEs), using data from the European Incoherent Scatter (EISCAT) Tromsø UHF and Svalbard radars between 1996 and 2015. The characteristics of ion upflows were compared with ion and electron temperature variations measured with the EISCAT radars, and also joule heating rate, electric field, and field-aligned current (FAC) distribution derived from the Weimer model. Upward ion velocity increases in the nighttime at Tromsø (66.2 ° N geomagnetic latitude) just after the CIR- and CME-driven storms, corresponding to electron temperature enhancements due to soft particle precipitation and also ion temperature enhancements in the strong westward electric field region. The CME-driven storms have larger upward ion flux (~1.7×10^{13} $m^{-2}s^{-1}$) than those under the CIR-driven storms (~0.3×10^{13} $m^{-2}s^{-1}$). In the daytime, ion upflows are seen at Longyearbyen, Svalbard (75.2 ° N geomagnetic latitude), with an upward flux of typically 10^{13} $m^{-2}s^{-1}$ for small CIR and CME storm cases. Substantial ion upflows last for a few days after the storm onsets under small CIR storms, whereas they last for only a day under small CME storms. Under both the cases, the substantial ion upflows are associated with an enhancement of the Region 1 FAC, eastward electric field and Joule heating rate. For large CME storms, substantial ion upflows are absent in the daytime probably due to equatorward expansion of the auroral oval.

キーワード：極域電離圏、磁気圏電離圏結合、EISCAT
Keywords: polar ionosphere, M-I coupling, EISCAT

©2019. Japan Geoscience Union. All Right Reserved.

SuperDARN Hokkaido Pair of (HOP) radars and mid-latitude SuperDARN: today and future

*西谷 望[1]
*Nozomu Nishitani[1]

1. 名古屋大学宇宙地球環境研究所
1. Institute for Space-Earth Environmental Research, Nagoya University

The Super Dural Auroral Radar Network (SuperDARN) is a network of HF radars. At present there are total of 36 SuperDARN radars located in high- to mid-latitude regions of both northern (23) and southern (13) hemispheres. Mid-latitude SuperDARN radars started operation about 15 years ago and have been acquiring scientific data, which could be obtained using the pre-existing high-latitude radars. The SuperDARN Hokkaido Pair of (HOP) radars consisting of Hokkaido East / West radars are located equatorward of 40 degrees geomagnetic latitude (currently located at the lowest geomagnetic latitude) and have been storing important scientific data during quiet to very active periods. In this presentation accomplishments, present status and future directions of the SuperDARN HOP radars and mid-latitude SuperDARN be reviewed.

キーワード：中緯度SuperDARN
Keywords: mid-latitude SuperDARN

©2019. Japan Geoscience Union. All Right Reserved.

南極昭和基地大型大気レーダー（39.6°E, 69.0°S）による適応的信号処理を用いた電離圏非干渉性散乱と沿磁力線不均一の同時観測
Simultaneous observation of Ionospheric Incoherent Scatter and Field Aligned Irregularities using adaptive signal processing techniques by the PANSY radar at Antarctic Syowa Station (39.6°E, 69.0°S)

*橋本 大志[1]、齊藤 昭則[2]、西村 耕司[3]、堤 雅基[3]、佐藤 薫[4]、佐藤 亨[1]
*Taishi Hashimoto[1], Akinori Saito[2], Koji Nishimura[3], Masaki Tsutsumi[3], Kaoru Sato[4], Toru Sato[1]

1. 京都大学大学院情報学研究科、2. 京都大学大学院理学研究科、3. 国立極地研究所、4. 東京大学大学院理学研究科
1. Graduate School of Informatics, Kyoto University, 2. Graduate School of Science, Kyoto University, 3. National Institute of Polar Research, 4. Graduate School of Science, The University of Tokyo

PANSYレーダーは南極昭和基地に設置された大型のVHF帯大気レーダーである。本レーダーは対流圏・成層圏・中間圏の観測を行うMSTレーダーとしての機能に加え、電離圏非干渉性散乱（IS）を用いて地表100㎞から500㎞にかけてのプラズマ物理量を観測することが可能であり、2015年に南極では初となる電離圏IS観測に成功した。

PANSYレーダーの電離圏観測が既存のより高い周波数を用いるISレーダーとは異なる点として、E層の沿磁力線不均一（FAI）エコーによる干渉が挙げられる。すなわち極域でVHF帯を用いる場合、地磁気の磁力線と電波の進行方向が直交条件を満たす高度は地表100㎞付近となるが、レーダーからの直線距離はF層においてISエコーが観測される高度と等しくなるため、強くコヒーレントなFAIエコーによる干渉が発生する。

このFAIエコーの混入によるPANSYレーダーのIS観測への影響に対処するため、我々は適応的ビーム形成技術を用いた信号処理法を開発した[1]。PANSYレーダーには三素子八木アンテナを12本ずつ直線状に配置したアレイアンテナが2組あり、方向拘束付き出力電力最小化法に基づく手法を用いて異なる角度からの信号を分離できる。すなわち、提案手法により背景の電子密度を精度良く観測できるだけでなく、FAIの構造や運動を同時に観測することが可能となる。

この発表では、PANSYレーダーの電離圏観測における信号処理法について概観する。また、ISとFAIの同時観測について、適応的信号処理によるFAIのイメージングなどを含む最新の成果を報告する。

[1] Hashimoto et al., 2018: “First incoherent scatter measurements and adaptive suppression of field-aligned irregularities by the PANSY radar at Syowa Station, Antarctic”, *J. Atmos. Oceanic Technol.*, conditional acceptance.

キーワード：PANSY、電離圏非干渉性散乱、適当的信号処理、沿磁力線不均一、南極昭和基地、ISレーダー
Keywords: PANSY, ionospheric incoherent scatter, adaptive signal processing, field aligned irregularities, Antarctic Syowa Station, IS radar

©2019. Japan Geoscience Union. All Right Reserved.

[E] 口頭発表 | セッション記号 P (宇宙惑星科学)：P-EM 太陽地球系科学・宇宙電磁気学・宇宙環境

2019年5月30日(木) 13:45 ~ 15:15 | A01 東京ベイ幕張ホール

[P-EM15] 太陽地球系結合過程の研究基盤形成

コンビーナ:山本 衛(京都大学生存圏研究所)、小川 泰信(国立極地研究所)、野澤 悟徳(名古屋大学宇宙地球環境研究所)、吉川 顕正(九州大学大学院理学研究院地球惑星科学部門)、座長:小川 泰信

地球には太陽から膨大なエネルギーと物質の流入がある。地球の環境はそれらの入出力のバランスの上に成り立っており、地球大気におけるエネルギーと物質の循環の理解が重要である。本セッションは、日本学術会議マスタープラン2011/2014/2017で継続的に重点大型研究計画とされ、2020年度に向けても提案準備中である研究プロジェクト「太陽地球系結合過程の研究基盤形成」に関する議論を目的として、国際セッションとして提案する。研究プロジェクトに関連する設備とネットワークとしては、赤道大気の全域を観測する赤道MUレーダーと極域の磁気圏ー電離圏結合過程の詳細な観測を主とするEISCAT_3Dレーダー、赤道から極域までをグローバルにつなぐ地上観測網と観測データ網が含まれている。本セッションでは、研究プロジェクトの内容と進捗状況を報告すると共に、国内外の関連研究者から幅広い話題を集約することで、研究の動向と方向性について議論を深める。大型大気レーダー、非干渉散乱レーダー、観測ネットワーク、衛星観測、モデル研究等を用いた多様な研究やプロジェクトとの連携が重要であり、多くの論文の参加を求める。

13:45 ~ 14:00

[PEM15-12] Mini/Micro Satellite Constelaltion for the study of LAI coupling

*小山 孝一郎[1,2,3] (1.国立成功プラズマ宇宙科学研究所　台湾、2.九州大学国際宇宙天気・教育センター、3.(株）アジア宇宙環境研究コンソーシアム)

14:00 ~ 14:15

[PEM15-13] Statistical study of daily and seasonal variation of the equatorial anomaly in Asia based on satellite-ground beacon experiment

*坂本 悠記[1]、山本 衛[1]、穂積 コンニャナット[2] (1.京都大学生存圏研究所、2.国立研究開発法人 情報通信研究機構)

14:15 ~ 14:30

[PEM15-14] Latest installation of FM-CW radar in Peru

*藤本 晶子[1]、池田 昭大[2]、吉川 顕正[3] (1.九州工業大学、2.鹿児島工業高等専門学校、3.九州大学)

14:30 ~ 14:45

[PEM15-15] Understanding the OH Meinel Band Emissions on the Terrestrial Planets

*Konstantinos S. Kalogerakis[1] (1.Center for Geospace Studies, SRI International, Menlo Park, California, U.S.A.)

14:45 ~ 15:00

[PEM15-16] Statistical study of Sporadic Sodium Layer (SSL) observed at Tromsø

*野澤 悟徳[1]、津田 卓雄[2]、斎藤 徳人[3]、高橋 透[4]、川原 琢也[5]、小川 泰信[4]、藤原 均[6]、和田 智之[3]、小川 洋平[1]、Hall Chris[7]、Brekke Asgeir[7] (1.名古屋大学宇宙地球環境研究所、2.電気通信大学情報理工学部、3.理化学研究所光量子工学研究センター、4.国立極地研究所、5.信州大学工学部、6.成蹊大学理工学部、7.UiTノルウェー北極大学)

15:00 ~ 15:15

[PEM15-17] 大型研究計画「太陽地球系結合過程の研究基盤形成」推進の議論（２）

*山本 衛[1] (1.京都大学生存圏研究所)

Mini/Micro Satellite Constelaltion for the study of LAI coupling

*小山 孝一郎[1,2,3]
*Koichiro Oyama[1,2,3]

1. 国立成功プラズマ宇宙科学研究所 台湾、2. 九州大学国際宇宙天気・教育センター、3. (株）アジア宇宙環境研究コンソーシアム
1. Institute of Plasma and Space Sciences,National Cheng Kung Univ., Taiwan, 2. International Ceneter for Space Weather Sudy and Education, Kyushu Univ.,, 3. CoLtd. Asia Space Environment Research Consortium, Japan

Recent Studies show that ionosphere influenced by Thunder cloud, Typhoon, Sudden Stratosphere warming, Earth quake, and so on. Possible atmosphere perturbation to generate Radio wave scintillation is still not confirmed by observation in spite of the long history of radio scintillation research. Since 1970’s, no break through is found in ionosphere physics. The reason is the lack of information of the atmosphere below which is needed simultaneously with ionopshere information. We propose here the satellite constellation of /Pico /mini satellites combined with one /two small satellite (200-500 Kg). Pico/mini satellite should be constellation to measure basic ionosphere parameter. These are electron density, temperature, ion temperature, ion mass, electric field, and neutral wind at ionosphere height. Information on the atmospheric wind down to ground surface below 120 km should be simultaneously measured. This means that we need photometric instruments such as TIDI and SABAR accommodated in TIMED satellite or instruments to measure electromagnetic waves radiated by neutral particles. These observations can be done through international collaboration.

References

Oyama, K.-I., J. T. Jhou, J. T. Lin, M. L. Hsu , C. Lin ,Y. S. Wu, H. Liu, and K.Yumoto, Behavior of the northern ionosphere during 2009 Sudden Stratosphere Warming, J.Geophys.Res., doi:10.1002/2014JA020014, 2014

Chou, M. Y., C. C. H. Lin, J. Yue, H. F. Tsai, Y. Y. Sun, J. Y. Liu, and C. H. Chen (2017), Concentric traveling ionosphere disturbances triggered by Super Typhoon Meranti (2016), Geophys. Res. Lett., 44, 1219–1226, doi:10.1002/2016GL072205.

Oyama, K. -I., Y.Kakinami, ,J.Y.Liu, T.Kodama, and C.Y.Chen, Micro/mini satellites for earthquake studies - toward international collaboration, Advances in Geoscience, 21, 251- 256, 2010.

Oyama, K.-I., Y. Kakinami, J. Y. Liu, M. A. Abdu, and C. Z. Cheng, Anomalous Ion Density Latitudinal Distribution as a precursor of large earthquake, J.Geophys. Res., 116, A04319, doi:10.1029/2010JA015948, 2011

キーワード：EAI結合、衛星観測、国際協力
Keywords: EAI coupling, Satellite Obserbation, International Collaboartion

©2019. Japan Geoscience Union. All Right Reserved.

Statistical study of daily and seasonal variation of the equatorial anomaly in Asia based on satellite-ground beacon experiment

*坂本 悠記[1]、山本 衛[1]、穂積 コンニャナット[2]
*Yuki Sakamoto[1], Mamoru Yamamoto[1], Kornyanat Hozumi[2]

1. 京都大学生存圏研究所、2. 国立研究開発法人 情報通信研究機構
1. Research Institute for Sustainable Humanosphere, Kyoto University, 2. National Institute of Information and Communications Technology

Studies of ionospheric structures by the satellite-ground beacon experiment were conducted in southeast Asia. We have deployed a meridional chain of five beacon receivers from 8S to 27N along 100E meridian, they showed meridional distribution of total-electron content (TEC) of the ionosphere. We revealed time and spatial variabilities of the equatorial anomaly in a certain period of time (Watthanasangmechai et al., 2014, 2015). The data analysis was, however, not easy mainly because of difficulty in estimating bias of the measurement to get the absolute TEC.
In this study, we developed the method of bias estimation. As a result, we can get TEC distribution by computers automatically. Using this method, we analyzed latitude distribution of TEC from Thai to Indonesia in 2012-2015. It is valuable to measure such latitudinal distribution of TEC in the wide latitudinal range from the ground fixed sites.
Using these data, we classified TEC distribution with the equatorial anomaly. It shows some distribution patterns depends on season or time. Classifying the TEC distribution data of LT14-17 and LT20-23, assuming after the formation of the equatorial anomaly (EIA), we take the average in 2012-2015. The plasma fountain makes the 2 peaks (northern and southern of the magnetic equator) in the TEC-Lat graph. In the northern hemisphere summer, the northern peak is larger than the southern one. In winter, the southern peak is larger than the northern one. Classifying the data of LT10-13, assuming the right after formation of the EIA. It shows the opposite result. In summer, the southern one is larger. In winter, the northern one is larger. We will compare these analysis results with atmospheric parameters from the whole atmosphere model GAIA and MSIS.

キーワード：全電子数、赤道異常
Keywords: total-electron content, equatorial anomaly

©2019. Japan Geoscience Union. All Right Reserved.

Latest installation of FM-CW radar in Peru

*藤本 晶子[1]、池田 昭大[2]、吉川 顕正[3]
*Akiko Fujimoto[1], Akihiro Ikeda[2], Akimasa Yoshikawa[3]

1. 九州工業大学、2. 鹿児島工業高等専門学校、3. 九州大学
1. Kyushu Institute of Technology, 2. National Institute of Technology,Kagoshima College, 3. Kyushu University

An FM-CW (Frequency Modulated Continuous Wave) radar is a type of HF (High Frequency) radar. The FM-CW radar can measure the range of target as well as Doppler shift for reflected radio waves from the target (e.g., ionized layer). From the observed Doppler shift, we can estimate east-west electric field in the ionosphere. Poole (1985) and Poole and Evans (1985) first used FM-CW radar for Doppler observation. Nozaki and Kikuchi (1987, 1988) made improvements to the design. We have installed three FM-CW stations along the Japanese longitude, at Japan, Russia and Philippine, in order to measure the electric fields that penetrate the ionosphere (Yumoto, 2006).

Our goals are, (i) to estimate EEJ (Equatorial Electrojet) structure including the generation, variance and modulation of EEJ, (ii) to understand the electrodynamics of EEJ and the generation mechanism of the Equatorial Spread F (ESF) associated with Plasma Bubbles (PBs) and (iii) to reveal the generation mechanisms of ULF pulsation waves at the lower and equatorial latitudes.

In 2018, the new FM-CW radar has been installed in Peru. This FM-CW observation will give the opportunity of the simultaneous ionospheric observation at the Japan local time and the opposite side of Japan (for example dayside and nightside). ICSWSE (International Center for Space Weather Science and Education, Kyushu University) also have the ground-based magnetometer network (MAGDAS) on the world including Peru MAGDAS chain. With the both magnetometer and FM-CW observations, we try to understand the energy transfer and propagation process from the poles to the equator, in the terms of the coupling the solar-magnetosphere-ionosphere-atmosphere.

We will give the detail and current status of FM-CW radar project.

©2019. Japan Geoscience Union. All Right Reserved.

Understanding the OH Meinel Band Emissions on the Terrestrial Planets

*Konstantinos S. Kalogerakis[1]

1. Center for Geospace Studies, SRI International, Menlo Park, California, U.S.A.

The OH Meinel band emissions, originating from vibrationally excited hydroxyl radicals, OH(v), represent some of the most important airglow features in the Earth’ s upper atmosphere. Such emissions were also observed on the night side of Venus during the Venus Express mission [*Piccioni et al.*, A&A 483, L29-L33 (2008)]. Data obtained by CRISM (Compact Reconnaissance Imaging Spectrometer for Mars) aboard the MRO (Mars Reconnaissance Orbiter) revealed OH(v) emissions in the nightglow of Mars [*Clancy et al.*, Icarus 226, 272-281 (2013)]. Modeling studies have shown that the predicted OH(v) emission intensities can vary dramatically depending on the nature of the vibrational relaxation mechanism assumed [e.g., *García Muñoz et al.*, Icarus 176, 75-95 (2005)]. Despite several investigations, the details of all the relevant OH(v) relaxation kinetics and pathways are not well understood.

Our recent studies demonstrated a previously unknown, efficient pathway for vibrational relaxation of OH(v) by O atoms that couples the mesospheric OH(v) emissions with the CO_2 4.3-micron emission and resolves a long-standing problem of severe discrepancies between model predictions and observations of the 4.3-micron emission in the Earth’ s atmosphere [*Panka et al.* , ACP 17, 9751-9760 (2017); *Kalogerakis et al.*, GRL 43, 8835-8843 (2016)]. This recent breakthrough development highlights the importance of investigating the mechanistic details of OH(v) collisional energy transfer.

We will discuss our efforts to investigate OH(v) vibrational relaxation relevant to the atmospheres of the terrestrial planets. Important areas of interest are the key OH(v) vibrational relaxation rate constants at temperatures relevant to the altitude of the emission layer and the pathways of OH(v) vibrational energy relaxation. The Meinel OH(v) emissions can be used as an indicator of atmospheric composition, variability, circulation, gravity waves, and as a probe of local temperature. A detailed understanding of the sources and sinks of these emissions is a prerequisite before they can be reliably used as a proxy for the aforementioned processes.

Keywords: OH Meinel band emission, Nightglow, vibrational relaxation, Terrestrial planets

©2019. Japan Geoscience Union. All Right Reserved.

Statistical study of Sporadic Sodium Layer (SSL) observed at Tromsø

*野澤 悟徳[1]、津田 卓雄[2]、斎藤 徳人[3]、高橋 透[4]、川原 琢也[5]、小川 泰信[4]、藤原 均[6]、和田 智之[3]、小川 洋平[1]、Hall Chris[7]、Brekke Asgeir[7]
*Satonori Nozawa[1], Takuo T. Tsuda[2], Norihito Saito[3], Toru Takahashi[4], Takuya Kawahara[5], Yasunobu Ogawa[4], Hitoshi Fujiwara[6], Satoshi Wada[3], Youhei Ogawa[1], Chris Hall[7], Asgeir Brekke[7]

1. 名古屋大学宇宙地球環境研究所、2. 電気通信大学情報理工学部、3. 理化学研究所光量子工学研究センター、4. 国立極地研究所、5. 信州大学工学部、6. 成蹊大学理工学部、7. UiTノルウェー北極大学
1. Institute for Space-Earth Environment Research, 2. The University of Electro-Communications, 3. RIKEN Center for Advanced Photonics, 4. National Institute of Polar Research, 5. Faculty of Engineering, Shinshu University, 6. Faculty of Science and Technology, Seikei University, 7. UiT The Arctic University of Norway

Based on about 3000 hours of sodium density data obtained with the Tromsø sodium LIDAR over 7 year seasons between 2012 and 2018, we have identified about 40 events of Sporadic Sodium Layer (SSL) in the polar mesosphere and lower thermosphere (MLT) region. A SSL is a thin sodium layer (about 1-2 km) with high sodium density (usually factor of 2 or more higher than that of a normal layer), and its life time is about a few minutes to a few hours. We have investigated an occurrence rate of sporadic sodium layer (SSL) as well as necessary conditions for a SSL to form in the polar MLT region. SSLs appeared for shorter than 5 % of the overall observational time, indicating it is a rare event. Auroral electron precipitation as well as appearance of a sporadic E layer would be necessary conditions to form a SSL.

The sodium LIDAR at Tromsø (69.6 deg N, 19.2 deg E) has made simultaneous five directional (vertical position, plus 4 horizontal positions with zenith angle = 30 deg or 12.5 deg and azimuth = 0, 90, 180, 270 deg) observations, and has obtained about 3000 hours of temperature, sodium density, and wind data between October 2012 and February 2019. Analyzing the datasets with temporal and height resolutions of 3 min and 500 m, respectively, we have identified about 40 SSL events over the seven winter seasons. By utilizing five point observations, we have determined if a SSL was in-situ generated or was advected. Most SSLs show feature of advection (systematic and similar temporal variations of sodium density), indicating associated sharp rise of sodium density, whose mechanism has long been not understood, can be explained with an advection effect.

Observational results can be summarized as follows:
(1) most SSLs found are probably advected, (2) ionization of aurora would be a necessary condition, (3) sporadic E (Es) layers are almost always associated, (4) local time dependence of appearance of SSL is found, suggesting convectional electric field and semidiurnal tide would play an important role. We will address a generation mechanism of SSL.

キーワード：ナトリウム層、トロムソ、スポラディックナトリウム層、スポラディックE層、ナトリウムライダー
Keywords: Sodium layer, Tromso, SSL, Es layer, Sodium LIDAR

©2019. Japan Geoscience Union. All Right Reserved.

大型研究計画「太陽地球系結合過程の研究基盤形成」推進の議論（２）
Discussion on large-scale research project "Study of coupling processes in solar-terrestrial system" (2)

*山本 衛[1]
*Mamoru Yamamoto[1]

1. 京都大学生存圏研究所
1. Research Institute for Sustainable Humanosphere, Kyoto University

大型研究計画「太陽地球系結合過程の研究基盤形成」は、マスタープラン2014と2017において重点大型研究計画に認められた。現在、マスタープラン2020への継続提案のための準備を進めている。本国際セッションにおいて、研究計画の推進に関する議論を実施するため、議論のための時間を申請する。

©2019. Japan Geoscience Union. All Right Reserved.

[E] 口頭発表 | セッション記号 A (大気水圏科学)：A-AS 大気科学・気象学・大気環境

2019年5月30日(木) 9:00 ~ 10:30 | 104 1F

[A-AS02] 台風研究の新展開～過去・現在・未来

コンビーナ:金田 幸恵(名古屋大学宇宙地球環境研究所)、和田 章義(気象研究所台風・災害気象研究部)、伊藤 耕介(琉球大学)、宮本 佳明(慶應義塾大学　環境情報学部)、座長:金田 幸恵(名古屋大学)、和田 章義(気象研究所)

台風は、大雨・暴風・高潮・高波により沿岸各地に甚大な被害を与えることから社会的関心の高い自然現象である。2018年は平成30年7月豪雨（前線及び台風第７号による大雨等）を皮切りに西日本を西進した台風第12号、８月の発生数の多さ（９個、観測史上三位）に加えて、９月には台風第21号及び台風第24号が強い勢力を保ったまま西日本を縦断し、日本各地に大きな爪痕を残した。また北大西洋ではハリケーンFlorenceが北米に上陸し、猛威を振るった。近年海面水温の上昇とともに、急発達する台風の増加傾向や、熱帯低気圧の最大強度到達緯度の北上傾向が報告されている。過去から現在、そして未来と地球温暖化が進む中で台風を理解し、その予測の高度化を実現することは、地球惑星科学上の重要な課題である。
台風をターゲットとした衛星観測・航空機観測、数値モデルを用いた大規模アンサンブル実験、最先端衛星観測や機械学習といった新しい手法の導入など、過去・現在・未来を通じた幅広い台風研究が国内外で展開されている。本セッションでは、台風をはじめとする熱帯低気圧に関わる幅広い話題に関する発表を募集し、今後の台風研究の方向性を探る。

9:00 ~ 9:15

[AAS02-01] A GRAPES-based mesoscale EPS for TC forecasting: configuration and performance

*Xubin Zhang[1] (1.Institute of Tropical and Marine Meteorology, CMA)

9:15 ~ 9:30

[AAS02-02] **Evaluation of operational Ensemble based Global Forecast System prediction for Tropical Cyclones over the North Indian Ocean**

*Medha Deshpande[1]、Radhika Kanase[1]、R P M Krishna[1]、Emmanuel Rongmie[1]、P Mukhopadhyay[1] (1.IITM, Pune, INDIA)

9:30 ~ 9:45

[AAS02-03] 270メンバーのアンサンブル実験から得られた急発達開始前の熱帯低気圧の構造変化

*宮本 佳明[1]、David Nolan[2] (1.慶應義塾大学　環境情報学部、2.Rosenstiel School of Marine and Atmospheric Science, University of Miami)

9:45 ~ 10:00

[AAS02-04] Potential impacts of tropical cyclone inner-core convective activity on the predictability of rapid intensification

*南出 将志[1]、Derek Posselt[1] (1.Jet Propulsion Laboratory, California Institute of Technology)

10:00 ~ 10:15

[AAS02-05] A link between high-speed solar wind streams and rapid intensification of tropical cyclones

*Paul Prikryl[1,2]、Lidia Nikitina[2]、Vojto Rušin[3] (1.Physics Department, University of New Brunswick, Fredericton, NB, Canada、2.Geomagnetic Laboratory, Natural Resources Canada, Ottawa, ON, Canada、3.Astronomical Institute, Slovak Academy of Sciences, Tatranská Lomnica, Slovak Republic)

10:15 ~ 10:30

[AAS02-06] Influence of Tropical Lower Stratospheric Cooling on Extreme Deep Convective Activity and Tropical Cyclones

*Kodera Kunihiko[1]、江口 菜穂[2]、Ueyama Rei[3]、Funatsu Beatriz[4]、Claud Chantal[5] (1.Meteorological Research Institute、2.Kyushu University、3.NASA Ames Research Center、4.Université de Nantes、5.Ecole Polytechnique)

A GRAPES-based mesoscale EPS for TC forecasting: configuration and performance

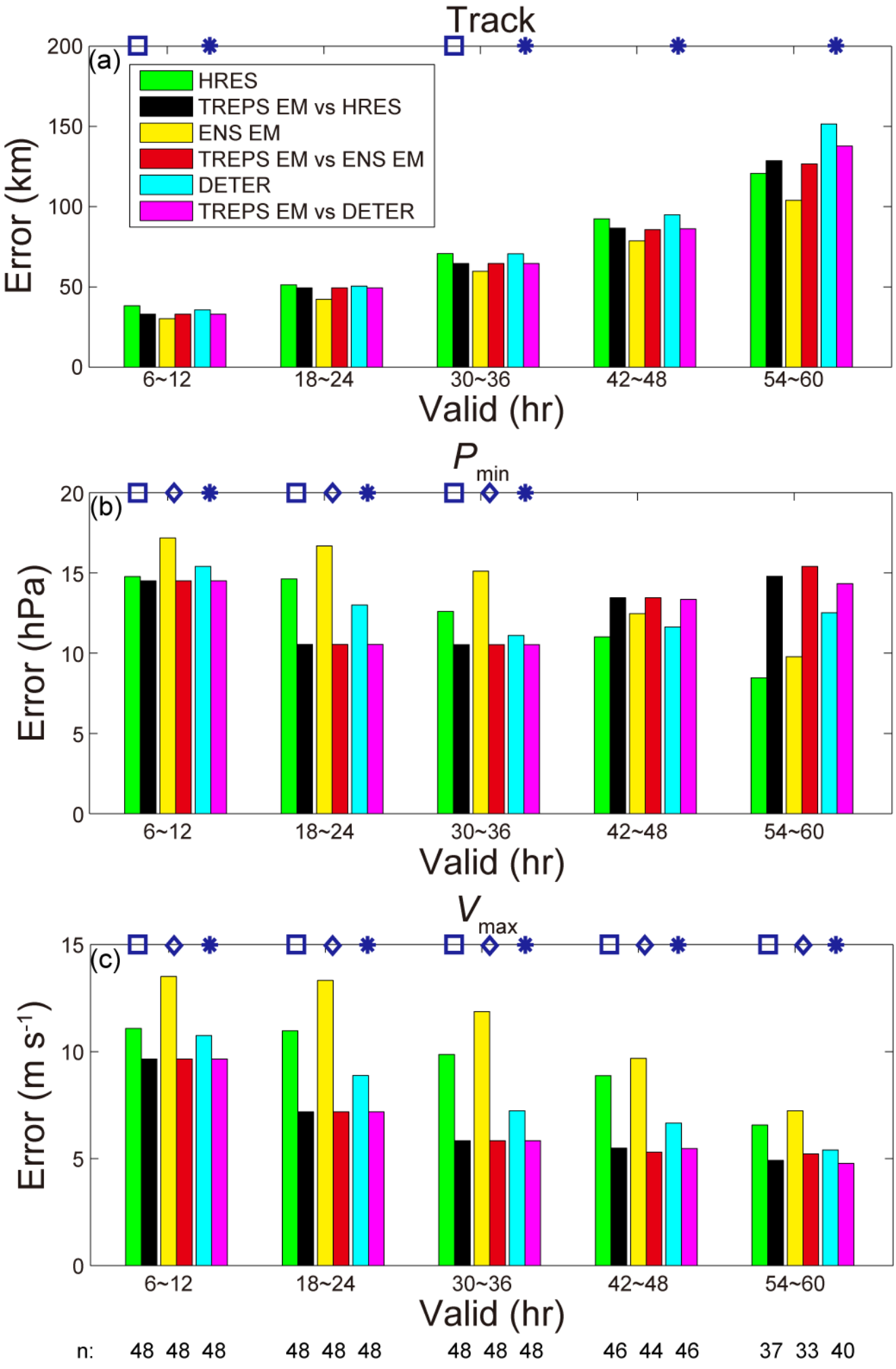
*Xubin Zhang[1]

1. Institute of Tropical and Marine Meteorology, CMA

To improve short-range tropical cyclone (TC) forecasting in China from both deterministic and probabilistic standpoints, a mesoscale ensemble prediction system (TREPS) based on the Global/Regional Assimilation and Prediction System (GRAPES) is constructed as a planned operational system. TREPS comprises one unperturbed and 30 perturbed forecasts ranging up to 60 h at horizontal resolution of 9 km. Downscaling perturbations from the ECMWF ensemble prediction system (ENS) are used to generate initial perturbations by blending them with balanced random perturbations implemented around the TC and to generate perturbations for lateral boundary conditions. The surface temperature around the TC is also perturbed, with a combination of multi-physics and stochastically perturbed parametrization tendencies considered to represent uncertainties in the model physics. These perturbation methods contribute a full-area, multi-scale and multi-variable mutual complement to increasing forecast perturbations. TREPS is evaluated for 19 TCs making landfall in China during 2014–2016. For deterministic guidance, TREPS significantly improves TC forecasting for intensity, rainfall and wind compared to ECMWF deterministic and ensemble forecasts. TREPS demonstrates significant advantages over its deterministic forecasts in predicting track, intensity, (extremely) heavy rainfall and wind. Furthermore, TREPS effectively reduces the degree of underdispersion in intensity forecasting compared to ENS. For probabilistic forecasting, TREPS outperforms ENS in accurately predicting extremely heavy rainfall and (extremely) strong wind owing to its better discriminating ability, but performs worse in predicting modest wind, light and heavy rainfall. Two post-processing techniques –optimal member and optimal probability –to improve, respectively, deterministic and probabilistic guidance of TREPS in rainfall and wind forecasting are proposed. The former is shown to be effective only for light rainfall, while the latter demonstrates consistent (partial) improvements in rainfall (wind). The superiorities and inferiorities of TREPS, as well as possible reasons for these, are intuitively illustrated in a case-study for Rammasun.

Keywords: ensemble prediction system, mesoscale, tropical cyclone

©2019. Japan Geoscience Union. All Right Reserved.



©2019. Japan Geoscience Union. All Right Reserved.

©2019. Japan Geoscience Union. All Right Reserved.

Evaluation of operational Ensemble based Global Forecast System prediction for Tropical Cyclones over the North Indian Ocean

*Medha Deshpande[1], Radhika Kanase[1], R P M Krishna[1], Emmanuel Rongmie[1], P Mukhopadhyay[1]

1. IITM, Pune, INDIA

The importance of accurate prediction of Tropical Cyclone (TC) genesis, rapid intensity changes, location and intensity during landfall is well known. Reliable prediction of these at 3-5 days lead time is crucial for disaster managing point of view. Bearing in mind the uncertainty in initial condition and model physics there was a need for high resolution ensemble based forecast system for region specific probabilistic prediction of weather over India. Considering this along with the existing Global Forecast System deterministic model (GFS T1534), the ensemble forecast system GEFS (T 1534) with 20 members is implemented and is in operation since June 2018 for the probabilistic prediction.

This paper evaluates the skill of operational high resolution (12.5 km) modelling system in predicting track and intensity of recent cases of TCs over North Indian Ocean at various lead time. Ensemble prediction of tracks of cyclones and its strike probability are evaluated. Ensemble mean track is better than the deterministic track particularly at longer lead time (figure 1). The vertical thermo-dynamic structure at the mature stage of the cyclone is well captured by the deterministic model. Evaluation of deterministic model (figure 2) specify average track error is ranging from < 100 km at Day 1 lead up to about 280 km at day 5 lead time and average error in intensity prediction is ranging from 10 kt –20 kts. In general model indicates early intensification and slightly overestimates the peak intensity in majority of the cases. It is challenging to predict the variation in the intensity. Skill in the prediction of genesis is also evaluated by calculating Genesis Potential Index (GPI). Further developments like improving the physics and dynamics of the model along with use of proper land use land cover data are underway.

Keywords: Tropical Cyclones, North Indian Ocean, High Resolution ensemble Prediction System

©2019. Japan Geoscience Union. All Right Reserved.

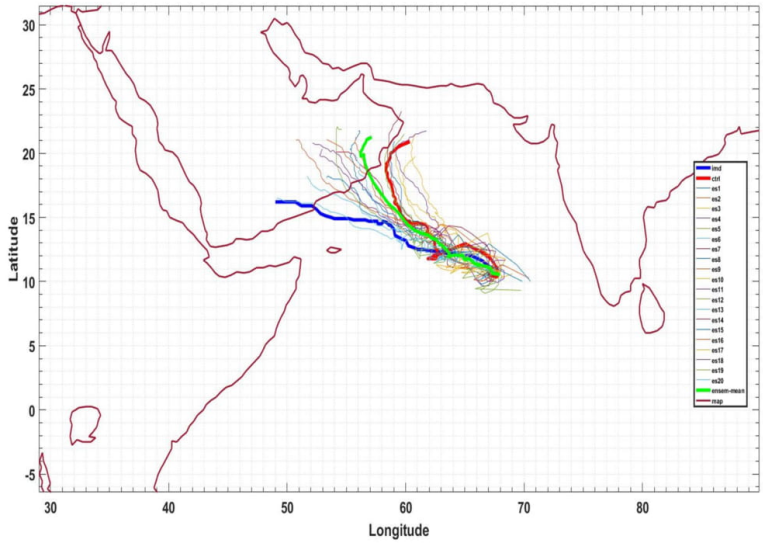


Figure1: Ensemble prediction of tracks based on 6 Oct Initial Condition for the case of Luban (6-14 Oct 2018)

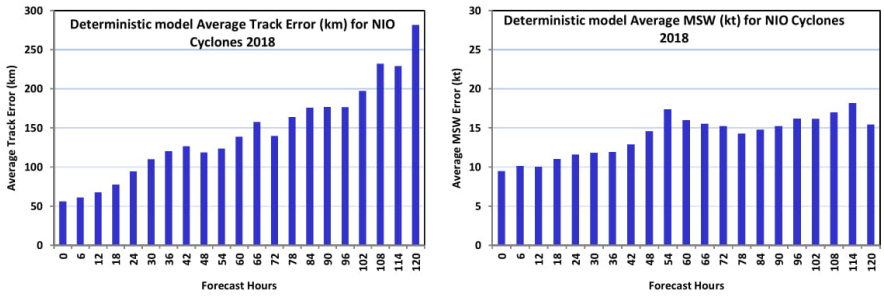


Figure 2: Deterministic model (GFS (T1534) average Track and intensity error for NIO cyclones 2018

©2019. Japan Geoscience Union. All Right Reserved.

270メンバーのアンサンブル実験から得られた急発達開始前の熱帯低気圧の構造変化

Structural Changes Preceding Rapid Intensification in Tropical Cyclones as shown in a Large Ensemble of Idealized Simulations

*宮本 佳明[1]、David Nolan[2]
*Yoshiaki Miyamoto[1], David S Nolan[2]

1. 慶應義塾大学　環境情報学部、2. Rosenstiel School of Marine and Atmospheric Science, University of Miami
1. Faculty of Environment and Information Studies, Keio University, 2. Rosenstiel School of Marine and Atmospheric Science, University of Miami

強い強度まで達する熱帯低気圧（Tropical Cyclone: TC）の多くが、その生涯に一度、急速に発達する過程（Rapid Intensification: RI）を経験している。防災上も重要となり、また、急激な強度変化の予測が難しいことから、近年盛んに研究されている。RIの研究には様々なものがあるが、RIそのもののメカニズムがまだ分かっていないことに加えて、一度RIが開始すると一気に強い強度まで達するため、RIが開始するメカニズムも重要なトピックである。

RIの開始メカニズムについて、これまでに観測データや数値シミュレーション結果を用いて研究がなされて来た。例えばMiyamoto and Takemi (2013, 2015) は、理想条件下でのシミュレーション結果から、渦が軸対称化し、最大風速半径より内側で熱的に不安定化する一方、境界層内で水平収束が最大となる半径が外側に移り、十分に最大風速半径に接近した時に眼の壁雲が形成し、RIが始まるというメカニズムを提案した。しかし彼らは鉛直シアーが無い時のみを調べており、より現実的な状況下での考察が必要となる。他の研究でも個々のTCのシミュレーションを行って結果を調べているのがほとんどで、一方で観測データを用いると時空間的に連続なデータを得ることが難しいため統計的に調べる研究がほとんどであり、普遍的なメカニズムは未だ不明である。

そこで本研究では、様々な環境下で発達するTCのRI開始前のメカニズムを明らかにするため、RIに重要と考えられるパラメータを変えた270アンサンブルのシミュレーションを実行した。その結果、RIを経験する・しないTCの頻度や、強度変化がこれまでの観測研究と整合的であった。また、鉛直シアーがあるときは、多くのTCがRI開始前に対流による上層の渦度強化で、直立した渦構造を作っていたことが分かった。その後に、Miyamoto and Takemiで提案したRI開始メカニズムによってRIが始まっていることが示された。

キーワード：熱帯低気圧、急発達
Keywords: Tropical Cyclone, Rapid Intensification

©2019. Japan Geoscience Union. All Right Reserved.

Potential impacts of tropical cyclone inner-core convective activity on the predictability of rapid intensification

*南出 将志[1]、Derek Posselt[1]
*Masashi Minamide[1], Derek J. Posselt[1]

1. Jet Propulsion Laboratory, California Institute of Technology
1. Jet Propulsion Laboratory, california institute of technology

Predictions of significant changes in tropical cyclone (TC) intensity, such as rapid intensification (RI), have emerged as a more challenging topic than forecasting TC tracks, since intensification of TCs involves multi-scale physical processes with significant contributions from convective-scale phenomena. Before the onset of RI, intensifying TCs are known to experience a precession process, in which tilted vortex rotates counter-clockwise to develop axisymmetric structure. From both modeling and observational studies, there is an agreement in the qualitative features of precession process among TCs, but the quantitative features, such as the vortex tilt magnitude, the duration of the precession process and whether or not the vortex is able to complete the precession process, vary among TCs. The predictability of the variety of precession process and subsequent RI is reported to be ultimately dominated by the chaotic nature of moist convection. Given the large influence of RI on the TC intensity forecasts, the further understandings in its uncertainty sources are necessary.

In this study, mechanisms that determine the variability of these precession processes are explored through sets of sensitivity and ensemble forecast experiments. We have used the Pennsylvania State University’s experimental real-time ensemble Kalman filter analysis of Hurricane Harvey (2017) that assimilated GOES-16 all-sky satellite radiances (which has an equivalent monitoring capability to Himawari-8) in convection-permitting Weather Research and Forecasting model (WRF-ARW) simulations. This analysis resulted in a highly accurate forecast of intensity and track, and realistically represented the storm’s rapid intensification. Starting with an analysis based on 18 hours of cycling data assimilation, we have conducted sensitivity experiments in which we reduced the initial atmospheric moisture amount by 5 to 20 %. Even initialized with the same wind field, and with fully developed convective updrafts and organization, the vortex tilt magnitude and the duration of precession are significantly modified by the inner-core moist processes. We explore the characteristics of the vortex structures that underwent short/long/uncompleted precession process, together with the theoretical background for these varieties of precession process by using a simplified toy-model. The results have implications for the design of future observation networks tasked with providing constraint on predictions of convections and rapidly intensifying tropical cyclones.

キーワード：台風、数値予報、全天輝度温度同化、対流
Keywords: tropical cyclones, numerical weather prediction, all-sky satellite radiance, convection

©2019. Japan Geoscience Union. All Right Reserved.

A link between high-speed solar wind streams and rapid intensification of tropical cyclones

*Paul Prikryl[1,2], Lidia Nikitina[2], Vojto Rušin[3]

1. Physics Department, University of New Brunswick, Fredericton, NB, Canada, 2. Geomagnetic Laboratory, Natural Resources Canada, Ottawa, ON, Canada, 3. Astronomical Institute, Slovak Academy of Sciences, Tatranská Lomnica, Slovak Republic

Physical processes responsible for changes of tropical cyclone intensity are not well understood [1]. To improve the current understanding of tropical cyclone structure and intensity changes the future research needs to focus on response to all external forcing [2]. We examined rapid intensification of tropical storms in the context of solar wind coupling to the magnetosphere-ionosphere-atmosphere system. Tropical cyclone “best tracks” in the southern and northern hemispheres are used in the superposed epoch analysis of time series of solar wind parameters. The results indicate that rapid intensification of tropical storms tends to follow arrivals of high-speed solar wind from coronal holes and coronal mass ejections [3]. The ensuing auroral and polar cap activity including ionospheric currents and ionospheric convection generates atmospheric gravity waves that propagate from the high-latitude lower thermosphere both upward and downward [4,5,6]. If ducted in the lower atmosphere, they can reach tropical troposphere. Despite significantly reduced wave amplitude, but subject to amplification upon reflection in the upper troposphere, these gravity waves can trigger/release moist instabilities to initiate convective bursts, with the latent heat release leading to intensification of storms [7]. Convective bursts have been linked to rapid intensification of tropical cyclones. Tropical cyclone intensifications are preceded by atmospheric gravity waves generated by the solar wind magnetosphere-ionosphere-atmosphere coupling process. The gravity waves are observed in the ionosphere as traveling ionospheric disturbances. Their propagation in the lower atmosphere is examined by ray tracing in a model atmosphere to show that they can reach tropical cyclones. It is suggested that the interaction of aurorally-generated gravity waves with the tropical cyclone vortex and the inner primary eyewall could play a role in the intensification process. Assuming that quasi-periodic convective bursts lead to vortex waves, a two-dimensional barotropic approximation [8] is used to obtain asymptotic solutions representing propagation of vortex waves. The absorption of vortex waves by the mean flow in the critical layer leads to formation of the secondary eyewall and ultimately to a process of eyewall replacement cycle, one of the well-established paradigms of intensity changes in tropical cyclones [9].

[1] Kaplan J., et al., Wea. Forecasting, 25, 220–241, 2010. https://doi.org/10.1175/2009WAF2222280.1
[2] Wang Y., Wu C.-C., Meteor. Atmos. Phys., 87, 257–278, 2004.
[3] Prikryl P., et al., J. Atmos. Sol.-Terr. Phys., 183, 36-60, 2019. https://doi.org/10.1016/j.jastp.2018.12.009.
[4] Mayr H.G., et al., J. Geophys. Res., 89, 10929–10959, 1984.
[5] Mayr H.G., et al., Space Sci. Rev. 54, 297–375, 1990.
[6] Prikryl P., et al., Ann. Geophys., 23, 401–417, 2005. doi:10.5194/angeo-23-401-2005
[7] Prikryl P., et al., Ann. Geophys. 27, 31–57, 2009. https://doi.org/10.5194/angeo-27-31-2009.
[8] Nikitina L.V., Campbell L.J., Stud. Appl. Math., 135, 377–446, 2015.
[9] Willoughby H.E., et al., J. Atmos. Sci., 39, 395–411, 1982.

Keywords: Solar wind-magnetosphere-ionosphere-atmosphere coupling, High-speed solar wind stream, Atmospheric gravity wave, Extratropical and tropical cyclones

©2019. Japan Geoscience Union. All Right Reserved.

©2019. Japan Geoscience Union. All Right Reserved.

Influence of Tropical Lower Stratospheric Cooling on Extreme Deep Convective Activity and Tropical Cyclones

*Kodera Kunihiko[1]、江口 菜穂[2]、Ueyama Rei[3]、Funatsu Beatriz[4]、Claud Chantal[5]
*Kunihiko Kodera[1], Nawo Eguchi[2], Rei Ueyama[3], Beatriz M Funatsu[4], Chantal Claud[5]

1. Meteorological Research Institute、2. Kyushu University、3. NASA Ames Research Center、4. Université de Nantes、5. Ecole Polytechnique
1. Meteorological Research Institute, 2. Kyushu University, 3. NASA Ames Research Center, 4. Université de Nantes, 5. Ecole Polytechnique

In previous studies we showed that stratospheric sudden warming (SSW) event can induce rapid cooling in the tropical stratosphere and impact on the tropical convective activity. Case studies on two large SSWs in January 2009 and January 2010, showed that convective activity increased along ascending branch of the Hadley circulation in the austral summer hemisphere. It is also found that frequency of the convective overshooting clouds, and the tropical cyclones (TCs) increased following the tropical stratospheric cooling. Detailed analysis on the relationship between the tropical stratospheric cooling and tropical cyclones are made for 2010 January case. In January 2010, TCs have been generated one after another over Indian Ocean, Maritime continent, and Pacific sectors following a eastward propagation of convective active center associated with the Madden-Julian Oscillation (MJO) until rapid cooling started in the tropical stratosphere in late January. Then, after that, MJO became stationary over the central Pacific and TCs developed or re-developed simultaneously over 3 different sectors: Southwest Indian Ocean, Australia, and central Pacific. TC does not form over the lands, however, extreme deep convective activity simultaneously enhanced with the TCs over African and South American continents. It is suggested that a decrease of static stability in the tropical tropopause layer (TTL) due to a cooling in the lower stratosphere, produced favorable condition for the development of extreme deep convection. The increase of extreme deep convection around 15˚ S latitudinal zone following the tropical stratospheric cooling can be characterized as a strengthening of deep ascending branch of the Hadley circulation connected to the Brewer-Dobson circulation.

キーワード：tropical cyclone、stratosphere、deep convection
Keywords: tropical cyclone, stratosphere, deep convection

©2019. Japan Geoscience Union. All Right Reserved.

[E] 口頭発表 | セッション記号 A (大気水圏科学)：A-AS 大気科学・気象学・大気環境

2019年5月30日(木) 10:45 ~ 12:15 | 104 1F

[A-AS02] 台風研究の新展開〜過去・現在・未来

コンビーナ:金田 幸恵(名古屋大学宇宙地球環境研究所)、和田 章義(気象研究所台風・災害気象研究部)、伊藤 耕介(琉球大学)、宮本 佳明(慶應義塾大学　環境情報学部)、座長:宮本 佳明、伊藤 耕介(琉球大学)

台風は、大雨・暴風・高潮・高波により沿岸各地に甚大な被害を与えることから社会的関心の高い自然現象である。2018年は平成30年7月豪雨（前線及び台風第７号による大雨等）を皮切りに西日本を西進した台風第12号、８月の発生数の多さ（９個、観測史上三位）に加えて、９月には台風第21号及び台風第24号が強い勢力を保ったまま西日本を縦断し、日本各地に大きな爪痕を残した。また北大西洋ではハリケーンFlorenceが北米に上陸し、猛威を振るった。近年海面水温の上昇とともに、急発達する台風の増加傾向や、熱帯低気圧の最大強度到達緯度の北上傾向が報告されている。過去から現在、そして未来と地球温暖化が進む中で台風を理解し、その予測の高度化を実現することは、地球惑星科学上の重要な課題である。
台風をターゲットとした衛星観測・航空機観測、数値モデルを用いた大規模アンサンブル実験、最先端衛星観測や機械学習といった新しい手法の導入など、過去・現在・未来を通じた幅広い台風研究が国内外で展開されている。本セッションでは、台風をはじめとする熱帯低気圧に関わる幅広い話題に関する発表を募集し、今後の台風研究の方向性を探る。

10:45 ~ 11:15

[AAS02-07] A change in the inner-core structure of Typhoon Trami (2018) as observed through upper-tropospheric aircraft reconnaissance of T-PARCII

★Invited Papers

*山田 広幸[1]、坪木 和久[2]、篠田 太郎[2]、久保田 尚之[3]、高橋 幸弘[3]、長浜 則夫[4]、清水 健作[4]、大東 忠保[5]、伊藤 耕介[1]、山口 宗彦[6]、中澤 哲夫[6] (1.琉球大学、2.名古屋大学、3.北海道大学、4.明星電気、5.防災科学技術研究所、6.気象庁気象研究所)

11:15 ~ 11:30

[AAS02-08] 台風第21号の上陸に伴う内部構造の劇的変化及びメソ渦と突風の関係

*嶋田 宇大[1]、小山 亮[1]、清水 慎吾[2] (1.気象庁気象研究所、2.防災科学技術研究所)

11:30 ~ 11:45

[AAS02-09] Revisiting Asymmetric CAPE in Sheared Tropical Cyclones

*Qingqing Li[1] (1.NUIST Nanjing University of Information Science and Technology)

11:45 ~ 12:00

[AAS02-10] Observed rainfall asymmetry of tropical cyclone in the process of making landfall in Guangdong, South China

*Guanhuan Wen[1] (1.Guangzhou Institute of Tropical and Marine Meteorology, China Meteorological Administation)

12:00 ~ 12:15

[AAS02-11] Volumetric Detection of Tornadic Vortices Associated with Typhoon Nanmadol (2017) Using PAWR and Deep Learning

*足立 透[1]、石津 尚喜[2]、楠 研一[1]、猪上 華子[1]、新井 健一郎[2]、藤原 忠誠[3]、鈴木 博人[3] (1.気象研究所、2.アルファ電子/気象研究所、3.東日本旅客鉄道)

A change in the inner-core structure of Typhoon Trami (2018) as observed through upper-tropospheric aircraft reconnaissance of T-PARCII

*山田 広幸[1]、坪木 和久[2]、篠田 太郎[2]、久保田 尚之[3]、高橋 幸弘[3]、長浜 則夫[4]、清水 健作[4]、大東 忠保[5]、伊藤 耕介[1]、山口 宗彦[6]、中澤 哲夫[6]
*Hiroyuki Yamada[1], Kazuhisa Tsuboki[2], Taro Shinoda[2], Hisayuki Kubota[3], Yukihiro Takahashi[3], Norio Nagahama[4], Kensaku Shimizu[4], Tadayasu Ohigashi[5], Kosuke Ito[1], Munehiko Yamaguchi[6], Tetsuo Nakazawa[6]

1. 琉球大学、2. 名古屋大学、3. 北海道大学、4. 明星電気、5. 防災科学技術研究所、6. 気象庁気象研究所
1. University of the Ryukyus, 2. Nagoya University, 3. Hokkaido University, 4. Meisei Electric, 5. National Research Institute for Earth Science and Disaster Resilience, 6. Meteorological Research Institute, Japan Meteorological Agency

Upper-tropospheric aircraft reconnaissance with dropsonde deployment using a Gulfstream-II aircraft was carried out for the inner core of Typhoon Trami on four successive days since 25 September 2018. According to the JMA best track, the central pressure reached its minimum value of 915 hPa on the first day and was subsequently maintained at 950 hPa for three days. Using dropsonde data, this study examined the change in the inner-core structure associated with the intensity change. Based on satellite imagery, this intensity change was associated with the rapid expansion of the eye (with radius increasing from 35 to 90 km) and the gradual increase in the eyewall cloud-top height. A composite analysis of dropsonde profiles in the radius-height domain on each day revealed a change in the flow structure, with the decrease (increase) in the tangential wind component near the radius of 40 km (120 km). This caused an increase in the radial gradient of angular momentum, corresponding to an increase in inertial stability. These results suggest that this typhoon underwent the structural change similar to eyewall replacement cycle while the central pressure was maintained.

Acknowledgements: This work was supported by JSPS KAKENHI Grant Numbers JP16H06311, JP16H04053, JP18H03805, and the Science and Technology Research Partnership for Sustainable Development (SATREPS) Understanding Lightning and Thunderstorm (ULAT) project.

キーワード：航空機観測、台風、北西太平洋
Keywords: aircraft reconnaissance, tropical cyclone, western North Pacific

©2019. Japan Geoscience Union. All Right Reserved.

台風第21号の上陸に伴う内部構造の劇的変化及びメソ渦と突風の関係
Dramatic changes in the inner-core structure of Typhoon Jebi (2018) at landfall and relationship between a mesovortex and strong wind gusts

*嶋田 宇大[1]、小山 亮[1]、清水 慎吾[2]
*Udai Shimada[1], Ryo OYAMA[1], shingo shimizu[2]

1. 気象庁気象研究所、2. 防災科学技術研究所
1. Meteorological Research Institute, 2. National Research Institute for Earth Science and Disaster Prevention

Landfalling tropical cyclones experience dramatic structural changes due to increased friction, topography, reduced surface heat fluxes, and reduced moisture supply. Typhoon Jebi (2018) made landfall in Shikoku Island on September 4, 2018, and then it caused record-breaking gust wind speeds greater than 40 m s^{-1} and heavy rainfall greater than 50 mm h^{-1} along its track. Dramatic changes in the inner-core structure of Jebi at landfall and the relationship between heavy rainfall and strong wind gusts, and structural features were examined by using observations. The azimuthal-mean structure of Jebi after landfall shows that while the tangential wind at 1-km altitude decreased from 45 m s^{-1} to 30 m s^{-1}, the structure became more compact, with the radius of maximum wind (RMW) at ~50 km and radar reflectivity increasing inside the RMW at altitudes from 1 to 5 km. Because of increasing forward speed and active convection inside the RMW, maximum wind speed below 6-km altitude did not decrease significantly even after landfall. Inside the RMW, a mesovortex with a scale of 50 km formed in the downshear-left quadrant. The formation of the mesovortex was likely attributed to dynamically forced updraft associated with the storm vortex tilted by vertical wind shear and attributed to tilting of horizontal vorticity associated with the convergence of enhanced frictional inflow. The mesovortex contributed to the strong wind gusts and heavy rainfall. Also, the fast forward speed of more than 15 m s^{-1} increased wind gusts on the right-hand side of Jebi’ s track.

キーワード：上陸台風、レーダー解析、メソ渦
Keywords: landfalling tropical cyclones, radar analysis, mesovortices

©2019. Japan Geoscience Union. All Right Reserved.

Revisiting Asymmetric CAPE in Sheared Tropical Cyclones

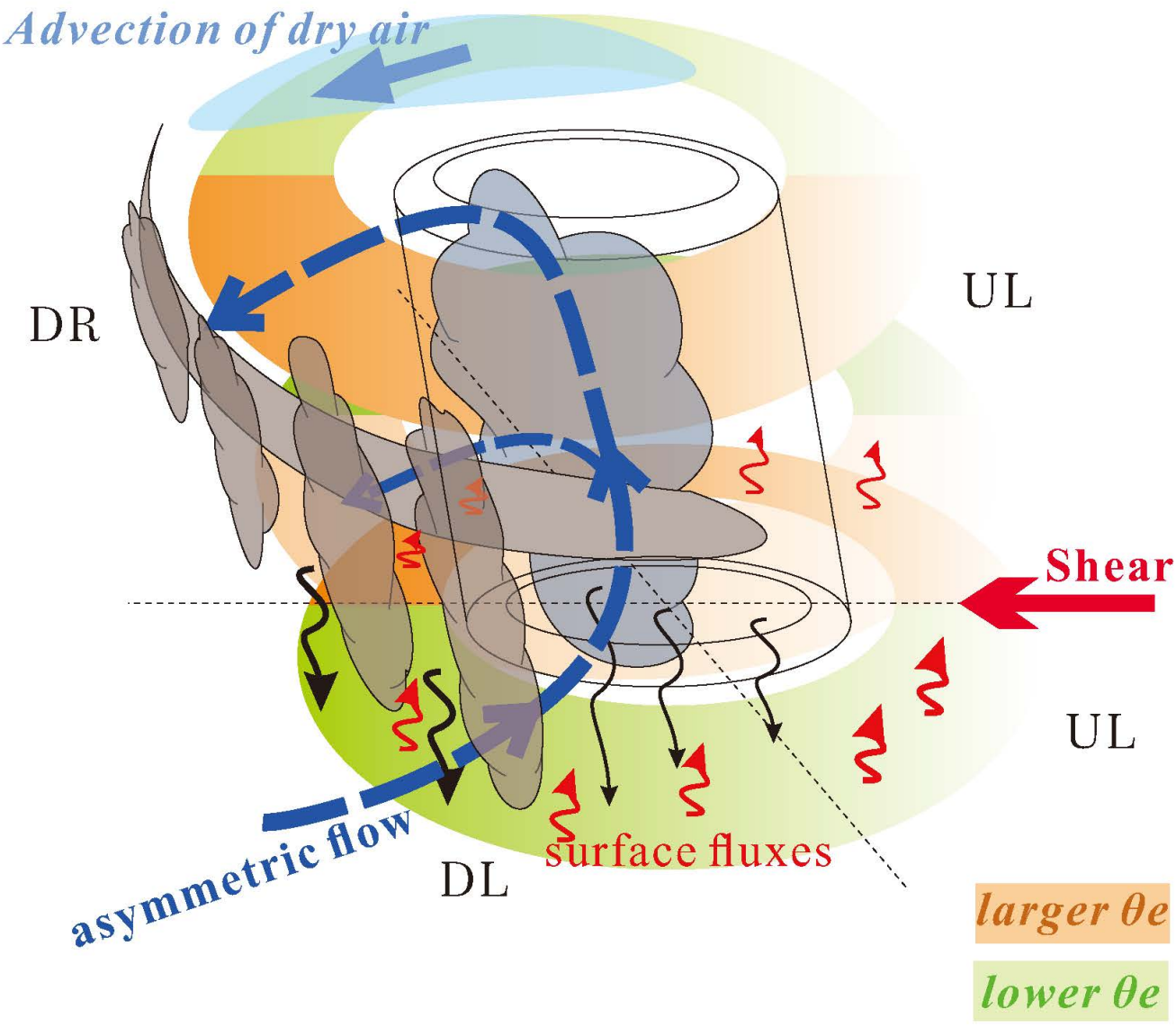
*Qingqing Li[1]

1. NUIST Nanjing University of Information Science and Technology

This study numerically revisits the characteristics and physical processes of azimuthally asymmetric convective available potential energy (CAPE) in the outer cores of vertically sheared tropical cyclones (TCs), which has been observed previously. The results indicate that a downshear-upshear contrast in CAPE occurs in weakly sheared TCs as pointed out in prior studies, while an enhanced downshear left-downshear right contrast is found in strongly sheared storms. Specifically, less (larger) CAPE values arise downshear left (right) under large shear environments. Downward transport of low entropy by the convective and mesoscale downdrafts in principal rainbands reduces the equivalent potential temperature (θe) in the downshear-left boundary layer, whereas positive horizontal advection by the asymmetric outflow contributes to the presence of a mid-level maximum of θe in the same quadrant. Resultantly, lower outer-core CAPE is present downshear left. In the downshear-right quadrant, a lack of convective downdrafts together with surface fluxes leads to higher θe in the boundary layer. The intrusion of dry air by ventilation produces lower θe in the upper troposphere on the right of the shear. Larger CAPE values thus arise downshear right. The effects of such azimuthally asymmetric CAPE on TC structure and intensity are also discussed.

Keywords: tropical cyclone, CAPE, shear

©2019. Japan Geoscience Union. All Right Reserved.



©2019. Japan Geoscience Union. All Right Reserved.

Observed rainfall asymmetry of tropical cyclone in the process of making landfall in Guangdong, South China

*Guanhuan Wen[1]

1. Guangzhou Institute of Tropical and Marine Meteorology, China Meteorological Administation

This study investigates the rainfall asymmetry of tropical cyclones (TCs) in the process of making landfall in Guangdong (GD), South China, on the basis of satellite-based and reanalysis precipitation data. We mainly focus on TC rainfall asymmetry, its main influencing factor, and its change in the process of landfall, and the difference between different ENSO phases. The results reveal that vertical wind shear (VWS) is the dominant influencing factor of TC rainfall asymmetry in GD. The rainfall maximum is located in downshear left of VWS. The TC rainfall asymmetry has little change in the process of making landfall, though the rain rate decreases. Both the phase and amplitude of TC rainfall asymmetry have no significant change from 24 hours prior to landfall to 12 hours after landfall. The rainfall maximum steadily lies in downshear left. The amplitude of rainfall asymmetry is about 50%, suggesting that the asymmetric rainfall is about half of the axisymmetric rainfall. There is no obvious difference in TC rainfall asymmetry between El Niño, La Niña, and neutral years.

Keywords: Tropical cyclone, Rainfall asymmetry, TRMM, Vertical wind shear

©2019. Japan Geoscience Union. All Right Reserved.

Volumetric Detection of Tornadic Vortices Associated with Typhoon Nanmadol (2017) Using PAWR and Deep Learning

*足立 透[1]、石津 尚喜[2]、楠 研一[1]、猪上 華子[1]、新井 健一郎[2]、藤原 忠誠[3]、鈴木 博人[3]
*Toru Adachi[1], Naoki Ishitsu[2], Kenichi Kusunoki[1], Hanako Inoue[1], Ken-ichiro Arai[2], Chusei Fujiwara[3], Hiroto Suzuki[3]

1. 気象研究所、2. アルファ電子/気象研究所、3. 東日本旅客鉄道
1. Meteorological Research Institute, 2. Alpha Denshi/Meteorological Research Institute, 3. East Japan Railway Company

Tornadoes spawned by miniature supercells associated with typhoon are one of critical issues for disaster risk reduction in Japan. However, it is not easy to monitor and predict their occurrence because the parent storm is considerably small compared with classic-type tornadic supercell. We try to overcome this problem by combining cutting-edge technologies using rapid-scan phased array weather radar (PAWR) and deep learning analysis. We present a case study of tornado-like vortices which caused damages in Souka city, Saitama, during the approach of Typhoon Nanmadol (2017). We performed data analysis of two rapid-scan phased array weather radars operated by Meteorological Research Institute in Tsukuba and operated by Japan Radio Co., Ltd. in Chiba. To detect vortices from the PAWR-observed Doppler velocity data, we employed a vortex pattern finding scheme using convolutional neural network. Since PAWR carries out quasi-simultaneous observation of multi-elevational angles, we considered a group of vortices located in a radius of 4-km as a single vertically-extending volumetric vortex. By analyzing the spatiotemporal structure, we found a significant growth of a tornadic vortex about five minutes prior to its passage over the ground damage area. This finding suggests that a combination of rapid-scan PAWR observation and deep learning analysis is useful for monitoring and short-term forecasting of tornadoes associated with typhoon.

Acknowledgement: This work is supported by JSPS KAKENHI Grant 17K13007. In this analysis, we used PAWR data operated by Japan Radio Co., Ltd.

キーワード：台風、竜巻、フェーズドアレイ気象レーダー、深層学習
Keywords: Typhoon, Tornado, Phased Array Weather Radar, Deep Learning

©2019. Japan Geoscience Union. All Right Reserved.

[E] 口頭発表 | セッション記号 A (大気水圏科学)：A-AS 大気科学・気象学・大気環境

2019年5月30日(木) 15:30 ~ 17:00 | 104 1F

[A-AS02] 台風研究の新展開～過去・現在・未来

コンビーナ:金田 幸恵(名古屋大学宇宙地球環境研究所)、和田 章義(気象研究所台風・災害気象研究部)、伊藤 耕介(琉球大学)、宮本 佳明(慶應義塾大学　環境情報学部)、座長:金田 幸恵(名古屋大学)、宮本 佳明

台風は、大雨・暴風・高潮・高波により沿岸各地に甚大な被害を与えることから社会的関心の高い自然現象である。2018年は平成30年7月豪雨（前線及び台風第７号による大雨等）を皮切りに西日本を西進した台風第12号、８月の発生数の多さ（９個、観測史上三位）に加えて、９月には台風第21号及び台風第24号が強い勢力を保ったまま西日本を縦断し、日本各地に大きな爪痕を残した。また北大西洋ではハリケーンFlorenceが北米に上陸し、猛威を振るった。近年海面水温の上昇とともに、急発達する台風の増加傾向や、熱帯低気圧の最大強度到達緯度の北上傾向が報告されている。過去から現在、そして未来と地球温暖化が進む中で台風を理解し、その予測の高度化を実現することは、地球惑星科学上の重要な課題である。
台風をターゲットとした衛星観測・航空機観測、数値モデルを用いた大規模アンサンブル実験、最先端衛星観測や機械学習といった新しい手法の導入など、過去・現在・未来を通じた幅広い台風研究が国内外で展開されている。本セッションでは、台風をはじめとする熱帯低気圧に関わる幅広い話題に関する発表を募集し、今後の台風研究の方向性を探る。

15:30 ~ 15:45

[AAS02-12] Evaluation of the monthly Potential of the 2018 typhoon activity and the effect of the positive PMM and SST of the eastern northwestern Pacific

*石山 尊浩[1]、佐藤 正樹[1] (1.東京大学大気海洋研究所)

15:45 ~ 16:00

[AAS02-13] **Contributions of different time scale variations to tropical cyclogenesis over the western North Pacific**

*Xi Cao[1] (1. Institute of Atmospheric Physics, Chinese Academy of Sciences)

16:00 ~ 16:15

[AAS02-14] Binary interaction between TC Chanthu (2016) and a nearby cold low

*伊藤 耕介[1]、比嘉 未雅[1]、Chan Johnny[2] (1.琉球大学、2.City University of Hong Kong)

16:15 ~ 16:30

[AAS02-15] **Response of landfalling North Indian Ocean cyclonic disturbances to warming climate and associated environmental parameters**

*JAGABANDHU PANDA[1]、KASTURI SINGH[1] (1.Department of Earth and Atmospheric Sciences, National Institute of Technology Rourkela, India)

16:30 ~ 16:45

[AAS02-16] **Rainfall contribution of North Indian Ocean cyclonic disturbances over India in a warming climate**

*KASTURI SINGH[1]、JAGABANDHU PANDA[1] (1.Department of Earth and Atmospheric Sciences, National Institute of Technology Rourkela, India)

16:45 ~ 17:00

[AAS02-17] Analysis of typhoon tracks and associated precipitation amount over western Japan: A case study with Typhoon Nancy and Typhoon Jebi

*Sridhara Nayak[1]、Tetsuya Takemi[1] (1.Disaster Prevention Research Institute, Kyoto University)

Evaluation of the monthly Potential of the 2018 typhoon activity and the effect of the positive PMM and SST of the eastern northwestern Pacific

*石山 尊浩[1]、佐藤 正樹[1]
*Takahiro Ishiyama[1], Masaki Satoh[1]

1. 東京大学大気海洋研究所
1. Atmosphere and Ocean Research Institute, The University of Tokyo

Typhoons in the northwest Pacific in 2018 exceeded the average for 29 occurrences, the number of landings to Japan to 5, and for the typhoon which became extreme strength it was updated with the most record and the activity was active. In the ENSO phase, La Niña phenomenon occurred in the beginning of 2018 but converged by early spring and El Niño phenomenon occurred in October. However, during the most active period of the typhoon (from June to November), the ENSO phase was still in a neutral state. Therefore, Pacific Meridional Mode (hereafter PMM) (Chiang and Vimont 2004) is focused recently. At the positive phase of PMM, a zone of warming sea surface temperature (hereafter SST) is formed in the northeast - southwest direction of 20 degrees north latitude, 120 degrees west latitude to 0 degrees north latitude and 180 degrees west longitude. Previous studies have pointed out that this positive PMM favors TC activities in the northwest Pacific (Zhang et al. 2016). Looking at the PMM index (SST) from 1948 to 2018, there was positive PMM in 2018 and the intensity was strong enough to be within 15th place of 71 in each month of active typhoon season. Especially, in August and September, strong positive PMM phenomenon was developed in 4th place and 2nd place.

The purpose of this research is to focus on the monthly SST variation such as ENSO and PMM and to evaluate the Potential of the 2018 typhoon activity. We also focus on the PMM and the SST over the eastern of northwest Pacific, and investigate how they affect the 2018 typhoon activity.

For the above purpose, we conducted perpetual experiments in which boundary conditions were fixed from July to October, respectively, using a nonhydrostatic model NICAM. The horizontal resolution was 56 km, and the number of vertical layers was 38 layers. In sensitivity experiments, PMM region and PMM + eastern northwest Pacific regions of SST in July 2018 sensitivity experiment 1 and sensitivity experiment 2 replaced with climate value were conducted. Comparing the experimental result of sea level pressure (hereafter SLP) with JRA-55, although the position of the maximum value of the high pressure in July is misaligned, the position and overhang of the high pressure does not differ greatly in each month, and perpetual experiments also reproduce the reality well. Both reanalysis and perpetual experiments have more typhoons in July and August than in September and October. Also, the occurrence position of the typhoon occurs more frequently in the eastern side of the northwestern Pacific in order of July, August, September. The same tendency was observed. Such differences in active areas of typhoon activity had an effect on the monsoon trough.
Subsequently, the SLPs of the 2018 experiment, sensitivity experiment 1 and sensitivity experiment 2 were compared. In comparison with the sensitivity experiment 1, the sensitivity experiment 1 became a lower pressure deviation in the west side of the northwest Pacific than 2018 experiment, whereas in the sensitivity experiment 2, the sensitivity experiment 2 had higher SLP in the whole northwest Pacific than 2018 experiment. From this, it was found that the positive SST deviation in the eastern northwest Pacific was more involved in the typhoon activity of 2018.

©2019. Japan Geoscience Union. All Right Reserved.

キーワード：熱帯低気圧、Pacific Meridional Mode、非静力学モデル
Keywords: tropical cyclone, Pacific Meridional Mode, nonhydrostatic model

©2019. Japan Geoscience Union. All Right Reserved.

Contributions of different time scale variations to tropical cyclogenesis over the western North Pacific

*Xi Cao[1]

1. Institute of Atmospheric Physics, Chinese Academy of Sciences

The present study investigates relative contributions of different time scale variations of environmental factors to the tropical cyclone (TC) genesis over the western North Pacific (WNP) during July-August-September-October (JASO). Distinct from previous studies that are concerned with large-scale spatial patterns during a certain period, the present study focuses on local and instantaneous conditions of the TC genesis. Analysis shows that the contribution of convection and lower-level vorticity to the TC genesis is mainly due to intraseasonal and synoptic variations. The contribution of vertical wind shear is largely related to synoptic variations. The contribution of mid-level specific humidity is almost two times more from intraseasonal variations than from synoptic variations. The contribution of sea surface temperature (SST) to the TC genesis is mainly due to interannual and intraseasonal variations. The barotropic energy for synoptic-scale disturbances during the TC genesis comes mainly from climatological mean flows over the southwest quadrant and from intraseasonal wind variations over the northeast quadrant of the WNP, respectively. The contribution of interannual variations to the TC genesis is enhanced over the southeast quadrant of the WNP. More TCs form under weak easterly and westerly vertical shears, respectively, during El Niño developing and decaying JASO. The contribution of interannual variations of SST tends to be larger during the El Niño decaying than developing JASO.

Keywords: tropical cyclone genesis, western North Pacific , different time scales

©2019. Japan Geoscience Union. All Right Reserved.

Binary interaction between TC Chanthu (2016) and a nearby cold low

*伊藤 耕介[1]、比嘉 未雅[1]、Chan Johnny[2]
*Kosuke Ito[1], Miyabi Higa[1], Johnny Chan[2]

1. 琉球大学、2. City University of Hong Kong
1. University of the Ryukyus, 2. City University of Hong Kong

Tropical cyclone (TC) Chanthu (2016) caused the heavy rainfall and strong wind on Hokkaido Prefecture, Japan. However, this was one of the "busted" cases in which the track forecast error reached up to 900 km in a 72-h forecast by the Regional Specialized Meteorological Center (RSMC) Tokyo. In fact, the re-forecast experiment with Japan Meterological Agency Non-Hydrostatic Model (JMA-NHM) that employed Kain-Fritsch scheme as a convective parameterization correctly captured the observed northward translation speed of TC Chanthu, while the JMA Global Spectral Model (JMA-GSM) and JMA-NHM that employed Arakawa-Schubert scheme failed to predict the accurate northward translation speed. The mesoscale analysis showed that there was a cold low located at 200km west of TC Chanthu (2016). With Kain-Frische scheme, the binary interaction between TC Chanthu and the nearby cold low was reproduced so that it contributed the faster translation to the north as consistent with the best track. In contrast, the binary interaction was not reproduced in the simulations with Arakawa-Schubert scheme because a triggered large-scale convection made TC Chanthu and the nearby cold low merged. It exemplifies that the reproduction of fine-scale features diminishes "busted" cases, which contributes to the disaster prevention and mitigation.

キーワード：tropical cyclone、Fujiwhara effect、track forecast
Keywords: tropical cyclone, Fujiwhara effect, track forecast

©2019. Japan Geoscience Union. All Right Reserved.

Response of landfalling North Indian Ocean cyclonic disturbances to warming climate and associated environmental parameters

*JAGABANDHU PANDA[1], KASTURI SINGH[1]

1. Department of Earth and Atmospheric Sciences, National Institute of Technology Rourkela, India

Most of the studies focusing on cyclonic disturbances (CDs) concentrate on their frequency. However, the system that causes destruction to nearby coastal areas is the landfalling one. The impact of warming climate on landfalling CD activity is an interesting topic. Thus, the present study focuses on the landfalling activity of CDs formed over North Indian Ocean (NIO) and associated environmental parameters responsible for the same. The study is divided into two epochs i.e. pre-warming period (PWP) 1891-1946 and current warming period (CWP) 1947-2016 based on the sea surface temperature anomaly variation.

Over NIO, nearly 88 and 84.80% of systems made landfall over coastal areas associated with Bay of Bengal (BOB) basin and the respective percentages are 53.03 and 39% for AS during PWP and CWP respectively. The percentage of landfalling CDs shows a decreasing and stable trend respectively during PWP and CWP for BOB sub-basin. Over AS, the Kendall’ s coefficients are found to be −0.255 and −0.0024 during PWP and CWP respectively. The study reveals that Bangladesh, Andhra Pradesh (AP), and Tamil Nadu (TN) are more vulnerable to severe cyclones formed over BOB during the current warming climate. Whereas, for Arabian Sea (AS) region, Gujrat (GJ) is prone to severe cyclones and Arabian Peninsula countries are vulnerable to cyclonic storms during the current warming climate. For pre-monsoon season, among all NIO coastal states, Bangladesh and Arakan face a greater number of CD landfalls during CWP for BOB systems. Whereas, for post-monsoon season, AP, TN and Bangladesh suffered maximum landfalls. The seasonal landfalling activity of CDs over AS shows that Arabian Peninsula is more vulnerable than GJ in pre-monsoon season during CWP. However, for post-monsoon season, both Arabian Peninsula and GJ are significantly prone to landfalling CDs. During PWP, most of the systems formed over middle sector of BOB recurve in north-eastward direction. Whilst, one climatological track is found to be recurving towards Bangladesh, another one is towards AP during CWP. CDs formed over southern sector of BOB prefers two tracks, one being westward towards TN and the other is in north-east direction towards Bangladesh during CWP. The enhanced genesis over southern and middle sector of BOB is mainly responsible for more landfalls over AP, TN and Bangladesh. The CDs formed over the eastern AS basin recurve to make landfall over GJ or Oman during PWP. However, during CWP, another preferable track towards Yemen is also seen for the systems formed over eastern AS.

The climatological vertically integrated (mass-weighted) tropospheric wind pattern near TN coast has changed direction from westward during PWP to north-westward during CWP (Figure 1), favouring more landfall over AP and TN. Over the central part near the latitude 14˚N, change in the magnitude has occurred with change in the direction of the winds from NW-N to NE. Because of the prevailing wind steering pattern, the systems that formed over the middle and southern BOB do not prefer to make landfall to WB and Odisha during CWP. Over AS, the wind is mostly directed towards GJ irrespective of the period considered, which favours more landfalling of CDs over the place. These winds are primarily part of mid-latitude westerly troughs. For BOB, the SST gradient is in meridional direction and hence most of the systems formed, suffer landfall over Indian coastal states and other rim countries face less landfalls. Over AS, SST gradient is zonally distributed and therefore, the eastward deflection of CDs is more observed, making the Indian state of GJ to be the most affected region. The study is expected to be helpful in the decision-making process in view of socio-economic impacts of landfalling CDs.

©2019. Japan Geoscience Union. All Right Reserved.

Keywords: Cyclonic disturbances, North Indian Ocean, Landfall, Bay of Bengal, Arabian Sea

©2019. Japan Geoscience Union. All Right Reserved.

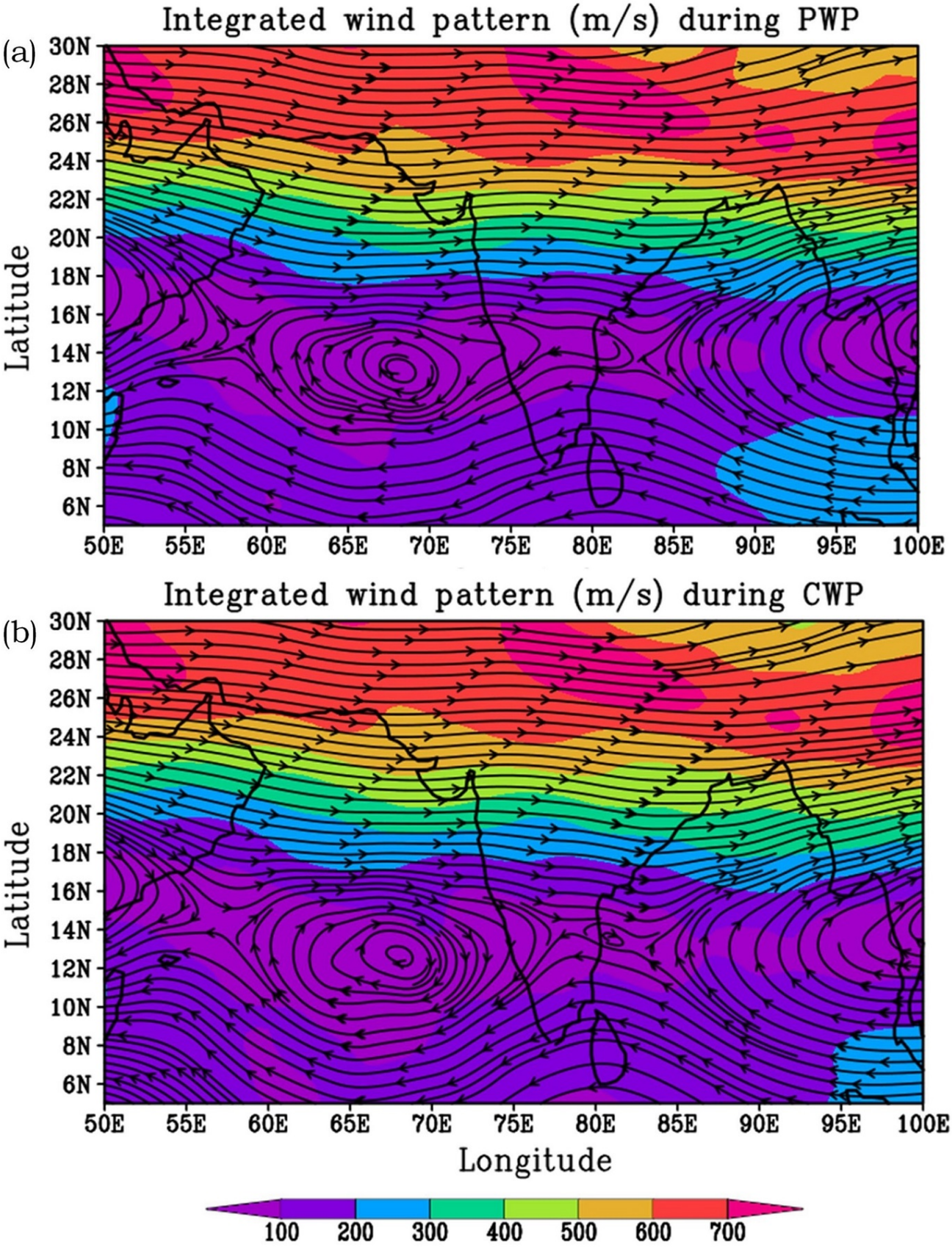


Figure 1: Climatological variation of mass weighted vertically integrated tropospheric wind magnitude (shaded) and wind pattern (vector) in m/s over NIO for the period 1891-2014 during PWP (a) and CWP (b). Here, NOAA-CIRES global re-analyses data set is used.

©2019. Japan Geoscience Union. All Right Reserved.

Rainfall contribution of North Indian Ocean cyclonic disturbances over India in a warming climate

*KASTURI SINGH[1], JAGABANDHU PANDA[1]

1. Department of Earth and Atmospheric Sciences, National Institute of Technology Rourkela, India

Rainfall associated with cyclonic disturbances (CDs) poses mostly significant threat to the society. Such type of systems and their remnants are capable of producing heavy rainfall, which often produce flash flooding. The warming climate is considered from 1947 onwards based on sea surface temperature anomaly variation over North Indian Ocean (NIO) basin. Nearly 71.42% of CDs in pre-monsoon and 87.07% CDs in post-monsoon season crossed or gazed the Indian coast during 140 cyclone seasons of the warming climate. The trend for annual variation of CD rainfall (CDR) anomaly is decreasing along with CD anomaly during pre-monsoon season (P=4.89901E-15). The trend for CDR anomaly is observed to be almost stable while the CD anomaly is decreasing drastically (P=1) in the post-monsoon season, indicating increased amount of rainfall is contributed by CDs over India in this period.

Among eastern coastal states, Andhra Pradesh (AP), Tamil Nadu (TN), Mizoram, Tripura and among western coastal states, Kerala (KL), Karnataka (KA) and Gujarat (GJ) received most of the accumulated rainfall in pre-monsoon season. The rainfall contributed by CDs during pre-monsoon season is limited to the coastal districts of India only. However, the rainfall occurrences during post-monsoon season could penetrate up to very interior districts. During post-monsoon season, Odisha (OD), AP and TN received the highest rainfall contribution from CDs. Jharkhand, KL, KA, parts of Maharashtra (MH) and coastal GJ received significantly higher amount of rainfall in comparison to other interior places. Up to ~70% of rainfall is contributed by CDs over GJ, nearly 20-30% over AP and 15-18% over western Rajasthan during pre-monsoon (Figure 1). During post-monsoon season, considerable rainfall (60% of annual value) contribution is seen over all states. The trend in CD rainfall is observed to be increasing over western GJ, western Rajasthan, northeast AP and southeast OD during pre-monsoon months. The spatio-temporal trend of CD rainfall over Bihar, Jharkhand, northern OD, northern Chhattisgarh, eastern Madhya Pradesh, Sikkim and Meghalaya are observed to be increasing during post-monsoon months. The rainfall contributed by CDs over the border regions of AP and TN is observed to be decreasing. Among eastern coastal states, AP has received 200cm of accumulated rainfall contribution during pre-monsoon season. The corresponding values for TN, OD and WB are 180, 140 and 140cm respectively. During post-monsoon season, AP received 1100cm of rainfall, OD and TN with 900cm of rainfall each, and WB received 450cm of accumulated rainfall contributed by CDs. For western coastal states, during pre-monsoon season, the maximum amount of accumulated rainfall contributions over GJ, MH, KA and KL are about 85, 75, 110 and 160cm respectively. During post-monsoon season, the corresponding values are nearly 134, 145, 320 and 350cm. Comparing the trend for maximum and minimum rainfall received by a coastal state, it can be concluded that even though the maximum values for some years are slightly less in comparison to other years, the minimum contribution is quite significant for those particular years. The possible reason can be due to larger and faster moving storms those result in longer precipitation durations with greater area coverage.

Further, the association of such rainfall contributions with ENSO, MJO and IOD cannot be undermined and thus, analyzed using observations and modeling output. The preliminary results indicate relative dominance of MJO in determining the CDR over Indian region during pre-monsoon months. During IOD –ve, heavy rainfall is contributed by CDs over AP and TN. The explicit discussion regarding the same will

©2019. Japan Geoscience Union. All Right Reserved.

be included in the presentation.

Keywords: cyclonic disturbances, rainfall, North Indian Ocean, India

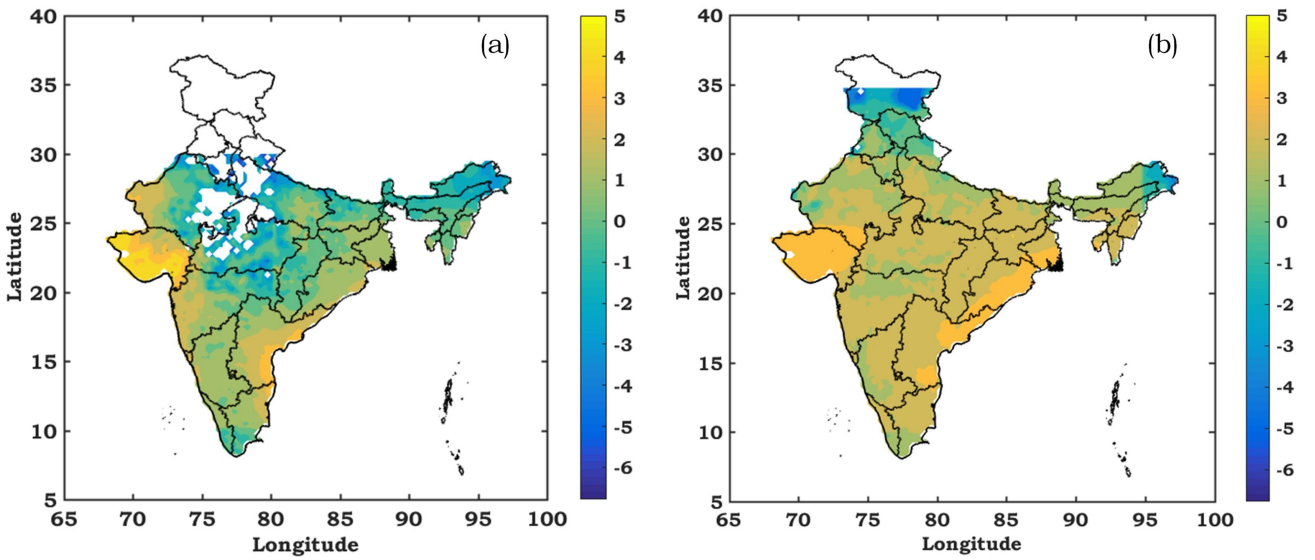


Figure 1: Percentage rainfall (cm) contributed by CDs formed over NIO during (a) pre-monsoon and (b) post-monsoon season respectively over India. Here, the percentage contribution of rainfall is shown in terms of logarithmic scale of actual value.

©2019. Japan Geoscience Union. All Right Reserved.

Analysis of typhoon tracks and associated precipitation amount over western Japan: A case study with Typhoon Nancy and Typhoon Jebi

*Sridhara Nayak[1], Tetsuya Takemi[1]

1. Disaster Prevention Research Institute, Kyoto University

Recent research suggests that typhoons under future warming climate will be more powerful and bring excessive precipitations to the landfall areas. In our study, we downscaled two very strong Typhoons [Typhoon Nancy (international #196118) and Typhoon Jebi (international #201821)] at 1-km grid resolution in present climate and with pseudo global warming (PGW) conditions by using Weather Research and Forecasting (WRF) model. An attempt is also made to examine whether the precipitation amounts carried by Typhoon Jebi can be projected from Typhoon Nancy with PGW conditions, because both typhoons made landfall over same region of Japan with a difference of 57 years. Our results indicate that the typhoon tracks in present climate simulation have good agreement with that of from the RSMC, Tokyo’ s best track datasets. The precipitation amounts over western Japan in the present climate simulation also follows the Radar-AMeDAS observed precipitation amounts. We again find similar typhoon tracks under PGW conditions for both typhoons with higher winds and precipitations compared to that of in present climate simulation. The precipitation amounts associated with the Typhoon Nancy in future climate is found to be higher than that of with Typhoon Jebi during the landfall. However, the 24 hours accumulated precipitation amount brought by Typhoon Nancy with PGW conditions has an overall good agreement with that of by Typhoon Jebi in present climate simulation especially over landfall region. Closer investigation on the typhoon tracks and typhoon induced precipitation amounts suggests that Typhoon Jebi is a possible projection of Typhoon Nancy although it was formed over different location.

Keywords: Typhoon Nancy, Typhoon Jebi, Typhoon track, Typhoon intensity

©2019. Japan Geoscience Union. All Right Reserved.

[E] 口頭発表 | セッション記号 A (大気水圏科学)：A-OS 海洋科学・海洋環境

2019年5月30日(木) 13:45 ~ 15:15 | 105 1F

[A-OS07] 季節内から十年規模の気候変動と予測可能性

コンビーナ:望月 崇(国立研究開発法人海洋研究開発機構)、V Ramaswamy(NOAA GFDL)、Doug Smith(Met Office)、森岡 優志(海洋研究開発機構)、座長:V Ramaswamy(NOAA GFDL)、望月 崇(海洋研究開発機構)

熱波や洪水、干ばつなどの異常気象の頻度や強度の変化を通じて、気候変動は我々の生命や生活、社会経済活動の大きな脅威となりつつある。これには、MJOやIOD、ENSO、PDV、AMVなど、季節内から季節、経年、十年といった幅広い時間スケールの気候現象が複雑に関係している。これまで、それぞれの時間スケールに注目しながら気候現象の理解と予測に対する努力が重ねられてきたが、それでもなお季節内から十年規模の気候変動を幅広く予測するには未だ大きな不確実性がある。個別の気候現象に対する不十分な理解に加えて、異なる時空間スケールで卓越する諸現象の相互作用（例えば、熱帯低気圧とENSO現象の相互作用）や、複数の場をまたぐ物理プロセス（例えば、成層圏-対流圏結合や大気海洋海氷相互作用）に対する理解の不足は特に強調されるべき点である。本セッションでは、季節内から十年規模の気候変動と予測可能性をターゲットにして、観測、理論、数値シミュレーションなど様々なアプローチによって得られている現在の知見を共有することにより、より良い理解と予測のために解決すべき問題点と進むべき方向性を明らかにする。

13:45 ~ 14:00

[AOS07-01] Seasonal Predictions of Tropical Cyclones in 2018 using GFDL and NICAM High-Resolution Global Models

★Invited Papers

*村上 裕之[1,2]、中野 満寿男[3]、V Ramaswamy[1]、Thomas Delworth[1]、Sarah Kapnick[1]、Rich Gudgel[1]、望月 崇[3]、土井 威志[3]、森岡 優志[3] (1.地球流体学研究所、2.大気研究大学連盟、3.海洋研究開発機構)

14:00 ~ 14:15

[AOS07-02] **Future change of tropical cyclone-induced waves in the Indian Ocean; An analysis based on super-high-resolution MRI-AGCM3.2 climate model**

*Bahareh Kamranzad[1,2]、Nobuhito Mori[1] (1.Disaster Prevention Research Institute, Kyoto University、2.Hakubi Center for Advanced Research, Kyoto University)

14:15 ~ 14:30

[AOS07-03] The ocean-coupled global cloud-resolving modeling era

★Invited Papers

*宮川 知己[1] (1.東京大学大気海洋研究所)

14:30 ~ 14:45

[AOS07-04] Westerly Wind Burst (WWB)/Easterly Wind Surge (EWS)-like stochastic forcing and the effects on ENSO prediction by the SINTEX-F system

*土井 威志[1]、Swadhin Behera[1]、山形 俊男[1] (1.JAMSTEC)

14:45 ~ 15:00

[AOS07-05] **The life-cycle of annual waves in the Pacific Ocean as identified by a seamless diagnosis for the energy flux**

*相木 秀則[1]、志村 貴寛[2] (1.名古屋大学宇宙地球環境研究所、2.名古屋大学大学院環境学研究科)

15:00 ~ 15:15

[AOS07-06] 気象研究所における弱結合同化システムの開発とその評価

★招待講演

*藤井 陽介[1]、小林 ちあき[1]、石橋 俊之[1]、高谷 祐平[1] (1.気象庁気象研究所)

Seasonal Predictions of Tropical Cyclones in 2018 using GFDL and NICAM High-Resolution Global Models

*村上 裕之[1,2]、中野 満寿男[3]、V Ramaswamy[1]、Thomas Delworth[1]、Sarah Kapnick[1]、Rich Gudgel[1]、望月 崇[3]、土井 威志[3]、森岡 優志[3]
*Hiroyuki Murakami[1,2], Masuo Nakano[3], V Ramaswamy[1], Thomas Delworth[1], Sarah Kapnick[1], Rich Gudgel[1], Takashi Mochizuki[3], Takeshi Doi[3], Yushi Morioka[3]

1. 地球流体学研究所、2. 大気研究大学連盟、3. 海洋研究開発機構
1. Geophysical Fluid Dynamics Laboratory, 2. University Corporation for Atmospheric Research, 3. JAMSTEC

We conduct real-time seasonal forecast using high-resolution global models (GFDL-FLOR, GFDL-HiFLOR, and NICAM) that have skill in predicting tropical cyclone statistics over the global ocean basins. The seasonal predictions starting from 2018 July initial conditions show above normal frequency of tropical cyclones in the Western North Pacific and Central Pacific Oceans as observed. To understand physical mechanisms behind the active storm season in the Pacific, we conducted idealized seasonal forecasts by changing sea surface temperature spatial patterns, which is so called "real-time attribution" simulations. We find out that warmer subtropical Pacific associated with positive Pacific Meridional Mode (PMM), rather than central Pacific El Nino, was responsible for the active storm season. In the presentation, we will also show preliminary results for impact of anthropogenic forcing on the 2018 active storm season.

キーワード：熱帯低気圧、季節予測、Pacific Meridional Mode、人為起源強制力、台風、地球温暖化
Keywords: Tropical Cyclone, Seasonal Prediction, Pacific Meridional Mode, Anthropogenic Forcing, Typhoon, Global Warming

©2019. Japan Geoscience Union. All Right Reserved.

Future change of tropical cyclone-induced waves in the Indian Ocean; An analysis based on super-high-resolution MRI-AGCM3.2 climate model

*Bahareh Kamranzad[1,2], Nobuhito Mori[1]

1. Disaster Prevention Research Institute, Kyoto University, 2. Hakubi Center for Advanced Research, Kyoto University

Indian Ocean experiences intensive tropical cyclones in both northern and southern parts. The Northern Indian Ocean (NIO) includes 7% of the global tropical cyclones which results in generating severe wave climate during the extreme events. In this study, future change of tropical cyclone-induced waves due to climate change is assessed in terms of change in the spatial distribution patterns and magnitude. The cyclone seasons in NIO are divided by pre-monsoon (especially May) and northeast monsoon (October–December). Moreover, there are few cyclones form the southwest monsoon during June and September. Hence, the assessment of future change of intensity of tropical cyclones and the generated waves is necessary to be performed on a monthly scale. For this purpose, wind field obtained from super-high-resolution atmospheric global climate model MRI-AGCM3.2S of the Japan Meteorological Agency (JMA) -with horizontal spatial and temporal output resolutions of 20 km and 1 hr., respectively- was used to force a numerical wave model (SWAN) in historical (1979-2003) and future (2075-2099) periods (based on Representative Concentration Pathway (RCP) 8.5 scenario).
Spatial distribution of annual extreme events in the domain shows that the concentration of tropical cyclones is in the NIO and around Madagascar (located in the Southern Indian Ocean (SIO)) generating high waves of the magnitudes of around 20 m during the events. Spatial distribution of monthly maximum values of the historical and future wind speed (WS) and significant wave height (SWH) indicates that according to historical projection, intense cyclones happen during May and June in NIO, while they can be observed mostly during December to April in the SIO. The future monthly distribution of cyclone induced waves in SIO shows a similar pattern to the historical events, except for winter tropical cyclones (November and December), which are decreased in the future, while increasing in the intensity can be observed during October and April in NIO.
Monthly variation of maximum events in the domain was assessed in the NIO and SIO, separately. According to the past studies, due to the global warming, tropical cyclones of hurricane intensity -which currently occur only in the pre and post-monsoon seasons- will likely be formed even during the summer monsoon in NIO. Our results illustrate an increase in the intensity of cyclones in the future, not only during the summer monsoon (July) but also during the winter monsoon (September and October). Results show that the range of change in the highest SWH in NIO is between -27% (in February) and +26% (in October). In the northern part of SIO, the intensity of future tropical cyclones will increase during the southwestern inter-monsoon season (March and April), whereas it will decrease at the end of southwestern monsoon season (September). In the southern part of SIO, the intensity of tropical cyclones will increase around 20% during northeastern monsoon (February and March), which results in a future increase of 40% in maximum SWH in February. Generally, change in highest SWH in the future follows the pattern of WS except for the northern parts of SIO when the highest increase in maximum SWH (21%) occurs in March whereas the highest increase in maximum WS occurs in April (25%). There is a 20% increase in maximum WS during February in southern parts of SIO which can be a reason for the increase of SWH during March in northern parts. It can be concluded that the change in the intensity of future tropical cyclones in NIO is higher than SIO. The range of change in highest SWH in NIO is larger than SIO, except for February when the maximum wave height in southern parts of SIO will increase about 40% in

©2019. Japan Geoscience Union. All Right Reserved.

the future. Furthermore, the change in maximum SWH in northern parts of SIO seems to be affected by the change of tropical cyclones in southern parts of SIO.

Keywords: Indian Ocean, tropical cyclone, wave climate, climate change

©2019. Japan Geoscience Union. All Right Reserved.

The ocean-coupled global cloud-resolving modeling era

*宮川 知己[1]
*Tomoki Miyakawa[1]

1. 東京大学大気海洋研究所
1. Atmosphere and Ocean Research Institute University of Tokyo

Developments of global cloud/cloud-system resolving models are recently in full activity in many modeling centers, with 9 members participating in a model inter-comparison project called the DYnamics of the Atmospheric general circulation Modeled On Non-hydrostatic Domains (DYAMOND). With the aid of the supercomputers, they are eyeing to become the main-stream in the next generation models for global simulations in the seasonal to multi-decadal range. Implementation of a fully dynamical ocean model is certainly an essential component in these developments. NICAM, a front-runner in DYAMOND project, can be coupled to COCO, the ocean component of a global climate model MIROC. The coupled version is called NICAM-COCO, or NICOCO, and is now being tested in pilot studies that involve atmosphere-ocean interactions.

An overview of these early studies will be presented, including how convection is affected by the existence of fine-scale ocean fronts, and how the Madden-Julian oscillation affects the initiation and termination of ENSO.

キーワード：海洋結合モデル、全球雲解像モデル、季節予測
Keywords: ocean-coupled model, global cloud-resolving model, seasonal prediction

©2019. Japan Geoscience Union. All Right Reserved.

Westerly Wind Burst (WWB)/Easterly Wind Surge (EWS)-like stochastic forcing and the effects on ENSO prediction by the SINTEX-F system

*土井 威志[1]、Swadhin Behera[1]、山形 俊男[1]
*Takeshi Doi[1], Swadhin Behera[1], Toshio Yamagata[1]

1. JAMSTEC
1. JAMSTEC

Intra-seasonal surface westerly wind bursts (WWB)/easterly wind surges (EWS) in the tropical Pacific play important roles in the onset of El Nino/La Nina. However, the latest version of the SINTEX-F seasonal prediction system tends to underestimate the chance of occurrence of those winds. This problem may cause the relatively low skill of predicting the onset of ENSO, and the over-confident problems of ENSO prediction. In this study, we developed the WWB/EWS-like stochastic forcing parameterization, and examined the effects on ENSO prediction by the SINTEX-F system. In my talk, failure of 2014 El Nino prediction is the focus.

キーワード：エルニーニョ予測、西風バースト、東風サージ
Keywords: ENSO prediction, Westerly Wind Burst, Easterly Wind Surge

©2019. Japan Geoscience Union. All Right Reserved.

The life-cycle of annual waves in the Pacific Ocean as identified by a seamless diagnosis for the energy flux

*相木 秀則[1]、志村 貴寛[2]
*Hidenori AIKI[1], Takahiro Shimura[2]

1. 名古屋大学宇宙地球環境研究所、2. 名古屋大学大学院環境学研究科
1. Institute for Space-Earth Environmental Research, Nagoya University, 2. Graduate School for Environmental Studies, Nagoya University

Synoptic-scale waves play an important role in tropical-extratropical interactions, that has been little investigated in terms of the transfers of wave energy owing to the lack of an appropriate diagnosis scheme in previous studies. A recent theoretical study has derived a seamless scheme that is able to identify the direction of group velocity for both gravity and planetary waves at all latitudes. This new scheme has been used in the present study to provide a first-ever energetic view for the life-cycle of annual waves in the Pacific Ocean in a set of shallow-water model experiments with climatological wind forcing. The new scheme is able to show, in particular for the third baroclinic mode, the signals of eastward energy flux associated with equatorial Kelvin waves that are distributed in the eastern part of the tropical Pacific Ocean. Waves in the tropical and subtropical regions are connected each other at the eastern boundary of the Pacific Ocean that has been viewed, for the first time in the history of geophysical fluid dynamics, in terms of the circulation of wave energy. Concerning the low-pass filtered time evolution of the energy flux, the reflection of equatorial waves at the western boundary is more clearly identified than that at the eastern boundary. These results for the analysis of climatological annual waves provide a basis for the analysis of waves with interannual variations in a future study to better understand, for example, tropical-extratropical interactions during El Nino and La Nina.

キーワード：熱帯中緯度相互作用、季節変動気候値実験、群速度
Keywords: tropical-extratropical interaction, seasonal climatology experiment, group velocity

©2019. Japan Geoscience Union. All Right Reserved.

気象研究所における弱結合同化システムの開発とその評価
Development of weakly coupled atmosphere-ocean data assimilation system and the evaluation of the coupled reanalysis in JMA/MRI

*藤井 陽介[1]、小林 ちあき[1]、石橋 俊之[1]、高谷 祐平[1]
*Yosuke Fujii[1], Chiaki Kobayashi[1], Toshiyuki Ishibashi[1], Yuhei Takaya[1]

1. 気象庁気象研究所
1. Meteorological Research Institute, Japan Meteorological Agency

気象研究所では気象庁の現業システムを用いて弱結合同化システムMRI-CDA1の開発を行っている。MRI-CDA1は数値天気予報用の4次元変分法（4DVAR）全球大気データ同化システムと季節予報用の3次元変分法全球海洋データ同化システム、大気海洋結合モデルで構成される。大気の4DVARデータ同化ルーチンにおいて、結合モデルはアウターループとして用いられが、インナーループでは非結合の大気モデルが用いられる。大気の4DVAR解析は6時間のサイクルで実行される一方、海洋解析は10日毎に実行され、海洋インクリメントがアウターループにおける結合モデルの積分時に適用される。

上記システムの検証のため、結合再解析実験を2013年1月から2015年12月にかけて実施したところ、気象庁55年再解析（JRA55）で見られた北太平洋の熱帯収束帯（ITCZ）などの降水過多が、結合再解析では解消することが確認された。また、結合再解析では、非結合の再解析では再現されない海面水温と降水量のラグ相関関係が正しく表現されていた。しかし、降水変動が改善するのは、大気について衛星データを除く従来型のデータのみを同化した場合のみであり、衛星データも同化した場合は、海洋同化で再現された海面水温に大気場が適応するのではなく、データ同化で決められた大気場に合うように海面水温の方が調節を受けていた。その他、大気の観測誤差共分散を大きく設定した実験も実施していて、元の設定での結合再解析に比べて、熱帯域での降水の変動が概ね改善していることを確認した。

キーワード：結合データ同化、結合再解析、季節内・季節予報、海面水温、降水
Keywords: coupled data assimilation, coupled analysis, Subseasonal-to-seasonal prediction, sea surface temperature, precipitation

©2019. Japan Geoscience Union. All Right Reserved.

[E] 口頭発表 | セッション記号 A (大気水圏科学)：A-OS 海洋科学・海洋環境

2019年5月30日(木) 15:30 ~ 17:00 | 105 1F

[A-OS07] 季節内から十年規模の気候変動と予測可能性

コンビーナ:望月 崇(国立研究開発法人海洋研究開発機構)、V Ramaswamy(NOAA GFDL)、Doug Smith(Met Office)、森岡 優志(海洋研究開発機構)、座長:森岡 優志(海洋研究開発機構)、望月 崇(海洋研究開発機構)

熱波や洪水、干ばつなどの異常気象の頻度や強度の変化を通じて、気候変動は我々の生命や生活、社会経済活動の大きな脅威となりつつある。これには、MJOやIOD、ENSO、PDV、AMVなど、季節内から季節、経年、十年といった幅広い時間スケールの気候現象が複雑に関係している。これまで、それぞれの時間スケールに注目しながら気候現象の理解と予測に対する努力が重ねられてきたが、それでもなお季節内から十年規模の気候変動を幅広く予測するには未だ大きな不確実性がある。個別の気候現象に対する不十分な理解に加えて、異なる時空間スケールで卓越する諸現象の相互作用（例えば、熱帯低気圧とENSO現象の相互作用）や、複数の場をまたぐ物理プロセス（例えば、成層圏-対流圏結合や大気海洋海氷相互作用）に対する理解の不足は特に強調されるべき点である。本セッションでは、季節内から十年規模の気候変動と予測可能性をターゲットにして、観測、理論、数値シミュレーションなど様々なアプローチによって得られている現在の知見を共有することにより、より良い理解と予測のために解決すべき問題点と進むべき方向性を明らかにする。

15:30 ~ 15:45

[AOS07-07] Decadal variability and predictability of the North Atlantic Oscillation

★Invited Papers

*Rosemary Eade[1,2]、David Stephenson[2]、Doug Smith[1]、Adam Scaife[1,2]、Leon Hermanson[1]、Nick Dunstone[1] (1.Met Office Hadley Centre、2.University of Exeter)

15:45 ~ 16:00

[AOS07-08] Seasonal to multi-year climate predictability in a climate model MIROC6

*片岡 崇人[1]、建部 洋晶[1]、小山 博司[1]、望月 崇[1] (1.研究開発法人　海洋研究開発機構)

16:00 ~ 16:15

[AOS07-09] Identifying the early 2000s hiatus associated with internal climate variability

*Xin-Gang Dai[1]、Ping Wang[2] (1.Institute of Atmospheric Physics, Chinese Academy of Sciences、2.Chinese Academy of Meteorological Sciences)

16:15 ~ 16:30

[AOS07-10] Decadal Evolution of the Surface Energy Budget during the Fast Warming and Global Warming Hiatus Periods in the ERA-Interim

*XIAOMING HU[1] (1.Sun Yat-sen University)

16:30 ~ 16:45

[AOS07-11] The role of ocean variability for multi-year droughts in Australia

*Andrea Taschetto[1,2]、Alex Sen Gupta[1,2]、Caroline C Ummenhofer[3]、Matthew H England[1,2] (1.Climate Change Research Centre, University of New South Wales, Sydney, Australia、2.ARC Centre of Excellence for Climate Extremes, University of New South Wales, Sydney, Australia、3.Department of Physical Oceanography, Woods Hole Oceanographic Institution, Woods Hole, MA, USA)

16:45 ~ 17:00

[AOS07-12] Decadal variability and predictability in the Southern Ocean - implications for interpreting recent observed trends

★Invited Papers

*Liping Zhang[1,2]、Thomas L Delworth[2]、William Cooke[2,3]、Xiaosong Yang[2,3] (1.Princeton University、2.Geophysical Fluid Dynamics Laboratory、3.UCAR)

Decadal variability and predictability of the North Atlantic Oscillation

*Rosemary Eade[1,2], David Stephenson[2], Doug Smith[1], Adam Scaife[1,2], Leon Hermanson[1], Nick Dunstone[1]

1. Met Office Hadley Centre, 2. University of Exeter

The winter of 1962/63 was the coldest in the UK in over a century while the mildest winter occurred in 1988/89. For countries to be resilient against the impacts of large weather variations in the future, it is important to assess the likelihood of seeing such extreme fluctuations and understand the physical drivers. In Europe and North America, these fluctuations are related to a combination of year-to-year variability and low-frequency variability of the North Atlantic Oscillation (NAO). The NAO is now a significant source of predictability for seasonal forecasts in these regions, however the signal-to-noise ratio of the ensemble mean to total variability in these ensemble predictions has been shown to be anomalously small, which means the real world is more predictable than our climate models suggest. Here we provide a new evaluation of the ability of climate models to simulate and predict longer-term variability and extreme trends in the NAO. For this we use statistical analyses of the observations and climate model simulations, and assess predictability with a large multi-model ensemble of decadal predictions. We also investigate the drivers of NAO variability and trends using new results from the CMIP6 Decadal Climate Prediction Project and the Polar Amplification MIP.

Keywords: Decadal variability, North Atlantic Oscillation, Polar Amplification, Trend analysis

©2019. Japan Geoscience Union. All Right Reserved.

Seasonal to multi-year climate predictability in a climate model MIROC6

*片岡 崇人[1]、建部 洋晶[1]、小山 博司[1]、望月 崇[1]
*Takahito Kataoka[1], Hiroaki Tatebe[1], Hiroshi Koyama[1], Takashi Mochizuki[1]

1. 研究開発法人　海洋研究開発機構
1. JAMSTEC Japan Agency for Marine-Earth Science and Technology

Seasonal to multi-year climate predictability is examined in hindcast experiments using the latest version of a climate model MIROC (MIROC6). The model is initialized by assimilating observed ocean temperature and salinity anomaly fields and full-filed of sea ice concentration. In addition, the atmospheric initial conditions are replaced with variables from JRA55 reanalysis and the hindcasts are issued on November 1st. On seasonal timescales, the MIROC6 prediction system shows an improvement in Niño3.4 prediction skill from that of MIROC5, though the skill itself is still modest. SLP variability around Japan appears to have predictive skill up to second winter (lead time of about 15 month) and summer (lead time of about 21 month) possibly due to the improved ENSO prediction skill and the better representation of East Asian monsoon. On longer timescales, although the predictive component largely originates from the externally forced variability, MIROC6 shows predictive skills in the surface air temperature particularly in the North Pacific and the North Atlantic.

キーワード：近未来予測、季節予測
Keywords: near-term prediction, seasonal prediction

©2019. Japan Geoscience Union. All Right Reserved.

Identifying the early 2000s hiatus associated with internal climate variability

*Xin-Gang Dai[1], Ping Wang[2]

1. Institute of Atmospheric Physics, Chinese Academy of Sciences, 2. Chinese Academy of Meteorological Sciences

This study focuses on re-examining the early 2000s hiatus and the associated key components of the global mean surface temperature (GMST) using multiscale statistics for five well-known gridded surface temperature and two reanalysis datasets. The hiatus is characterized as a near-zero trend on the decadal scale corresponding to the maximum P-value via an F-test in statistics. The results reveal that the hiatus exists in both the GMST and global mean air temperature (GMAT) time series, rather than in global warming component, which has maintained an approximately constant rate of change of approximately 0.08ºC/decade over the past three decades. The hiatus' s duration is different from that of time series such as 2002-2012/2001-2013/2002-2014 in HadCRUT4, NOAA-old, ERA-Interim and NCEP-R2. The newly gridded datasets with data infilling or bias correction for interpreting the sea surface temperature (SST) measurement from the old versions show a slightly higher trend from for 2002-2012 than the hiatus, which is thus regarded as a slowdown. Comparison suggests that the hiatus should be during the period 2002-2012. Orthogonal wavelet decomposition of the temperature time series shows that the hiatus was merely a decadal balance between cooling from interannual variability and global warming, in addition to weak warming from interdecadal and multidecadal climate oscillations. In addition, the evolutions of the GMST' s interannual composite well coincided with Niño3.4 SST anomalies, which is consistent with the numerical simulation performed by Kosaka and Xie in 2013. Hence, it is the anomalous El Niño Southern Oscillation (ENSO) events in the early 2000s that caused the hiatus despite a constant rate of global warming and the maximum magnitude of the multidecadal composite that led to the limited contribution to the trend during this period. The multidecadal composite follows a downward path, which implies that future climate conditions will likely rely on competition between multidecadal cooling and global warming if the multidecadal climate cycle repeats, as was experienced during the second half of the twentieth century.

Keywords: Global mean temperature, early 2000s hiatus, multiscale decomposition, global warming, multidecadal oscillation, interannual variability

©2019. Japan Geoscience Union. All Right Reserved.

Decadal Evolution of the Surface Energy Budget during the Fast Warming and Global Warming Hiatus Periods in the ERA-Interim

*XIAOMING HU[1]

1. Sun Yat-sen University

The global-mean surface temperature has experienced a rapid warming from the 1980s to early-2000s but a muted warming since, referred to as the global warming hiatus in the literature. Decadal changes in deep ocean heat uptake are thought to primarily account for the accelerated warming rate and subsequent slowdown. Here, we examine the role of ocean heat uptake in establishing the fast warming and warming hiatus periods in the ERA-Interim through a decomposition of the global-mean surface energy budget. We find the increase of carbon dioxide alone yields a nearly steady increase of the downward longwave radiation at the surface from the 1980s to the present, but neither accounts for the fast warming nor warming hiatus periods. During the global warming hiatus period, the transfer of latent heat energy from the ocean to atmosphere increases and the total downward radiative energy flux to the surface decreases due to a reduction of solar absorption caused primarily by an increase of clouds. The reduction of radiative energy into the ocean and the surface latent heat flux increase cause the ocean heat uptake to decrease and thus contribute to the slowdown of the global-mean surface warming. Our analysis also indicates that in addition to a reduction of deep ocean heat uptake, the fast warming period is also driven by enhanced solar absorption due predominantly to a decrease of clouds and by enhanced longwave absorption mainly attributed to the air temperature feedback.

Keywords: global warming, global warming hiatus, surface energy budget

©2019. Japan Geoscience Union. All Right Reserved.

The role of ocean variability for multi-year droughts in Australia

*Andrea Taschetto[1,2], Alex Sen Gupta[1,2], Caroline C Ummenhofer[3], Matthew H England[1,2]

1. Climate Change Research Centre, University of New South Wales, Sydney, Australia, 2. ARC Centre of Excellence for Climate Extremes, University of New South Wales, Sydney, Australia, 3. Department of Physical Oceanography, Woods Hole Oceanographic Institution, Woods Hole, MA, USA

Australian climate is strongly affected by variations in sea surface temperature in the Pacific, Indian and Southern Oceans. Over the northern and eastern regions of Australia, the El Niño –Southern Oscillation (ENSO) is the main phenomenon causing profound impacts in rainfall. On the southern regions, a large proportion of rainfall comes from synoptic weather systems at the mid-latitudes, such as cold fronts and cut-off lows. The interaction between the tropical modes of variability and the atmosphere dynamics at mid-latitudes makes difficult to understand the role of the oceans for droughts relative to the atmosphere internal variability.

The contribution of ocean versus atmosphere variability for Australian rainfall is investigated in this study. Numerical experiments are performed using the National Center for Atmospheric Research (NCAR) Community Earth System Model (CESM). Three multi-century simulations are integrated to address the role of the oceans for rainfall variability: (i) a fully coupled climate system run, (ii) an run forced with climatological cycle of SST, i.e. no SST variability beyond one year, and (iii) a run forced with varying SST, i.e. containing SST variability but no air-sea feedback.

Our results show that interannual variations in sea surface temperature has a significant impact on rainfall variability and extremes, such as multi-year droughts and pluvials. Ocean variability makes droughts more intense and modulates the duration of short-term dry spells. However, interannual variability in the oceans does not significantly affect the duration of droughts longer than 3 years. On the other hand, in a world with no year-to-year ocean variability, multi-year dry spells can last longer than oceanic-driven droughts. This can be explained by the influence that ENSO has over the tropics:ENSO is a crucial phenomenon for restoring droughts and pluvials. In the absence of ocean variability, there is no dominant climate driver that can act to terminate extended dry or wet periods.

Keywords: Precipitation variability, Droughts, El Niño - Southern Oscillation, atmospheric variability , ocean variability

©2019. Japan Geoscience Union. All Right Reserved.

Decadal variability and predictability in the Southern Ocean - implications for interpreting recent observed trends

*Liping Zhang[1,2], Thomas L Delworth[2], William Cooke[2,3], Xiaosong Yang[2,3]

1. Princeton University, 2. Geophysical Fluid Dynamics Laboratory, 3. UCAR

While decadal variability and predictability in the North Atlantic and North Pacific have received considerable attention, there has been less work on decadal variability and predictability in the Southern Ocean. As shown previously, a coherent mode of decadal to centennial variability exists in multiple climate models. The mechanism involves a multidecadal accumulation of heat in the subsurface of the Southern Ocean, which is then rapidly discharged through intense oceanic convection when the accumulation of subsurface heat reduces the stratification of the water column. The release of this accumulated subsurface heat can have considerable regional scale climatic impacts, along with substantial impacts on ocean heat uptake. Using a large suite of perfect predictability experiments, in concert with long control simulations, we show that this variability has a high degree of predictability. We present further results that show this type of variability may play an important role for interpreting recently observed trends of sea ice and temperature in the Southern Ocean. Specifically, observed trends over the last several decades resemble a particular phase of this variability in which reduced oceanic convection leads to subsurface warming and surface cooling, with associated increases in sea ice extent. This phase of natural variability may substantially contribute to observed decadal trends, working in concert with other factors.

©2019. Japan Geoscience Union. All Right Reserved.

[E] 口頭発表 | セッション記号 A (大気水圏科学)：A-OS 海洋科学・海洋環境

2019年5月30日(木) 9:00 ~ 10:30 | 105 1F

[A-OS10] Atlantic climate variability, and its global impacts and predictability

コンビーナ:Ingo Richter(JAMSTEC Japan Agency for Marine-Earth Science and Technology)、時長 宏樹(九州大学応用力学研究所)、Noel S Keenlyside(Geophysical Institute Bergen)、Carlos R Mechoso(University of California Los Angeles)、座長:時長 宏樹(京都大学白眉センター)、Ingo Richter

The Atlantic Ocean is subject to pronounced climate variations that occur on a wide range of time scales, including interannual variability in the equatorial and subtropical regions, and Atlantic multi-decadal variability (AMV), which has been linked with the Atlantic meridional overturning circulation (AMOC). These are connected to other climate variations across the globe. The AMV, e.g., has long been known to have global impacts, such as changes in the Indian, Asian and South American summer monsoons, and changes in the Pacific associated with the "global hiatus". Interannual variability in the equatorial and subtropical Atlantic has also been shown to influence global climate, including over Asia, while the freshening of the North Atlantic by melting of the Greenland ice cap is expected to influence all ocean basins via atmospheric bridges. Likewise, misrepresentation of the Atlantic can have global ramifications in climate models. Misrepresentation of the AMOC, e.g., has been associated with model biases in the entire Northern Hemisphere.

This session seeks observational, modeling, and theoretical studies on the mechanisms that determine the Atlantic mean climate and variability, as well as the predictability and global impacts of such variability. We also seek studies that evaluate climate model performance in the region. Topics include atmosphere-ocean-cloud interactions in the tropical Atlantic and their remote impacts; relationships between tropical and mid/high latitude variability; air-sea interaction along the Gulf Stream and its influence on cyclones and storm track evolution; variability in the Benguela upwelling region; influence of Agulhas leakage on the South Atlantic; coupled climate models biases in the region and their impacts; AMOC and long-term climate change.

9:00 ~ 9:15

[AOS10-01] Atlantic impacts on the tropical Pacific climate in the 2000s

*望月 崇[1]、渡部 雅浩[2]、木本 昌秀[2] (1.国立研究開発法人海洋研究開発機構、2.東京大学大気海洋研究所)

9:15 ~ 9:30

[AOS10-02] Recent acceleration of Arabian Sea warming induced by the Atlantic-western Pacific trans-basin multidecadal variability

*Cheng Sun[1] (1.Beijing Normal University)

9:30 ~ 9:45

[AOS10-03] **Westward Wind Changes over the Tropical and Mid-latitude Pacific in the Past Three Decades Driven by the Inter-basin Teleconnections**

★Invited Papers

*Xichen Li[1] (1.Institute of Atmospheric Physics)

9:45 ~ 10:00

[AOS10-04] On the Usefulness of the Atlantic Multidecadal Oscillation Index for Identifying Origins of North Atlantic Sea Surface Temperature Variability

*Jing Sun[1,2]、Mojib Latif[1,3]、Wonsun Park[1]、Taewook Park[1,4] (1.GEOMAR Helmholtz Centre for Ocean Research Kiel、2.Ocean University of China、3.University of Kiel、4.Korea Polar Research Institute)

10:00 ~ 10:15

[AOS10-05] Atlantic Multidecadal SST Signal Modulated by the Low-Frequency Mixed Layer Depth Variability

*Ayako Yamamoto[1]、Hiroaki Tatebe[1]、Masami Nonaka[1] (1.Japan Agency for Marine-Earth Science and Technology)

10:15 ~ 10:30

[AOS10-06] A High-Resolution Future Wave Climate Projection for the Northwestern Atlantic

*Adrean Webb[1]、Tomoya Shimura[1]、Nobuhito Mori[1] (1.Kyoto University, Disaster Prevention Research Institute)

Atlantic impacts on the tropical Pacific climate in the 2000s

*望月 崇[1]、渡部 雅浩[2]、木本 昌秀[2]
*Takashi Mochizuki[1], Masahiro Watanabe[2], Masahide Kimoto[2]

1. 国立研究開発法人海洋研究開発機構、2. 東京大学大気海洋研究所
1. Japan Agency for Marine-Earth Science and Technology, 2. Atmosphere-Ocean Research Institute, The University of Tokyo

A subdecadal (i.e., 3-year-running means) variation over the tropical Pacific is very distinctively observed in the 2000s. Here, we have demonstrated that sea surface temperature (SST) anomalies in the tropical Atlantic contribute to forming high ocean temperature anomalies of the tropical Pacific in the early-2000s, by performing partial data assimilation of global climate model. Low SST over the equatorial Atlantic changes the Walker circulation and the associated weakening of the Pacific trade wind raises the equatorial SST on the subdecadal timescales. At the same time, high SST anomaly is generated also in the off-equatorial North Pacific through deepening of the upper ocean thermocline due to an accompanying anti-cyclonic surface wind anomaly aloft. In addition, the north tropical Atlantic SST may help the subdecadal warming in the equatorial Pacific, similar to the common changes working as a seasonal trigger of the so-called central Pacific El Nino Southern Oscillation event.

キーワード：subdecadal variability、interbasin influence、partial data assimilation、Pacific trade wind
Keywords: subdecadal variability, interbasin influence, partial data assimilation, Pacific trade wind

©2019. Japan Geoscience Union. All Right Reserved.

Recent acceleration of Arabian Sea warming induced by the Atlantic-western Pacific trans-basin multidecadal variability

*Cheng Sun[1]

1. Beijing Normal University

The rapid warming of the Arabian Sea (AS) brings an increased risk of extreme weather and climate events,
e.g., flood, heat wave and cyclone. AS warming has significantly accelerated since the 1990s, in particular in the
spring season, stemming from the multidecadal variability of AS sea surface temperature (SST). Here, we show
that this variability is closely related to the Atlantic multidecadal oscillation (AMO). A set of Atlantic pacemaker
experiments with slab mixed-layer ocean model successfully reproduce the AS spring multidecadal variability and
its connection with the AMO. An atmospheric teleconnection from the Atlantic to the AS in the preceding winter
and associated thermodynamic air-sea feedback are found important. The teleconnection can be recreated by the
atmospheric model when the SSTs of AMO and its trans-basin footprint over western Pacific (WP) are prescribed
simultaneously. The WP SST warming associated with AMO positive phase induces a Gill-type Rossby wave
response over the AS, showing an anomalous low and converging southerlies that weaken the winter northerly.
A positive wind-evaporation-SST feedback further develops, leading to the AS SST anomalies being formed and
maintained to the subsequent spring. The concurrent cold-to-warm phase shift of AMO and its WP SST footprint
since the 1990s contributes constructively to the rapid warming of AS. Our results suggest a key role of trans-basin
interactions in the attribution of historical regional SST warming and constraint of projected future warming.

Keywords: Atlantic multidecadal oscillation , Trans-basin variability, Arabian Sea warming

©2019. Japan Geoscience Union. All Right Reserved.

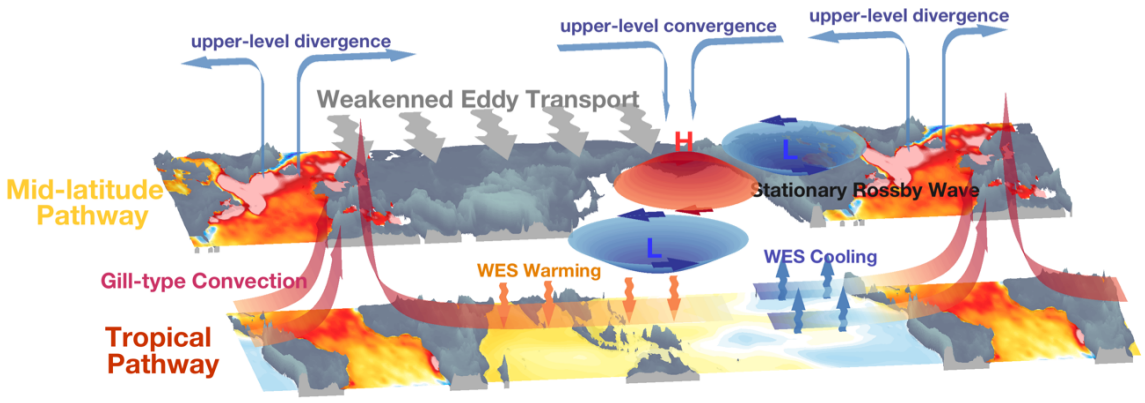
Westward Wind Changes over the Tropical and Mid-latitude Pacific in the Past Three Decades Driven by the Inter-basin Teleconnections

*Xichen Li[1]

1. Institute of Atmospheric Physics

Due to its active role in the atmosphere-ocean interactions and in the global climate variability, the trade wind regime over the Pacific Ocean has been receiving increased attention. Although the intensification of the equatorial trade wind in recent decades has been widely investigated, the meridional extension of this easterly wind change and the associated mechanism remain unclear. To untangle this problem, we combine observations, reanalysis datasets, and a hierarchy of climate model simulations. Analysis based on measurements and reanalysis datasets show that the intensified easterly wind anomaly is not only confined within the tropical basin, but also extends to the mid-latitude Pacific, from 40˚S to 40˚N. In the tropics, the trade wind change is primarily attributed to the enhanced Walker circulation driven by the inter-basin teleconnection and further the decadal variability over the Atlantic and the Pacific oceans, whereas in the mid-latitudes, the changes in sub-tropical highs and Aleutian Low become more dominant. While the altered winds can contribute to the observed sea surface temperature (SST) changes in both tropical and mid-latitude Pacific, they are not driven by the regional Pacific SST changes. Instead, the wind changes are mostly caused by remote influences originated from the tropical Atlantic and Indian Ocean SST changes through stationary Rossby waves. This finding builds a direct pathway linking the tropical Atlantic and Indian Ocean to the mid-latitude Pacific. This pathway has a broad implication for understanding air-sea interactions and sea level changes over the Pacific, and may have an important impact on the interannual and decadal predictability of the Pacific climate variability, such as Pacific Decadal Oscillation and El Niño –Southern Oscillation.

Keywords: Pacific, Westerly Wind, Interbasin Teleconnection



©2019. Japan Geoscience Union. All Right Reserved.

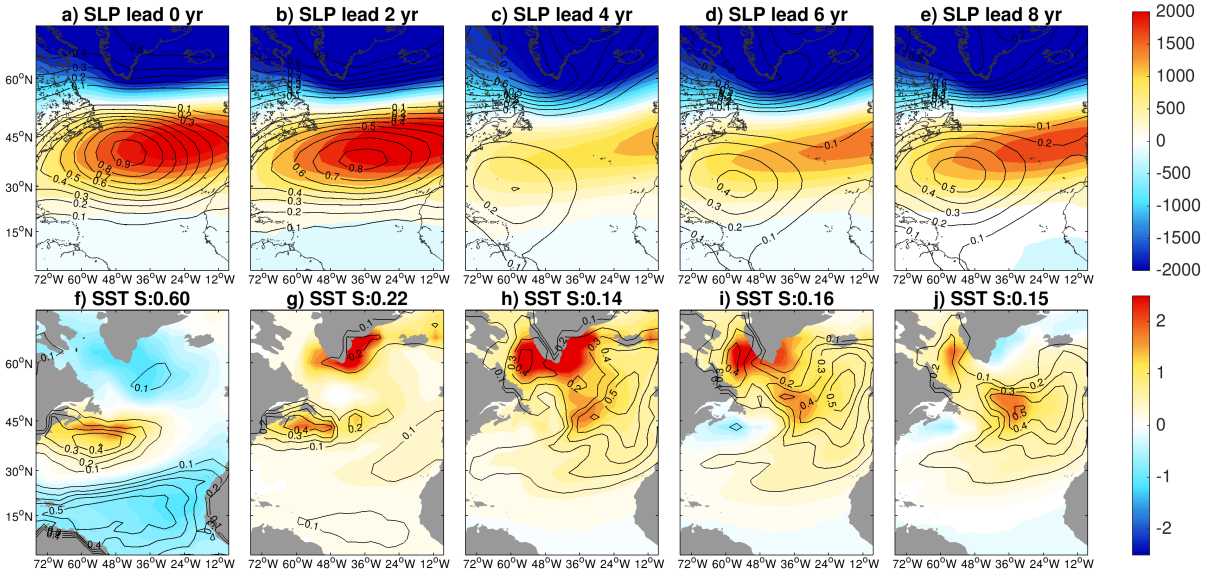
On the Usefulness of the Atlantic Multidecadal Oscillation Index for Identifying Origins of North Atlantic Sea Surface Temperature Variability

*Jing Sun[1,2], Mojib Latif[1,3], Wonsun Park[1], Taewook Park[1,4]

1. GEOMAR Helmholtz Centre for Ocean Research Kiel, 2. Ocean University of China, 3. University of Kiel, 4. Korea Polar Research Institute

We provide, on the basis of observations and climate models, an interpretation of the Atlantic Multidecadal Oscillation (AMO) index which is widely used in studies addressing sea surface temperature (SST) variability over the North Atlantic (NA). In particular, the AMO index is often used as an index of the Atlantic Meridional Overturning Circulation (AMOC). The AMO index, defined here as the anomalous North Atlantic SST averaged over 0˚ - 60˚ N, accounts for significant SST variability over the tropical and subpolar NA. Climate models analyzed in this study suggest that the AMOC only accounts for significant SST variability over the subpolar NA. In these models, a low-pass filtered AMO index also is associated with SST variability only over the subpolar NA and tracks well multidecadal AMOC variability. SST variability over the tropical NA has previously been suggested to be largely governed by local surface wind variability, which can be amplified the wind-evaporation-SST feedback, and remote forcing by El Niñ o/Southern Oscillation, the leading mode of interannual variability over the tropical Pacific. The AMO index lumps together SST variability associated with different physical mechanisms, which limits the usefulness of the index to understand the origins of NA SST variability. Our results may help to reconcile seemingly competing results about the role of ocean dynamics in NA SST variability.

Keywords: Atlantic Multidecadal Oscillation/Variability, Atlantic Meridional Overturning Circulation, North Atlantic sea surface temperature



©2019. Japan Geoscience Union. All Right Reserved.

Atlantic Multidecadal SST Signal Modulated by the Low-Frequency Mixed Layer Depth Variability

*Ayako Yamamoto[1], Hiroaki Tatebe[1], Masami Nonaka[1]

1. Japan Agency for Marine-Earth Science and Technology

Atlantic Multidecadal Oscillation (AMO) has conventionally been attributed to the heat transport associated with the Atlantic Meridional Overturning Circulation. A recent study, however, challenged this paradigm and indicated that the North Atlantic basin-wide sea surface temperature (SST) pattern analogous to AMO can emerge owing to the atmospheric stochastic forcings in slab ocean models, without an active ocean. Subsequent studies have disputed this finding, arguing that the cause of the SST warming differ between the slab ocean models and fully-coupled models; however, a consensus is yet to be reached.

In this study, we take an approach to resolve this conundrum, by partitioning the multidecadal SST tendency into a part that is induced by the surface heat fluxes and another by the ocean, using a latest version of a fully-coupled climate model, MIROC6. We found that the heat flux term is primarily responsible for the North Atlantic subpolar SST warming, opposing the cooling caused by the oceanic term, despite that the associated heat flux anomalies are upward. Further decomposition of the heat flux term indicates that it is the mixed layer depth (MLD) deepening that makes the ocean less susceptible for cooling. This MLD variability is essentially induced by the anomalous salinity transport by the Gulf Stream modulated by the multidecadal North Atlantic Oscillation. The tropical North Atlantic SST signal, in contrast, arises due to the surface heat fluxes. Our study thus implies the key role of both air-sea fluxes and the ocean dynamics in the emergence of the AMO signal.

Keywords: Atlantic Multidecadal Oscillation/Variability, Gulf Stream, mixed-layer depth

©2019. Japan Geoscience Union. All Right Reserved.

A High-Resolution Future Wave Climate Projection for the Northwestern Atlantic

*Adrean Webb[1], Tomoya Shimura[1], Nobuhito Mori[1]

1. Kyoto University, Disaster Prevention Research Institute

A high-resolution wave climate projection for the Northwestern Atlantic has been conducted to help assess possible regional impacts under an RCP8.5 climate forcing scenario. Here, NOAA WAVEWATCH III is utilized to resolve the Northwestern Atlantic and US Eastern Coast at approximately 21 km and 7 km, respectively. Hourly wind field forcings are provided by MRI-AGCM 3.2S at a 21 km/lat resolution and the increased temporal frequency and spatial resolution allow for better modeling of large storm events. Climatological (25-year) significant wave height differences between future and historical periods indicate that a seesaw effect will occur, with decreases occurring in the Northwest Atlantic and Gulf of Mexico and increases occurring in the Caribbean Sea. Other notable changes include decreases in incident shoreline energy along the US East Coast. Further details of the projection will be discussed, including underlying wind field changes and extreme wave statistics.

Keywords: wave climate, Northwest Atlantic, WaveWatch III

©2019. Japan Geoscience Union. All Right Reserved.

[E] 口頭発表 | セッション記号 A (大気水圏科学)：A-OS 海洋科学・海洋環境

2019年5月30日(木) 10:45 ~ 12:15 | 105 1F

[A-OS10] Atlantic climate variability, and its global impacts and predictability

コンビーナ:Ingo Richter(JAMSTEC Japan Agency for Marine-Earth Science and Technology)、時長 宏樹(九州大学応用力学研究所)、Noel S Keenlyside(Geophysical Institute Bergen)、Carlos R Mechoso(University of California Los Angeles)、座長:Ingo Richter、時長 宏樹(京都大学白眉センター)

The Atlantic Ocean is subject to pronounced climate variations that occur on a wide range of time scales, including interannual variability in the equatorial and subtropical regions, and Atlantic multi-decadal variability (AMV), which has been linked with the Atlantic meridional overturning circulation (AMOC). These are connected to other climate variations across the globe. The AMV, e.g., has long been known to have global impacts, such as changes in the Indian, Asian and South American summer monsoons, and changes in the Pacific associated with the "global hiatus". Interannual variability in the equatorial and subtropical Atlantic has also been shown to influence global climate, including over Asia, while the freshening of the North Atlantic by melting of the Greenland ice cap is expected to influence all ocean basins via atmospheric bridges. Likewise, misrepresentation of the Atlantic can have global ramifications in climate models. Misrepresentation of the AMOC, e.g., has been associated with model biases in the entire Northern Hemisphere.

This session seeks observational, modeling, and theoretical studies on the mechanisms that determine the Atlantic mean climate and variability, as well as the predictability and global impacts of such variability. We also seek studies that evaluate climate model performance in the region. Topics include atmosphere-ocean-cloud interactions in the tropical Atlantic and their remote impacts; relationships between tropical and mid/high latitude variability; air-sea interaction along the Gulf Stream and its influence on cyclones and storm track evolution; variability in the Benguela upwelling region; influence of Agulhas leakage on the South Atlantic; coupled climate models biases in the region and their impacts; AMOC and long-term climate change.

10:45 ~ 11:00

[AOS10-07] Tropical Atlantic Impact on ENSO predictability

★Invited Papers

*Belen Rodriguez-Fonseca[1,2]、Irene - Polo[1]、Elsa - Mohino[1]、Teresa - Losada[1]、Marta - Martin-Rey[5]、Roberto - Mechoso[3]、Noel - Keenlyside[4] (1.Department of Physics of the Earth and Astrophysics, UCM, Madrid, Spain、2.Institute of Geosciences, IGEO, UCM-CSIC, Madrid, Spain、3.Department of Atmospheric and Oceanic Sciences, UCLA, Los Angeles, USA、4.Geophysical Institute, University of Bergen, Norway、5.Instituto de Ciencias del Mar, Barcelona, Spain)

11:00 ~ 11:15

[AOS10-08] Interannual variability of Antarctic Intermediate Water in the tropical North Atlantic

*Yao Fu[1]、Chunzai Wang[1]、Peter Brandt[2,3]、Richard J. Greatbatch[2,3] (1.State Key Laboratory of Tropical Oceanography, South China Sea Institute of Oceanology, Chinese Academy of Sciences, Guangzhou, China、2.GEOMAR Helmholtz Centre for Ocean Research Kiel, Kiel, Germany 、3.Christian-Albrechts-Universität zu Kiel, Kiel, Germany)

11:15 ~ 11:30

[AOS10-09] Understanding the mechanisms of the Atlantic meridional climate variability

*Hyacinth C Nnamchi[1]、Riccardo Farneti[2]、Noel S Keenlyside[3]、Fred Fred Kucharski[2]、Mojib Latif[1] (1.GEOMAR Helmholtz Centre for Ocean Research Kiel, Kiel, Germany、2.Abdus Salam International Centre for Theoretical Physics, Trieste, Italy、3.Geophysical Institute, University of Bergen, and Bjerknes Centre for Climate Research, Bergen, Norway)

11:30 ~ 11:45

[AOS10-10] The corss-equatorical gradient variability: The role of heat, momentum, and freshwater flux

*片岡 崇人[1] (1.研究開発法人　海洋研究開発機構)

11:45 ~ 12:00

[AOS10-11] Generation mechanisms of the Benguela Nino with a focus on local amplification

*東塚 知己[1]、小林 諒[1] (1.東京大学大学院理学系研究科地球惑星科学専攻)

12:00 ~ 12:15

[AOS10-12] **Seasonal energy analysis for baroclinic waves in equatorial Atlantic through a diagnostic scheme for energy flux**

*Qingyang Song[1]、Hidenori AIKI[1] (1.Institute of space-earth environmental research, Nagoya University)

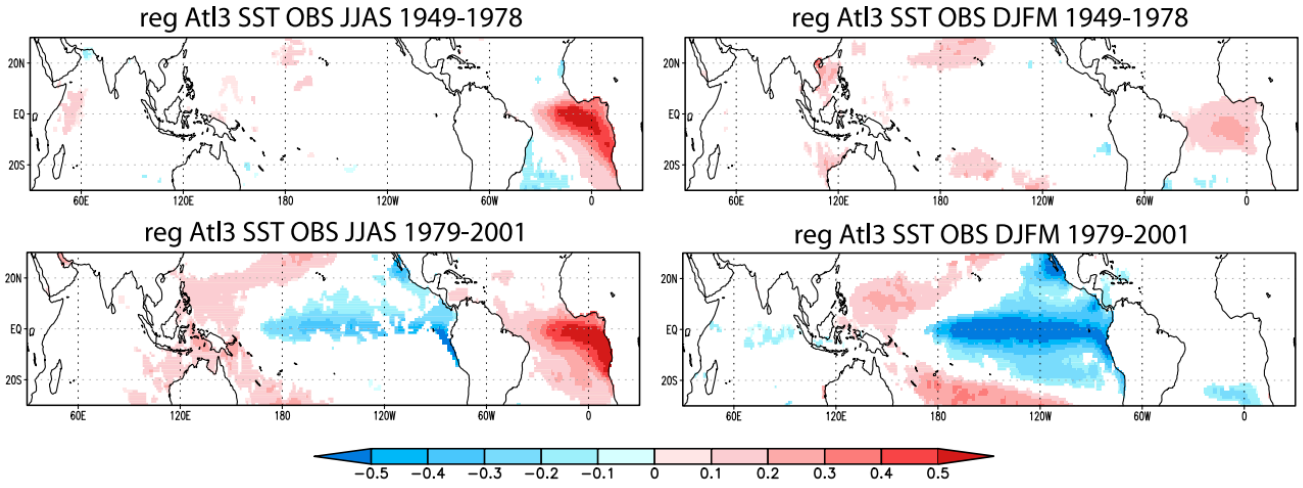
Tropical Atlantic Impact on ENSO predictability

*Belen Rodriguez-Fonseca[1,2], Irene - Polo[1], Elsa - Mohino[1], Teresa - Losada[1], Marta - Martin-Rey[5], Roberto - Mechoso[3], Noel - Keenlyside[4]

1. Department of Physics of the Earth and Astrophysics, UCM, Madrid, Spain, 2. Institute of Geosciences, IGEO, UCM-CSIC, Madrid, Spain, 3. Department of Atmospheric and Oceanic Sciences, UCLA, Los Angeles, USA, 4. Geophysical Institute, University of Bergen, Norway, 5. Instituto de Ciencias del Mar, Barcelona, Spain

Observational studies have identified periods of enhanced ENSO predictability from tropical Atlantic variability. Some works have found that this enhancement is provided by the boreal summer Atlantic Equatorial Mode (EM) impact on the atmospheric processes that trigger the following winter ENSO phenomenon. Other works have found how the variability of sea surface temperature (SST) in the northern tropical Atlantic (NTA) during boreal spring acts as ENSOs optimal predictor. The periods of enhanced ENSO predictability appear in phase with the Atlantic Multidecadal Variability (AMV) but no physical explanation has been posed so far. Here we present a hypothesis that conciliates for the first time the existence of both relationships in observations . The results are tested in CMIP5 PI-Control simulations, which allows consideration of a large number of time-periods in which either the NTA or the EM impact ENSO are tested. Model results are consistent with our hypothesis about the switch for the inter-basin connections and the proposed mechanisms. In addition, the model bias in global SST consisting of too high values south of the equator favors some interbasin teleconnections more than others.

Keywords: Atlantic-Pacific interbasin connections, tropical Atlantic variability, ENSO predictability, CMIP5



©2019. Japan Geoscience Union. All Right Reserved.

Interannual variability of Antarctic Intermediate Water in the tropical North Atlantic

*Yao Fu[1], Chunzai Wang[1], Peter Brandt[2,3], Richard J. Greatbatch[2,3]

1. State Key Laboratory of Tropical Oceanography, South China Sea Institute of Oceanology, Chinese Academy of Sciences, Guangzhou, China, 2. GEOMAR Helmholtz Centre for Ocean Research Kiel, Kiel, Germany , 3. Christian-Albrechts-Universität zu Kiel, Kiel, Germany

Interannual variability of Antarctic Intermediate Water (AAIW) in the tropical North Atlantic is investigated using the GECCO2 ocean state estimate and Argo data. AAIW salinity variability near the western boundary is shown to be highly correlated with the western boundary current (WBC) transport on interannual timescales. Northward propagating anomalies are associated with the WBC variability that, in turn, is related to the large-scale wind stress curl forcing by means of the Sverdrup balance. AAIW anomalies also propagate westward with the speed of baroclinic Rossby waves, indicating that the westward propagation of baroclinic Rossby waves also plays a role in the variability of AAIW characteristics. Slow eastward spreading of AAIW anomalies is also identified on decadal timescales. Understanding the observed interannual and decadal variability of AAIW salinity is important to properly interpret salinity changes with respect to changes in the hydrological cycle.

Keywords: Interannual variability of Antarctic Intermediate Water (AAIW) in the tropical North Atlantic, Meridional propagating AAIW salinity anomalies associated with the western boundary current variability, Zonal propagating AAIW anomalies related to baroclinic Rossby wave propagation

©2019. Japan Geoscience Union. All Right Reserved.

Understanding the mechanisms of the Atlantic meridional climate variability

*Hyacinth C Nnamchi[1], Riccardo Farneti[2], Noel S Keenlyside[3], Fred Fred Kucharski[2], Mojib Latif[1]

1. GEOMAR Helmholtz Centre for Ocean Research Kiel, Kiel, Germany, 2. Abdus Salam International Centre for Theoretical Physics, Trieste, Italy, 3. Geophysical Institute, University of Bergen, and Bjerknes Centre for Climate Research, Bergen, Norway

Decadal climate variability over tropical Atlantic is dominated by the Atlantic meridional mode (AMM). The AMM is characterized by opposite sea surface temperature anomalies to the north and south of the equator, anomalous wind flow from the cooler to the warmer hemisphere and meridional shift of the inter-tropical convergence zone. The tropical variability has also been linked to meridional variability in the South Atlantic and the extratropics of North Atlantic, with far-reaching impacts over the adjacent continents. The AMM is primarily understood in terms of the thermodynamic ocean-atmosphere interactions, particularly, the wind-evaporation sea surface feedback. Using a global ocean model forced by atmospheric observations, this study suggests that the Atlantic meridional overturning circulation may affect the Atlantic-scale meridional climate variability.

Keywords: Atlantic meridional mode, AMOC, WES feedback

©2019. Japan Geoscience Union. All Right Reserved.

The corss-equatorical gradient variability: The role of heat, momentum, and freshwater flux

*片岡 崇人[1]
*Takahito Kataoka[1]

1. 研究開発法人　海洋研究開発機構
1. JAMSTEC Japan Agency for Marine-Earth Science and Technology

The ocean-atmosphere feedback associated with the thermodynamic coupling among wind speed, evaporation, and sea surface temperature (SST), called the wind-evaporation-SST (WES) feedback, contributes to the cross-equatorial SST gradient over the tropical oceans. By conducting an eigenanalyses of simple linear air-sea coupled models, it is shown that three additional feedback processes are present when the variable oceanic mixed layer depth (MLD) is considered. The horizontal structures of the leading modes are similar to the WES mode, which shows a meridional dipole in the SST anomalies straddling the equator with cross-equatorial wind anomalies that represent the weakening/strengthening of the trade winds over the warm/cool SST anomalies.
In the presence of the damping term, the WES mode exists as a least damped mode consistent with previous studies. When the buoyancy flux anomaly associated with the latent heat flux anomaly is considered, a similar dipole mode in obtained, but the decaying time scale is about 40 % smaller. The freshwater flux coupling also gives a cross-equatorial gradient mode, but its stability is even smaller (decaying time scale is about 30 % of that of the WES). On the other hand, the momentum coupling allows a strongest meridional dipole variability, which is weakly unstable, indicating the importance of the wind mixing effect on the tropical meridional modes.

キーワード：大気海洋相互作用、熱帯、海洋混合層
Keywords: air-sea interaction, tropics, ocean mixed layer

©2019. Japan Geoscience Union. All Right Reserved.

Generation mechanisms of the Benguela Nino with a focus on local amplification

*東塚 知己[1]、小林 諒[1]
*Tomoki Tozuka[1], Ryo Kobayashi[1]

1. 東京大学大学院理学系研究科地球惑星科学専攻
1. Department of Earth and Planetary Science, Graduate School of Science, The University of Tokyo

Benguela Nino is associated with positive sea surface temperature (SST) anomalies off the west coast of Angola and Namibia in the South Atlantic. Although both local and remote forcing have been indicated to contribute to the development of Benguela Nino, the reason why their relative contribution varies among the events has not been clarified. Thus, the generation mechanisms of the Benguela Nino are investigated in this study by categorizing the events into locally amplified and non-locally amplified events depending on whether alongshore wind anomalies contribute to the development of the Benguela Nino. It is found that the locally events are associated with alongshore northerly wind anomalies related to anomalous weakening of the subtropical anticyclone in the South Atlantic known as St. Helena High and the continental low named Angola Low. On other hands, no alongshore wind anomalies that favor the development of SST anomalies exist in the non-locally amplified events. A mixed layer heat budget analysis reveals that the surface heat flux term is greater in the locally amplified events owing to smaller latent heat release associated with the weakening of the climatological southerly winds, while the anomalous warming by the advection term is stronger in the non-locally amplified events.

キーワード：沿岸ニーニョ、南大西洋、経年変動、セントヘレナ高気圧、アンゴラ低気圧
Keywords: Coastal Nino, South Atlantic, Interannual variation, St. Helena High, Angola Low

©2019. Japan Geoscience Union. All Right Reserved.

Seasonal energy analysis for baroclinic waves in equatorial Atlantic through a diagnostic scheme for energy flux

*Qingyang Song[1], Hidenori AIKI[1]

1. Institute of space-earth environmental research, Nagoya University

This study applied a gravity-reduced ocean model to simulate three baroclinic normal modes covering 20 years for energy analysis in Atlantic Ocean. The model, considering lateral mixing, is driven by decomposed wind forcing for each mode. Energy flux were calculated through a recently proposed diagnostic scheme with model output for all the three modes. The scheme is capable of altering pressure flux to the direction parallel to group velocities of Rossby and mixed Rossby waves in equatorial region (4° N to 4°S) without affecting the divergence. The obtained annual energy flux confirmed the dominant of westward Rossby waves in the northern and southern part of the equatorial region, while eastward Kelvin and mixed Rossby waves are most prevail in central and eastern part. The results are consistent with the fact that in the west tropical Atlantic, the most prominent signal is annual and in the central and east Atlantic, is semi-annual. Additionally, three monthly averaged energy flux revealed the seasonal energy cycle of baroclinic waves in equatorial Atlantic. Two energy sources in August and April emerged in western (around 35°W) and central part (around 15°W) of the equator in Atlantic ocean respectively. Those results suggested that the energy flux calculated by new proposed scheme in Atlantic Ocean can provide a powerful tool for energy analysis making significant contributions for further climate predictions.

Keywords: Equatorial basin mode, Energy flux, Tropical Atlantic, Seasonal variability

©2019. Japan Geoscience Union. All Right Reserved.

[E] 口頭発表 | セッション記号 A (大気水圏科学)：A-HW 水文・陸水・地下水学・水環境

2019年5月30日(木) 9:00 ~ 10:30 | 201B 2F

[A-HW22] 流域の物質輸送と栄養塩循環ー源流域から沿岸海域までー

コンビーナ:小林 政広(国立研究開発法人森林研究・整備機構　森林総合研究所)、吉川 省子(農業・食品産業技術総合研究機構　農業環境変動研究センター)、安元 純(琉球大学　農学部　地域農業工学科)、Adina Paytan(University of California Santa Cruz)、座長:Adina Paytan(University of California, Santa Cruz)

本セッションでは，源流部から沿岸海域を含む流域における物質輸送および栄養塩循環について，幅広い研究分野（陸水学，水文学，地下水学，沿岸海洋学，気象学，土壌学，堆積学，林学，農学，水産学，生態学，社会科学など）からの話題提供を踏まえて，持続可能な流域環境に関する分野横断的な議論を行うことを目的としている．特に，人間活動や気候変動の影響下における複雑で動的な水系における自然現象やその時間変化に主眼をおいた物理，化学，生物学的メカニズムを明瞭にするために，トレーサー技術，分子レベルの技術，水理モデル，古生物学的手法，屋内やフィールドでの試験，生態系サービスや社会ー生態学システムについての社会科学的評価など，流域科学のための新しい手法に基づく研究発表を歓迎する．このセッションを通して，新しい流域科学を創造するために，分野を超えた参加者相互の議論と協力体制作りを目指したい．

9:00 ~ 9:15

[AHW22-06] 沿岸食物網における底生無脊椎動物群集の多様性と統合栄養位置（*i*TP）の関係：「栄養位置の多様性仮説」の検証

*奥田 昇[1]、苅部 甚一[2]、酒井 陽一郎[3]、武山 智博[4]、陀安 一郎[1]、由水 千景[1]、永田 俊[5] (1.総合地球環境学研究所、2.近畿大学、3.琵琶湖環境科学研究センター、4.岡山理科大学、5.東京大学)

9:15 ~ 9:30

[AHW22-07] The analysis of the community composition of riverine bacteria and microalgae in relation to nutrient status and diversity: the case in irrigation season in the Yasu River, Japan

*池谷 透[1]、石田 卓也[1]、上原 佳敏[1]、淺野 悟史[2]、陀安 一郎[1]、奥田 昇[1]、潮 雅之[3,4,5]、藤永 承平[4]、Chia-Ying Ko[6]、Elfritzson Peralta[7]、石川 尚人[8]、岩田 智也[9] (1.総合地球環境学研究所、2.滋賀県琵琶湖環境科学研究センター、3.京都大学白眉センター、4.京都大学生態学研究センター、5.さきがけ 科学技術振興機構、6.National Taiwan University、7.University of Santo Tomas、8.海洋研究開発機構生物地球化学研究分野、9.山梨大学生命環境学部)

9:30 ~ 9:45

[AHW22-08] **Multiple stressors and protection efforts in highly urbanized watersheds in the Philippines**

*Elfritzson M. Peralta[1,3]、Leocris S. Batucan Jr.[4,6]、Alexis E. Belen[2,3]、Irisse Bianca B. De Jesus[1,3]、Takuya Ishida[5]、Chia-Ying Ko[7]、Yuki Kobayashi[5]、Tohru Ikeya[5]、Yoshitoshi Uehara[5]、Tomoya Iwata[8]、Adelina S. Borja[9]、Jonathan Carlo A. Briones[1,2,3]、Francis S. Magbanua[4]、Rey Donne S. Papa[1,2,3]、Noboru Okuda[5] (1.Research Center for the Natural and Applied Sciences, University of Santo Tomas, PH、2.Department of Biological Sciences, University of Santo Tomas, PH、3.The Graduate School, University of Santo Tomas, PH、4.Institute of Biology, University of the Philippines Diliman, PH、5.Research Institute for Humanity and Nature, JP、6.Academia Sinica and Department of Life Science, National Taiwan Normal University, TW、7.Institute of Fisheries Science and Department of Life Science, National Taiwan University, TW、8.Faculty of Life and Environmental Sciences, University of Yamanashi, JP、9.Resource Management and Development Department, Laguna Lake Development Authority, PH)

9:45 ~ 10:00

[AHW22-09] ベトナム中部の野菜畑における浅層地下水のアンモニア態窒素汚染

★招待講演

*前田 守弘[1]、藤村 拓也[1]、Hoang Ngoc Tuong Van [2]、井上 大介[3]、近森 秀高[1]、兵藤 不二夫[1] (1.岡山大学、2.フエ大学、3.大阪大学)

10:00 ~ 10:15

[AHW22-10] Modelling nutrient and organic waste behaviour in a tropical wetland in Singapore under projected anthropogenic scenarios

*Swee Yang Edmund Low[1]、Dong Eon Kim[1]、Canh Tien Trinh Nguyen[1]、Yixiong Cai、Shie-Yui Liong[1] (1.National University of Singapore)

10:15 ~ 10:30

[AHW22-11] **Benthic macroinvertebrate assemblages and water quality reflect the impacts of land use and land cover in Marikina Watershed, Philippines**

*Julie - An N. Gregorio[1,2]、Elfritzson M. Peralta[3,5]、Irisse Bianca B. de Jesus[3,5]、Tohru Ikeya[6]、Jonathan Carlo A. Briones[3,4,5]、Rey Donne S. Papa[3,4,5]、Francis S. Magbanua[1]、Noboru Okuda[6] (1.Institute of Biology, University of the Philippines, Diliman, Quezon City, 1101 Philippines、2.Institute of Environmental Science and Meteorology, University of the Philippines, Diliman, Quezon City 1101 Philippines、3.Research Center for the Natural and Applied Sciences, University of Santo Tomas, España Boulevard, Manila, 1015, Philippines、4.Department of Biological Sciences, University of Santo Tomas, España Boulevard, Manila, 1015, Philippines、5.The Graduate School, University of Santo Tomas, España Boulevard, Manila, 1015, Philippines、6.Research Institute for Humanity and Nature, 457-4 Motoyama, Kamigamo, Kyoto, 603-8047, Japan)

沿岸食物網における底生無脊椎動物群集の多様性と統合栄養位置（*i*TP）の関係：「栄養位置の多様性仮説」の検証

Biodiversity increases integrated trophic position of macroinvertebrate communities in coastal food webs: testing the vertical diversity hypothesis

*奥田 昇[1]、苅部 甚一[2]、酒井 陽一郎[3]、武山 智博[4]、陀安 一郎[1]、由水 千景[1]、永田 俊[5]
*Noboru Okuda[1], Jin'ichi Karube[2], Yoichiro Sakai[3], Tomohiro Takeyama[4], Ichiro Tayasu[1], Chikage Yoshimizu[1], Toshi Nagata[5]

1. 総合地球環境学研究所、2. 近畿大学、3. 琵琶湖環境科学研究センター、4. 岡山理科大学、5. 東京大学
1. Research Institute for Humanity and Nature, 2. Kindai University, 3. Lake Biwa Environmental Research Institute, 4. Okayama University of Science, 5. University of Tokyo

Introduction

Study on relationships between biodiversity and ecosystem functioning (BEF) has attracted social as well as ecological interests because the biodiversity can affect ecosystem processes, especially productivity, which determines provisioning service for humanity. Because of difficulty in accurate measurement of the productivity, however, biomass has been traditionally used as its proxy to assess the BEF. Positive correlations between biodiversity and biomass-based productivity indices have been reported for many plants both in terrestrial and aquatic ecosystems. Such correlations are also true for consumers in terrestrial systems. In aquatic ecosystems, in contrast, the biomass-based BEF relationships are inconsistent among consumer communities: some are positive or convex and others non-significant (Waide et al. 1999).

Such an inconsistency can be explained by vertical diversity, i.e., diversity of trophic positions. In systems with multitrophic interactions, in theory, consumer biomass exponentially decreases with the increasing trophic position, while underlying more primary products. The use of the consumer biomass as a proxy of its productivity is, therefore, inappropriate to view the BEF relationships in complex multitrophic systems, as in the case of aquatic food webs. Considering the multitrophic and multifunctional nature of real food webs, Wang & Brose (2018) recently have constructed a theoretical model to test vertical diversity hypothesis (VDH), predicting that functional diversity across the TPs can enhance trophic biomass flows from basal resources to top predators.

In the multitrophic and multifunctional systems, one of better ways for full-understanding of the BEF is to estimate trophic biomass flows, using carbon ($\delta^{13}C$) and nitrogen ($\delta^{15}N$) stable isotope analysis, which is a powerful tool for the food web analysis. Taking advantage of this analysis, Ishikawa et al. (2017) have proposed a novel index of food web properties, integrated trophic position (hereafter, *i*TP), defined as the summed TPs of all taxa in a focal food web weighed by the relative biomass of each taxon. The *i*TP can provide appropriate estimate for ecosystem functioning of vertical diversity because it indicates how many times consumer biomass experiences metabolic turnover as a whole of community within its food web. Here we test how the biodiversity can affect *i*TP for benthic macroinvertebrates in coastal waters of Lake Biwa, focusing on within-lake variation in coastal environments which can alter their local communities and thus food web properties.

©2019. Japan Geoscience Union. All Right Reserved.

Materials & Methods

We collected benthic macroinvertebrates and their basal food sources from 33 shallow coastal waters of Lake Biwa. For each sampling site, the macroinvertebrates were sorted, identified and counted to calculate Shannon-Wiener diversity index (H'). For each taxon at each site, its dry mass was measured to calculate its biomass per unit area. Individual taxa and their basal foods at each site were provided for $\delta^{13}C$ and $\delta^{15}N$ stable isotope analysis. After this analysis, we calculated *i*TP, according to Ishikawa et al. (2017).

Results & Discussion

A total of 27 benthic macroinvertebrate taxa were found in coastal waters of Lake Biwa. In the coastal communities, oligochaetes and chironomids are the most dominant taxa in numerical abundance, while gazing snails and a suspension-feeding bivalve were the most dominant in biomass abundance. Most taxa of grazers and deposit feeders located around TP=2, while carnivorous leeches and a freshwater prawn had the highest TP, regarded as top predators of macroinvertebrate communities.
The community biomass tended to increase significantly but weakly with macroinvertebrate diversity H'. By contrast, *i*TP of coastal macroinvertebrate communities markedly increased when they have the higher H' (Fig. 1). The within-lake variation in their *i*TPs was better accounted for not only by the relative biomass abundance of top predators with highest TPs and lower numerical abundance but also by that of deposit feeders with lower TP and highest numerical abundance: the former can increase the relative contribution of predator TPs to the *i*TP, while the latter can have negative effects not only on the *i*TP but also on H' because of its numerical abundance. This is possible explanation for such a correlational pattern of BEF found in the coastal macroinvertebrate communities, empirically supporting the VDH. Our study demonstrated that the *i*TP rather than the consumer community biomass can be a promising indicator for BEF related to vertical diversity in aquatic food webs with multitrophic interactions.

キーワード：生物多様性－生態系機能、食物網、統合栄養位置、琵琶湖、安定同位体分析、栄養段階の多様性
Keywords: Biodiversity-Ecosystem functioning, Food web, Integrated trophic position, Lake Biwa, Stable isotope analysis, Vertical diversity

©2019. Japan Geoscience Union. All Right Reserved.

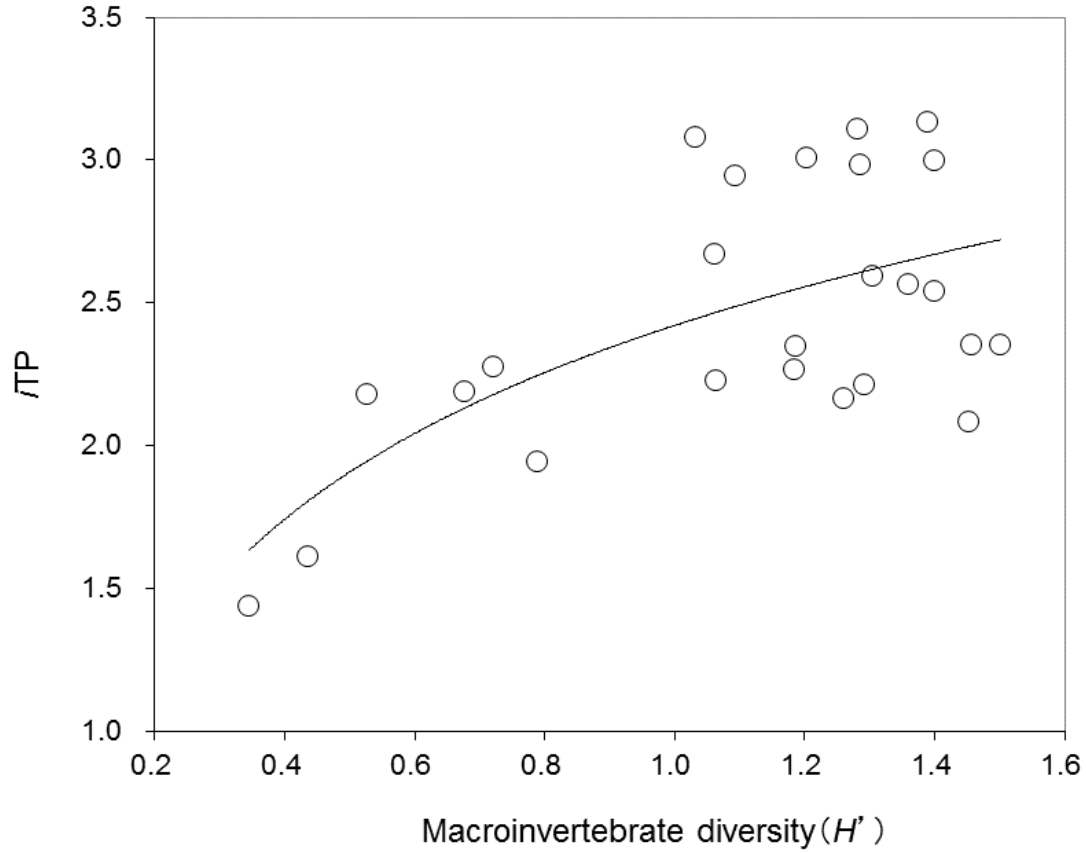


Fig. 1 A positive correlation between diversity (H') and integrate trophic position (iTP) for benthic macroinvertebrate communities in coastal waters of Lake Biwa.

©2019. Japan Geoscience Union. All Right Reserved.

The analysis of the community composition of riverine bacteria and microalgae in relation to nutrient status and diversity: the case in irrigation season in the Yasu River, Japan

The analysis of the community composition of riverine bacteria and microalgae in relation to nutrient status and diversity: the case in irrigation season in the Yasu River, Japan

*池谷 透[1]、石田 卓也[1]、上原 佳敏[1]、淺野 悟史[2]、陀安 一郎[1]、奥田 昇[1]、潮 雅之[3,4,5]、藤永 承平[4]、Chia-Ying Ko[6]、Elfritzson Peralta[7]、石川 尚人[8]、岩田 智也[9]
*Tohru Ikeya[1], Takuya Ishida[1], Yoshitoshi Uehara[1], Satoshi Asano[2], Ichiro Tayasu[1], Noboru Okuda[1], Masayuki Ushio[3,4,5], Shohei Fujinaga[4], Chia-Ying Ko[6], Elfritzson Martin Peralta[7], Naoto F. Ishikawa[8], Tomoya Iwata[9]

1. 総合地球環境学研究所、2. 滋賀県琵琶湖環境科学研究センター、3. 京都大学白眉センター、4. 京都大学生態学研究センター、5. さきがけ 科学技術振興機構、6. National Taiwan University、7. University of Santo Tomas、8. 海洋研究開発機構生物地球化学研究分野、9. 山梨大学生命環境学部
1. Research Institute for Humanity and Nature, 2. Lake Biwa Environmental Research Institute, 3. Hakubi Center, Kyoto University, 4. Center for Ecological Research, Kyoto University, 5. PRESTO, Japan Science and Technology Agency, 6. National Taiwan University, 7. University of Santo Tomas, 8. Department of Biogeochemistry, Japan Agency for Marine-Earth Science and Technology, 9. Faculty of Life and Environmental Sciences, Yamanashi University

The previous our analysis based on the community composition of microalgae and bacteria have shown that; 1) the beta diversity distances of algae and bacteria were significantly different between the four categories of land use in the Yasu River, 2) the ordinations of the sampling sites by the riverine microbial composition can be regressed by the environmental gradients between the sites in the watershed, 3) the diversity indices of bacteria increased with diversity index of algae. The further analyses of elemental composition of epilithic matter, most of which may be constituted from algae and bacteria, were made in order the assess the internal nutrient status of the epilithon. Both phosphorus amount per unit area and chlorophyll per carbon showed a significant positive correlation with phosphorus per carbon ($P < 10^{-8}$). Such ordination may help to realize whether phosphorus availability is limited to sustain the biofilm abundance or microbial activities so as to consider the possible impact of land use on the community composition and diversity of algae and bacteria. The richness of algae decreased with the decline of phosphorus per carbon of epilithic matter whereas that of bacteria was bifurcated. So, the richness and the Shannon diversity index (H') of algae showed a significant positive relationship with the phosphorus per carbon (possible index of phosphorus availability) ($P < 10^{-4}$), whereas those of bacteria showed insignificant relationship ($P > 0.2$). Most of low bacteria richness sites at low phosphorus per carbon corresponded to those where chlorophyll abundance per unit area is relatively high in spite of low phosphorus availability.

キーワード：バクテリア、微細藻類、16S、次世代シーケンサー、リン
Keywords: bacteria, microalgae, 16S, MiSeq, phosphorus

©2019. Japan Geoscience Union. All Right Reserved.

Multiple stressors and protection efforts in highly urbanized watersheds in the Philippines

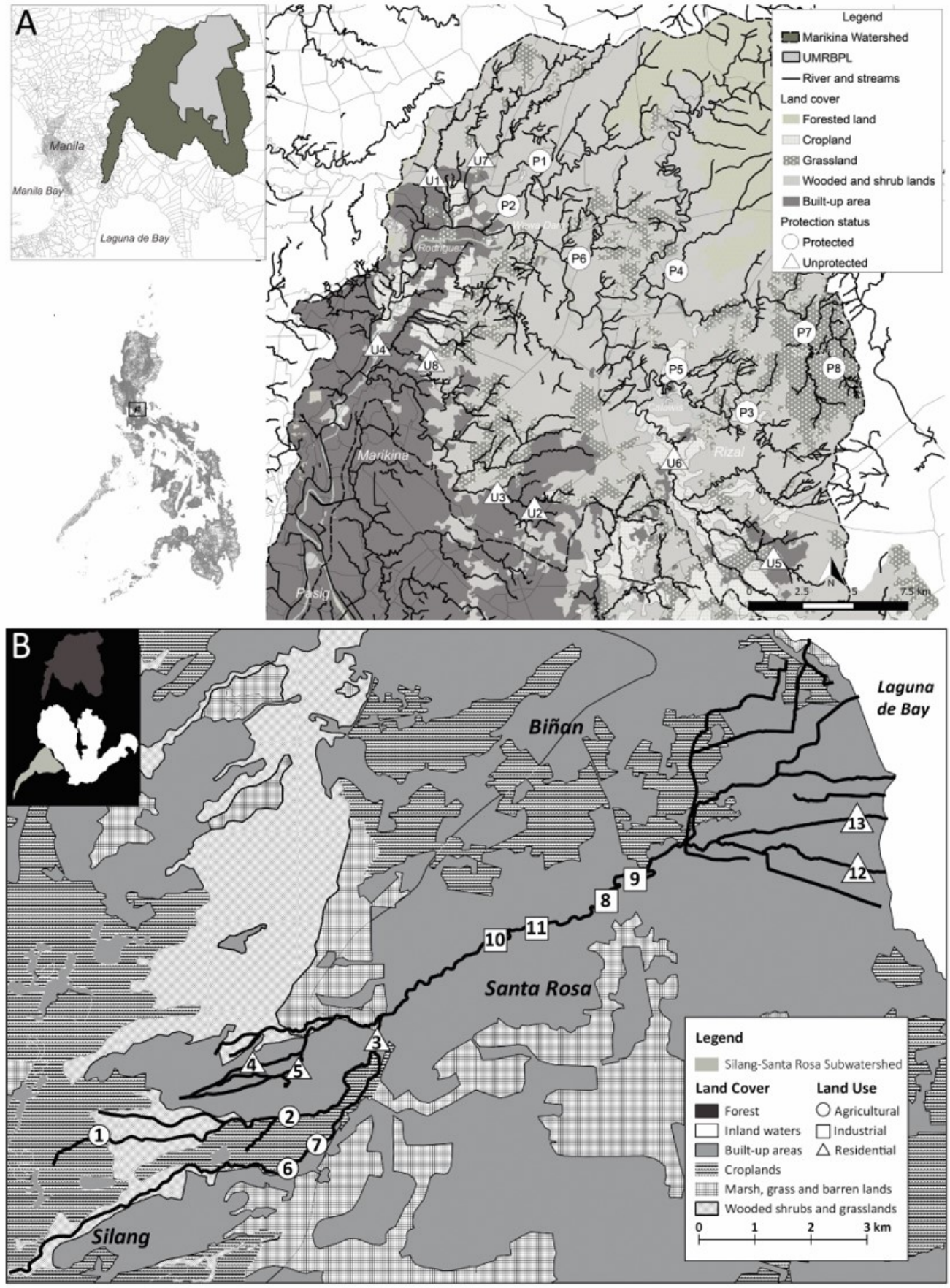
*Elfritzson M. Peralta[1,3], Leocris S. Batucan Jr.[4,6], Alexis E. Belen[2,3], Irisse Bianca B. De Jesus[1,3], Takuya Ishida[5], Chia-Ying Ko[7], Yuki Kobayashi[5], Tohru Ikeya[5], Yoshitoshi Uehara[5], Tomoya Iwata[8], Adelina S. Borja[9], Jonathan Carlo A. Briones[1,2,3], Francis S. Magbanua[4], Rey Donne S. Papa[1,2,3], Noboru Okuda[5]

1. Research Center for the Natural and Applied Sciences, University of Santo Tomas, PH, 2. Department of Biological Sciences, University of Santo Tomas, PH, 3. The Graduate School, University of Santo Tomas, PH, 4. Institute of Biology, University of the Philippines Diliman, PH, 5. Research Institute for Humanity and Nature, JP, 6. Academia Sinica and Department of Life Science, National Taiwan Normal University, TW, 7. Institute of Fisheries Science and Department of Life Science, National Taiwan University, TW, 8. Faculty of Life and Environmental Sciences, University of Yamanashi, JP, 9. Resource Management and Development Department, Laguna Lake Development Authority, PH

Among developing countries in the tropics, urban stream syndrome is primarily driven by multiple environmental stressors, such as nutrient pollution and habitat degradation, due to social-economic developments in the catchment. To aid in environmental mitigation, improved conservation effort was recently set based on the Convention of Biological Diversity Aichi Target 11 that underscores global expansion of protected areas in terrestrial and aquatic environments. As such, this study aims to disentangle the overlaying effects of nutrient pollution and deforestation on benthic macroinvertebrate communities and assess the recent protection efforts in the watersheds of Laguna de Bay, Philippines. Study sites in Silang-Santa Rosa Subwatershed (13) and Marikina Watershed (16) were sampled for benthic macroinvertebrates and surveyed for environmental factors such as land cover and land use patterns, human population density (HPD), and stream physicochemistry including nutrient concentrations. Multivariate and multiple regression analyses on macroinvertebrate assemblages and environmental variables efficiently delineated sites according to degree of human impacts in Silang-Santa Rosa Subwatershed and the status of protection in Marikina Watershed. Canopy openness, HPD, conductivity, dissolved oxygen, and nutrients (total phosphorus, nitrates, ammonia) appeared to be the most important variables in predicting assemblages of benthic macroinvertebrates. This study effectively demonstrated how Silang-Santa Rosa Subwatershed’ s HPD and canopy openness, as proxies for human activities and deforestation, respectively, impact stream environments and the benthic communities. Furthermore, the recent establishment of Upper Marikina River Basin Protected Landscape inside Marikina Watershed was successfully used to show how freshwater protected areas are effective in combatting stream habitat destruction and biodiversity loss. Our findings timely show the crucial role of freshwater protected areas in conserving stream ecosystems from the effects of unsustainable urbanization in a developing country like the Philippines.

Keywords: Human population density, Deforestation, Freshwater protected area, Aichi Target 11, Biodiversity loss

©2019. Japan Geoscience Union. All Right Reserved.



©2019. Japan Geoscience Union. All Right Reserved.

ベトナム中部の野菜畑における浅層地下水のアンモニア態窒素汚染
Ammonium contamination of shallow groundwater beneath vegetable fields in Central Vietnam

*前田 守弘[1]、藤村 拓也[1]、Hoang Ngoc Tuong Van [2]、井上 大介[3]、近森 秀高[1]、兵藤 不二夫[1]
*Maeda Morihiro[1], Takuya Fujimura[1], Van Ngoc Tuong Hoang[2], Daisuke Inoue[3], Hidetaka Chikamori[1], Fujio Hyodo[1]

1. 岡山大学、2. フエ大学、3. 大阪大学
1. Okayama University, 2. Hue University, 3. Osaka University

Nitrogen contamination in shallow groundwater occurs in a coastal area in Central Vietnam. In agricultural fields close to the residential area, high concentrations of NH_4^+ and NO_3^- in groundwater was attributed to unintended inflow of livestock wastes and/or domestic wastewater. On the other hand, NH_4^+ concentration reaches to several milligrams N per liter even in vegetable fields away from the residential area. The objective of this study was to determine NH_4^+ contamination mechanisms of the shallow groundwater without domestic wastewater inflow. In this study, we tested three hypotheses: (i) NH_4^+ derived from fertilizer or manure applied to the fields was transported to groundwater thorough soil, (ii) nitrate (NO_3^-) produced as a result of nitrification in topsoil was transferred to deep soil and again transformed to NH_4^+, or (iii) nitrogen mineralization occurred in deep soil. Soil samples were collected up to 240 cm from a vegetable production field in Quang Thang Commune, Central Vietnam in June (dry season) and November (rainy season) of 2016 and 2017. The groundwater table existed at 57 or 67 cm in June and 33 cm from the soil surface in November. Concentrations of NH_4^+ in PVC pipe wells fluctuated between 1 and 3 mg N L^{-1} in accordance with the detection of soil NH_4^+ content (5-20 mg kg^{-1}) in the 150-240 cm layer. On the other hand, soil NH_4^+ was not detected in the 30-80 cm layer whereas it was 2-6 mg kg^{-1} in the 0-10 cm layers, indicating that NH_4^+ was not transferred to layers deeper than 30 cm. The absence of a functional gene of dissimilatory nitrate reduction to NH_4^+ (DNRA) in the 150-240 cm soil layer shows that DNRA did not occur in this deep layer. Natural abundance values of ^{15}N ($\delta^{15}N$) for soil NH_4^+ (+3.6 to 5.5‰) were similar to those in soil total N (+1.9 to 3.6‰) in the 150-240 cm layer. In addition, anaerobically incubated soil from the 140-160 cm layer was mineralized by 1-2 mg NH_4^+-N kg^{-1} for 8 weeks. These experimental results suggest that the high concentration of NH_4^+ found in wells was originated from mineralization of deep soil.

キーワード：アンモニア態窒素、異化型硝酸還元アンモニウム、窒素無機化
Keywords: ammonium , dissimilatory nitrate reduction to ammonium, nitrogen mineralization

©2019. Japan Geoscience Union. All Right Reserved.

Modelling nutrient and organic waste behaviour in a tropical wetland in Singapore under projected anthropogenic scenarios

*Swee Yang Edmund Low[1], Dong Eon Kim[1], Canh Tien Trinh Nguyen[1], Yixiong Cai, Shie-Yui Liong[1]

1. National University of Singapore

Nee Soon swamp forest is one of the last vestiges of tropical wetland in Singapore, and is important both as a site for ecological preservation, as well as a source of water for potable treatment. Understanding the hydrological regime of the swamp forest and implications for water quality is critical to guide stakeholders in implementing effective measures to preserve the wetland against anthropogenic impacts. In particular, although current field measurement data do not indicate a concern with organic or nutrient pollution, reviewing the ways in which the wetland responds to elevated waste discharges can help identify potential hotspots, and the impact on the outflow from the catchment which drains into downstream controlled watercourses. An integrated water quality model is therefore developed in this study to investigate spatial and temporal concentrations of DO levels, organic pollution (as quantified by biochemical oxygen demand, BOD), and nutrient pollution (NH3-N and NO3-N) within the catchment’s river network under projected scenarios of upstream wastewater inflow. The model was developed using MIKE HYDRO for modelling the study domain, as well as the MIKE ECO Lab numerical laboratory for characterising water quality processes. Model parameters are calibrated against time series of observed discharges and dissolved oxygen levels at measurement stations along the river network. The calibrated model was then applied to study downstream impact due to elevated BOD and ammonia from upstream wastewater discharge. Over a simulation period of April 2014 to December 2015, the model predicted that a spiked inflow of 400 mg/l BOD and 30 mg/l NH3-N upstream will elevate downstream concentrations at the catchment outlet to an average of 13 mg/l BOD, and 0.7 mg/l nitrogen (NH3-N, NO3-N), from a baseline of 0.4 mg/l BOD, 0.03 mg/l NH3-N, and 0.07 mg/l NO3-N. Levels of DO were decreased from an initial 5.4 mg/l to 3.6 mg/l. Though a scenario of spiked pollutant influx at the swamp forest’s undeveloped upstream sub-catchments is currently unlikely to occur, the outcomes nevertheless will be beneficial for future planning studies in understanding how the water quality of the catchment will be impacted should urban redevelopment works be considered around the swamp forest.

Keywords: Wetland, Organic waste impact, Nutrient impact, Water quality, Modeling

©2019. Japan Geoscience Union. All Right Reserved.

Benthic macroinvertebrate assemblages and water quality reflect the impacts of land use and land cover in Marikina Watershed, Philippines

*Julie - An N. Gregorio[1,2], Elfritzson M. Peralta[3,5], Irisse Bianca B. de Jesus[3,5], Tohru Ikeya[6], Jonathan Carlo A. Briones[3,4,5], Rey Donne S. Papa[3,4,5], Francis S. Magbanua[1], Noboru Okuda[6]

1. Institute of Biology, University of the Philippines, Diliman, Quezon City, 1101 Philippines, 2. Institute of Environmental Science and Meteorology, University of the Philippines, Diliman, Quezon City 1101 Philippines, 3. Research Center for the Natural and Applied Sciences, University of Santo Tomas, España Boulevard, Manila, 1015, Philippines, 4. Department of Biological Sciences, University of Santo Tomas, España Boulevard, Manila, 1015, Philippines, 5. The Graduate School, University of Santo Tomas, España Boulevard, Manila, 1015, Philippines, 6. Research Institute for Humanity and Nature, 457-4 Motoyama, Kamigamo, Kyoto, 603-8047, Japan

Watershed systems provide various ecological services such as good water quality, regulate water flow, maintain water balance and biodiversity conservation. However, human disturbances greatly affect the water quality and composition of biotic communities. Although anthropogenic changes in freshwater systems were truly evident, studies focusing on the human impacts on tropical watersheds are still limited in developing countries. Thus, this study aims to investigate the response of freshwater macroinvertebrates to varying land use patterns and land cover characteristics in Marikina Watershed, Philippines. For a total of 30 streams, which were categorized into 7 protected, 3 forested, 8 agricultural, and 12 residential streams based on land use and cover in their catchments, were collected benthic macroinvertebrates and measured environmental variables. PCA plots were not able to classify water quality according to land use and was supported with no significant difference in Kruskal –Wallis test. However, water quality of primarily vegetated and primarily non-vegetated sites as well as protected and protected streams had delineation, as accorded with the results of independent *t* - tests with significant differences ($p<0.05$) on dissolved oxygen, conductivity, total dissolved solids and salinity. While the forested streams are clustered together in the NMDS plot but there is no clear pattern in the assemblage of benthic macroinvertebrates. The similarities in the composition of macroinvertebrates could be attributed to the similar magnitude and intensity of landscape alteration of each land use among the streams. Interestingly, the nMDS plot shows strong separation of macroinvertebrate assemblages across gradient of vegetation area (Global $R = 0.388$, $P = 0.001$) and were supported independent *t*- test where with macroinvertebrate diversity, density and abundance of pollution-sensitive taxa on primarily vegetated areas exhibited significant differences from non-vegetated areas ($p < 0.05$). Additionally, biotic indices such as such as SingScore, Average Score per Taxon THAI ($ASPT^{THAI}$), Biological Monitoring Working Party ($BMWP^{THAI}$), and Stream Invertebrate Grade Number Average Level version 2 (SIGNAL 2) reveal significant differences among protection status, land use types and land cover ($p<0.05$). CCA plot also revealed pollution –sensitive taxa with primarily vegetated sites were associated with pollution-sensitive taxa and primarily non-vegetated sites are associated with pollution-tolerant organisms to on CCA plot. The findings of this study demonstrate the effects of land alteration to the macroinvertebrate community and water quality. Furthermore, it emphasizes the importance of vegetation cover and designation of protected areas to have better ecological quality in a watershed. This study thus suggests for an extensive and improved policy development and implementation. Furthermore, extensive biomonitoring and formulation of Marikina Watershed Biotic Index are recommended.

Keywords: Marikina Watershed, land use, land cover, water quality, benthic macroinvertebrates

©2019. Japan Geoscience Union. All Right Reserved.

[E] 口頭発表 | セッション記号 A (大気水圏科学)：A-HW 水文・陸水・地下水学・水環境

2019年5月30日(木) 10:45 ~ 12:15 | 201B 2F

[A-HW22] 流域の物質輸送と栄養塩循環ー源流域から沿岸海域までー

コンビーナ:小林 政広(国立研究開発法人森林研究・整備機構　森林総合研究所)、吉川 省子(農業・食品産業技術総合研究機構　農業環境変動研究センター)、安元 純(琉球大学　農学部　地域農業工学科)、Adina Paytan(University of California Santa Cruz)、座長:安元 純(琉球大学　農学部　地域農業工学科)

本セッションでは，源流部から沿岸海域を含む流域における物質輸送および栄養塩循環について，幅広い研究分野（陸水学，水文学，地下水学，沿岸海洋学，気象学，土壌学，堆積学，林学，農学，水産学，生態学，社会科学など）からの話題提供を踏まえて，持続可能な流域環境に関する分野横断的な議論を行うことを目的としている．特に，人間活動や気候変動の影響下における複雑で動的な水系における自然現象やその時間変化に主眼をおいた物理，化学，生物学的メカニズムを明瞭にするために，トレーサー技術，分子レベルの技術，水理モデル，古生物学的手法，屋内やフィールドでの試験，生態系サービスや社会ー生態学システムについての社会科学的評価など，流域科学のための新しい手法に基づく研究発表を歓迎する．このセッションを通して，新しい流域科学を創造するために，分野を超えた参加者相互の議論と協力体制作りを目指したい．

10:45 ~ 11:00

[AHW22-12] **Characterization, distribution and degradation of environmental plastics in inland river system of Mongolia**

*Batdulam Battulga[1]、Masayuki Kawahigashi[1]、Bolormaa Oyuntsetseg[2] (1.Department of Geography, Tokyo Metropolitan University, Tokyo, 192-0397, Japan 、2.Department of Chemistry, National University of Mongolia, Ulaanbaatar, 210646, Mongolia)

11:00 ~ 11:15

[AHW22-13] Multi-site and multi-approach sediment transport modeling in tropical watersheds

★Invited Papers

*Assefa M Melesse[1]、Alemu Osore Aga[2]、Hagos Gebreselassie[2] (1.Florida International University、2.Addis Ababa University)

11:15 ~ 11:30

[AHW22-14] 流域土地利用モデルによるSS濃度係数の算出

*吉川 省子[1]、馬 東来[1,2]、齋藤 忠将[1,3]、松森 堅治[4]、伊藤 優子[5]、小林 政広[5] (1.農業・食品産業技術総合研究機構　農業環境変動研究センター、2.筑波大学大学院、3.茨城大学農学部、4.農業・食品産業技術総合研究機構　西日本農業研究センター、5.国立研究開発法人　森林研究・整備機構森林総合研究所)

11:30 ~ 11:45

[AHW22-15] Evaluation of long term variation in water balance and discharge of sediment and nitrogen in the urbanized catchment of Yamato River, using SWAT model

*王 崑陽[1,2]、清水 裕太[3]、小野寺 真一[1]、齋藤 光代[4]、友澤 裕介[1] (1.広島大学、2.首都師範大学、3.農研機構、4.岡山大学)

11:45 ~ 12:00

[AHW22-16] Causal correlation between water-use of the Tedori River and coastal erosion of Chirihama Nagisa Driveway, Ishikawa, Japan

*百瀬 年彦[1] (1.石川県立大学)

12:00 ~ 12:15

[AHW22-17] セレンガ河における元素動態への懸濁粒子の役割

★招待講演

*川東 正幸[1]、Orgilbold Myangan[2]、Bolormaa Oyuntsetseg[2] (1.首都大学東京、2.モンゴル国立大学)

Characterization, distribution and degradation of environmental plastics in inland river system of Mongolia

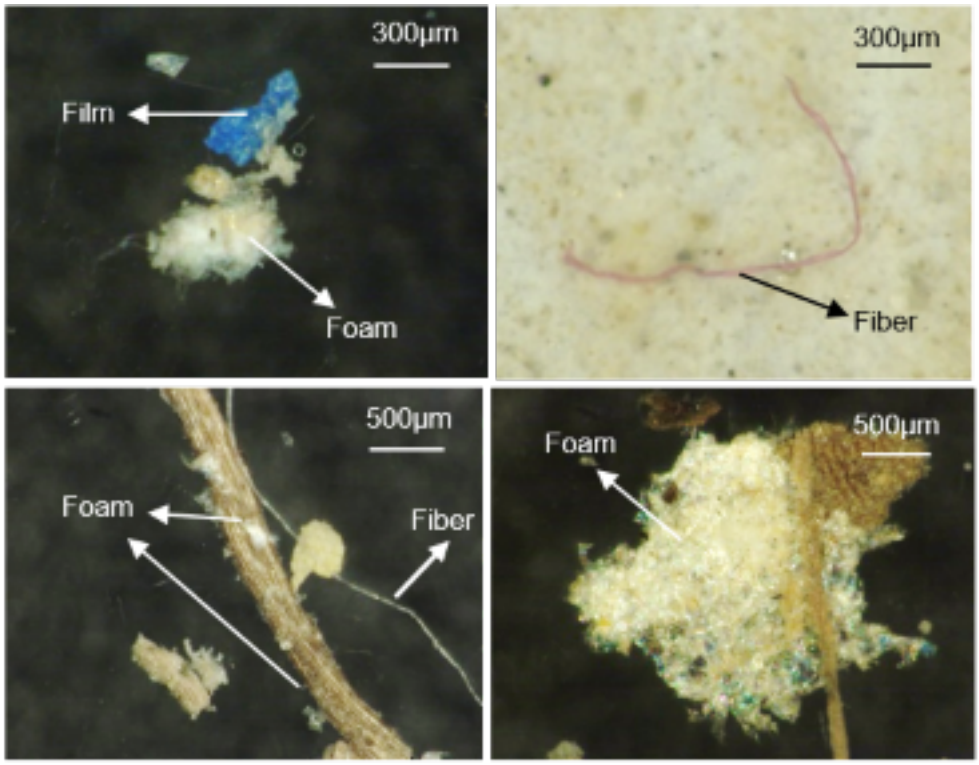
*Batdulam Battulga[1], Masayuki Kawahigashi[1], Bolormaa Oyuntsetseg[2]

1. Department of Geography, Tokyo Metropolitan University, Tokyo, 192-0397, Japan , 2. Department of Chemistry, National University of Mongolia, Ulaanbaatar, 210646, Mongolia

Marine plastic abundance and distribution have been reported toward increasing importance of their behavior as anthropogenic influences on aquatic environment. However, remains of plastics particularly in freshwater are largely unknown. Tributaries in the Selenga River system are important sources of fresh water in Central and Northern Mongolia, although the river system has been alarmed by various kinds of pollution because of growing population and increasing demand of land and resources. Evaluating fate of plastics in the river is vital to assess how the urban system affects plastic pollution in Selenga River. This study aimed to identify the fate of environmental plastics in the Selenga River system of Mongolia.
In 2017 and 2018, totally 18 sampling sites have been surveyed according to geographical locations from the capital city, Ulaanbaatar. Collected plastics were classified as their sizes (micro, meso, macro and mega) and materials such as films, foams, fragments and fibers. Visually sorted plastics identified by FTIR micro-spectroscopy to determine chemical characterization. Furthermore, a degradation index of collected plastics was examined using a ratio of two specific IR absorptions. Invisible microplastics (MP) attached onto the collected plastics were separated mainly from polystyrene foam (PSF), which was the most dominant environmental plastics in the research field. Characterization of the invisible MP was conducted using a digital microscope and an FTIR micro-spectroscopy.
Plastic films and foams were largely occupied in the collected plastics from the researched rivers. Surprisingly great amount of PSF were found in micro and meso size ranges. The results illustrate that on-site fragmentation and degradation of bulk PSF occurred in the research sites probably due to solar radiation and freeze-thaw cycles. A broad range of the degradation index was recorded in micro, meso and macro sized PSF, indicating that various stages of degradation occurred in the river environment. Apart from the other plastics types, PSF was considered as a carrier of invisible MP. A greater diversity of invisible MP types and numbers were found in a microscopic view using a digital microscope on the surface of PSF. Polyethylene (PE) and polystyrene (PS) were major components of the sorbed MP.
This study represents the first detailed examination of the distribution, types and degradation processes of plastics in the Mongolian river system. Environmental plastics were widespread litter in the investigated Mongolian river shores due to low-level of waste management with rapidly growing population and urbanization.

Keywords: Plastic debris, River shore, Mongolia, Degradation, Microplastics

©2019. Japan Geoscience Union. All Right Reserved.



Microscopic view of microplastics attached onto visible polystyrene foam (PSF).

©2019. Japan Geoscience Union. All Right Reserved.

Multi-site and multi-approach sediment transport modeling in tropical watersheds

*Assefa M Melesse[1], Alemu Osore Aga[2], Hagos Gebreselassie[2]

1. Florida International University, 2. Addis Ababa University

Land degradation and poor watershed management have been the major factors that led to severe soil erosion and hence sedimentation in receiving water bodies and reservoirs. The environmental impacts of sediment transport and loading is highly pronounced in tropical watersheds where rainfall is erratic and torrential and soil and conservation measures are poor. In this study, a soil erosion, sediment yield and transport modeling were conducted in three tropical watersheds in Ethiopia and Kenya. Field plot experiment, model development and evaluation were conducted. The impact of land use, rainfall intensity and slope were evaluated at plot and watershed scales. Three models (WEPP, SWAT and Erosion 3D) were tested and compared. The results indicate that the models performed differently with Erosion 3D and WEPP performed better in sediment load simulation. In the absence of the observed sediment data, sediment rating curves developed and validated were useful and are promising.

Keywords: Sediment flux, Sediment modeling, Erosion 3D, SWAT, WEPP, Tropical watersheds

©2019. Japan Geoscience Union. All Right Reserved.

流域土地利用モデルによるSS濃度係数の算出
Calculation of SS concentration coefficients of river water for each land use by a simple watershed model.

*吉川 省子[1]、馬 東来[1,2]、齋藤 忠将[1,3]、松森 堅治[4]、伊藤 優子[5]、小林 政広[5]
*Seiko Yoshikawa[1], Donglai Ma[1,2], Tadamasa Saito[1,3], Kenji Matsumori[4], Yuko Itoh[5], Masahiro Kobayashi[5]

1. 農業・食品産業技術総合研究機構　農業環境変動研究センター、2. 筑波大学大学院、3. 茨城大学農学部、4. 農業・食品産業技術総合研究機構　西日本農業研究センター、5. 国立研究開発法人　森林研究・整備機構森林総合研究所
1. Institute for Agro-environmental Sciences, National Agriculture and Food Research Organization, 2. Graduate Scool, Tsukuba University , 3. Faculty of Agriculture, Ibaraki University , 4. Western Region Agricultural Research Center, National Agriculture and Food Research Organization, 5. Forestry and Forest Products Research Institute

近年、降雨の気候変動に起因する降雨の激化や局所化により、土砂災害が増加している。土砂災害の起きる場所や程度を予測することは困難であるが、まず、近年の平均的な土砂流出程度を把握し、それに基づき、雨の降り方が変わった場合の土砂量の増減を予測する方法が合理的であると考えられる。

土砂流出は、土地利用、植生、保全策、立地条件、降水などの気象条件等により左右される。なかでも、平水年では土地利用の影響が大きいと予想される。ここでは、今後の土砂災害の予測に資するために、全国の河川流域を対象に、土地利用毎の水系へのSSの負荷強度を示す濃度係数を、簡易な流域土地利用モデルにより算出する。公開されているDEM(国土地理院、10B、ラスターデータ)、および高解像度土地利用土地被覆図（JAXA、ALOS AVNIR-2、10mメッシュデータ）を用いて、公共用水域測定地点を下端とする流域と、その流域の土地利用（水田、畑、森林、市街地）面積割合を求めた。一方、環境省の公共用水域測定地点データについて、2000~2009年の10年間の測定データの揃っている地点について、SS濃度の算術平均値を求めた。そして流域ごとの土地利用比率を説明変数、流域ごとのSS濃度を目的変数とする以下の重回帰式により、各土地利用の負荷強度の指標となる濃度係数を算出した。

$$C = a_1 x_1 + a_2 x_2 + a_3 x_3 + a_4 x_4$$

Cは河川SS濃度 (mg L^{-1})　a_iは土地利用iのSS濃度係数　x_iは土地利用iの面積率
土地利用 i は 1;水田 2;畑 3;森林 4;市街地

SS濃度係数は、水田、畑、森林、市街地で、15.4（下限95%値12.0～上限95%値18.8）、11.5（7.4～15.6）、3.9（2.6~5.1)、11.2（9.2～13.2）（n=5103）であった。さらに詳細に調べるには、施肥管理、土壌の性質、流域の畜産業、気象条件（特に降水量）、地形、地質などの影響を考慮した詳細な解析が必要である。

キーワード：流域土地利用モデル、SS、濃度係数
Keywords: watershed land-use model, SS, concentration coefficient

©2019. Japan Geoscience Union. All Right Reserved.

Evaluation of long term variation in water balance and discharge of sediment and nitrogen in the urbanized catchment of Yamato River, using SWAT model

*王 崑陽[1,2]、清水 裕太[3]、小野寺 真一[1]、齋藤 光代[4]、友澤 裕介[1]
*Kunyang Wang[1,2], Yuta Shimizu[3], Shin-ichi Onodera[1], Mitsuyo Saito[4], Yusuke Tomozawa[1]

1. 広島大学、2. 首都師範大学、3. 農研機構、4. 岡山大学
1. Graduate School of Integrated Arts and Science, Hiroshima University, 2. Capital Normal University, 3. National Agriculture and Food Research Organization, 4. Okayama University

Land-use changes, freshwater use, and the biochemical flow are important factors affecting the Earth's environmental threshold. In the research topics of Planetary Boundaries (PB), these factors have been defined as entering high-risk levels. One-third of the planet's freshwater resources come from groundwater, and now, in some countries and regions, it is also exposed to the risk of groundwater depletion. Large-scale urbanization brings economic development but also increases the possibility of urban waterlogging.

Yamato river is the highest-level river in Japan. It has a watershed area of 1067 square kilometers, covering almost half area of Nara prefecture. Yamato river catchment includes Nara basin which as an important agricultural base, Nara city and part of Sakai city. The water environment in the catchment is closely related to the healthy life of human beings. Especially in recent years, there are frequent flooding in the catchment. Therefore, the study of Yamato river is very necessary.

This thesis uses the SWAT (Soil and Water Assessment Tool) model and Geographic Information System (GIS) methodology. The SWAT model can not only simulate the water discharge and nutrient load but also find the essence of the change of water environment through the change of parameter sensitivity. Select Coefficient of determination (R2), Nash–Sutcliffe efficiency (NSE), and percentage of bias (PBIAS) as a factor of assessing results and obtained the experimental results with credibility.

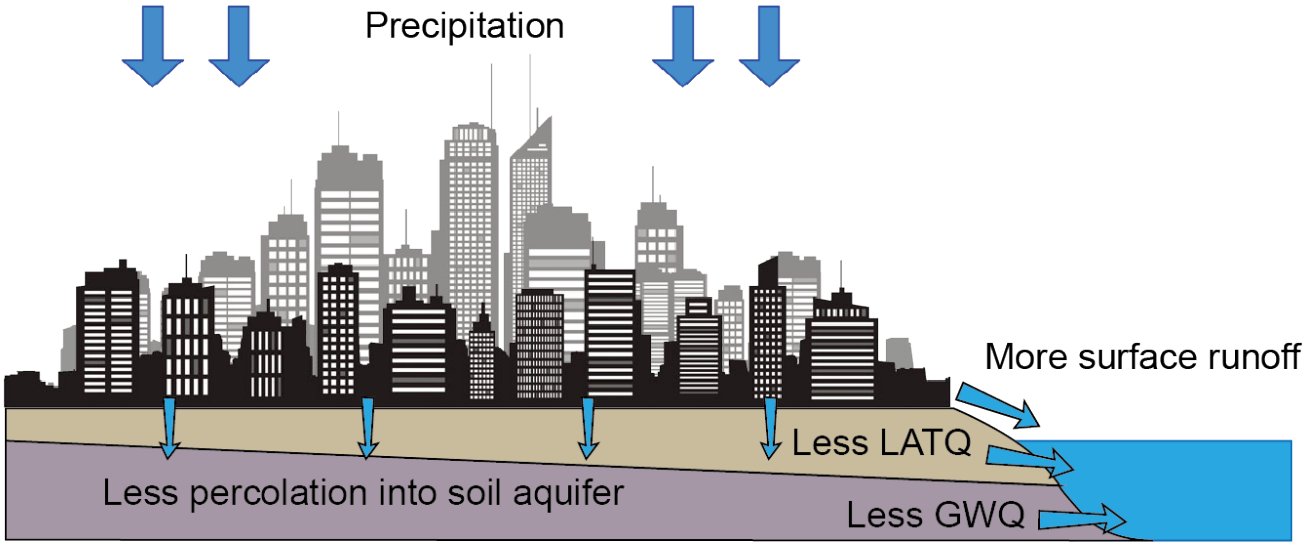
It is found that the land use in the basin is mainly manifested in the change from farmland to urban land use type, which probably accounts for 1/3 of the total area of land use type changed. Over a period of 2009-2016, the average of water discharge from the total outlet in the main channel is 2.37 million m3/day while it's 2.06 million m3/day in 1971-1978. As a result of changes in land use, water yield from farmland decreased by 45% compared with the 1970s, while the yield from the city increased by 43%. Among them, Surface runoff generated increase by about 70%. In Sakai and its surrounding cities, surface runoff generated increased by 18% per 100 mm precipitation. Curb length density in the high-density urban area increased about one time. That means Sakai now, in the face of flooding caused by torrential rains, needs to take on higher risks.

Sediment yield reducing by more than 70% from 1988 to 2014. The change comes mainly from the management of the river channel. The non-point source load of nitrate increased from 1096 tons to 1534 tons, this is mainly due to the increase in precipitation and the increase in population. The growth of forests also has a certain impact. This is because the type of land used in farmland and forests, there has a large number of fertilizers on the surface of the soil from human agriculture activities or the decay of animal and plant debris. Under the driving effect of precipitation, it mainly transported by the lateral flow

©2019. Japan Geoscience Union. All Right Reserved.

in farmland and forest area and the surface runoff in the urban area, a large part will enter the river channel.

キーワード：土地利用変化、水平衡、窒素負荷、SWATモデル、長期変動
Keywords: Land use change, Water balance, Nitrogen load, SWAT Model, Long term variation



©2019. Japan Geoscience Union. All Right Reserved.

Causal correlation between water-use of the Tedori River and coastal erosion of Chirihama Nagisa Driveway, Ishikawa, Japan

*百瀬 年彦[1]
*Toshihiko Momose[1]

1. 石川県立大学
1. Ishikawa Prefectural University

Awarded as the best beach of Japan (Reported by TripAdvisor, Inc. 2016), Chirihama Nagisa Driveway is a sandy beach located in Ishikawa, attracting people as the place that allows for driving cars and even large tourist buses along the shore. The source of the Chirihama sand is debris from Mt. Haku-san, which is transferred by the Tedori River and the Tsushima Current. At the river mouth, the finer sands are transferred to further offshore, and then drifted to further beach such as the Chirihama coast (50 km far from the river mouth). Due to the natural sand drifting process, the Chirihama coast is composed of the sands with fine and uniform grain size, the feature which guarantees for comfortable drive on the beach. The Chirihama coast is a treasure of Ishikawa; however, it faces a crisis of disappearance due to beach erosion.

According to Ishikawa prefectural government, the amount of sand loss of the Chirihama coast is 70000 m^3/year and its width decreases at 1 m/year. While the Chirihama coast is disappearing, a large-scale landslide of 1300000 m^3 occurred at upstream region of the Todori River in 2015 and the massive derbies moved downstream. The turbid water released for the ocean seemed to contribute to the formation of the Chirihama coast, but there are no reports on the recovery of the Chirihama coast. Where do the sands released from the Tedori River move?

Field investigations along the coast have found that the beach sediment at 4 –5 km far from the river mouth has the same feature as the Chirihama sand. From the viewpoint of recent water-use of the Tedori river, this presentation explains a possible reason why the fine sand released from the Tedori River cannot move to the Chirihama coast.

キーワード：千里浜なぎさドライブウェイ、海岸浸食、手取川、河川構造物
Keywords: Chirihama Nagisa Driveway, Coastal erosion, Tedori River, River structure

©2019. Japan Geoscience Union. All Right Reserved.

セレンガ河における元素動態への懸濁粒子の役割
Role of suspended solids on elemental dynamics in the Selenga River system

*川東 正幸[1]、Orgilbold Myangan[2]、Bolormaa Oyuntsetseg[2]
*Masayuki Kawahigashi[1], Orgilbold Myangan[2], Bolormaa Oyuntsetseg[2]

1. 首都大学東京、2. モンゴル国立大学
1. Tokyo Metropolitan University, 2. National University of Mongolia

Lake Baikal is one of the cleanest lake in the world. However, there are many sources of pollution such as mining, industry and agriculture in the river basin of the main tributary, Selenga River which is flowing into Lake Baikal. Lake Baikal actually face to severe pollution affected by anthropogenic activities in the watershed. Natural cleaning mechanism can still be functioning to prevent pollutants flow into the Baikal. Since suspended solids (SS) in the Selenga River can play a role as carriers of heavy metals and organic pollutants, their dynamics should be addressed to know the mechanism.

Water and sediment samples were collected in the Russian territory from the Mongolian border to the shore of the Baikal including the Selenga Delta. SS samples were further recovered using a glass fiber filter from the water samples. Surface sediments and SS samples were digested with the mixture of nitric acid and perchloric acid for determination of elements using Inductively Coupled Plasma Atomic Emission Spectrometry (ICP-AES).

Elemental concentrations were changeable depending on SS concentration along the tributary. Changes in SS concentration can be controlled by flow rate of the tributary. The significant relationship were observed between SS and sesquioxides mainly consisting of Fe and Al. Both of Mn and Cr were also common constituents of the SS oxides despite of their low concentration in SS. In contrast, Zn and Cu have no correlation with SS, indicating that they are specifically accumulated onto SS surface at a point where the two elements were released. The concentration of SS gradually decreased accompanied by decrease in heavy metals in SS in the delta region. On the contrary, those elements in the surface sediments increased to downstream in the delta region. Deposition process of SS in the delta can be occurred due to decrease in flow rate by channel bifurcation of tributaries, back water effect from Lake Baikal and SS trapping by vegetation in the delta. The delta has a potential to trap SS, resulting that water quality in the Lake Baikal has been protected of water quality in Lake Baikal.

キーワード：バイカル湖、懸濁粒子沈降、支流分岐
Keywords: Lake Baikal, SS deposition, channel bifurcation

©2019. Japan Geoscience Union. All Right Reserved.

[E] 口頭発表 | セッション記号 A (大気水圏科学)：A-HW 水文・陸水・地下水学・水環境

2019年5月30日(木) 13:45 ~ 15:15 | 201B 2F

[A-HW22] 流域の物質輸送と栄養塩循環ー源流域から沿岸海域までー

コンビーナ:小林 政広(国立研究開発法人森林研究・整備機構　森林総合研究所)、吉川 省子(農業・食品産業技術総合研究機構　農業環境変動研究センター)、安元 純(琉球大学　農学部　地域農業工学科)、Adina Paytan(University of California Santa Cruz)、座長:吉川 省子(国立研究開発法人 農業・食品産業技術総合研究機構 農業環境変動研究センター)

本セッションでは，源流部から沿岸海域を含む流域における物質輸送および栄養塩循環について，幅広い研究分野（陸水学，水文学，地下水学，沿岸海洋学，気象学，土壌学，堆積学，林学，農学，水産学，生態学，社会科学など）からの話題提供を踏まえて，持続可能な流域環境に関する分野横断的な議論を行うことを目的としている．特に，人間活動や気候変動の影響下における複雑で動的な水系における自然現象やその時間変化に主眼をおいた物理，化学，生物学的メカニズムを明瞭にするために，トレーサー技術，分子レベルの技術，水理モデル，古生物学的手法，屋内やフィールドでの試験，生態系サービスや社会ー生態学システムについての社会科学的評価など，流域科学のための新しい手法に基づく研究発表を歓迎する．このセッションを通して，新しい流域科学を創造するために，分野を超えた参加者相互の議論と協力体制作りを目指したい．

13:45 ~ 14:00

[AHW22-18] Relationship between topographical characteristics in catchment area and dissolved iron concentration of river in permafrost area

*田代 悠人[1]、楊 宗興[1]、白岩 孝行[2]、大西 健夫[3] (1.東京農工大学、2.北海道大学、3.岐阜大学)

14:00 ~ 14:15

[AHW22-19] Water Source Zones and Hydrochemical Properties of Fluoride Water in Mt. Meru Watershed, Tanzania

*中屋 眞司[1]、高田 遼吾[1]、安元 純[2]、吉谷 純一[1]、ルゴディシャ イノセント[3]、ルインボ ズベリ[3]、コマケッチ ハンス[4]、モレル トーマス[5] (1.信州大学工学部水環境・土木工学科、2.琉球大学農学部地域農業工学科、3.ネルソンマンデラ科学技術大学、4.ネルソンマンデラ科学技術大学ワイズフューチャー、5.タンザニアさくら女子中学)

14:15 ~ 14:30

[AHW22-20] 水質総負荷量の計測システム開発とその適用例
★招待講演

*高瀬 恵次[1]、伊藤 優子[2] (1.石川県立大学、2.国立研究開発法人　森林総合研究所)

14:30 ~ 14:45

[AHW22-21] Water infiltration and uptake around a Japanese cypress growing on a flat upland

*小林 政広[1]、小野寺 真一[2]、伊藤 優子[1]、阪田 匡司[1] (1.国立研究開発法人森林研究・整備機構　森林総合研究所、2.広島大学大学院総合科学研究科)

14:45 ~ 15:00

[AHW22-22] Innovative Rainfall Simulator Design for Moving Storm Scenarios with Different Storm Patterns

*RAVI KUMAR MEENA[1]、SUMIT SEN[2] (1.M.Tech Student, Department of Hydrology, Indian Institute of Technology Roorkee, Roorkee, Uttarakhand, India、2. Associate Professor, Department of Hydrology, Indian Institute of Technology Roorkee, Roorkee, Uttarakhand, India)

15:00 ~ 15:15

Discussion

Relationship between topographical characteristics in catchment area and dissolved iron concentration of river in permafrost area

*田代 悠人[1]、楊 宗興[1]、白岩 孝行[2]、大西 健夫[3]
*Yuto Tashiro[1], Muneoki Yoh[1], Takayuki Shiraiwa[2], Takeo Onishi[3]

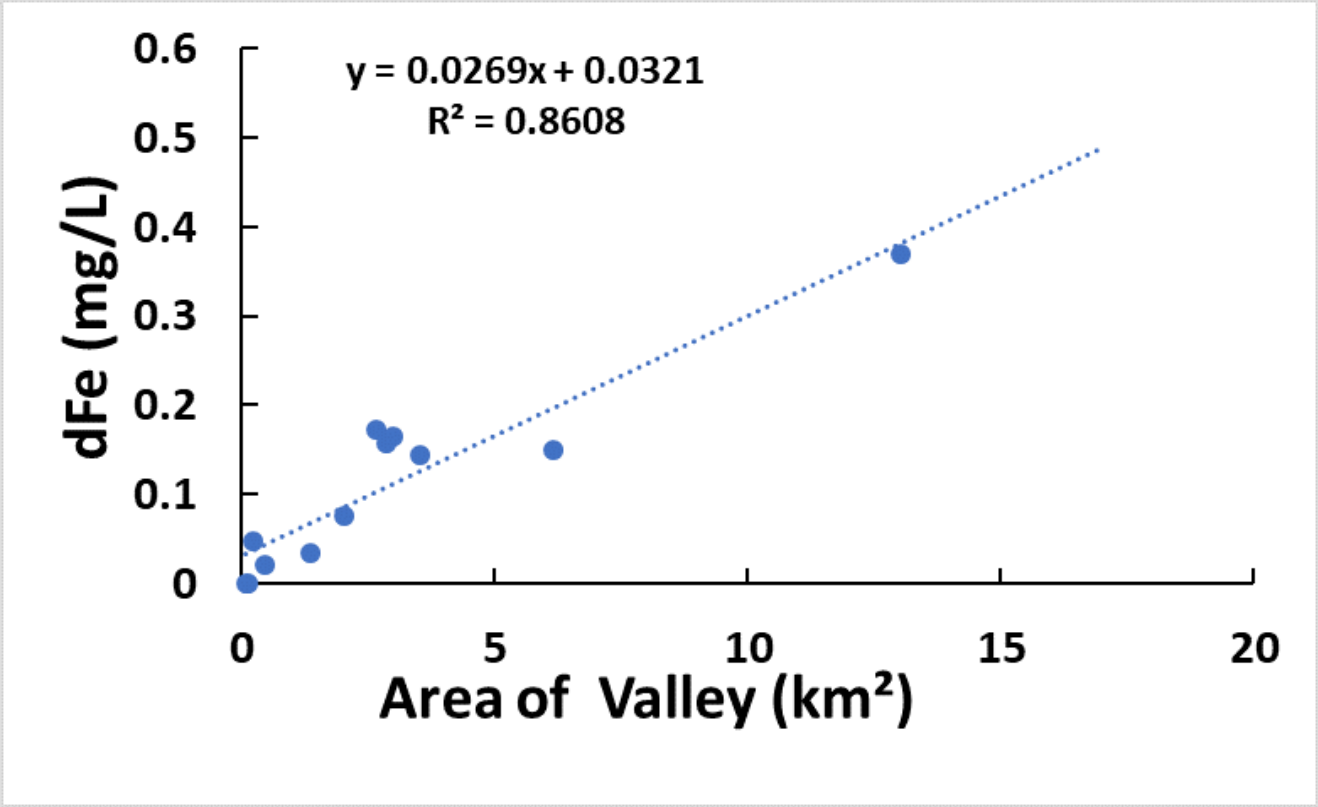
1. 東京農工大学、2. 北海道大学、3. 岐阜大学
1. Tokyo University of Agriculture and Technology, 2. Hokkaido University, 3. Gifu University

[Background]
Dissolved iron flowing out from the wetlands in the Amur River basin is an important nutrient that supports the primary production of phytoplankton in the Sea of Okhotsuk. Therefore, the amount of iron supplied to the sea is supposed to change due to the increase and/or decrease of the wetland area within the Amur basin. However, in the longterm observation of the dissolved iron concentration in the Amur River, the considerably high concentration, which can not be explained by the land-use change of the wetland, was observed in the latter of the 1990s. In the 1990s, because the relatively higher temperature had been continued, Shamov et al.,2014 speculated that permafrost thawing might be caution. Therefore, we hypothesized that permafrost thawing might promote the forming of humid and reductive condition which was suited to dFe generation in active layer, and have been conducting research on the mechanism of dissolved iron production and the distribution of permafrost. It has become clear that permafrost exists under the vegetation called Mari. Mari is the wetland which is covered by hygrophyte and sphagnum in a valley, and thick peat soil is accumulated underground.On the other hand, forest areas where birch or larch are densely spread with thin peat layers on the slope and ridge. Thus, the topographical features such as valley, slope and ridge in the catchment area dominate the vegetation and soil properties, and the dissolved iron cycling. In this study, we focused on the area of the valley as a topographical feature within the catchment area, and researched with the aim to discover the relationship to dissolved iron concentration in the river.
[Materials and Methods]
The research was conducted in the Tyrma River basin, which is a further tributary of the Tributary of the Amur River, in Khabarovsk. This area corresponds to the sporadic permafrost zone. In September 2018, we collected the water from 12 rivers in total; 5 rivers flowing into the Tyrma River and 5 rivers flowing into the Gujar river which is a tributary of the Tyrma River (basin area 7 to 200 km2). After sampling the water, immediately filtration was carried out with a disposable 0.45 μm filter and stored in polyethylene containers. Dissolved iron concentration was measured by the phenanthroline method after adding a few drops of HNO3- to the sample water to adjust pH <2.
We extracted the valley area using GIS soft "QGIS". The altitude data of field site, a global numerical surface model (DSM) corresponding to a resolution of 30 m by a panchromatic stereoscopic sensor (PRISM) equipped with JAXA 's Land Observing Satellite "ALOS" was used. The catchment area on the upstream side from the sampling point of each river was extracted and the Topographic Position Index (TPI) and the inclination (degree) were calculated. Next, the cells with TPI <0 - [standard deviation of TPI ×1/2] and inclination <3 (degree) were judged as a valley and these areas were calculated. The radius(R) of TPI was set to R = 500 m or R = 1000 m according to the valley width of the river. The reason why the condition of inclination <3 (degree) was added was that if only the condition of TPI was included, even the lower part of the slope was included, so that the valley area could be overestimated.
[Results and Discussion]
Dissolved iron concentrations in some rivers showed a very low concentration of <0.02 mg / L, which is below the detection limit, while others showed high concentrations of 0.37 mg / L. The relationship

©2019. Japan Geoscience Union. All Right Reserved.

between these concentration differences and the valley area in the catchment area is shown in Fig.1. In the rivers whose valley area was less than 1 km2, the concentration of dissolved iron was less than 0.05 mg / L. On the other hand, it was revealed that the concentration of dissolved iron tended to be higher with larger valley area in the catchment area. For the rivers with the low dFe concentrations, the catchment areas ware less than 15 km2, and the valley area occupied as low as 3% or less. The other rivers whose the dissolved iron concentration higher than 0.1 mg / L, the valley area accounted for 5-8% of the catchment area. The flat valley exists along the river is a typical topography in the Tyrma basin. In such places where the inclination is small, since the movement of water is also limited and make the residence time longer, the moisture and reductive environment can be maintained in the active layer on the permafrost, and wetland like Mari which is taken precedence by hygrophyte is widely formed in the valley. As the result, this study showed that Mari covering the valley has the function of dissolved iron generation and dissolved iron flow out into rivers.

キーワード：溶存鉄、永久凍土、湿地
Keywords: Dissolved Iron, Permafrost, Wetland



©2019. Japan Geoscience Union. All Right Reserved.

Water Source Zones and Hydrochemical Properties of Fluoride Water in Mt. Meru Watershed, Tanzania

*中屋 眞司[1]、高田 遼吾[1]、安元 純[2]、吉谷 純一[1]、ルゴディシャ イノセント[3]、ルインボ ズベリ[3]、コマケッチ ハンス[4]、モレル トーマス[5]
*Shinji Nakaya[1], Ryogo Takada[1], Jun Yasumoto[2], Junichi Yoshitani[1], Innocent Lugodisha[3], Zuberi Dominicus Lwimbo[3], Hans Komakech[4], Thomas Reuben Mollel[5]

1. 信州大学工学部水環境・土木工学科、2. 琉球大学農学部地域農業工学科、3. ネルソンマンデラ科学技術大学、4. ネルソンマンデラ科学技術大学ワイズフューチャー、5. タンザニアさくら女子中学
1. Department of Water Environment and Civil Engineering, Faculty of Engineering, Shinshu University, Japan, 2. Department of Regional Agriculture Engineering, University of the Rykuyus, Japan, 3. School of Materials, Energy, Water and Environmental Sciences, NM-AIST, Tanzania, 4. WISE-Future, NM-AIST, Tanzania, 5. SGSS and Institute of resources assessment-UDSM, Tanzania

Fluoride is leaching to natural water system from volcanic rocks and ashes with alkali volcanic activity along Great Lift Valley in east Africa. Tanzanian people in Great Lift Valley are also suffering drinking water including high fluoride (> 1.5 mgF/L of WHO) and water shortage. We investigated the groundwater and river water fluoride pollutions in area between Arusha of Mt. Meru watershed and Moshi of Mt. Kilimanjaro watershed in September, 2018 to provide the solutions to these issues as No. 6 of SDGs. We find some results below:

1. Average fluoride content is 4.0 mgF/L in Mt. Meru watershed, and 0.5 mgF/L in Mt. Kilimanjaro watershed.

2. Fluoride concentrates in Na-HCO_3 type water, and Fluoride tend to increase with Na and pH.

3. Groundwater fluoride tends to be increasing with residence time, but in recent twenty five years, fluoride is
higher in younger groundwater.
4. Well waters supplied to Arusha city come from the recharge zone of 2,000 m to 3,000 m in altitude of Mt. Meru, and the fluoride content tend to increase with the recharge altitude.

キーワード：フッ素、大地溝帯、タンザニア、メルー山流域
Keywords: Fluoride, Great Lift Valley, Tanzania, Mt. Meru watershed

©2019. Japan Geoscience Union. All Right Reserved.

水質総負荷量の計測システム開発とその適用例
Development and Application of a System for Measurement of Total Load of Water Quality

*高瀬 恵次[1]、伊藤 優子[2]
*Keiji Takase[1], Yuko Itoh[2]

1. 石川県立大学、2. 国立研究開発法人　森林総合研究所
1. Ishikawa Prefectual University, 2. Forestry and Forest Products research Institute, Japan

水質の保全・管理は安全な水資源の確保のみならず、地域の水環境保全にとって重要な課題である。これまで、水質管理は濃度規制的な立場に重きを置いて行われてきたが、近年の排出物質の多様化と排出水量の増加は総量規制による水質管理が重要になることを示唆している。また、流域における物質循環・物質収支を理解する上で負荷量を正確に把握することは、基本的事項である。しかしながら、負荷量の計測には多大の労力と時間あるいは経費を必要することが多く、その正確な把握はそれほど容易ではないのが現状である。そこで、本研究では流出負荷量を対象として、これを簡便に正確に計測できるシステムを構築した。そして、これを積雪地の森林理水試験地に適用し、従来からよく用いられてきたコンポジットサンプラーによる定時間間隔採水による負荷量算定値と比較することによって、その有効性を検討した。その結果、両者はよく一致し、本計測システムを用いれば、面源からの長期間にわたる流出負荷量を簡便に正確に計測できることが示された。

キーワード：水質、濃度、総負荷量、採水システム、森林流域
Keywords: Water Quality, Concentration, Total load of water quality, System for collecting water, Forested watershed

©2019. Japan Geoscience Union. All Right Reserved.

Water infiltration and uptake around a Japanese cypress growing on a flat upland

*小林 政広[1]、小野寺 真一[2]、伊藤 優子[1]、阪田 匡司[1]
*Masahiro Kobayashi[1], Shin-ichi Onodera[2], Yuko Itoh[1], Tadashi Sakata[1]

1. 国立研究開発法人森林研究・整備機構　森林総合研究所、2. 広島大学大学院総合科学研究科
1. Forestry and Forest Products Research Institute, 2. Graduate School of Integrated and Arts Sciences, Hiroshima University

In forest ecosystems, trees strongly influence the water movement above and below the ground. During rainfall events, some rainwater flows as stemflow, which provides concentrated water input into soil. The redistribution of soil water during periods without rainfall is affected by water uptake by roots. To clarify the effects of trees on soil water dynamics during and after rainfall events, we monitored the distribution and temporal dynamics of the soil water potential around the stem of a Japanese cypress (*Chamaecyparis obtusa*) using a two-dimensional array of tensiometers installed at multiple soil depths and distances from the tree. During rainfall events with wet antecedent moisture conditions, stemflow infiltrated into the soil and recharged the shallow groundwater near the stem. The matric potential often increased at lower positions before upper positions, indicating bypass flow through macropores. After large rainfall events, once the matric potential distribution became uniform horizontally, gravity-driven drainage proceeded. During the drying process, the matric potential decreased markedly proximal to the stem compared to distally. A horizontal gradient in the matric potential was observed in both the shallow and deeper soil layers. This indicates an intense sink caused by water uptake by roots from the deeper soil layer. Upon excavating the roots after monitoring the matric potential, dense fine roots were observed in the deeper soil layer. The tree studied may feed the deeper soil around its root zone with rainwater as stemflow and use the water advantageously following the drying process.

キーワード：樹木、樹幹流、吸水
Keywords: tree, stemflow, water uptake

©2019. Japan Geoscience Union. All Right Reserved.

Innovative Rainfall Simulator Design for Moving Storm Scenarios with Different Storm Patterns

*RAVI KUMAR MEENA[1], SUMIT SEN[2]

1. M.Tech Student, Department of Hydrology, Indian Institute of Technology Roorkee, Roorkee, Uttarakhand, India, 2. Associate Professor, Department of Hydrology, Indian Institute of Technology Roorkee, Roorkee, Uttarakhand, India

Rainfall simulators are widely used in the field of hydrology, biosystem engineering, agronomy, and geomorphology to understand the processes involved in these disciplines. Usually, rainfall simulators are not able to generate spatio-temporal variation in rainfall intensity simultaneously unlike natural conditions. Majority of methods used in rainfall simulator studies assumes that the rainstorm reaches instantaneously and remains steady over an area for a certain time period. Hence, most of the rainfall experiments ignore the effect of runoff response caused by moving storm across a watershed which results in under or over estimation of runoff peaks. Considering these limitations of traditional rainfall simulators, we are developing an advanced rainfall simulator using eleven full cone nozzles to simulate moving front storm. These nozzles can generate rainfall intensity in the range of 65 to 190 mm/hr at a pressure range of 50 kPa to 180 kPa with a varying height from 1.5m to 4m above the ground surface. All the eleven nozzles are controlled by flow control valves and the valves are individually regulated by servo motors. Arduino Mega microcontroller system is used to control all the servo motors to generate variable rainfall intensities. Further, we have developed a mobile application for Android users to regulate all the valves of rainfall simulator. This simulator is able to simulate nearly natural rainfall conditions in the controlled environment in four different patterns i.e. uniform, advanced, delayed and intermediate. A tray of 250cm×140cm×50cm has also being designed and fabricated to conduct different hydrological experiments. This tray is designed with a provision to generate and record overland, subsurface and base flow. Tray area can also be divided in three partition to analyze three different soil conditions simultaneously. Slope adjustment, leachate collection unit and piezo metric head measurement unit are also incorporated in this experimental tray. Overall, the whole rainfall simulator with tray can be used to study the impact of moving storm on soil erosion, infiltration, and runoff in the simulated near natural environment along with pollutant transport mechanisms. This study is being focused on detailed analysis of moving storms and their impact on hydrograph characteristics, especially in terms of time of concentration (tc), time to peak (tp), and peak discharge (Qp) for two different storm directions (upstream and downstream) with different storm movement velocity and rainfall intensity.

Keywords: Rainfall simulator, Moving Storm experiments, Spatio-temporal variation

©2019. Japan Geoscience Union. All Right Reserved.

[E] 口頭発表 | セッション記号 A (大気水圏科学)：A-GE 地質環境・土壌環境

2019年5月30日(木) 9:00 ~ 10:30 | 301A 3F

[A-GE28] 地質媒体における物質移動，物質循環と環境評価

コンビーナ:小島 悠揮(岐阜大学工学部)、濱本 昌一郎(東京大学大学院農学生命科学研究科)、斎藤 広隆(東京農工大学大学院農学研究院)、森 也寸志(岡山大学大学院環境生命科学研究科)、座長:小島 悠揮(岐阜大学)、濱本 昌一郎(東京大学)、森 也寸志(岡山大学)、斎藤 広隆(東京農工大学)

土壌や岩石からなる地質媒体における物質の移動と循環，並びにエネルギーの輸送について，室内実験，現位置試験，フィールド調査，解析・評価モデル及び関連応用分野への適用など，広い視点から議論し，国内外における最新成果の交流を図る。地質汚染，環境修復，地層処分，地中熱利用等未解明部分の多いヴェイドスゾーン（不飽和帯）における物質移動，熱輸送，衛星観測等を用いた土壌水分モニタリング及び環境影響評価に関する研究発表を特に歓迎する。

9:00 ~ 9:25

[AGE28-01] **Humic substances in deep sedimentary groundwater**

★Invited Papers

*斉藤 拓巳[1] (1.東京大学大学院工学研究科)

9:25 ~ 9:40

[AGE28-02] Nano-Bubble Retention in Saturated Porous Media under Different Solution Chemistry

*濱本 昌一郎[1]、杉本 卓也[1]、竹村 貴人[2]、西村 拓[1]、Bradford Scott[3] (1.東京大学大学院農学生命科学研究科、2.日本大学文理学部、3.アメリカ農務省塩類研究所)

9:40 ~ 9:55

[AGE28-03] **Geochemical Investigation of Metals and Trace Elements around the Abandoned Cu – Ni Mine Site in Selibe Phikwe, Botswana**

*Fiona Segolame Motswaiso[1]、Kengo - Nakamura[1]、Noriaki - Watanabe[1]、Takeshi - Komai[1] (1.Tohoku Univeristy Graduate School of Environmental Studies)

9:55 ~ 10:10

[AGE28-04] Removal of Arsenic (III) From Aqueous Solution Using Pumice and Zeolite Supported Zero-Valent Iron Nanoparticle

*Shashi Ranjan[1]、Brijesh kumar yadav[1]、Himanshu Joshi[1] (1.Indian Institute of Technology Roorkee)

10:10 ~ 10:25

[AGE28-05] **Unsaturated Hydraulic Conductivity Estimation from Multi-step Centrifuge Outflow**

*Thanh Long Bui[1]、Yasushi Mori[1] (1.Graduate School of Environmental and Life Science, Okayama University)

10:25 ~ 10:30

Discussion

Humic substances in deep sedimentary groundwater

*斉藤 拓巳[1]
*Takumi Saito[1]

1. 東京大学大学院工学研究科
1. School of Engineering, The University of Tokyo

Humic substances (HSs) are ubiquitous in various environments and play important roles for the fate of nutrients and pollutants. Deep underground environment is not an exception, although the properties of HSs there are largely unknown due to their limited availability. Recently, we reported the physicochemical and ion-binding properties of HSs extracted from sedimentary groundwater at -250 m below ground surface of the Horonobe underground research center operated by the Japan Atomic Energy Agency. The Horonobe HSs (HHSs) consist of relatively small organic molecules rich in aliphatic carbon and reduced sulfur. The densities of acidic functional groups such as carboxylic groups are relatively high for HHSs, and they are chemically homogenous. Nevertheless, the binding of Cu^{2+} to HHSs are smaller than that to surface HSs, suggesting the presence of different coordination environments for Cu^{2+} in HHSs. Cadmium, a thiophilic metal, tends to form CdS(s) nano-particles with HHSs likely due to the high concentrations of reduced sulfur. In this talk, the particularity of the HHSs will be discussed, comparing their properties with those of their counterparts in surface environments.

キーワード：腐植、地下水
Keywords: Humic substance, Groundwater

©2019. Japan Geoscience Union. All Right Reserved.

Nano-Bubble Retention in Saturated Porous Media under Different Solution Chemistry

*濱本 昌一郎[1]、杉本 卓也[1]、竹村 貴人[2]、西村 拓[1]、Bradford Scott[3]
*Shoichiro Hamamoto[1], Takuya Sugimoto[1], Takato Takemura[2], Taku Nishimura[1], Scott A Bradford[3]

1. 東京大学大学院農学生命科学研究科、2. 日本大学文理学部、3. アメリカ農務省塩類研究所
1. Department of Biological and Environmental Engineering, The University of Tokyo, 2. College of Humanities and Sciences, Nihon University, 3. U. S. Salinity Laboratory

An understanding of nano-bubble (NB) migration in porous media is needed for potential environmental applications. This research investigates factors that control the transport, retention, and release of air NBs in repacked glass beads. One-dimensional column transport studies with air NBs were conducted under different solution IS, ionic composition, and pH conditions. Collected data were simulated using a mathematical model that considered advective and dispersive transport, first-order kinetic retention, and transient release. Results were interpreted with the aid of interaction energy calculations that considered electric double layer, van der Waals, and Lewis acid-base interactions on surfaces with different amounts of nanoscale roughness. NB concentrations in the effluent were reduced with an increase in ionic strength (IS) or a decrease in pH due to a reduction in the repulsive force between the glass surface and NBs, especially when the solution contained Ca^{2+} as compared to Na^{+} and for larger NBs. NB retention on the surface was explained by ubiquitous nanoscale roughness on the glass beads that significantly lowered the energy barrier, and localized attractive charge heterogeneity and/or hydrophobic interactions.

キーワード：ナノバブル、輸送、多孔質体、溶液化学性
Keywords: Nano bubble, Transport, Porous media, Solution chemistry

©2019. Japan Geoscience Union. All Right Reserved.

Geochemical Investigation of Metals and Trace Elements around the Abandoned Cu –Ni Mine Site in Selibe Phikwe, Botswana

*Fiona Segolame Motswaiso[1], Kengo - Nakamura[1], Noriaki - Watanabe[1], Takeshi - Komai[1]

1. Tohoku Univeristy Graduate School of Environmental Studies

Metals and trace elements may occur naturally in rocks and soils, but elevated quantities of them are gradually released into the environment by anthropogenic activities such as mining. In order to address issues of trace element water and soil pollution, a distinction needs to be made between natural and anthropogenic anomalies. The current study aims at characterizing the spatial distribution of trace elements and evaluate site-specific geochemical background concentrations of trace elements in the mine soils and river sediments and also to discriminate between lithogenic and anthropogenic sources of enrichment around a copper-nickel mining town in Selibe-Phikwe, Botswana.

A total of 43 soil, 30 river sediments, and 9 river water samples were collected from an area of 500m2 within the precincts of the mine. The total concentration of Cu, Ni, Pb, Cr, As, and Co in soils and sediments were determined using ED-XRF while river water samples were analyzed by ICP-AES. Geochemical pollution indices such as Geo-accumulation Index (Igeo), Enrichment Factor (EF) and Integrated Pollution Index (IPI) were employed for the assessment of metal and trace element contamination. The average metal concentration in soil of Cu, Ni, Pb, Cr, As, and Co in the study area were 73.27, 78.10, 25.83, 61.43, 4.28 and 6.43 mg/kg, respectively. To calculate the geochemical baseline, Relative cumulative frequency curves and the 4 s -outlier test methods suggested by Matschullat (2000) were incorporated. The estimated average baseline concentrations of Cr, Cu, Ni, Co, Zn and As are 53.8, 51.85, 53.95, 5.6, 32.36 and 4.27 mg kg 1, respectively. Soil leachate, sediment leachate, and river water pH levels ranged from basic (9) to very acidic (3) in areas closer to the mine. There is high variation in heavy metal concentration, eg. Cu, depicting regional natural background concentrations while others depict anthropogenic sources. The calculated Igeo values revealed moderate pollution level by the same metals. The result of integrated pollution indices suggested a generally deteriorating site quality. The results of chemical analysis also indicate that the trace elements in soils decreased with respect to distance from the mine; controlled mainly by water movement, wind direction, and topography.

Keywords: Soil Contamination, Geochemical baseline, Pollution indices, Trace elements

©2019. Japan Geoscience Union. All Right Reserved.

Removal of Arsenic (III) From Aqueous Solution Using Pumice and Zeolite Supported Zero-Valent Iron Nanoparticle

*Shashi Ranjan[1], Brijesh kumar yadav[1], Himanshu Joshi[1]

1. Indian Institute of Technology Roorkee

Arsenic is a naturally occurring toxic element and is widely distributed in natural ecosystems. Due to the natural as well as human-induced actions, its presence in groundwater is expanding its horizons and is becoming a major concern in lower Gangetic plains. Large active surface area and high arsenic adsorption capacity make nano-zero valent iron nanoparticle (nZVI) a promising adsorbent to remove arsenic species but due to high surface energy and the inherent magnetic forces of nZVI, it gets agglomerated and reduces its efficiency for adsorption. The objective of the present study was to develop supported nZVI over the porous material (pumice and zeolite) and their use for As (III) removal from aqueous solution. The chemical approach, i.e., Liquid Phase Synthesis, was used to infuse the iron nanoparticle on the surface of the porous material via reduction of iron in the presence of the base material by sodium borohydride. The shape, size, and surface morphology studied by Fe-SEM and shows a uniform distribution of nZVI over the surface of granular (0.5-1 mm) base materials. Batch studies were performed to determine the applicability of prepared composites as an adsorbent for As (III) removal at varying initial As (III) concentration (0.5 -5 mg/L), adsorbent dose (1-10 g/L) and pH (3-12). Adsorption kinetics and isotherms were studied in detail for the synthesized adsorbent to deduce the overall performance. Batch experiments demonstrated the quick removal of As (III) at initial stages followed by a slower removal rate, making it a two-stage process. The supported nZVI was found to be an effective adsorbent for As (III) removal and due to its mechanical strength, it can be applied for in-situ remediation of arsenic-polluted groundwater

Keywords: Arsenic, Nano Zerovalent Iron, Remediation, Pumice and Zeolite

©2019. Japan Geoscience Union. All Right Reserved.

Unsaturated Hydraulic Conductivity Estimation from Multi-step Centrifuge Outflow

*Thanh Long Bui[1], Yasushi Mori[1]

1. Graduate School of Environmental and Life Science, Okayama University

In the age of blooming technologies, direct and indirect laboratory methods, which identified soil function, are developed to shorten experiment time. In developing countries of Asia area, research on soil physic is sometimes limited because it is not easy to bring samples from those countries. In addition, it is impossible to identify soil function from the soil sample without original structure. Therefore if we can measure soil hydraulic conductivity or water holding capacity with small volume of samples, it is very beneficial for the region where soil data is limited. In this study, centrifuge multi-step outflow method was examined to estimate drainage process, i.e., unsaturated hydraulic properties.

The experiment was conducted using 2-mL centrifuge tube with two pin-holes at the top and bottom of the tube. After saturated from the bottom, multi-step pressurized outflow was performed on four kinds of soil samples including standard soil, granite decomposed soil, rice paddy field soil and volcanic ash soil. Transient outflow volume was measured using small centrifuge machine within 5 and 15 minutes at room temperature (25oC). The centrifuge pressure step was 1000, 2000, 3000, 4000, and 5000rpm, which was approximately 90, 360, 810, 1400, and 2250cmH2O respectively. Based on the outflow volume and accumulated time as input data for inverse solution model (HYDRUS 1D v4.6), hydraulic conductivity was optimized.

We found out that the optimization was successful with clayey soils and volcanic ash soils, but not with granite decomposed soil and standard sandy soils. The more sand particles it contained, the less convergence for hydraulic conductivity optimization we had obtained.

Keywords: Unsaturated Hydraulic Conductivity, Multi-step outflow, Centrifuge

©2019. Japan Geoscience Union. All Right Reserved.

[E] 口頭発表 | セッション記号 A (大気水圏科学)：A-GE 地質環境・土壌環境

2019年5月30日(木) 10:45 ~ 12:15 | 301A 3F

[A-GE29] エネルギ・環境・水ネクサスと持続的発展

コンビーナ:張 銘(産業技術総合研究所地質調査総合センター地圏資源環境研究部門)、川本 健(埼玉大学大学院理工学研究科)、Jet-Chau Wen(National Yunlin University of Science and Technology)、? 永紅(天津師範大学)、座長:張 銘(産業技術総合研究所)、斎藤 広隆(東京農工大学)、郝 永紅(Tianjin Normal University)

このセッションは、社会の持続的発展を目指し、クリーンエネルギー生産、環境修復と保全、廃棄物管理、水循環、水質モニタリング、水資源管理及びエネルギ・環境・水連鎖作用に係る基礎的及び最新研究成果を幅広く発表と議論する場として提供する。また、水・エネルギ及び環境管理に係る市民意識の向上やステークホルダーエンパワーメントと参加の促進並びに政策決定に関連する社会科学的話題の発表も歓迎する。

10:45 ~ 10:50

Introduction

10:50 ~ 11:05

[AGE29-01] Input-Output Analysis of Taiwan’s Food-Energy-Water Risk

*CHU-CHUN YAO[1]、Gene Jiing-yun You[1] (1.National Taiwan University)

11:05 ~ 11:20

[AGE29-02] **Groundwater potential analysis using the multiple spatiotemporal remote sensing approach in fractured rock of mountainous region**

*Jung-Jun Lin[1,2]、Yuei-An Liou[1]、Chien-Chung Ke[2]、Su-Yun Chi[2]、Jia-Hung Liang[3] (1.National Central Univ.、2.Sinotech Engineering Consultants, Inc.、3.Ministry of Economic Affairs)

11:20 ~ 11:35

[AGE29-03] Estimating Soil Water Content with Color Calibration Method in the Image of Remote Sensing by Unmanned Aerial Vehicle

*Hong-Yi Li[1]、Hong-Ru Lin[1]、Jyun-Lin Chen[1]、Shao-Yang Huang[1]、Jet-Chau Wen[1] (1.National Yunlin University of Science and Technology)

11:35 ~ 11:50

[AGE29-04] **Characterizing Geotechnical Properties of Drinking Water Sludge Blended with Graded Crushed Clay Brick for Road Subgrade: Effects of Gradation and Mixing Proportion of Crushed Clay Brick on CBR and Water Permeability**

*Muhammad Rashid Iqbal[1]、Akihiro Matsuno[1]、Ken Kawamoto[1] (1.Graduate School of Science and Engineering, Saitama University)

11:50 ~ 12:05

[AGE29-05] Investigation and Evaluation of the Multiple-liquefaction Site at the Southern Taiwan

*Chih-Sheng KU[1] (1.I-Shou University)

12:05 ~ 12:15

Discussion

Input-Output Analysis of Taiwan’s Food-Energy-Water Risk

*CHU-CHUN YAO[1], Gene Jiing-yun You[1]

1. National Taiwan University

The water, energy, and food (WEF) nexus means that the three sectors are inextricably linked and that actions in one area more often than not have impacts in one or both of the others. From a national planning perspective, it is necessary to more precisely investigate the relationships among food-energy-water sectors. This study applies input-output analysis based on interdependencies between economic sectors or industries in Taiwan’s food-energy-water challenge and risk. In this study, the research data is based on Taiwan’s trade association tables of 52 economic sectors (including food, energy, and water-related sectors) for the year 1996, 2001, 2006, and 2011. We develop the extrapolation method to produce available I-O table. The future I-O table can be forecasted by applying different predictive models (e.g., linear or nonlinear regressions). We will observe the changes in Taiwan’s economic structures during the time period (e.g., between 1996 and 2001) and also investigate the uncertainty of economic impact focusing on food, energy, and water. Based on the results of analysis of Taiwan’s trade association tables, we can predict the risks that Taiwan’s industries may face under different conditions in the future and might provide some useful information to the government for taking countermeasures.

Keywords: WEF, input-output analysis, extrapolation, I-O table, economic structures, risk

©2019. Japan Geoscience Union. All Right Reserved.

Groundwater potential analysis using the multiple spatiotemporal remote sensing approach in fractured rock of mountainous region

*Jung-Jun Lin[1,2], Yuei-An Liou[1], Chien-Chung Ke[2], Su-Yun Chi[2], Jia-Hung Liang[3]

1. National Central Univ., 2. Sinotech Engineering Consultants, Inc., 3. Ministry of Economic Affairs

Because of the costly field investigation, an optimum benefit technique, the multiple spatiotemporal remote sensing analysis, was used for long-term monitoring and assessment of groundwater potential capacity. In this study, we used the mentioned approach to derive the spatiotemporal index from Landsat imagery for identifying the land use change and understanding the regional hydrogeological characteristics, such as normalized difference vegetation index (NDVI), soil moisture index (SMI), land surface temperature (LST) and so on. To verify the index evaluation results, the hydrogeological properties including the core inspection, geophysical logging and hydraulic testing of totally 108 boreholes drilling in the fractured rock mass in mountainous region were collected. The pumping test results such as well capacity from 76 groundwater monitoring wells were also used to compare the potential groundwater capacity evaluated from remote sensing analysis. It was found a good agreement between the field investigation data and remote sensing analysis results. Therefore, the multi-scaled comprehensive analyses of natural and anthropogenic geomorphic features are suitable for providing more information to qualify and estimate the selections of investigated sites in the future.

Keywords: groundwater, fractured rock, remote sensing

©2019. Japan Geoscience Union. All Right Reserved.

Estimating Soil Water Content with Color Calibration Method in the Image of Remote Sensing by Unmanned Aerial Vehicle

*Hong-Yi Li[1], Hong-Ru Lin[1], Jyun-Lin Chen[1], Shao-Yang Huang[1], Jet-Chau Wen[1]

1. National Yunlin University of Science and Technology

From the previous research results, there are many methods for measuring soil water content (SWC), but most of the SWC measurement methods are destructive methods for soil structure. Moreover, it takes a lot of time and manpower. In recent years, the method of estimating SWC from digital images of unmanned aerial vehicle (UAV) is a novel and rapid for measuring SWC non-destructive. While estimating SWC in the field using digital images, the effects are produced sunlight and climates and setting of the camera white balance. While estimating the SWC by digital images, these influences will let these methods have a bias between the hue value of digital images and the color of actual soil. So, the purpose of this study is to add a color calibration method while the process of estimating to remove the influences of sunlight, climates and white balance of camera, to improve the accuracy of estimating SWC by digital images.

At first, this study collected the surface soil samples from 0 to 5 cm below the ground surface at the study site which is the sampling range of in-situ planning. A standard color card (ColorChecker) is placed at the study site as a basis for image color calibration. After that, this study used UAV to take a photo-shooting at 30 meters above the ground, and obtain the digital images of the study site. After the sampling is completed, the surface soil sample is obtained its gravimetric water content by thermogravimetry in the laboratory. Next, the digital images taken by the UAV is used to cut the study area and image color calibration using the image processing software.

Then, using Matlab 2018b software to calculates the hue value of RGB color space (Red (R), Green (G), and Blue (B)) of the digital images before and after the color calibration separately, and transforms them into other six color spaces (normalized RGB, HIS, I1I2I3, Lab, YCbCr, and Lch). At last, this study used multiple linear regression to establish the SWC estimation models separately, and then compare the influences which before and after color calibration.

The results of this study show the influences of sunlight, climates and white balance of camera make a significant bias when estimating SWC using the digital images before color calibration. However, this study which added color calibration improves the accuracy in the estimation of SWC by digital images. Finally, the achievements of this study can apply in reducing the number of water resources of the agriculture irrigation widely.

Keywords: Surface soil, Aerial photo-shooting, Digital image processing, Color calibration

©2019. Japan Geoscience Union. All Right Reserved.

Characterizing Geotechnical Properties of Drinking Water Sludge Blended with Graded Crushed Clay Brick for Road Subgrade: Effects of Gradation and Mixing Proportion of Crushed Clay Brick on CBR and Water Permeability

*Muhammad Rashid Iqbal[1], Akihiro Matsuno[1], Ken Kawamoto[1]

1. Graduate School of Science and Engineering, Saitama University

Effective uses of construction and demolition waste, sludge, and industrial by-products for engineering purposes are highly demanded in developing countries. Currently, these materials are used for other construction works such as ground levelling and backfilling without any quality control of materials and/or directly dumped at the landfill site. In this research, an attempt was made to use drinking water sludge (DWS) by blending with crushed clay bricks (CCB) to propose their utilization for constructing road subgrade. DWS with less than 2-mm was blended with CCB with three different particles range; (a) finer fraction having particle size 2-10mm, (b) Coarser fraction 10-30mm, and (c) graded fraction 2-30mm. The mixing proportion has been controlled from 0 to 100% on the dry mass basis. Geotechnical properties such as California bearing ratio (CBR) and water permeability were investigated in the laboratory. Experimental results showed that addition of a finer fraction of CCB from 0 to 100% with DWS improved CBR values from 45% to 88% which was almost double than the DWS itself and captured a well linear relationship. Up to 60% addition of a coarser and graded fraction of CCB increased CBR value from 45% to 110% which was 2.44 times higher than the DWS itself. However, at 80% addition of CCB, graded fraction enhanced the CBR value more as compared to coarser fraction which was due to the well packing and reduction of the voids. On the other hand, at 100% blend of CCB coarser fraction showed quite higher values which could be due to the breakage of the bigger particles and filling the voids effectively. The water permeabilities of all these blended samples showed a very well relationship with Hazen model as compared to Kozeny-Carman model. It can be concluded that graded and coarser fraction 60% blend had an equal or superiority effect than the 100% of the finer fraction blends. All the tested sample fulfilled the improved subgrade requirement to utilize for the road subgrade.

Keywords: Drinking water sludge, Crushed Clay bricks, California Bearing Ratio (CBR), Water Permeability

©2019. Japan Geoscience Union. All Right Reserved.

Investigation and Evaluation of the Multiple-liquefaction Site at the Southern Taiwan

*Chih-Sheng KU[1]

1. I-Shou University

Southern Taiwan experienced several large earthquakes on 5 December 1946 (M_w=6.3), 4 March 2010 (M_w=6.4) and 6 February 2016 (M_w=6.6), respectively. Liquefaction phenomenon evidences was observed at Hsinhwa district, Tainan city, Taiwan during the 1964, 2010, and 2016 earthquake. Re-liquefaction at this site was confirmed by GPS surveying at the sand boiling locations after last two earthquakes. Seismic cone penetration test (SCPT) and boring were conducted at this site after 2010, and 2016 earthquake. The recurrence of liquefaction, availability of pre-earthquake logging, and high fine content in the liquefied soil stratum make this case valuable for detail study. This paper presents the results of the investigation and evaluates the liquefaction potential of the reliquefied site by different period exploration data. The comparison of the SCPT strength profile before and after the last earthquakes seems to indicate that no significant variation has occurred in this multiple liquefied site, making the area vulnerable to liquefaction induced sand boiling in future large-scale earthquakes. Liquefaction analyses with in situ test data show that this site is still highly susceptible to liquefaction.

Keywords: Earthquake, Liquefaction, Seismic Cone Penetration Test



03-05-2010



02-13-2016

©2019. Japan Geoscience Union. All Right Reserved.

[E] 口頭発表 | セッション記号 A (大気水圏科学)：A-GE 地質環境・土壌環境

2019年5月30日(木) 13:45 ~ 15:15 | 301A 3F

[A-GE29] エネルギ・環境・水ネクサスと持続的発展

コンビーナ:張 銘(産業技術総合研究所地質調査総合センター地圏資源環境研究部門)、川本 健(埼玉大学大学院理工学研究科)、Jet-Chau Wen(National Yunlin University of Science and Technology)、? 永紅(天津師範大学)、座長:川本 健(埼玉大学)、温 志超(雲林科技大学)

このセッションは、社会の持続的発展を目指し、クリーンエネルギー生産、環境修復と保全、廃棄物管理、水循環、水質モニタリング、水資源管理及びエネルギ・環境・水連鎖作用に係る基礎的及び最新研究成果を幅広く発表と議論する場として提供する。また、水・エネルギ及び環境管理に係る市民意識の向上やステークホルダーエンパワーメントと参加の促進並びに政策決定に関連する社会科学的話題の発表も歓迎する。

13:45 ~ 13:50

Introduction

13:50 ~ 14:05

[AGE29-06] Investigating the Reproducibility of Hydraulic Tomography Estimates with Time-Variable Boundary Conditions

*Jian-Dao Li[1]、Jyun-Lin Chen[1]、Hong-Ru Lin[1]、Shao-Yang Huang [1]、Tian-Chyi Jim Yeh[2]、Jet-Chau Wen[1] (1.National Yunlin University of Science and Technology、2.The University of Arizona)

14:05 ~ 14:20

[AGE29-07] **Applying river pollution index and QUAL2K model for water quality assessment and management in Ke-Ya river, Taiwan**

*Hong-Syuan Li[1]、Yu-Chih Lin[1] (1.Department of Environmental Engineering & Health, Yuanpei University of Medical Technology)

14:20 ~ 14:35

[AGE29-08] Environmental assessment at CDW disposal sites in Vietnam: Case study in Thanh Tri landfill, Hanoi

*Thanh Ha Ngo[1]、Akihiro Matsuno[1]、Ken Kawamoto[1] (1.Graduate School of Science and Engineering, Saitama University)

14:35 ~ 14:50

[AGE29-09] **Modeling Study on the Impacts of Groundwater Pumping to Regional Hydroclimatology in 37 World Major Aquifers**

*Pat J.-F. Yeh[1] (1.Monash University Malaysia)

14:50 ~ 15:05

[AGE29-10] CHRATERIZING BURIED WASTE COMPOSITION AT CONSTRUCTION AND DEMOLITION WASTE (CDW) DISPOSAL SITE IN VIETNAM: A CASE STUDY IN THANH TRI LANDFILL IN HANOI

*Tselmeg Aldarjav[1]、Akira Kato[1]、Akihiro Matsuno[1]、Ken Kawamoto[1,2] (1.Graduate School of Science and Engineering, Saitama University, Japan 、2.International Institute for Resilient Society, Saitama University, Japan)

15:05 ~ 15:15

Discussion

Investigating the Reproducibility of Hydraulic Tomography Estimates with Time-Variable Boundary Conditions

*Jian-Dao Li[1], Jyun-Lin Chen[1], Hong-Ru Lin[1], Shao-Yang Huang [1], Tian-Chyi Jim Yeh[2], Jet-Chau Wen[1]

1. National Yunlin University of Science and Technology, 2. The University of Arizona

In recent years, the hydraulic tomography (HT) is a popular method for the delineation of the spatial distributions of hydraulic properties in the groundwater aquifer. Previous researches investigated the spatial distributions of hydraulic properties by the HT survey using the constant head boundary condition. However, the constant head is not the real condition in the boundary condition at the field. The study purpose is the case studies of two years at the same site using the time-variable boundary conditions to delineate the reproducibility of hydraulic properties.

The study area is located in National Yunlin University of Science and Technology (NYSUT) campus in Taiwan. The sequential pumping test is carried in 2010 and 2012 were used for the inverse modeling effort to estimate the hydraulic properties. The boundary condition is applied to the HT method using the sensitivity equation method (SEM) to calibrate the time-variable heads. Then, the reproducibility of estimates and prediction were analyzed in two different years. The results show that the more heterogeneity of hydraulic properties. The HT method can be improved using the time-variable boundary conditions.

Keywords: Sensitivity equation method, Boundary condition, Hydraulic tomography, Sequential pumping test, Heterogeneity, Hydraulic property

©2019. Japan Geoscience Union. All Right Reserved.

Applying river pollution index and QUAL2K model for water quality assessment and management in Ke-Ya river, Taiwan

*Hong-Syuan Li[1], Yu-Chih Lin[1]

1. Department of Environmental Engineering & Health, Yuanpei University of Medical Technology

Waste water from hundreds of factories in Hsiang-Shan industrial park, Hsinchu Science Park, animal husbandry, metal surface electroplating industries, and domestic sewage are discharged into Keiya River HshinChu, Taiwan. In this study, monitoring data of the Keya River was collected, the river pollution index (RPI) and QUAL2K models were utilized for analysis and assessment of water quality. The divide of pollution collection area and evaluation of the assimilative capacity were also discussed.
The results indicated that the main pollutant in the water quality of Keiya River was ammonia nitrogen, which was contained in wastewater discharged from residential areas and Hsinchu Science Park etc., the second was biochemical oxygen demand (BOD). In order to improve the problem of ammonia nitrogen in the rivers, the Taiwan Environmental Protection Agency has tightened the emission limits of ammonia and nitrogen concentrations in wastewater discharges from 2012. The ammonia nitrogen wastewater treatment modules were also installed in the Hsinchu Science Park to reduce ammonia nitrogen emissions into rivers. In addition, the Hsinchu City Environmental Protection Bureau has strengthened the control of the copper standard for discharge water upto 1.5mg/L from 2017, so that the copper concentration in the current river water was maintained at <0.001-0.03mg/L, which was compliance with the environmental standards related to human health protection.

Keywords: river pollution index, assimilative capacity, ammonia nitrogen

©2019. Japan Geoscience Union. All Right Reserved.

Environmental assessment at CDW disposal sites in Vietnam: Case study in Thanh Tri landfill, Hanoi

*Thanh Ha Ngo[1], Akihiro Matsuno[1], Ken Kawamoto[1]

1. Graduate School of Science and Engineering, Saitama University

In the last recent decade, Vietnam has become one of most developing countries within South East Asia. Due to a rapid increasing of economic and industrial, the amount of construction and demolition waste (CDW) in Vietnam also increasing fast and becoming one of the biggest issue for the surrounding environment. According to MONRE, in 2015, Vietnam produced 1.9 million tons of CDW, while the recycling rate was only accounted for 1 −2%. In particularly, 30% of total solid waste generated in Hanoi was reported as CDW during the period of 2010 −2014. Currently, most of generated CDW from construction and demolition sites is reused on-/off sites without any quality control of materials and dumped at disposal sites along with collected waste from town cleaning (e.g., sludge and soil). At CDW disposal site, there is a potential risk of accepting hazardous and scheduled waste together with non-hazardous waste due to lack of management and control of waste acceptance. Therefore, in order to have environmental risk assessment of CDW disposal sites in Vietnam, it is important to identify the current environmental status of CDW dumping sites according to an appropriate monitoring program. In this study, we assessed qualities of water, gas, and fine residues (soil and fines of dumped CDW) inside the disposal site and its surrounding at Thanh Tri Landfill CDW disposal site in Hanoi as a case study. The final goal of study is to develop a standard monitoring/operating procedure for environmental assessment of CDW disposal sites in Vietnam. The field monitoring of surface gas emission and the sampling of internal gas, water, and fine residues, and investigation of dumped scheduled waste at the site were carried out on December 2018. The internal gas samples were collected at six different points from 0.5 - 1m depth and a flux chamber method applied to determine surface gas emission. The groundwater sample was taken from a well inside the disposal site. Results showed very low concentration of methane (CH4) and Carbon Dioxide (CO2). In the meantime, groundwater quality showed that the amount of Ferrous and Arsenic became higher than Vietnam technical regulation on drinking water (QCVN 01:2009/BYT) and Vietnam technical regulation on domestic water (QCVN 02:2009/BYT).

Keywords: Environmental assessment, CDW disposal sites

©2019. Japan Geoscience Union. All Right Reserved.

Modeling Study on the Impacts of Groundwater Pumping to Regional Hydroclimatology in 37 World Major Aquifers

*Pat J.-F. Yeh[1]

1. Monash University Malaysia

Groundwater pumping (GWP) introduces dormant fossil waters into the active hydrologic cycle and alters the mand and atmosphere water budgets, but its effects are poorly understood due to the lack of large-scale GWP information and hydrometeorological data to estimate these changes. In this study, two sets of global-scale model simulations by a fully-coupled climate-hydrologic model, one with GWP and the other one without, are conducted for the 1900-1999 period. The effects of GWP in affecting the land and atmospheric water budgets are investigated over the selected 37 major aquifers worldwide by analyzing the output data from both sets of simulations. The entire set of the internally-consistent water budget components, includ precipitation (P), evaporation (E), runoff (R), atmospheric vapor convergence (C), and changes in land, ocean and atmosphere water storages, are analyzed, and their differences between tow simulations are considered the effects due to GWP. The contribution of GWP to global sea level rise (GSLR) as a result of the changes in the land and atmospheric water budgets is also estimated via (1) the direct R contribution from land to ocean and (2) the indirect C contribution via atmospheric interactions.

Keywords: groundwater, water budget, sea level rise, model simulations

©2019. Japan Geoscience Union. All Right Reserved.

CHRATERIZING BURIED WASTE COMPOSITION AT CONSTRUCTION AND DEMOLITION WASTE (CDW) DISPOSAL SITE IN VIETNAM: A CASE STUDY IN THANH TRI LANDFILL IN HANOI

*Tselmeg Aldarjav[1], Akira Kato[1], Akihiro Matsuno[1], Ken Kawamoto[1,2]

1. Graduate School of Science and Engineering, Saitama University, Japan , 2. International Institute for Resilient Society, Saitama University, Japan

In recent years building and construction work has been growing rapidly in Vietnam, as construction sector expanded simultaneously the waste generated have increased as well. Due to increasing cost and handling availability of CDW disposal the landfilling approach is the most common and cost-efficient way of disposal in developing countries, including Vietnam. On the other hand, due to lack of technical and management abilities, it is very difficult to collect the data on amount and composition of CDW dumped to the landfilling site. The data on amount and composition of dumped CDW is necessary to evaluate the remaining lifetime of present CDW landfills and to examine the possible recycling strategy and method of CDW fills in future. Besides, the waste composition data contributes to classify the type of CDW landfills. The data on the ratio of each amount is currently not available. In this study, a field survey including pit sampling of buried waste, size grading, weighting of graded fractions, and categorization of waste has been done at Thanh Tri landfill site located on the south-eastern side of Hanoi, Vietnam. The final goals of study are 1) to develop a technical manual to investigate buried CDW at disposal sites, and 2) to characterize waste composition, physical and chemical characteristics of dumped waste in Vietnam. The overall procedure of the manual includes 5 parts: 1. Preliminary survey work, 2. Design of CDW composition survey, 3. Set-up of CDW composition survey, 4. Excursion of CDW composition survey, and 5. data analysis. The proposed manual enables not only to measure the waste composition but also to characterize particle size distribution of buried waste.

Keywords: Construction and Demolition Waste , Waste composition, Landfill, Survey, Manual, Vietnam

©2019. Japan Geoscience Union. All Right Reserved.

[E] 口頭発表 | セッション記号 A (大気水圏科学)：A-CG 大気海洋・環境科学複合領域・一般

2019年5月30日(木) 9:00 ~ 10:30 | 302 3F

[A-CG34] 衛星による地球環境観測

コンビーナ:沖 理子(宇宙航空研究開発機構)、本多 嘉明(千葉大学環境リモートセンシング研究センター)、高薮 縁(東京大学 大気海洋研究所)、松永 恒雄(国立環境研究所地球環境研究センター／衛星観測センター)、座長:鈴木 健太郎

近年、我々は様々な時空間スケールで起こる地球環境変動の問題を意識せざるを得ない状況下にある。衛星による地球環境観測データは、その問題への対処や解決に向けて必要不可欠な基礎データとなっている。衛星観測の分野は、近年の観測センサ技術とデータ処理技術の進歩により急速な進展を見せつつあり、個々の観測センサデータの精度を吟味する時代から、より高度なデータ利用の時代に入り、ユーザーの裾野も広がっている。また40年以上に渡る観測データの蓄積により、長期変動の解析がもたらす成果に期待が持てるようになり、長期継続観測の重要性が益々増している。利用が複合的になった今日において、大気、海洋、陸域の分野を包含できる本連合大会の大気水圏科学分野のセッションで包括的に取り上げ、関係者の知恵と知識を集結することで地球環境変動の問題に向けた更なる研究と利用の進展、将来の衛星地球観測計画の議論を促進することを目的としてセッション提案を行う。

9:00 ~ 9:15

[ACG34-07] GCOM-C「しきさい」による初年の観測について

★招待講演

*村上 浩[1]、堀 雅裕[1]、宮崎 理紗[1]、小林 利行[1]、永尾 隆[1]、緒方 一紀[1]、島田 利元[1]、高久 淳一[2] (1.宇宙航空研究開発機構地球観測研究センター、2.リモートセンシング技術センター)

9:15 ~ 9:30

[ACG34-08] Algorithm improvement for GCOM-C/SGLI Above Ground Biomass Standard product.

*梶原 康司[1]、本多 嘉明[1] (1.千葉大学)

9:30 ~ 9:45

[ACG34-09] Common retrieval of Atmospheric Aerosol Properties for geostationary and polar-orbital Satellite Imaging Sensors: Himawari8/AHI and GCOM-C/SGLI results

*吉田 真由美[1]、菊池 麻紀[1]、永尾 隆[1]、村上 浩[1]、弓本 桂也[2] (1.宇宙航空研究開発機構、2.九州大学)

9:45 ~ 10:00

[ACG34-10] Cloud optical properties from various ground and satellite instruments evaluated during an intensive campaign

*Alessandro Damiani[1]、Hitoshi Irie[1]、Takashi Horio[1]、Tamio Takamura[1]、Rei Kudo[2]、Pradeep Khatri[3]、Hironobu Iwabuchi[3]、Ryosuke Masuda[3]、Takashi M. Nagao[4] (1.CEReS, Chiba University、2.Meteorological Research Institute, Japan Meteorological Agency、3.Graduate School of Science, Tohoku University、4.Earth Observation Research Center, JAXA)

10:00 ~ 10:15

[ACG34-11] Issues in aerosol-cloud-climate interaction: Needs for future satellite mission

★Invited Papers

*鈴木 健太郎[1] (1.東京大学大気海洋研究所)

10:15 ~ 10:30

[ACG34-12] Impact of aerosol vertical profile and optical parameters on the accuracy of satellite AOD retrieval

*Jing Li[1]、Chong Li[1] (1.Peking University)

GCOM-C「しきさい」による初年の観測について
GCOM-C “Shikisai” FIRST YEAR OBSERVATIONS

*村上 浩[1]、堀 雅裕[1]、宮崎 理紗[1]、小林 利行[1]、永尾 隆[1]、緒方 一紀[1]、島田 利元[1]、高久 淳一[2]
*Hiroshi Murakami[1], Masahiro Hori[1], Risa Miyazaki[1], Toshiyuki Kobayashi[1], Takashi M. Nagao[1], Kazunori Ogata[1], Rigen Shimada[1], Junichi Takaku[2]

1. 宇宙航空研究開発機構地球観測研究センター、2. リモートセンシング技術センター
1. Earth Observation Research Center, Japan Aerospace Exploration Agency, 2. Remote Sensing Technology Center of Japan

One-year observation results of Global Change Observation Mission-Climate (GCOM-C) called “SHIKISAI” are introduced.

JAXA polar-orbit satellite, GCOM-C, which carries Second-generation Global Imager (SGLI), has been launched on 23 Dec. 2017, and operated in orbit during 2018. The key characteristics of the SGLI are (1) 250-m spatial resolution with 1150 km or 1400 km swath, and (2) nineteen bands in 0.38-12 um including two polarimetry bands (at 672 nm and 866 nm) with +/- 45 degree along-track tilt.

The SGLI radiometric gain was evaluated by the on-board calibration functions (solar, lamp, lunar, and electric calibrations) and vicarious calibration over the land, ocean and ice sheet. The radiometric gain was stable during the first year except for slight degradation (<2 %/year) in 380-565 nm bands. The geometric correction accuracy was evaluated by the Ground Control Point (GCP) matching. The deviation from the GCPs was stable and kept less than about 0.3 pixels.

The SGLI 250-m bands could capture seasonal change of the vegetation and the snow cover, the large-scale red tide, and the fine structures of land-surface temperature and coastal sea-surface temperature. Especially, unique functions of SGLI, the 380-nm band and polarimetry revealed the fine-mode aerosol distribution around wild fires (e.g., California, Africa, and Siberia) and Asian city areas (e.g., North India, and East China). The polarimetry seemed to improve estimation of the aerosols emitted densely from the fires. Difference of the 250-m land-surface temperature between the day and nighttime may give us information about the heat budget in the various land covers including city and crop areas. The GCOM-C standard products have been evaluated and open to public freely through JAXA data portal, G-portal, since Dec. 2018. The re-process of the 2018 data will be completed in the early summer 2019. The accumulating GCOM-C data products are expected to be used in the wide areas of the earth environment researches.

キーワード：GCOM-C、SGLI、リモートセンシング
Keywords: GCOM-C, SGLI, remote sensing

©2019. Japan Geoscience Union. All Right Reserved.

Algorithm improvement for GCOM-C/SGLI Above Ground Biomass Standard product.

Algorithm improvement for GCOM-C/SGLI Above Ground Biomass Standard product.

*梶原 康司[1]、本多 嘉明[1]
*KAJIWARA Koji[1], Yoshiaki HONDA[1]

1. 千葉大学
1. Chiba University

On 23rd Dec., 2017, Japan Aerospace Exploration Agency (JAXA) has launched new Earth observation satellite GCOM-C . GCOM-C equips Second-generation Global Land Imager (SGLI) as core sensor. Since SGLI can observe nadir and off-nadir angle with along-track direction simultaneously, it is expected to retrieve forest Above Ground Biomass (AGB) using bi-directional spectral data.

For the estimation of forest AGB, difference of bi-directional reflectance of each observation angle caused by forest canopy structure will be key information.

Authors have been developed basic AGB estimation algorithm for SGLI AGB standard product. This algorithm is based on the empirical model related to the relationship between reflectance shift on the Red-NIR plane for different viewing angle and AGB. The algorithm requires optimum approximation coefficients directly related AGB amount in observed area for each forest type. In 1st stage product algorithm, we have decided these coefficients using AGB in-situ dataset collected from literature survey which work has been conducted by JAMSTEC. While the AGB estimation results using SGLI reflectance data achieved success criteria for initial stage, it is required for getting better accuracy to achieve the full success criteria.

In this paper, development of algorithm for aimed at improving accuracy was discussed. The improved algorithm which adopting the rasterized AGB existed data base and change the zoning method, has been tested. The result of the trial, the accuracy of estimation has been confirmed.

キーワード：Second Generation Global Imager (SGLI)、Multi-angular observation、Forest canopy、Biomass Estimation
Keywords: Second Generation Global Imager (SGLI), Multi-angular observation, Forest canopy, Biomass Estimation

©2019. Japan Geoscience Union. All Right Reserved.

Common retrieval of Atmospheric Aerosol Properties for geostationary and polar-orbital Satellite Imaging Sensors: Himawari8/AHI and GCOM-C/SGLI results

*吉田 真由美[1]、菊池 麻紀[1]、永尾 隆[1]、村上 浩[1]、弓本 桂也[2]
*Yoshida Mayumi[1], Maki Kikuchi[1], Takashi M. Nagao[1], Hiroshi Murakami[1], Keiya Yumimoto[2]

1. 宇宙航空研究開発機構、2. 九州大学
1. Japan Aerospace Exploration Agency, 2. Kyusyu University

Aerosols influence the energy budget of the earth’ s climate system through scattering and absorbing solar radiation. The Intergovernmental Panel on Climate Change Fifth Assessment Report (IPCC, 2014) reported that the radiative forcing of the total aerosol effect in the atmosphere, which includes cloud adjustments due to aerosols, is −0.9 W m^{-2} and results from a negative forcing from most aerosols with a positive contribution from black carbon absorption of solar radiation. However, the range of the uncertainties remains large (−1.9 W m^{-2} to −0.1 W m^{-2}).

For a more precise estimation of the impact of aerosols on climate systems, investigation of the behavior of aerosols on a global scale is essential but challenging because aerosol amounts and characteristics vary over space and time.

Aerosol remote sensing studies have been carried out using polar-orbital Earth observation satellites. JAXA has launched Global Change Observation Mission-Climate (GCOM-C)/Second-generation GLobal Imager (SGLI) at the end of 2017, and Greenhouse gases Observing SATellite- 2 (GOSAT-2)/Cloud and Aerosol Imager 2 (CAI-2) in 2018. In several years, Earth Clouds Aerosols and Radiation Explorer (EarthCARE)/ Multi-Spectral Imager (MSI) will be launched.

In addition, the next-generation geostationary satellite of the Japan Meteorology Agency (JMA), Himawari-8, was launched on October 7, 2014. It carries the Advanced Himawari Imager (AHI), which has six bands from visible to near-infrared wavelengths. It is significantly different from the previous Himawari-6/7 having only one channel in the wavelengths, which made the estimation of aerosol difficult because the assumption of aerosol type is necessary. Himawari-8/AHI observes the top of atmosphere (TOA) visible and near-infrared radiance at a resolution of 0.5–2.0 km over Asia and Oceania at every 10 min, which enables frequent aerosol estimation over the same ground targets.

The synergistic uses of these various imaging sensors on both geostationary and polar-orbital satellites are helpful to understand a complete picture of aerosol distribution in the global scale. For this purpose, we developed the common retrieval algorithm of the atmospheric aerosol properties for various satellite sensors and over both land and ocean.

The algorithm is based on the method developed by Higurashi and Nakajima (1998) and Fukuda et al. (2013). The three main features in the concept of this algorithm are as follows: (1) automatic selection of the optimum channels for aerosol retrieval by introducing a weight for each channel to the object function, (2) setting common candidate aerosol models over land and ocean, and (3) preparation of lookup tables for every 1 nm in the range of 300 to 2500 nm of wavelength and weighting the radiance using the response function for each sensor.

©2019. Japan Geoscience Union. All Right Reserved.

The method was applied to Himawari-8/AHI and GCOM-C/SGLI. The validation study indicated that aerosol optical thickness estimated from our algorithm was generally consistent with the products from Moderate Resolution Imaging Spectro-radiometer (MODIS) and Aerosol Robotic Network, and SKYNET.

In addition, the utilization of the aerosol properties forecasted by a global aerosol transport model for the retrieval are discussed.

キーワード：エアロゾル、リモートセンシング、ひまわり、SGLI
Keywords: earosol, remote-sensing, Himawari, SGLI

©2019. Japan Geoscience Union. All Right Reserved.

Cloud optical properties from various ground and satellite instruments evaluated during an intensive campaign

*Alessandro Damiani[1], Hitoshi Irie[1], Takashi Horio[1], Tamio Takamura[1], Rei Kudo[2], Pradeep Khatri[3], Hironobu Iwabuchi[3], Ryosuke Masuda[3], Takashi M. Nagao[4]

1. CEReS, Chiba University, 2. Meteorological Research Institute, Japan Meteorological Agency, 3. Graduate School of Science, Tohoku University, 4. Earth Observation Research Center, JAXA

An intensive campaign to monitor the atmospheric environment (i.e., aerosols, clouds, and gases) has been carried out at the SKYNET station of Chiba University in November 2018. The station is equipped with a broad range of meteorological instruments as well as sky radiometers and is part of various international research networks. Due to their challenging estimation from ground observations and the typical discrepancy between satellite and surface-based estimates, here we focus on cloud optical properties taking a particular interest in cloud optical depth (COD). First, we conducted a careful evaluation of four COD datasets retrieved from surface observations of i) zenith radiance recorded by a sky-radiometer (based on two independent algorithms), ii) solar radiation taken by a pyranometer and iii) spatial distribution of radiance recorded by a camera system equipped with fisheyes lens. Then, we assessed satellite-based estimations of COD retrieved from AHI/Himawari-8 and SGLI/GCOM-C observations trying to explain the differences between satellite and ground data in term of atmospheric conditions, acquisition geometry and COD spatial distribution. Preliminary results achieved from this activity will be presented.

Keywords: satellite, clouds, solar radiation

©2019. Japan Geoscience Union. All Right Reserved.

Issues in aerosol-cloud-climate interaction: Needs for future satellite mission

*鈴木 健太郎[1]
*Kentaroh Suzuki[1]

1. 東京大学大気海洋研究所
1. Atmosphere and Ocean Research Institute, University of Tokyo

The aerosol forcing is the largest source of uncertainty in determining climate forcing that drives global climate change. The aerosol forcing consists of the so-called direct (aerosol-radiation interaction) and indirect (aerosol-cloud interaction) effects, both of which are subject to significant uncertainty. This uncertainty arises from our lack of understanding on key processes that govern interactions between aerosol, cloud and climate. Precipitation, among those processes, is central to the aerosol-cloud-climate interaction through its effect of depleting both clouds and aerosols. The aerosol-induced precipitation change influences the cloud lifetime and amount, whereas the precipitation change also modulates the wet removal of aerosols. This underscores a fundamental role of precipitation in shaping the aerosol-cloud-climate interaction. Recent advance in satellite observations by multiple sensors and platforms enabled us to observationally diagnose the precipitation processes on the global scale particularly, which also offers a process-level constraint on model representation of the processes. Such a “bottom-up” model constraint, however, turned out to be inconsistent with “top-down” energy balance requirement on model performance, exposing error compensations in state-of-the-art climate models at a fundamental level. This proposes that there is still a gap in our understanding of the aerosol-cloud-climate processes that hampers their reliable modeling. This presentation discusses what is required to observe in future satellite missions for filling the gap in understanding and modeling the aerosol-cloud-climate interaction. In particular, observational needs for aerosol, cloud and precipitation will be argued to better quantify aerosol-induced climate forcing in the context of recent Aerosol-Cloud-Convection-Precipitation (A-CCP) discussion emerging from the US Decadal Survey and multiple community efforts for process-oriented model diagnostics in an attempt to advance climate modeling.

キーワード：エアロゾル、雲・降水、気候モデリング、衛星観測
Keywords: Aerosol, Cloud and precipitation, Climate modeling, Satellite observation

©2019. Japan Geoscience Union. All Right Reserved.

Impact of aerosol vertical profile and optical parameters on the accuracy of satellite AOD retrieval

*Jing Li[1], Chong Li[1]

1. Peking University

Satellite sensors are widely used to monitor large scale aerosol variability from space. However, current aerosol retrieval algorithm used by passive sensors still suffers from uncertainties in a series of assumptions, with two important ones being aerosol vertical distribution and scattering/absorbing parameters. In this study, we investigate the effect of these two assumptions on the accuracy of retrieved aerosol optical depth (AOD) using both sensitivity experiments and actual retrieval practices. Using the 6S and Modtran radiative transfer model, we find that the retrieved AOD is very sensitive to the height of absorbing aerosols, and the effect increases with surface albedo. In extreme cases, the error can be as large as 80%. The retrieval results are also quite sensitive to aerosol single scattering albedo, compared to other parameters such as asymmetry parameter and effective radius. Using the aerosol profiles and optical parameters measured by lidar and sunphotometer at the PKU site, we find that the retrieval accuracy can be greatly improved by ~50%. Our results highlight the necessity to refined aerosol profile and optical parameters in the passive retrieval algorithms, possibly through space born lidars and ground based observations.

Keywords: aerosol satellite retrieval, aerosol vertical profile, aerosol single scattering abledo, lidar

©2019. Japan Geoscience Union. All Right Reserved.

[E] 口頭発表 | セッション記号 A (大気水圏科学)：A-CG 大気海洋・環境科学複合領域・一般

2019年5月30日(木) 10:45 ~ 12:15 | 302 3F

[A-CG34] 衛星による地球環境観測

コンビーナ:沖 理子(宇宙航空研究開発機構)、本多 嘉明(千葉大学環境リモートセンシング研究センター)、高薮 縁(東京大学 大気海洋研究所)、松永 恒雄(国立環境研究所地球環境研究センター／衛星観測センター)、座長:高橋 暢宏(名古屋大学宇宙地球環境研究所)

近年、我々は様々な時空間スケールで起こる地球環境変動の問題を意識せざるを得ない状況下にある。衛星による地球環境観測データは、その問題への対処や解決に向けて必要不可欠な基礎データとなっている。衛星観測の分野は、近年の観測センサ技術とデータ処理技術の進歩により急速な進展を見せつつあり、個々の観測センサデータの精度を吟味する時代から、より高度なデータ利用の時代に入り、ユーザーの裾野も広がっている。また40年以上に渡る観測データの蓄積により、長期変動の解析がもたらす成果に期待が持てるようになり、長期継続観測の重要性が益々増している。利用が複合的になった今日において、大気、海洋、陸域の分野を包含できる本連合大会の大気水圏科学分野のセッションで包括的に取り上げ、関係者の知恵と知識を集結することで地球環境変動の問題に向けた更なる研究と利用の進展、将来の衛星地球観測計画の議論を促進することを目的としてセッション提案を行う。

10:45 ~ 11:00

[ACG34-13] GPM/DPRの推定する雨滴粒径分布の統計的手法による検証

*高橋 暢宏[1] (1.名古屋大学　宇宙地球環境研究所)

11:00 ~ 11:15

[ACG34-14] Impact study of DPR SLH nudging method for data assimilation in the JMA Local NWP system

★Invited Papers

*幾田 泰酵[1] (1.気象庁)

11:15 ~ 11:30

[ACG34-15] Precipitation Extremes Monitoring using Global Satellite Mapping of Precipitation (GSMaP) Product

*久保田 拓志[1]、田島 知子[1]、沖 理子[1]、妻鹿 友昭[2]、牛尾 知雄[2] (1.宇宙航空研究開発機構　地球観測研究センター、2.首都大学東京　システムデザイン学部)

11:30 ~ 11:45

[ACG34-16] Estimation of cloud water content over land using satellite-based passive microwave observations with a coupled land and atmosphere assimilation method

*瀬戸 里枝[1]、鼎 信次郎[1] (1.東京工業大学)

11:45 ~ 12:00

[ACG34-17] Ensemble-Based Data Assimilation of GPM/DPR Reflectivity into the Nonhydrostatic Icosahedral Atmospheric Model NICAM

*小槻 峻司[1]、寺崎 康児[1]、三好 建正[1] (1.国立研究開発法人　理化学研究所　計算科学研究センター)

12:00 ~ 12:15

[ACG34-18] **An ecohydrological land reanalysis by integrating simulation and satellite observations**

*澤田 洋平[1]、仲江川 敏之[1]、岡本 幸三[1]、入口 武史[1]、藤井 秀幸[2] (1.気象庁気象研究所、2.宇宙航空研究開発機構)

GPM/DPRの推定する雨滴粒径分布の統計的手法による検証
Statistical validation of drop size distribution estimated by GPM/DPR

*高橋 暢宏[1]
*Nobuhiro Takahashi[1]

1. 名古屋大学　宇宙地球環境研究所
1. Institute for Space-Earth Environmental Research, Nagoya University

The dual-frequency precipitation radar (DPR) onboard Global Precipitation Measurement (GPM) core satellite provides the information of the model parameter of the drop size distribution (DSD) assuming the Gamma type DSD model by using Ku-band (KuPR) and Ka-band (KaPR) radar observations. In the current DPR algorithm introduces ε (epsilon) as a DSD parameter that is constant in the vertical profile. The ε is defined as a control parameter in k-Z relationship as $k=\varepsilon \alpha Z^{\wedge}\beta$, where k is specific attenuation in (dB/km) and, α and β is constant value, respectively. Therefore, once ε and Z are determined, DSD (and then R) and Z(Ku) - Z (Ka) relationship are determined.

The purpose of this study is to evaluate ε estimated from DPR algorithm by statistical approach. In this study, two methods are implemented: 1) Histogram matching between Z from KuPR and KaPR, and 2) Estimation of ε from PIA-zeta relationship that can be calculated both KuPR and KaPR individually (single frequency method).

Data used in this study are DPR level-2 (Matched swath) in 2015, 2016 and 2017. Before applying the methods, backscattering database for Ku, Ka and W band using Mie theory and Z(Ku)-Z(Ka), Z(Ku)-Z(W) table for various ε ranging from 0.3 to 2.0 with 0.05 intervals, are prepared.

The histogram method compares histograms of Z (Ku) and Z (Ka). In this analysis, the average ε at a certain area (e.g. 10 x 10 degrees box in latitude and longitude) represent the typical value of the area. Since the difference in the histograms of Z both from the KuPR and KaPR reflects the difference in Mie effect between KuPR and KaPR and therefore ε represents the corresponding DSD model. In other words, if we know the ε, we can reproduce the KaPR histogram from KuPR histogram. In this analysis, starting from KuPR histogram, the most appropriate KaPR histogram is tried to find by changing the ε. The advantage of this approach is that ε can be estimated various height (e.g. 1 km, 2 km) if the both KuPR and KaPR data exist. This method, however, is not independent estimation of ε from the standard algorithm of DPR because this method uses the attenuation corrected Z by the standard algorithm that implicitly include the ε. For the calculation of ε, exceedance probability of Z histogram is used. This method can be utilized for different orbital sensors such as the comparison between CloudSat and TRMM/PR.

The next method is to utilize the path integrated attenuation (PIA)- zeta(ζ) relationship (regression method). According to Iguchi et al. (2000),
$1-10^{\wedge}(-PIA\beta/10)=\varepsilon\zeta$, where ζ is the integral of specific attenuation using the observed Z(Zm) instead of attenuation corrected Z multiplied by $0.2\ln(10)\beta$. PIA is estimated by the observation of the surface echo (surface reference method). By making a scatter plot of $1-10^{\wedge}(-PIA\beta/10)$ and ζ, ε corresponds to the slope of this plot. The slope in Ku-band corresponds to the ε in this study. Ka-band epsilon is calculated using the same k-Z relationship with Ku-band.

©2019. Japan Geoscience Union. All Right Reserved.

The ε estimated by these two methods are compared with the average value of ε from standard algorithm. Basically ε from both methods correlate well with the ε from the standard algorithm. Note that the variance ε from the regression method is twice large as the standard algorithm. This result may be caused by that the standard algorithm not to determine the ε under less attenuated situation. The regression method can be utilized to assess the k-Z relationship between Ku and Ka and the histogram method of various height indicates the constant ε of the throughout the profile may not be valid.

キーワード：降水、レーダ、雨滴粒径分布
Keywords: Precipitation, radar, drop size distribution

©2019. Japan Geoscience Union. All Right Reserved.

Impact study of DPR SLH nudging method for data assimilation in the JMA Local NWP system

*幾田 泰酵[1]
*Yasutaka Ikuta[1]

1. 気象庁
1. Japan Meteorological Agency

GPM DPR Spectral Latent Heating (GPM-SLH) profile is a very valuable product with three-dimensional latent heating information of precipitation system. The data assimilation of this GPM-SLH is expected to improve the precipitation prediction in numerical weather prediction. The impact of SLH data assimilation is investigated in the Local NWP system which includes the high-resolution numerical prediction model called Local Forecast Model (LFM) of Japan Meteorological Agency.

The purpose of the operation of LFM is to provide information on very-short range precipitation forecast and aviation weather forecasting. The initial condition for the LFM is created by hourly data assimilation in the Local NWP system because the forecast immediacy is important for the achievement of the LFM's aims. Thus the forecast of LFM from the initial condition has latest information of real atmosphere by the hourly assimilation. However, this data assimilation system consists of simple 3D-VAR combined with prediction which is capable of performing speedy calculation for rapidly updating the forecast.

GPM-SLH nudging method corrects the latent heating in cloud microphysics scheme while the numerical prediction model is running in the assimilation window. It is a very efficient method that can input SLH information into the model with keeping immediacy of forecast. In the Local NWP system, the nudging method was implemented and impact studies of SLH assimilation were conducted in typical cases of mid-latitude precipitation system. In this presentation, I will show the result of impact study of GPM-SLH assimilation and the problems to be addressed.

©2019. Japan Geoscience Union. All Right Reserved.

Precipitation Extremes Monitoring using Global Satellite Mapping of Precipitation (GSMaP) Product

*久保田 拓志[1]、田島 知子[1]、沖 理子[1]、妻鹿 友昭[2]、牛尾 知雄[2]
*Takuji Kubota[1], Tashima Tomoko[1], Riko Oki[1], Tomoaki Mega[2], Tomoo Ushio[2]

1. 宇宙航空研究開発機構　地球観測研究センター、2. 首都大学東京　システムデザイン学部
1. Earth Observation Research Center,Japan Aerospace Exploration Agency, 2. Department of Aerospace Engineering, Tokyo Metropolitan University

Natural hazards caused by weather and climate tend to increase in recent years, and it is recognized that there is a need to better utilize and improve the monitoring of extreme weather and climate events from space. Recently, satellite-based precipitation datasets have been developed to achieve higher spatial and temporal resolutions using combined data from passive microwave (PMW) sensors in low Earth orbit and infrared (IR) radiometers in geostationary Earth orbit. Global Satellite Mapping of Precipitation (GSMaP) is a blended PMW–IR precipitation product and has been developed in Japan for the Global Precipitation Measurement (GPM) mission. In this study, detections of drought and heavy precipitation events are examined using standardised precipitation index (SPI) and a statistical value, to demonstrate a capability of the GSMaP. Such efforts will contribute to precipitation extremes monitoring activities using satellite data, such as the World Meteorological Organization (WMO) Space-based Weather and Climate Extremes Monitoring Demonstration Project (SEMDP) with focus on monitoring drought and heavy precipitation in countries of the South-East Asia and the Pacific.

In this study, GSMaP Near-real-time Gauge-adjusted Rainfall Product (GSMaP_Gauge_NRT) for algorithm version 6 is used. This product is adjusted using an optimization model with parameters calculated from data during the past 30 days. As for weather and climate extremes, here it is defined as an extreme precipitation, when a mean rainfall for a specified period is higher than a threshold based on the percentiles (ex. 95th, 99th percentile). Whereas, drought is diagnosed based on SPI over 1, 2 and 3 months. Percentiles and SPI are calculated in 0.1x0.1 grid at lat/lon resolution from the dataset during 18 years from April 2000 to March 2018. To demonstrate feasibilities of GSMaP_Gauge_NRT (v6) for climate extremes monitoring, we evaluated past cases of drought and heavy rainfall.

The first case is drought in south-eastern Australia during July-September 2007. A drought area where 3-month SPI is less than -1.2 spreads widely around the south of Australia. The detected drought area is roughly consistent with an area above 9th decile (Very Much Below Average) shown by the Bureau of Meteorology (BoM) in Australia. However, because there are few rain gauges in Western Australia’s eastern part, distributions between both are different. The second case is heavy rainfall events in western and eastern Australia in December 2010. Monthly mean precipitation exceeds 95th percentile in western and eastern Australia. These detected heavy rainfall area roughly corresponds to an area below 2nd decile (Very Much Above Average) shown by the BoM. The last case is heavy rainfall events in Malay Peninsula in December 2014, which extreme rainfall caused widespread flooding over Thailand and the east coast of Peninsular Malaysia. Time-fluctuation of GSMaP_Gauge_NRT (v6) daily precipitation averaged over these areas is roughly in good agreement with that of CPC Gauge Analysis. A series of heavy rainfall events beginning on 14 December 2014 can be confirmed from space-based observations. Especially, pentad precipitation for 22-26 December 2014, is higher than 99th percentile over large portion of Peninsular Malaysia. Actually, floods caused by heavy rain hit in this area.

©2019. Japan Geoscience Union. All Right Reserved.

キーワード：降水、衛星、極値
Keywords: Precipitation, Satellite, Extreme

©2019. Japan Geoscience Union. All Right Reserved.

Estimation of cloud water content over land using satellite-based passive microwave observations with a coupled land and atmosphere assimilation method

*瀬戸 里枝[1]、鼎 信次郎[1]
*Rie Seto[1], Shinjiro Kanae[1]

1. 東京工業大学
1. Tokyo Institute of Technology

We proposed a method to estimate the cloud water content (CWC) over land at multiple-kilometer resolutions and to concurrently assimilate the estimated CWC into the model by using multi-frequency satellite-based passive microwave brightness temperatures (TBs) and coupled land and atmosphere assimilation.
The need for a better understanding and more accurate representation of clouds in atmospheric models has been apparent for decades. However, a lack of sufficient observations and reanalysis products is a major obstacle. The use of TBs is an effective way to retrieve CWC of extensive and heterogeneous cloud systems all at once, but it is challenging to estimate CWC over land due to complexities of cloud processes and uncertainties in strong and heterogeneous land emissions. Our method overcomes the difficulty of retrieving clouds over land from TBs and representing them in models by simultaneously optimizing land emissions and CWC over land, and assimilating the estimations into models.
The estimated CWC was in good accordance with vertical two-dimensional products of CloudSat in terms of cloud water path and the vertical distribution of CWC. In addition, we examined the uncertainties of this method by sensitivity analysis of CWC estimates of TBs and cloud top height. The results suggested that the error in TBs is not large, and that cloud top height affects the estimated CWC more sensitively than TBs. The addition of cloud top height information from other satellite observations as a constraint of optimization allows further improvement of the vertical distributions of CWC.
This study revealed that the proposed method has great potential to provide unprecedented data for CWC with adequate accuracy, which are continuously distributed over land and ocean.

キーワード：陸域雲水量の推定、衛星搭載マイクロ波放射計、陸面と大気の同時同化
Keywords: estimation of cloud water content over land, satellite-based passive microwave brightness temperature, coupled assimilation of land and atmosphere

©2019. Japan Geoscience Union. All Right Reserved.

Ensemble-Based Data Assimilation of GPM/DPR Reflectivity into the Nonhydrostatic Icosahedral Atmospheric Model NICAM

*小槻 峻司[1]、寺崎 康児[1]、三好 建正[1]
*Shunji Kotsuki[1], Koji Terasaki[1], Takemasa Miyoshi[1]

1. 国立研究開発法人　理化学研究所　計算科学研究センター
1. RIKEN Center for Computational Science

This study aims to improve the precipitation forecasts from numerical weather prediction models through effective assimilation of satellite-observed precipitation data. The assimilation of precipitation data is known to be difficult mainly due to highly non-Gaussian statistics of precipitation-related variables. We have been developing a global atmospheric data assimilation system NICAM-LETKF, which comprises the Nonhydrostatic ICosahedral Atmospheric Model (NICAM) and Local Ensemble Transform Kalman Filter (LETKF). Using the NICAM-LETKF system, Kotsuki et al. (2017, JGR) successfully improved the weather forecasts by assimilating the Japan Aerospace eXploration Agency (JAXA)’s Global Satellite Mapping of Precipitation (GSMaP) data into the NICAM at 112-km horizontal resolution. However, assimilating space-borne precipitation radar data remains to be a challenging issue.

This study pioneers to assimilate radar reflectivity measured by the Dual-frequency Precipitation Radar (DPR) onboard the Global Precipitation Measurement (GPM) core satellite into the NICAM. We conduct the NICAM-LETKF experiments at 28-km horizontal resolution with explicit cloud microphysics of a single-moment 6-class bulk microphysics scheme. To simulate GPM/DPR reflectivity from NICAM model outputs, the joint-simulator (Hashino et al. 2013; JGR) is used. Our initial tests showed a better match with the observed reflectivity by assimilating GPM/DPR reflectivity into NICAM forecasts. However, the results from a 1-month data assimilation cycle experiment showed general degradation by assimilating GPM/DPR reflectivity. For better use of GPM/DPR reflectivity data, we are exploring to estimate model cloud physics parameters by assimilating them. This presentation will include the most recent progress up to the time of the meeting.

キーワード：GPM、データ同化、NICAM-LETKF、降水、レーダー反射強度、アンサンブルカルマンフィルタ
Keywords: GPM, Data Assimilation, NICAM-LETKF, Precipitation, Radar Reflectivity, Ensemble Kalman Filter

©2019. Japan Geoscience Union. All Right Reserved.

An ecohydrological land reanalysis by integrating simulation and satellite observations

*澤田 洋平[1]、仲江川 敏之[1]、岡本 幸三[1]、入口 武史[1]、藤井 秀幸[2]
*Yohei Sawada[1], Tosiyuki Nakaegawa[1], Kozo Okamoto[1], Takeshi Iriguchi[1], Hideyuki Fujii[2]

1. 気象庁気象研究所、2. 宇宙航空研究開発機構
1. Meteorological Research Institute, 2. Japan Aerospace Exploration Agency

Monitoring terrestrial water, energy, and ecosystem is crucially important to understand global environmental changes. Land reanalysis, in which a land surface model (LSM) is driven by bias-corrected atmospheric forcing based on an atmospheric reanalysis dataset, has greatly contributed to generating the long-term and spatiotemporally homogeneous dataset of terrestrial environmental condition. Here we propose a new land reanalysis called ECoHydrological Land reAnalysis (ECHLA). Compared with the other existing land reanalyses, the characteristics of ECHLA are: (1) ECHLA can simulate not only water and energy, but also vegetation dynamics; (2) ECHLA is generated by sequential data assimilation of satellite microwave observation, which is sensitive to soil moisture and vegetation water content, into a LSM; (3) ECHLA can quantify the uncertainty in its simulated variables by an ensemble method. In this presentation, we will show the concept of ECHLA and the preliminary results of the validation of the ECHLA’s prototype and its application to drought quantification.

Sawada, Y. (2018), Quantifying drought propagation from soil moisture to vegetation dynamics using a newly developed ecohydrological land reanalysis, ***Remote Sensing**, 10,* 1197

キーワード：陸域再解析、マイクロ波リモートセンシング、衛星データ同化
Keywords: land reanalysis, microwave remote sensing, satellite data assimilation

©2019. Japan Geoscience Union. All Right Reserved.

[E] 口頭発表 | セッション記号 A (大気水圏科学)：A-CG 大気海洋・環境科学複合領域・一般

2019年5月30日(木) 15:30 ~ 17:00 | 302 3F

[A-CG34] 衛星による地球環境観測

コンビーナ:沖 理子(宇宙航空研究開発機構)、本多 嘉明(千葉大学環境リモートセンシング研究センター)、高薮 縁(東京大学 大気海洋研究所)、松永 恒雄(国立環境研究所地球環境研究センター／衛星観測センター)、座長:松永 恒雄

近年、我々は様々な時空間スケールで起こる地球環境変動の問題を意識せざるを得ない状況下にある。衛星による地球環境観測データは、その問題への対処や解決に向けて必要不可欠な基礎データとなっている。衛星観測の分野は、近年の観測センサ技術とデータ処理技術の進歩により急速な進展を見せつつあり、個々の観測センサデータの精度を吟味する時代から、より高度なデータ利用の時代に入り、ユーザーの裾野も広がっている。また40年以上に渡る観測データの蓄積により、長期変動の解析がもたらす成果に期待が持てるようになり、長期継続観測の重要性が益々増している。利用が複合的になった今日において、大気、海洋、陸域の分野を包含できる本連合大会の大気水圏科学分野のセッションで包括的に取り上げ、関係者の知恵と知識を集結することで地球環境変動の問題に向けた更なる研究と利用の進展、将来の衛星地球観測計画の議論を促進することを目的としてセッション提案を行う。

15:30 ~ 15:45

[ACG34-19] How GOSAT has survived in-orbit anomalies and calibrated radiance spectra for 10 years.

★Invited Papers

*久世 暁彦[1]、hiroshi Suto[1]、Kei Shiomi[1]、菊地 信弘[1]、橋本 真喜子[1]、Fumie Kataoka[2] (1.宇宙航空研究開発機構、2.リモート・センシング技術センター)

15:45 ~ 16:00

[ACG34-20] Estimating regional anthropogenic methane emissions with GOSAT satellite retrievals and ground-based observations

*Shamil Maksyutov[1]、Aki Tsuruta[2]、Rajesh Janardanan[1]、Fenjuan Wang[1]、Akihiko Ito[1]、Motoki Sasakawa[1]、Toshinobu Machida[1]、Isamu Morino[1]、Yukio Yoshida[1]、Johannes Kaiser[3]、Greet Janssens-Maenhout[4]、Ed Dlugokencky[5]、Tsuneo Matsunaga[1] (1.National Institute for Environmental Studies、2.Finnish Meteorological Institute、3.Deutscher Wetterdienst、4.European Commission, Joint Research Centre 、5.National Oceanic and Atmospheric Administration, Global Monitoring Division)

16:00 ~ 16:15

[ACG34-21] The Status and the Future Plan of GOSAT-2 Level 2 and 4 Products

★Invited Papers

*松永 恒雄[1]、森野 勇[1]、吉田 幸生[1]、齊藤 誠[1]、野田 響[1]、大山 博史[1]、亀井 秋秀[1]、河添 史絵[1]、今須 良一[2]、中島 映至[4]、中島 孝[5]、齋藤 尚子[3]、橋本 真喜子[4] (1.国立環境研究所地球環境研究センター／衛星観測センター、2.東京大学、3.千葉大学、4.宇宙航空研究開発機構、5.東海大学)

16:15 ~ 16:30

[ACG34-22] 温室効果ガス観測技術衛星2号機搭載CAI-2による雲判別プロダクトの初期確認

*石原 吉明[1]、大石 優[2]、石田 春磨[3]、中島 孝[4] (1.国立環境研究所、2.農研機構、3.気象庁、4.東海大学)

16:30 ~ 16:45

[ACG34-23] Drought monitoring and evaluation performance of temperature vegetation drought index (TVDI) over Eurasia

*Fengmei Yao[1]、Siqi Shi[1]、Jiahua Zhang[2] (1.UCAS University of Chinese Academy of Sciences、2.Institute of Remote Sensing and Digital Earth, Chinese Academy of Sciences)

16:45 ~ 17:00

[ACG34-24] IMPACT OF CHANGE IN LAND USE AND LAND COVER PATTERN ON LAND SURFACE TEMPERATURE AND THERMAL COMFORT USING MICRO-SCALE AREA MODEL: CASE STUDY OF

AN EDUCATIONAL CAMPUS.

*DILJIT KUMAR NAYAK[1]、MANJU MOHAN[1] (1.IIT DELHI)

How GOSAT has survived in-orbit anomalies and calibrated radiance spectra for 10 years.

*久世 暁彦[1]、hiroshi Suto[1]、Kei Shiomi[1]、菊地 信弘[1]、橋本 真喜子[1]、Fumie Kataoka[2]
*Akihiko Kuze[1], hiroshi Suto[1], Kei Shiomi[1], Nobuhiro Kikuchi[1], Makiko Hashimoto[1], Fumie Kataoka[2]

1. 宇宙航空研究開発機構、2. リモート・センシング技術センター
1. Japan Aerospace Exploration Agency, 2. RESTEC

Since 2009 Thermal And Near infrared Sensor for carbon Observation Fourier-Transform Spectrometer (TANSO-FTS) onboard the Greenhouse gases Observing SATellite (GOSAT) TANSO-FTS onboard GOSAT has provided 0.2 cm-1-step radiance spectra from solar reflected light in shortwave infrared (SWIR) to thermal infrared (TIR) light using the FTS multiplex-advantage.
The SWIR light passes from the top of the atmosphere to the Earth’s surface providing column-averaged dry air mole fractions of carbon dioxide (CO2) and methane (CH4). TIR light is the thermal emission from the Earth’s atmosphere and surface. By combining these wide spectral data, GOSAT can extract the partial column density of lower troposphere, which shows enhanced density from local anthropogenic emission sources.
For SWIR data analysis, we use robust algorithm of differential optical absorption spectroscopy and optical path modification by thin clouds and aerosol can be calibrated by simultaneously observed oxygen (O2) data. On the other hand, thermal emission measurements need absolute radiometric calibration. Furthermore, the PC-MCT detector for TIR is less linear than the Si and InGaAs detectors for SIWR.
During the 10-year operation in orbit, TANSO-FTS had system-shut-down in May 2014, May 2018, and November 2018 due to satellite anomalies and cryo-cooler shutdown in August 2018. Every time TANSO-FTS restarted, the thermal condition of the TIR detector and optics had changed and parameters for non-linearity corrections had to be updated. We present how we can calibrate SWIR and TIR spectra for 10 years for decade-long uniform quality.

キーワード：Green House Gases、Fourier Transform Spectrometer、CO2、CH4、Thermal Infrared、Shortwave Infrared
Keywords: Green House Gases, Fourier Transform Spectrometer, CO2, CH4, Thermal Infrared, Shortwave Infrared

©2019. Japan Geoscience Union. All Right Reserved.

Estimating regional anthropogenic methane emissions with GOSAT satellite retrievals and ground-based observations

*Shamil Maksyutov[1], Aki Tsuruta[2], Rajesh Janardanan[1], Fenjuan Wang[1], Akihiko Ito[1], Motoki Sasakawa[1], Toshinobu Machida[1], Isamu Morino[1], Yukio Yoshida[1], Johannes Kaiser[3], Greet Janssens-Maenhout[4], Ed Dlugokencky[5], Tsuneo Matsunaga[1]

1. National Institute for Environmental Studies, 2. Finnish Meteorological Institute, 3. Deutscher Wetterdienst, 4. European Commission, Joint Research Centre , 5. National Oceanic and Atmospheric Administration, Global Monitoring Division

GOSAT satellite observations of methane are being used for regional and national methane emission estimates in a number of studies using either high resolution regional inverse models or global medium resolution models. We perform global high-resolution methane flux inversion to estimate global methane emissions using atmospheric methane data collected at global in-situ network, which is archived at WDCGG and NIES, and GOSAT satellite retrievals. High resolution tracer transport is implemented by coupling Lagrangian model FLEXPART to a global atmospheric tracer transport model (NIES-TM) and its adjoint. Prior fluxes at 0.1˚ resolution were prepared for anthropogenic emissions (EDGAR 4.3.2), biomass burning (GFAS), and wetlands (VISIT). The inverse model based on NIES-TM-FLEXPART applies variational optimization to two categories of fluxes: anthropogenic and natural (wetlands). Bi-weekly emissions are estimated for years 2009 to 2017. To reduce GOSAT retrieval biases, the monthly mean difference between GOSAT data and the inversion-optimized forward simulation is estimated for each 5˚ latitude band and it is subtracted from GOSAT retrievals (NIES Level 2 retrievals, v. 02.72) before including them in the inversion. The bias correction is designed to remove large scale biases in GOSAT retrievals, while retaining local scale variability that contains most information on anthropogenic emissions from intense sources such as megacities. Estimated anthropogenic emissions over large regions (US, China, India) are compared to GCP-CH4 top-down estimates. The sensitivity of the estimated emissions to prior fluxes is tested by adjusting the prior fluxes to match UNFCCC reports for selected large countries.

Keywords: methane , inverse model, GOSAT, anthropogenic emissions

©2019. Japan Geoscience Union. All Right Reserved.

The Status and the Future Plan of GOSAT-2 Level 2 and 4 Products

*松永 恒雄[1]、森野 勇[1]、吉田 幸生[1]、齊藤 誠[1]、野田 響[1]、大山 博史[1]、亀井 秋秀[1]、河添 史絵[1]、今須 良一[2]、中島 映至[4]、中島 孝[5]、齋藤 尚子[3]、橋本 真喜子[4]
*Tsuneo Matsunaga[1], Isamu Morino[1], Yukio Yoshida[1], Makoto Saito[1], Hibiki M Noda[1], Hirofumi Ohyama[1], Akihide Kamei[1], Fumie Kawazoe[1], Ryoichi Imasu[2], Teruyuki Nakajima[4], Takashi Nakajima[5], Naoko Saitoh[3], Makiko Hashimoto[4]

1. 国立環境研究所地球環境研究センター／衛星観測センター、2. 東京大学、3. 千葉大学、4. 宇宙航空研究開発機構、5. 東海大学
1. Center for Global Environmental Research and Satellite Observation Center, National Institute for Environmental Studies, 2. The University of Tokyo, 3. Chiba University, 4. Japan Aerospace Exploration Agency, 5. Tokai University

GOSAT-2 (Greenhouse Gases Observing Satellite 2), launched in October, 2018, is the second Japanese Earth observation satellite for greenhouse gas observation from space. It is a joint mission promoted by Ministry of the Environment, JAXA (Japan Aerospace Exploration Agency), and NIES (National Institute for Environmental Studies) as similar to the first satellite, GOSAT, launched in and operated since 2009. Both satellites are designed to measure atmospheric concentrations of carbon dioxide (CO_2) and methane (CH_4) using Fourier transform spectrometers, FTS and FTS-2, with a help of moderate resolution imagers, CAI and CAI-2, for aerosol and cloud observation. The design lifetime of GOSAT-2 is five years and the 15-year record of atmospheric $CO_2$and $CH_4$is now expected from these two satellites.

NIES is responsible for the generation of GOSAT-2's Level 2 and Level 4 standard products which are

1) GOSAT-2 TANSO-CAI-2 L2 Cloud Discrimination Product
2) GOSAT-2 TANSO-CAI-2 L2 Aerosol Property Product
3) GOSAT-2 TANSO-FTS-2 SWIR L2 Chlorophyll Fluorescence and Proxy-method Product
4) GOSAT-2 TANSO-FTS-2 SWIR L2 Column-averaged Dry-air Mole Fraction Product
5) GOSAT-2 TANSO-FTS-2 TIR L2 Cloud and Aerosol Property Product
6) GOSAT-2 TANSO-FTS-2 TIR L2 Temperature and Gas Profile Product
7) GOSAT-2 L4A Global CO2 Flux Product
8) GOSAT-2 L4A Global CH4 Flux Product
9) GOSAT-2 L4B Global CO2 Distribution Product
10) GOSAT-2 L4B Global CH4 Distribution Product

The public release of GOSAT-2 Level 2 and Level 4 products will start by the end of October 2019 and 2020, respectively.

In this presentation, the latest status and the future plan of these products will be introduced.

キーワード：温室効果ガス、気候変動、衛星
Keywords: greenhouse gas, climate change, satellite

©2019. Japan Geoscience Union. All Right Reserved.

温室効果ガス観測技術衛星2号機搭載CAI-2による雲判別プロダクトの初期確認

A preliminary initial check of the cloud discrimination products by CAI-2 onboard GOSAT-2

*石原 吉明[1]、大石 優[2]、石田 春磨[3]、中島 孝[4]
*Yoshiaki Ishihara[1], Yu Oishi[2], Haruma Ishida[3], Takashi Nakajima[4]

1. 国立環境研究所、2. 農研機構、3. 気象庁、4. 東海大学
1. NIES, 2. NARO, 3. JMA, 4. Tokai Univ.

GOSAT-2, which is a successor of Japanese GOSAT (Greenhouse Gases Observing Satellite) which was launched in January 2009 and has been operated for about ten years, is successfully launched on Oct. 29, 2018. Both satellites are jointly developed and operated by Ministry of the Environment, Japan Aerospace Exploration Agency, and National Institute for Environmental Studies. GOSAT-2 carries two mission instruments, Fourier Transform Spectrometer 2 (FTS-2) and Cloud and Aerosol Imager 2 (CAI-2). They are successors of GOSAT FTS and CAI.

Several publicly available standard products will be generated from GOSAT-2 FTS-2 and CAI-2 data. One of these is CAI-2 Level 2 Cloud Discrimination Product and will be used for the detection of clouds within the field of view of FTS-2. CAI-2 cloud discrimination product is generated by one of two different algorithms. One of those is CLAUDIA1 used for GOSAT CAI Level 2 cloud mask product and the other is newly developed CLAUDIA3. And CLAUDIA3 is default algorithm for CAI-2 cloud discrimination product generation.

In this presentation, we will present a very preliminary initial check results of CAI-2 Level 2 cloud discrimination products, including comparison of cloud discrimination results by CLAUDIA1 and CLAUDIA3.

キーワード：GOSAT-2、雲識別
Keywords: GOSAT-2, Cloud Discrimination

©2019. Japan Geoscience Union. All Right Reserved.

Drought monitoring and evaluation performance of temperature vegetation drought index (TVDI) over Eurasia

*Fengmei Yao[1], Siqi Shi[1], Jiahua Zhang[2]

1. UCAS University of Chinese Academy of Sciences, 2. Institute of Remote Sensing and Digital Earth, Chinese Academy of Sciences

Drought has been a common concern recent years as it is one of the high frequent nature disasters in Eurasia that is included in the Belt and Road Initiative under the background of global warming. Thus, it is of great significance to study the drought monitoring and assessment in the region to develop effective plans to mitigate the effects of disasters. This study explored applicability of Temperature Vegetation Drought Index (TVDI) derived from MODIS normalized difference vegetation index (NDVI) and land surface temperature (LST) data as an index for drought monitoring in Eurasia in growing season (April - September) from 2005 to 2014. Three methods were used to compare TVDI against Standardized Precipitation Evapotranspiration Index in three time scales (SPEI-01, SPEI-03, SPEI-06) and the Essential Climate Variable surface soil moisture product (ECV-SM) at continental scales and Land Cover scales, as well as records of drought events from Emergency Events Database (EM-DAT) and relative literatures. The results indicated acceptable correlations between TVDI and SPEIs, ECV-SM in most areas, and TVDI had higher coefficients of correlation with ECV-SM than SPEIs at continental scale. Then we found that the correlation coefficient maps at continental scales were visually consistent with the land cover types, thus correlations between TVDI and SPEIs, ECV-SM were analyzed at Land Cover scales. TVDI showed strong correlation with SPEIs and ECV-SM in evergreen Needle leaf forest, deciduous broad leaf forest and grasslands. However, the accuracy of TVDI in open shrub lands that mainly distributed at high-latitudes remains to be further validated in the future. Finally, a comparison with typical drought-year and typical drought events also demonstrated TVDI could be used as a drought index to monitor drought events in study area over study time.

Keywords: drought monitoring, Temperature Vegetation Drought Index, growing season, continental scale, land cover, drought records

©2019. Japan Geoscience Union. All Right Reserved.

IMPACT OF CHANGE IN LAND USE AND LAND COVER PATTERN ON LAND SURFACE TEMPERATURE AND THERMAL COMFORT USING MICRO-SCALE AREA MODEL: CASE STUDY OF AN EDUCATIONAL CAMPUS.

*DILJIT KUMAR NAYAK[1], MANJU MOHAN[1]

1. IIT DELHI

The influence of change in Land Use Land Cover pattern of an area due to rapid urbanization, over the increment in the Land Surface Temperature (LST) has always been a challenging area for research. This study covers the analysis of the influence of freshly built structure and the storey increment on the thermal comfort of the outdoor environment and Land Surface Temperature with a periodic remotely sensed observation for every three years at IIT Delhi (an educational institute campus). Numerical modelling approach using a 3D microclimate model ENVIMET is implemented for simulating the surface temperature in the presence of hostel residences and in the absence of hostel residences during a summer month of May during the period from 2002 to 2018. The effect of the Sky View Factor on Mean Radiant Temperature is likely to play a key role in influencing the thermal comfort of the residents of the campus. The entire IIT Delhi was classified under open high-rise as per Local Climate Zone (LCZ) categories. It was classified into 17 classes which included eight types of building classification from 4m to 36m and the rest of the nine classes included soil layer, asphalt roads, vegetation cover like trees, dense and light bushes, concrete roads, granite concrete and swimming pool PVC liner. The building class was sub-divided into different classes based on their height to study the effect of high rise buildings on the surface temperature. The model validation is carried out with the LST values obtained from the satellite observation of LANDSAT thermal band. The model estimated the surface temperature giving a correlation of (r=0.95) with the observed values. The RMSE value was found to be 1.28 for the student residence and 2.34 for the non-building structures. Temperature difference over the years as built structure influence was assessed approximately to the tune of 10 degrees. The model performed well in estimating the surface temperature with an accuracy of 94.97 per cent.

Keywords: ENVI-met, 3D microclimate model, Land surface temperature(LST), Land Use Land Cover(LULC), Local Climate Zone(LCZ), Landsat

©2019. Japan Geoscience Union. All Right Reserved.

IMPACT OF CHANGE IN LAND USE AND LAND COVER PATTERN ON LAND SURFACE TEMPERATURE AND THERMAL COMFORT USING MICRO-SCALE AREA MODEL: CASE STUDY OF AN EDUCATIONAL CAMPUS

DILJIT KUMAR NAYAK AND MANJUMOHAN

Centre for Atmospheric Sciences,

Indian Institute of Technology Delhi, Hauz Khas,

New Delhi, India 110016

ABSTRACT

The influence of change in Land Use Land Cover pattern of an area due to rapid urbanization, over the increment in the Land Surface Temperature (LST) has always been a challenging area for research. This study covers the analysis of the influence of freshly built structure and the storey increment on the thermal comfort of the outdoor environment and Land Surface Temperature with a periodic remotely sensed observation for every three years at IIT Delhi (an educational institute campus). Numerical modelling approach using a 3D microclimate model ENVIMET is implemented for simulating the surface temperature in the presence of hostel residences and in the absence of hostel residences during a summer month of May during the period from 2002 to 2018. The effect of the Sky View Factor on Mean Radiant Temperature is likely to play a key role in influencing the thermal comfort of the residents of the campus. The entire IIT Delhi was classified under open high-rise as per Local Climate Zone (LCZ) categories. It was classified into 17 classes which included eight types of building classification from 4m to 36m and the rest of the nine classes included soil layer, asphalt roads, vegetation cover like trees, dense and light bushes, concrete roads, granite concrete and swimming pool PVC liner. The building class was sub-divided into different classes based on their height to study the effect of high rise buildings on the surface temperature. The model validation is carried out with the LST values obtained from the satellite observation of LANDSAT thermal band. The model estimated the surface temperature giving a correlation of (r=0.95) with the observed values. The RMSE value was found to be 1.28 for the student residence and 2.34 for the non-building structures. Temperature difference over the years as built structure influence was assessed approximately to the tune of 10 degrees. The model performed well in estimating the surface temperature with an accuracy of 94.97 per cent.

***Key Words*:** ENVI-met, 3D microclimate model, Land surface temperature(LST), Landsat, Land Use Land Cover, Local Climate Zone(LCZ)

©2019. Japan Geoscience Union. All Right Reserved.

[E] 口頭発表 | セッション記号 H (地球人間圏科学)：H-TT 計測技術・研究手法

2019年5月30日(木) 13:45 ~ 15:15 | 301B 3F

[H-TT19] Geographic Information Systems and Cartography

コンビーナ:小口 高(東京大学空間情報科学研究センター)、村山 祐司(筑波大学大学院生命環境科学研究科地球環境科学専攻)、若林 芳樹(首都大学東京大学院都市環境科学研究科)、座長:村山 祐司、若林 芳樹

地球惑星科学分野で展開されている自然・人文現象に関する地理空間情報を取得，加工，蓄積，分析，可視化するための汎用的な理論と方法を検討する．また，デジタル空間データとGISを用いた実証研究や，地図による具体的な空間表現の成果を発表する．対象を広く設定しているので，GISや地図に関連する隣接諸分野の研究の発表も歓迎する．また，純粋科学的な課題のみならず，教育や社会におけるGISや地図の活用といった応用的な課題や，地球惑星科学分野における意義なども幅広く取り上げる．本セッションは英語で行う．

13:45 ~ 14:00

[HTT19-01] **A study on geographical changes in main roads and coastlines in the 200 years in Japan**

*岩井 優祈[1]、村山 祐司[1] (1.筑波大学大学院生命環境科学研究科地球環境科学専攻)

14:00 ~ 14:15

[HTT19-02] Comparative analysis of foreign tourists' spatial behavior in Tokyo using locational data from the photo-sharing service of Flickr

*Bochra Bettaieb[1]、Yoshiki Wakabayashi[1] (1.Tokyo Metropolitan University)

14:15 ~ 14:30

[HTT19-03] Neighborhood Walkability and its Potential Associations with Residents' Walking Habits

★Invited Papers

*山田 育穂[1]、眞田 佳市郎[2] (1.中央大学理工学部、2.中央大学理工学研究科)

14:30 ~ 14:45

[HTT19-04] **THE STUDY OF USING PARTICLE FILTER METHOD COMBINED INDOOR MAGNETIC MAP AND PEDESTRIAN DEAD RECKONING FOR INDOOR POSITIONING.**

*Yu-Chun Chen[1] (1.Department of Land Economics, National Chengchi University)

14:45 ~ 15:00

[HTT19-05] Assessing the Agriculture Sustainability based on Geospatial Technique in a Tropical Mountain Area : A Case Study in Kotmale Catchment in Sri Lanka.

*DM Sanjeewa Lasantha Bandara[1]、Takehiro Morimoto [2] (1.Division of Spatial Information Science, Graduate School of Life and Environmental Sciences, University of Tsukuba、2.Faculty of Life and Environmental Sciences, University of Tsukuba)

15:00 ~ 15:15

[HTT19-06] **Spatial Evaluation of Potential Tsunami Vertical Evacuation: A Case Study of the Western Coastal Belt in Sri Lanka**

*Ranagalage Mahinda Manjula[1]、Yuji Murayama[1] (1.Division of Spatial Science, Graduate School of Life and Environmental Sciences, University of Tsukuba, Japan)

A study on geographical changes in main roads and coastlines in the 200 years in Japan

*岩井 優祈[1]、村山 祐司[1]
*Yuki IWAI[1], Yuji Murayama[1]

1. 筑波大学大学院生命環境科学研究科地球環境科学専攻
1. Graduate School of Life and Environmental Sciences, University of Tsukuba

This study analyzed the changes in the spatial distribution of main roads and coastlines and its determining factors between 1818 and 2018. These changes are important social and natural foundations for the Japanese national land formation, and the knowledge of the spatial changes is useful for promoting the sustainable society. Previous studies have focused on the regional transformation using aerial photographs, drilling surveys, and some old paper maps. They used the geographical data after modernization and targeted the specific region. In our study, an attempt is made to compare the long term of 200 years on the national scale by using INŌ's digital map.
Digital data of main roads and coastlines on the INŌ's map are included in the “Digital INŌ's Map, Professional Edition”. This is digitized by using the INŌ's large paper map which is the largest scale in the INŌ's map. In the analysis of the changes in main roads, we used the attribute information of Digital INŌ's Map. The changes in coastlines were derived by overlay analysis with coastlines of Digital INŌ's Map and the present national land. In the overlay analysis, each section of coastlines which did not overlap with the present national land was defined as the section changed by the backward movement of the coastline. On the other hand, each section of coastlines which overlapped with the present national land contained both the section changed by the reclamation and the section almost unchanged. In analyzing the determining factors, land use data (100m gridded area) and coastal ocean data (1km gridded area) were mainly used.
As a result, it was found that the route changes in main roads were 18.3% of the total (Fig.1), and the changes in coastlines were 28.9% of the whole length. In the changed coastlines, the changed section by the backward movement was 66.3% (Fig.2A), and the changed section due to the reclamation was 33.7% (Fig.2B). Main roads drawn on the INŌ's large map had different density depending on the region, because only main roads surveyed by INŌ's team were drawn on the INŌ's large map. Therefore, the distance of the changed section was summarized at the regional level. The rate of the change was the largest in Kyushu region (27.8%), and the smallest in Shikoku region (2.8%). On the other hand, coastlines drawn on the INŌ's large map distribute uniformly at the national scale. The rate of the change was the largest in the eastern Japan (Fig.2A) and the industrial areas (Fig.2B). Details on determining factors of changes will be discussed on the day of the presentation.

キーワード：街道変化、海岸線変化、伊能図、GIS、日本
Keywords: Changes in Roads, Changes in Coastlines, INŌ's Map , GIS, Japan

©2019. Japan Geoscience Union. All Right Reserved.

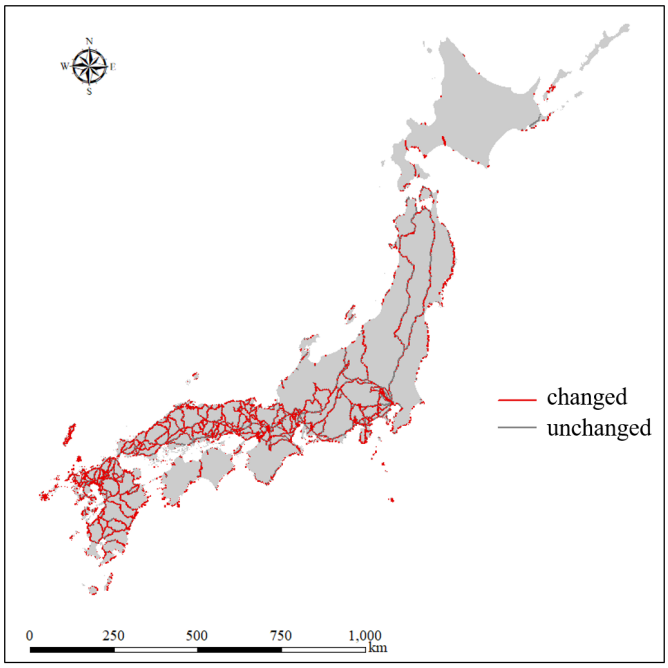


Figure 1 The main roads drawn in the INŌ's large map

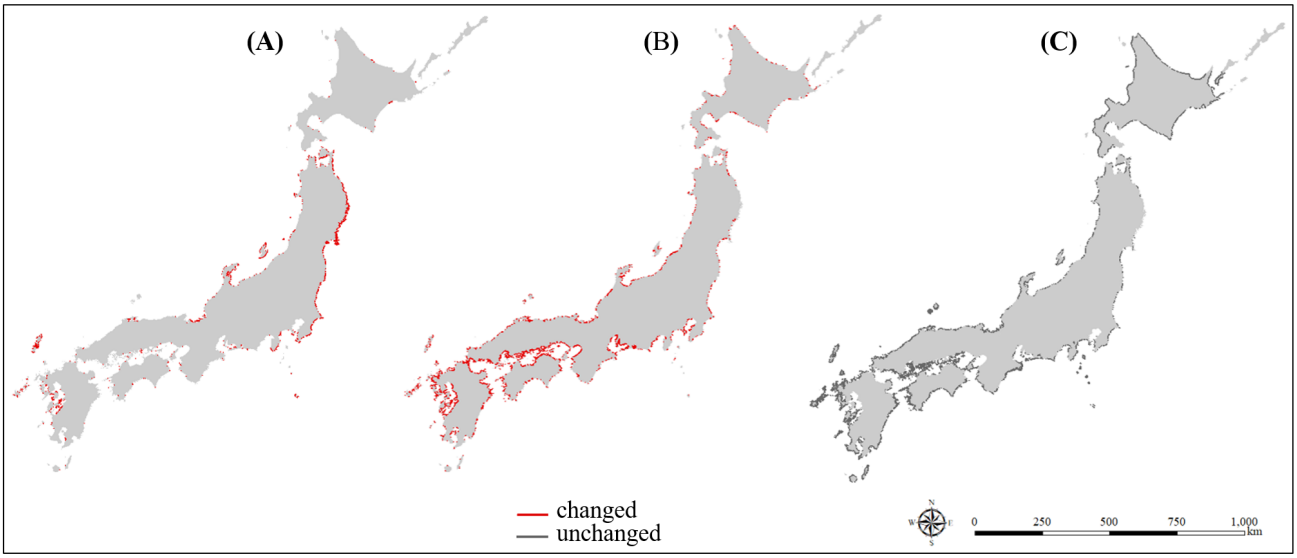


Figure 2 The coastlines drawn in the INŌ's large map; (A) coastlines occurred by backward movement, (B) coastlines occurred by reclamation, (C) coastlines unchanged

©2019. Japan Geoscience Union. All Right Reserved.

Comparative analysis of foreign tourists' spatial behavior in Tokyo using locational data from the photo-sharing service of Flickr

*Bochra Bettaieb[1], Yoshiki Wakabayashi[1]

1. Tokyo Metropolitan University

These new sources of geospatial data, such as smartphones, global positioning systems, and travel cards, provide the possibility of analyzing high-resolution big data to capture patterns of human spatial behavior across space and time. This study analyzes the geocoded photos from a photo-sharing service to make a comparison of the tourist behavior in Tokyo between countries of foreign visitors.

We selected three places (Shinjuku, Asakusa, and Ginza) as study districts. The data were downloaded from Flickr, one of the most popular online platforms for people to share their travel experiences by uploading photos. We used the data of geocoded photos from 2014, taken within 1.5 km from Shinjuku, Ginza, and Asakusa stations. Information on the nationality of contributors recorded in the Flickr data was used to compare the tourist spots of foreign visitors. To summarize the distribution of the points of photos, we aggregated the point features into a rectangular polygon feature with 100 meter grid square, then we made dot maps and mesh maps to capture the overall distribution of the photos.

The obtained results showed that some tourist spots common to foreign visitors in three study areas, namely, places close to railroad stations. However, spatial patterns of tourist spots varied with the study district in question. In Shinjuku and Ginza, there are differences in tourist spots between Asians and Europeans. Particularly, European tourists' hot spots tend to be more scattered than Asians. However, such differences are not observed in Asakusa, where tourists' hot spots are concentrated around Sensoji Temple and Tokyo Sky Tree. The reason for this is that tourist attractions are concentrated in and around specific facilities in the Asakusa district. Hence, the variations of tourist spots obtained by analyzing the geotagged photographs on Flickr can be explained by the difference in behavior and interest of foreign tourists between countries, as well as the spatial distribution of tourist attractions.

Keywords: social media, Flickr, spatial behavior, mesh map, Tokyo

©2019. Japan Geoscience Union. All Right Reserved.

Neighborhood Walkability and its Potential Associations with Residents' Walking Habits

*山田 育穂[1]、眞田 佳市郎[2]
*Ikuho Yamada[1], Keiichiro Sanada[2]

1. 中央大学理工学部、2. 中央大学理工学研究科
1. Faculty of Science and Engineering, Chuo University, 2. Graduate School of Science and Engineering, Chuo University

Walkability is a concept that embraces various aspects of physical neighborhood environments that may support and promote walking in a neighborhood. Walkable neighborhoods are expected to improve residents' physical activity level and thus health because such environments may be able to implicitly encourage residents to choose walking over driving as a daily transportation mode. While research on walkability originated in western countries, where obesity and lifestyle-related illnesses has been a longstanding public health problem, such research in Japan is also useful and necessary because improving healthy life expectancy among the elderly in an undemanding way is critical in our super-aging society. The concept of walkability is also closely related to that of the compact city, which is considered to be a promising form of sustainable cities in the field of urban planning, as walking is expected to be a major transportation mode in such cities.

This research therefore aims to investigate potential associations between neighborhood walkability and residents' walking habits with specific consideration to characteristics of Japanese cities. Here, we consider two types of walking, namely walking for transportation and walking for leisure, separately because they may relate to neighborhood walkability in different ways. Moreover, we assess neighborhood walkability both subjectively and objectively so as to capture the neighborhood situations in a more comprehensive manner.

An Internet-based questionnaire survey was conducted in January 2018 in order to collect information about residents' walking habits, subjective evaluations of neighborhood environments, and health in selected 49 municipalities in Tokyo. The survey was implemented via an Internet research company, and about 4000 individuals who had registered as a panel of the ompany responded. Questions related to the residents' subjective evaluations of neighborhoods were based on an internationally used standard questionnaire named ANEWS (Abbreviated Neighborhood Environment Walkability Scale). In addition, objective measures of neighborhood walkability were computed using various GIS datasets such as the small area statistics of 2015 Population Census, road network data, and facility location data. Then, statistical analysis was conducted to assess potential associations between residents' walking habits and both subjectively and objectively measured neighborhood walkability.
Results indicated that the two types of walking habits related to different aspects of neighborhood walkability. For example, neighborhood community was found to have positive association with walking for leisure, but no such association was found with walking for transportation. Further, it was suggested that the associations between residents' walking habits and neighborhood walkability would potentially vary depending on neighborhood settings such as urban and suburban regions. Our results also suggested that subjective and objective measures of walkability might have different associations with the two types of walking even when they were assumed to measure the same aspect of neighborhood environments.

©2019. Japan Geoscience Union. All Right Reserved.

キーワード：ウォーカビリティ、近隣住環境、移動歩行、余暇歩行、簡易版歩行環境調査質問紙
Keywords: walkability, neighborhood environments, walking for transportation, walking for leisure, ANEWS (Abbreviated Neighborhood Environment Walkability Scale)

©2019. Japan Geoscience Union. All Right Reserved.

THE STUDY OF USING PARTICLE FILTER METHOD COMBINED INDOOR MAGNETIC MAP AND PEDESTRIAN DEAD RECKONING FOR INDOOR POSITIONING.

*Yu-Chun Chen[1]

1. Department of Land Economics, National Chengchi University

In the past, we often needed a map to find out the destination in an unfamiliar environment. With the appearance of Global Positioning System, the outdoor positioning performance has approached perfection. However, due to the environment obstruction, the indoor signal will reduce the positioning accuracy. Therefore, indoor positioning technology has become the focus of research and development in recent years.
In the history of indoor positioning technology, target positions were detected by sensors, radio signals and image or Pedestrian Dead Reckoning (PDR). All the technologies above have their own advantages and disadvantages, like costly or low accuracy. It is necessary to combine the different technologies to achieve a comprehensive consideration of cost, efficiency and accuracy. This study used the built-in magnetometer of the smart phones to build the magnetic field maps of the floor and also accelerometer as an aid to achieve indoor positioning. This study effectively improved the accuracy and efficiency of indoor positioning by using the particle filter method combine PDR with the magnetic positioning.

Keywords: Indoor positioning, Magnetic field map, Pedestrian Dead Reckoning, Particle filter

©2019. Japan Geoscience Union. All Right Reserved.

THE STUDY OF USING PARTICLE FILTER METHOD COMBINED INDOOR MAGNETIC MAP AND PEDESTRIAN DEAD RECKONING FOR INDOOR POSITIONING.

Yu-Chun Chen , Fang-Shii Ning

Department of Land Economics, National Chengchi University,
NO.64, Sec.2, ZhiNan Rd., Wenshan District,Taipei City 11605, Taiwan (R.O.C)
Email: 106257031@nccu.edu.tw; fsn@nccu.edu.tw

Abstract: In the past, we often needed a map to find out the destination in an unfamiliar environment. With the appearance of Global Positioning System, the outdoor positioning performance has approached perfection. However, due to the environment obstruction, the indoor signal will reduce the positioning accuracy. Therefore, indoor positioning technology has become the focus of research and development in recent years.

In the history of indoor positioning technology, target positions were detected by sensors, radio signals and image or Pedestrian Dead Reckoning (PDR). All the technologies above have their own advantages and disadvantages, like costly or low accuracy. It is necessary to combine the different technologies to achieve a comprehensive consideration of cost, efficiency and accuracy. This study used the built-in magnetometer of the smart phones to build the magnetic field maps of the floor and also accelerometer as an aid to achieve indoor positioning. This study effectively improved the accuracy and efficiency of indoor positioning by using the particle filter method combine PDR with the magnetic positioning.

Keywords: Indoor positioning, Magnetic field map, Pedestrian Dead Reckoning, Particle filter

©2019. Japan Geoscience Union. All Right Reserved.

Assessing the Agriculture Sustainability based on Geospatial Technique in a Tropical Mountain Area : A Case Study in Kotmale Catchment in Sri Lanka.

*DM Sanjeewa Lasantha Bandara[1], Takehiro Morimoto [2]

1. Division of Spatial Information Science, Graduate School of Life and Environmental Sciences, University of Tsukuba,
2. Faculty of Life and Environmental Sciences, University of Tsukuba

Sustainable agricultural systems aim at developing new farming practices that do not degrade the environment. It should be catering to the future societal needs for food and feed, ecosystem services and human health, maximizing the net benefit for people, without compromising the ability of future generations to meet their own needs. The agricultural land where located in the tropical mountain area has been becoming a dilapidated situation due to the unplanned agricultural practices coupled with the physical properties of the area and socioeconomic factors. The Kotmale catchment area is located in the central highland of Sri Lanka and covers 572 km^2 with altitude ranges from 681 to 2,505 meters above mean sea level. It is extended from latitude 7˚6'32.80"N to 6˚47'33.12"N and from longitude 80˚ 50'21.26"E to 80˚34'31.34"E which encompasses in the south-central mountainous. The primary objective of this study is to assess the sustainability of agriculture based on the environmental and socioeconomic indicators in the Kotmale catchment using geospatial techniques. The Analytic Hierarchy Process (AHP) combined with Multi-Criteria Decision Making (MCDM) methods was used as data computation method, and both spatial and non-spatial data were used under the three main criteria, such as environment, social and economic. The results of the analysis show that soil erosion is one of the major issues and it is reported as mean erosion is 9.8 t ha^{-1} yr^{-1}. The mean annual rainfall in this area has decreased over the study period (1986-2016) while temperature has increased up to 2-3 ^{0}C. In view of socioeconomic factors, education level of the farmers, lack of labor force, fluctuation of the unit price of the agricultural production, insufficient income of the farmers was negatively affected to the current agricultural activities of the research area. The result would be an aid and sources for assessing the sustainability of agricultural land and decision makers will be able to use this result for future planning.

Keywords: Kotmale watershed, Soil erosion, Agriculture land sustainability , MCDA , AHP

©2019. Japan Geoscience Union. All Right Reserved.

Spatial Evaluation of Potential Tsunami Vertical Evacuation: A Case Study of the Western Coastal Belt in Sri Lanka

*Ranagalage Mahinda Manjula[1], Yuji Murayama[1]

1. Division of Spatial Science, Graduate School of Life and Environmental Sciences, University of Tsukuba, Japan

On December 26, 2004, a massive tsunami resulted to recode extensive damages in the Indian Ocean. The recorded death toll was more than 35,000, and approximately one million people were affected in Sri Lanka. Lack of awareness was the main reason for massive damage. After this tsunami incident, Sri Lanka was also categorized as a tsunami-vulnerable country. Several past studies have contributed to introducing proper mechanisms that would minimize the damages from the next tsunami incident. Most tsunami-vulnerable areas have been covered by horizontal tsunami evacuation after 2004, and people need to travel great distances to reach tsunami evacuation centers due to the lower elevation profile of the coastal area. The purpose of this study was to spatially evaluate the potential for tsunami vertical evacuation in the western coastal belt in Sri Lanka. The western coastal belt selected by considering the existing urban structure and tsunami vulnerability. Several criteria and assumptions have been computed to achieve the goal of the study. In this analysis, three tsunami scenarios 4 m, 8 m, and 12 m were used to identify potential vertical evacuation sites. According to the results of the inundation ratio, the category of critical buildings can be increased to 1.7% and 67.0% in 4 m and 12 m scenarios, respectively. It was indicated that the 12 m scenario consisted of more damage than the other two scenarios. Tsunami evacuation sites were selected based on the three tsunami scenarios and 220, 232 and 122 sites were selected for the 4 m, 8 m and 12 m tsunami scenarios, respectively. According to the calculations of the capacity of each site, the selected 220 sites will facilitate 17,594 people during the 4 m tsunami scenario. The selected 232 sites will accommodate 25,677 people during the 8 m scenarios. All selected sites are capable of accommodating the affected population in both the 4 m and the 8 m scenarios. However, the selected evacuation sites are not sufficient for accommodating the affected population in the 12 m scenario. In the 12 m scenario, 12,221 people are affected. However, the evacuation sites can only accommodate 10,165 people. The finding of vertical evacuation by considering the existing urban structure of the city is essential to save human lives during the next tsunami incident. The adopted methodology can be used as an example for other lowland coastal cities to select vertical evacuation to protect human life.

Keywords: tsunami scenario, building volume, vertical evacuation, tsunami , Sri Lanka

©2019. Japan Geoscience Union. All Right Reserved.

[E] 口頭発表 | セッション記号 H (地球人間圏科学)：H-TT 計測技術・研究手法

2019年5月30日(木) 15:30 ~ 17:00 | 301B 3F

[H-TT19] Geographic Information Systems and Cartography

コンビーナ:小口 高(東京大学空間情報科学研究センター)、村山 祐司(筑波大学大学院生命環境科学研究科地球環境科学専攻)、若林 芳樹(首都大学東京大学院都市環境科学研究科)、座長:小口 高、山田 育穂(中央大学)

地球惑星科学分野で展開されている自然・人文現象に関する地理空間情報を取得，加工，蓄積，分析，可視化するための汎用的な理論と方法を検討する．また，デジタル空間データとGISを用いた実証研究や，地図による具体的な空間表現の成果を発表する．対象を広く設定しているので，GISや地図に関連する隣接諸分野の研究の発表も歓迎する．また，純粋科学的な課題のみならず，教育や社会におけるGISや地図の活用といった応用的な課題や，地球惑星科学分野における意義なども幅広く取り上げる．本セッションは英語で行う．

15:30 ~ 15:45

[HTT19-07] A Framework for Assessing the Spatial Distribution of Vulnerability of Communities to Landslides in Tropical Mountainous Region: A Case study from Kegalle District – Sri Lanka.

★Invited Papers

*Nimala Chinthake Perera[1] (1.SANASA CAMPUS - SRI LANKA, IHRA - UNIVERSITY OF COLOMBO - SRI LANKA)

15:45 ~ 16:00

[HTT19-08] Applications of WebGIS to Educating Disaster Risk Reduction for Chinese and Japanese Students

*Jiali SONG[1]、Takashi Oguchi[2]、Hiroyuki Yamauchi[2]、Takuro Ogura[1] (1.Graduate School of Frontier Sciences, The University of Tokyo、2.Center for Spatial Information Science, The University of Tokyo)

16:00 ~ 16:15

[HTT19-09] Solar System Treks - GIS that provides interactive visualization and analysis for planetary science and exploration

★Invited Papers

*Emily Law[1]、Brian Hamilton Day[2] (1.NASA Jet Propulsion Laboratory、2.NASA Ames Research Center)

16:15 ~ 16:30

[HTT19-10] **Landslide Recognition using Remote Sensing Images and PCANet**

*魏 伊梅[1]、小口 高[1] (1.東京大学 新領域創成科学研究科)

16:30 ~ 16:45

[HTT19-11] Estimating the fractional vegetation cover using fixed-wing drone and multiple vegetation indices

★Invited Papers

*飯塚 浩太郎[1] (1.東京大学　空間情報科学研究センター)

16:45 ~ 17:00

[HTT19-12] スバールバル・ニーオーレスン地域における地形調査とマッピング手法の改善

*李 在庸[1]、小口 高[2] (1.東京大学大学院新領域創成科学研究科自然環境学専攻、2.東京大学空間情報科学研究センター)

A Framework for Assessing the Spatial Distribution of Vulnerability of Communities to Landslides in Tropical Mountainous Region: A Case study from Kegalle District –Sri Lanka.

*Nimala Chinthake Perera[1]

1. SANASA CAMPUS - SRI LANKA, IHRA - UNIVERSITY OF COLOMBO - SRI LANKA

Landslide vulnerability refers to the degree of loss to a given element at risk due to the occurrence of a landslide event. The concept of vulnerability is difficult to quantify due to the involvement of some social and physical indicators to determine vulnerability to a landslide in a given location. Therefore, limited research has been carried out to determine the spatial distribution of landslide vulnerability. This study attempt to map the spatial distribution of vulnerability to landslide using vulnerability index developed by entropy method abstracting information from fourteen indicators. The study was based on primary sources of data, obtained from 402 elements including associated human capital from Kegalle District-Sri Lanka. Then the Entropy method was used to estimate the level of vulnerability in sample locations (elements). Computed vulnerably vales were imported into Geodatabase which was used to evaluate element at vulnerability and map the spatial distribution of vulnerability. The spatial distribution of vulnerability was obtained from interpolating vulnerability values of sample locations (elements) by using Kriging interpolation method. Results were expressed on maps on which different spatial patterns of levels of vulnerability were found for the study area. According to the map, landslide vulnerabilities in the study area demonstrate notable regional specification. In general, vulnerability reflects expected degree of damage to the considered element or location by the adjacent to occurred landslides. Also, the spatial distribution of vulnerability has shown a close relationship with the rural-urban divide. According to landslide vulnerability analyses, 14.6% (247 sq Km) of the entire area is found to be the highest vulnerable zone for a landslide.

Further, 32% (544 sq Km) of the total land area categorized under very high or high vulnerable zones. Moderately vulnerable zones take part 13.4% (227 sq Km) of the total area. However, 26.4% (448 sq Km) of land area categorized as low or very low vulnerability, while 13.4% (227 sq Km) area categorize under the lowest zone it can be concluding that entropy method has a sufficient level of capacity to defined weigh for indicators which use for vulnerability assessment

Keywords: Element at risk , Entropy method, Spatial distribution, Vulnerability

©2019. Japan Geoscience Union. All Right Reserved.

Applications of WebGIS to Educating Disaster Risk Reduction for Chinese and Japanese Students

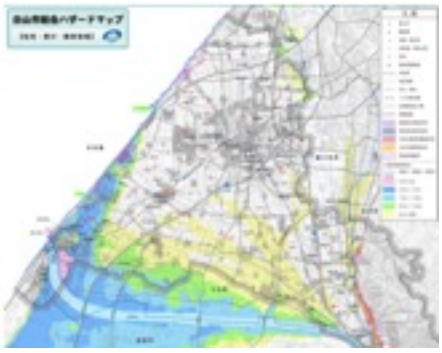
*Jiali SONG[1], Takashi Oguchi[2], Hiroyuki Yamauchi[2], Takuro Ogura[1]

1. Graduate School of Frontier Sciences, The University of Tokyo, 2. Center for Spatial Information Science, The University of Tokyo

In this world of globalization and information explosion, WebGIS (Web Geographic Information Systems) can effectively support education in natural and social sciences. We should utilize this technology and for better human life. Research on mortality due to natural disasters has shown that nations with higher levels of education experience lower levels of mortality. This suggests that young students are knowledgeable and will contribute to future disaster risk reduction (DRR) if they are well educated. Hence, it is important to introduce DRR into high school education such as classes of geography. At present Chinese researchers are preparing disaster-related compulsory curricula for high school DDR education, and are designing special textbooks for this purpose. In Japan, some researchers have already constructed online WebGIS systems for DRR education using hazard maps available on the Internet. However, such DRR activities tend to be insufficient because of limited cognition of citizens about information related to hazards and risks. This study aims to construct an improved online DRR system for high school education using WebGIS technology along with hazard information including maps for China and Japan. In August 2018, Japanese students used the system in an event funded by the Japan Society for the Promotion of Science. After that, a similar educational event was held in a high school in China. During these activities, students compared paper hazard maps with electronic hazard maps and used both of them for consideration. At the end of each event, the feasibility and effectiveness of the system were surveyed by questionnaires to evaluate the understanding of students about WebGIS and relevant knowledge. The results indicate that students in both countries prefer teaching materials like the constructed DRR system for school classes. However, there are some differences between the two countries. For example, the Chinese students thought that analysis of dangerous areas using the layer of flooding areas was more difficult than the Japanese students, reflecting differences in DDR knowledge. To improve the applicability of the system, further educational activities will be conducted in the near future.

Keywords: WebGIS, Disaster risk reduction, Geography education





©2019. Japan Geoscience Union. All Right Reserved.

Solar System Treks - GIS that provides interactive visualization and analysis for planetary science and exploration

*Emily Law[1], Brian Hamilton Day[2]

1. NASA Jet Propulsion Laboratory, 2. NASA Ames Research Center

Meeting the challenges of space exploration has resulted in new knowledge that has kept NASA and JPL world leaders in big data science and technology. We, NASA’s Solar System Treks Project (SSTP – https://trek.nasa.gov) development team at JPL, under the management of Solar System Exploration Virtual Research Institute (SSERVI, https://sservi.nasa.gov/), have developed a Geographic Information Sysetms (GIS) based system that includes a set of web-based portals that provide a suite of interactive visualization and analysis tools to enable mission planners, scientists, and engineers to access a large volume of cartographic products and models from a growing number of spacecraft. Currently, various web-based portals are available for discovering and exploring the Moon, Mars, Vesta, Ceres, Titan and Icy Moons of Saturn, and hydrology on Earth. This presentation will provide an overview of this GIS-based system highlighting its high level architecture, technologies and capabilities that was designed and developed specifically for exploration of any Solar System bodies. We will also describe its uses, features and capabilities, highlighting visualization and analysis innovations.

Keywords: GIS, Visualization, Analysis, Solar System

©2019. Japan Geoscience Union. All Right Reserved.

Landslide Recognition using Remote Sensing Images and PCANet

*魏 伊梅[1]、小口 高[1]
*Yimei Wei[1], Takashi Oguchi[1]

1. 東京大学 新領域創成科学研究科
1. Graduate School of Frontier Science, the University of Tokyo

Landslides are complex geological phenomena that can cause serious damage to the natural and social environments and may result in a significant loss of lives and properties. Consequently, landslide recognition, mapping, and monitoring are important for the prevention of secondary disasters and post-disaster relief. Since various remote sensing images have become more accessible in recent years, the use of satellite and aerial imagery for geological disasters has become a hot research topic. When remote sensing images are used to recognize landslides, image feature extraction is the main technical issue, and inefficiency in extracting ground object features has been a major challenge. This study explores the use of a simplified deep learning network structure, PCANet, to learn image features from post-disaster remote sensing images and train the classifier. This approach reduces the computation time of feature extraction and improves the efficiency of landslide recognition. The materials for training PCANet are image data sets for several areas in Japan including both landslide and non-landslide samples. They were collected from vertical aerial photographs and orthophotographs provided by the Geospatial Information Authority of Japan (GSI). In addition, post-disaster landslide distribution maps provided by the National Institute of Geosciences and Disaster Recovery (NIED) and GSI were utilized in the selection of sample images. As the analyzed remote sensing images were taken in a short time after a serious geological disaster, this research also contributes to future rapid responses to landslide hazards.

キーワード：地すべり認識、画像特徴抽出 、PCANet、機械学習
Keywords: Landslide recognition, Image feature extraction, PCANet, Machine learning

©2019. Japan Geoscience Union. All Right Reserved.

Estimating the fractional vegetation cover using fixed-wing drone and multiple vegetation indices

*飯塚 浩太郎[1]
*Kotaro Iizuka[1]

1. 東京大学　空間情報科学研究センター
1. Center for Spatial Information Science, The University of Tokyo

Fractional vegetation cover (percentage of vegetation cover) plays a key role in characterizing the conditions of the terrestrial environment. To analyze the distribution of the vegetation conditions, several methods and models can be found for estimating its coverage. Remote sensing techniques, especially utilizing the satellite imagery is one of the major approaches due to its applicability in larger spatial extent and multiple channels observed from different electromagnetic spectra. Although, in cases of high frequent cloud covering regions such as the tropical regions, usually this is difficult to conduct. Thus, in this work, we seek in alternatively collecting a remotely sensed imagery from a fixed-wing drone and analyze to estimate the fractional vegetation cover of the study site. Normal RGB camera and multispectral sensors were carried onboard the fixed-wing drone, and multiple images were collected. The Structure from Motion method was implemented to develop an ortho image of the whole study site. The imageries were used to further develop a general land use/land cover (LULC) map of the site, and within the determined gridded area, the fraction of each LULC types were examined with different vegetation indices (VIs) computed from the multispectral data. Clear positive trend was found with increasing VIs and increasing fractional cover of healthy trees, and clear negative trend was found with decreasing VIs and increasing fractional cover of soils. This approach demonstrates that it is possible to analyze the coverage information through the utilization of drones, which can be also used as ground truthing, moreover, the findings would play an important role in further simulating such as the water cycles.

キーワード：ドローン、森林、リモートセンシング、植生指数、土地被覆、Structure from Motion
Keywords: Drone, Forests, Remote Sensing, Vegetation Index, Land Cover, Structure from Motion

©2019. Japan Geoscience Union. All Right Reserved.

スバールバル・ニーオーレスン地域における地形調査とマッピング手法の改善

Topographic surveys in Ny-Alesund, Svalbard, and improvement of mapping methods

*李 在庸[1]、小口 高[2]
*Jaeyong Lee[1], Takashi Oguchi[2]

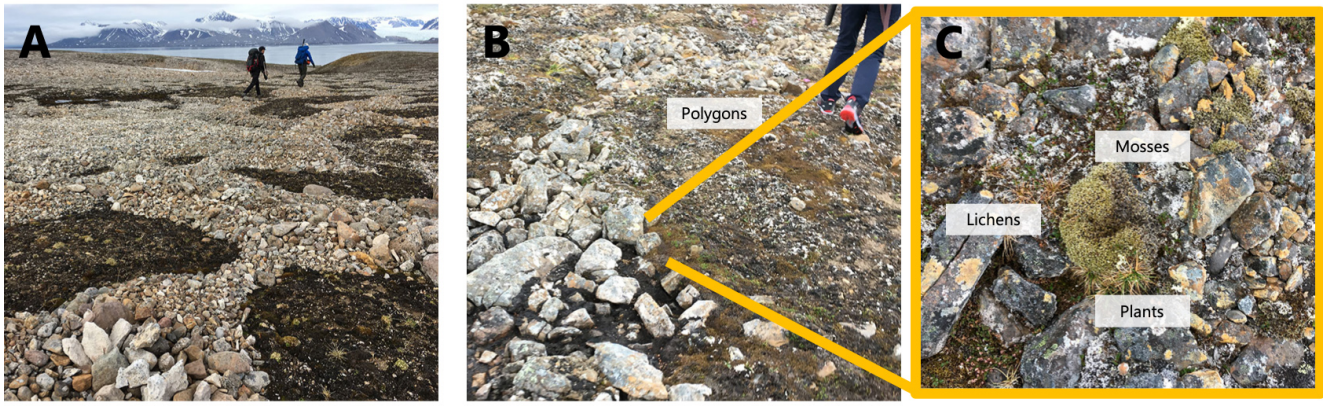
1. 東京大学大学院新領域創成科学研究科自然環境学専攻、2. 東京大学空間情報科学研究センター
1. Department of Environmental Studies, Graduate School of Frontier Sciences, The University of Tokyo, 2. Center for Spatial Information Science, The University of Tokyo

スバールバル諸島のニーオーレスンには凍土層が広範囲に分布しており、夏季にのみ融解する活動層と、常時凍結している不透水性の永久凍土層で構成されている。このような垂直構造は、表層の環境のみならず地下水の分布にも影響を与えている。また、反復的な凍結・融解により形成される構造土と植生の分布なども含めて、極地に固有の生態系の基盤となっている。最近、温暖化により活動層が拡大して流水が増加しているため、植生や斜面の物質移動などの表層環境が変化している。このような凍土層と表層環境の変化の定量的な把握のために、ニーオーレスン地域の高解像度のマッピングに関する技術的検討を行った。極地における現地調査には、調査可能な範囲や日程上の制約があるため、過去の現地調査の資料、衛星・航空画像、及びGISデータも活用して地形分析の妥当性を調べた。

2017年の現地調査の際に訪れたニーオーレスン科学基地村の周辺地域を対象に、ノルウェー極地研究所のDEMを利用して傾斜度、斜面方向、曲率、日射量、高度などの地形量を算出した。また、夏季に撮影されたTopoSvalbard衛星の画像と航空写真の判読を通じて、地形量の分析の妥当性を検討した。さらに、地上で撮影された写真を用いて衛星・航空画像からは判読不可能な表層環境を記載し、SfM-MVS手法を用いた高解像度の写真測量も活用して地形図を作成した。無線周波数の利用に法的制約のあるニーオーレスンでは、UAVの使用が制限されるため、スタビライザー機能を持つポールカメラを製作した。改善されたポールカメラで得られる写真の解像度は3 mm前後である。これは狭い地域における超高解像度マップピングの有用な手法になると期待される。

キーワード：ニーオーレスン、凍土層、超高解像度マップピング
Keywords: Ny-Alesund, Permafrost, High-resolution mapping

©2019. Japan Geoscience Union. All Right Reserved.



The images of frozen layer taken in field survey in Ny-Alesund, 2017.
A) Well-developed polygon shape patterned ground., **B)**, **C)** Vegetation on the polygons.

©2019. Japan Geoscience Union. All Right Reserved.

[E] 口頭発表 | セッション記号 S (固体地球科学)：S-IT 地球内部科学・地球惑星テクトニクス

2019年5月30日(木) 9:00 ~ 10:30 | A09 東京ベイ幕張ホール

[S-IT25] Planetary cores: Structure, formation, and evolution

コンビーナ:寺崎 英紀(大阪大学大学院理学研究科)、大谷 栄治(東北大学大学院理学研究科地学専攻)、William F McDonough(University of Maryland College Park)、George Helffrich(Earth-Life Science Institute, Tokyo Institute of Technology)、座長:George Helffrich(ELSI, Tokyo Institute of Technology)、寺崎 英紀

There are fundamental links between the formation and evolution of planets and their satellites to that of their cores. Defining the physical and chemical properties of the cores of these terrestrial bodies are fundamental for understanding their internal structures and thermal profile. Recent advances in experimental and theoretical studies provide new insights and applications to the Earth's cores and other terrestrial bodies. Near-future exploration missions will obtain data on the internal structure of terrestrial planets (e.g., Mars and Mercury) and planet-satellite systems. We anticipate presentations on recent advances on the physical and chemical properties of cores and discussions regarding the latest views of their formation and evolution. We welcome contributions from mineral/rock physics, geophysics, geochemistry, geodynamics, and planetary science.

9:00 ~ 9:15

[SIT25-01] **High-pressure Equation of State of Schreibersite $Fe_{2.15}Ni_{0.85}P$: Implications for the Martian Core**

*Xuejing He[1]、Jiazeng Guo[2]、Xiang Wu[3]、Shengxuan Huang[1]、Fei Qin[1]、Xiangping Gu[4]、Shan Qin[1] (1.Peking Univ.、2.Nanyang Normal Univ.、3.China Univ. of Geosciences、4.Central South Univ.)

9:15 ~ 9:30

[SIT25-02] Bottom-up solidification versus top-down solidification of the liquid core of the relatively small planetary bodies

*浦川 啓[1]、寺崎 英紀[2] (1.岡山大学大学院自然科学研究科、2.大阪大学大学院理学研究科)

9:30 ~ 9:45

[SIT25-03] P-wave velocity of Fe_3S under high pressure and temperature

*鎌田 誠司[1,2]、寺崎 英紀[3]、福井 宏之[4,5]、坂巻 竜也[2]、内山 裕士[6]、筒井 智嗣[6]、大谷 栄治[2]、Baron Alfred[5] (1.東北大学学際科学フロンティア研究所、2.東北大学大学院理学研究科地学専攻、3.大阪大学大学院理学研究科宇宙地球科学専攻、4.兵庫県立大学物質理学研究科物質科学専攻、5.RIKEN、6.JASRI)

9:45 ~ 10:00

[SIT25-04] The sound velocity of liquid Fe-Ni-S-Si alloys under Mercury’s core condition

*山田 伊織[1]、寺崎 英紀[1]、神谷 朝香[1]、鶴岡 椋[1]、肥後 祐司[2]、町田 晃彦[3] (1.大阪大学大学院理学研究科、2.(財)高輝度光科学研究センター、3.量子科学技術研究開発機構)

10:00 ~ 10:15

[SIT25-05] レーザー衝撃実験によるFe-Si融体の重力不安定性成長のその場観察

*寺崎 英紀[1]、境家 達弘[1]、重森 啓介[2]、加藤 弘樹[2]、弘中 陽一郎[2]、近藤 忠[1] (1.大阪大学大学院理学研究科、2.大阪大学レーザー科学研究所)

10:15 ~ 10:30

Discussion

High-pressure Equation of State of Schreibersite $Fe_{2.15}Ni_{0.85}P$: Implications for the Martian Core

*Xuejing He[1], Jiazeng Guo[2], Xiang Wu[3], Shengxuan Huang[1], Fei Qin[1], Xiangping Gu[4], Shan Qin[1]

1. Peking Univ., 2. Nanyang Normal Univ., 3. China Univ. of Geosciences, 4. Central South Univ.

Phosphorus is thought to be an important light element existing in planetary cores. The phosphorus abundance is evaluated to be ~0.20 wt% in the Earth’ s core, and ~0.32 wt% in the Martian core. To fully understand its existence in planetary cores, structural and physical properties of iron-nickel phosphides should be investigated under high pressure and high temperature. $(Fe,Ni)_3P$-schreibersite is observed as a common accessory in the veinlet of iron and stony-iron meteorites, so that it is of significance to discuss and constrain the properties of planetary cores. The equation of state of a natural single-crystal schreibersite, $Fe_{2.15}Ni_{0.85}P$, has been studied up to ~50 GPa at room temperature in a diamond anvil cell using *in situ* synchrotron-radiation X-ray diffraction. The sample kept its tetragonal structure ($I\bar{4}$) up to the highest pressure with no observation of phase transition. Experimental results have shown that the magnetic collapse of $Fe_{2.15}Ni_{0.85}P$ is weakened because of the substitution of nickel, leading to an isotropic axial compressibility. The pressure-volume data were fitted by the third-order Birch-Murnaghan equation of state, yielding K_0 = 184(4) GPa, K_0' = 4.1(2), V_0 = 365.9(1) $Å^3$. The density of $Fe_{2.15}Ni_{0.85}P$, along with several iron sulfides and iron phosphides has been calculated under relative pressure-temperature conditions of the Martian core. The comparison with that of γ-Fe and a density model of the Martian core evidences that nickel and phosphorus dopant would result in density reduction of iron sulfides, suggesting that $(Fe,Ni)_3(S,P)$ might be a possible compound existing in the Martian core.

Keywords: schreibersite, high pressure, equation of state, Martian core

©2019. Japan Geoscience Union. All Right Reserved.

Bottom-up solidification versus top-down solidification of the liquid core of the relatively small planetary bodies

*浦川 啓[1]、寺崎 英紀[2]
*Satoru Urakawa[1], Hidenori Terasaki[2]

1. 岡山大学大学院自然科学研究科、2. 大阪大学大学院理学研究科
1. Department of Earth Sciences, Okayama University, 2. Department of Earth and Space Science, Osaka University

Some planetary bodies, such as Mercury and Ganymede, have their own magnetic fields and other bodies, such as the Moon and Mars, once had a magnetic field. These magnetic fields of the relatively small bodies are thought to be originated from core dynamo driven by compositional convection. Compositional convection is related to the density fluctuation due to partial crystallization of liquid core. The phenomenon that iron solidified at the upper part of the core settles is called ‘Fe snowing’ and it is considered as the main cause of compositional convection in the core of the small planetary bodies. However, crystallization of iron occurs from the top of the core in some cases and from the bottom of the core in another case, due to the complexity of melting relationships of iron-light element system under pressure. Whether the top-down freezing occurs or the bottom-up freezing occurs depends on the adiabat in the liquid core and the melting slope of the constituent substance of the core. We have investigated the adiabatic temperature gradient of the Fe-S liquid core based on the thermal expansivity which is determined by X-ray absorption density measurements at high pressures. Then, we divided the pressure-composition space for the Fe-FeS system into the bottom-up solidification field and the top-down solidification field at the pressures up to 10 GPa. These would contribute to understand the generation of magnetic field in the relatively small bodies.

キーワード：惑星磁場、惑星核、組成対流、断熱温度勾配、Fe-Sメルト
Keywords: Planetary magnetic field, planetary core, compositional convection, adiabat, Fe-S liquid

©2019. Japan Geoscience Union. All Right Reserved.

P-wave velocity of Fe_3S under high pressure and temperature

*鎌田 誠司[1,2]、寺崎 英紀[3]、福井 宏之[4,5]、坂巻 竜也[2]、内山 裕士[6]、筒井 智嗣[6]、大谷 栄治[2]、Baron Alfred[5]
*Seiji Kamada[1,2], Hidenori Terasaki[3], Hiroshi Fukui[4,5], Tatsuya Sakamaki[2], Hiroshi Uchiyama[6], Satoshi Tsutsui[6], Eiji Ohtani[2], Alfred Q.R. Baron[5]

1. 東北大学学際科学フロンティア研究所、2. 東北大学大学院理学研究科地学専攻、3. 大阪大学大学院理学研究科宇宙地球科学専攻、4. 兵庫県立大学物質理学研究科物質科学専攻、5. RIKEN、6. JASRI
1. Frontier Research Institute for Interdisciplinary Sciences, Tohoku University, 2. Department of Earth Science, Graduate School of Science, Tohoku University, 3. Department of Earth and Space Science, Graduate School of Science, Osaka University, 4. Graduate School of Material Science, University of Hyogo, 5. RIKEN, 6. JASRI

Martian cores have been thought to include a certain amount of sulfur as a light element. Sohl and Spohn (1997) proposed seismic wave velocity and density profiles of the interior of Mars based on equations of state of core matrials although seismic wave velocities of core materials are needed for presice estimation. However, there have been only a limited number of works for V_P of Fe alloys with sulfur. In the Fe-FeS system, V_P of FeS and FeS_2 have been studied (e.g. Badro et al. 2007) but these compounds are not appropriate for the core materials of Mars because Fe_3S is a stable phase above 20 GPa corresponding to Martian core conditions (Fei et al., 1997, 2000) up to at least 200 GPa (Kamada et al., 2010, 2012). Therefore, Fe_3S is a subsolidus phase together with ε -Fe in the Fe-Fe_3S system at Martian core conditions and it is essential to study V_P of Fe_3S to understand seismic properties of the Martian core. We have measured sound V_P of Fe_3S under high temperature and pressure at BL35XU of SPring-8.
In this study, a synthesized Fe_3S was used as a starting material. A symmetric diamond anvil cell was used to generate high pressures. IXS(Inelastic X-ray Scattering) and XRD experiments were performed at the beamline 35XU of SPring-8, Japan (Baron et al., 2000). V_P of Fe_3S were measured up to 100 GPa and 2000 K. We will discuss temperature effect on the V_P of Fe_3S and the Birch's law and seismic wave velocity profile of the Martian core.

キーワード：非弾性X線散乱法、ダイヤモンドアンビルセル、レーザー加熱
Keywords: Inelastic X-ray scattering, diamond anvil cell, laser heateting

©2019. Japan Geoscience Union. All Right Reserved.

The sound velocity of liquid Fe-Ni-S-Si alloys under Mercury’s core condition

*山田 伊織[1]、寺崎 英紀[1]、神谷 朝香[1]、鶴岡 椋[1]、肥後 祐司[2]、町田 晃彦[3]
*Iori Yamada[1], Hidenori Terasaki[1], Asaka Kamiya[1], Ryo Tsuruoka[1], Yuji Higo[2], Akihiko Machida[3]

1. 大阪大学大学院理学研究科、2. (財)高輝度光科学研究センター、3. 量子科学技術研究開発機構
1. Graduate School of Science, Osaka University, 2. Japan Synchrotron Radiation Research Institute, 3. National Institute for Quantum and Radiological Science and Technology

Mercury has a large liquid core and it mainly consists of Fe-Ni and possibly contains some light elements. The X-ray spectroscopy measurements by the MESSENGER spacecraft indicates that surface on Mercury contains 1-4wt% S (Nittler et al. 2011). When silicate containing 1-4 wt%S coexists with liquid metal, S and Si tend to dissolve into liquid metal based on partitioning of S and Si between metal and silicate melts. This suggests that both S and Si are likely to be included in the outer core of Mercury (Chabot et al. 2014). Thus, elastic properties of liquid Fe-Ni-S-Si at BL04B1 and BL22XU beamlines, SPring-8 Facility. High pressure was generated using 1500ton Kawai-type or 180 ton cubic multianvi press. The sound velocity was measured using the pulse-echo overlap method. We used two kinds of compositions (Fe-11wt%Ni-6wt%S-4wt%Si and Fe-11wt%Ni-3wt%S-8wt%Si) for Fe-Ni-S-Si sample. The P-wave velocity (V_P) was measured up to 16 GPa and 2000 K and it increases with pressure. Temperature dependence on the V_P of liquid Fe-Ni (Kuwabara et al. 2016), the V_P of liquid Fe-Ni decreases approximately 1.6 % by addition of 6 wt%S and 4 wt%Si and increases approximately 3.1 % by addition of 3wt%S and 8wt%Si. This suggests that the effect of S reduces the V_P effectively also in the Fe-Ni-S-Si system.

キーワード：水星、核、音速、軽元素
Keywords: Mercury, Core, Sound velocity, Light element

©2019. Japan Geoscience Union. All Right Reserved.

レーザー衝撃実験によるFe-Si融体の重力不安定性成長のその場観察
In situ observation of Rayleigh–Taylor instability growth of liquid Fe-Si using laser shock

*寺崎 英紀[1]、境家 達弘[1]、重森 啓介[2]、加藤 弘樹[2]、弘中 陽一郎[2]、近藤 忠[1]
*Hidenori Terasaki[1], Tatsuhiro Sakaiya[1], Keisuke Shigemori[2], Hiroki Kato[2], Yoichiro Hironaka[2], Tadashi Kondo[1]

1. 大阪大学大学院理学研究科、2. 大阪大学レーザー科学研究所
1. Graduate School of Science, Osaka University, 2. Institute of Laser Engineering, Osaka University

Rayleigh–Taylor instability occurs at the interface between two fluids with different densities when a heavy fluid overlies a light one in a gravitational field. The RT instability is considered as one of the important core formation mechanism beneath the magma ocean. This mechanism has been discussed from simulations (e.g., Honda et al. 1993, Ricard et al. 2009) and analog experiment (e.g., Olson and Weeraratne, 2008). However, experimental approach using liquid Fe-alloys for this mechanism has never been performed under high pressure. In this study, we applied the laser-shock technique to observe *in situ* the Rayleigh–Taylor instability of liquid Fe-Si alloy under high pressure. The growth of the Rayleigh–Taylor instability was successfully observed using *in situ* x-ray radiography under shock compression. The growth rate of the Rayleigh–Taylor instability was estimated to 0.3 ns^{-1}. The present results provide useful information to constrain the time scale of the Earth’s and planetary core formation.

キーワード：核形成、レイリー・テーラー型重力不安定、鉄合金融体
Keywords: Core formation, Rayleigh–Taylor instability, liquid Fe-alloy

©2019. Japan Geoscience Union. All Right Reserved.

[E] 口頭発表 | セッション記号 S (固体地球科学)：S-IT 地球内部科学・地球惑星テクトニクス

2019年5月30日(木) 10:45 ~ 12:15 | A09 東京ベイ幕張ホール

[S-IT25] Planetary cores: Structure, formation, and evolution

コンビーナ:寺崎 英紀(大阪大学大学院理学研究科)、大谷 栄治(東北大学大学院理学研究科地学専攻)、William F McDonough(University of Maryland College Park)、George Helffrich(Earth-Life Science Institute, Tokyo Institute of Technology)、座長:William McDonough(University of Maryland / Tohoku University)、大谷 栄治(東北大学)

There are fundamental links between the formation and evolution of planets and their satellites to that of their cores. Defining the physical and chemical properties of the cores of these terrestrial bodies are fundamental for understanding their internal structures and thermal profile. Recent advances in experimental and theoretical studies provide new insights and applications to the Earth's cores and other terrestrial bodies. Near-future exploration missions will obtain data on the internal structure of terrestrial planets (e.g., Mars and Mercury) and planet-satellite systems. We anticipate presentations on recent advances on the physical and chemical properties of cores and discussions regarding the latest views of their formation and evolution. We welcome contributions from mineral/rock physics, geophysics, geochemistry, geodynamics, and planetary science.

10:45 ~ 11:00

[SIT25-06] *P-V-T* equation-of-state of liquid Fe from *ab-initio* simulations to the TPa regime

*Gerd Steinle-Neumann[1]、Fabian Wagle[1] (1.Bayerisches Geoinstitut, University of Bayreuth, Germany)

11:00 ~ 11:15

[SIT25-07] ***Ab initio* study of Iron-Nickel alloys in Super-Earths cores**

*Francois Soubiran[1]、Razvan Caracas[1] (1.Ecole normale superieure de Lyon, Laboratoire de Géologie de Lyon, Université Lyon 1, CNRS UMR 5276, Lyon, France)

11:15 ~ 11:30

[SIT25-08] **Impurity effect on the iron's transport properties at Earth's core conditions: A key constraint for the evolution of the Earth's core**

*Youjun Zhang[1]、Mingqiang Hou[2]、Nilesh Salke[2]、Jung-Fu Lin[3] (1.Sichuan University、2.HPSTAR、3.University of Texas at Austin)

11:30 ~ 11:45

[SIT25-09] 214 GPaまでのFe-FeO系の共融点組成の決定

*岡 健太[1]、木所 佑斗、廣瀬 敬[1]、中島 陽一[2]、Guillaume Morard[3]、Guillaume Fiquet[3]、Nicolas Coudurier[3] (1.東京大学大学院理学系研究科地球惑星科学専攻、2.熊本大学大学院先導機構、3.ソルボンヌ大学)

11:45 ~ 12:00

[SIT25-10] B2 phase in the inner core: constraints from high pressure experiments

*Eiji Ohtani[1]、Daijo Ikuta[1]、Seiji Kamada[2]、Tatsuya Sakamaki[1]、Naohisa Hirao[3] (1.Department of Earth and Planetary Materials Science, Graduate School of Science, Tohoku University、2.Frontier Institute for Interdisciplinary Research, Tohoku University、3.SRring-8, Japan Synchrotron Research Institute)

12:00 ~ 12:15

Discussion

P-V-T equation-of-state of liquid Fe from *ab-initio* simulations to the TPa regime

*Gerd Steinle-Neumann[1], Fabian Wagle[1]

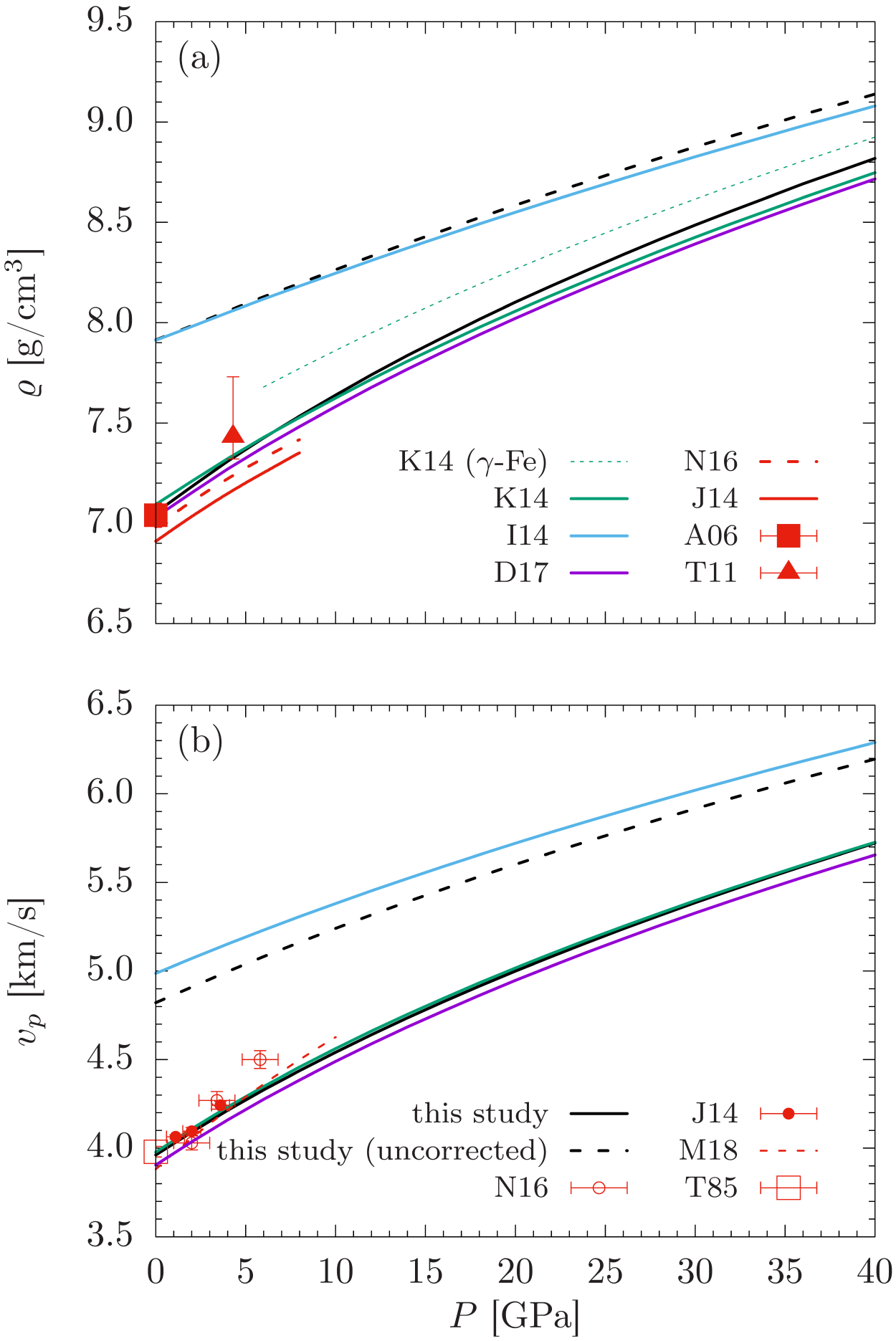
1. Bayerisches Geoinstitut, University of Bayreuth, Germany

The pressure-volume-temperature (*P-V-T*) equation-of-state (EoS) of liquid iron provides important information (reference adiabat, density ρ, and higher order thermodynamic parameters) in the modelling of the internal structure of planetary bodies with Fe-based cores. Relevant P-conditions range from a few GPa (Moon, Mercury) through the Mbar range (Earth) to several TPa (super-Earth exoplanets). Experimental data on ρ in the liquid stability field are scarce and a thermodynamic assessment of ρ depends on matching Gibbs energy along the melting line which remains controversial to this day. The alternative determination of a *P-V-T* EoS based on ab-initio simulations, on the other hand, suffer from the fact that ρ at ambient P is predicted too large by as much as 20% in the simulations [e.g., 1]. Here, we have fitted *P-V-T* triplets from *ab-initio* molecular dynamics simulations with an EoS formulation that is thermodynamically self-consistent [2] and combined it with a correction formalism that accounts for the known ρ-mismatch at ambient *P* [3]. As the correction is additive to the Helmholtz potential and shows the correct limiting behavior at high and low ρ, the thermodynamic self-consistency of the results is not affected. Using this combination, the EoS we have developed reproduces ρ from shock-wave experiments as well as previous models, but shows a significantly improved agreement at ambient *P*, the critical point and the sole low ρ measurement at 4.3 GPa [4] (T11 in Figure). We explore the performance of our thermodynamic potential and various previously published models [1,5,6] for liquid iron over a wide range of conditions: (i) at ambient pressure as a function of temperature, (ii) along the melting curve of Fe to 40 GPa, relevant for the cores of smaller terrestrial bodies in our solar system (Figure), (iii) along isentropes in the Earth's outer core and (iv) for the core of super-Earth Kepler-36b. The correction term significantly improves the agreement of computed properties with experiments and other thermodynamic models that are based on an assessment of the phase diagram at ambient and moderate pressure, showing how *ab-initio* molecular dynamics simulations can be used at par with other thermodynamic techniques. For the Earth's core, densities from the various models are similar, but higher-order derivatives (acoustic velocities and Grüneisen parameter) show significant differences. Evaluated along a core-temperature profile in Kepler-36b, differences in density from various models are negligible, for core mass they do not exceed 2%, showing robust extrapolation of all equation of state models.

[1] Ichikawa et al., JGR 119, 240 (2014) (I14); [2] Vlček et al., PRB 85, 184201 (2012); [3] French & Mattsson, JAP 116, 013510 (2014); [4] Tateyama et al., PCM 38, 801 (2011) (T11); [5] Komabayashi, JGR 119, 4164 (2014) (K14); [6] Dorogokupets et al., SciRep 7, 41,863 (2017) (D17); [7] Nishida et al., PEPI 257, 230 (2016) (N16); [8] Jing et al., EPSL 396, 78 (2014) (J14); [9] Assael et al., JPCRD 35, 285 (2006) (A06); [10] Morard et al., AmMin 103, 1770 (2018) (M18); [11] Tsu et al., BRIMDM 41, 1 (1985) (T85).

Keywords: planetary cores, iron, equation of state

©2019. Japan Geoscience Union. All Right Reserved.



©2019. Japan Geoscience Union. All Right Reserved.

Ab initio study of Iron-Nickel alloys in Super-Earths cores

*Francois Soubiran[1], Razvan Caracas[1]

1. Ecole normale superieure de Lyon, Laboratoire de Géologie de Lyon, Université Lyon 1, CNRS UMR 5276, Lyon, France

Iron-nickel alloys are considered the main components of Earth and Super-Earth cores, which make them crucial systems in order to comprehend the properties of these planets. While the relative nickel content is anticipated to be around 10% in the Earth, this value could differ slightly in other planets because of different host star metallicity and formation history. It is thus important to understand the properties of iron-nickel systems with various compositions in the multi-megabar regime.

While pure iron is anticipated to have hexagonal close packing at high pressure, nickel is expected to have face-centered cubic packing. This means there is a structural change as the composition is modified, which can also mean a limited stability of the solid solutions of iron-nickel.

We will discuss the properties of iron-nickel alloys in the megabar regime as predicted by *ab initio* simulations. We will examine the relative stability of different iron-nickel solid solution compositions and the interplay of the spin states. After characterizing the properties of these alloys at pressure-temperature conditions relevant for Super-Earth, we will discuss possible consequences their cores.

Keywords: Super-Earth, iron core, Ab initio simulations

©2019. Japan Geoscience Union. All Right Reserved.

Impurity effect on the iron’s transport properties at Earth’s core conditions: A key constraint for the evolution of the Earth’s core

*Youjun Zhang[1], Mingqiang Hou[2], Nilesh Salke[2], Jung-Fu Lin[3]

1. Sichuan University, 2. HPSTAR, 3. University of Texas at Austin

The Earth’s core is mainly composed of Fe-Ni alloyed with some light elements, such as Si, S, O and C [1]. The transport properties of Fe alloys at Earth’s core conditions constrain the heat flow from the core into mantle, which governs the geodynamo, dynamics and thermal evolution of Earth’s core [2,3]. While, this property is still not well understood and remains controversial in previous work due to the experimental challenging at very high pressure and temperature [4,5]. Here, we directly measure the electrical resistivity of hcp-Fe-Ni and hcp-Fe-Si alloys at the relevant conditions of Earth’s core using double-side laser-heated Diamond Anvil Cells. Our results show a quasi-linear relation between temperature and resistivity in hcp-Fe-Ni and hcp-Fe-Si at the core pressures. Compared with hcp-Fe [6], the impurities like Ni and Si can elevate iron’s resistivity but they show different magnitude. Thermal conductivity of an Fe-Ni-Si alloy as a candidate core composition was modelled via the Wiedemann-Franz law based on our measured resistivity. Our results show that the core’s thermal conductivity could be strongly reduced by impurities, supporting a Mesoproterozoic inner core age and a self-consistent convection-driven geodynamo.

Refs:
[1] Li and Fei. Treat. Geochem., 527-557 (2014)
[2] Davies et al. Nat. Geosci. 8, 678-685 (2015)
[3] Williams. Annu. Rev. Earth Planet. Sci. 46: 47-66 (2018)
[4] Ohta et al. Nature 534, 95-98 (2016)
[5] Konôpková et al. Nature 534, 99-101 (2016)
[6] Zhang et al. Submitted, (2019)

Keywords: Fe alloys, Transport properties, High pressure-temperature, Geodynamo, Thermal evolution of the core

©2019. Japan Geoscience Union. All Right Reserved.

214 GPaまでのFe-FeO系の共融点組成の決定
Melting in the Fe-FeO system to 214 GPa

*岡 健太[1]、木所 佑斗、廣瀬 敬[1]、中島 陽一[2]、Guillaume Morard[3]、Guillaume Fiquet[3]、Nicolas Coudurier[3]
*Kenta Oka[1], Yuto Kidokoro, Kei Hirose[1], Yoichi Nakajima[2], Guillaume Morard[3], Guillaume Fiquet[3], Nicolas Coudurier[3]

1. 東京大学大学院理学系研究科地球惑星科学専攻、2. 熊本大学大学院先導機構、3. ソルボンヌ大学
1. Department of Earth and Planetary Science, The University of Tokyo, 2. Priority Organization for Innobation and Excellence, 3. Sorbonne Université

Oxygen is one of the likely candidates as the light elements in the Earth’ s core. If oxygen is the primary one, the oxygen content in the outer core should be less than that of the eutectic liquid composition in the Fe-FeO system, which is required to explain the dense solid inner core compared to the liquid outer core. The eutectic liquid composition in the Fe-FeO system has been estimated under high pressures, on the basis of thermodynamic calculations and high-pressure experiments. However, large inconsistency is found among these previous studies, especially below 100 GPa.

In this study, we have conducted high-temperature and high-pressure experiments up to 214 GPa and 3650 K. Liquidus phase relations were determined from textural and chemical characterizations of recovered samples using FIB/FE-EDS/FE-EPMA. Liquid-liquid immiscibility reported below 21 GPa in previous multi-anvil studies (Tsuno et al., 2007) was not observed above 42 GPa in the present DAC experiments. Our results demonstrate that the eutectic liquid composition in the Fe-FeO binary system changed largely from Fe+1.3wt.%O at 15 GPa (Tsuno et al., 2007) to >8 wt.% O at 42 GPa. It then further increased gradually to ~13 wt.% O with increasing pressure to 214 GPa.

These results are in reasonably good agreement with the previous DAC experiments by Seagle et al. (2008) based on XRD measurements and the earlier thermodynamic model by Komabayashi (2014) that considered non-ideal mixing between liquid Fe and FeO. Our data also showed contamination by variable amounts of carbon in liquid, which may explain the difference from the results by Morard et al. (2017) below 80 GPa. The large change in the liquidus phase relations in the Fe-FeO system observed between 15 and 42 GPa is likely related to the disappearance of liquid-liquid immiscibility.

The outer core may include 5.5 wt.% O if oxygen is a sole light element (Badro et al., 2014). When extrapolating our data to 330 GPa, the eutectic liquid in the Fe-FeO binary system includes about 15 wt.% O, which is much higher than the 5.5 wt.% O and therefore allows the outer core liquid containing oxygen as one of important light elements to crystallize solid Fe at the ICB. These results support the presence of oxygen in the core.

キーワード：外核、軽元素、融解実験、鉄-酸素系
Keywords: outer core, light elements, melting experiment, Fe-FeO System

©2019. Japan Geoscience Union. All Right Reserved.

B2 phase in the inner core: constraints from high pressure experiments

*Eiji Ohtani[1], Daijo Ikuta[1], Seiji Kamada[2], Tatsuya Sakamaki[1], Naohisa Hirao[3]

1. Department of Earth and Planetary Materials Science, Graduate School of Science, Tohoku University, 2. Frontier Institute for Interdisciplinary Research, Tohoku University, 3. SRring-8, Japan Synchrotron Research Institute

The Earth inner core is considered to be composed of hcp-iron alloy with small amounts of light elements, and intensive efforts have been made to clarify the physical properties of hcp-iron. On the other hand, there are many seismological observations on existence of heterogeneities, layering, and anisotropy in the inner core, which cannot be accounted for only by hcp-iron.

It has been suggested that B2 or bcc phase can exit in the inner core mainly by theoretical calculations (e.g., Belonoshko et al., 2003). Therefore, it has been a debated matter on the existence of a stable B2 structure of iron alloys in the inner core. There is experimental reports suggesting existence of B2 phase in Fe-Si alloy (Fischer et al., 2013). Coexistence of hcp+B2 is observed by Fishcer et al. (2013) in the Fe-Si system with silicon greater than 6 wt. %.

Nickel is an important metallic component in meteorites, and it can modify the phase relations of iron alloy systems significantly. In order to clarify the stability of B2 phase in the inner core, we studied the phase relations of the Fe-Ni-Si system at high pressure and temperature relevant in the core. The in-situ X-ray observations of the Fe-Ni-Si alloys at high pressure and temperature were conducted at BL10XU of SPring-8 by using the double sided laser heating diamond anvil cell. We observed a wide stability field of coexistence of B2 phase and hcp at high pressure and temperature above 100 GPa and 2500 K in the composition of Fe7wt%Ni5wt%Si alloy.

The nickel and silicon contents in the inner core were estimated to be 0~8 wt% and 3-6 wt% respectively in order to account for the PREM inner core based on the equation of state of hcpFe-Ni-Si alloy (Asanuma et al., 2013) and the sound velocity of hcpFe-Si alloy (Sakairi et al., 2018). Combined with the phase relations together with the sound velocity measurements, we can suggest that the inner core is mainly composed of hcp-iron with a small amount of B2 phase. Coexistence of B2 phase with hcp-Fe alloy in the inner core can explain the heterogeneity and fine structure of the inner core reported in seismology.

Reference: Belonoshki et al. (2003) Nature, 466, 744-747. Fischer et al. (2015) Am Min, 100, 2718-2724. Asanuma et al. (2011) EPSL, 310, 113-118. Sakairi et al. (2018), Am Min., 102, 85-90.

Keywords: inner core, bcc, hcp, Fe-Ni-Si alloy, phase relation, sound velocity

©2019. Japan Geoscience Union. All Right Reserved.

[E] 口頭発表 | セッション記号 S (固体地球科学)：S-VC 火山学

2019年5月30日(木) 9:00 ~ 10:30 | A07 東京ベイ幕張ホール

[S-VC34] Connecting magma dynamics in vent-conduit system with surface expression of volcanic eruption

コンビーナ:三輪 学央(防災科学技術研究所)、下司 信夫(産業技術総合研究所　活断層・火山研究部門)、座長:三輪 学央、Jacopo Taddeucci

Magma dynamics within a shallow conduit system control the diversity of behavior of volcanic eruptions. Recent advancements in geophysical, airborne and ground-based observation techniques provide quantitative data about the dynamic behavior of volcanic eruptions. New analytical methods of the macro and microtextures of eruptive products also open new insights on detailed dynamics of magmas within conduit. The aim of this session is the integration of these new techniques to approach the dynamics of magma ascending from a shallow part of conduit to vent. This session seeks submissions that explore magma dynamics controlling the behaviors of volcanic eruption by integrated investigation of 1) degassing, outgassing, crystallization, and fragmentation of ascending magma, 2) emission and recycling of eruptive product, and 3) morphological characterization of the vent-conduit system. We encourage contributions based on textural-petrological analyses of eruptive product, experimental study reproducing magma in the conduit, geophysical observation on surface expression of volcanic eruption, and related numerical modeling.

9:00 ~ 9:15

[SVC34-01] An experimental basis for estimating particle properties following volcanic ash emissions

★Invited Papers

*Adrian Hornby[1]、Ulrich Kueppers[1]、Hanna Horsch[2]、Paul Ayris[1]、Nick Varley[3]、Daniele Andronico[4]、Boris Behncke[4]、Yan Lavallée[5]、Jackie E Kendrick[5]、James Utley[5]、Amy Hughes[5]、David Damby[6]、Benedikt Maurer[1]、Marlin Juchem[1]、Donald B Dingwell[1] (1.Ludwig-Maximilians-Universität München, DE、2.Hazen Research, Golden, USA、3.University of Colima, MX、4.INGV Catania, IT、5.University of Liverpool, UK、6.USGS Cascades Volcano Observatory, USA)

9:15 ~ 9:30

[SVC34-02] **Vapor transport in shallow intruded magmas: insights from diktytaxitic texture**

*櫻井 亮輔[1]、中村 美千彦[2]、奥村 聡[2]、無盡 真弓[2]、中谷 貴之[2] (1.東北大学理学部地球惑星物質科学科、2.東北大学大学院理学研究科地学専攻地球惑星物質科学講座)

9:30 ~ 9:45

[SVC34-03] First observation of nanolites and ultrananolites in alkaline volcanic glasses (Eifel, Germany)

*Marija Putak Juricek[1]、Michihiko Nakamura[2]、Mayumi Mujin[2]、Hans-Ulrich Schmincke[3]、Mari Sumita[3]、Nobuyoshi Miyajima[1] (1.BGI、2.Tohoku Univ.、3.GEOMAR)

9:45 ~ 10:00

[SVC34-04] Textural Study of Pumice Clasts from The Youngest Toba Tuff Eruption

*Gabriela Nogo Retnaningtyas Bunga Naen[1]、Atsushi Toramaru[1]、Tomoharu Miyamoto[1]、Haryo Edi Wibowo[2] (1.Department Earth and Planetary Sciences, Graduate School of Sciences, Kyushu University, Nishiku, 744, Motooka, Fukuoka, 819-0395, Japan、2.Geological Engineering Department, Universitas Gadjah Mada, 55284, Yogyakarta, Indonesia)

10:00 ~ 10:15

[SVC34-05] **Oomurodashi volcano: Past effusive and phreatomagmatic activity revealed by submarine and subaerial deposits**

*Iona McIntosh[1]、Kenichiro Tani[2]、Alexander Nichols[3]、Qing Chang[1]、Jun-Ichi Kimura[1] (1.Japan Agency for Marine-Earth Science and Technology, Yokosuka、2.National Museum of Nature and Science,

Tsukuba、3.University of Canterbury, Christchurch, New Zealand)

10:15 ~ 10:30

[SVC34-06] Mechanism of volatile transport from mafic to silicic magma upon mixing

*吉村 俊平[1]、松本 亜希子[1]、中川 光弘[1] (1.北海道大学・地球惑星科学)

An experimental basis for estimating particle properties following volcanic ash emissions

*Adrian Hornby[1], Ulrich Kueppers[1], Hanna Horsch[2], Paul Ayris[1], Nick Varley[3], Daniele Andronico[4], Boris Behncke[4], Yan Lavallée[5], Jackie E Kendrick[5], James Utley[5], Amy Hughes[5], David Damby[6], Benedikt Maurer[1], Marlin Juchem[1], Donald B Dingwell[1]

1. Ludwig-Maximilians-Universität München, DE, 2. Hazen Research, Golden, USA, 3. University of Colima, MX, 4. INGV Catania, IT, 5. University of Liverpool, UK, 6. USGS Cascades Volcano Observatory, USA

In recent years, mitigating the impact of volcanic ash emissions has risen up political and research agendas. Despite intense research efforts, challenges remain as to the detection and forecasting of emissions, and subsequent interactions in the earth system. Monitoring instruments and ash dispersal models usually require the input of volcanic ash properties in order to operate effectively, however forensic methods are poorly suited to volcanic eruptions where near-real-time data is required, and default values are commonly used. Here, we take an experimental approach to demonstrate that the surface composition and the initial size and shape distribution of volcanic ash particles depends upon (i) the initial rock texture, chemistry and mineralogy and (ii) the fragmentation processes that produced the particles.

We compare natural pyroclasts produced during recent eruptive activity at Volcán de Colima, Mt Etna, Santiaguito, Mt Agung and Tungurahua, with particles produced in fragmentation experiments using fresh rock samples from Volcán de Colima and Mt Etna. Sets of experiments were conducted under varying conditions in shock tube, tumbling and fault friction apparatuses to simulate natural eruption processes. Using QEMSCAN, an SEM-based automated mineralogy technique, we produce micron-scale maps showing the size, shape and phase distribution of thousands of ash particles in each sample. We measure particle size-, shape- and phase distribution in each sample and show that particle sizes and shapes show characteristic variation between different experimental methods and eruptive activity. Some phases, particularly groundmass glass (or tachylite), feldspars and pyroxenes are found to vary significantly at particles boundaries compared to the bulk. The pattern of enrichment and depletion of phases is shown to relate to the fragmentation mechanism and the rock texture at the macro- and micro-scale, and correlations between experimental and natural samples indicate a robust signal.

Volcanic ash presents unique hazards to aviation, health and the environment and better constraints on ash particle properties immediately following activity may improve estimations of the intensity and spatial extent of ash-related hazards. Our results may benefit local hazard management, monitoring and forecasting efforts at the case study volcanoes.

Keywords: Volcanic ash, Fragmentation processes, Experimental volcanology, Hazards, Ash dispersal and monitoring, QEMSCAN

©2019. Japan Geoscience Union. All Right Reserved.

Vapor transport in shallow intruded magmas: insights from diktytaxitic texture

*櫻井 亮輔[1]、中村 美千彦[2]、奥村 聡[2]、無盡 真弓[2]、中谷 貴之[2]
*Ryosuke Sakurai[1], Michihiko Nakamura[2], Satoshi Okumura[2], Mayumi Mujin[2], Takayuki Nakatani[2]

1. 東北大学理学部地球惑星物質科学科、2. 東北大学大学院理学研究科地学専攻地球惑星物質科学講座
1. Division of Earth and Planetary Materials Science, Faculty of Science, Tohoku University, 2. Division of Earth and Planetary Materials Science, Department of Earth Science, Graduate School of Science, Tohoku University

Volcanic ashes from Vulcanian explosions derived from shallow-intruded magmas and dome lavas often include microporous and glass-free groundmass in which lath-shaped plagioclase microlites form angular voids. Such texture, generally described as diktytaxitic texture, is known to control the permeability of bulk rock significantly when the connected porosity of bubbles and cracks is small (Kushnir et al., 2016). How and under what conditions diktytaxitic texture is formed is, however, not precisely known. In this study we simulated the formation of diktytaxitic groundmass through a series of isobaric-isothermal (IBIT) crystallization experiments in order to clarify its formation kinetics. As a result, diktytaxitic texture was formed at 850 and 900℃ and at 10 and 20 MPa, and almost entire groundmass became diktytaxitic (i.e. glass-free) in the experiment kept at 850℃ and 20 MPa for 189 h. At 850℃ and 10 MPa for >24 h, interstitial melt completely disappeared to form the groundmass composed of feldspar microlites with angular voids. Cristobalite crystals were found in the groundmass and on the interior walls of capsules. The glass compositions form liner trends between the plagioclase microlites and the precipitated silica on the SiO_2-Al_2O_3 diagram. These observations indicate that evaporation of SiO_2-rich melt and condensation of cristobalite are the dominant process for the formation of microporous groundmass characteristic of dixtytaxitic texture. The wide range of K_2O contents in the glass can be explained as a result of vapor-phase growth of ~10 μm K-feldspar microlites in the diktytaxitic groundmass. Hence, we conclude that diktytaxitic texture is formed through (1) enrichment of silicon and potassium in the melt by microlite crystallization, (2) evaporation of SiO_2-rich constituents from the melt accompanied by breakage of Si-O covalent bond, and (3) precipitation of cristobalite and K-feldspar from vapor. The present study indicates that the late stage magma crystallization in shallow intrusions and lava domes proceeds dominantly through a vapor phase.

キーワード：結晶化実験、蒸発凝縮作用、クリストバライト、ディクティタキシティック組織、気相成長、溶岩ドーム
Keywords: crystallization experiment, evaporation-condensation, cristobalite, diktytaxitic texture, vapor-phase growth, lava dome

©2019. Japan Geoscience Union. All Right Reserved.

First observation of nanolites and ultrananolites in alkaline volcanic glasses (Eifel, Germany)

*Marija Putak Juricek[1], Michihiko Nakamura[2], Mayumi Mujin[2], Hans-Ulrich Schmincke[3], Mari Sumita[3], Nobuyoshi Miyajima[1]

1. BGI, 2. Tohoku Univ., 3. GEOMAR

Nanolites are the smallest, less than <1 μm wide, crystals observed in groundmass of volcanic rocks. They are believed to be the last solid phases that crystallize from the melt during eruptions. Understanding mechanisms of nucleation and subsequent growth of nanolites could potentially provide information about the physiochemical conditions of magma just prior to eruption.

Since nanolite studies are scarce in literature and experimental observation of crystal nucleation and growth is challenging, few constraints on kinetics of nanolite crystallization are available at present. Furthermore, previous studies have investigated nanolites from exclusively calc-alkaline volcanic products. Since melt composition may have a significant effect on crystal nucleation and growth, detailed and systematic descriptions of nanolites occurring in eruptive products of different magma series are required.

The purpose of this study is to present a preliminary overview of nanolite nucleation and growth mechanisms in alkaline melts. Due to high concentrations of network modifying Na and K atoms and considerable volatile budgets, alkaline magmas have very low viscosities. As chemical diffusion is highly dependent on viscosity, nucleation and growth of nanolites in alkaline melts may be governed by different mechanisms from those observed in previous studies.

Variously differentiated samples produced by different eruption styles were collected from West and East Eifel Volcanic Fields (Germany). Samples were observed using a combination of polarized microscopy, FE-SEM and TEM.

Preliminary observation suggests that average nanolite nucleation density in mafic and ultramafic Eifel samples is noticeably higher in comparison to calc-alkaline rocks. In general, nanolites in alkaline eruptive products display a wide range of morphologies with a tendency towards acicular and dendritic habits. Examples of both homogeneous and heterogeneous nucleation were observed. The most abundant phase in the nanolite population of mafic and ultramafic samples is magnetite. The only highly differentiated sample, a phonolitic glass, contained very few nanolites.

In a recently published experimental study it was suggested that precipitation of magnetite nano-crystals may increase magma viscosity by modifying the melt composition. Considering the abundance of magnetite nanolites in Eifel scoria fragments, these magmas may have experienced a severe viscosity increase at shallow crustal levels. We suspect that the presence of extensive interconnected networks of acicular and dendritic magnetite nanolites may have mechanically impeded magma flow as well, contributing to the explosive nature of Eifel eruptions that was previously attributed to magma-water mixing.

Keywords: nanolites, alkaline, nucleation, dendrites

©2019. Japan Geoscience Union. All Right Reserved.

©2019. Japan Geoscience Union. All Right Reserved.

Textural Study of Pumice Clasts from The Youngest Toba Tuff Eruption

*Gabriela Nogo Retnaningtyas Bunga Naen[1], Atsushi Toramaru[1], Tomoharu Miyamoto[1], Haryo Edi Wibowo[2]

1. Department Earth and Planetary Sciences, Graduate School of Sciences, Kyushu University, Nishiku, 744, Motooka, Fukuoka, 819-0395, Japan, 2. Geological Engineering Department, Universitas Gadjah Mada, 55284, Yogyakarta, Indonesia

Toba Caldera Complex, North Sumatra, Indonesia is well known as the largest Quaternary caldera (87×33 km) that formed by four major eruptions with magnitude of VEI 8 among which the biggest one is the latest eruption of the Youngest Toba Tuff (YTT) about 74,000 years ago. The conduit dynamics of Toba caldera forming eruption is still poorly understood. Bubbles in pumice, which are produced by an explosive eruption possibly record dynamic processes in the conduit during eruption. This textural study aims to estimate the decompression rate of the biggest event of Toba eruption (YTT) by using textural data from Bubble Number Density (BND) together with geochemical, petrographical, grain size distribution (GSD), and bulk density data. In general, only a few data of decompression rate from caldera forming eruption events are available because the products were mostly welded and the original texture has been erased. Meanwhile, Toba eruption produced non-welded to welded deposit. Therefore, we focus on the nonwelded part of the biggest Quaternary caldera forming eruption localized on the northern part of the caldera in order to extract the original condition of the bubble formation. Samples from three different locations were employed for the analyses. Whole rock geochemical data of pumices were obtained by XRF. Petrography analysis for 21 thin sections were conducted using optical microscope. Bulk density measurement for 338 individual pumices with the size range of 4-8 mm and 8-16 mm were conducted using Laser 3D scanner. Textural analysis was carried out for 6 particles of 3 selected thin sections using microphotographs taken by SEM and further analyzed using image processing software. Geochemical data showed that the YTT magma is rhyodacitic to rhyolitic in whole rock compositions with the narrow range of SiO_2 (69.15 - 72.17 wt. %). Phenocrysts are plagioclase, biotite, quartz, and sanidine, most of which are fractured. The vesicle has a variety in size from 2.5 μm to 97 μm and in shape from rounded, elongated, to complex. GSD for each location are dominated by fine size (phi=1). Bulk density of individual pumice ranges from 0.4 to 1.1 gcm^{-3}. BND calculation were done in carefully selected area where is uniform in size of bubbles to represent samples in estimating the decompression rate in the conduit. BND value ranges from 10^5 - 10^7 mm^{-3} showing a wide range of BND magnitude. Qualitatively, higher magnitude of BND is correlated with higher silica content, higher frequency of crystal fracture, complex vesicle shape, smaller vesicle size, and lower bulk density, and vice versa . The decompression rate was calculated using the BND decompression rate meter from Toramaru (2006). The result showed that Toba caldera forming eruption has high decompression rate ranging from 10^7 –10^8 Pa/s. Those fact shows that Toba experienced with rapid decrease of pressure in the conduit. Moreover, this idea could be an important factor to reveals the conduit dynamic system of YTT super eruption.

Keywords: Toba Caldera, Pumice of the Youngest Toba Tuff (YTT), Textural Study, Conduit Dynamics, Bubble Number Density, High Decompression Rate

©2019. Japan Geoscience Union. All Right Reserved.

Oomurodashi volcano: Past effusive and phreatomagmatic activity revealed by submarine and subaerial deposits

*Iona McIntosh[1], Kenichiro Tani[2], Alexander Nichols[3], Qing Chang[1], Jun-Ichi Kimura[1]

1. Japan Agency for Marine-Earth Science and Technology, Yokosuka, 2. National Museum of Nature and Science, Tsukuba, 3. University of Canterbury, Christchurch, New Zealand

Oomurodashi is a recently discovered active, shallow (~140 mbsl), silicic submarine volcano in the northern Izu-Bonin arc, only 60 km from the entrance to Tokyo Bay. Past activity at Oomurodashi spans a wide range of eruption styles and includes small lava effusions, submarine pumice, and subaerial tephra deposits on nearby Izu-Oshima and Toshima islands. Here we present volatile and textural data that reveal contrasting degassing, quench and fragmentation processes occurring in the shallow conduit and overlying water column.

H_2O data for pumiceous pyroclasts and lavas were obtained using new Fourier Transform Infrared spectroscopy (FTIR) analytical techniques for vesicular and hydrated glasses. Although the Oomurodashi glasses are extensively hydrated, the interconversion of H_2O species (i.e. molecular water, H_2O_m, and hydroxyl groups, OH) stops at the glass transition temperature, and low temperature hydration occurs via diffusive addition of H_2O_m only, leaving OH contents unchanged. OH data can therefore be interpreted according to the known pressure-dependence of H_2O solubility and temperature dependence of H_2O speciation.

Pumice clasts within the subaerial tephra layer have OH contents that are consistent with quench fragmentation at depths of ~60 –150 m depth within the shallow edifice. Moreover, the majority of this tephra deposit consists of ‘mosslike’ particles formed by annealing of extremely fine-grained material, which are typically formed by explosive phreatomagmatic activity. We therefore propose that this tephra represents the distal deposits from the explosive formation of the shallow (~100 m depth) summit crater by a shallow submarine, phreatomagmatic maar-type eruption.

By contrast, two in situ submarine lavas have lower OH contents than expected for their current water depths. Comparison with past sea level variation suggests that these effusive eruptions occurred at ~8-9 and ~12 ka during times of lower sea level. Loose submarine pumice also sampled from the edifice has a range of OH contents and vesicularities, reflecting different quench depths and dispersal histories within the water column.

Keywords: Submarine volcanism, FTIR, Volatiles, Magma fragmentation

©2019. Japan Geoscience Union. All Right Reserved.

Mechanism of volatile transport from mafic to silicic magma upon mixing

*吉村 俊平[1]、松本 亜希子[1]、中川 光弘[1]
*Shumpei Yoshimura[1], Akiko Matsumoto[1], Mitsuhiro Nakagawa[1]

1. 北海道大学・地球惑星科学
1. Department of Earth and Planetary Sciences, Hokkaido University

Introduction
Deep-derived, high-temperature mafic magma often injects into shallow-stored, low-temperature silicic magma, producing either well-mixed intermediate magma or mafic enclaves floating in host magma. Volatile transport from mafic to silicic magma accompanies magma mixing, and it may control volcanic activity (e.g., Roberge et al., 2009). However, the detailed mechanism of such volatile transport is unclear. In this study, we investigated how the gas was generated in mafic magma and transported to the silicic magma based on S and Cl analysis of Atchiyama rhyolitic lava that contains abundant basaltic enclaves.

Method
We observed Atchiyama biotite-rhyolite lava that erupted 1600 BP in Niijima Island (Isshiki, 1997), and analysed compositions of host rhyolite and basaltic enclaves. Cl mapping analysis was also performed on the area of enclave-host boundary to track the volatile transfer paths.

Results and discussion
Basaltic enclaves exhibited fine-grained groundmass composed of dendritic crystals, rhyolitic interstitial melt, and bubbles. The interstitial melt, which was compositionally distinguishable from the host rhyolite, was S-free (<50 ppm) and Cl-rich (1200 ppm). Melt inclusion analysis showed that the initial basaltic melt before mixing was S-rich (~4000 ppm) and Cl-poor (~430 ppm). These observations indicate that the basaltic magma cooled and crystallised rapidly upon injection, and the interstitial rhyolitic melt was produced as a result of crystallisation fractionation. Crystallisation-induced vesiculation (second boiling) occurred and S degassed completely, while Cl was concentrated in the interstitial melt.
Groundmass glass of host rhyolite was S-free and Cl-poor (~800 ppm). However, Cl mapping analysis revealed that the Cl content increased to 1200 ppm near the enclave margin. In addition, finger-like veins containing vapour-phase crystals developed from the enclave to far afield in host rhyolite, and the Cl content was also high near such veins. All these observations indicate that S- and Cl-rich gas was generated in crystallising enclave, and it was transported to the host rhyolitic magma via gas flow and diffusion.

キーワード：マグマ、混合、揮発性成分
Keywords: magma, mixing, volatile

©2019. Japan Geoscience Union. All Right Reserved.

[E] 口頭発表 | セッション記号 S (固体地球科学)：S-VC 火山学

2019年5月30日(木) 10:45 ~ 12:15 | A07 東京ベイ幕張ホール

[S-VC34] Connecting magma dynamics in vent-conduit system with surface expression of volcanic eruption

コンビーナ:三輪 学央(防災科学技術研究所)、下司 信夫(産業技術総合研究所　活断層・火山研究部門)、座長:下司 信夫(産総研　活断層・火山研究部門)、Adrian Hornby(Ludwig-Maximilians-University Munich)

Magma dynamics within a shallow conduit system control the diversity of behavior of volcanic eruptions. Recent advancements in geophysical, airborne and ground-based observation techniques provide quantitative data about the dynamic behavior of volcanic eruptions. New analytical methods of the macro and microtextures of eruptive products also open new insights on detailed dynamics of magmas within conduit. The aim of this session is the integration of these new techniques to approach the dynamics of magma ascending from a shallow part of conduit to vent. This session seeks submissions that explore magma dynamics controlling the behaviors of volcanic eruption by integrated investigation of 1) degassing, outgassing, crystallization, and fragmentation of ascending magma, 2) emission and recycling of eruptive product, and 3) morphological characterization of the vent-conduit system. We encourage contributions based on textural-petrological analyses of eruptive product, experimental study reproducing magma in the conduit, geophysical observation on surface expression of volcanic eruption, and related numerical modeling.

10:45 ~ 11:00

[SVC34-07] The in-flight grain size distribution of lapilli and bombs from Strombolian explosions

*Jacopo Taddeucci[1]、Piergiorgio Scarlato[1]、Elisabetta Del Bello[1]、Tullio Ricci[1]、Ulrich Kueppers[2]、Bruce Houghton[3] (1.Istituto Nazionale di Geofisica e Vulcanologia, Rome, Italy、2.Department of Earth and Environmental Sciences. Ludwig-Maximilians-Universität (LMU). Munich, Germany、3.Department of Earth Sciences, University of Hawai‘i at Mānoa, Honolulu, USA)

11:00 ~ 11:15

[SVC34-08] **Pyrrotite oxidation as a proxy for air entrainment in eruption columns**

*松本 恵子[1]、中村 美千彦[2] (1.産業技術総合研究所地質調査総合センター、2.東北大学大学院理学研究科)

11:15 ~ 11:30

[SVC34-09] **Thermal signals in volcano monitoring: combining MODIS-MIROVA data with ground-based measurements at Aso Volcano, Japan**

*Corrado CIGOLINI[1]、Akihiko Yokoo[2]、Diego Coppola[1]、Marco Laiolo[1] (1.Department of Earth Sciences, University of Torino, Italy、2.Aso Volcanological Laboratory, Institute for Geothermal Sciences, Kyoto University, Japan)

11:30 ~ 11:45

[SVC34-10] Magma transfer processes in the NE Japan arc: insights from crustal ambient noise tomography combined with volcanic eruption records

*Georg F Zellmer[1]、Kai-Xun Chen[2]、Yuancheng Gung[2]、Ban-Yuan Kuo[3]、Takeyoshi Yoshida[4] (1.Massey University, Palmerston North, New Zealand、2.National Taiwan University, Taipei, Taiwan、3.Academia Sinica, Taipei, Taiwan、4.Tohoku University, Sendai, Japan)

11:45 ~ 12:00

[SVC34-11] **STRATIGRAPHY RENEWAL, MAGMA CHAMBER STRATIFICATION, AND CONDUIT PROCESS OF THE 1815 TAMBORA CALDERA FORMING ERUPTION**

*Indranova Suhendro[1]、Atsushi Toramaru[1]、Yasuo Miyabuchi[2]、Tomoharu Miyamoto[1] (1.Department of Earth and Planetary Sciences, Graduate School of Sciences, Kyushu University, Japan、2.Faculty of Advanced Science and Technology, Kumamoto University, Kurokami 2-40-1, Chuo-ku, Kumamoto 860-8555, Japan)

12:00 ~ 12:15
Discussion

The in-flight grain size distribution of lapilli and bombs from Strombolian explosions

*Jacopo Taddeucci[1], Piergiorgio Scarlato[1], Elisabetta Del Bello[1], Tullio Ricci[1], Ulrich Kueppers[2], Bruce Houghton[3]

1. Istituto Nazionale di Geofisica e Vulcanologia, Rome, Italy, 2. Department of Earth and Environmental Sciences. Ludwig-Maximilians-Universität (LMU). Munich, Germany, 3. Department of Earth Sciences, University of Hawai‘i at Mānoa, Honolulu, USA

Grain size distribution is one of the fundamental physical parameters of pyroclastic deposits, key to understanding both magma fragmentation and tephra emplacement processes during an explosive eruption. Most commonly, the grain size distribution of pyroclasts from one eruption is obtained from field sampling and analysis of the resulting tephra deposit; integration of multiple analyses gives a total grain size distribution. In this process it is often assumed that the grain size distribution of the deposit reflects that of the assemblage of pyroclasts that left the eruptive vent. However, observations suggest that multiple processes may act to change the size of erupted pyroclasts during their emplacement, so that the grain size distribution of a deposit may differ, to a variable degree, from that at the vent. Here, we use high-speed imaging to measure the in-flight grain size distribution of pyroclasts for the first tens of meters above an eruptive vent.

We focus on lapilli and bombs from Strombolian- explosions at Stromboli volcano (Italy) in September 2018. At that time, multiple, well-collimated jets with incandescent pyroclasts and no visible ash erupted from a vent about one meter in diameter and in plain view. The activity was recorded by using a high-speed camera filming with a temporal and spatial resolution of 500 frames per second and 0.012 m/pixel, respectively. The high-speed videos were pre-processed for background subtraction, then thresholded for gray level intensity, and finally the individual particles measured for their 2-D size and shape by using image processing. Particle velocity and size was also measured using particle tracking algorithms.

In a parametric study, the effect of different thresholding levels and frame sampling has been investigated. The results define the best parameters and the most effective truncation limits of the measured grain size distributions. Modal values of the grain size are broadly centered around the phi -4 to -5 size classes (16-32 mm) by particle number and the phi -5 to -6 size classes (32 to 64) by particle mass, respectively. The grain size distribution of erupted pyroclasts shifts considerably over time, with smaller clasts being ejected at the beginning of an explosion, and larger median diameters recorded at instants of higher pyroclast volume fluxes.

These results highlight the complexity and variability of the erupted size distributions at the vent, but also the need for a careful assessment of analytical error and methodological limitations.

Keywords: strombolian, explosion, grain size distribution

©2019. Japan Geoscience Union. All Right Reserved.

Pyrrotite oxidation as a proxy for air entrainment in eruption columns

*松本 恵子[1]、中村 美千彦[2]
*Keiko Matsumoto[1], Michihiko Nakamura[2]

1. 産業技術総合研究所地質調査総合センター、2. 東北大学大学院理学研究科
1. Geological Survey of Japan, The National Institute of Advanced Industrial Science and Technology, 2. Faculty of Science, Tohoku University

Entrainment of air by turbulent mixing into eruption columns is a primary control of explosive eruption styles. Pyrrhotite (Po; $Fe_{1-x}S$) in erupted materials is oxidized to form magnetite (Mt) and hematite (Hm) at the oxygen fugacity (fO_2) on the Earth's surface and at magmatic temperature. Degree of Po breakdown has been proposed as a proxy for magma oxidation and cooling by entrained air through examination of the Plinian pumice and lavas from the 1914 eruption at Sakurajima volcano (VEI4). To verify and further investigate the potential use of Po oxidation for estimating eruption intensities from pyroclasts, we have examined the pumice clasts from three andesitic explosive eruptions with similar magmatic temperature and different eruption intensity: the 1783 Plinian eruption of the Asama volcano (VEI4), the 2011 sub-Plinian eruption of the Shinmoedake volcano (VEI2) and the 2010 Vulcanian explosion of the Sakurajima volcano (VEI1).
Mineral phases of magmatic sulfide and occurrence of pseudomorph (Mt and Hm) are different among the three eruption samples. Po is observed in the groundmass of the pumice from the Asama 1783 eruption and the Sakurajima 2010 eruption, whereas the sulfide in the Shinmoedake 2011 groundmass is intermediate solid solution (iss; $Cu_{1-x}Fe_{2+y}S_{2-z}$). Po is sometimes replaced to form pseudomorph, while iss shows no replacement. The porous texture of the Po pseudomorph, which indicates a reaction of Po with air, is similar to that observed for the oxidation product having columnar microstructure reported in the pumice from the Sakurajima 1914 eruption (Matsumoto and Nakamura, 2017). Approximately half of the Po grains are partly or entirely replaced by the pseudomorph in the Asama 1783 pumice, as observed in the Sakurajima 1914 samples. On the other hand, proportion of the pseudomorphic Po grains is less than 20% in the Sakurajima 2010 pumice. This difference indicates that the Asama 1783 pumice, together with the Sakurajima 1914 pumice, has been more efficiently oxidized than the Sakurajima 2010 pumice. The preservation of iss in the Shinmoedake 2011 pumice is probably due to the difference in oxidation mechanism between iss and Po. The efficient oxidation of Po during the two Plinian eruptions (i.e., the Asama 1783 and the Sakurajima 1914 eruptions) can be attributed to the longer duration in which temperature of pumice were kept high in the eruption columns than that in the Vulcanian column. These results underscore the potential use of Po oxidation for the purpose of constraining the temperature and fO_2 of eruption columns that reflect eruption intensity of explosive eruptions.

キーワード：磁硫鉄鉱、酸化、爆発的噴火、噴煙柱
Keywords: pyrrhotite, oxidation, explosive eruption, eruption column

©2019. Japan Geoscience Union. All Right Reserved.

Thermal signals in volcano monitoring: combining MODIS-MIROVA data with ground-based measurements at Aso Volcano, Japan

*Corrado CIGOLINI[1], Akihiko Yokoo[2], Diego Coppola[1], Marco Laiolo[1]

1. Department of Earth Sciences, University of Torino, Italy, 2. Aso Volcanological Laboratory, Institute for Geothermal Sciences, Kyoto University, Japan

Active volcanoes bearing crater lakes are rather challenging targets for thermal monitoring since their anomalies are rather small when compared to lava flows and/or domes. Thus, we have combined satellite data with ground-based measurements at Aso Volcano during its recent activity.
The thermal signals of Aso Volcano (Nakadake) during unrest episodes have been analyzed by means of the MODIS-MIROVA data set and high resolution images (LANDSAT 8 OLI and Sentinel 2) cross-checked with ground-based thermal observations. The Volcanic Radiative Power (VRP) detected by nighttime satellite data during the time span considered was mainly below 3 MW. This value is a thermal threshold that marks the transition from high fumarole activity (HFA) to Strombolian eruptions (SE). Periods with the occurrence of sporadic phreatic eruptions (PE, eventually bearing phreatomagmatic episodes), is the dominant phase during unrest episodes, with VRP values around 0.5 MW. However, during sustained Strombolian phases (November-December 2014) the radiative power was higher than 4 MW, reaching peak values up to 15.6 MW (on December 7, 2014, 10 days after the major Strombolian explosion of November 27). Ground-based measurements, recorded by FLIR T440 Thermo-camera on the fumarole field of the South Area, shows that the heat-flux stabilized around 2 MW until February 2015. Apparent temperatures measured on the fumarole field were around 490-575˚C before the major Strombolian explosive event, whereas those recorded at the active vent (Central Pit) reached their maxima around 600 ˚C. In the following days they both exhibited a decreasing trend. However, during the Strombolian phase the crater lake dried out and was then replenished by early July, 2016. Then volcanic activity shifted back to phreatic-phreatomagmatic and the eruptive cycle was completed; in this period ground measurements were fluctuating around 1 MW. Following the major phreatic explosion of October 8, 2016 satellite VRP were moderately above 2 MW and then progressively decreased. During 2018, they were essentially below 1 MW (with a mean of 0.75 Mw and few peaks above 1 MW).
We estimated the total amount of Magma Equivalent Volume (MEV) responsible for satellite thermal anomalies during the Strombolian phase (from the end of November 2014 to May 2015). The cumulative volume involved in this phase reached 4.5 x 10^5 m^3, which is two order of magnitude lower than the total volume of magma undergoing degassing (estimated by means of the petrologic models based on SO_2 degassing). This indicates that thermal anomalies during the Strombolian phases detect the magma that is reaching the surface and through a feeder dike, or conduit, connected at depth with a major reservoir.

Keywords: Aso Volcano, unrest episodes, thermal anomalies, Strombolian activity, major explosions

©2019. Japan Geoscience Union. All Right Reserved.

Magma transfer processes in the NE Japan arc: insights from crustal ambient noise tomography combined with volcanic eruption records

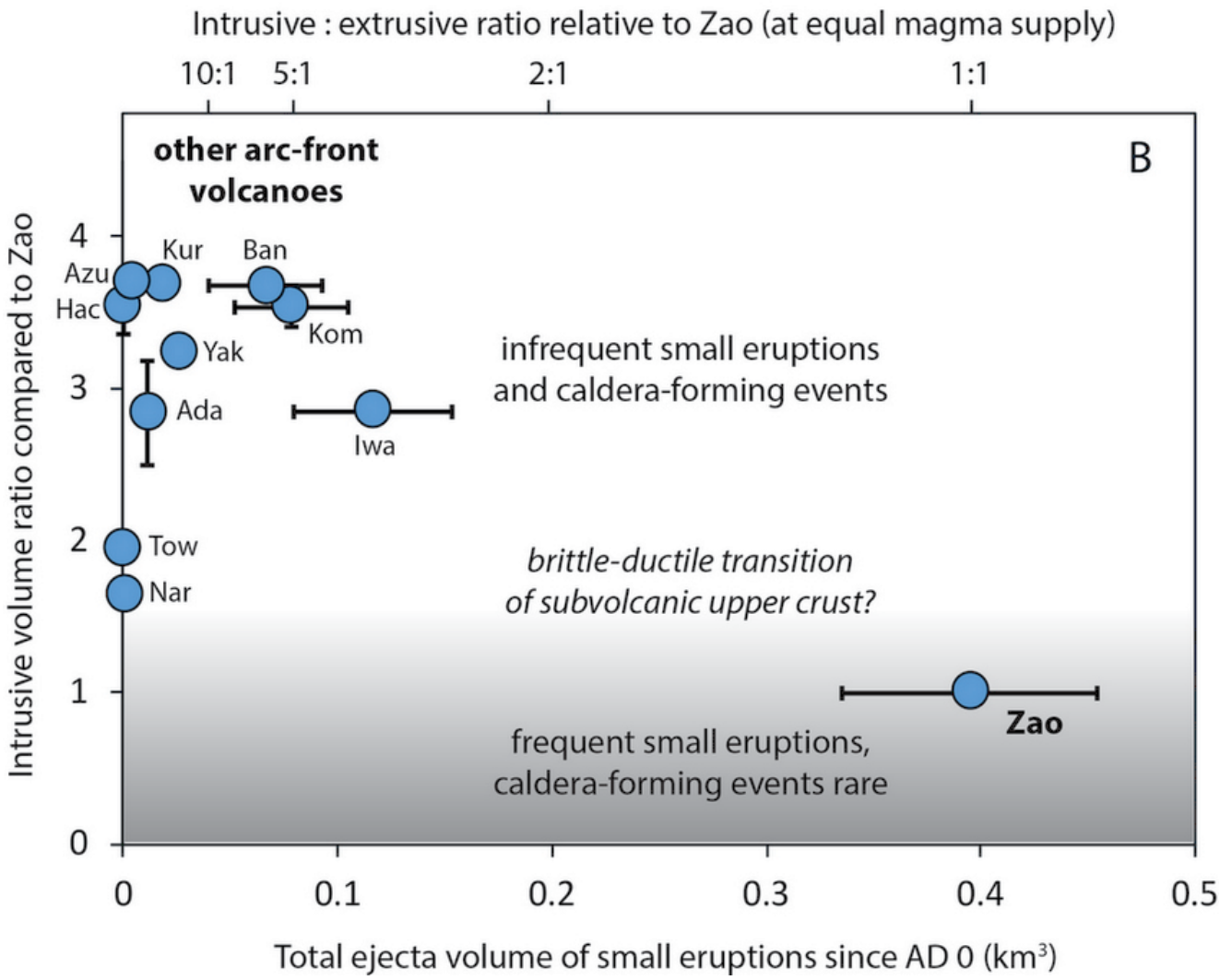
*Georg F Zellmer[1], Kai-Xun Chen[2], Yuancheng Gung[2], Ban-Yuan Kuo[3], Takeyoshi Yoshida[4]

1. Massey University, Palmerston North, New Zealand, 2. National Taiwan University, Taipei, Taiwan, 3. Academia Sinica, Taipei, Taiwan, 4. Tohoku University, Sendai, Japan

Subduction zone magmatic budgets and crustal growth processes depend on poorly constrained intrusive : extrusive ratios of arc magmas. Published ambient noise tomography data from northeast Japan reveal upper crustal low-V_S bodies, indicating elevated temperatures of plutonic rocks, beneath most sites of active arc-front volcanoes, with the exception of Zao volcano. Strikingly, when small eruptions (VEI 1 to VEI 3) from arc-front volcanoes in the last 2 kyr are considered, Zao has erupted most frequently and has produced a more than three times greater tephra volume than any of the other volcanoes. We propose that the frequent low-volume volcanism at Zao is fed by dikes that traverse the crustal section rapidly, fracturing through brittle lithologies. Beneath the other volcanoes, hotter and more ductile plutonic bodies have developed through repeated intrusive activity, hindering magma transport to the surface. This positive feedback mechanism ultimately results in cataclysmic caldera-forming events. We show that the number of late Cenozoic calderas is higher above the imaged low-V_S crust, consistent with this interpretation. We propose that generation of plutonic bodies is facilitated by volcaniclastic materials buried in a Miocene rift graben, which dampen fracture propagation and promote repeated sill intrusion. In contrast, transcurrent faulting has moved cold Cretaceous basement of the fore-arc range into the arc-front beneath Zao. These brittle rocks instead provide fracture pathways explored by magmas rapidly rising to the surface. The combined data imply that millions of years of crustal growth and tectonic history have a direct control on present-day volcanic eruption style.

Keywords: heat incubation, crustal magma ascent, crustal growth history, volcanic eruption style, Tohoku volcanism, brittle-ductile transition

©2019. Japan Geoscience Union. All Right Reserved.



©2019. Japan Geoscience Union. All Right Reserved.

STRATIGRAPHY RENEWAL, MAGMA CHAMBER STRATIFICATION, AND CONDUIT PROCESS OF THE 1815 TAMBORA CALDERA FORMING ERUPTION

*Indranova Suhendro[1], Atsushi Toramaru[1], Yasuo Miyabuchi[2], Tomoharu Miyamoto[1]

1. Department of Earth and Planetary Sciences, Graduate School of Sciences, Kyushu University, Japan, 2. Faculty of Advanced Science and Technology, Kumamoto University, Kurokami 2-40-1, Chuo-ku, Kumamoto 860-8555, Japan

The 1815 eruption of Tambora volcano was initiated by two precursory Plinian falls and terminated by pyroclastic density current (PDC) deposits. Although the occurrence of fall deposits and pumice rich PDC has been well-described by previous researchers, we discover scoria rich PDC deposits. However, the presence and relationship of scoria rich PDC with another well-described 1815 eruption deposit has never been discussed in detail. Moreover, several aspects of the magma chamber and conduit dynamics are still poorly understood. In order to that, we conducted petrography by optical microscope, chemical anlyses by XRF, SEM-EDS, and FE-EPMA, and textural analyses of BND and MND. Systematic change in the phenocryst, vesicle, microlite, and chemical compositions also observed through the stratigraphic position. Plinian fall units are characterized by relatively low crystal abundance and small average phenocryst size (0.44 - 0.52 mm) with higher silica content (56.8-58.05 wt.% SiO_2). In contrast, PDC deposits are characterized by relatively higher crystal abundance and greater average phenocryst size (0.53 - 0.59 mm) with lower silica content (56.5-57.5 wt.% SiO_2). There is no evidence of magma mixing because no bimodal distribution in anorthite content and no reverse zoning pattern in plagioclase phenocryst. Large phenocrysts (>1 mm) have less variation than small phenocrysts (<1 mm) in chemistry. Core compositions of large phenocrysts are An_{70}-$_{90,}$ while those of small phenocrysts are An_{40}-$_{95}$. The correlation between crystal size, chemical composition, and stratigraphic position suggests that stratification of crystals and chemical compositions in the magma chamber was established prior to 1815 eruption. Juveniles from Plinian eruption are composed of higher BND and lower MND value, compared to juveniles from PDC. As a result, we explained negative correlation of BND and MND by the control of decompression rate (dP/dt). Namely, high decompression rate will induce high nucleation rate of bubble thus facilitate magma to ascent rapidly and limiting the growth of microlite. The increase of lithic population from precursory Plinian towards PDC can be regarded as vent-widening process. Therefore, the decrease of decompression rate accompanied by conduit widening during the early to later phase has shifted the eruption style, from buoyant Plinian column to PDC. Finally, rapid and voluminous magma withdrawal from the chamber has led to the formation of caldera.

Keywords: Tambora, caldera forming eruption, textural analyses, detailed stratigraphy, bubble number density, microlite number density

©2019. Japan Geoscience Union. All Right Reserved.

[E] 口頭発表 | セッション記号 S (固体地球科学)：S-CG 固体地球科学複合領域・一般

2019年5月30日(木) 9:00 ~ 10:30 | コンベンションホールA 2F

[S-CG48] Science of slow earthquakes: Toward unified understandings of whole earthquake process

コンビーナ:井出 哲(東京大学大学院理学系研究科地球惑星科学専攻)、廣瀬 仁(神戸大学都市安全研究センター)、氏家 恒太郎(筑波大学生命環境系)、波多野 恭弘(東京大学地震研究所)、座長:望月 公廣(東京大学地震研究所)、新井 隆太

Accumulating observational studies on various types of slow deformation events, such as tectonic tremors, very low frequency events, and slow slip events, portrays some universal characteristics in generally complex behavior, including interaction among events and influence by various outer loadings. Some of these phenomena seem to have causal relation with the occurrence of very large earthquakes. A unified understanding of these slow and fast earthquake processes requires an approach integrating geophysics, seismology, geodesy, geology, and non-equilibrium statistical physics. We welcome presentations based on, but not limited to, geophysical observation, data analysis, analytical theory, numerical simulation, field study, and laboratory experiments.

9:00 ~ 9:15

[SCG48-17] Three-dimensional seismic structure of the shallow plate boundary in the northern Hikurangi margin from NZ3D OBS data

*新井 隆太[1]、小平 秀一[1]、Kellett Richard[2]、Stucker Valerie[2]、Bassett Dan[2]、Henrys Stuart[2]、尾鼻 浩一郎[1]、Bangs Nathan[3]、Barker Dan[2]、Bell Rebecca[4]、望月 公廣[5]、藤江 剛[1]、三浦 誠一[1]、Fry Bill[2]、NZ3D team (1.国立研究開発法人海洋研究開発機構、2.GNS Science、3.University of Texas Institute for Geophysics、4.Imperial College London、5.東京大学地震研究所)

9:15 ~ 9:45

[SCG48-18] **Using earthquake focal mechanisms to investigate slow slip driving forces in the northern Hikurangi**

★Invited Papers

*Emily Warren-Smith[1]、Bill Fry[1]、Laura Wallace[1] (1.GNS Science)

9:45 ~ 10:00

[SCG48-19] 広帯域レシーバ関数が示す南海トラフ沈み込み帯スロー地震発生域の地震学的構造変化

*佐脇 泰典[1]、伊藤 喜宏[2]、太田 和晃[2]、澁谷 拓郎[2]、岩田 知孝[2] (1.京都大学大学院理学研究科、2.京都大学防災研究所)

10:00 ~ 10:15

[SCG48-20] Slip tendency maps for compressional and extensional stress states on a shallow decollement in Nankai Trough

*橋本 善孝[1]、佐藤 茂行[1]、グレゴリー ムーア[2]、木下 正高[3]、木村 学[4]、宮川 歩夢[5]、白石 和也[6]、山田 泰広[6] (1.高知大学、2.ハワイ大学、3.東京大学、4.東京海洋大学、5.産業技術総合研究所、6.海洋研究開発機構)

10:15 ~ 10:30

[SCG48-21] Permeability and its anisotropy on creeping Chihshang Fault, Taiwan

*Tyas Dwi Aprilniadi[1]、Wen-Jie Wu[1]、Li-Wei Kuo[1]、Jian-Cheng Lee[2]、Jia-Jyun Dong[3] (1.Department of Earth Sciences, National Central University、2.Institute of Earth Sciences, Academia Sinica、3.Graduate Institute of Applied Geology, National Central University)

Three-dimensional seismic structure of the shallow plate boundary in the northern Hikurangi margin from NZ3D OBS data

*新井 隆太[1]、小平 秀一[1]、Kellett Richard[2]、Stucker Valerie[2]、Bassett Dan[2]、Henrys Stuart[2]、尾鼻 浩一郎[1]、Bangs Nathan[3]、Barker Dan[2]、Bell Rebecca[4]、望月 公廣[5]、藤江 剛[1]、三浦 誠一[1]、Fry Bill[2]、NZ3D team
*Ryuta Arai[1], Shuichi Kodaira[1], Richard Kellett[2], Valerie Stucker[2], Dan Bassett[2], Stuart Henrys[2], Koichiro Obana[1], Nathan Bangs[3], Dan Barker[2], Rebecca Bell[4], Kimihiro Mochizuki[5], Gou Fujie[1], Seiichi Miura[1], Bill Fry[2], team NZ3D

1. 国立研究開発法人海洋研究開発機構、2. GNS Science、3. University of Texas Institute for Geophysics、4. Imperial College London、5. 東京大学地震研究所
1. Japan Agency for Marine-Earth Science and Technology, 2. GNS Science, 3. University of Texas Institute for Geophysics, 4. Imperial College London, 5. Earthquake Research Institute, University of Tokyo

Slow earthquakes occur around the seismogenic zones of the plate boundary faults and they have so far been largely studied on the deep portions of the plate interface based on land-based geophysical observations. On the other hand, recent marine studies reveal that shallow slow earthquakes at the up-dip portions of seismogenic zones are also common in subduction zones. These shallow slow earthquakes have been found to occur from near the trench to ~10 km depth of the plate interface and their genesis is thought to be closely linked to fluid pressures and effective stresses at the fault. However, primary controls on seismogenesis at these depths, such as fault structures and stratigraphic/hydrogeologic properties around the subduction megathrust faults, are highly complex in three dimensions and poorly understood.

In order to refine our understanding of structural characteristics regulating slow earthquakes occurring at shallow plate boundaries, we collected 3-D seismic refraction/wide-angle reflection data from offshore Gisborne at the northern Hikurangi subduction margin, New Zealand, as part of an international collaborative project, NZ3D. The dataset covers an area of 60 km x 14 km ranging from the northern Tuaheni landslide complex and the easterly forearc slope to the subduction trench and was recorded on 97 ocean bottom seismographs deployed with an average spacing of 2 km on 4 parallel lines with over 140,000 airgun sources. In the study area, shallow slow slip events and tectonic tremor have been well documented (Wallace et al., 2016; Todd et al., 2018). Previous 2-D seismic reflection studies also show that the subduction of large-scale seamounts facilitates the transport of fluid-rich sediments deep into the subduction zone and produces conditions of high fluid pressures along the plate interface and pathways for fluid migration into the overriding plate (Bell et al., 2010; Barker et al., 2018).

Using the very dense airgun-OBS data, we constructed a preliminary three-dimensional P-wave velocity structure model of the accretionary forearc and the plate boundary from first arrival tomography. The velocity images from over 250,000 first arrivals revealed a thick low-velocity (Vp < 5.0 km/s) volume along the plate interface down to a depth of at least ~10 km. This velocity structure may represent a thick subduction channel filled with fluid-rich sediments associated with seamount subduction.

キーワード：浅部プレート境界、ヒクランギ沈み込み帯、３次元地震波速度構造
Keywords: Shallow plate boundary, Hikurangi margin, 3-D seismic structure

©2019. Japan Geoscience Union. All Right Reserved.

Using earthquake focal mechanisms to investigate slow slip driving forces in the northern Hikurangi

*Emily Warren-Smith[1], Bill Fry[1], Laura Wallace[1]

1. GNS Science

Understanding the processes that drive slow slip events (SSEs) may assist in improving our understanding of the physics of both slow and fast earthquakes. Recent work has shown that the stress ratio, R, retrieved by focal mechanism inversion systematically decreases prior to SSEs in New Zealand's northern Hikurangi subduction zone, and subsequently increases during the evolution of each SSE. These R fluctuations are proposed to represent slow, precursory increases and fast concurrent decreases in fluid pressure within overpressured subducting oceanic crust during the SSE cycle.

These observations represent an exciting opportunity to improve forecasts of SSE occurrence via monitoring of R changes. Thus far, this cyclic behaviour has only been observed over a short time-period (9 months, 4 SSE cycles) when ocean-bottom seismographs were deployed.

Here we present the results of a waveform cross-correlation study that aims to extend the catalogue in time and reduce the magnitude of completeness for focal mechanisms of northern Hikurangi seismicity. This enables improved temporal coverage and statistical analysis of stress tensor changes across multiple SSE cycles. By using well constrained focal mechanisms of events recorded on >30 OBS and land stations as templates, we automatically assign correlation-derived relative polarities to waveforms and subsequently invert for focal mechanisms and R using many more earthquakes complete to a lower magnitude. This approach offers an important step towards accurate SSE forecasting and an improved understanding of the physical processes leading to slow rupture nucleation.

Keywords: slow slip, seismology, focal mechanisms, stress inversions, Hikurangi, fluid pressure

©2019. Japan Geoscience Union. All Right Reserved.

広帯域レシーバ関数が示す南海トラフ沈み込み帯スロー地震発生域の地震学的構造変化

Seismological structural changes around source regions of slow earthquakes in Nankai subduction zone inferred from broadband receiver functions

*佐脇 泰典[1]、伊藤 喜宏[2]、太田 和晃[2]、澁谷 拓郎[2]、岩田 知孝[2]
*Yasunori Sawaki[1], Yoshihiro Ito[2], Kazuaki Ohta[2], Takuo Shibutani[2], Tomotaka Iwata[2]

1. 京都大学大学院理学研究科、2. 京都大学防災研究所
1. Graduate School of Science, Kyoto University , 2. Disaster Prevention Research Institute, Kyoto University

Coupled phenomena of tremors accompanying short-term slow slip events and very low frequency earthquakes (Ito et al., 2007) have been detected at deeper parts of seismogenic regions on the Nankai Subduction Zone in southwestern Japan. Elucidating detailed seismological structures on plate interfaces hosting slow earthquakes is very important to understand mechanisms and relationships of slow earthquakes and megathrust earthquakes. Few studies, however, have proposed detailed velocity structure models and their spatio-temporal variations with high resolution receiver functions (RFs) on plate interfaces. In this study, we calculate broadband RFs around source regions with slow earthquake events in the Nankai Subduction Zone. We also investigate frequency dependency of RFs to constrain detailed physical features near the plate interface.

RF method is one of the best approaches to estimate the velocity structure beneath seismic stations by extracting P-to-S phases converted on velocity discontinuity from teleseismic waveforms. In southwestern Japan, Shiomi et al. (2008) confirmed the oceanic Moho discontinuity in the Philippine Sea Slab. In usual cases, high cut filter (e.g. 0.6Hz: Shiomi et al., 2008) is used when deconvoluting vertical component waveforms from horizontal ones in order to avoid instability on calculation. Akuhara et al. (2017) recently calculated high frequency RFs up to 4 Hz using ocean bottom seismometers equipped off the Kii peninsula, and confirmed the existence of a thin low velocity zone composed of a fluid-rich sediment layer along the Nankai trough megathrust fault. In this study, we calculate RFs applying the Extended-Time Multitaper method modified by Shibutani et al. (2008) and the frequency dependency of RFs is examined by taking different frequency ranges up to 0.5, 1, 2, 3 and 4 Hz.

We have used Hi-net and F-net seismograms provided by National Research Institute for Earth Science and Disaster Resilience in Japan. We confirm that spectra of teleseismic waveforms have sufficient SN ratios up to 3 or 4 Hz. Fig.1 shows an example of the RFs at NKTH located on the Kii peninsula. The RFs at most of the stations contain positive and negative phases around 3-4 s after P-wave arrival, which correspond to oceanic Moho discontinuity and the plate interface, respectively. The amplitude and the arrival time of these phases depend on backazimuth, suggesting that dependency on the incident angle of a ray to the subducting plate interface. In case of a downdip for the subducting slab, incoming P-waves have lower incident angles and generate smaller convert S-waves. On the contrary, an updip case, incoming P-waves have higher incident angles and generate larger convert S-waves.

At higher frequency RFs (Fig.1, right), the phases from the plate interface are generally sharper than those at lower frequency, whereas the phases corresponding to oceanic Moho seems to tend to be broader or split into several phases, suggesting that the oceanic Moho is not a simple velocity discontinuity but would consists of several layers. The split positive phase just after the negative phase from the plate interface may relate to the thin low velocity zone inferred from Akuhara et al. (2017).

©2019. Japan Geoscience Union. All Right Reserved.

キーワード：レシーバ関数、広帯域レシーバ関数、スロー地震、南海トラフ沈み込み帯
Keywords: Receiver function, Broadband receiver function, Slow earthquake, Nankai subduction zone

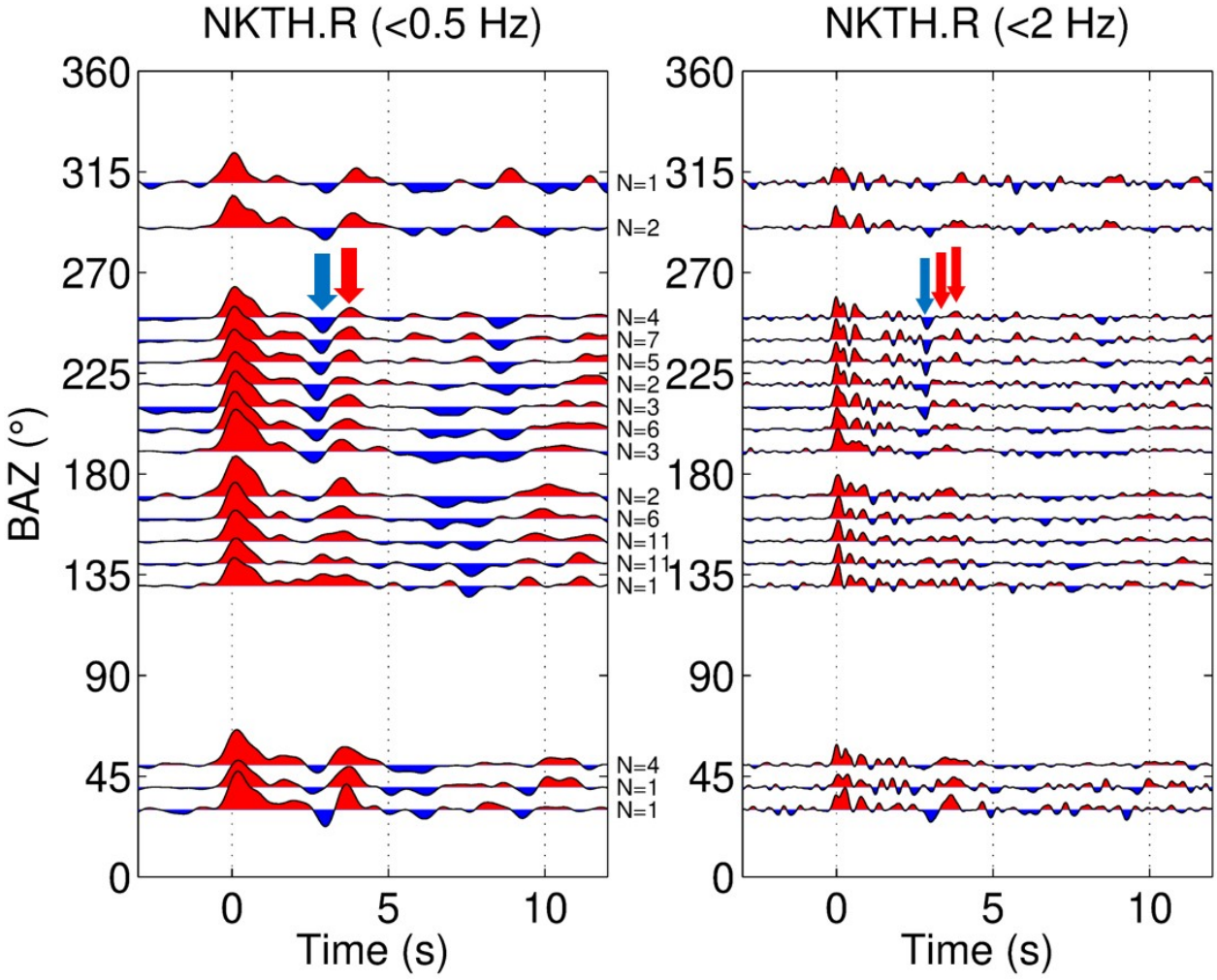


Fig. 1 Radial receiver functions (RFs) on NKTH with frequency ranges up to (left) 0.5 Hz and (right) 2 Hz. The vertical and horizontal axes denote delay time from P-wave arrival [s] and backazimuth [degree], respectively. Areas colored in red and blue show the positive and negative amplitudes, respectively. N is the number of RFs stacked every 10 degrees. Red and blue arrows indicate later phases from the oceanic Moho and the plate interface, respectively.

©2019. Japan Geoscience Union. All Right Reserved.

Slip tendency maps for compressional and extensional stress states on a shallow decollement in Nankai Trough

*橋本 善孝[1]、佐藤 茂行[1]、グレゴリー ムーア[2]、木下 正高[3]、木村 学[4]、宮川 歩夢[5]、白石 和也[6]、山田 泰広[6]
*Yoshitaka Hashimoto[1], Shigeyuki Sato[1], Gregory F Moore[2], Masataka Kinoshita[3], Gaku Kimura[4], Ayumu Miyakawa[5], Kazuya Shiraishi[6], Yasuhiro Yamada[6]

1. 高知大学、2. ハワイ大学、3. 東京大学、4. 東京海洋大学、5. 産業技術総合研究所、6. 海洋研究開発機構
1. Kochi University, 2. University of Hawaii, 3. University of Tokyo, 4. Tokyo University of Marine Science and Technology, 5. AIST, 6. JAMSTEC

Stress state along a subduction plate interface is one of important controls for wedge architectures, fault activations and seismogenic behaviors. In a shallow portion of a subduction plate interface, a large displacement along decollement could be expected for tsunamigenic events (Fujiwara et al., 2012) as well as slow earthquakes such as very low frequency earthquakes and slow slips have been observed (Araki et al., 2017, Nakano et al., 2018). Paleo-stress state has been estimated using micro-fault inversion method from exhumed accretionary complexes and oceanic accretionary wedges, which shows the stress state changes between compression and extension states with almost horizontal and vertical principal stress axes. The stress change could be related to seismic cycle.

In this study, we examined geographical features of a shallow decollement using 3D seismic profiles and mapped slip tendencies on the decollement with compressional and extensional stress state to discuss an effect of distribution of slip tendency on the fault slip behaviors. Slip tendency is a shear stress ratio to normal stress on a fault surface when a regional stress state is applied on a fault surface.

The target transect of the 3D seismic profiles is located at the Nankai Trough off Kii Peninsula, SW Japan where Philippine Sea Plate subducted into Eurasian Plate, and IODP NantroSEIZE project has been operated. The 3D seismic profiles had been reprocessed to make reflectors clear using an updated technology. We traced the shallow decollement to make geographic features (3D surface) by Petrel. We analyzed dip angle and dip azimuth for 50 m mesh of the surface. The characteristics of geographic features of the shallow decollement are 1) almost horizontal with dip angle ranging 5-15, 2) dip azimuth directing 300-350˚ (NW-NWN) in average. In addition, some narrow zones with dip azimuth directing 50-150˚ (SE-SES) are identified, which shows a relatively high frequency reliefs striking NE-SW direction. Some of these are related to the geography of oceanic basement.

Compressional and extensional stress states were applied on the surface to examine a change in slip tendency with change in stress state. We assumed that compressional one has (150, 0) sigma 1 and (90, 90) sigma 3 and others has (150, 0) sigma 3 and (90, 90) sigma 1. The 0.6 of friction coefficient was assumed as the maximum value. We calculated differential stresses for compressional and extensional stress states to make a plane with idealized attitude to applied stress state reactivated. This assumption implies that the estimated slip tendency is the maximum value.

Resulted slip tendency represents a strong relationship with geomorphic features. In compressional stress state, large slip tendency (0.4-0.5) distributes on the surface with dip azimuth directing 300-350˚ whereas small slip tendency (0.1-0.2) corresponds to the surface with dip azimuth directing 50-150˚. In extensional stress state, the similar distribution with that in compressional stress state is identified but the

©2019. Japan Geoscience Union. All Right Reserved.

difference between the dip azimuths is very small; slip tendency ranges 0.1-0.2. The differences between slip tendencies in compressional and extensional stress states is almost similar to that for compressional stress state because slip tendency for extensional stress state is almost 0.1-0.2.

If we take the difference in slip tendency as a kind of stress drop, relatively small stress drop are observed on the surface with dip azimuth directing 50-150˚, which is distributed in NE-SW zones. Nakano et al. (2018) found that VLFs in the region migrates toward NE, which is consistent with the directions of zones with stress drop is small. The area for VLFEs could be limited in these zones where the slip tendency is small both in compressional and extensional stress states, implying that the material with very low friction coefficient and/or high pore fluid pressure are expected to make a plane reactivated with small slip tendency.

キーワード：スリップテンデンシー、地震サイクル、南海トラフ、超低周波地震
Keywords: Slip tendency, seismic cycle, Nankai Trough, very low frequency earthquake

©2019. Japan Geoscience Union. All Right Reserved.

Permeability and its anisotropy on creeping Chihshang Fault, Taiwan

*Tyas Dwi Aprilniadi[1], Wen-Jie Wu[1], Li-Wei Kuo[1], Jian-Cheng Lee[2], Jia-Jyun Dong[3]

1. Department of Earth Sciences, National Central University, 2. Institute of Earth Sciences, Academia Sinica, 3. Graduate Institute of Applied Geology, National Central University

The Chihshang Fault in eastern Taiwan is a 20-km-long segment of the Longitudinal Valley Fault that a plate-suture boundary fault between the Eurasian continental margin and the Philippine Sea Plate has fastest shallow creep in the world and infrequently occurs earthquakes (Magnitude greater than 6). Here we performed permeability measurements on Lichi Mélange and conglomerate with an intra-vessel oil pressure apparatus (YOKO2) at room temperature at isotropic confining pressure, using helium as pore fluid. We made samples, with dip and normal direction of fault, from retrieved rock cores in WAN-2 borehole and attempted to build the permeability structure across creeping Chihshang Fault. Generally, intrinsic permeabilities of Lichi Mélange were lower than that of conglomerate and intrinsic permeabilities in dip direction were higher than that in normal direction. But the permeability differed in rock type and was associated with shear structures that fault zone architecture is not typical as simple mode suggested by Caine et al. (1996). The results show Lichi Mélange was a natural aquifuge blocking the fluid flow that may be responsible for fluid-rock interaction and seasonal fluctuation on creeping Chihshang Fault. The heterogeneous Lichi Mélange has complicated composition as other Mélange that the microstructural observation would be conducted for investigating the relationship between microstructures and permeability in creeping Chihshang Fault. Taking microstructures, permeability anisotropy and the fault zone architecture into consideration, we may depict the permeability structures of Chihshang Fault and further provide the information of matrix permeability for hydraulic properties in the field.

Keywords: creeping Chihshang Fault, Lichi Mélange, permeability anisotropy

©2019. Japan Geoscience Union. All Right Reserved.

[E] 口頭発表 | セッション記号 S (固体地球科学)：S-CG 固体地球科学複合領域・一般

2019年5月30日(木) 10:45 ~ 12:15 | コンベンションホールA 2F

[S-CG48] Science of slow earthquakes: Toward unified understandings of whole earthquake process

コンビーナ:井出 哲(東京大学大学院理学系研究科地球惑星科学専攻)、廣瀬 仁(神戸大学都市安全研究センター)、氏家 恒太郎(筑波大学生命環境系)、波多野 恭弘(東京大学地震研究所)、座長:氏家 恒太郎(筑波大学生命環境系)、ウォリス サイモン(Nagoya University)

Accumulating observational studies on various types of slow deformation events, such as tectonic tremors, very low frequency events, and slow slip events, portrays some universal characteristics in generally complex behavior, including interaction among events and influence by various outer loadings. Some of these phenomena seem to have causal relation with the occurrence of very large earthquakes. A unified understanding of these slow and fast earthquake processes requires an approach integrating geophysics, seismology, geodesy, geology, and non-equilibrium statistical physics. We welcome presentations based on, but not limited to, geophysical observation, data analysis, analytical theory, numerical simulation, field study, and laboratory experiments.

10:45 ~ 11:00

[SCG48-22] Short fluid infiltration events in the low permeable metamorphic rocks triggered by crustal fracturing at amphibolite–granulite facies conditions

*Diana Mindaleva[1]、Masaoki Uno[1]、Fumiko Higashino[1]、Atsushi Okamoto[1]、Noriyoshi Tsuchiya[1] (1.Graduate school of environmental studies, Tohoku University)

11:00 ~ 11:15

[SCG48-23] Generation of high fluid pressure at the base of the shallow mantle wedge—evidence from serpentinite of the Sanbagawa belt, SW Japan

*ウォリス サイモン[1]、纐纈 佑衣[2]、横田 麻莉[1,2] (1.東京大学、2.名古屋大学)

11:15 ~ 11:30

[SCG48-24] **Overpressured subduction plate boundary caused by infiltration of mantle-derived fluids: Evidence from helium isotope analysis on veins in subduction mélange**

*西山 直毅[1]、氏家 恒太郎[1]、角野 浩史[2] (1.筑波大学　生命環境系、2.東京大学)

11:30 ~ 11:45

[SCG48-25] **Geological and rheological conditions of subduction plate boundary between the seismogenic zone and the ETS zone in warm-slab environments**

*氏家 恒太郎[1]、野呂 和也[1]、重松 紀生[2]、Fagereng Ake[3]、西山 直毅[1]、Tulley Christopher[3]、増山 春菜[1]、森 康[4] (1.筑波大学生命環境系、2.産業技術総合研究所活断層・火山研究部門、3.カーディフ大学、4.北九州市立自然史・歴史博物館)

11:45 ~ 12:00

[SCG48-26] Temperature variation in tectonic mélanges of the Shimanto Belt, SW Japan

*Tsai-Wei Chen[1]、Donald M Fisher[1]、Andrew J Smye[1]、Yoshitaka Hashimoto[2] (1.Penn State Univ.、2.Kochi Univ.)

12:00 ~ 12:15

[SCG48-27] Frictional properties of opal gouge at low-temperature hydrothermal conditions and their implications for seismogenic faulting along subduction-zone megathrusts

*金川 久一[1]、中西 智哉[2]、桑名 盛人[3]、澤井 みち代[1]、廣瀬 丈洋[4] (1.千葉大学理学研究院、2.千葉大学大学院融合理工学府、3.千葉大学理学部、4.海洋研究開発機構高知コア研究所)

Short fluid infiltration events in the low permeable metamorphic rocks triggered by crustal fracturing at amphibolite–granulite facies conditions

*Diana Mindaleva[1], Masaoki Uno[1], Fumiko Higashino[1], Atsushi Okamoto[1], Noriyoshi Tsuchiya[1]

1. Graduate school of environmental studies, Tohoku University

Aqueous fluids flow could be responsible for changing hydrologic and thermodynamic properties of rocks. It is generally accepted that fluids play a key role in the generation of earthquakes, tremors, and slow slip events. For example, it was suggested that tremors are related to fluids released during dehydration processes in the subduction slab (e.g., Abers et al., 2009; Katsumata and Kamaya, 2003; Obara et al., 2004). Hydrous minerals in subducting slabs release H_2O due to dehydration reactions. Released water increases fluid pressure rapidly. However, fluid pressure gradients within the crust remain poorly constrained due to their heterogeneity. Therefore, it is important to constrain timescales of fluid infiltration to understand fluid pressure gradient, permeability, and tectonic evolution.

We have investigated fluid-rock reaction zones in mafic granulite and amphibolite samples from Mefjell, south-central part of the Sør Rondane Mountains (SRM), East Antarctica, and constrained pressure gradient and permeability. Mafic granulite and amphibolite samples are cut by numerous randomly-oriented veins. Samples are partially hydrated along veins associated with mm-scale hydration reactions zones. Reaction zones fingerprint relationship between fluid infiltration and rock response. We divide samples into several reaction zones increasing distance from the vein center by modal amount of minerals, reaction textures, and trace elements concentrations distributions profiles in apatite. The P-T conditions for the fluid infiltration in mafic granulite were estimated to be 0.65 GPa, 650˚C , and that for peak P-T conditions were 850˚C, 0.55-1.0 GPa. On the other hand, P-T conditions for the fluid infiltration in amphibolite were estimated to be around 500˚C.

Trace elements concentrations (Cl, Sr, and some REE) measured by EPMA and LA-ICP-MS in several apatite grains were gradually decreasing with distance from the vein. Cl distributions profiles were analyzed by a reactive-transport model to define transport mechanism by fitting to Peclet number (Pe#=vL/D, where v is pore velocity, L is length of reaction zone, D is self-diffusion coefficient) and time-scales of fluid infiltration. For mafic granulite Pe# is 0.025, for amphibolite is 90. Whereas diffusion transport is revealed to be dominant for mafic granulite, advection transport is likely for amphibolite. Duration of fluid infiltration was estimated to be 5.5 h for mafic granulite and 1-3 h for amphibolite, which is very short in geological timescales. This suggests rapid and intense fluid flux through the mantle wedge and onto overlying crust. Short timescales of fluid infiltration may reflect linkage to the seismic events.

To estimate permeability, the pressure gradient for the reaction zones was calculated from the water and other elements activities constrained by pseudosection analysis for different reaction zones. Bulk compositions at each reaction zone were used to create pseudosections. Permeability was calculated from the estimated pressure gradient and total flux $q=-\kappa(\partial P/\partial x)/\eta$, where q is total flux, k is permeability, η is viscosity, and $(\partial P/\partial x)$ is pressure gradient. Results suggest low and contrasting permeability between mafic granulite dominated by diffusion and amphibolite dominated by advection mass transport mechanisms. This difference may be explained by different P-T conditions for fluid infiltration and heterogeneity of the pressure gradients. Therefore, it suggest that fluid infiltration in low

©2019. Japan Geoscience Union. All Right Reserved.

permeable rocks caused fracturing and formed narrow reaction zones, which released fluid pressure in a short time. Above results of our study suggest importance of fluid transport phenomena in relation to the evolution of rocks hydrological properties.

Abers G. A. et al. Geology 37.12 (2009): 1119-1122.

Katsumata A., Kamaya N. Geophysical Research Letters 30.1 (2003): 20-1.

Obara K. et al. Geophysical Research Letters 31.23 (2004).

Keywords: Pressure gradient, Permeability, Water-rock interaction

©2019. Japan Geoscience Union. All Right Reserved.

Generation of high fluid pressure at the base of the shallow mantle wedge—evidence from serpentinite of the Sanbagawa belt, SW Japan

*ウォリス サイモン[1]、纐纈 佑衣[2]、横田 麻莉[1,2]
*Simon Richard Wallis[1], Yui Kouketsu[2], Mari Yokota[1,2]

1. 東京大学、2. 名古屋大学
1. University of Tokyo, 2. Nagoya University

Serpentinite units derived from the mantle wedge in the Sanbagawa subduction-type metamorphic belt record interaction between the shallow mantle-wedge and the flow of SiO2-bearing fluids at two different depths in the paleo subduction zone. The mineralogy and geochemistry of two units indicate there was a major increase in the fluid flow perpendicular to the subduction boundary with decreasing pressure. The rate of flow can be related to the presence or absence of a thick shear zone. Estimates of fluid flux from subducted slabs combined with experimentally determined permeability of serpentinite suggests that the presence of a zone of gently dipping strongly foliated serpentinite is a key component of developing high fluid pressures at depths of 30–50 km in subduction zones—a key requirement for the development of slow earthquakes. Most of the SiO2 in these subduction fluids will be absorbed in the serpentinite and is unlikely to be available for precipitation and formation of an impermeable cap at higher levels in the system.

キーワード：流体圧、深部スロー地震、蛇紋岩、三波川帯
Keywords: Fluid pressure, Deep slow earthquakes, Serpentinite, Sanbagawa belt

©2019. Japan Geoscience Union. All Right Reserved.

Overpressured subduction plate boundary caused by infiltration of mantle-derived fluids: Evidence from helium isotope analysis on veins in subduction mélange

*西山 直毅[1]、氏家 恒太郎[1]、角野 浩史[2]
*Naoki Nishiyama[1], Kohtaro Ujiie[1], Hirochika Sumino[2]

1. 筑波大学　生命環境系、2. 東京大学
1. University of Tsukuba, 2. The University of Tokyo

Fluid overpressures have been invoked as one of the key factors controlling slow earthquakes in subduction zones. The generation of fluid overpressures has been thought to occur by in-situ processes such as compaction disequilibrium and mineral dehydration in sediment and oceanic crust. To determine the origin of fluid responsible for overpressured subduction plate boundary, we examined noble gas and microthermometric analyses on quartz-calcite veins in the subduction mélange deformed at ~10–15 km depth.
The analyzed veins are sigmoidal extension vein arrays and shear veins. The former represents Riedel shear zones formed during subduction under vertical σ_1. The latter records the numerous low-angle brittle thrusting at very small shear strength with recurrence time comparable to that of slow earthquakes, which could account for the generation of tectonic tremors [1]. Homogenization and ice melting temperatures of fluid inclusions indicate that the both types of veins recorded the fluids with salinity of 3–7 wt% and near-lithostatic fluid pressures at 10–15 km depth. The measured $^3He/^4He$ range 1.6–2.5 Ra (Ra is the $^3He/^4He$ of air) regardless of types of veins, indicating the presence of mantle helium. The ratios of non-radiogenic heavy noble gas isotopes (^{36}Ar, ^{84}Kr, and ^{130}Xe) are similar to those of seawater and serpentinite in slab mantle [2]. Because porosity in sediments already decreased to <1 % at depths of 4–5 km [3], seawater captured in the pores would be completely expelled from the subducting sediments before reaching to 10–15 km depth, and thus the serpentinized slab mantle is the likely origin of the ^{36}Ar, ^{84}Kr, and ^{130}Xe. The measured $^3He/^4He$, non-radiogenic heavy noble gas ratios, and salinity are consistent with those of slab-derived fluids observed in mantle wedge peridotites from subduction zones [4, 5], suggesting that fluids released from subducted serpentinite to the mantle wedge migrate toward shallow depths along subduction boundary. From a mixing calculation using ^{36}Ar, ^{84}Kr, and ^{130}Xe data, more than 64% of vein-forming fluids were originated from the subducted serpentinite. Therefore, the migration of mantle-derived fluids has a potential to induce brittle failures in plate boundaries via increasing fluid pressures.

[1] Ujiie *et al.* (2018) *Geophys. Res. Lett.* **45**, 5371–5379. [2] Kendrick *et al.* (2013) *Earth Planet. Sci. Lett.* **365**, 86–96. [3] Kato *et al.* (2004) *Geophys. Res. Lett.* **31**, L06602. [4] Sumino *et al.* (2010) *Earth Planet. Sci. Lett.* **294**, 163–172. [5] Kobayashi *et al.* (2017) *Earth Planet. Sci. Lett.* **457**, 106–116.

キーワード：過剰間隙圧、マントル由来流体、ヘリウム同位体、鉱物脈
Keywords: Fluid overpressure, Mantle-derived fluids, Helium isotopes, Crack-seal vein

©2019. Japan Geoscience Union. All Right Reserved.

Geological and rheological conditions of subduction plate boundary between the seismogenic zone and the ETS zone in warm-slab environments

*氏家 恒太郎[1]、野呂 和也[1]、重松 紀生[2]、Fagereng Ake[3]、西山 直毅[1]、Tulley Christopher[3]、増山 春菜[1]、森 康[4]
*Kohtaro Ujiie[1], Kazuya Noro[1], Norio Shigematsu[2], Ake Fagereng[3], Naoki Nishiyama[1], Christopher Tulley[3], Haruna MASUYAMA[1], Yasushi Mori[4]

1. 筑波大学生命環境系、2. 産業技術総合研究所活断層・火山研究部門、3. カーディフ大学、4. 北九州市立自然史・歴史博物館
1. Graduate School of Life and Environmental Sciences, University of Tsukuba, 2. Research Institute of Earthquake and Volcano Geology, National Institute of Advanced Industrial Science and Technology, Japan, 3. Cardiff University, 4. Kitakyushu Museum of Natural History and Human History

In subduction zones particularly under warm-slab environments, the transition zone between the locked seismogenic zone and the deeper, stably sliding zone is the site of slow earthquakes such as episodic tremor and slip (ETS) and long-term slow slip events (L-SSEs). Exhumed subduction mélanges on Kyushu Island, Japan, were deformed at depths of ~15–30 km and temperatures of ~370–500 ˚C under warm-slab environments and thus provide an invaluable opportunity to examine geological and rheological conditions that may responsible for slow earthquakes. The mélanges record low-angle thrust sense, viscous shear associated with metasomatic reactions. The metasomatism is caused by the infiltration of sodium-bearing fluid between pelitic schist and mafic to ultramafic rocks, resulting in albitization of pelitic schist. Microstructural observations and electron backscatter diffraction analysis show that viscous shear was accommodated by dislocation creep, mechanical rotation, and possible diffusion creep, resulting in dynamic recrystallization of quartz, strong shape and crystal preferred orientations of actinolite and chlorite, and random orientation of albite, respectively. Strain rate of viscous shear zones, estimated from the recrystallized grain size piezometer and flow law for quartz, increases with depth from ~$10^{-13}s^{-1}$to ~$10^{-10}s^{-1}$. The upper value of strain rate is consistent with the strain rate of L-SSEs in subduction zones, when the thickness of viscous shear zone is orders of 10–100 m, compatible with our field observation. Lattice-preferred orientation patterns of quartz c-axes also changes with depth from Type I crossed girdle to c-axis maximum subparallel to shear direction, showing a shear sense consistent with low-angle thrust faulting. Albitized pelitic schist formed by metasomatic reactions and associated viscous shear zones are absent in the mélange deformed at temperatures less than ~330 ˚C. In total, viscous shear associated with metasomatic reactions may account for strain rate, kinematics, and lower limit temperature of L-SSEs zone.

キーワード：テクトニックメランジュ、交代変成作用、粘性剪断
Keywords: subduction mélange, metasomatism, viscous shear

©2019. Japan Geoscience Union. All Right Reserved.

Temperature variation in tectonic mélanges of the Shimanto Belt, SW Japan

*Tsai-Wei Chen[1], Donald M Fisher[1], Andrew J Smye[1], Yoshitaka Hashimoto[2]

1. Penn State Univ., 2. Kochi Univ.

Silica redistribution along plate interfaces is a fault zone aging process likely to affect the slip behavior of subduction interfaces. Numerical modeling for slip according to the rate law based on silica kinetics reproduces the characteristics of real-world subduction zones, such as an updip limit to the seismogenic zone, earthquake clustering, and a power-law size distribution of earthquake magnitudes. In the field, the structure of subduction fault zones is typically marked by veined sandstone blocks within mudstones with scaly fabric, with mudstones providing a local source of silica and other elements that precipitate as minerals veins, which act as a sink for mobile elements. The silica kinetics related to diffusion from shearing mudstones to cracking sandstone blocks in mélange provides a temperature dependent mechanism for fault zone aging whereby the contact area across the fault zone increases in the time between slip instabilities. In the Shimanto belt of Japan, scaly fabric and vein microstructures show textural variability as a function of temperature. There is a gradient in the age of paleosubducting oceanic crust from north to south within the inner Shimanto belt, from the Yokonami mélange, with a thick pelagic chert section and older basalt and younger mélanges in the south (Okitsu, Hyuga, and Mugi) with little or no chert section, suggesting younger subducting crust. Thus, the mélanges of the Shimanto belt were accreted at different temperatures and depths along the interface, and there also may have been differences in the subduction geotherm. We suggest that these variations in temperature are likely to lead to different silica kinetics and rates of mineral redistribution, recorded in microstructural variations that may reflect different frictional properties along the plate interface. The slip behavior of the plate interface depends on temperature as evidenced by down dip variations in slip mode and differences in earthquake size distributions for subduction zones with different age crust. We therefore have undertaken a study of oxygen isotope thermometry using coexisting mineral pairs of quartz-albite-calcite observed in the tectonic mélanges from the Shimanto belt at a variety of estimated temperatures. This data provides an independent method for evaluating the temperature during mineral redistribution that can be compared with current estimates based on vitrinite reflectance and fluid inclusion analyses.

Keywords: Subduction zone processes, Shimanto Belt , Silica redistribution, Oxygen isotope thermometry

©2019. Japan Geoscience Union. All Right Reserved.

Frictional properties of opal gouge at low-temperature hydrothermal conditions and their implications for seismogenic faulting along subduction-zone megathrusts

*金川 久一[1]、中西 智哉[2]、桑名 盛人[3]、澤井 みち代[1]、廣瀬 丈洋[4]
*Kyuichi Kanagawa[1], Tomoya Nakanishi[2], Morito Kuwana[3], Michiyo Sawai[1], Takehiro Hirose[4]

1. 千葉大学理学研究院、2. 千葉大学大学院融合理工学府、3. 千葉大学理学部、4. 海洋研究開発機構高知コア研究所
1. School of Science, Chiba University, 2. Graduate School of Science and Engineering, Chiba University, 3. Faculty of Science, Chiba University, 4. Kochi Institute for Core Sample Research, Japan Agency for Marine-Earth Science and Technology

We conducted a series of triaxial friction experiments on opal gouge at low-temperature (≦200˚C) hydrothermal conditions, in order to address the change in frictional stability along subduction-zone megathrusts. The results revealed frictional properties of opal gouge dependent on temperature (*T*), displacement (*V*) or pore water presure (P_p), as described below.

When fitted by the rate- and state-friction constitutive law, friction parameter *a* does not change much with *T*, *V* or P_p, while friction parameter *b* increases, and resultantly (*a* −*b*) value decreases with increasing *T*, decreasing *V* or increasing P_p. Microstructural observations revealed that densification and coalescence of gouge particles occurred at higher *T*, suggesting the operation of pressure solution. Thus increasing activity of thermally activated pressure solution with increasing *T*, decreasing *V* or increasing P_p promotes gouge lithification to increase frictional strength, by which (*a* −*b*) value decreases to <0, and thereby the transition from aseismic faulting to seismic faulting along subduction-zone megathrusts. Our results also imply that increasing P_p at that transition region where (*a* −*b*) ≈0 would decrease (*a* −*b*) value to <0, and hence promote slow seismic faulting with small negative (*a* −*b*) values, which is consistent with high V_P/V_S ratios observed in the regions of slow earthquakes.

キーワード：摩擦特性、オパールガウジ、低温熱水条件
Keywords: frictional properties, opal gouge, low-temperature hydrothermal conditions

©2019. Japan Geoscience Union. All Right Reserved.

[E] 口頭発表 | セッション記号 S (固体地球科学)：S-CG 固体地球科学複合領域・一般

2019年5月30日(木) 13:45 ~ 15:15 | コンベンションホールA 2F

[S-CG48] Science of slow earthquakes: Toward unified understandings of whole earthquake process

コンビーナ:井出 哲(東京大学大学院理学系研究科地球惑星科学専攻)、廣瀬 仁(神戸大学都市安全研究センター)、氏家 恒太郎(筑波大学生命環境系)、波多野 恭弘(東京大学地震研究所)、座長:波多野 恭弘、鈴木 岳人

Accumulating observational studies on various types of slow deformation events, such as tectonic tremors, very low frequency events, and slow slip events, portrays some universal characteristics in generally complex behavior, including interaction among events and influence by various outer loadings. Some of these phenomena seem to have causal relation with the occurrence of very large earthquakes. A unified understanding of these slow and fast earthquake processes requires an approach integrating geophysics, seismology, geodesy, geology, and non-equilibrium statistical physics. We welcome presentations based on, but not limited to, geophysical observation, data analysis, analytical theory, numerical simulation, field study, and laboratory experiments.

13:45 ~ 14:00

[SCG48-28] **Rate and State Dependent Friction Law and Static Friction Force**

*松川 宏[1] (1.青山学院大学)

14:00 ~ 14:30

[SCG48-29] **Stable sliding, slow and silent slip events and laboratory earthquakes across the brittle ductile transition**

★Invited Papers

*Alexandre Schubnel[1]、Aubry Jérôme[1]、François Passelègue[2] (1.Laboratoire de Géologie, ENS, PARIS, France、2.EPFL, Switzerland)

14:30 ~ 14:45

[SCG48-30] Dramatic velocity weakening of dry quartz friction at relatively slow slip velocities

*堤 昭人[1]、飯田 大貴[2]、 尾上 裕子[1] (1.京都大学大学院理学研究科、2.地熱エンジニアリング（株）)

14:45 ~ 15:00

[SCG48-31] ゲルの摩擦実験における微動とゆっくりすべりを伴う破壊核形成過程

*山口 哲生[1] (1.九州大学)

15:00 ~ 15:15

[SCG48-32] 多孔質媒質中の乱流におけるk-εモデルの解軌道

*鈴木 岳人[1] (1.青山学院大学理工学部物理・数理学科)

Rate and State Dependent Friction Law and Static Friction Force

*松川 宏[1]
*Hiroshi Matsukawa [1]

1. 青山学院大学
1. Aoyama Gakuin University

It is well known that the Rate and State Dependent Friction Law (RSF) plays an important role in the study of earthquake including slow-earthquake [1, 2]. RSF was introduced by Dietrich [3] and Ruina [4] based on the laboratory experiments and describes the sliding velocity and state-variable dependences of the friction coefficient. The dependences are analyzed by the thermal activation process of the deformation and detachment of actual contact points [5-7]. The thermal activation of the deformation of actual contact points, which is called the indirect process, cause the increase of the actual contact area and then the friction force with increasing contact time of actual contact point, which is inversely proportional to the sliding velocity. The thermal activation of the detachment of actual contact points, which is called the direct process, cause the increase of the friction force with increasing sliding velocity. Such analysis discuss the change of friction coefficient depending on the sliding velocity and state-variable. Here we extend the analysis and discuss the absolute value of the friction coefficient. In the case that the direct process overwhelm the indirect process, the friction coefficient can vanish in the limit of vanishing sliding velocity, that means the vanishing static friction force. The vanishing static friction force results from the thermal activation of the detachment of the actual contact points. The velocity dependence of the friction coefficient in the low velocity regime is investigated. It is also shown that even in the case that the indirect process overwhelm the direct process in the usual velocity regime, the direct process overwhelm the indirect process in the law velocity limit. In this case the steady state friction coefficient once increase from zero in the low velocity regime, shows a peak and then decreases with increasing sliding velocity. The relations with the laboratory experiment [8] and slow earthquake are discussed.

References

1, Scholz, C., “*Earthquakes and friction laws*”, Nature **391**, 37 (1998).

2, Saito, T., Ujiie, K., Tsutsumi, A., & Kameda, J., “*Geological and frictional aspects of very-low-frequency earthquakes in an accretionary prism*”, Geophysical Research Letters **40**, 703 (2013).

3, Dieterich, J., “*Modeling of rock friction 1. Experimental results and constitutive equations*” and “*Modeling of rock friction 2. Simulation of preseismic slip”*, Journal of Geophysical Research **80,** 2161 and 2169 (1979).

4, Ruina, A. , “*Slip instability and state variable friction law*”, Journal of Geophysical Research: Solid Earth **88,** 10359 (1983).

5, Heslot, F., Baumberger, T., Perrin, B., Caroli, B., & Caroli, C. *“Creep, stick-slip, and dry-friction dynamics: Experiments and a heuristic model”*, Physical Review E **49**, 4973 (1994).

©2019. Japan Geoscience Union. All Right Reserved.

6, Hatano T., “*Rate and state friction law as derived from atomistic processes at Asperities*”, arXiv:1512.05078v1 (2015).

7. Aharonv, E., & Scholz, C.H., “*A physics based rock friction constitutive law: Steady state friction*”, Journal of Geophysical Research: Solid Earth **123**, 1591 (2018).

8. Yamaguchi, T., private communication.

キーワード：速度状態依存摩擦則、静摩擦力
Keywords: Rate and State Dependent Friction Law, Static Friction Force

©2019. Japan Geoscience Union. All Right Reserved.

Stable sliding, slow and silent slip events and laboratory earthquakes across the brittle ductile transition

*Alexandre Schubnel[1], Aubry Jérôme[1], François Passelègue[2]

1. Laboratoire de Géologie, ENS, PARIS, France, 2. EPFL, Switzerland

The transition from brittle to plastic deformation corresponds to the regime where brittle fracturing and plastic flow co-exist. This transition is of fundamental importance to understand how natural faults behave differently at the bottom of the seismogenic zone, at PT conditions where the deformation regime is not fully brittle anymore.

Here, we reproduced the complete spectrum of natural faulting at laboratory scale, from stable slip to slow earthquakes and up to fast instabilities, on samples of dolostones and carbonates. Transitions from creep to slow ruptures and from slow to fast ruptures, are obtained by increasing both pressure and temperature up to conditions encountered at 3 km depth (i.e. 100 MPa confining pressure and 100 ˚C), which corresponds to the onset of seismicity in nature. Increasing confining pressure and temperature augments the fault elastic stiffness, which decreases the nucleation length and enhances the slip velocities during the nucleation to values allowing flash weakening and decarbonation processes.

From our experimental results, we conclude that: (i) laboratory earthquakes may nucleate on inherited fault interfaces at brittle-ductile transition conditions; (ii) in this regime where plastic deformation of the bulk and dynamic fault slip may co-exist, laboratory earthquakes are promoted when the interface is smooth, or when the loading rate is slow; (iii) stable sliding tends to produce mirror-like surface, while stick-slips is associated with matte surfaces, on which the size of the asperities grows with increasing confining pressure, (iv) slower loading rates and higher confining pressures promote the occurrence of laboratory earthquakes associated with increasing plastic deformation, while increasing initial roughness promotes stable sliding and slow stick-slip.

Keywords: slow and silent earthquakes, stick slip, brittle ductile transition

©2019. Japan Geoscience Union. All Right Reserved.

Dramatic velocity weakening of dry quartz friction at relatively slow slip velocities

*堤 昭人[1]、飯田 大貴[2]、 尾上 裕子[1]
*Akito Tsutsumi[1], Hirotaka Iida[2], Yuko Onoe[1]

1. 京都大学大学院理学研究科、2. 地熱エンジニアリング（株）
1. Graduate School of Science, Kyoto University, 2. Geothermal Engineering. Co. Ltd.

Understanding the frictional properties of subduction-zone fault materials is crucial to understanding subduction-zone seismogenesis. Previous experimental studies have demonstrated that fault weakening in siliceous rocks occurred at relatively low slip velocities ($V > 0.01$ mm/s) [Goldsby and Tullis, 2002; Di Toro et al., 2004; Hayashi and Tsutsumi, 2010], under which conditions transformation reactions are unable to proceed because of low temperatures. Formation of a silica gel layer has been suggested as a possible cause of the weakening behavior [Goldsby and Tullis, 2002]. However, there exists only limited information on the frictionally generated material and little is known about the weakening mechanism. To study the effect of moisture on the fault zone process in siliceous material, we have performed friction experiments on a synthetic quartz sample under two different humidity conditions: in room humidity (relative humidity RH = 20 to 75%) and in dry (RH < 3%) conditions. to

Three types of friction experiments were performed using a rotary-type testing machine on a pair of hollow-cylindrical specimens of quartz with outer and inner diameter of 25 and 5 mm, respectively, at a constant normal stress of 1.5 MPa. Constant velocity tests and velocity stepping tests were conducted under a range of slip velocities from 0.005 to 105 mm/s. In slide-hold-slide (SHS) tests, samples were first slid at $v = 105$ mm/s, by which sliding friction coefficient f decreases to attain a steady-state value of about $f = 0.2$. Then, rotation of the sample was stopped for periods of 1 to 10000s, after which rotation of the sample at the same rate was restarted.

In room humidity conditions, steady state friction shows velocity weakening at $v > 0.01$ mm/s, which is consistent to the previous studies. We find that steady-state friction values measured at the dry condition are almost constant at $f = 0.2$ for slip velocities v from 0.1 to 100 mm/s. SHS tests show that time-dependent frictional healing is observed for hold time duration $t > 10$s in room humidity condition. On the contrary, the time-dependent frictional healing is negligible when tested in the dry condition.

Our results imply that the moisture-absorption strengthening, which has been proposed to be an effective mechanism for time-dependent healing of high-velocity friction of gabbro (Mizoguchi et al. 2006) is an important underlying mechanism of the frictional weakening of quartz rocks observed in ambient humidity conditions.

キーワード：高速摩擦、速度弱化、ゲル潤滑
Keywords: high-velicity friction, velocity weakening, gel lubrication

©2019. Japan Geoscience Union. All Right Reserved.

ゲルの摩擦実験における微動とゆっくりすべりを伴う破壊核形成過程
Rupture nucleation processes accompanying tremor and slow slip in gel friction experiments

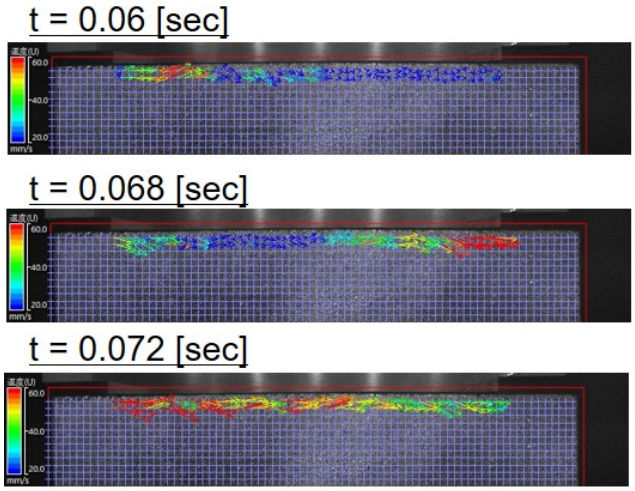
*山口 哲生[1]
*Tetsuo Yamaguchi[1]

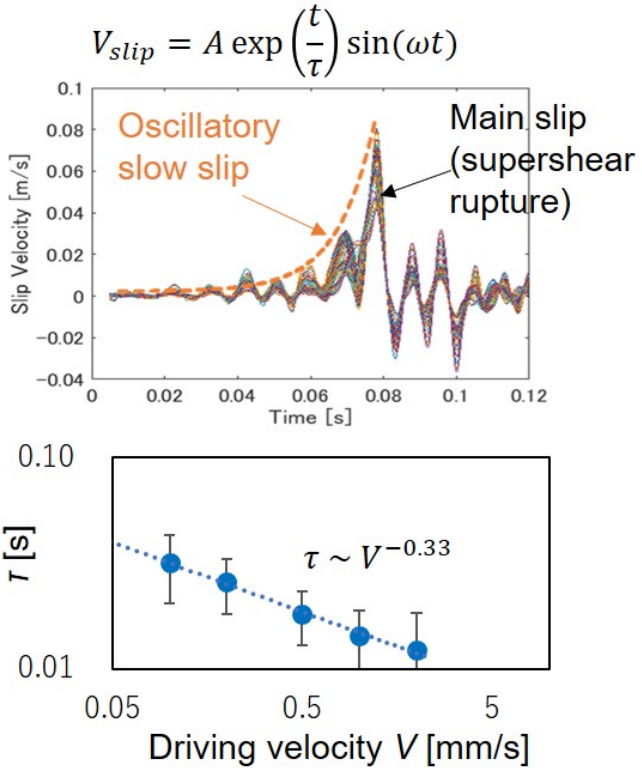
1. 九州大学
1. Graduate school of Engineering, Kyushu University

我々はこれまで，ゲルと呼ばれるやわらかい弾性体を用いた摩擦実験を通して，速いすべりとゆっくりすべりの共存，GR則，サイズ-持続時間スケーリング，スーパーシアー破壊など，実際の地震現象との類似性を見出してきた．

本研究では，破壊核形成過程の詳細な観察を行ったところ，ゆっくりすべりと微動が同期して発生していることが分かった．また，駆動速度をさまざまに変えて摩擦実験を行った結果，ゆっくりすべりの継続時間が駆動速度の-0.33乗に比例していることが分かった．本研究で用いたゲルは，低すべり速度で速度強化，高すべり速度で速度弱化を示す非単調な摩擦構成関係に従うが，このべき的な振る舞いは，摩擦力が極大となる臨界速度とは無関係に決まることを示唆している．数値計算との比較によって，摩擦構成関係と巨視的なすべり挙動との関連を明らかにするとともに，プレート境界での実現可能性についても議論したい．

キーワード：ゆっくりすべり、微動、アナログ実験、ゲル
Keywords: Slow slip, Tremor, Analogue experiment, Gel





©2019. Japan Geoscience Union. All Right Reserved.

多孔質媒質中の乱流におけるk-ε モデルの解軌道
Solution Orbit for k and epsilon Model for Turbulent Flow in Porous Media

*鈴木 岳人[1]
*Takehito Suzuki[1]

1. 青山学院大学理工学部物理・数理学科
1. Department of Physics and Mathematics, Aoyama Gakuin University

断層岩のような多孔質媒質中における乱流は動的地震破壊過程に影響を与え、多くの研究者の関心を集めてきた。それを取り扱うモデルの中で、k-ε モデルというものが幅広く用いられてきた。ここでkは乱流エネルギーであり、 ε はkの単位時間当たりの散逸率である。しかしながら、それらの初期値が最終状態に与える影響についての解析的取り扱いはなされていない。

１次元で均質な多孔質媒質を考え、等方的な乱れを考える。また流体の密度 ρ と空隙率 φ も一定であるとし、 φ kと φ ε の統計平均を以下ではk及び ε と書く。これらの仮定から、epsilon=c_k u_D k /\sqrt{*K*}で与えられるk-ε 相空間上の直線がkと ε の共通のヌルクラインになることに注意する。ここでc_kは正定数、u_Dは平均ダルシー速度、*K*は透水係数である。このヌルクラインはSuzuki (2017)に見られるように線状のアトラクタかリペラーになる。なお、直線epsilon=0（k軸）も ε に対するヌルクラインになる。

解軌道の解析的表現はepsilon=$epsilon_0$ (k/k_0)^C_2と得られる。ここでC_2は定数でおよそ1.9である。この結果を用いて、先の共通のヌルクラインepsilon=c_k u_D k/\sqrt{*K*}は解軌道のアトラクタであることが以下のように示される。まず領域Iというものを相空間上で0< epsilon < c_k u_D k/\sqrt{*K*}を満たす領域と定義する。同様に領域IIをepsilon > c_k u_D k/\sqrt{*K*}>0を満たす領域とする。また点(k_0, $epsilon_0$)を通る解軌道がヌルラインと交わる点を点 (k_f, $epsilon_f$)と定義する。ここでk_0, $epsilon_0$はそれぞれkと ε の初期値である。これらの定義から、もし(k_0, $epsilon_0$)が領域Iにあればk_0f及び$epsilon_0$fが成り立つことが分かる。なぜならヌルライン上では ε がkに比例するのに対して、解軌道上では ε がk^C_2に比例しかつC_2 >1だからである。同様に、もし(k_0, $epsilon_0$)が領域IIにあればk_0>k_f及び$epsilon_0$>$epsilon_f$ を得る。次に、領域I（II）ではkとepsilonが時間と共に増加（減少）することに注意する。これは\partial k/\partial tと\partial epsilon/\partial tが正（負）だからである。従って、もし(k_0, $epsilon_0$)が領域I（II）にあるならば、解軌道は右上（左下）方向に動き、時刻無限大でヌルラインに吸収される。すなわちヌルラインは（リペラーではなく）線状のアトラクタであることが分かる。定常状態は(k, epsilon)=(k_f, $epsilon_f$)である。

流体のみの系に見られる通常の乱流においては、kと ε は時刻無限大で消滅するが、上述の取り扱いはその場合にも有効である。通常の乱流は*K*が無限大の極限で記述されることに注意する。このとき共通のヌルクラインはk軸になり、領域Iが消滅する。ゆえに全ての解軌道が原点に吸収される。有限の*K*により、多孔質媒質中では定常状態においても乱流が存在できるのである。

キーワード：多孔質媒質、k-epsilonモデル、解軌道
Keywords: porous media, k-epsilon model, solution orbit

©2019. Japan Geoscience Union. All Right Reserved.

[E] 口頭発表 | セッション記号 S (固体地球科学)：S-CG 固体地球科学複合領域・一般

2019年5月30日(木) 15:30 ~ 17:00 | コンベンションホールA 2F

[S-CG48] Science of slow earthquakes: Toward unified understandings of whole earthquake process

コンビーナ:井出 哲(東京大学大学院理学系研究科地球惑星科学専攻)、廣瀬 仁(神戸大学都市安全研究センター)、氏家 恒太郎(筑波大学生命環境系)、波多野 恭弘(東京大学地震研究所)、座長:麻生 尚文、波多野 恭弘

Accumulating observational studies on various types of slow deformation events, such as tectonic tremors, very low frequency events, and slow slip events, portrays some universal characteristics in generally complex behavior, including interaction among events and influence by various outer loadings. Some of these phenomena seem to have causal relation with the occurrence of very large earthquakes. A unified understanding of these slow and fast earthquake processes requires an approach integrating geophysics, seismology, geodesy, geology, and non-equilibrium statistical physics. We welcome presentations based on, but not limited to, geophysical observation, data analysis, analytical theory, numerical simulation, field study, and laboratory experiments.

15:30 ~ 16:00

[SCG48-33] **Modelling precursory seismicity in the laboratory using a roughness derived rate and state friction model**

★Invited Papers

*Paul A Selvadurai[1]、Percy Galvez[2]、Stefan Wiemer[1]、P. Martin Mai[2] (1.Swiss Seismological service, ETH Zurich, Switzerland、2.King Abdullah University of Science and Technology, Thuwal, Saudi Arabia)

16:00 ~ 16:15

[SCG48-34] Exponential dependence on perturbation stress of earthquake nucleation

*齋藤 拓也[1]、波多野 恭弘[1] (1.東京大学)

16:15 ~ 16:30

[SCG48-35] Stochastic modeling of slow earthquakes comparable to observations

*麻生 尚文[1]、安藤 亮輔[2]、井出 哲[2] (1.東京工業大学、2.東京大学)

16:30 ~ 16:45

[SCG48-36] Migration of aqueous fluid near the subducting plate interface

*森重 学[1] (1.国立研究開発法人海洋研究開発機構)

16:45 ~ 17:00

[SCG48-37] EnKF estimation of frictional properties and slip evolution on a LSSE fault and the changing slip deficit rate on a megathrust fault

*平原 和朗[1,2] (1.香川大学四国危機管理教育・研究・地域連携推進機構、2.理化学研究所　AIPセンター)

Modelling precursory seismicity in the laboratory using a roughness derived rate and state friction model

*Paul A Selvadurai[1], Percy Galvez[2], Stefan Wiemer[1], P. Martin Mai[2]

1. Swiss Seismological service, ETH Zurich, Switzerland, 2. King Abdullah University of Science and Technology, Thuwal, Saudi Arabia

Growing amounts of seismologic observations appear to be capturing a larger diversity in slip behavior along natural faults. One such behavior is the appearance of localized high-frequency events occurring within a larger preparatory region of accelerated preslip. A mechanism explaining this phenomenon is that fault zones have contrasting strength, which may affect the spatial variability of seismic coupling. Recent numerical studies of faults governed by rate-and-state (RS) friction, show that systematic variations in the strength heterogeneity could explain diverse slip behaviors, such as, stable sliding without spontaneous slip transients, or unstable with spontaneous rupture [Liu and Ampuero, 2017].

Here we detail results from a direct shear friction experiment where a well-instrumented fault was formed by pressing together mature (worn) surfaces of poly(methyl methacrylate), then subjecting it to shear, until gross ‘stick-slip’ failure occurred. Prior to failure, spontaneous ruptures were found to nucleate within a region of accelerated slip, but *arrested locally within a seismogenic section* of the interface. Seismic waves produced by these high-frequency events were measured by an array of calibrated piezoelectric transducers. The seismogenic section was found to form where a slow slip front propagated into a relatively locked region [Selvadurai and Glaser, 2015].

To model the behavior of this lab-scale seismogenic region, we use multi-cycle simulations and linear stability analysis in the open source software QDYN, which utilizes boundary element method and adaptive time-stepping [Luo et al., 2017]. We studied the postmortem surfaces and found that the worn fault displayed a clear bimodal Gaussian distribution of surface height. This unique distribution of surface roughness was determined to be a proxy for a heterogeneous description of the critical slip distance D_c used in numerical calculation that modelled the seismogenic region as a VW section with constant normal stress that obeyed the slip law in terms of RS friction.

Our model showed that it was capable of producing the same diversity in slip behaviors from stable sliding to unstable with localized spontaneous ruptures and this was dependent on parameter selection. Preferentially smooth (polished) sections of fault exhibited low D_c and were susceptible to rupture nucleation. However, the extent to which they propagated along the fault depended on the level strength heterogeneity. Wearing of the fault also led to a natural periodicity in the spatial distribution of strength, which produced numerical estimates of source characteristics that matched those made from an independent analysis of seismic waves. Matching numerical and experimental estimates of source characteristics (seismic moment, source length scale and stress drop) was used a calibration tool to accurately tune the model behavior and better understand conditions leading to the production of seismicity attributed to the interaction of a slow slip front into a relatively locked section of fault.

References:

Luo, Y., Ampuero, J.-P. (2017), Stability of faults with heterogeneous friction properties and effective normal stress, *Tectonophysics*, doi:10.1016/j.tecto.2017.11.006

©2019. Japan Geoscience Union. All Right Reserved.

Luo, Y., Ampuero, J.P., Galvez, P., Ende, M., Idini, B., (2017). *QDYN: a Quasi-DYNamic Earthquake simulator (V1.1).* http://dx.doi.org/10.5281/zenodo.322459.

Selvadurai, P. A., and S. D. Glaser (2015), Laboratory-developed contact models controlling instability on frictional faults, *J. Geophys. Res. Solid Earth*, 120, doi:10.1002/2014JB011690.

Keywords: Foreshocks, Linear stability analysis, Strength heterogeneity, Laboratory studies

©2019. Japan Geoscience Union. All Right Reserved.

Exponential dependence on perturbation stress of earthquake nucleation

*齋藤 拓也[1]、波多野 恭弘[1]
*Saito Takuya[1], Takahiro Hatano[1]

1. 東京大学
1. The University of Tokyo

Recent observations have reported that some tremors in slow earthquake are sensitive to stress perturbations caused by ocean tides [1]. According to the preceding studies [1], occurrence frequencies of the susceptible tremors display exponential dependence on the stress magnitude. This study numerically investigates effects on earthquake nucleation growths of the periodic stress perturbations to see if the nucleation developed under the rate-and-state friction law reproduces the stress dependence. The numerical results suggest the exponential dependence on the perturbation stress magnitudes even in the presence of superimposed sinusoidal waves with the different periods. In addition, the exponential rates are found not to be sensitive to a change in the perturbation period or the superposition components of the sinusoidal perturbations, which implies the critical stresses magnitude are independent of a variety of the perturbations.

[1] S. Ide and Y. Tanaka, Geophys. Res. Lett. 41, 3842 (2014); S. Ide, S. Yabe, H.-J. Tai, and K. H. Chen, Geophys. Res. Lett., 42, 3248 (2015).

©2019. Japan Geoscience Union. All Right Reserved.

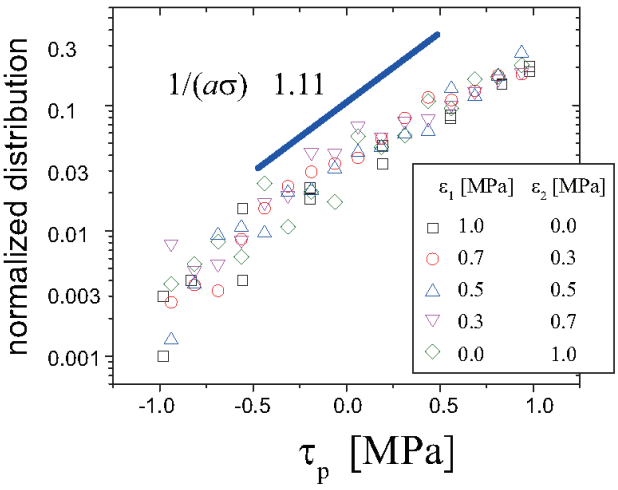


FIG. 1: Numerical results of stress dependence of the nucleation growth under the perturbation $\tau_p = \epsilon_1 \sin(\omega_1 t) + \epsilon_2 \sin(\omega_2 t + \phi_{2,ini})$. Horizontal or vertical axes represents stress magnitude or the normalized distribution, respectively. For each parameter condition, we measured the stresses of 1000 nucleation samples, which grow from randomly generated initial conditions, when the nucleation slip reaches the threshold velocity $V_{thr} = 1.0$ mm/s.

©2019. Japan Geoscience Union. All Right Reserved.

Stochastic modeling of slow earthquakes comparable to observations

*麻生 尚文[1]、安藤 亮輔[2]、井出 哲[2]
*Naofumi Aso[1], Ryosuke Ando[2], Satoshi Ide[2]

1. 東京工業大学、2. 東京大学
1. Tokyo Institute of Technology, 2. University of Tokyo

Slow earthquakes are often modeled using rate-and-state friction law with heterogeneously distributed parameters. However, we never know the exact friction law nor the perfect distribution of frictional parameters. Also, other physics are also proposed to contribute to the slow process, including pore fluid. Since any deterministic approaches cannot adequately capture the temporal stress change at a specific site because of the inherent unpredictability caused by various nonlinear processes, we instead focus on the stochastic approach to model slow earthquakes.
In stochastic modeling, we artificially add stochastic fluctuations in numerical simulations. When the result agrees with observations, the stochastic fluctuations are found to represent underlying physics. Then, we can make some predictions that could be evaluated by further observations. After capturing many characteristics of the stochasticity, we could finally approach physics. Although the deductive approach based on specific physics is often taken in earthquake source physics, the experimental approach has the potential to fill the gap between modeling and observations.
Here, we demonstrate that the consideration of stochastic stress fluctuations in ordinary crack simulations can reproduce a variety of observations of slow earthquakes, including burst-like tremor initiation, the existence of tremor front, decelerating tremor migration, and precursory slow earthquakes. The identical model can also reproduce both crack-like and pulse-like ordinary earthquakes by simply changing the strength drop and initial stress level.

©2019. Japan Geoscience Union. All Right Reserved.

Migration of aqueous fluid near the subducting plate interface

*森重 学[1]
*Manabu Morishige[1]

1. 国立研究開発法人海洋研究開発機構
1. Japan Agency for Marine-Earth Science and Technology

At least in several subduction zones including Tohoku, Japan, and Cascadia, low surface heat flow has been observed in the forearc, which suggests the existence of a cold fore-arc mantle. This low heat flow has been explained by a thin, low-viscosity layer (LVL) on top of the subducting slab that decouples the movement between the slab and the overriding mantle wedge. Although the formation mechanism of the LVL remains unclear, hydrous minerals such as serpentine may play an essential role in it. The effects of the LVL on solid (or rock) velocity have been extensively investigated. However, little is known of aqueous fluid migration in and around the LVL, despite its importance to our understanding of seismic activity along the subducting plate interface which includes slow earthquakes. In this presentation, I propose a mechanism of fluid flow through the LVL based on a numerical modeling of two-phase flow.

It has been shown that the equations for the solid and fluid phases can be decoupled if porosity is small. I therefore take the following two-step approach based on this assumption. I first solve for solid velocity and the dynamic pressure gradient in and around the LVL. These results are then used to solve for the porosity and compaction pressure in this region.

Preliminary results show that a large amount of fluid is trapped within the LVL by the effects of compaction, that is, the fluid cannot easily flow into the overriding mantle wedge with high viscosity. Dynamic pressure gradient within the LVL becomes large when a thin LVL or high solid viscosity within the LVL is assumed, which leads to a faster fluid flow in the updip direction. These findings suggest that the effects of compaction and dynamic pressure gradient are critical to understand the fluid flow near the subducting plate interface. I also find that the fluid tends to stay near the basal region of the LVL when a non-linear solid viscosity is applied.

キーワード：スロー地震、水流体、沈み込み帯、低粘性層
Keywords: slow earthquakes, aqueous fluid, subduction zones, low-viscosity layer

©2019. Japan Geoscience Union. All Right Reserved.

EnKF estimation of frictional properties and slip evolution on a LSSE fault and the changing slip deficit rate on a megathrust fault

*平原 和朗[1,2]
*Kazuro Hirahara[1,2]

1. 香川大学四国危機管理教育・研究・地域連携推進機構、2. 理化学研究所　AIPセンター
1. Institute of Education, Research and Regional Cooperation for crisis Management Shikoku, Kagawa University , 2. Riken, AIP center

With EnKF(Ensemble Kalman Filter), we are developing a system of real-time estimation of frictional properties and slip evolution on LSSE(long-term slow slip event) faults together with the slip deficit rate of the megathrust existing at the up-dip portion of the LSSE faults from the observed GNSS data, through numerical experiments. In the present system, the state vector to be forecasted and updated includes slip rates, state variables and frictional parameters on a LSSE fault, and the slip deficit rate in the megathrust fault. The first 3 parameters are constrained by a RSF(rate and state friction) law and data, but the last one is only by data in a kinematic way. Nishikiori and Hirahara (2017) have shown that the system with EnKF has successfully estimated the slip deficit rate together with frictional properties and slip evolution on the assumed Bungo-Channel LSSE fault for the station distribution corresponding to the GEONET one. So far, we have mainly examined the case of the constant slip deficit rate of the locked megathrust fault, assuming a short and stationary period in the Nankai earthquake cycle.
Several simulation studies have suggested the activity of LSSE is changing during the megaquake cycle, and the real-time monitoring of LSSE activity is important for understanding the stress state of the megaquake fault. Hirahara and Nishikiori (2018) have preliminarily examined the effect of changing deficit rate of the locked region. This study is an extension of theirs. A time series of slip deficit rate derived from a simple simulation of the Nankai earthquake cycle with a RSF law produces shorter reoccurrence time and larger slip rate of the Bungo-Channel LSSE fault toward the occurrence of Nankai megaquake. Based on this simulation model, we produce the simulated deformation rate data at GEONET stations. Then we try to estimate the changing slip deficit rate of the Nankai earthquake fault together with frictional parameters and slip evolution on the LSSE fault. Here, we define v_lock=V_lock -Vpl, and assign Vpl=6.5cm/yr. We can correctly trace the v_lock around -6cm/y during almost locked period. However, when v_lock is larger than -4 cm/yr, our system can not trace v_lock and underestimate the value. Then other parameters become to be also estimated as values deviated from the true ones. Therefore, we try to apply covariance inflation to enlarge the error covariance of the forecast state vector. There are two types of covariance inflation to enlarge the error covariance of the forecast vector. One is multiplicative inflation, where the forecast vector is artificially enlarged. Another is additive inflation, where we add random perturbation to the analysis vector in the previous time step, and obtain the forecast one in the next time step. In the latter one, the perturbation is not added directly to the forecast vector but to the analyzed one in the previous time step, so that the dynamical balances are kept when the next forecast is obtained. We use the approach of additive inflation of covariance. Then, we can correctly estimate the value of v_lock as well as other parameters up to a high value of v_lock around 25 cm/yr. We discuss such problems of abrupt breaks when we encounter in applying our system in numerical experiments.

キーワード：アンサンブルカルマンフィルタ、スロースリップイベント、速度状態摩擦、巨大地震、共分散膨張
Keywords: Ensemble Kalman Filter, Slow Slip Events, Rate and State Friction, Megaquake, Covariance Inflation

©2019. Japan Geoscience Union. All Right Reserved.

©2019. Japan Geoscience Union. All Right Reserved.

[E] 口頭発表 | セッション記号 S (固体地球科学)：S-CG 固体地球科学複合領域・一般

2019年5月30日(木) 9:00 ~ 10:30 | A02 東京ベイ幕張ホール

[S-CG50] Intraslab and intraplate earthquakes

コンビーナ:北 佐枝子(建築研究所)、大内 智博(愛媛大学地球深部ダイナミクス研究センター)、Marcel Thielmann(Bavarian Geoinstitute, University of Bayreuth)、奥脇 亮(産業技術総合研究所 地質調査総合センター 活断層・火山研究部門)、座長:北 佐枝子(建築研究所)、大内 智博(愛媛大学地球深部ダイナミクス研究センター)、Marcel Thielmann(University of Bayreuth)、奥脇 亮(筑波大学)、Thomas Ferrand(UC San Diego)

The purpose of this session is to share recent advances of geo-scientifical studies for intraslab and shallow-depth intraplate earthquakes. We seek to formulate future directions of the interdisciplinary study of the occurrence of intermediate-depth and deep earthquakes from the viewpoint of seismology, geodynamics and mineral physics. We welcome presentations from a wide variety of scientific disciplines, including seismology, seismotectonics, geodynamics, mineral and rock physics, other geophysics, geology, and numerical modeling.

9:00 ~ 9:15

[SCG50-01] On a reversely-dipping low-velocity layer in the Tohoku-slab beneath the forearc: unbending induced fluid pathway?

★招待講演
発表キャンセル

*川勝 均[1]、Kim HyeJeong[1] (1.東京大学地震研究所)

9:15 ~ 9:30

[SCG50-02] Evidence for transient fluid pathways in the mantle of the subducting Nazca slab from seismological observations and modeling of the Poisson's ratio

★Invited Papers

*Wasja Bloch[1,2]、Timm John[2]、Jörn Kummerow[2]、Bernd Schurr[1]、Pablo Salazar[3,4]、Serge A. Shapiro[2] (1.GeoForschungszentrum GFZ, Potsdam, Germany、2.Freie Universität Berlin, Germany、3.Universidád Católica del Norte, Antofagasta, Chile、4.National Research Center for Integrated Natural Disasters Management (CIGIDEN), Santiago, Chile)

9:30 ~ 9:45

[SCG50-03] Numerical simulation of water transportation along subducting slabs and implications for intraslab earthquakes

★Invited Papers

*中尾 篤史[1]、岩森 光[1,2,3]、中久喜 伴益[4]、鈴木 雄治郎[1]、中川 貴司[5]、中村 仁美[2,3,6,7] (1.東京大学地震研究所、2.海洋研究開発機構地球内部物質循環研究分野、3.東京工業大学理学院、4.広島大学大学院理学研究科、5.Department of Earth Sciences, The University of Hong Kong、6.産業技術総合研究所地質調査総合センター、7.千葉工業大学次世代海洋資源研究センター)

9:45 ~ 10:00

[SCG50-04] Subduction of serpentinized fracture zone and intraslab earthquakes in southern Mexico

★Invited Papers

*Marina Manea[1,2] (1.Computational Geodynamics Laboratory, Geosciences Center, National Autonomous University of Mexico、2.Institute of Astronomy, Romanian Academy)

10:00 ~ 10:15

[SCG50-05] Reaction-induced embrittlement of the lower continental crust

*Alexandre Schubnel[1]、Sarah Incel[2]、Julien Gasc[1]、Nadège Hilairet[5]、Yanbin Wang[3]、Feng Shi[3]、Loic Labrousse[4] (1.Laboratoire de Géologie, ENS、2.University of Oslo、3.GCECARS, University of Chicago、4.ISTEP, Sorbonne Université、5.UMET, Université de Lille)

10:15 ~ 10:30

[SCG50-06] **Transformation-induced, melt-enhanced faulting in orthoenstatite: implications for global intermediate-depth earthquakes**

Feng Shi[1]、Jianguo Wen[2]、Tony Yu[1]、Lupei Zhu[3]、*Yanbin Wang[1] (1.Center for Advanced Radiation Sources, University of Chicago, Chicago, IL, USA、2.Center for Nanoscale Materials, Argonne National Laboratory, Argonne, IL, USA、3.Department of Earth & Atmospheric Sciences, Saint Louis University, St. Louis, MO, USA)

On a reversely-dipping low-velocity layer in the Tohoku-slab beneath the forearc: unbending induced fluid pathway?

On a reversely-dipping low-velocity layer in the Tohoku-slab beneath the forearc: unbending induced fluid pathway?

*川勝 均[1]、Kim HyeJeong[1]
*Hitoshi Kawakatsu[1], HyeJeong Kim[1]

1. 東京大学地震研究所
1. Earthquake Research Institute, University of Tokyo

Kawakatsu & Kim (2018, SSJ) have recently updated the receiver function reflectivity images beneath the Japanese islands reported earlier in a series of papers by Kawakatsu and others(e.g., Kawakatsu & Watada, 2007, Science). We collected data from recent 14 years (April 2004 to April 2018) of Hi-net recordings; the resulting new dataset is 2.4, 6.4 and 4.8 times larger in terms of the time period, the number of earthquakes, and the number of RF waveforms compared to the earlier works. New images obtained are generally consistent with the previous ones; as the data quantity increases, the covered area widens and images tend to be clearer and smoother. One exception is that there is a glimpse of reversely-dipping low-velocity layer (LVL) within the slab beneath the forearc region dipping toward the Japan trench. When compared with the recent tomographic model that incorporates data from a seafloor cable seismic network S-net, the LVL appears to correspond to a strong P-wave LVL dipping also toward the trench that is imaged from the slab surface at around a depth of 40km to at least 60km. As this LVL is observed along the entire Tohoku Japan arc, it might be a representation of some mechanical process associated with subduction, unless some systematic bias is introduced in tomography (e.g., mis-location of off-shore earthquake depths). We speculate that this structure may continue to the bottom of the slab as imaged by the tomography though not resolved, and be related with the slab unbending that straightens the slab in the mantle (e.g., Kawakatsu, 1986, JGR). Tensile stress caused by unbending near the slab bottom may open a pathway for the sub-slab fluid to migrate upwards all the way to the slab top to further supply fluids around the slab surface, as well as to hydrate the lower-layer of the double seismic zone as suggested by Seno & Yamanaka (1996, AGU Monograph). Geophysical and geochemical consequences of this hypothesis that might be testable via various ways may be discussed.

キーワード：アンベンディング、スラブ、流体
Keywords: unbending, slab, fluid

©2019. Japan Geoscience Union. All Right Reserved.

Evidence for transient fluid pathways in the mantle of the subducting Nazca slab from seismological observations and modeling of the Poisson's ratio

*Wasja Bloch[1,2], Timm John[2], Jörn Kummerow[2], Bernd Schurr[1], Pablo Salazar[3,4], Serge A. Shapiro[2]

1. GeoForschungszentrum GFZ, Potsdam, Germany, 2. Freie Universität Berlin, Germany, 3. Universidád Católica del Norte, Antofagasta, Chile, 4. National Research Center for Integrated Natural Disasters Management (CIGIDEN), Santiago, Chile

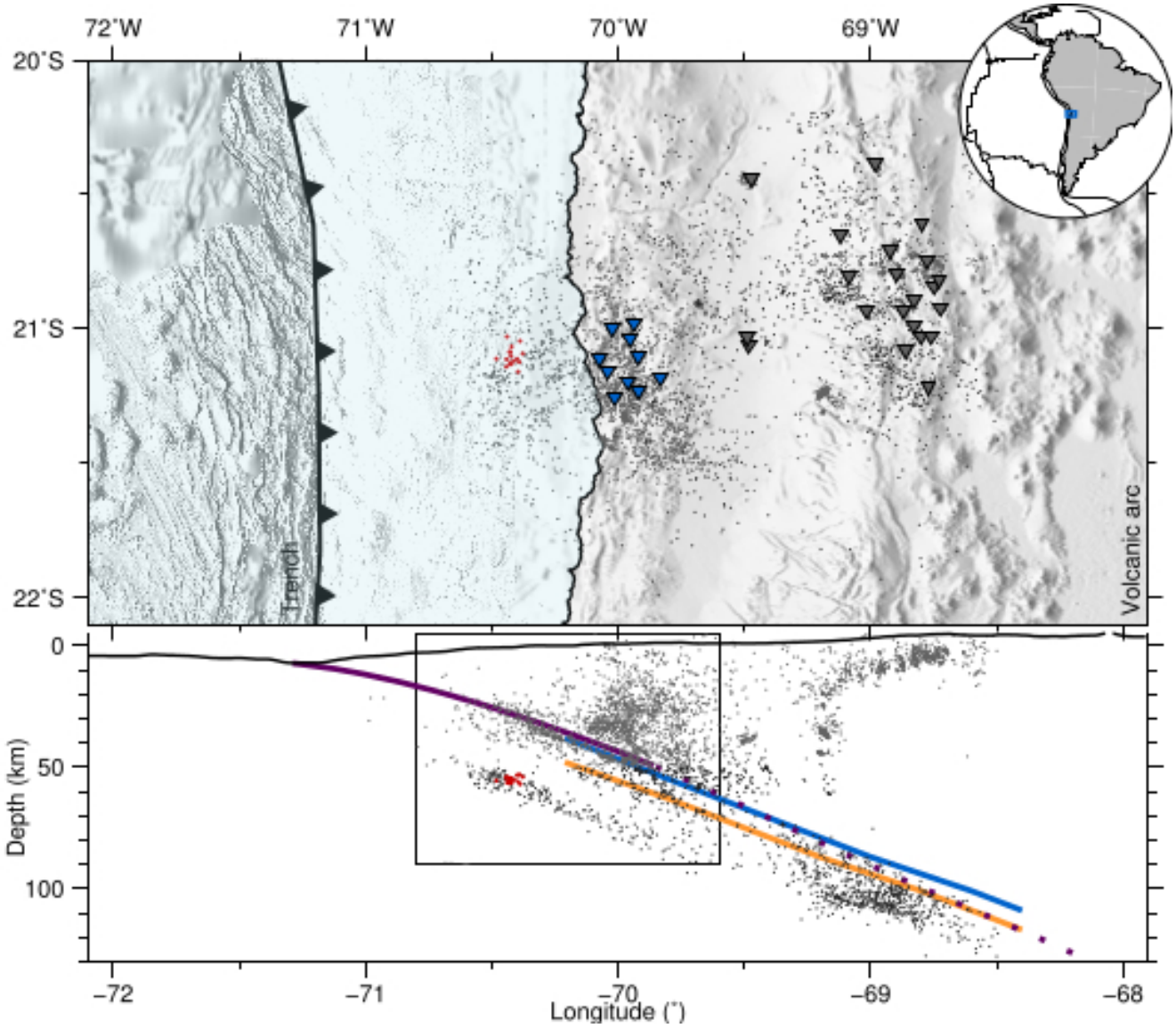
Subduction zones worldwide show the common pattern of a lower seismicity plane, where earthquakes occur at intermediate depth within the mantle of the subducting slab. In order to explain the occurrence of these earthquakes different earthquake nucleation mechanisms have been proposed. Some of them attribute seismicity to different transient phenomena that accompany the metamorphic breakdown of water bearing mineral phases. Event though such mechanisms can well explain the distinct shape of the lower seismicity plane and can well be reproduced in laboratory experiments, they are based on the assumption that the subducting plate is hydrated tens of kilometers below the oceanic Moho. Direct evidence for this assumption is scarce.

To detect the possible presence of fluids in the slab mantle, as predicted by the dehydration hypotheses, we estimated the Poisson's ratio of a small rock volume that hosts intra-slab earthquakes by employing a non-tomographic seismic method that has its greatest sensitivity in the direct vicinity of the earthquakes and delivers unique results. We interpret our results by means of a state-of-the-art coupled thermodynamic-poroelastic model. We additionally determine focal mechanisms in the lower seismicity plane to gain information about the prevailing stresses.

The joint interpretation yields a picture in which seismicity occurs at a low rate at 50km depth in a dehydrating but not over-pressured environment at low, overall tensile differential stresses. The modeling results indicate that the fluid occupies a minor volume fraction in the order of only 0.1% and constitutes an interconnected, vein-shaped and therefore transient pore network. These findings are in agreement with results from laboratory experiments, numerical simulations and outcrop studies. They imply that the oceanic mantle of the subducting Nazca slab must be at least weakly hydrated to a depth of 20-30km below the seafloor. Our interpretation can also be applied to tomographic images of other lower seismicity planes, e.g. in Japan.

Keywords: Mantle dehydration, Fluid processes, Seismology

©2019. Japan Geoscience Union. All Right Reserved.



©2019. Japan Geoscience Union. All Right Reserved.

Numerical simulation of water transportation along subducting slabs and implications for intraslab earthquakes

*中尾 篤史[1]、岩森 光[1,2,3]、中久喜 伴益[4]、鈴木 雄治郎[1]、中川 貴司[5]、中村 仁美[2,3,6,7]
*Atsushi Nakao[1], Hikaru Iwamori[1,2,3], Tomoeki Nakakuki[4], Yujiro Suzuki[1], Takashi Nakagawa[5], Hitomi Nakamura[2,3,6,7]

1. 東京大学地震研究所、2. 海洋研究開発機構地球内部物質循環研究分野、3. 東京工業大学理学院、4. 広島大学大学院理学研究科、5. Department of Earth Sciences, The University of Hong Kong、6. 産業技術総合研究所地質調査総合センター、7. 千葉工業大学次世代海洋資源研究センター
1. Earthquake Research Institute, University of Tokyo, 2. Department of Solid Earth Geochemistry, Japan Agency for Marine-Earth Science and Technology, 3. Department of Earth and Planetary Sciences, Tokyo Institute of Technology, 4. Department of Earth and Planetary Systems Science, Hiroshima University, 5. Department of Earth Sciences, The University of Hong Kong, 6. Geological Survey of Japan, National Institute of Advanced Industrial Science and Technology, 7. Ocean Resource Research Center for Next Generation, Chiba Institute of Technology

It has been argued that water is abundant enough across subducting slabs to trigger lower seismic planes (i.e., >40-km-thick hydrous mantle; Peacock, 2001). Geodynamic modeling, however, suggests that the Pacific slab has a low water content beneath Northreast Japan (NEJ) (Nakao et al., 2018), despite presence of the clear lower seismic plane. The model shows that the thickly serpentinized slab mantle (>10 km for 100-Ma slab) causes slow plate convergence, stationary trenches, and slab penetration into the 660-km boundary, in contrast to the case of NEJ (Lallemand et al., 2008; Fukao & Obayashi, 2013). Moreover, seismic velocity and anisotropy structures also indicate a small amount of water around the lower plane in the Pacific slab (Zhang et al., 2004; Reynard et al., 2010). To address this discrepancy, we performed numerical simulations of water transport within and along the subducting slab of a variable age and initial water content. It is demonstrated that the loci of fluid liberation from the subducted slab of an old age (130 Ma) broadly correspond to the upper seismic plane beneath NEJ. On the other hand, loci of any dehydration reaction within the old slab may not explain the lower seismic plane. Instead, the loci of chlorite breakdown for a 36-Ma slab correspond to the lower plane beneath NEJ. In this case, the breakdown and formation of chlorite repeatedly occur, and liberated fluid forms a long curved-linear locus similar to the shape and extent of lower seismic plane in the Pacific slab beneath NEJ. We suggest that the repeated chlorite breakdown which effectively reutilizes a small amount of water contained initially in the slab may trigger the long lower seismic plane beneath NEJ.

キーワード：Wadati-Benioff zone、intermediate-depth earthquake、plate tectonics、phase relation、thermal structure
Keywords: Wadati-Benioff zone, intermediate-depth earthquake, plate tectonics, phase relation, thermal structure

©2019. Japan Geoscience Union. All Right Reserved.

Subduction of serpentinized fracture zone and intraslab earthquakes in southern Mexico

*Marina Manea[1,2]

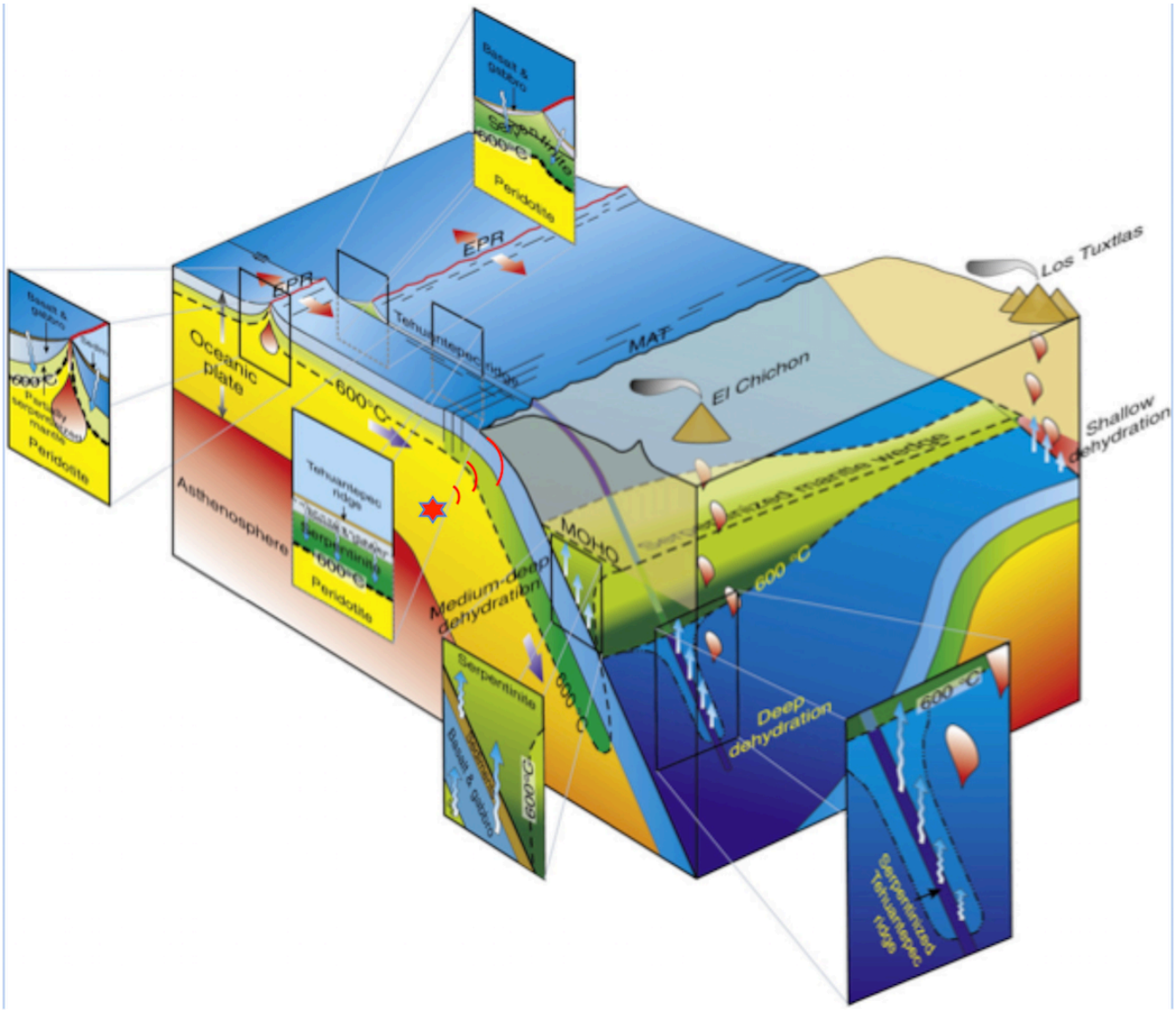
1. Computational Geodynamics Laboratory, Geosciences Center, National Autonomous University of Mexico, 2. Institute of Astronomy, Romanian Academy

Oceanic fracture zones are born where spreading centers are offset, creating strong gradients in oceanic floor age and vertical offsets in the oceanic lithosphere. Several lines of evidence, such as tectonic uplift and localized volcanic activity distributed along fracture zones, suggest that oceanic fracture zones represent zones of weakness where seawater can infiltrate several kilometers down into the lithosphere and transform mantle peridotites into serpentinites. Such major serpentinized fracture zones are often consumed into subduction zones where they release large quantities of fluids. The southern Mexican subduction zone is similarly characterized by the presence of a large fracture zone, the Tehuantepec fracture zone (TFZ), which presumably is serpentinized. Moreover, the region where TFZ enters into subduction is marked by a relatively low intraplate seismic activity and a large seismic gap where no large megathrust occurred in the last 100 years or more.

In general the physical processes associated with such seismic gaps are not well understood. However, the presence of TFZ in this area can provide a unique opportunity to advance our knowledge into earthquake mechanics linked to mantle thermal structure. The peculiar 2017 M8.2 Tehuantepec intraslab earthquake nucleated in the vicinity of TFZ, and, from analyses of regional geophysical observations, it is demonstrated that this large normal faulting event ruptured the entire ~26 Ma Cocos slab right beneath the megathrust region. The faulting most likely reactivated a bend fault fabric and ruptured to a depth well below the predicted brittle-ductile transition for the Cocos slab, including regions where temperature is expected to exceed 1000˚C, at far greater P-T conditions than previously considered. Additionally, since the rupture area also propagated laterally along the trench and stopped abruptly when encountered the subducted TFZ, we propose that large and serpentinized fracture zones can act as barriers for intraslab earthquakes. I have to acknowledge that all numerical computations were performed at the National Laboratory for Advanced Scientific Visualization at UNAM (LAVIS).

Keywords: intraslab earthquakes, fracture zone, serpentinization , southern Mexico

©2019. Japan Geoscience Union. All Right Reserved.



©2019. Japan Geoscience Union. All Right Reserved.

Reaction-induced embrittlement of the lower continental crust

*Alexandre Schubnel[1], Sarah Incel[2], Julien Gasc[1], Nadège Hilairet[5], Yanbin Wang[3], Feng Shi[3], Loic Labrousse[4]

1. Laboratoire de Géologie, ENS, 2. University of Oslo, 3. GCECARS, University of Chicago, 4. ISTEP, Sorbonne Université, 5. UMET, Université de Lille

Field observations and geophysical data reveal a causal link between brittle seismic failure and eclogitization of the lower continental crust. We present results from experimental deformation of plagioclase-rich samples at eclogite-facies conditions and quantify the link between rock rheology and the kinetics of the eclogitization reactions. The deformation was ductile both in the absence of reaction and when the progress of eclogitization was fast compared to the imposed strain rate. However, when the reaction rate was relatively slow, the breakdown of plagioclase into nanocrystalline reaction products induced a weakening that triggered seismic failure. Fluid-induced plagioclase breakdown under eclogite-facies conditions is an exothermic reaction accompanied by a negative change in solid volume. This is similar to other mineral transformations that are known to trigger transformational faulting. We demonstrate that mineral reactions lead to brittle deformation in situations where reaction rates are slow compared to the deformation rate. This reaction-induced instability may provide a generic mechanism for embrittlement at depths beyond the normal seismogenic zone.

Keywords: lower crust, Eclogitisation, Granulite

©2019. Japan Geoscience Union. All Right Reserved.

Transformation-induced, melt-enhanced faulting in orthoenstatite: implications for global intermediate-depth earthquakes

Feng Shi[1], Jianguo Wen[2], Tony Yu[1], Lupei Zhu[3], *Yanbin Wang[1]

1. Center for Advanced Radiation Sources, University of Chicago, Chicago, IL, USA, 2. Center for Nanoscale Materials, Argonne National Laboratory, Argonne, IL, USA, 3. Department of Earth & Atmospheric Sciences, Saint Louis University, St. Louis, MO, USA

Intermediate-depth earthquakes, which occur at ~50-300 km depths and account for ~90% of all deep earthquakes between 50 and 700 km, are ubiquitously observed along convergent plate margins and post great hazards in many regions of the world. Earthquake-depth distribution in oceanic subduction zones exhibits a prevalent secondary seismicity peak between 180 and 240 km, where major dehydration reactions are expected to have completed [1, 2]. This secondary seismcity peak is a direct manifestation of earthquake activities in the lower plane of the double seimic zone [3]. One of the main constituents of oceanic slabs is harzburgite, which consists mainly of olivine and orthoenstatite (OEn) [4]. The latter transforms to high-pressure clinoenstatite (HP-CEn) at ~120 –210 km depths, depending on aluminum content and slab temperature [5, 6]. We conducted deformation experiments on OEn at conditions corresponding to ~ 40 –250 km depths. Within its stability field, OEn deforms plastically; no brittle failure is detected with acoustic emission (AE) monitoring. In the HP-CEn stability field, metastable OEn generates numerous AEs generated, and fails by macroscopic faulting between ~773 and 1373 K. Outside this temperature range, metastable OEn flows plastically again with no AEs detected. Recovered failed samples contain large conjugated faults, with ultrafine-grained gouge layers containing melts that are more Al-rich. OEn grain boundaries are decorated with fine grained (grainsize < 1 micron) garnet and clinoenstatite (CEn). The latter is interpreted as back-transformed HP-CEn upon pressure release. Within large OEn grains, finer-grained garnet forms thin lamellae preferentially parallel to the OEn (100) twin planes. These results suggest that micro-ruptures start in metastable OEn by syn-deformational transformation, which, aided by exothermic latent heat production, results in exsolution lamellae of garnet and CEn, both along the OEn (100) planes, associated with intragranular ruptures. These micro-ruptures conglomerate along weakened grain boundaries to form intergragular faults consisting of ultrafine grained reaction and shear zones, which, through adiabatic heating and local melting, self-organize into macroscopic faults. We propose that in harzburgite, the observed OEn instability triggers shear localization in olivine, resulting in adiabatic instability, a mechanism hypothesized on theoretical grounds [7, 8] and recently observed in laboratory experiments [9].

References:

[1] Hacker, B.R., Peacock, S.M., Abers, G.A., Holloway, S.D., 2003. J Geophys Res 108, 2019.
[2] Syracuse, E.M., van Keken, P.E., Abers, G.A., 2010. Phys Earth Planet In 183, 73–90.
[3] Brudzinski, M.R., C.H. Thurber, B. R. Hacker, E.R. Engdahl, Science, 316, 1472-1474.
[4] Ringwood, A.E., Irifune, T., 1988. Nature 331, 131–136.
[5] Gasparik, T., 2003. Phase diagrams for geoscientists. An Atlas of the Earth's Interior.
[6] Akashi, A.,et al., 2009. J Geophys Res 114, 322.
[7] Ogawa, M., 1987. J Geophys Res 92, 13801-13810.
[8] Hoobs, B.E., Ord, A., 1988. J. Geophys Res 93, 10521-10540.
[9] Ohuchi, T., et al., 2017. Nature Geoscience 10, 771.

©2019. Japan Geoscience Union. All Right Reserved.

[E] 口頭発表 | セッション記号 S (固体地球科学)：S-CG 固体地球科学複合領域・一般

2019年5月30日(木) 10:45 ~ 12:15 | A02 東京ベイ幕張ホール

[S-CG50] Intraslab and intraplate earthquakes

コンビーナ:北 佐枝子(建築研究所)、大内 智博(愛媛大学地球深部ダイナミクス研究センター)、Marcel Thielmann(Bavarian Geoinstitute, University of Bayreuth)、奥脇 亮(産業技術総合研究所 地質調査総合センター 活断層・火山研究部門)、座長:北 佐枝子(建築研究所)、大内 智博(愛媛大学地球深部ダイナミクス研究センター)、Marcel Thielmann(University of Bayreuth)、奥脇 亮(筑波大学)、Thomas Ferrand(UC San Diego)

The purpose of this session is to share recent advances of geo-scientifical studies for intraslab and shallow-depth intraplate earthquakes. We seek to formulate future directions of the interdisciplinary study of the occurrence of intermediate-depth and deep earthquakes from the viewpoint of seismology, geodynamics and mineral physics. We welcome presentations from a wide variety of scientific disciplines, including seismology, seismotectonics, geodynamics, mineral and rock physics, other geophysics, geology, and numerical modeling.

10:45 ~ 11:00

[SCG50-07] The Isolated M7.9 Deep Earthquake of 30 May 2015 Under the Present Bonin Wadati-Benioff Zone: Evidence from the New ISC-EHB Earthquake Catalogue (1930-2015) and CMT Focal Mechanisms

*Kirby Stephen[1]、Engdahl E.[2]、Okal Emile[3] (1.United States Geological Survey, Menlo Park、2.University of Colorado、3.Northwestern University)

11:00 ~ 11:15

[SCG50-08] What Can M_W –4 Lab-Quakes Teach Us About Deep-Focus Earthquakes?

★Invited Papers

*Julien Gasc[1]、Julien Fauconnier[1]、Clémence Daigre[1]、Arefeh Moarefvand[1]、Damien Deldicque[1]、Blandine Gardonio[1]、Alexandre Schubnel[1]、Pamela Burnley[2] (1.Laboratoire de Géologie, ENS-CNRS, Paris, FRANCE、2.University of Nevada Las Vegas, Las Vegas, USA)

11:15 ~ 11:30

[SCG50-09] Deep intraslab earthquake rupture due to grain size assisted thermal runaway

*Marcel Thielmann[1]、Thibault Duretz[2] (1.Bavarian Geoinstitute, University of Bayreuth, Germany、2.Université de Rennes, Rennes, France)

11:30 ~ 11:45

[SCG50-10] 2012年宮城沖プレート内ダブレット地震の震源断層モデルから検討した日本海溝近傍における海洋プレート内レオロジー

*久保田 達矢[1]、日野 亮太[2]、鈴木 秀市[2] (1.国立研究開発法人防災科学技術研究所、2.東北大学大学院理学研究科)

11:45 ~ 12:00

[SCG50-11] Source-rupture process of the intraplate earthquake; its diversity related to the fault geometry and damaged fault zone

*奥脇 亮[1]、八木 勇治[1] (1.筑波大学大学院生命環境科学研究科)

12:00 ~ 12:15

[SCG50-12] **Aftershocks of the NEXT Cascadia Intraslab Earthquake**

*Paul Bodin[1,2] (1.University of Washington Seattle、2.Pacific Northwest Seismic Network)

The Isolated M7.9 Deep Earthquake of 30 May 2015 Under the Present Bonin Wadati-Benioff Zone: Evidence from the New ISC-EHB Earthquake Catalogue (1930-2015) and CMT Focal Mechanisms

The Isolated M7.9 Deep Earthquake of 30 May 2015 Under the Present Bonin Wadati-Benioff Zone: Evidence from the New ISC-EHB Earthquake Catalogue (1930-2015) and CMT Focal Mechanisms

*Kirby Stephen[1]、Engdahl E.[2]、Okal Emile[3]
*Stephen Kirby[1], E. Robert Engdahl[2], Emile Andre Okal[3]

1. United States Geological Survey, Menlo Park、2. University of Colorado、3. Northwestern University
1. United States Geological Survey, Menlo Park, 2. University of Colorado, 3. Northwestern University

The M7.9 deep earthquake of 30 May 2015 at a depth of about 680 km was surprising in that it occurred more that 150 km distant from any event in the main Bonin sector Wadati-Benioff Zone (WBZ) above it and more than 120 km deeper than any well-recorded event in the Bonin subduction system. We applied the recently developed ISC-EHB methodology (GJI, 2018, v. 214, 474-484) to produce a comprehensive catalogue of hypocenters for the Izu-Bonin-Marianas region from 1904 to 2015. This methodology, which utilizes only events well-recorded telesesismically along with reported depth phases, ensures that the hypocenters in any given region are relatively well constrained in both location and depth. Individual trench-normal cross sections though the Southern-Bonin/Northern-Marianas subduction systems (including the transition through the Ogasawara Plateau collision zone) display a very sharply defined Bonin inclined seismic zone with no ISC-EHB events at depths and positions between the 2015 deep event and the Izu-Bonin Wadati Benioff Zone (WBZ) above it. Moreover the 2015 deep event occurred at least 200 km north of a possible tear in the main slab at about latitude about 25-26 ˚N where the deep WBZ bends back under the intermediate-depth segment. Most of the CMT focal mechanisms deeper than 300 km within the Bonin WBZ have normal-faulting mechanisms. Some published papers have claimed that the 2015 deep Bonin earthquake occurred in a steeply-dipping sector of the Bonin slab based largely on seismic tomography, but none of these studies have demonstrated sufficient resolution for convincing evidence of high-wave-speed slab material clearly linking the 2015 hypocenter with the main Bonin WBZ. Other published papers show independent evidence that the 2105 event occurred below the Bonin WBZ. We are left with the interpretation that the 2015 event occurred in a slab fragment separated from the main Bonin WBZ. We offer a possible fragmentation scenario involving a oceanic plateau collision, a consequent slab detachment, and an eastward trench stepback. Isolated deep earthquakes in slab fragments can rupture by transformational faulting in metastable olivine (MO) where stresses can originate by the residual stresses caused by heterogeneous volume changes associated with the MO->Spinel transformation (Okal and Kirby, PEPI, 1998).

キーワード：Deep earthquakes、Bonin seismic zone、2015 Ultra-deep earthquake、Metastable olivine
Keywords: Deep earthquakes, Bonin seismic zone, 2015 Ultra-deep earthquake, Metastable olivine

©2019. Japan Geoscience Union. All Right Reserved.

What Can M_w −4 Lab-Quakes Teach Us About Deep-Focus Earthquakes?

*Julien Gasc[1], Julien Fauconnier[1], Clémence Daigre[1], Arefeh Moarefvand[1], Damien Deldicque[1], Blandine Gardonio[1], Alexandre Schubnel[1], Pamela Burnley[2]

1. Laboratoire de Géologie, ENS-CNRS, Paris, FRANCE, 2. University of Nevada Las Vegas, Las Vegas, USA

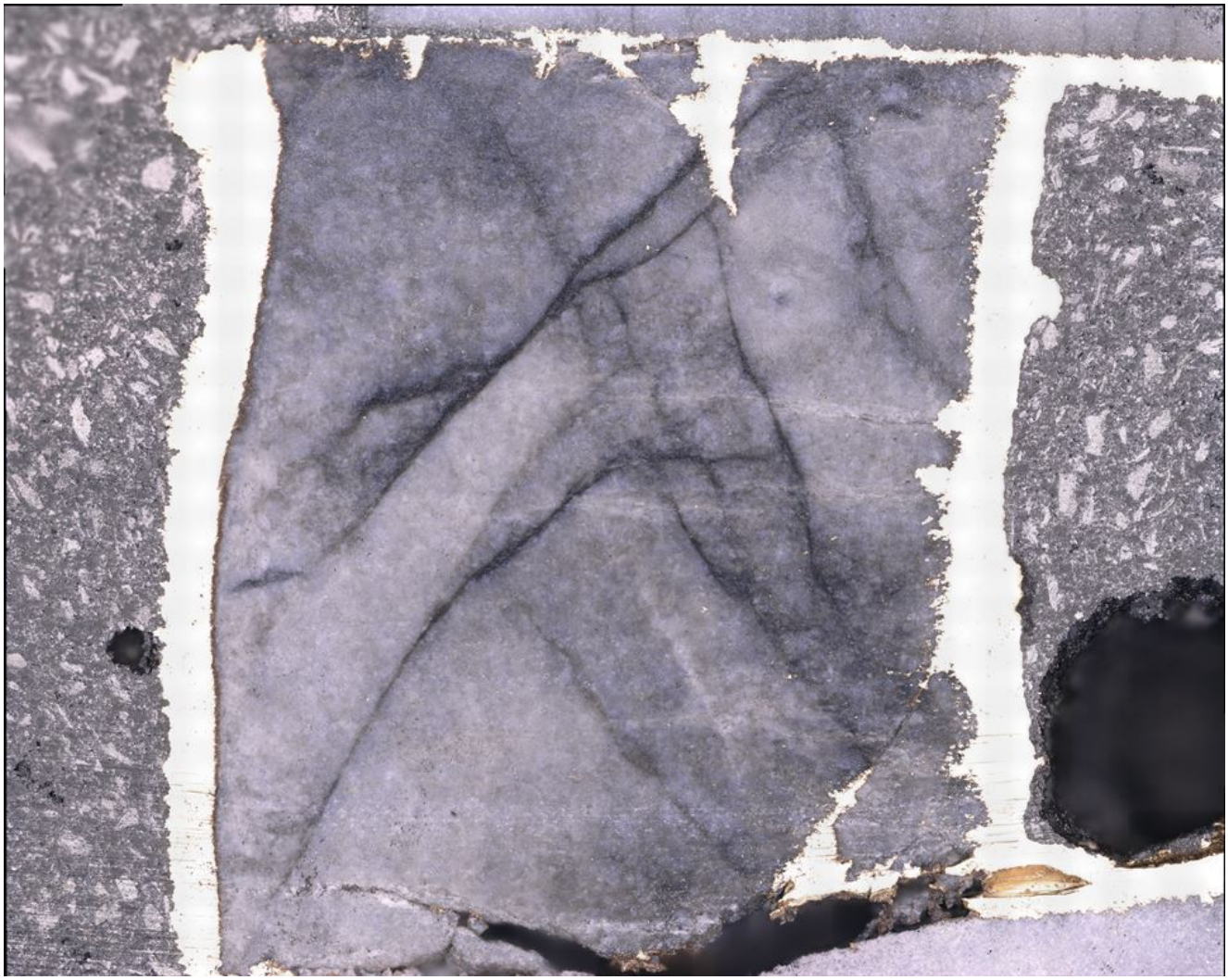
In recent years, several experimental studies have shed new light on possible faulting mechanisms responsible for intermediate and deep-seated earthquakes. These studies rely not only on the traditional analysis of mechanical data and recovered microstructures, but also on the in situ collection of acoustic data −in the form of Acoustic Emissions (AEs)− used to identify possible co-seismic faulting, i.e., brittle failure.

I will give an overview of this recent work and detail how, recently, deep-focus earthquakes mechanisms could be investigated at 1.5 GPa and 750-900˚C, in a new-generation Griggs-type apparatus using sintered Mg_2GeO_4 samples. This compound is an analogue of natural olivine for which the transition towards the high pressure phase (spinel structure) occurs at atmospheric pressure, instead of ~14 GPa for the silicate. This transition induces a mechanical instability −the so-called *transformational faulting*− that leads to macroscopic failure of the samples in a narrow temperature window. The boundaries of this brittle window, as for other reactions (quartz-coesite, antigorite dehydration, plagioclase breakdown and so on), are defined by the reaction kinetics. Here, faulting only occurs in cases where spinel nucleates but hardly grows, i.e., when reaction rates are slow.

At 900˚C mechanical data show a softening, indicative of ductile plastic flow, whereas large amounts of hardening followed by rapid stress drops (and audible stick slips) are recorded at 750˚C. AEs were detected in both cases and differences between P and S waves arrival times suggest that the majority of AEs originate inside the sample. Coherence analysis of the AEs seems to suggest that some bursts of events have similar sources. Surprisingly, AEs are more numerous (~600) at higher temperature, where deformation takes place in a ductile way, accommodated by the development of a wide mylonitic shear band. However, at 750˚C, far more energy is released acoustically upon brittle faulting despite a lower number of AEs (~100). Therefore, higher temperatures favor larger reaction rates, which, in turn, allow the growth of ductile fine-grained spinel. Our results confirm that the brittle temperature window (1) is a function of both equilibrium overstep (reaction kinetic) and strain rate and (2) seems to shift towards lower temperatures with decreasing strain rates, which may explain how earthquakes can occur in a slowly reacting metastable olivine wedge at strain rates orders of magnitude lower than in the lab.

Keywords: deep focus earthquakes, high pressure deformation experiments, transformational faulting, olivine spinel transition, acoustic emissions

©2019. Japan Geoscience Union. All Right Reserved.



©2019. Japan Geoscience Union. All Right Reserved.

Deep intraslab earthquake rupture due to grain size assisted thermal runaway

*Marcel Thielmann[1], Thibault Duretz[2]

1. Bavarian Geoinstitute, University of Bayreuth, Germany, 2. Université de Rennes, Rennes, France

The rupture of the 2017 Mw 8.2 Tehuantepec earthquake has been shown to extend to temperatures above 1,000 ˚C. Ruptures penetrating to regions of such temperatures are highly unusal and raise the question whether the governing rupture mechanisms at these temperatures are comparable to shallow earthquakes. It has been suggested that dehydration embrittlement could result in deep intraslab earthquakes. However, dehydration embrittlement requires the presence of fluids. In the case of the Tehuantepec earthquake, this means that fluids would have to infiltrate the slab to depths that have not been observed.
An alternative mechanism that may lead to failure at these temperatures and depths is thermal runaway, in particular in conjunction with grain size reduction. Due to the conversion from mechanical work to heat during irreversible deformation, this mechanism weakens the rock. In certain conditions, it then results in zones of highly localized viscous creep along which a significant amount of displacement can be accumulated.
Here, we investigate the onset and formation of a ductile shear zone nucleating a cold temperatures and then propagating to regions of higher temperature using 2D numerical models with a nonlinear viscoelastic rheology. We show that it is indeed possible to form a ductile shear zone through the combined action of grain size reduction and shear heating and determine the parameter ranges where this feedback loop may result in ductile shear zone formation and thus also deep earthquake rupture.

Keywords: intraslab earthquakes, deep earthquakes, thermal runaway, grain size evolution

©2019. Japan Geoscience Union. All Right Reserved.

2012年宮城沖プレート内ダブレット地震の震源断層モデルから検討した日本海溝近傍における海洋プレート内レオロジー
Fault model of the 2012 off-Miyagi intraslab earthquake doublet and its implication for rheological signature of incoming Pacific plate

*久保田 達矢[1]、日野 亮太[2]、鈴木 秀市[2]
*Tatsuya Kubota[1], Ryota Hino[2], Syuichi Suzuki[2]

1. 国立研究開発法人防災科学技術研究所、2. 東北大学大学院理学研究科
1. National Research Institute for Earth Science and Disaster Resilience, 2. Graduate School of Science, Tohoku University

2012年12月7日，日本海溝そばのプレート内において深い逆断層型地震(~60km，Mw7.2，サブイベント1)と浅い正断層型地震(~20km，Mw7.1，サブイベント2；時間差は約10秒) からなるMjma7.3の地震が発生した．震源域の周辺では，プレートの折れ曲がりによって浅部と深部それぞれで引張・圧縮の応力場が発達していることが知られている(e.g., Chapple and Forsyth, 1979 JGR)．両サブイベントのメカニズムはそれぞれが発生した深さにおける応力場と対応するため，この地震の破壊過程はプレート内部の応力場について議論するのに有用と考えられる．我々はこれまで，沖合津波記録と遠地地震波形記録からこの地震について詳細な震源モデルの推定を行ってきた(久保田, 2017 東北大博論)．本研究は，この地震の震源断層モデルの推定精度を評価したうえで，東北沖地震前後の地震活動や室内実験で得られた岩石の強度などと比較し，プレート内部の応力場やレオロジー的性質について考察を行った．

震源断層モデルの推定では，まず津波記録の逆解析から津波の波源分布を推定し，Global CMT解から期待される各サブイベントの海底変動分布と比較した．その結果，波源の沈降域はサブイベント2により，隆起域は両方のサブイベントの変動の重ね合わせにより生じていることが分かった．次に，サブイベント2について，津波波源分布の沈降域をもっともよく説明する一様すべり矩形断層モデルを，余震分布(Obana et al. 2015, AGU FM) を参考にしながらグリッドサーチにより探索した．最後に，津波波源分布からサブイベント2の断層モデルから計算される上下変動を差し引いてサブイベント1による上下変動を抽出し，これを最もよく説明するサブイベント1の矩形断層モデルを，遠地実体波から得られたCMT解の情報を参考にしながら探索した．探索結果のうち，変動分布の説明度が比較的良い断層モデルを抽出し，それに基づいて断層モデルの推定精度を考察した結果，得られた断層モデルの深さ方向の広がりは，サブイベント1が~ 45 –70 km，サブイベント2が~5 –35 km (上端は海底と一致) の範囲にあることが分かった．

推定された正断層サブイベントの下端の深さ(~35 km)は，2007年に同海域で海底地震計を用いた観測により得られた正断層型地震の下端(~25km，Hino et al., 2009 G3) より有意に深い．この正断層型地震の深さ変化(~10 km)は，プレートの折れ曲がりによって生じる応力の深さ勾配(~ 15 MPa/km) を考えると，東北沖地震によってサブイベント2の震源域周辺に生じる水平引張の静的応力変化(~20MPa)では説明できない．そのため，東北沖地震発生前の時点ですでにプレートが深さ35km近くまで降伏し，強度と同程度の応力レベルまで低下しており，東北沖地震による静的応力変化が加わることで強度レベルを超え地震活動が活発化したと考える必要がある．このような応力場を説明するには，正断層型地震発生域下限の近傍において，室内実験から期待される岩石強度(e.g., Byerlee, 1978) よりも強度が顕著に低下している必要がある．構造探査の結果から示唆される海洋プレート表層部(< ~5km) に存在する流体(Fujie et al., 2018 Nature Comm) や，プレート表層に発達する正断層を介した流体のプレート内部への流入(e.g., Faccenda et al., 2009 Nature Geo) を考えると，この強度低下の原因は流体によるものと推測され，日本海溝付近において流体は深さ35 km程度まで流入していると示唆される．

©2019. Japan Geoscience Union. All Right Reserved.

サブイベント1の断層下端の深さは70kmと推定されたが，この深さはプレート年代から期待される脆性一延性(brittle-ductile)の遷移深さ(~55km) よりも有意に深い．これは，東北沖地震後に起こる粘弾性緩和(e.g., Tomita et al. 2017 Science Adv) に伴ってプレート深部での歪み蓄積速度が大きくなり，それによって延性破壊強度が増加(e.g., Scholtz, 1988) してbrittle-ductileの遷移深さが深部に移動したことで，脆性破壊ができる深さ範囲が深くなったことで断層破壊がプレートの深部まで及んだと考えられる．この結果は，東北沖地震のような，粘弾性緩和の影響が大きい巨大プレート境界型地震の後には，沈み込むプレート内の深部で発生する逆断層型地震の規模が大きくなる可能性を示唆している．

キーワード：2011年東北沖地震、プレート内地震、レオロジー、応力、津波
Keywords: The 2011 Tohoku-Oki earthquake, Intraplate earthquake, Rheology, Stress, Tsunami

©2019. Japan Geoscience Union. All Right Reserved.

Source-rupture process of the intraplate earthquake; its diversity related to the fault geometry and damaged fault zone

*奥脇 亮[1]、八木 勇治[1]
*Ryo Okuwaki[1], Yuji Yagi[1]

1. 筑波大学大学院生命環境科学研究科
1. Graduate School of Life and Environmental Sciences, University of Tsukuba

Supershear rupture is one of the features that characterizes the earthquake-rupture complexity. Both the theoretical analyses and the laboratory experiments suggests that the rupture-front propagation can exceed the shear wave velocity of the medium due to the excess of the energy flux into the rupture tip. However in real earthquakes, extrinsic factor that controls the manner of supershear rupture has yet been well captured and a relationship between the geometric complexity of the fault and the supershear rupture propagation has been elusive. Geometrical complexity of the fault system is a challenging feature against a reliable estimate of kinematic slip evolution on the basis of finite-fault inversion, since the presumed, fixed rectangle-fault plane or even configuration of the multiple rectangles may not necessarily, fully represent a real fault geometry. Especially for the strike-slip (mode-II rupture) earthquake, the radiation pattern of the wave is sensitive around nodal-shear planes, and if the earthquake involves the geometric complexity in the fault system, the radiation pattern at a certain location on a fault cannot be reproduced when the presumed model fault geometry deviates from the real one. Although supershear-rupture propagation has often been observed in the large strike-slip earthquake (e.g. Mw 7.8 2001 Kunlun, Tibet and Mw 7.9 2002 Denali, Alaska earthquakes), such limitations of finite-fault modeling has prevented us to discuss a relationship between supershear rupture and the fault geometry.

Here we present a kinematic rupture model for the intraplate, Mw 7.5 2018 Palu, Indonesia, earthquake. The 2018 Palu earthquake occurred along the strike-slip Palu-Koro fault zone, which is located around the triple junction of the Australia, Eurasia, and Philippines sea plates. The trace of the surface rupture of the 2018 Palu earthquake, mapped by the Interferometric Synthetic Aperture Rader (InSAR), shows the geometric complexity around the epicenter and south of the Palu bay. We inverted the teleseismic waveforms to resolve both the spatiotemporal evolution of shear slip and the variation of fault geometry by representing slip with five-basis potency-density tensors, without forcing a shear plane to be consistent with a pre-fixed model plane. A possibility of supershear rupture was taken into account by resolving slip in a wide parametric-model space with longer duration of slip-rate function and faster maximum rupture velocity.

The resultant model showed that a rupture front persistently propagated at a high speed (~5 km/s) that exceeds the local shear wave velocity throughout 200-km long within 40 s, but also showed the transient deceleration and acceleration of slip migration, which can be seen as an inchworm walking. The transient deceleration and acceleration of the slip migration was resolved in the area where the strike angle was rotated from the reference-model strike (358°), which also coincides with the geometric discontinuity of the surface rupture resolved by the InSAR analyses. We will then discuss possible roles of geometric discontinuity that develops inchworm-like slip evolution and damaged fault zone that enables long-lived supershear rupture propagation, which may be characteristic factors that control diverse rupture process of the intraplate earthquake.

©2019. Japan Geoscience Union. All Right Reserved.

キーワード：プレート内地震、波形インバージョン、断層形状、Supershear rupture、震源過程
Keywords: Intraplate earthquake, Waveform inversion, Fault geometry, Supershear rupture, source rupture process

©2019. Japan Geoscience Union. All Right Reserved.

Aftershocks of the NEXT Cascadia Intraslab Earthquake

*Paul Bodin[1,2]

1. University of Washington Seattle, 2. Pacific Northwest Seismic Network

In 1949, 1965, and 2001 damaging (M6.5-M6.8) deep (~60 km) earthquakes ruptured faults within the Juan de Fuca slab beneath the Puget Sound region of the Cascadia subduction zone in the Pacific Northwest of the U.S.. Each had only a few and very small (approximately M<4) aftershocks. Immediately after the *next* such damaging intraslab earthquake shall we tell the public and first responders that there will likely be no damaging aftershocks? While this low likelihood of aftershocks seems probable based on the historical record, there is no compelling well-agreed-upon physical reason to expect this behavior. For example, recent deep intraslab earthquakes in Japan, Alaska, and Mexico have been followed by strong aftershock sequences. Is the lack of aftershocks following Cascadian intraslab earthquakes unique or extreme? And is it expected and explainable? Possible explanations for regulating the production rate of aftershocks include physical environmental characteristics such as pressure and temperature, geological differences like rock types and faulting geometry, dynamic frictional factors like slip rates, afterslip, and stress drop, and possible roles of fluids. We survey aftershock occurrence following recent smaller Cascadian intraslab earthquakes and following recent large intraslab earthquakes in a number of subduction zones and attempt to classify and distinguish between hypotheses for the lack of Cascadian deep earthquake aftershocks. Is this another possibly unique feature of Cascadia, like the nearly complete lack of instrumentally observed interface earthquakes of any size?

Keywords: intraslab, aftershock, Cascadia, intraplate

©2019. Japan Geoscience Union. All Right Reserved.

[E] 口頭発表 | セッション記号 S (固体地球科学)：S-CG 固体地球科学複合領域・一般

2019年5月30日(木) 13:45 ~ 15:15 | A11 東京ベイ幕張ホール

[S-CG51] Role of volatiles on Earth and planetary dynamics

コンビーナ:石井 貴之(バイロイト大学バイエルン地球科学研究所)、大谷 栄治(東北大学大学院理学研究科地学専攻)、中村 美千彦(東北大学大学院理学研究科地学専攻地球惑星物質科学講座)、Mysen Bjorn(Geophysical Laboratory, Carnegie Inst. Washington)、座長:中村 美千彦、大谷 栄治(東北大学)

This session addresses how volatile species affect dynamics of the
Earth and planets from natural observations, laboratory experiments, and
numerical modeling in the temperature, pressure, and oxygen activity
range from the early stage of the planet formation to the present. The
volatiles can be critical in zones of magma storage and ascent, mantle
upwelling and melting in the fluid-enriched subduction zones, in the
mantle transition zone, in the lower mantle, in the core-mantle boundary,
and in Earth and planetary cores. However, volatiles affect properties
and processes differently depending on their pressure, temperature, and
redox conditions, which vary in time and space.
 This session aims to address how volatiles control the dynamic
processes of the Earth and planets, governed by their geophysical and
geochemical properties. We welcome papers dealing with geological and
laboratory observations coupled with numerical modeling on the role of
volatiles. The topics include (1) Stability relations, chemical and
physical properties of crystalline, molten and fluid phases,
partitioning of volatiles among these phases, (2) Rheological and other
physical properties of minerals, and the effects of intergranular fluid
on the properties, (3) Volatiles and dehydration induced seismicity and
volcanism in various tectonic regions including subduction zones, and (4)
Effects of volatiles in numerical simulation of geo-tectonics, and (5)
Magma outgassing and its control of volcanic eruption dynamics.

13:45 ~ 14:00

[SCG51-01] Constraining the degassing rate of the mantle since 3 Ga using the deficit of xenon-129 in the ancient atmosphere

★Invited Papers

*Bernard Marty[1]、David Bekaert[1]、Michael Broadley[1] (1.Centre de Recherches Pétrographiques et Géochimiques/ CNRS - Universite de Lorraine France)

14:00 ~ 14:15

[SCG51-02] **Investigating volatile cycles in the terrestrial mantle by incorporating He and Ar isotopes into geodynamical models of mantle convection**

★Invited Papers

*Rosie Ellen Jones[1]、Peter van Keken[2]、Jonathan M Tucker[2]、Chris J Ballentine[1] (1.Department of Earth Sciences, University of Oxford, Oxford, UK、2.Department of Terrestrial Magnetism, Carnegie Institution of Washington, Washington, USA)

14:15 ~ 14:30

[SCG51-03] Fluid circulation in the forearc mantle wedge inferred from the dihedral angle in an olivine-H_2O-NaCl system

*Yongsheng HUANG[1]、Takayuki Nakatani[1]、Michihiko Nakamura[1]、Catherine McCammon[2] (1.Graduate School of Science, Tohoku University、2.Byerisches Geoinstitut, University of Bayreuth)

14:30 ~ 14:45

[SCG51-04] The oxygen fugacity of serpentinites: implications for subduction zone redox evolution

*Lisa Eberhard[1]、Dan Frost[1]、Catherine McCammon[1] (1.BGI)

14:45 ~ 15:00

[SCG51-05] Experimental study of the effect of composition on water solubility in natural silicate melts

*山下 茂[1] (1.岡山大学惑星物質研究所)

15:00 ~ 15:15

[SCG51-06] Deep mantle volatile cycle and plate tectonics: Impact to the climate evolution

*中川 貴司[1]、門屋 辰太郎[2]、田近 英一[3] (1.香港大学、2.ワシントン大学、3.東京大学)

Constraining the degassing rate of the mantle since 3 Ga using the deficit of xenon-129 in the ancient atmosphere

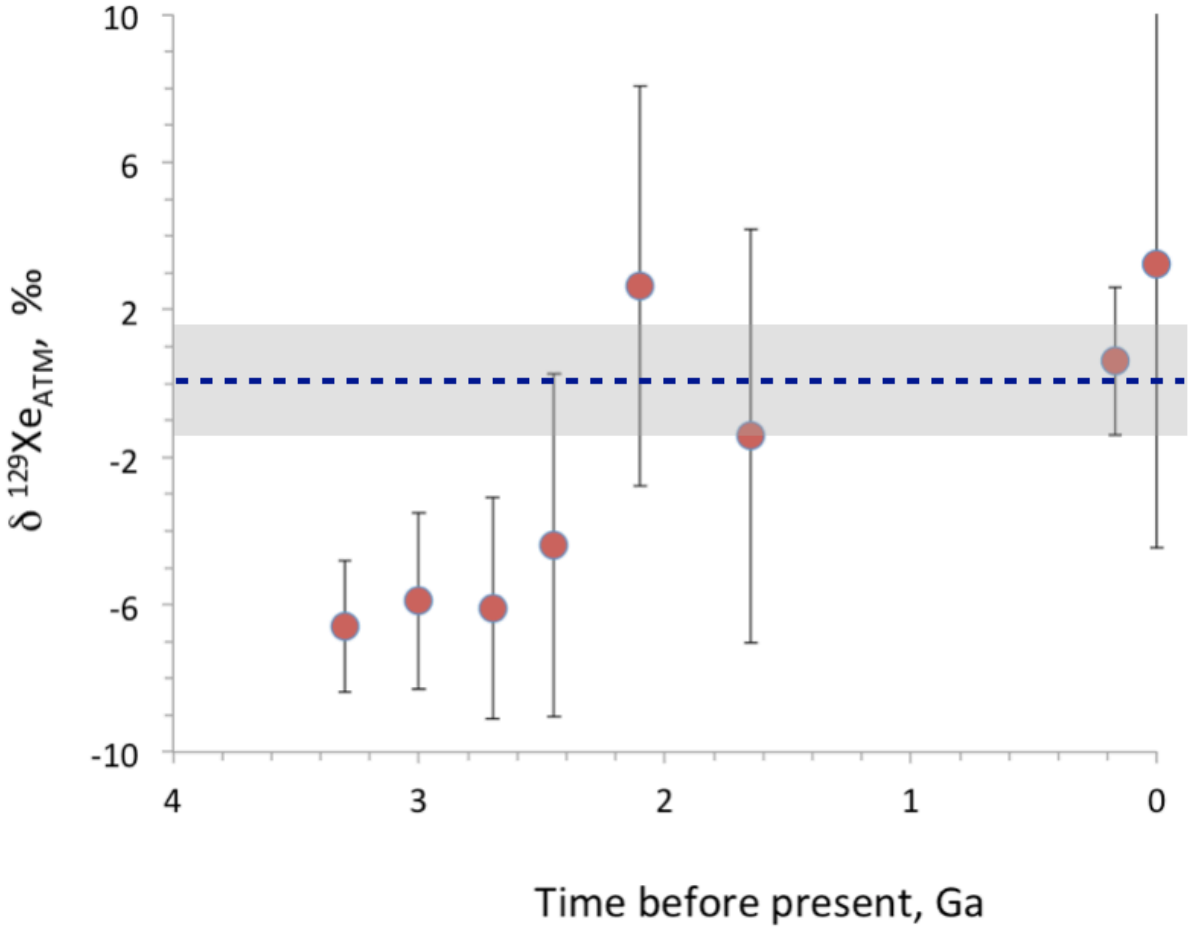
*Bernard Marty[1], David Bekaert[1], Michael Broadley[1]

1. Centre de Recherches Pétrographiques et Géochimiques/ CNRS - Universite de Lorraine France

Degassing of volatile elements from the mantle to the atmosphere requires decompression melting, magma generation and degassing, and is therefore linked to mantle convection. Mantle convection is a physical process that tends to minimize temperature contrasts between the Earth's surface and the deep regions of the mantle. Hence its strength was variable through geological periods of time as it depended on heat generation within the Earth as well as heat dissipation to space. Convection of planetary mantles is a key driver of the evolution of planets and on Earth has been modulating the generation and stabilization of the continental crust. Still the thermal regime of the Earth, and notably the radiogenic/total heat production ratio (the Urey number) are not precisely known. It is related to the distribution of radioactive isotopes (mainly ^{238,235}U, ^{232}Th, ^{40}K) among Earth's reservoirs which varied through time, on the latent heat of core crystallization, on the residual energy of accretion, and on the heat dissipation from the Earth's interior, which depends on mantle convection, a self-regulating process. Geological and geochemical observations have the potential to set constraints on variations of mantle convection in the distant time. Atmospheric xenon presents excesses in ^{129}Xe, an isotope contributed by the decay of extinct iodine-129 ($T_{1/2}$ = 16 Ma). Part of this excess resulted from early degassing of the mantle and, possibily from contributions of comet to early Earth. Mantle degassing also contributed ^{129}Xe to the atmosphere through time since the solid Earth is rich in ^{129}Xe compared to the atmosphere. In agreement with this possibility, remnants of the Archean atmosphere trapped in fluid inclusions (Avice et al *Nature Comm*, 2017, GCA 2018) and in organic matter (Bekaert et al Science Adv 2018) show that xenon in Archean air was depleted in ^{129}Xe compared to the modern composition (see Figure; error bars at 2 s; the grey area represents the reproducibility of air standards at the 2 slevel). However, this deficit cannot be accounted for by the modern degassing rate (as estimated from noble gas fluxes from the mantle), and requires degassing rates two orders of magnitude larger in the distant past than at present. This discrepancy implies a more vigorously convecting Archean-Proterozoic Earth, and suggests a potential impact on the composition of the Archean atmosphere. It also leads credence to models advocating a magmatic origin for drastic environmental changes like the great oxidation event.

Keywords: mantle degassing, Archean, noble gases

©2019. Japan Geoscience Union. All Right Reserved.



©2019. Japan Geoscience Union. All Right Reserved.

Investigating volatile cycles in the terrestrial mantle by incorporating He and Ar isotopes into geodynamical models of mantle convection

*Rosie Ellen Jones[1], Peter van Keken[2], Jonathan M Tucker[2], Chris J Ballentine[1]

1. Department of Earth Sciences, University of Oxford, Oxford, UK, 2. Department of Terrestrial Magnetism, Carnegie Institution of Washington, Washington, USA

The dichotomy in $^{3}He/^{4}He$ isotopes ratios between mid ocean ridge and ocean island basalt samples (MORB and OIB) has provided a fundamental cornerstone in defining the need for a long-lived, volatile rich, and possibly primordial, geochemical reservoir within the deep mantle. However, this is somewhat at odds with evidence from other radiogenic isotope systems (e.g., U-Th-Pb, Lu-Hf, Sm-Nd, Rb-Sr), as well as geophysical evidence, for recycled surficial/crustal material in the deep mantle. Geodynamic models of mantle convection have been developed to incorporate earth-like phase and viscosity changes and can reproduce earth-like surface heat flow and plate motion. When such models take into account the higher density of the subducting oceanic crust, compared to the surrounding mantle, it provides a mechanism of retarding convection in the deepest mantle and reproduces observed geochemical distributions in multiple isotope systems (U-Th-Pb, Rb-Sr, Sm-Nd, Lu-Hf and Re-Os) that define the DMM, HIMU and EMI mantle endmembers (Brandenburg et al., 2008, Jones et al., 2017). Here we use a geodynamical model of mantle convection (Brandenburg et al., 2008), and combine it with geochemical input parameters, to investigate whether the subduction of dense eclogite can retard lower mantle convection sufficiently to explain the observed differences in $^{3}He/^{4}He$ obtained for MORB and OIB. We go on to analyse the effect of ^{3}He outgassing from the Earth's core and early recycling of extra-terrestrial material containing high ^{3}He (e.g., interplanetary dust particles (IDPs)) into the mantle. The K-Ar system is also incorporated into the model and earth-like ^{40}Ar planetary degassing from the mantle is reproduced. We explore the impact of ^{36}Ar recycling on the $^{40}Ar/^{36}Ar$ compositions of MORB and OIB. The results suggest recycling of atmospheric Ar can produce the observed $^{40}Ar/^{36}Ar$ compositions of the upper and lower mantle.

Brandenburg, J.P., Hauri, E.H., van Keken, P.E., Ballentine, C.J., 2008. Earth and Planetary Science Letters 276, 1-13.

Jones, R., van Keken, P. E., Hauri, E., Vervoort, J. D., & Ballentine, C. J., 2017. AGU Fall Meeting Abstracts.

Keywords: He isotopes, Ar isotopes, Mantle convection, Geodynamic model, Geochemistry, Volatiles

©2019. Japan Geoscience Union. All Right Reserved.

Fluid circulation in the forearc mantle wedge inferred from the dihedral angle in an olivine-H_2O-NaCl system

*Yongsheng HUANG[1], Takayuki Nakatani[1], Michihiko Nakamura[1], Catherine McCammon[2]

1. Graduate School of Science, Tohoku University, 2. Byerisches Geoinstitut, University of Bayreuth

In subduction zones, the circulation of slab-released aqueous fluids is crucial to understand the generation of arc magma and recycle of materials, and further to constrain the global geodynamics. The infiltration of aqueous fluids plays an important role in controlling geophysical properties of the mantle wedge such as elasticity, permeability and electrical conductivity. Recently, magnetotellulic studies found a high electrical conductor beneath the fore-arc region which was interpreted as a storage of voluminous slab-derived fluid, implying the presence of permeable mantle wedge at fore-arc depths. By contrast, experimental constraints on dihedral (wetting) angle (θ) in the olivine-H_2O system indicated the fluid is once trapped in isolated pores ($\theta > 60^\circ$) within the down-dragging mantle matrixat fore-arc depths and finally released just beneath the arc volcano where $\theta < 60^\circ$. Here we present the precisely determined dihedral angles in the olivine and NaCl-bearing aqueous fluid (5–27.5 wt% NaCl) system at 1–4 GPa and 800–1100˚C to reveal the influence of NaCl on the fluid connectivity because the NaCl is now recognized to be an important constituent of subduction zone fluids. We found that NaCl significantly decreases θ down to below 60˚ at all the investigated temperature and pressure conditions even at 5 wt% NaCl. Our results suggest that released NaCl-bearing aqueous fluid begins to form an interconnected network in the mantle at relatively shallow depths of ~80 km and can partly penetrate the fore-arc crust without causing mantle melting, which could account for the high electrical conductivity anomalies beneath the for-are region. Our model also emphasizes that partial melting of peridotite triggered by the addition of aqueous fluid can occur more widely than that previously thought, and implies that the release depth of aqueous fluid is not a primary control on the volcanic front position. This work was supported by the JSPS Japanese-German Graduate Externship.

Keywords: dihedral angle, NaCl-bearing, fluid network, mantle wedge, subduction zone

©2019. Japan Geoscience Union. All Right Reserved.

The oxygen fugacity of serpentinites: implications for subduction zone redox evolution

*Lisa Eberhard[1], Dan Frost[1], Catherine McCammon[1]

1. BGI

At subduction zones H_2O and CO_2 are returned to the Earth’ s mantle, bound within hydrous and carbonate minerals. Serpentinites are considered to be major carriers of H_2O into the mantle but natural exposures indicate that some sections of serpentinized mantle also contain significant amounts of carbonate minerals. Determining the fate of so called ophicarbonate rocks presents an important challenge because it involves the interaction between both H_2O- and CO_2- bearing fluids. A further aspect however is that serpentine minerals also contain ferric in addition to ferrous iron. Natural serpentinites record in fact a very wide range of Fe^{3+}/Fe^{tot} ratio but the effect of this ratio on the high pressure stability of serpentine and the relationship with the speciation of coexisting C-O-H fluid phases is unknown.

We have examined the stability of the serpentinite mineral antigorite within ophicabonate assemblages at subarc conditions as a function of P, T and fO_2. Multi-anvil experiments were performed both inside the stability field of antigorite, but also at conditions where antigorite starts to dehydrate. Natural serpentinites are used as starting materials with initially high and low Fe^{3+}/Fe^{tot} ratios. Calcium carbonate was then added to these assemblages to simulate ophicarbonate composition. Iridium metal was added to some nominally unbuffered experiments to allow the oxygen fugacity to be determined, whereas in other experiments the oxygen fugacity was fixed using powders of Ru + RuO_2 and Re + ReO_2 distributed throughout the sample. Ferrous Fe is located in the octahedral site of antigorite whereas ferric Fe may additionally occupy the tetrahedral site of the trioctahedral 1:1 sheet silicates, providing charge balance. We have determined the location and speciation of the Fe atoms in serpentinites as a function of fO_2, P and T by using Mössbauer spectroscopy to examine the run products of the multi-anvil experiments.

The experiments were run for approximately 3 days during which it was possible to change the Fe^{3+}/Fe^{tot} ratios of the starting materials to both higher and lower ratios depending on the redox buffers employed. We found that the relationship between the Fe^{3+}/Fe^{tot} ratio of antigorite and the oxygen fugacity is very temperature dependent with antigorite Fe^{3+}/Fe^{tot} ratios decreasing sharply at the same oxygen fugacity as dehydration commences. This behaviour should cause the oxygen fugacity within subducting lithosphere to increase as dehydration takes place, which will have important implications for fluid speciation. On the other hand the stabilisation of ferric iron in antigorite at high oxygen fugacities appears to have a minimal effect on the temperature of dehydration.

Keywords: Serpentine, subduction zone, f(O2), Multi-anvil, Mössbauer spectroscopy

©2019. Japan Geoscience Union. All Right Reserved.

Experimental study of the effect of composition on water solubility in natural silicate melts

*山下 茂[1]
*Shigeru Yamashita[1]

1. 岡山大学惑星物質研究所
1. Institute for Planetary Materials, Okayama University

Water is the first dominant volatile dissolved in magmas. Oversaturation and exsolution of the water in magmas affects the buoyancy and excess vapor pressure of the system, and hence the water solubility in silicate melts is fundamental in controlling magma transport beneath volcanoes. Many experimental studies of the solubility for water in natural silicate melts are now available, but most of them were performed over a limited range of composition. For example, published solubility data for water are rather sparse for the natural silicate melts having moderate SiO_2 contents. This has resulted in insufficient data coverage of composition space, which makes difficult to precisely model if a melt is subject of compositional change due to partial crystallization, assimilation, or magma hybridization. This study presents results from experimental determinations of the solubility for water in a natural dacitic melt at near-the liquidus and the superheated conditions.

The starting material for the experiments was the natural subalkaline dacite JA1 (GSJ standard reference material, ~65 wt% SiO_2). A nominally anhydrous glass was prepared from the starting material, and the glass was equilibrated with water in an internally heated pressure vessel for ~24 hours at 1000-1200 ˚C and 100-200 MPa. Double capsule technique was employed to control the oxygen fugacity in the sample along Ni-NiO buffer during the experiments. The water content in the quenched glass was determined from the near infrared absorption intensities of the hydroxyl groups band at ~4500 cm^{-1} and the molecular water band at ~5200 cm^{-1} using the molar absorption coefficients of Ohlhost et al. (2001).

Results of this study are overall consistent with previous determinations of pressure- and temperature-dependence of water solubility in rhyolitic melts. Water solubility in the dacitic melt increases with pressure at a fixed temperature, and decreases with temperature at a fixed pressure. On the other hand, the water solubility in the dacitic melt was found to be 10-20 % (relative, on the mole fraction basis) greater than those previously determined by Holtz et al. (1992; 1995) and Yamashita (1999) for the rhyolitic melts when compared at the same pressure and temperature condition. This advocates that the effect of melt composition play a noticeable role in controlling the degree of water oversaturation during magmatic processes. When a hotter basaltic magma is injected to a colder rhyolitic magma body, a purely thermal effect on water solubility enhances formation of vapor bubbles in the rhyolitic magma (e.g., Yamashita, 1999). Once hybridization between the melt portions of the two magmas proceeds, the effect of melt composition on water solubility becomes important, i.e., already present, sub-millimeter size bubbles (thus their buoyant separation is limited) can be resorbed by the hybridized melt which has an intermediate composition.

References: Holtz et al., Chem. Geol., 96, 289-302, 1992; Holtz et al., Amer. Mineral., 80, 94-108, 1995; Ohlhost et al., Chem. Geol., 174, 5-20, 2001; Yamashita, J. Petrol., 40, 1497-1507, 1999.

キーワード：マグマ、水の溶解度、組成依存性

©2019. Japan Geoscience Union. All Right Reserved.

Keywords: magma, water solubility, composition dependence

©2019. Japan Geoscience Union. All Right Reserved.

Deep mantle volatile cycle and plate tectonics: Impact to the climate evolution

*中川 貴司[1]、門屋 辰太郎[2]、田近 英一[3]
*Takashi Nakagawa[1], Shintaro Kadoya[2], Eiichi Tajika[3]

1. 香港大学、2. ワシントン大学、3. 東京大学
1. Department of Earth Sciences, The University of Hong Kong, 2. Department of Earth and Space Sciences, University of Washington, 3. Department of Earth and Planetary Sciences, The University of Tokyo

We investigate the deep mantle volatile (water and carbon) cycle and its impact to plate tectonics and climate evolution in the numerical mantle convection simulations couping with the energy balance model of the surface climate model. To calculate the mantle water cycle, the storage capacity model of water in each mantle minerals as functions of temperature and pressure is incorporated into numerical mantle convection simulations so that the dehydration process can be included in the numerical model of mantle water cycling as well as the regassing and degassing processes. However, the decarbonation process cannot be included because the storage capacity model of carbon is not well-established. In three migration processes of mantle volatiles, the volcanic degassing plays a significant role because the volatile composition of the atmosphere-ocean system can be described as a balance between degassing flux and silicate weathering effects as uptake of the volatile components. As a result, the optical properties of the atmosphere-ocean system such as the Albedo and planetary radiation are changed with the volcanic degassing. Other two migration processes may be worked for regulating the volatile content stored in the deep planetary interior and inventory of surface volatile reservoir. The style of plate tectonics driven by mantle convection may strongly affect the style of climate evolution and inventory of surface volatile reservoir. In the stagnant lid mode of mantle convection, the snowball climate is dominated for over a few billion years because the strong radiative cooling is controlled due to less amount of volcanic degassing associated with the stagnant lid convection. Whereas, the continuous carbon degassing is expected in the continuous surface plate motions so that the mild climate can be found, which allows having the liquid water over a few billion years on the planetary surface. In order to preserve the amount of surface seawater on the planetary surface as the present-day amount of surface seawater on the Earth, the required amount of the water in the entire planetary system may be around 10 to 12 Ocean Masses of present-day Earth's water ocean. Therefore, the mantle volatile cycle concerning with the plate tectonics driven by mantle convection may control the habitability of the rocky planets such as the Earth.

キーワード：プレートテクトニクス、揮発性元素サイクル、気候進化
Keywords: plate tectonics, volatile cycle, climate evolution

©2019. Japan Geoscience Union. All Right Reserved.

[E] 口頭発表 | セッション記号 S (固体地球科学)：S-CG 固体地球科学複合領域・一般

2019年5月30日(木) 15:30 ~ 17:00 | A11 東京ベイ幕張ホール

[S-CG51] Role of volatiles on Earth and planetary dynamics

コンビーナ:石井 貴之(バイロイト大学バイエルン地球科学研究所)、大谷 栄治(東北大学大学院理学研究科地学専攻)、中村 美千彦(東北大学大学院理学研究科地学専攻地球惑星物質科学講座)、Mysen Bjorn(Geophysical Laboratory, Carnegie Inst. Washington)、座長:石井 貴之(バイロイト大学バイエルン地球科学研究所)、Bjorn Mysen(Carnegie Institution of Washington)

This session addresses how volatile species affect dynamics of the
Earth and planets from natural observations, laboratory experiments, and
numerical modeling in the temperature, pressure, and oxygen activity
range from the early stage of the planet formation to the present. The
volatiles can be critical in zones of magma storage and ascent, mantle
upwelling and melting in the fluid-enriched subduction zones, in the
mantle transition zone, in the lower mantle, in the core-mantle boundary,
and in Earth and planetary cores. However, volatiles affect properties
and processes differently depending on their pressure, temperature, and
redox conditions, which vary in time and space.
 This session aims to address how volatiles control the dynamic
processes of the Earth and planets, governed by their geophysical and
geochemical properties. We welcome papers dealing with geological and
laboratory observations coupled with numerical modeling on the role of
volatiles. The topics include (1) Stability relations, chemical and
physical properties of crystalline, molten and fluid phases,
partitioning of volatiles among these phases, (2) Rheological and other
physical properties of minerals, and the effects of intergranular fluid
on the properties, (3) Volatiles and dehydration induced seismicity and
volcanism in various tectonic regions including subduction zones, and (4)
Effects of volatiles in numerical simulation of geo-tectonics, and (5)
Magma outgassing and its control of volcanic eruption dynamics.

15:30 ~ 15:45

[SCG51-07] The nature of water induced small degree melts in the deep mantle

★Invited Papers

*Daniel James Frost[1]、Pierre Condamine[3]、Davide Novella[2]、Rong Huang[1] (1.University of Bayreuth、2.University of Cambridge、3.Université de Lorraine)

15:45 ~ 16:00

[SCG51-08] **Phase separation of hydrous Vesuvius melt: vesicle nucleation or spinodal decomposition?**

★Invited Papers

*Anja Allabar[1]、Marcus Nowak[1] (1.University of Tuebingen)

16:00 ~ 16:15

[SCG51-09] Role of water on dynamics in the lower mantle and core-mantle boundary regions

*Eiji Ohtani[1]、Takayuki Ishii[2]、Liang Yuan[1]、Daijo Ikuta[1]、Tomoo Katsura[2]、Dan Frost[2] (1.Department of Earth and Planetary Materials Science, Graduate School of Science, Tohoku University、2.Bavarian Research Institute, University of Bayreuth)

16:15 ~ 16:30

[SCG51-10] Stability of Fe-bearing hydrous phases and element partitioning in the system MgO-Al_2O_3-Fe_2O_3-SiO_2-H_2O in Earth's lowermost mantle

*Hongsheng Yuan[1]、Li Zhang[1]、Eiji Ohtani[2]、Yue Meng[3]、Eran Greenberg[4]、Vitali B. Prakapenka[4] (1.Center for High Pressure Science and Technology Advanced Research、2.Department of Earth Science, Graduate School of Science, Tohoku University、3.HPCAT, X-Ray Science Division, Argonne National Laboratory、4.Center for Advanced Radiation Sources, University of Chicago)

16:30 ~ 16:45

[SCG51-11] **Laboratory Micro-Seismicity during Serpentinite Deformation as a Potential Analogue for Lower Wadati-Benioff Plane Seismicity**

*Julien Gasc[1,3]、Nadège Hilairet[2]、Tony Yu[3]、Yanbin Wang[3]、Thomas P. Ferrand[1]、Alexandre Schubnel[1] (1.Laboratoire de Géologie, CNRS - ENS, Paris, FRANCE、2.Unité Matériaux et Transformations, CNRS - Lille University, Villeneuve d'Ascq, FRANCE、3.GeoSoilEnviro-CARS, University of Chicago, Argonne IL, USA)

16:45 ~ 17:00

[SCG51-12] Water transport and mixing in the whole-mantle scale convection

*金子 岳郎[1]、中久喜 伴益[1]、亀山 真典[2]、岩森 光[3] (1.広島大学大学院理学研究科地球惑星システム学専攻、2.愛媛大学地球深部ダイナミクス研究センター、3.東京大学地震研究所)

The nature of water induced small degree melts in the deep mantle

*Daniel James Frost[1], Pierre Condamine[3], Davide Novella[2], Rong Huang[1]

1. University of Bayreuth, 2. University of Cambridge, 3. Université de Lorraine

Slow S-wave velocities in the deep mantle have been used to argue for the presence of hydrous silicate melts. Small degree partial melts could potentially be formed due to a reduction in the H_2O storage capacity of mantle minerals due to pressure induced phase transitions or as a result of redox processes. Hydrous melt layers could accumulate at certain depths in the mantle due to neutral buoyancy. Water concentrations in the ambient mantle are at most likely to lead to only small degrees of melting. Such incipient melts would be in equilibrium with a peridotite assemblage containing minerals that would be practically identical in major elements as the unmelted assemblage. The compositions of such melts are important because their water contents constrain the relationship between melt fraction and the bulk water content. Furthermore, the water content and the iron content would mainly determine their buoyancy. To assess if neutrally buoyant small degree hydrous melt layers exist in the mantle and to determine how much water would need to be present to create them requires experimental determination of their compositions.

Determining the chemical composition of low degree melts and particularly their water contents is experimentally very challenging. At pressures higher than 2 GPa melts no longer quench to form glasses and can therefore not be analyzed to determine water contents. Small melt fractions are very hard to analyze due to their very small volume and due to modification through reaction with solid phases during quenching. One way to overcome these problems and produce an analyzable portion of incipient melt composition is by performing sandwich experiments. In this method an initial first guess melt composition is equilibrated with a sub-equal proportion of peridotite. The resulting melt is then re- equilibrated with peridotite in a series of iterative experiments until a composition is obtained that is in equilibrium with the entire peridotite assemblage.

We have used this procedure to determine the compositions of incipient melts at depths equivalent to around 200 and 400 km in the mantle at adiabatic temperatures. The sandwich technique has to be modified in a number of ways when used at very high pressures, mainly to ensure that water contents can be accurately determined through mass balance. The resulting melts have affinities with the major classes of kimberlite magmas and their compositions can be used to assess their buoyancy in the deep mantle.

Keywords: Pressure, Transition zone

©2019. Japan Geoscience Union. All Right Reserved.

Phase separation of hydrous Vesuvius melt: vesicle nucleation or spinodal decomposition?

*Anja Allabar[1], Marcus Nowak[1]

1. University of Tuebingen

The phase separation of H_2O fluids from supersaturated hydrous silicate melts determines the starting point of explosive volcanic eruptions. The number of fluid vesicles per unit volume of silicate melt (*VND*) is a basic property that controls the efficiency of fluid-melt separation and as a result the acceleration of magma ascent. To simulate the phase separation of single phase hydrous silicate melts during ascent, continuous decompression experiments were performed at superliquidus temperatures with AD79 Vesuvius white pumice composition. This pumice buried Herculaneum and Pompeii and is representative of other catastrophic phonolitic and trachytic explosive eruptions like the violent 39 ka Campi Flegrei and the 1815 AD Tambora eruption.
Experiments were conducted in an internally heated pressure vessel equipped with a high-pressure valve that facilitates continuous decompression. 5.3 wt% H_2O were dissolved in the melts at 200 MPa and 1523 K for 96 h. Subsequently, the slightly H_2O undersaturated melts were isothermally decompressed at 1323 or 1373 K with rates of 0.024-1.7 MPa·s^{-1}. At final pressures (P_{final}) between 110 and 70 MPa, the samples were isobarically quenched with ~150 K·s^{-1} to room temperature. The *VND* of the vitreous samples were determined with optical microscopy and quantitative backscattered electron image analysis combined with computational 2D to 3D transformation.
Homogeneously dispersed vesicles are observed in the samples decompressed to a P_{final} ≦100 MPa which corresponds to a ΔP of ~95 MPa that is necessary to induce homogeneous phase separation. High log *VND*'*s* of ~5.2 (in mm^{-3}), corresponding to average vesicle distances of 10 μm, are observed irrespective of decompression rate within the investigated range. A nucleation theory based decompression rate meter (Toramaru, 2006), which is commonly used to estimate magma ascent velocity from *VND* of volcanic ejecta, fails to explain the experimentally observed decompression rate independent *VND*. Alternatively, decompression induced H_2O-silicate melt phase separation may be described by the theory of spinodal decomposition (Cahn, 1965) at the limit of thermodynamic stability. Critical behavior of hydrous silicate melt has already been evidenced experimentally by e.g. Shen and Keppler (1997) and is attributed to spinodal decomposition.
Irrespective of the phase separation mechanism, a decompression rate independent *VND* has profound consequences for the degassing dynamics of natural polyphase hydrous magma, that contain crystals and pre-existing fluid vesicles. During ascent, H_2O supersaturation is decreased in melt shells surrounding pre-existing vesicles by H_2O diffusion. Homogeneous phase separation occurs in interstitial melt volumes in which sufficient supersaturation is still preserved. If the decompression rate is fast enough to maintain such supersaturated volumes, the formation of vesicles with high log*VND* of 5.2 inevitably causes efficient melt degassing within seconds due to short H_2O diffusion distances on a 10 μm scale from the melt into fluid vesicles. This causes rapid density decrease accompanied by sudden increase of magma buoyancy required for explosive volcanism.

Cahn, J.W., 1965. J. Chem. Phys. 42, 93–99.
Shen, A.H., Keppler, H., 1997. Nature 385, 710–712.
Toramaru, A., 2006. J. Volcanol. Geotherm. Res. 154, 303–316.

©2019. Japan Geoscience Union. All Right Reserved.

Keywords: magma degassing, magma ascent rate, vesicle number density, spinodal decomposition, phase separation

©2019. Japan Geoscience Union. All Right Reserved.

Role of water on dynamics in the lower mantle and core-mantle boundary regions

*Eiji Ohtani[1], Takayuki Ishii[2], Liang Yuan[1], Daijo Ikuta[1], Tomoo Katsura[2], Dan Frost[2]

1. Department of Earth and Planetary Materials Science, Graduate School of Science, Tohoku University, 2. Bavarian Research Institute, University of Bayreuth

Recent experimental evidence indicated that the Earth’ s transition zone contains some amount of water at least locally. Subduction of the slabs into the lower mantle can transport water further into the lower mantle. One of the most important candidates of the water carrier into the lower mantle is hydrous phase delta-AlOOH and phase H-$MgSiO_4H_2$ solid solution. Our works on the stability of this solid solution revealed that it coexists with bridgmanite under the lower mantle conditions [1, 2].

We studied the hydrogen and aluminum partitioning between alumina and hydrogen between the delta-H solid solution and aluminous bridgmanite at high pressure and temperature. We observed that bridgmanite under the wet conditions depleted in aluminum, and it contains almost no water under the wet lower mantle conditions at 28 GPa and 800-1400°C. This partitioning of H and Al can provide significant effect on lower mantle dynamics through the change of the garnet-bridgmanite phase boundary, the pressure of the spin transition of both bridgmanite and delta-H solid solution, and bridganite-postperovskite transition.

The supply of water to the core-mantle boundary can create a reaction of water and iron in the core to produce FeO_2H and its reaction product postperovskite Fe_2O_3. These phases together with the delta-H solid solution can play important roles at the bottom of the lower mantle. Physical properties of these phases can account for the sound velocity and density anomalies in the regions such as ULVZ (ultra-low velocity zone) and LLSVP (large low shear velocity province) [3].

References:

[1] Ohira et al. (2014) Earth Planet. Sci. Lett., 401: 12–17, [2] Ohtani et al. (2018) Jour. Asian Earth Sci. 2018, [3] Yuan et al. (2018) Geophys. Res. Lett.,45. doi.org/10.1002/2017GL0757

Keywords: Water, lower mantle, hydrous mineral, phase delta, phase H, bridgmanite

©2019. Japan Geoscience Union. All Right Reserved.

Stability of Fe-bearing hydrous phases and element partitioning in the system MgO-Al_2O_3-Fe_2O_3-SiO_2-H_2O in Earth's lowermost mantle

*Hongsheng Yuan[1], Li Zhang[1], Eiji Ohtani[2], Yue Meng[3], Eran Greenberg[4], Vitali B. Prakapenka [4]

1. Center for High Pressure Science and Technology Advanced Research, 2. Department of Earth Science, Graduate School of Science, Tohoku University, 3. HPCAT, X-Ray Science Division, Argonne National Laboratory, 4. Center for Advanced Radiation Sources, University of Chicago

We performed experiments on a synthetic hydrous gel consisting of a model composition of subducted slabs in the MgO–Al_2O_3–Fe_2O_3–SiO_2–H_2O system and containing ~7 wt.% water. The experiments were conducted in laser-heated diamond anvil cells under high pressure–temperature (*P-T*) conditions corresponding to the lowermost mantle using *in situ* synchrotron X-ray diffraction and *ex situ* transmission electron microscope techniques. The hydrous δ-phase AlOOH–FeOOH–$MgSiO_2(OH)_2$–SiO_2 (with an orthorhombic symmetry and the space group of *Pnnm*) coexists with bridgmanite (Bdg), post-perovskite (pPv), or both in a broad *P-T* range of 104–126 GPa and 1900–2500 K, whereas the pyrite-type (py) $FeOOH_x$ phase was only observed to coexist with the pPv phase by *in situ* XRD. Chemical analysis on recovered samples showed that (i) in the Bdg-bearing assemblage quenched from 104 GPa and 1900 K, the Bdg phase contains ~8 at.% Al and ~11 at.% Fe, and the coexisting hydrous δ-phase contains ~70 at.% Al and ~14 at.% Fe; (ii) in the pPv-bearing assemblage quenched from 117 GPa and 2050 K, the pPv phase contains ~7 at.% Al and ~16 at.% Fe, and the coexisting hydrous δ-phase contains ~81 at.% Al and ~9 at.% Fe. The considerable $Fe_2O_2(OH)_2$ (8–13 mol%) and SiO_2 (9–13 mol%) content in the δ-phase does not reduce its thermal stability; therefore, the Fe-bearing δ-phase can transport water to the lowermost mantle along the mantle geotherm. The dense py-phase may accumulate in the lowermost mantle in the presence of the pPv phase. In a hydrous system, Al_2O_3 depletion in both the Bdg and pPv phases can significantly reduce the width of the Bdg to pPv transition compared with the width in a dry system. On the other hand, significant Fe enrichment in pPv relative to the coexisting Bdg lowers the transition pressure to the depth of the D'' discontinuity. Accordingly, the depth and thickness of the Bdg to pPv transition in subducted hydrous basaltic crustal materials might explain the seismically detected D'' discontinuity. The formation of the dense hydrous py-phase in subducted slabs may contribute to chemical heterogeneities in the lowermost mantle.

Keywords: deep lower mantle, hydrous phase, bridgmanite to post-perovskite transition, synchrotron X-ray diffraction, multigrain analysis

©2019. Japan Geoscience Union. All Right Reserved.

Laboratory Micro-Seismicity during Serpentinite Deformation as a Potential Analogue for Lower Wadati-Benioff Plane Seismicity

*Julien Gasc[1,3], Nadège Hilairet[2], Tony Yu[3], Yanbin Wang[3], Thomas P. Ferrand[1], Alexandre Schubnel[1]

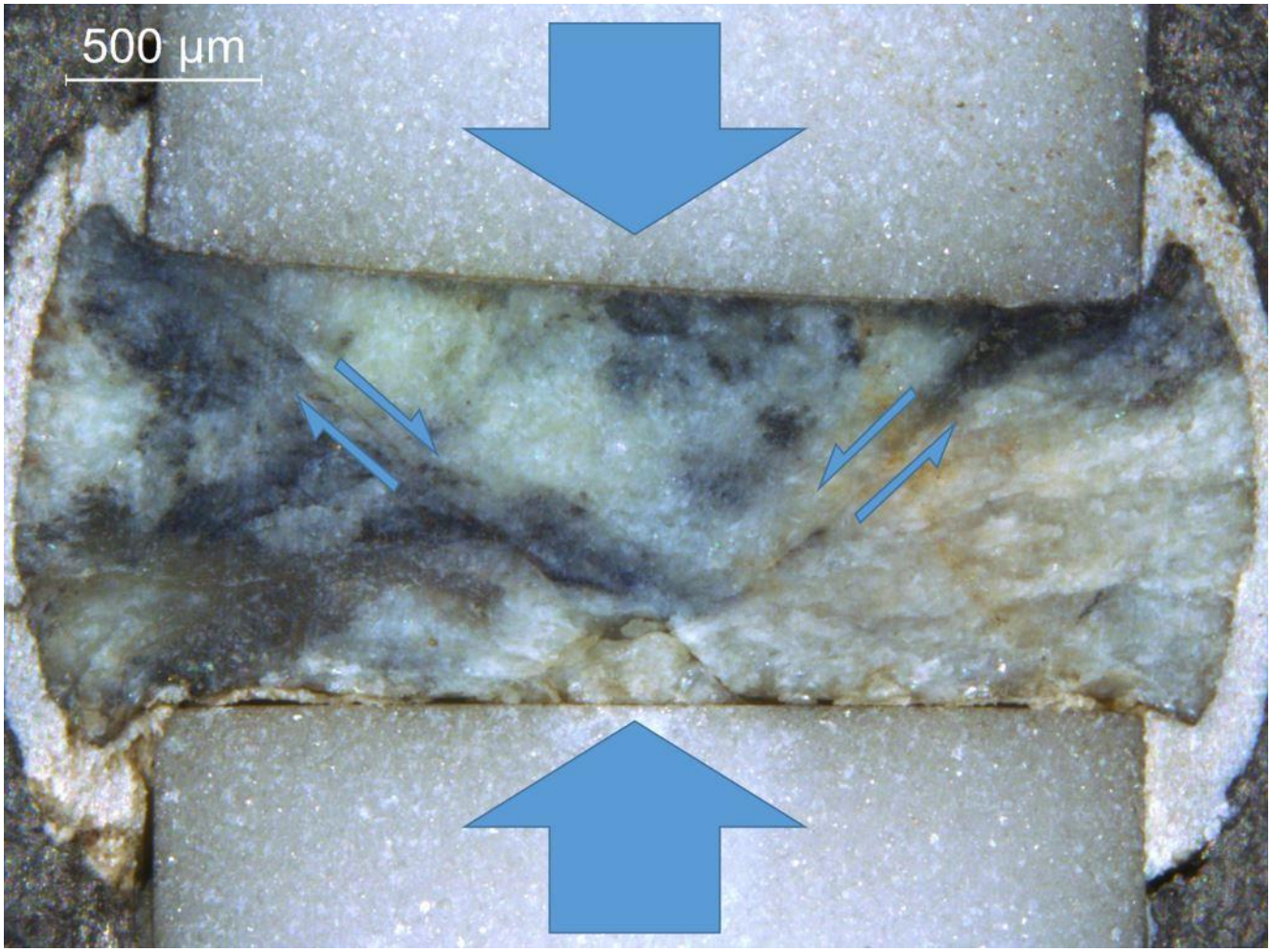
1. Laboratoire de Géologie, CNRS - ENS, Paris, FRANCE, 2. Unité Matériaux et Transformations, CNRS - Lille University, Villeneuve d'Ascq, FRANCE, 3. GeoSoilEnviro-CARS, University of Chicago, Argonne IL, USA

The origin of intermediate-depth earthquakes, which occur at depths of 60-300 km along subducting slabs, remains somehow enigmatic. In the pressure and temperature conditions involved, rocks should indeed deform in a ductile fashion. Dehydration embrittlement, due to serpentine breakdown, was long considered a good candidate to explain lower Wadati-Benioff plane seismicity. However, unlike in the classic dehydration embrittlement theory, dehydration induced volume changes are negative at such depths and cannot trigger instabilities via pore pressure buildup. Accordingly, some experimental studies have shown that faulting of serpentinites related to dehydration, occurs in a stable and aseismic way (Chernak and Hirth, 2011; Gasc et al., 2011). Nevertheless, tremendous progress was recently made in understanding the mechanics of intermediate earthquakes, notably thanks to the combination of high pressure deformation experiments and in-situ synchrotron techniques. In order to assess the seismic potential of serpentinites, micro-seismicity was monitored during high pressure experiments by recording Acoustic Emissions (AE’s) –or labquakes. A D-DIA apparatus was used to deform natural antigorite-rich samples at pressures of 1-5 GPa, both within and outside antigorite’s stability field.

Below 400˚C, the deformation of fully hydrated serpentinite samples involves aseismic ductile cataclastic flow. Above 600˚C, despite conditions propitious to dehydration embrittlement (i.e., with fast strain rates and reaction kinetics), joint deformation and dehydration also lead to ductile shear, without generation of AE’s. However, samples show a brittle temperature window around 500˚C that seems to correlate with the very onset of the mineral’s breakdown, and is therefore not associated to significant release of water. In this latter case, AE’s are consistently collected upon faulting and extremely sharp strain localization is observed (Gasc et al., 2017). In addition, brittle faulting of partly hydrated samples (a mixture of olivine and antigorite) can also occur with minor amounts of antigorite, due to stress percolation upon antigorite breakdown. Unlike for low-pressure dehydration embrittlement, faulting is also enabled here by the metastability of the solid phase rather than by fluid overpressure and dynamic fault propagation occurs concomitantly with the appearance of pseudotachylites along the fault plane (Ferrand et al., 2017).
Both brittle failure mechanisms identified in these studies share major similarities with the now-classic concept of transformational faulting (Burnley et al., 1991), often invoked for deep-focus earthquakes, and both may be a source of seismicity in subducting slabs. We provide evidence that destabilizing antigorite at mantle depths can initiate faulting and thus be involved in intermediate-depth earthquakes. However, analysis of the acoustic signal shows that it is relatively weaker than its real-earth counterpart, once scaled relative to standard brittle faulting. This suggests that other mechanisms are responsible for large intermediate-depth earthquakes, which may reflect fault propagation in the adjacent peridotitic mantle.

Keywords: intermediate-depth earthquakes, serpentinite, high pressure, deformation experiments, acoustic emissions

©2019. Japan Geoscience Union. All Right Reserved.



©2019. Japan Geoscience Union. All Right Reserved.

Water transport and mixing in the whole-mantle scale convection

*金子 岳郎[1]、中久喜 伴益[1]、亀山 真典[2]、岩森 光[3]
*Takeo Kaneko[1], Tomoeki Nakakuki[1], Masanori Kameyama[2], Hikaru Iwamori[3]

1. 広島大学大学院理学研究科地球惑星システム学専攻、2. 愛媛大学地球深部ダイナミクス研究センター、3. 東京大学地震研究所
1. Department of Earth and Planetary Systems Science, Graduate School of Science, Hiroshima University, 2. Geodynamics Research Center, Ehime University, 3. Earthquake Research Institute, University of Tokyo

The subduction of oceanic plates transports sea water with the basaltic crust to the Earth’ s interior. High-pressures experiments reveal that nominally anhydrous minerals (NAMs) contain the water of a few thousands ppm in the weight fraction. On the other hand, numerical simulations show that the NAMs layer above the subducted slab plays an important role in water transport into the deep mantle. However, the details of the water circulation and distribution processes on the whole mantle has still not been understood well.
We perform numerical simulations of isoviscous mantle convection in a two-dimensional cylinder in which hydrous-mineral phase changes and the hydration-dehydration reaction are considered. We systematically examined the effects of parameters that control activity and mixing efficiency of the mantle convection, i.e., the Rayleigh number, the internal heating rate, and the water storage capacity of the lower mantle, on the water transport into the deep mantle.
The distribution and total amount of the water transported into the mantle strongly depends on the convection style. When the internal heating is absent, stable cellular flow dominates the mantle convection. The stable convection does not mix water well so that the water distributes only near the convection cell boundary. When the mantle has the internal heating, the mantle flow becomes strongly time-dependent by thermal boundary layer instabilities. Migration of the convection cell boundary enhances the mixing of the water into the whole mantle. In addition, mixing efficiency increases with the Rayleigh number, which is an index indicating convective vigor. When the water storage capacity of the lower mantle is much smaller than the NAMs, the ejected water forms the regional hydrous layer with high water content over the 660 km discontinuity near the downwellings. However, these hydrous regions are hindered from globally spreading to the mantle transition zone. The water content in most of the mantle rocks becomes equal to the smaller value among water storage capacities of the NAMs in the upper mantle and the lower mantle finally, though the upper mantle can accommodate more water. The amount of the water stored in the whole mantle rocks is, therefore, smaller than the summation of their capacities. As a result, the equilibrium of the water regassing and degassing is realized more rapidly than the whole mantle rocks are completely saturated.

©2019. Japan Geoscience Union. All Right Reserved.

[E] 口頭発表 | セッション記号 M (領域外・複数領域)：M-IS ジョイント

2019年5月30日(木) 13:45 ~ 15:15 | 304 3F

[M-IS03] アジア・モンスーンの進化と変動，新生代全球気候変化におけるモンスーンの位置づけ

コンビーナ:山本 正伸(北海道大学大学院地球環境科学研究院)、多田 隆治(東京大学大学院理学系研究科地球惑星科学専攻)、座長:山本 正伸(北海道大学)、入野 智久、久保田 好美(国立科学博物館)、多田 隆治(東京大学)

The Asian Monsoon (AM) is a part of interhemispheric atmospheric phenomena that is driven by the thermal gradient between ocean and land. Contrasts of insolation, heat content and latent heat transfer between ocean and land may have affected the behavior of the AM in the past, but the proxy records are occasionally controversial and do not show a clear picture of the AM variability. Recent proxy and modeling studies suggest that glacial pCO2 cycles could be related to the position of southern westerlies, which is sensitive to interhemispheric heat imbalance. Because monsoon is driven by the heat imbalance, knowledge on the variability of the AM is important to understand the behavior of the global climate system. In this session, presentations on the reconstruction of long-term AM variability from various archives such as IODP expedition cores, discussion on its forcing, and the roles of the AM in global climate changes are welcome.

13:45 ~ 14:00

[MIS03-01] Reconstruction of Indian summer monsoon variability during the last 1,460,000 years

*山本 正伸[1]、クレメンス スティーブ[2] (1.北海道大学大学院地球環境科学研究院、2.ブラウン大学地球環境惑星科学科)

14:00 ~ 14:20

[MIS03-02] Pleistocene Seawater $\delta^{18}O$ reconstructions from the Indian and East Asian Monsoon Regions

★Invited Papers

*Steven C Clemens[1]、Masanobu Yamamoto[2] (1.Brown University、2.Hokkaido University)

14:20 ~ 14:40

[MIS03-03] The Monsoon Erosion Pump

★Invited Papers
Cancelled

*Liviu Giosan[1] (1.Woods Hole Oceanographic Institution)

14:40 ~ 15:00

[MIS03-04] East Asian winter monsoon intensity in the Pleistocene based on seasonal land snail shell stable isotope ratios

★Invited Papers

*David L Dettman[1,3]、Xin Wang[2]、Mi Wang[2]、Junhui Zhang[2] (1.University of Arizona, Geosciences Dept., Environmental Isotope Lab.、2.Lanzhou University, Key Laboratory of Western China's Environmental Systems, College of Earth and Environmental Sciences、3.Shimane University, Estuary Research Center)

15:00 ~ 15:15

[MIS03-05] Reconstruction of ventilation history of the Japan Sea based on physical properties data collected during IODP Exp. 346

*入野 智久[1]、Liviu Giosan[2]、多田 隆治[3]、池原 研[4] (1.北海道大学　大学院地球環境科学研究院、2.Woods Hole Oceanographic Institution、3.東京大学大学院　理学系研究科、4.産業技術総合研究所　地質情報部門)

Reconstruction of Indian summer monsoon variability during the last 1,460,000 years

*山本 正伸[1]、クレメンス スティーブ[2]
*Masanobu Yamamoto[1], Steven Clemens[2]

1. 北海道大学大学院地球環境科学研究院、2. ブラウン大学地球環境惑星科学科
1. Faculty of Environmental Earth Science, Hokkaido University, 2. Department of Earth, Environmental and Planetary Sciences, Brown University

Monsoon is an atmospheric phenomenon dominant in low and mid-latitudes and determines the temporal and spatial distributions of rainfall that govern vegetation. A classical model assumes that monsoon responds to precession-controlled changes in seasonal insolation. Speleothem records show a precession cycle in oxygen isotope variation consistent with this model, but marine and loess records generally do not show strong precession variation. This mismatch has long been debated. Key approach is the precipitation reconstruction to understand past changes in summer monsoon. In this study, we generated an Indian summer monsoon (ISM) record by evaluating riverine discharge. We used GDGT indices, i.e., CBT and MBT, as a proxy of soil organic matter contribution and generated a 1,700-year resolution record of Mahanadi River soil discharge in IODP Site U1446 to understand changes in the ISM rainfall during the last 1,460,000 years. The CBT and BIT show a similar variation according to glacial-interglacial cycles. Maxima appeared after the peak of interglacial. Minima appeared during deglaciations. Their variations are reversely correlated with the sea water $\delta^{18}O$ obtained based on *G. ruber* $\delta^{18}O$, global $\delta^{18}O$ and TEX_{86}-based SST. The records are consistent with previously-reported ISM records from marine archives and Borneo speleothems in the overlap periods and different from Chinese speleothem records. Spectral analysis indicates that BIT and CBT show 100,000, 41,000, 30,000, 23,000 and 19,000-year cycles during the last 800,000 years, the variation was out of phase with variation in northern hemisphere summer insolation. This suggests that the ISM did not respond directly to orbital forcing, in contrast to the classical hypothesis, but was driven by internal feedback processes. Orbital cycles were not clearly shown prior to 800,000 years ago. This suggests that the strong response of the ISM to orbital forcing was initiated around 800,000 years ago, which coincided with the onset of glacial 100,000 year cycles.

キーワード：インド夏季モンスーン、更新世、IODP
Keywords: Indian summer monsoon, Pleistocene, IODP

©2019. Japan Geoscience Union. All Right Reserved.

Pleistocene Seawater $\delta^{18}O$ reconstructions from the Indian and East Asian Monsoon Regions

*Steven C Clemens[1], Masanobu Yamamoto[2]

1. Brown University, 2. Hokkaido University

The study of orbital-scale climate change during the late Pleistocene is unique in that the signal-to-noise ratio is large, the external forcing (insolation) is known, and the critical internal forcings (greenhouse gases and terrestrial ice volume) are well constrained. As such, it should be possible to assess the underlying mechanisms driving climate change at this time scale, as well as the relative sensitivity to these forcing mechanisms.

We present three reconstructions of local seawater $\delta^{18}O$, including previously published records from the East China Sea (U1429)[*S. C. Clemens et al.*, 2018], the Andaman Sea (NGHP 17)[*Gebregiorgis et al.*, 2018], and our new work from the northeast Indian Margin, Bay of Bengal (U1446). Local seawater $\delta^{18}O$ is based on removal of the SST and global seawater $\delta^{18}O$ from planktonic foraminifer $\delta^{18}O$ and reflects changes in surface salinity driven by rainfall and runoff from surrounding catchment basins. This proxy offers an independent reconstruction for comparison to speleothem $\delta^{18}O$ and other proxies in order to assess driving mechanisms and the extent to which the Indian and East Asian subsystems covary with one another.

In the northern East China Sea, *G. ruber* $\delta^{18}O$ has the same precession- and millennial-scale structure as the onshore speleothem $\delta^{18}O$ record from the Yangtze River Valley[*Cheng et al.*, 2016]. However, after removing the temperature and global seawater $\delta^{18}O$ signals, the offshore seawater $\delta^{18}O$ has almost no precession-scale (23 kyr) variance)[*S. C. Clemens et al.*, 2018]. This result contrasts with the speleothem record, which is almost exclusively dominated by precession-scale variance, and argues against external insolation as the primary driver of East Asian monsoon rainfall in the Yangtze River Valley region.

The Andaman Sea record monitors direct rainfall and runoff from the Irrawaddy and Salween catchment basins. The precession-band timing of low seawater $\delta^{18}O$ (increased rainfall, low mixed-layer salinity) indicates that strong monsoonal rainfall lags maximum northern hemisphere insolation by ~9 kyrs at the precession band[*Gebregiorgis et al.*, 2018]. Our new Indian Margin record resides within the low-salinity East India Coastal Current fed by runoff from the Ganges-Brahmaputra complex, the Mahanadi Basin, and direct rainfall. The Indian Margin seawater $\delta^{18}O$ reconstruction also demonstrates this large lag. The lag in both these records agrees with that of the summer-season (southwest) monsoon wind strength records from the NW Arabian Sea[*S.C. Clemens and Prell*, 2003; *S.C. Clemens et al.*, 1991].

This precession-band timing (lagging minimum precession by 7-9 kyrs) precludes insolation as a direct forcing for Indian monsoon rainfall and wind strength, pointing instead to decreased high-latitude ice volume, increased greenhouse gasses, and latent heat export from the southern hemisphere as the primary drivers of monsoon circulation at these time scales[*S.C. Clemens and Prell*, 2003].

©2019. Japan Geoscience Union. All Right Reserved.

Cheng, H., et al. (2016), The Asian monsoon over the past 640,000 years and ice age terminations, Nature, 534(7609), 640-646, doi: 10.1038/nature18591

Clemens, S. C., and W. L. Prell (2003), A 350,000 year summer-monsoon multi-proxy stack from the Owen Ridge, Northern Arabian Sea, Marine Geology, 201, 35-51.

Clemens, S. C., W. L. Prell, D. Murray, G. Shimmield, and G. Weedon (1991), Forcing mechanisms of the Indian Ocean monsoon, Nature, 353, 720-725.

Clemens, S. C., A. Holbourn, Y. Kubota, K. E. Lee, Z. Liu, G. Chen, A. Nelson, and B. Fox-Kemper (2018), Precession-band variance missing from East Asian monsoon runoff, Nature Communications, 9(1), 3364, doi: 10.1038/s41467-018-05814-0.

Gebregiorgis, D., E. C. Hathorne, L. Giosan, S. Clemens, D. Nürnberg, and M. Frank (2018), Southern Hemisphere forcing of South Asian monsoon precipitation over the past ~1 million years, Nature Communications, 9(1), 4702, doi: 10.1038/s41467-018-07076-2.

Keywords: East Asian Monsoon, Indian Monsoon, East China Sea, Bay of Bengal, Paleoclimate, Greenhouse Gas

©2019. Japan Geoscience Union. All Right Reserved.

The Monsoon Erosion Pump

*Liviu Giosan[1]

1. Woods Hole Oceanographic Institution

Understanding the factors controlling the flux of materials from land to oceans has key implications for global biogeochemical cycling and the links between the sedimentary record and landscape evolution. Monsoonal climates are recognized as prodigious sediment producers but conflicting proxy reconstructions limit assessing their influence on land-sea material transfers at various timescales. Here I discuss the concept of a monsoon erosion pump based on terrestrial and oceanic records reconstructed from recent Indian National Gas Hydrate Program and IODP drilling in the Bay of Bengal, Arabian and Andaman Seas. From millennial to orbital to tectonic timescales, these records suggest that vegetation land cover interacts and modulates the regime of erosion and weathering under perennial but variable monsoonal rain conditions. Under this new proposed interpretation the Indian monsoon exhibits two distinct flavours during the Cenozoic that can be largely explained by its heartbeat, or astronomical forcing. This erosional regime is mediated by the global glacial state and attendant sea level and by limiting conditions imposed by the paleogeography of Asia.

Keywords: monsoon, India, erosion

©2019. Japan Geoscience Union. All Right Reserved.

East Asian winter monsoon intensity in the Pleistocene based on seasonal land snail shell stable isotope ratios

*David L Dettman[1,3], Xin Wang[2], Mi Wang[2], Junhui Zhang[2]

1. University of Arizona, Geosciences Dept., Environmental Isotope Lab., 2. Lanzhou University, Key Laboratory of Western China's Environmental Systems, College of Earth and Environmental Sciences, 3. Shimane University, Estuary Research Center

Monsoon climates are characterized by strong seasonal oscillations between a very wet season and very dry conditions. The study of ancient variation in monsoon climate strength and its impact on regional environments is difficult because geological materials rarely record individual seasons. It is difficult to infer seasonal change through time when working with oxygen isotope records that average multiple years or centuries. One solution is to use high-resolution sampling of land snail shells as monitors of wet-season and dry-season differences. Although land snail fossils are often rare, in many cases they are well preserved and widely distributed across the planet. We subsampled shells along the spiral growth axis, producing 15 to 35 samples per shell to document maximum and minimum oxygen and carbon stable isotope ratios. The most robust signal in land snail shell oxygen isotope records is connected to evaporation. The arid dry-season leads to significant evaporation in the land snail body water, which elevates the δ18O values recorded in the shell. Wet-season oxygen isotope ratios are more negative and can be tied roughly to the δ18O of wet season precipitation and summer temperatures. Carbon isotope ratios are tied to the diet of the animals, and reveal the proportion of C3 and C4 plants in the landscape.

Larger land snail (> 1.5 cm diameter) taxa have behaviors that can lead to significant evaporation of body water, as they are willing to range away from local water sources. Modern samples show that the total amplitude in oxygen isotope variation in a shell can be related to the intensity and duration of the dry season. This suggests that amplitudes in ancient shells are indicators of the winter monsoon strength. Although under extremely arid conditions snail growth occurs only when surface water is available and d18O amplitudes collapse in desert conditions. The most negative δ18O values are not correlated with the intensity of the summer monsoon, suggesting that δ18O values are not good indicators of summer monsoon strength.

Data from one genus of land snail (*Cathaica* species) living on the Chinese loess plateau throughout the late Pleistocene allow us to make some generalizations about monsoon climate in this region. In general, the oxygen isotope amplitude in shells from glacial periods are larger than those from the interglacial periods. This suggests that the East Asian Winter Monsoon was strongest during glacial intervals on the Loess Plateau. The largest δ18O amplitude observed was 19.2 ‰. Marine Isotope Stages 2, 6, and 8 have the largest amplitudes and, by inference, the strongest winter monsoons in our record. Older glacial intervals seem to have weaker winter monsoons. However, glacial amplitudes were not always larger, just as climate undergoes significant short-term variation in glacial intervals (such as D-O cycles and Heinrich events) oxygen isotope amplitudes show large amounts of variability in glacial times. In contrast, interglacial intervals tend to have smaller δ18O amplitudes, pointing to warmer and wetter winters in interglacial times. But like the glacial data, some interglacial amplitudes are larger than some glacial records. These data show that the differences in high frequency climate variability is as large as the differences between glacial and interglacial climates.

©2019. Japan Geoscience Union. All Right Reserved.

Keywords: Winter Monsoon, Seasonality, Oxygen isotopes, Land Snails

©2019. Japan Geoscience Union. All Right Reserved.

Reconstruction of ventilation history of the Japan Sea based on physical properties data collected during IODP Exp. 346

*入野 智久[1]、Liviu Giosan[2]、多田 隆治[3]、池原 研[4]
*Tomohisa Irino[1], Liviu Giosan[2], Ryuji Tada[3], Ken Ikehara[4]

1. 北海道大学　大学院地球環境科学研究院、2. Woods Hole Oceanographic Institution、3. 東京大学大学院　理学系研究科、4. 産業技術総合研究所　地質情報部門
1. Faculty of Environmental Earth Science, Hokkaido University, 2. Woods Hole Oceanographic Institution, 3. Graduate School of Science, University of Tokyo, 4. Institute of Geology and Geoinformation, National Institute of Advanced Industrial Science and Technology

The Japan Sea is a semi-enclosed marginal sea located at the eastern edge of Asian continent and under the influence of east Asian monsoon. The primary production is controlled by nutrient supply from the East China Sea by summer monsoon, while deep water ventilation is promoted by winter monsoon cooling of the surface water of the Japan Sea. Perfectly continuous sediment splice sequences were established at Sites U1422-U1427 and U1430 which have been correlated among others using apparent dark-light cycles. The coverage of water depths are, in ascending order, 330 m at Site U1427, 903 m at Site U1426, 1072 m at Site U1430, 1785 m at Site U1423, 1909 m at Site U1425, 2808 m at Site U1424, and 3429 m at Site U1422, which enable us to reconstruct the temporal variation of depth distribution of organic carbon flux related to the past primary production and deep water ventilation in the Japan Sea.

For calculation of the mass accumulation of organic carbon (OC flux) at each site, we used the perfectly continuous records of dry bulk density (DBD) and total organic carbon content (TOC) calculated from shipboard measurements such as gamma-ray attenuation (GRA) density with grain density and a strong negative correlation between TOC and photo RGB values, respectively. Linear sedimentation rate (LSR) of each site was estimated based on the projection of the age model established at Site U1424 by tuning the GRA variation onto LR04 benthic oxygen isotope curve. Based on the consistent correlation among sites, depth distribution of OC flux was reconstructed for 1 ky step during the last 1.5 million years.

Princple component analysis for depth-temporal OC flux distribuion suggests that three princple component explain 74% of the total variance. Principle component (PC) 1 loading was positively correlated with all the sites except for the U1427 (330 m), while PC2 loading was correlated positively with sites shallower than 1000 m and negatively with those deeper than 2000 m. PC3 loading was correlated negatively with sites around 1000 m and positively with other sites. Such depth dependent patterns suggest that primary production (PC2) and ventilation (PC1) at middle to deeper depth were primary controls on the OC deposition. PC3 may indicate stronger middle depth ventilation or (oppositely) formation of oxygen minimum zone.

We also examined the color variation of these sediments using metric hue. Sediment color varies between dull green (higher hue) and olive (lower hue). Average metric hue is about 88 degree for all the site and variability is smaller for shallower sites. The metric hue at Site U1425 (1909 m) varies in harmony with the score of PC1, and lower metric hue is associated with larger PC1 score. Namely, higher OC flux (a lower oxygenation level) was associated with more olive color, which could be interpreted that dull green background (detritus) color was overridden by olive color reduced iron. Such an agreement between independently estimated variables suggests that the deep water ventilation intensity in the Japan Sea could be independently reconstructed as a proxy of winter monsoon intensity.

©2019. Japan Geoscience Union. All Right Reserved.

キーワード：日本海、有機物フラックス、中深層水換気、IODP Expedition 346
Keywords: Japan Sea, Organic carbon flux, Ventilation, IODP Expedition 346

©2019. Japan Geoscience Union. All Right Reserved.

[E] 口頭発表 | セッション記号 M (領域外・複数領域)：M-IS ジョイント

2019年5月30日(木) 15:30 ~ 17:00 | 304 3F

[M-IS03] アジア・モンスーンの進化と変動，新生代全球気候変化におけるモンスーンの位置づけ

コンビーナ:山本 正伸(北海道大学大学院地球環境科学研究院)、多田 隆治(東京大学大学院理学系研究科地球惑星科学専攻)、座長:多田 隆治(東京大学)、久保田 好美(国立科学博物館)、山本 正伸(北海道大学)

The Asian Monsoon (AM) is a part of interhemispheric atmospheric phenomena that is driven by the thermal gradient between ocean and land. Contrasts of insolation, heat content and latent heat transfer between ocean and land may have affected the behavior of the AM in the past, but the proxy records are occasionally controversial and do not show a clear picture of the AM variability. Recent proxy and modeling studies suggest that glacial pCO2 cycles could be related to the position of southern westerlies, which is sensitive to interhemispheric heat imbalance. Because monsoon is driven by the heat imbalance, knowledge on the variability of the AM is important to understand the behavior of the global climate system. In this session, presentations on the reconstruction of long-term AM variability from various archives such as IODP expedition cores, discussion on its forcing, and the roles of the AM in global climate changes are welcome.

15:30 ~ 15:45

[MIS03-06] The spatial-temporal patterns of Indian monsoonal variations during the past 80 kyr recorded in NGHP-02 Hole 19B, western Bay of Bengal: Implications from chemical and mineral properties

*太田 雄貴[1,2,3,4]、川幡 穂高[4]、黒田 潤一郎[4,3]、鈴木 淳[2]、荒岡 大輔[2]、山口 飛鳥[4]、阿部 彩子[4] (1.東京大学大学院理学系研究科地球惑星科学専攻、2.産業技術総合研究所、3.海洋開発研究機構、4.東京大学大気海洋研究所)

15:45 ~ 16:05

[MIS03-07] **400,000 years millennial scale temperature and rainfall in East Asia deduced from paired Mg/Ca and oxygen isotope of planktic foraminifera from the East China Sea**

★Invited Papers

*久保田 好美[1]、Steven Clemens[2]、Kyung-Eun Lee[3]、Ann Holbourn[4]、脇坂 恵都子[5]、堀川 恵司[5]、多田 隆治[6]、木元 克典[7] (1.国立科学博物館、2.ブラウン大学、3.韓国海洋大学、4.クリスチャンアルブレヒト大学、5.富山大学、6.東京大学、7.海洋研究開発機構)

16:05 ~ 16:20

[MIS03-08] 日本海堆積物に記録された東アジアモンスーン千年スケール変動の開始と時代変化：新しいデータによる新しい解釈

*多田 隆治[1]、入野 智久[2]、関 有沙[3]、村山 雅史[4]、三武 司[1]、池田 昌之[5] (1.東京大学大学院理学系研究科地球惑星科学専攻、2.北海道大学大学院地球環境科学研究院、3.信州大学理学部、4.高知大学農林海洋科学部海洋資源科学科、5.静岡大学)

16:20 ~ 16:40

[MIS03-09] Interhemispheric linkages of Australian and Asian monsoons on a warmer-than-modern Earth

★Invited Papers

*Ann E Holbourn[1]、Wolfgang Kuhnt[1]、Janika Joehnck[1]、Sebastian Beil[1]、Julia Luebbers[1]、Kenji Marc Raymond Matsuzaki[2]、Yair Rosenthal[3]、Denise Kulhanek[4]、IODP Expedition 363 Scientists (1.University of Kiel、2.University of Tokyo、3.Rutgers University、4.Texas A&M University)

16:40 ~ 17:00

[MIS03-10] **Miocene evolution of the Asian Monsoon from climate and productivity proxies in the Bay of Bengal and South China Sea**

★Invited Papers

*Wolfgang Kuhnt[1]、Julia Luebbers[1]、Ann Holbourn[1]、Karlos GD Kochhann[2]、Steven C Clemens[3]、Clara T Bolton[4]、Yoichi Usui[5] (1.University of Kiel、2.UNISINOS University、3.Brown University、4.Aix-Marseille Université、5.Japan Agency for Marine-Earth Science and Technology)

The spatial-temporal patterns of Indian monsoonal variations during the past 80 kyr recorded in NGHP-02 Hole 19B, western Bay of Bengal: Implications from chemical and mineral properties

*太田 雄貴[1,2,3,4]、川幡 穂高[4]、黒田 潤一郎[4,3]、鈴木 淳[2]、荒岡 大輔[2]、山口 飛鳥[4]、阿部 彩子[4]
*Yuki Ota[1,2,3,4], Hodaka Kawahata[4], Junichiro Kuroda[4,3], Atsushi Suzuki[2], Daisuke Araoka[2], Asuka Yamaguchi[4], Ayako Abe-Ouchi[4]

1. 東京大学大学院理学系研究科地球惑星科学専攻、2. 産業技術総合研究所、3. 海洋開発研究機構、4. 東京大学大気海洋研究所
1. Department of Earth and Planetary Science, The University of Tokyo, 2. Geological Survey of Japan, National Institute of Advanced Industrial Science and Technology, 3. Department of Biogeochemistry, Japan Agency for Marine-Earth Science and Technology, 4. Atmosphere and Ocean Research Institute, The University of Tokyo

Detailed reconstruction of Indian summer monsoons is necessary to better understand the late Quaternary climate history of the Bay of Bengal and Indian peninsula. We established a chronostratigraphy for a sediment core from Hole 19B in the western Bay of Bengal, extending to approximately 80 kyr BP, and examined major and trace element compositions and clay mineral components of the sediments. Lower lithogenic matter flux, higher $\delta^{18}O$ values, and weaker weathering in the sediment source area during marine isotope stages (MIS) 2 and 4 compared to MIS 1, 3, and 5 are explained by increased Indian summer monsoonal precipitation and river discharge around the western Bay of Bengal. Chemical components indicate a felsic sediment source, suggesting the Precambrian gneissic complex of the eastern Indian peninsula as the dominant sediment source at this site since 80 kyr. Trace element ratios indicate increased sediment contributions from mafic rocks during MIS 2 and 4. We interpret these results as reflecting the changing influences of the eastern and western branches of the Indian summer monsoon, and a greater decrease in rainfall in the eastern and northeastern parts of the Indian peninsula than in the western part during MIS 2 and 4.

キーワード：インドモンスーン、ベンガル湾堆積物、後期第四紀
Keywords: Indian Monsoon, Bay of Bengal sediments, late Quaternary

©2019. Japan Geoscience Union. All Right Reserved.

400,000 years millennial scale temperature and rainfall in East Asia deduced from paired Mg/Ca and oxygen isotope of planktic foraminifera from the East China Sea

*久保田 好美[1]、Steven Clemens[2]、Kyung-Eun Lee[3]、Ann Holbourn[4]、脇坂 恵都子[5]、堀川 恵司[5]、多田 隆治[6]、木元 克典[7]
*Yoshimi Kubota[1], Steven Clemens[2], Kyung-Eun Lee[3], Ann Holbourn[4], Etsuko Wakisaka[5], Keiji Horikawa[5], Ryuji Tada[6], Katsunori Kimoto[7]

1. 国立科学博物館、2. ブラウン大学、3. 韓国海洋大学、4. クリスチャンアルブレヒト大学、5. 富山大学、6. 東京大学、7. 海洋研究開発機構
1. National Museum of Nature and Science, 2. Brown University, 3. Korea Maritime and Ocean University, 4. Christian-Albrechts-University, 5. University of Toyama, 6. The University of Tokyo, 7. Japan Agency for Marine-Earth Science and Technology

Abrupt millennial-scale climate changes during the late Quaternary were widely recognized in the East Asian monsoon region from deep-sea sediments in the Japan Sea and more recently from oxygen isotope ($\delta^{18}O$) variability in Chinese speleothems ($\delta^{18}O_{sp}$). The finely ^{230}Th-dating method on the speleothems enables comparison to climate records from other regions on millennial scale, and there is little doubt that the variability of these $\delta^{18}O_{sp}$ records is synchronized with climate perturbation in the North Atlantic high latitude, known as Heinrich events and with Dansgaard-Oeschger (D-O) oscillations in Greenland. However, mechanisms of the climate response in East Asia remain unclear due to the lack of fundamental agreement on what the $\delta^{18}O_{sp}$ climate signal represents. A primary impediment to interpreting the variability in $\delta^{18}O_{sp}$ is the lack of the means to decompose $\delta^{18}O_{sp}$ into constituent components. By contrast, the $\delta^{18}O$ of calcite planktic foraminifers ($\delta^{18}O_p$) from nearshore marine sediments can be quantitatively partitioned into sea surface temperature (SST) and $\delta^{18}O_w$ of seawater ($\delta^{18}O_w$), a function of sea surface salinity (SSS). In this study, millennial-scale climate variability in East Asia is investigated using 400,000-yr records of SST, $\delta^{18}O_p$, and $\delta^{18}O_w$ from the East China Sea (IODP Site U1429). $\delta^{18}O_w$ can be interpreted as reflecting SSS, hence rainfall, as the monsoonal runoff from the Yangtze River determines summer SSS in the northern East China Sea. As a result, SST and $\delta^{18}O_w$ variability accounts for 58% and 35% of the total variability of $\delta^{18}O_p$ and the rest (6%) is the ice volume component or noise; the primary contributor to $\delta^{18}O_p$ variations is SST, and the secondary is $\delta^{18}O_w$. Foraminiferal $\delta^{18}O_p$ shows the strongest similarly with Chinese $\delta^{18}O_{sp}$, indicating that $\delta^{18}O_{sp}$ is best interpreted as the combination of changes in surface temperature and monsoon rainfall; it is not indicative of summer monsoon rainfall alone. Partitioning of variance between temperature and rainfall does not change on glacial-interglacial timescales indicating that the hemispheric teleconnection mechanism between the Atlantic and East Asia does not depend on the global climate background status (CO_2, ice volume). In comparison with the millennial scale Greenland temperature, the East China Sea SST decreases and $\delta^{18}O_w$ increases (rainfall deceases) in most of the North Atlantic cold events (e.g., Heinrichs). However, SST and $\delta^{18}O_w$ exhibit overall poor coherence, revealing that these climate parameters fundamentally behave differently on the millennial scale, but tend to respond in the manner described above (decrease in temperature and rainfall) once a severe cold event occurs in the North Atlantic.

キーワード：アジアモンスーン、東シナ海、千年スケール気候変動、酸素同位体比、マグネシウム・カルシウム比、IODP Exp.346

©2019. Japan Geoscience Union. All Right Reserved.

Keywords: Asian Monsoon, East China Sea, Millennial-scale climate variability, oxygen isotope, Mg/Ca, IODP Exp.346

©2019. Japan Geoscience Union. All Right Reserved.

日本海堆積物に記録された東アジアモンスーン千年スケール変動の開始と時代変化：新しいデータによる新しい解釈
Onset and evolution of millennial-scale variability of East Asian Monsoon recorded in the Japan Sea sediments: New data with new interpretation

*多田 隆治[1]、入野 智久[2]、関 有沙[3]、村山 雅史[4]、三武 司[1]、池田 昌之[5]
*Ryuji Tada[1], Tomohisa Irino[2], Arisa Seki[3], Masafumi Murayama[4], Kaz Mitake[1], Masayuki Ikeda[5]

1. 東京大学大学院理学系研究科地球惑星科学専攻、2. 北海道大学大学院地球環境科学研究院、3. 信州大学理学部、4. 高知大学農林海洋科学部海洋資源科学科、5. 静岡大学
1. Department of Earth and Planetary Science, Graduate School of Science, The Univeristy of Tokyo, 2. Faculty of Environmental Earth Science, Hokkaido University, 3. Faculty of Science, Shinshu University, 4. Faculty of Agriculture and Marine Science, 5. Shizuoka University

New XRF scanner data from U1426 on Oki Ridge and comparison with those of the deeper sites U1424 and 1425 revealed Br (MOC proxy) profile of deeper sites are significantly influenced by post-depositional oxidation during the early diagenesis while Br profile of shallower site (U1426) better preserve surface productivity signal. Thus we use Br profile of U1426 during the last 3 Ma to analyze past changes in millennial-scale variability of East Asian Summer Monsoon intensity and the response of the Japan Sea to such changes. The result suggests several new information which will be presented at 2019JpGU.

キーワード：東アジア夏季モンスーン、日本海
Keywords: East Asian Summer Monsoon, Japan Sea

©2019. Japan Geoscience Union. All Right Reserved.

Interhemispheric linkages of Australian and Asian monsoons on a warmer-than-modern Earth

*Ann E Holbourn[1], Wolfgang Kuhnt[1], Janika Joehnck[1], Sebastian Beil[1], Julia Luebbers[1], Kenji Marc Raymond Matsuzaki[2], Yair Rosenthal[3], Denise Kulhanek[4], IODP Expedition 363 Scientists -

1. University of Kiel, 2. University of Tokyo, 3. Rutgers University, 4. Texas A&M University

The large-scale Asian-Australian monsoon system consists of several regional subsystems that are dynamically linked through the annual migration of the Intertropical Convergence Zone across the equator, but exhibit distinct responses to external (local insolation) and internal (e.g., ice volume, greenhouse gas concentrations) forcings. Here we provide a long-term perspective of regional variability under different mean-state climate conditions. We focus on the 8 to 5 Ma period, which was characterized by warmer-than-modern climate conditions, but was also marked by distinct reversals in climate trends including transient cooling events exhibiting similarities to late Pleistocene Heinrich stadials. Extended sediment archives recovered by the Ocean Drilling Program (ODP) and the International Ocean Discovery Program (IODP) in the South China Sea, Bay of Bengal and off Northwest Australia allow direct comparison of Northern and Southern Hemisphere monsoonal subsystems on orbital timescales. High-resolution XRF-scanner derived estimates of terrigenous discharge, foraminiferal Mg/Ca derived mixed layer temperatures and stable isotopes reveal cooling and strengthening of the Northern Hemisphere winter monsoon starting at ~7 Ma. This intensification occurred synchronously with an increase in monsoonal seasonality in the Southern Hemisphere. In all regions, summer monsoonal precipitation intensified after ~5.5 Ma in tandem with globally rising sea surface temperatures. Our results suggest that changes in latitudinal temperature gradients, greenhouse gas concentrations and moisture budgets strongly influenced the long-term evolution of the Australian and Asian monsoons during the transition from a unipolar to a bipolar glaciated Earth.

Keywords: Asian-Australian Monsoon, late Miocene, International Ocean Discovery Program, Foraminiferal stable isotopes, Foraminiferal Mg/Ca, X-ray fluorescence scanner elemental data

©2019. Japan Geoscience Union. All Right Reserved.

Miocene evolution of the Asian Monsoon from climate and productivity proxies in the Bay of Bengal and South China Sea

*Wolfgang Kuhnt[1], Julia Luebbers[1], Ann Holbourn[1], Karlos GD Kochhann[2], Steven C Clemens[3], Clara T Bolton[4], Yoichi Usui[5]

1. University of Kiel, 2. UNISINOS University, 3. Brown University, 4. Aix-Marseille Université, 5. Japan Agency for Marine-Earth Science and Technology

Export particle flux from primary production and terrigenous input in combination with planktic and benthic foraminiferal isotope records were used to monitor monsoon-related paleoceanographic changes in the Bay of Bengal (Indian Monsoon) and South China Sea (East Asian Monsoon) through the middle to late Miocene. Proxy indicators of carbon export flux to the seafloor and carbonate accumulation rates at International Ocean Discovery Program (IODP) Site U1443 located in 2925 m water depth at the northern end of the Ninetyeast Ridge closely track changes in the carbonate budget of the deep Indian Ocean. Prolonged intervals of low carbonate concentrations and accumulation rates from ~17 to 15 Ma and from ~13.2 to 8.7 Ma indicate episodes of reduced carbonate deposition, which correlate with the globally recognized early to middle Miocene “Carbonate Drought” and the middle to late Miocene “Carbonate Crash”. The global occurrence of these events implies that changes in chemical weathering and in the riverine input of calcium and alkalinity into the ocean reservoir (rather than changes in circulation or inter-ocean carbonate fractionation) drove carbonate accumulation in the deep Indian Ocean. Higher XRF-scanner derived Log(Ba/Ti) together with a change in the redox state of deep sea sediments at ~11.2 Ma indicate a rise in biological production and export flux to the sea floor. A contemporaneous stepwise steepening of the gradient between mixed layer and deep ocean $\delta^{13}C$ starting from a minimum at ~11 Ma also indicates intensification of the biological pump at Ocean Drilling Program (ODP) Site 1146 (2091 m water depth) in the South China Sea. We suggest that the attendant increase in carbonate accumulation in the Indian Ocean was linked to increased nutrient flux and intensification of upper ocean mixing, associated with changes in the seasonality and intensity of the Asian monsoon.

Keywords: Asian Monsoon, Miocene, International Ocean Discovery Program , Foraminiferal stable isotopes, Foraminiferal Mg/Ca, X-ray fluorescence scanning elemental data

©2019. Japan Geoscience Union. All Right Reserved.

[E] 口頭発表 | セッション記号 M (領域外・複数領域)：M-IS ジョイント

2019年5月30日(木) 13:45 ~ 15:15 | A02 東京ベイ幕張ホール

[M-IS04] Interdisciplinary studies on pre-earthquake processes

コンビーナ:服部 克巳(千葉大学大学院理学研究科)、劉 正彦(国立中央大学太空科学研究所)、Ouzounov Dimitar(Center of Excellence in Earth Systems Modeling & Observations (CEESMO) , Schmid College of Science & Technology Chapman University, Orange, California, USA)、Qinghua Huang(Peking University)、座長:Jann-Yenq Liu(National Central University, Taiwan)、長尾 年恭

This session expands the interdisciplinary discussions on preparation process of earthquake and earthquake predictability by presenting the latest progress in studying the physically based pre-earthquake phenomena. New observations from space and ground have provided
evidences, which may enhance better understanding of tectonic activity. The session anticipates talks that include but not limited to observations and analyses of seismic, electrical, electromagnetic, electro-chemical and thermodynamic processes related to stress changes in the lithosphere along with their statistical and physical validation. Presentations on the latest observational results associated with major earthquakes obtained by different methodologies are welcomed. The topics of the session are as follows but not limited.

-General discussion on earthquake preparation process and the physics of pre-earthquake signals

- Theory, modeling, laboratory experiments, computational simulation for generation and propagation of pre-earthquake signals and their connection with seismic cycle

 - Multi-parameter observations, detection, and validation of pre-earthquake signals

 - Cross-disciplinary studies, practical and technical approaches for better understanding of earthquake preparation processes and their connection with seismicity

13:45 ~ 14:00

[MIS04-01] Application of blind source separation method in seismo-magnetic data analysis

★Invited Papers

*Peng Han[1]、Yi Zhong[1]、Yuanyuan Zhou[1]、Yonghui Ma[2]、Chengliang Xie[3]、Katsumi Hattori[4]、Chie Yoshino[4] (1.Southern University of Science and Technology, Shenzhen, China、2.Harbin Institute of Technology (Shenzhen), Shenzhen 518055, China、3.China University of Geosciences (Beijing), Beijing, 100083, China、4.Chiba University, Chiba, Japan)

14:00 ~ 14:15

[MIS04-02] 房総旭観測点近傍の地震活動と地中ラドン濃度変動

*小島 春奈[1]、服部 克巳[2]、吉野 千恵[2]、下 道國[3]、小西 敏春[4]、古屋 隆一[5] (1.千葉大学大学院融合理工学府地球環境科学専攻地球科学コース、2.千葉大学大学院理学研究院、3.藤田保健衛生大学、4.応用光研株式会社、5.コムシステム株式会社)

14:15 ~ 14:30

[MIS04-03] Geochemical evidence for the occurrence of 2018 Hualien earthquake triggered by earlier earthquake swarm

*Ching-Chou Fu[1]、Lou-Chuang Lee[1]、Cheng-Horng Lin[1]、Vivek Walia[2]、Dimitar Ouzounov[3] (1.Institute of Earth Sciences, Academia Sinica、2.National Center for Research on Earthquake Engineering, NARL, Taiwan、3.Chapman University, One University Drive, Orange, CA, USA)

14:30 ~ 14:45

[MIS04-04] b値の時間変化及び統計的評価

*謝 蔚云[1]、服部 克巳[1]、韓 鵬[2] (1.千葉大学、2.中国南方科技大学)

14:45 ~ 15:00

[MIS04-05] The S-K characteristics of the borehole areal strains associated with the Ms 8.0 Wenchuan and Ms 7.0 Lushan earthquakes

★Invited Papers

*Kaiguang Zhu [1]、Zining Yu[1]、Chenquan Chi[1]、Mengxuan Fan[1]、Kaiyan Lii[1] (1.Jilin University)

15:00 ~ 15:15

[MIS04-06] The Relationship between Earthquakes and Lightning Events of the globe during 2009-2017

*Ching-Chung Cheng[1]、JANN-YENQ Liu[1,2,3] (1.Graduate Institute of Space Science, National Central University, TAIWAN、2.Center for Astronautical Physics and Engineering, National Central University, TAIWAN、3.Center for Space and Remote Sensing Research, National Central University, TAIWAN)

Application of blind source separation method in seismo-magnetic data analysis

*Peng Han[1], Yi Zhong[1], Yuanyuan Zhou[1], Yonghui Ma[2], Chengliang Xie[3], Katsumi Hattori[4], Chie Yoshino[4]

1. Southern University of Science and Technology, Shenzhen, China, 2. Harbin Institute of Technology (Shenzhen), Shenzhen 518055, China, 3. China University of Geosciences (Beijing), Beijing, 100083, China, 4. Chiba University, Chiba, Japan

Along with the development of urban constructions, artificial disturbances in geomagnetic observations are becoming more and more tremendous. The near-field noises produced by human activities such as vehicles, subway and high-speed railways make it difficult to precisely measure geomagnetic pulsations on the ground, thus reducing the practical application value of geomagnetic data. Therefore, suppressing near-field noises has scientific significance and application value. In this study, by combining remote reference and blind source separation analysis methods, we proposed a new signal processing approach which is able to separate geomagnetic pulsation from near-field noise. First, we demonstrated the effectiveness of the new approach by separating signals of different sources in the simulation analysis. Then, we applied this method to geomagnetic field data observed in Chiba, Japan where DC-driven train noises were intense. The results showed that geomagnetic pulsations and train noises are separated clearly, and near-field train noise could be reduced effectively on that basis. It is concluded that the reference-based blind source separation analysis is useful in extracting geomagnetic pulsations and suppressing near-field noises, and may have potential application value in electromagnetic exploration.

Keywords: blind source separation, seismo-magnetic data analysis, Boso, Japan

©2019. Japan Geoscience Union. All Right Reserved.

房総旭観測点近傍の地震活動と地中ラドン濃度変動
Rn flux anomaly and local seiemicity around Asahi station,Boso,Japan

*小島 春奈[1]、服部 克巳[2]、吉野 千恵[2]、下 道國[3]、小西 敏春[4]、古屋 隆一[5]
*Haruna Kojima[1], Katsumi Hattori[2], Chie Yoshino[2], Michikuni Shimo[3], Toshiharu Konishi[4], Ryuichi Furuya[5]

1. 千葉大学大学院融合理工学府地球環境科学専攻地球科学コース、2. 千葉大学大学院理学研究院、3. 藤田保健衛生大学、4. 応用光研株式会社、5. コムシステム株式会社
1. Graduate School of Science and Engineering,Chiba University, 2. Department of Earth Sciences,Graduate School of Science,Chiba University, 3. Fujita Hearth University, 4. OHYO KOKEN KOGYO Co.,Ltd, 5. COM SYSTEM ,INC.

近年、地震に先行する電離層異常や衛星赤外異常などの電磁気学的な地震前兆現象が多く報告されている。これらの前兆現象と地震を結びつける理論として地圏一大気圏一電離圏結合（LAIC）が提案されている。本研究では、旭観測点にて大気電場、大気イオン濃度、ラドン濃度の同時観測を行い、LAICの化学チャネルについて観測学的検証を行っている。大気電気パラメータは主に気象要素の影響を受けるため、これらの影響を除去する必要がある。我々はMSSA(マルチチャンネル特異スペクトル解析)を用いて、地中ラドン濃度から気象による影響を除去し、地中からのRnフラックスを推定し、フラックスの変動と地震との関連について調査した。地震のパラメータとして観測点から50kmおよび100kmの累積地震モーメントとEs指数（観測点の感じる1日あたりの地震エネルギー）を用いて解析を行った結果、Rnフラックスの変動は、観測点近傍の地震活動と相関があることがわかった。この結果から、地中ラドン濃度のモニタリングは地域的な地震活動を監視する指標として有効であるといえる。より詳細な調査のために、地中ラドン濃度のネットワーク観測などを実施し、Rnフラックス変動の地震のマグニチュード依存性や距離依存性等の関係を調査する必要がある。

キーワード：地圏-大気圏-電離圏結合、大気電場、大気イオン濃度、地中ラドン濃度
Keywords: Lithosphere-Atmosphere-Ionosphere Coupling, atmospheric electric field, atmospheric ion concentration, ground Rn concentration

©2019. Japan Geoscience Union. All Right Reserved.

Geochemical evidence for the occurrence of 2018 Hualien earthquake triggered by earlier earthquake swarm

*Ching-Chou Fu[1], Lou-Chuang Lee[1], Cheng-Horng Lin[1], Vivek Walia[2], Dimitar Ouzounov[3]

1. Institute of Earth Sciences, Academia Sinica, 2. National Center for Research on Earthquake Engineering, NARL, Taiwan, 3. Chapman University, One University Drive, Orange, CA, USA

The continuous observations of soil radon for earthquake studies at the Tapingti station (TPT) have been recorded and are compared with the data from gamma rays observations at the Taiwan Volcano Observation station (YMSG), located north to the TPT station. The previous significant increases of gamma rays and radon were observed at both stations before the earthquakes, which occurred in eastern and northeastern Taiwan, suggest that anomalies in gamma and radon may provide the good indicator for exploring earthquake precursor in eastern Taiwan. A Mw 6.4 Hualien earthquake struck eastern Taiwan on 6 February 2018. Based on seismological studies, this earthquake may be triggered by the earthquake swarm that shook eastern Taiwan on 4 February 2018. In this study, both stations recorded significant changes about two weeks before the Hualien Earthquake. However, we provide the possible evidences from geochemical data for the occurrence of 2018 Hualien earthquake was triggered by earlier earthquake swarm. The continuous monitoring on the multiple parameters can improve our understanding of the relationship between the observed radon and gamma-ray variations and the regional crustal stress/strain in the area.

©2019. Japan Geoscience Union. All Right Reserved.

b値の時間変化及び統計的評価
Temporal Variation and Statistical Assessment of b value

*謝 蔚云[1]、服部 克巳[1]、韓 鵬[2]
*weiyun xie[1], Katsumi Hattori[1], Peng Han[2]

1. 千葉大学、2. 中国南方科技大学
1. chiba university, 2. Southern University of Science and Technology

The Gutenberg-Richter Law describes frequency-magnitude distribution of earthquakes. A number of studies have shown that the slope (b value) of the relationship between frequency and magnitude decreased before large earthquakes. In this paper, we investigate the temporal variation of the b value in the Hokkaido and Tohoku regions, Japan and the Wenchuan region, China, respectively, where M 8.0+ earthquakes occurred in the new century. The magnitude of completeness (Mc) in the catalog is evaluated by combining the maximum curvature (MAXC) technique and the bootstrap approach. Then, the b value and its uncertainty is computed by using the maximum likelihood estimation. The Akaike Information Criterion (AIC) with the bootstrap approach is introduced to statistically assess the temporal variation of b values and quantify the significance level. The results show decrease trends of the b value prior to the 2003 Tokachi Earthquake (M8.0) in Hokkaido, the 2011 Tohoku Earthquake (M9.0), and the 2008 Wenchuan Earthquake in China. In addition, the decrease of b values shows certain statistical significance few months before the three M8.0+ great earthquakes. It is concluded that the b value with statistical assessment may contain potential information for future large earthquake preparation.

キーワード：b値、赤池情報量基準
Keywords: b-value, AIC

©2019. Japan Geoscience Union. All Right Reserved.

The S-K characteristics of the borehole areal strains associated with the Ms 8.0 Wenchuan and Ms 7.0 Lushan earthquakes

*Kaiguang Zhu [1]、Zining Yu[1]、Chenquan Chi[1]、Mengxuan Fan[1]、Kaiyan Lii[1]
*Kaiguang Zhu[1], Zining Yu[1], Chenquan Chi[1], Mengxuan Fan[1], Kaiyan Lii[1]

1. Jilin University
1. Jilin University

The skewness and kurtosis of daily borehole areal strain at Guza station are jointly analysed on the S-K plane for the Wenchuan and Lushan earthquakes. We define a crustal stationary background to distinguish possible anomalies related to the earthquakes on the assumption that the background exhibits a quasi-Gaussian distribution. By calculating the S-K biases of the daily areal strain from the crustal stationary background, we found that before the Wenchuan earthquake, the large S-K bias anomalies were always negative, implying that the crust was compressed near the station. Whereas for the Lushan earthquake, clustered positive bias anomalies appeared within two time periods, revealing tensile changes in the crust. In addition, the S-K distributions of two arthquakes are separated on the S-K plane, further indicating differences in the associated deformation. These results demonstrate that the S-K characteristics of borehole areal strain data are potentially promising as earthquake precursors.

キーワード：borehole areal strain、S-K biases、S-K distributions、Wenchuan and Lushan earthquakes
Keywords: borehole areal strain, S-K biases, S-K distributions, Wenchuan and Lushan earthquakes

©2019. Japan Geoscience Union. All Right Reserved.

The Relationship between Earthquakes and Lightning Events of the globe during 2009-2017

*Ching-Chung Cheng[1], JANN-YENQ Liu[1,2,3]

1. Graduate Institute of Space Science, National Central University, TAIWAN, 2. Center for Astronautical Physics and Engineering, National Central University, TAIWAN, 3. Center for Space and Remote Sensing Research, National Central University, TAIWAN

Lightning activities observed by WWLLN (World-Wide Lightning Location Networks) and 95 magnitude greater than 7.0 earthquakes within 30 degrees north and south latitude during 2009 - Nov. 2017 have been statistically examineed. In particular, we investigate how the lightning activities relate to the magnitude, depth, and distance to the epicenter of the earthquakes. Results show that the lightning events 12-22 days before the magnitude greater than 7.9 earthquakes significantly increase around the epicenter. Furthermore, the area size around the epicenter with the statistical significance of lightning activity enhancements is proportional to the earthquake magnitude. These results suggest that lightning activities can be used to find the possible location of forthcoming large earthquakes.

Keywords: Earthquake, Lightning

©2019. Japan Geoscience Union. All Right Reserved.

[E] 口頭発表 | セッション記号 M (領域外・複数領域)：M-IS ジョイント

2019年5月30日(木) 15:30 ~ 17:00 | A02 東京ベイ幕張ホール

[M-IS04] Interdisciplinary studies on pre-earthquake processes

コンビーナ:服部 克巳(千葉大学大学院理学研究科)、劉 正彦(国立中央大学太空科学研究所)、Ouzounov Dimitar(Center of Excellence in Earth Systems Modeling & Observations (CEESMO) , Schmid College of Science & Technology Chapman University, Orange, California, USA)、Qinghua Huang(Peking University)、座長:Peng Han、服部 克巳

This session expands the interdisciplinary discussions on preparation process of earthquake and earthquake predictability by presenting the latest progress in studying the physically based pre-earthquake phenomena. New observations from space and ground have provided
evidences, which may enhance better understanding of tectonic activity. The session anticipates talks that include but not limited to observations and analyses of seismic, electrical, electromagnetic, electro-chemical and thermodynamic processes related to stress changes in the lithosphere along with their statistical and physical validation. Presentations on the latest observational results associated with major earthquakes obtained by different methodologies are welcomed. The topics of the session are as follows but not limited.

-General discussion on earthquake preparation process and the physics of pre-earthquake signals

- Theory, modeling, laboratory experiments, computational simulation for generation and propagation of pre-earthquake signals and their connection with seismic cycle

 - Multi-parameter observations, detection, and validation of pre-earthquake signals

 - Cross-disciplinary studies, practical and technical approaches for better understanding of earthquake preparation processes and their connection with seismicity

15:30 ~ 15:45

[MIS04-07] 3D-Tomography of the Ionospheric Anomalies Preceding the 2011 Tohoku-Oki (M_W9.0) Earthquake

*Ihsan Naufal Muafiry[1,2]、Kosuke Heki[1] (1.Hokkaido University, Japan、2.Universitas Esa Unggul, Indonesia)

15:45 ~ 16:00

[MIS04-08] Statistical Analysis of Pre-seismic Ionospheric Electron Density Anomalies and Investigation of Precursor

*齊藤 央[1]、吉野 千恵[1]、服部 克巳[1] (1.千葉大学)

16:00 ~ 16:15

[MIS04-09] Spatial clustering of pre-earthquake anomalies as an indicator of the preparation/activation zone

*Dimitar Ouzounov[1]、Sergey Pulinets[2]、Tiger Liu[3]、Katsumi Hattori[4] (1.Center of Excellence in Earth Systems Modeling & Observations (CEESMO) , Schmid College of Science & Technology Chapman University, Orange, California, USA、2.Space Research Institute, RAS, Moscow, Russia、3.National Central University, Taoyuan City, Taiwan、4. Chiba University, Chiba, Japan)

16:15 ~ 16:30

[MIS04-10] **Application of the ionospheric parameters on the seismic research**- -Seismic-ionospheric effect detected from China Seismo-Electromagnetic Satellite

★Invited Papers

*Rui Song[1]、Hattori Katsumi[2]、Xuemin Zhang[3] (1.Graduate School of Science and Engeering, Chiba University、2.Graduate School of Science, Chiba University、3.Institute of Earthquake Science, China Earthquake Administration)

16:30 ~ 16:45

[MIS04-11] ROC curve analyses on the ionospheric TEC of M>=6.0 earthquakes in Japan during 1998-2015

★Invited Papers

*JANN-YENQ Liu[1]、Yuh-Ing Chen[2]、Pei-Jung Lee[1] (1.Center for Astronautical Physics and Engineering; Graduate Institute of Space Science, National Central University, Taiwan、2.Graduate Institute of Statistics, National Central University, Taiwan)

16:45 ~ 17:00

[MIS04-12] FORMOSAT-5/AIP observes seismo-ionospheric precursors

*JANN-YENQ Liu[1]、Chi-Kuang Chao[1] (1.Center for Astronautical Physics and Engineering; and Graduate Institute of Space Science, National Central University, TAIWAN)

3D-Tomography of the Ionospheric Anomalies Preceding the 2011 Tohoku-Oki (M_w9.0) Earthquake

*Ihsan Naufal Muafiry[1,2], Kosuke Heki[1]

1. Hokkaido University, Japan, 2. Universitas Esa Unggul, Indonesia

The vertical deformation of solid earth could trigger direct acoustic wave propagating upward and will reach the F-layer of the ionosphere ~10 minutes after earthquakes (Cahyadi & Heki, 2015). Such an acoustic disturbance may also make long-lasting electron depletion (Shinagawa et al., 2013). These phenomena can be studied through Total Electron Content (TEC) data using Global Navigation Satellite System (GNSS) receivers. The GNSS phase difference can be converted to slant TEC (STEC) integrated along its line-of-sight (LoS), which are further converted to absolute vertical TEC (VTEC) by removing inter-frequency biases and multiplying with the cosine of the incidence angle of LoS to the ionosphere.

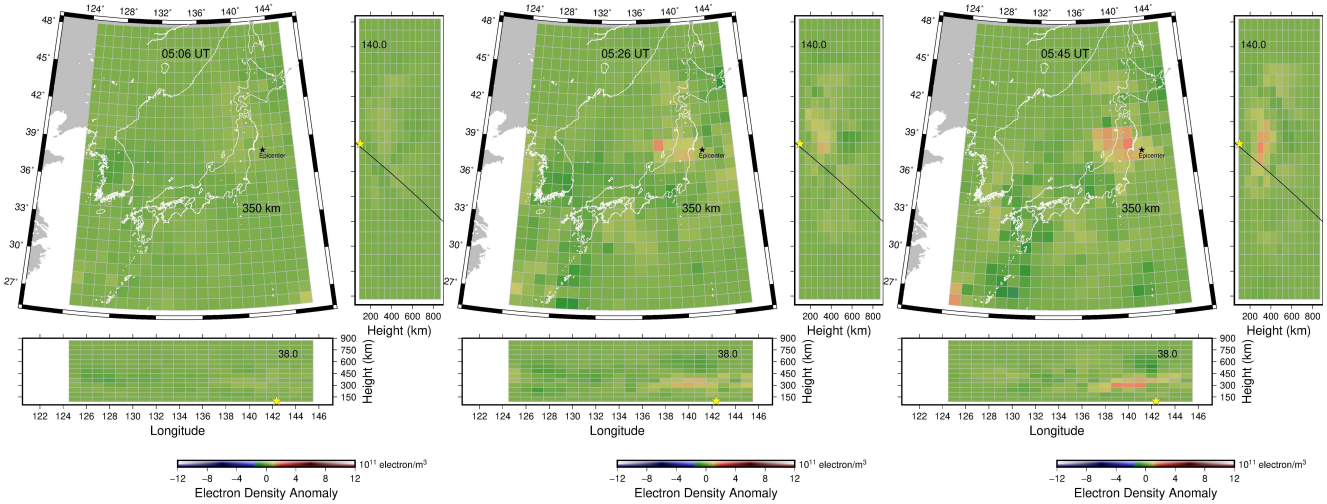
Shortly after the 2011 Tohoku-Oki M_w9.0 earthquake, Heki (2011) reported a significant positive anomaly in TEC starting ~40 minutes before the earthquake above the focal area, and He & Heki (2017) found similar TEC enhancements before 18 earthquakes with M_w 7.3-9.2. He & Heki (2016; 2018) investigated the spatial structure of the electron density anomalies before the 2015 Illapel earthquake, Chile (M_w8.3) using three-dimensional (3D) tomography technique. The result showed that positive electron density anomaly at ~200 km and negative anomalies at high altitudes line up along the geomagnetic field. This suggests their origin by electron redistribution caused by electric field made by surface positive electric charge (e.g. Freund, 2011).

Here, we report the 3D structure of the ionospheric electron density anomalies immediately before the 2011 Tohoku-Oki Earthquake using data from GEONET, a dense GNSS arrays in Japan, and the dense network in South Korea, with the 3D tomography technique similar to He & Heki (2018) and Muafiry et al. (2018). We set up more than 1500 blocks over the region covering the whole Japanese Islands, the Japan Sea, and the Korean Peninsula, with the size of 1.0° (E-W) x 0.9° (N-S) x 60 km (U-D) up to 900 km altitude. By using STEC residuals of pairs of thousand stations and 8 GPS satellites from reference curves, carefully determined by the L-curve method, as the input, we estimated the number of electron density anomalies within individual blocks. To stabilize and regularize the solution, we applied two types of constraints, i.e. continuity constraint and altitude-dependent absolute value constraint assuming the Chapman distribution. Before using the real data, we performed various tests to confirm the reliability of the solution including the checkerboard test, the test assuming realistic preseismic anomaly pattern, and comparing observed STEC anomalies of 10 % of the observation data with those calculated using the electron density anomalies estimated from the remaining 90% of data. These tests showed that our tomography results are robust with its difference is below 0.5 total electron content unit (TECU).

The attached figure shows the map view of our result at a height of 350 km with longitudinal and latitudinal profiles at three different epochs. The results show that positive electron density anomalies occurred at ~300 km altitude. They become large without spatial drifts as the main-shock approaches. Negative anomalies surround this compact and strong positive anomaly. The anomaly is situated just above to the focal area, suggesting its origin as the concentration of ionospheric electrons in response to surface positive electric charges appearing immediately before the 2011 Tohoku-Oki earthquake.

©2019. Japan Geoscience Union. All Right Reserved.

Keywords: Ionosphere-Anomalies, Earthquake Precursor, GPS-TEC, 3D-tomography



©2019. Japan Geoscience Union. All Right Reserved.

Statistical Analysis of Pre-seismic Ionospheric Electron Density Anomalies and Investigation of Precursor

*齊藤 央[1]、吉野 千恵[1]、服部 克巳[1]
*Sanaka Saito[1], Chie Yoshino[1], Katsumi Hattori[1]

1. 千葉大学
1. Chiba University

Recently, many papers have been published on the earthquake-related ionospheric anomalies. In particular, event studies and statistical studies on Ionospheric electrons using Ionosonde and GPS TEC (total electron content) indicate the pre-seismic anomalies. In Japan region, the previous statistical study during 1998-2010 shows that there is an increase anomaly 1-5 days before the earthquake with M>=6 D<=40 km. In this study, we performed statistical analysis on ionosonde data observed at Kokubunji (35.71N, 139.49E), Japan over 60 years of 1958 ~ 2017 in order to investigate the earthquake-related ionospheric anomalies. The ionosonde is operated by the National Institute of Information and Communication Technology, Japan. The studied parameters are NmF2, which indicates the maximum electron density in the F2 layer, hmF2, which shows the NmF2 altitude, and foEs which is the critical frequency of the Es layer. We select earthquakes occurred within 1000 km and 350 km radius from the ionosonde station, and M >= 6 and D <= 40 km. There are 352 and 148 earthquakes. Ionospheric anomalies are also induced by geomagnetic storm. Therefore, to remove the geomagnetic storm effects, we adopt the Dst index. We divided the values into some classes by onset time and intensity. For each class, we performed statistical processes to calculate duration of ionospheric anomalies triggered by a geomagnetic storm. We found these anomalies last about 1-3 days, and we remove the data based on results. To investigate the correlation between ionospheric anomalies and earthquakes, we perform the Superposed Epoch Analysis (SEA). We define the anomaly as 15 days backward median value ±1.5 IQR and an anomalous day has the anomaly with more than 10 hours. Then, we make up the binary time series data on the earthquake-related anomaly. We extract dataset 30 days before and after the earthquake day for the all selected earthquakes and perform SEA. To evaluate the statistical significance, we compute the random test. SEA results show that there is a significant positive anomalies 1-10 days before the earthquakes in NmF2 data. For hmF2 data, we can find there are no clear correlation. As for foEs, we need further investigation. For NmF2, we checked Molchan’ s Error Diagram (MED). From the results of MED, NmF2 may be precursor for earthquakes. The detailed will be given in the presentation.

©2019. Japan Geoscience Union. All Right Reserved.

Spatial clustering of pre-earthquake anomalies as an indicator of the preparation/activation zone

*Dimitar Ouzounov[1], Sergey Pulinets[2], Tiger Liu[3], Katsumi Hattori[4]

1. Center of Excellence in Earth Systems Modeling & Observations (CEESMO) , Schmid College of Science & Technology Chapman University, Orange, California, USA, 2. Space Research Institute, RAS, Moscow, Russia, 3. National Central University, Taoyuan City, Taiwan, 4. Chiba University, Chiba, Japan

We present an interdisciplinary study of observations of pre-earthquake processes associated with major earthquakes based on integrating space and ground- data. We are exploring the general temporal-spatial and evolution patterns of these pre-earthquake signals as a function of both their type and the earthquake magnitude. We examined the possible correlation between the spatial clustering of pre-Earthquake anomalies and the size of earthquake preparation/activation (Dobrovolsky-Bowman zone) in the framework of the Lithosphere-Atmosphere-Ionosphere Coupling (LAIC) concept. For this analysis we selected six most massive earthquakes from the last decade with differing geographic and seismo-tectonics regions: (1) M9.3, Off the West Coast of Northern Sumatra, Dec 26, 2004; (2) M9.0 Great Tohoku Earthquake, , Japan, March 11, 2011; (3 and (4) M7.8 and M7.3 Gorkha, Nepal, 2015; (5); M8.2 Tehuantepec, Mexico, September 8, 2017 and; (6) M7.1, Puebla central Mexico earthquakes, Mexico, September 19, 2017.
Four physical parameters were measured from ground and satellite were used in the temporal-spatial patterns: 1) Ground Radon variation; 2) Outgoing Long-wavelength Radiation (OLR obtained from NPOESS, NASA/AQUA) on top of the atmosphere (TOA); 3) Atmospheric Chemical Potential (ACP) obtained from NASA assimilation models and; 4) electron density variations in the ionosphere via GPS Total Electron Content (GPS/TEC).

Our preliminary results of temporal-evolution patterns indicate an enhancement of radon (about a week to ten days prior) followed by the increase in the atmospheric chemical potential measured near the epicenter from both satellite and subsequently with an increase of OLR observed on the TOA from NOAA/NASA (a week in advance). Finally, GPS/TEC data indicate an increase in electron concentration 1-4 days before the earthquakes. Although the radon variations, some of satellite OLR and GPS/TEC anomalies were observed far (>2000km) from the epicenter areas, the anomalies were always inside the estimates of the Dobrovolsky-Bowman area of preparation. This finding provides new metrics in the assessment of pre-earthquake signals according to LAIC for both sea and land earthquakes possible only by integrating satellite and ground observations. A detailed summary of our approach to this study of pre-earthquake research has just been published as AGU/Wiley Geophysical Monograph Series No. 234.

Keywords: earthquake forecasting, pre-earthquake, LAIC, GPS/TEC, satellite thermal anomaly, radon

©2019. Japan Geoscience Union. All Right Reserved.

Application of the ionospheric parameters on the seismic research --Seismic-ionospheric effect detected from China Seismo-Electromagnetic Satellite

*Rui Song[1], Hattori Katsumi[2], Xuemin Zhang[3]

1. Graduate School of Science and Engeering, Chiba University, 2. Graduate School of Science, Chiba University, 3. Institute of Earthquake Science, China Earthquake Administration

The ionosphere is located at the altitude of 60 kilometers above the earth surface and the top of the ionosphere is about 500km. Figure 1 shows the basic structure of the ionosphere, where D, E and F layers are all clearly concluded. In addition, F layer can be divided into F1 and F2 layers. F1 layers and D region always disppear in nighttime. The seismic-ionospheric research began in 1960s, when American scientists studied the Alaska M8.5 earthquake in 1964, they first found that the disturbance of plasma density before this earthquake. Since then, many researchers engaged in this field. Based on the promising seismic-ionospheric research, China government launched the Seismo-electromagnetic satellite, CSES for short, on February, 2018 for both the earthquake observation and geophysical research. As the data is available now, in this research we adopt the observed data from CSES. The basic information of this satellite is listed in Table 1. There are four consecutive shallow focus earthquakes in a short period in Indonesia during July to Augst, 2018, where Table 2 shows the detailed information about these four earthquakes, and figure 2 shows the specific locations of four epicenters on the map. As for the data sources, there are mainly three kinds of data. The first kind is the Ionospheric Electron density (Ne for short) from CSES satellite. Figure 3 shows the launch and flight status of CSES satellite where a total of 8 payloads concluded, and we adopted the electron density from Langmuir Probe PayloadIn this research. The second kind of data is Ne corresponding with the observed data from International Reference Ionosphere model 2016 (IRI 2016). The third kind is the global ionosphere map from CODE whose time resolution is 1 hour, spatial resolution is 2.5deg*5deg. We adopt these data to evaluate the reliability of the CSES satellite data. First, we used the following formula to calculate the percent disturbance of electron density from CSES satellite. After calculation, we found that there are mainly four significant anomalies on July 27, 31, August 07, and 14 respectively, shown as figure 3. Compared with the earthquake time listed in table 2, these four disturbances just happened before the four earthquakes, which maybe the seismic-ionospheric effect. And the red star in these figures represent the epicenter. After checking different kinds of space weather index, we can exclude that the disturbance is caused by space weather. As for the IRI 2016 model can be seen as the background data without any seismic factors, so we adopt the corresponding Ne from IRI model to evaluate the reliability of CSES data. From figure 4, it is clear the abnormal orbits in figure 3 also show the similar disturbance. As the orbit revisiting period is 5 days, figure 5 shows the comparison between the revisiting orbits of CSES on July 31 and August 14, the other two orbits go through the same location 5 or 10 days before. From this figure, the electron density shows obvious swelling on the abnormal days while the electron temperature shows the opposite trend. Then we used the grid data from CODE to calculate the disturbance about VTEC. Figure 6 (a) shows the percent disturbance of VTEC on August 1, 2018, from 5:00UT the abnormal around the epicenter is gradually increased, till 15:00UT the abnormal area disappeared. It is worth noting that the anomaly did not change with time, which means it is not triggered by sun activity. The percent disturbance of VTEC on Aug. 14, 2018 also shows the similar results from figure 6 (b). In the following research, we counted all the earthquakes that occurred in Indonesia over a 10-year period during 2007-2017 between 106.45 E-126.45 E and 8.3 S-1.7 N from USGS to check the anomalies of

©2019. Japan Geoscience Union. All Right Reserved.

ionospheric vertical TEC from CODE. After selecting the earthquake accidents whose depth is less than 50km, and magnitude is greater than M5.8, there are a total of 35 earthquakes in the end, shown as figure 7. Figure 8 shows the statistical results of the count of TEC anomalies 15 days before and after these 35 earthquakes. It is obvious that 1-7 days before one earthquake in Indonesian region, the number of ionospheric parameter anomalies is more than other time.

Keywords: Seismic-ionospheric effect, Electron density, Total electron contents, CSES satellite

©2019. Japan Geoscience Union. All Right Reserved.

ROC curve analyses on the ionospheric TEC of M>=6.0 earthquakes in Japan during 1998-2015

*JANN-YENQ Liu[1], Yuh-Ing Chen[2], Pei-Jung Lee[1]

1. Center for Astronautical Physics and Engineering; Graduate Institute of Space Science, National Central University, Taiwan, 2. Graduate Institute of Statistics, National Central University, Taiwan

To verify the pre-earthquake ionospheric anomaly (PEIA), statistical analyses are implemented on the relationship between the total electron content (TEC) of global ionosphere map (GIM) and M>=6.0 earthquakes in Japan during 1998-2018. A median-based method together with z test is employed to find the criteria and/or characteristics of TEC anomalies related to earthquakes. It is found that the GIM TEC over the Japan significantly increases 1-3 days before the earthquakes. The receiver operating characteristic (ROC) curve is used to compare the TEC anomaly-based method with some competitive alternatives for predicting the earthquakes under study. We find, based on possible TEC anomalies, that the observed PEIAs are significantly earthquake-related. Moreover, the results of regression analyses show that the PEIA strength is associated with the magnitude of earthquakes.

Keywords: pre-earthquake ionospheric anomaly (PEIA), total electron content (TEC), earthquake, receiver operating characteristic (ROC)

©2019. Japan Geoscience Union. All Right Reserved.

FORMOSAT-5/AIP observes seismo-ionospheric precursors

*JANN-YENQ Liu[1], Chi-Kuang Chao[1]

1. Center for Astronautical Physics and Engineering; and Graduate Institute of Space Science, National Central University, TAIWAN

FORMOSAT-5 (F5) was launched at 18:51 UT (universal time) on 24 August 2017 with a sun-synchronous orbit at 720 km altitude and 98.28° inclination, which passes at almost the same local time everywhere in the daytime of about 10:30 LT and the nighttime of about 22:30 LT. It carries a primary payload, optical RSI (Remote Sensing Instrument), and a science payload, AIP (Advanced Ionospheric Probe), which are normally operating in the daytime and nighttime, respectively. The AIP mission is to monitor seismo-ionospheric precursors (SIPs) and observe ionospheric space weather. It is basically a multi-grid planar ion probe integrated with a planar Langmuir probe within a 10 cm ×10 cm aperture, which consists of Retarding Potential Analyzer (RPA), and Ion Drift Meter (IDM)/Ion Trap (IT) to maximize the total availability of ionospheric ion concentration (or density), ion velocities, and ion/electron temperatures at a sample rate up to 8192 Hz over a wide range of spatial scales in ionospheric plasma. The electroformed gold grids used has almost no hysteresis in sweeping current-voltage curves, and results in that the AIP can accurately probe plasma quantities in the ionosphere. The RPA and IDM/IT have been alternatively operating on every other orbit since end of October 2017. The RPA probes the ion density, while the IDM/IT derives the ion density and ion drift velocity. This paper combines in situ plasma measurements of F5/AIP and remote sensing of the TEC (total electron content) derived by ground-based GNSS (global navigation satellite system) receivers to three-dimensionally study SIPs of the 12 November 2017 M7.3 Iran-Iraq Border Earthquake and disturbances of ionospheric storms on 1 and 21 November 2017. The F5/AIP ion density is employed to confirm the SIP signatures and storm signatures being observed, while the F5/AIP ion velocity is employed to find electric fields associated with the SIPs and the ionospheric storms.

Keywords: FORMOSAT-5, AIP (Advanced Ionospheric Probe), seismo-ionospheric precursors

©2019. Japan Geoscience Union. All Right Reserved.

[E] 口頭発表 | セッション記号 M (領域外・複数領域)：M-IS ジョイント

2019年5月30日(木) 13:45 ~ 15:15 | 202 2F

[M-IS06] ジオパーク、ジオサイト、石造文化財の保存修復：風化プロセスとダメージアセスメント

コンビーナ:小口 千明(埼玉大学大学院理工学研究科)、藁谷 哲也(日本大学大学院理工学研究科)、目代 邦康(東北学院大学)、Magdalini Theodoridou(School of Engineering, Cardiff University)、座長:藁谷 哲也(日本大学大学院　理工学研究科)、目代 邦康(ジャパンジオサービス)

ジオパークや世界遺産、石造文化財など、価値の高い自然遺産や文化遺産は、地質学的時間スケールだけでなく、人間的時間スケールでも風化の影響を受け劣化に直面している。美しい景観や、地質材料である岩石や土を用いた価値ある文化財など、これらの遺産を保存するためには、保全対策について科学的な視点から考慮されなければならない。既に、地形学、地質工学、環境地質学、材料科学、岩石物理学、地球化学など、幅広い研究分野においてこのテーマについて、研究が進められている。本セッションは、ドキュメンテーション手法や事例、測定・モニタリング技術、実験的アプローチ、予測モデル、損傷評価（ダメージアセスメント）など、多方面からの研究発表を歓迎します。

13:45 ~ 14:00

[MIS06-01] 自然災害発生時におけるジオサイトの保全についてのジオパークの対応

*目代 邦康[1]、長谷川 修一[2] (1.日本ジオサービス株式会社、2.香川大学)

14:00 ~ 14:15

[MIS06-02] Physical and mechanical properties for damage assesment of Taya Cave rocks, central Japan

*小口 千明[1]、秋元 友理奈[2]、田村 裕彦[3]、坂根 海征[1] (1.埼玉大学大学院理工学研究科、2.埼玉大学工学部、3.田谷の洞窟保存実行委員会)

14:15 ~ 14:30

[MIS06-03] **多分野統合共同調査から地域づくりへ展開させる地下文化財「田谷の洞窟」保存活動の実践的試行**

★招待講演

*田村 裕彦[1,2]、小口 千明[4]、早川 裕弋[5,2]、小倉 拓郎[2]、緒方 啓介[6]、守田 正志[3] (1.田谷の洞窟保存実行委員会、2.東京大学空間情報科学研究センター、3.横浜国立大学大学院都市イノベーション学府・研究院、4.埼玉大学理工学研究科 環境科学・社会基盤部門、5.北海道大学大学院地球環境科学研究院、6.鶴見大学文学部文化財学科)

14:30 ~ 14:45

[MIS06-04] **Italian underground cultural heritage: from monitoring to enhancement**

★Invited Papers

*Mario Parise[1]、Tiziana Vitolo[2]、Roberta Varriale[2] (1.Univ. Aldo Moro, Dept. Earth and Environmental Sciences, Bari, Italy、2.CNR-ISSM, Italy)

14:45 ~ 15:00

[MIS06-05] アンコール遺跡を構成する砂岩ブロックの日射による風化の可能性

*藁谷 哲也[1] (1.日本大学大学院理工学研究科)

15:00 ~ 15:15

[MIS06-06] **Durability evaluation of pyroclastic rocks used in the historical built environment of Hungary**

*Luigi Germinario[1,2]、Ákos Török[1] (1.Budapest University of Technology and Economics, Hungary、2.Saitama University, Japan)

自然災害発生時におけるジオサイトの保全についてのジオパークの対応
Geopark's response to conservation of geosites from natural hazards

*目代 邦康[1]、長谷川 修一[2]
*Kuniyasu Mokudai[1], Shuichi Hasegawa[2]

1. 日本ジオサービス株式会社、2. 香川大学
1. Japan Geoservice Incorporated, 2. Kagawa Univ.

湿潤変動帯である日本列島においては，洪水や斜面崩壊，地震動など様々な自然災害が発生する．こうした自然災害はジオサイトの状態に大きく影響する．ジオパークは，自然災害発生時に活動を行うが，そのノウハウは蓄積されていない．四国西予ジオパークでは，2018年の西日本豪雨時には，ジオパーク事務局は行政としての災害復旧作業をする必要があった．そのため，ジオパークとしての情報発信やサイトの保全は困難であった．

キーワード：ジオパーク、地質遺産の保護、自然災害
Keywords: geopark, geoconservation, natural hazard

©2019. Japan Geoscience Union. All Right Reserved.

Physical and mechanical properties for damage assesment of Taya Cave rocks, central Japan

*小口 千明[1]、秋元 友理奈[2]、田村 裕彦[3]、坂根 海征[1]
*Chiaki T. Oguchi[1], Yurina Akimoto[2], Yasuhiko TAMURA[3], Kaisei Sakane[1]

1. 埼玉大学大学院理工学研究科、2. 埼玉大学工学部、3. 田谷の洞窟保存実行委員会
1. Institute for Environmental Science and Technology, Graduate School of Science and Engineering, Saitama University, 2. Faculty of Engineering, Saitama University, 3. The Exective Committee for the Preservation of TAYA CAVERN

Taya cave, an artificial cave in a hill in south Yokohama, was excavated from the Kamakura period through the late Edo period. There are many sculptures and bas-reliefs on the surface of the cave wall made of soft rock which deposited in Pleistocene. Those sculptures has been suffering from weathering and deterioration, especially exfoliation of the wall and ceiling. In this study, for the purpose of conservation and restoration of sculptural murals, rock physical properties were investigated to assess the current situation. As a result, the possibility of surface exfoliation is considered to be affected by moisture difference, whereas the possibility of collapse of ceilings or floors between stairs becomes higher if too much water infiltrate.

キーワード：物理的性質、力学的性質、田谷洞窟
Keywords: Phisical property, Mechanical property, Taya Cave

©2019. Japan Geoscience Union. All Right Reserved.

多分野統合共同調査から地域づくりへ展開させる地下文化財「田谷の洞窟」保存活動の実践的試行

Interdisciplinary approaches on conservation of underground geoheritage for community development of Taya Cave and its adjacent area

*田村 裕彦[1,2]、小口 千明[4]、早川 裕弋[5,2]、小倉 拓郎[2]、緒方 啓介[6]、守田 正志[3]
*Yasuhiko TAMURA[1,2], Chiaki T. Oguchi[4], Yuichi S. Hayakawa[5,2], Takuro Ogura[2], OGATA KEISUKE[6], Masashi MORITA[3]

1. 田谷の洞窟保存実行委員会、2. 東京大学空間情報科学研究センター、3. 横浜国立大学大学院都市イノベーション学府・研究院、4. 埼玉大学理工学研究科 環境科学・社会基盤部門、5. 北海道大学大学院地球環境科学研究院、6. 鶴見大学文学部文化財学科
1. The Executive Committee for the Preservation of TAYA CAVERN , 2. The University of Tokyo, Center for Spatial Information Science, 3. Yokohama National University, Institute of Urban Innovation, 4. Saitama University, Graduate School of Science and Engineering, 5. Hokkaido University, Faculty of Environmental Earth Science, 6. Tsurumi University, The Department of Cultural Properties

1.はじめに

横浜市栄区田谷町にある真言宗定泉寺の境内の山中に「田谷の洞窟」と呼ばれる全長570ｍの地下文化財がある。この洞窟は、真言宗の修行洞窟であり、横浜市登録地域文化財である。約800年前の鎌倉時代にその起源があるとされ、三層構造の人工の素掘りのトンネルである。その内部には、300を超える美しい浮彫のレリーフが施されている。近年、この「田谷の洞窟」は、劣化風化による損傷が激しい。この地下文化財の3Dデジタルデータ保存を目的とした、多分野統合による基礎調査を実践的に進めている。これまでの実践的な試行からその効果と課題等を明らかにする。

2.背景

日本は口減少問題と直面する時代に入った。人間活動空間は「都市」と「農村」に大別され二項対立的に考え易いが、これらの中間に「都市近郊農村」と呼べる人間活動空間が存在している事を忘れてはならない。「都市近郊農村」は、「都市と農村の両問題」を抱え、多層的で実践的な「自立的地域力」の獲得が急務となる。本洞窟のある田谷町はまさに「都市近郊農村」であり、このような地下文化財が存在する事は、非常に強い地域力（良好なコンテンツ）の一つと言える。洞窟の未来を思考する事は、地域の在り方を思考する事と充分な相関関係があると言える。洞窟との地域共生の為に、実践的な試行を同時多層的に進め、多分野の専門家の異種交流議論を通し、都市近郊農村の新たな地域力（展望）を探る必要があると考えた。

3.多分野統合型の共同基礎調査の実践

多分野統合基礎調査は、「地盤・石造の劣化等の基礎調査（埼玉大学小口千明）」、「地理・地形・空間把握調査（北海道大学早川裕弋と東京大学小倉拓郎）」及び「文化財基礎調査（鶴見大学緒方啓介）」と共同基礎調査を実施し、地下文化財と都市近郊農村の地域共生に関する「地域資質調査（横浜国立大学守田）」を実施し、合計4分野の5大学研究機関と共同して実施している。

4.地域づくりへの展開（地域連携の実践）

近隣の公立小学校と大学が連携した「小大連携プロジェクト」として、小学6年生の地域学習の授業において、洞窟保存活動と研究者による専門的な授業を実施し、卒業制作を兼ねた洞窟保全検討に必要な巨大模型の製作による教育との連携による人づくりを実践している。また、地域イベントや報告会を通し地域啓蒙・アウトプットを実践している。大学研究者と地域社会が直接つながる場の提供による相乗効果を期待した試行を進めている。

5.効果と課題

これまでの多分野統合調査の様々な活動により、田谷の洞窟に対する地域の見方や感心に変化が生じ始め

©2019. Japan Geoscience Union. All Right Reserved.

た。小学校の教育現場との連携が大人に広がり始め、地域社会に望ましい変化がみられる。一方で、課題も挙げられる。第一に「地域と研究者との相互理解の向上」、第二に「地域の人的資源の確保」、第三に「面的な広がりを持つ啓蒙手法の確立」、第四に「多言語対応」、そして第五に「資金調達」である。

6.おわりに

これまでの多分野統合調査により、周辺環境と地下文化財保全が密接な関係である事が判明し、地下文化財保全の為に里山や農村風景の保全が重要である事が判った。今日的な研究が直接地域社会に貢献できることが実践された。一方、地域は地下文化財の希少性と重要性を再認識し始めており、各種メディアでも本活動が取り上げられる機会が増えた。これまでの試行により、今後も継続的に展開させていく必要性を確認できた。

キーワード：文化財保存、地下文化財、多分野共同調査、地域連携、小大連携、田谷の洞窟
Keywords: Preservation of cultural property, underground heritage, multi-field joint basic survey, regional cooperation, Elementary school - University collaboration, TAYA Cave



©2019. Japan Geoscience Union. All Right Reserved.

Italian underground cultural heritage: from monitoring to enhancement

*Mario Parise[1], Tiziana Vitolo[2], Roberta Varriale[2]

1. Univ. Aldo Moro, Dept. Earth and Environmental Sciences, Bari, Italy, 2. CNR-ISSM, Italy

Italy is among the European countries with the highest number of artificial cavities, many of which represent a precious testimony of past civilizations and cultures, and of the continuous link between town development and the underground as well. The Italian underground has historically managed several environmental conflicts and social interactions, in both urban and rural settings. Nowadays the artificial cavities represent a significant segment within the local cultural heritage and have become in the last decades the object of strategic planning addressed towards their regeneration, valorization and public fruition. All these actions, however, need to be based on sound studies and researches aimed at evaluating the opportunity to open to the public sites that could potentially be unsafe. At this regard, monitoring plans and activities, and careful assessment of the susceptibility to failure and collapses, must be performed. Only after the stability conditions have been positively ascertained, underground sites might be considered for valorization, public visits and other activities.
In such a framework, we present in this contribution some case studies (including the underground tanks Cisternone in Formia, Latium, and Palombaro in Matera, Basilicata), also to describe their use at the time of realization, and to illustrate the related "sense of place". Environmental, social, historical and economic reconstructions have been carried out to generate and manage the knowledge of the places selected in order to facilitate their use and contribute to their development, in direct link with the cities where they are hosted. The methodology adopted aims at highlighting the cultural vitality and the identity of these places for the benefit of the local populations, and of tourists as well.

Keywords: artificial cavity, underground, stability, monitoring, enhancement

©2019. Japan Geoscience Union. All Right Reserved.

アンコール遺跡を構成する砂岩ブロックの日射による風化の可能性
Possibility of insolation weathering of sandstone blocks composing Angkor temples, Cambodia

*藁谷 哲也[1]
*Tetsuya Waragai[1]

1. 日本大学大学院理工学研究科
1. Graduate School of Science and Engineering, Nihon University

Angkor temples such as Angkor Wat and Bayon temples built from 9th to 13th century are mainly composed of sandstone blocks. However, as a result of tree cutting that has been proceeded to protect the temples from rootwedging processes, most of temples are exposed to direct insolation. Possibility of insolation weathering of the sandstone blocks are pointed out, since the sandstone blocks can keep high temperature condition during daytime. Therefore, this study carried out field experiments that expose a sandstone cylindrical specimen in a dry season as a trial experiment using an acoustic emission (AE) method that may detect microcracks in the specimen by temperature changes. The experiment was carried out at the test site of Angkor Wat temple by measuring surface temperatures and AE signals of the specimen in December 2018. As the results, the surface temperatures of the specimen were 51.5 ˚C in maximum and 20.8 ˚C in minimum, and diurnal difference was 30.3 ˚C. In addition, the maximum elevation rate of the temperature was 1.50 ˚C/min and the minimum descending rate of the temperature was -1.88 ˚C/min. Although the surface temperature measurement could not synchronize to the AE measurement, an AE signal that is 40% bigger than ordinal value, was detected at the time of 0.43 ˚C/min of the elevation rate of temperature. This is though that sandstone blocks maybe deteriorate due to temperature changes by insolation.

キーワード：アンコール遺跡、砂岩、日射風化、アコースティックエミッション
Keywords: Angkor temples, sandstone, insolation weathering, acoustic emission

©2019. Japan Geoscience Union. All Right Reserved.

Durability evaluation of pyroclastic rocks used in the historical built environment of Hungary

*Luigi Germinario[1,2], Ákos Török[1]

1. Budapest University of Technology and Economics, Hungary, 2. Saitama University, Japan

Pyroclastic rocks of diverse composition have experienced a broad historical usage in the built environment of Hungary, especially from the Middle Ages. In the northern regions, for instance, acid ignimbrites have been widely used as building stones in monumental construction, e.g., churches and castles, Ottoman architectures like mosques and spas, as well as common dwellings. Their characterization reveals a small-scale inconstancy of their physico-mechanical performance and petrographic features, which affects weathering susceptibility. That involves most significantly porosity, pore-size distribution, and tensile strength, considering the technical properties; on the other hand, texture must be accounted for in terms of changing quantity and size of pumice clasts, phenocrysts, and crystals, and amount of the weak and porous groundmass. The behavior of the ignimbrites when subjected to artificial weathering, by freeze-thaw and salt attack tests, alters accordingly. The variability of open porosity represents the most important factor marking a possible dramatically diverse durability. It turns out to be proportional to water absorption, controlling the amount of infiltrating water or salt solutions, at the base of potential rock failure due to ice or salt crystallization. The sole high moisture may also lead to an extreme and hazardous deterioration of the mechanical properties. Finally, high porosity is correlated with low welding degree and, in turn, low strength. Such outcomes suggest criteria for evaluating the vulnerability of these volcanic rocks in cultural heritage, and directing reasonable material selections for stonework restorations.

Keywords: Stone decay, Freeze-thaw, Salt weathering, Petrophysical properties, Mechanical properties, Rhyolite tuff

©2019. Japan Geoscience Union. All Right Reserved.

[E] 口頭発表 | セッション記号 M (領域外・複数領域)：M-IS ジョイント

2019年5月30日(木) 9:00 ~ 10:30 | 201A 2F

[M-IS07] アストロバイオロジー

コンビーナ:薮田 ひかる(広島大学大学院理学研究科地球惑星システム学専攻)、杉田 精司(東京大学大学院理学系研究科地球惑星科学専攻)、深川 美里(国立天文台)、藤島 皓介(東京工業大学地球生命研究所)、座長:薮田 ひかる(広島大学大学院 理学研究科)、杉田 精司(東京大学大学院 理学系研究科)、深川 美里(名古屋大学大学院 理学研究科)、藤島 皓介(ELSI 地球生命研究所)

様々な分野を横断し、宇宙における生命の起源と進化、生命存在可能性の解明を目的とするアストロバイオロジーが発祥して20年。太陽系物質進化、惑星系形成、初期地球の前生物的化学、地球と生命の共進化、極限環境生物、ハビタブルな惑星環境、といった個々のテーマが複数分野の知見や手法で研究されるようになり、「我々はどこから来たか」を或る幾つかの形では示すことができるようになってきた。しかし、最終的には成し遂げるべき、挑戦的な領域が残っている。それは、地球惑星環境で生じた非生物的な物質は、どのように生命機能を獲得したのか？　生命の起源に至る、または、生命存在可能な条件を満たす、有機化学と生化学の接点には未だに隔たりが大きい。そこで、これからのJpGUアストロバイオロジーセッションでは、これまで以上の取り組みが重要と考えられる「天文学、地球科学、生化学の融合」を模索し、この未知領域の開拓に臨む。例えば系外惑星と分子進化など、試験管の中の知見を超えた、”場”と対応づけた生化学的・分子生物学的な事象を議論し「生命とはなにか」の理解に近づけ、将来の宇宙生命探査に必要な非生命と生命の識別法の議論や開発に繋げる。

9:00 ~ 9:20

[MIS07-06] How to find and characterize nearby habitable exoplanets

★Invited Papers

*成田 憲保[1] (1.アストロバイオロジーセンター)

9:20 ~ 9:40

[MIS07-07] **Organic Matter Preserved in Mudstones of a 3-Billion-Year-Old Lake Deposit in Gale Crater, Mars**

★Invited Papers

*Jennifer L Eigenbrode[1]、Roger E Summons[2]、Andrew Steele[3]、Caroline Freissinet[4]、Maëva Millan[5]、Rafael Navarro-González[6]、Paul Mahaffy[1] (1.NASA Goddard Space Flight Center、2.Massachusetts Institute of Technology、3.Carnegie Institution of Washington、4.Institut Pierre Simon Laplace, CNRS、5.Georgetown University、6.Universidad Nacional Autónoma de México)

9:40 ~ 9:55

[MIS07-08] **The third year sample return of Tanpopo: Capture and Exposure Experiment of Micrometeorite and Microbes on Exposure Facility of International Space Station**

*山岸 明彦[1]、Hashimoto Hirofumi[2]、Yano Hajime[2]、Yokobori Shin-ichi[3]、Kobayashi Kensei[4]、Mita Hajime[5]、Yabuta Hikaru[6]、Higashide Masumi[7]、Tabata Makoto[8]、Kawai Hideyuki[8]、Imai Eiichi[9] (1.Tokyo University of Pharmacy and Life Science, Department of Molecular Biology、2.ISAS/JAXA, Sagamihara, Japan、3.Tokyo University of Pharmacy and Life Science, Tokyo, Japan、4.Yokohama National University, Yokohama, Japan、5.Fukuoka Institute of Technology, Fukuoka, Japan、6.Hiroshima University, Hirosima, Japan、7.Japan Aerospace Exploration Agency (JAXA), Tokyo, Japan、8.Chiba University, Chiba, Japan、9.Nagaoka University of Technology, Nagaoka, Japan)

9:55 ~ 10:10

[MIS07-09] 低温度周りに適応可能な光合成色素の理論的探索：中心金属による物理化学的特性の調整

*小松 勇[1,2]、滝澤 謙二[1,3] (1.アストロバイオロジーセンター 、2.国立天文台、3.基礎生物学研究所)

10:10 ~ 10:25

[MIS07-10] 地球類似惑星の気候安定性とハビタビリティにおける炭化水素エアロゾルの影響

*渡辺 泰士[1]、田近 英一[1]、尾崎 和海[2]、洪 鵬[3] (1.東京大学、2.東邦大学、3.千葉工業大学)

10:25 ~ 10:30
Discussion

How to find and characterize nearby habitable exoplanets

*成田 憲保[1]
*Norio Narita[1]

1. アストロバイオロジーセンター
1. Astrobiology Center

In this review, I will summarize previous and ongoing efforts to find habitable exoplanets in the vicinity of the Solar system and future prospects to characterize such planets with next generation telescopes and instruments. In addition, I will talk about the importance and some examples of interdisciplinary studies of astrobiology to consider future missions.

キーワード：系外惑星、アストロバイオロジー
Keywords: Exoplanets, Astrobiology

©2019. Japan Geoscience Union. All Right Reserved.

Organic Matter Preserved in Mudstones of a 3-Billion-Year-Old Lake Deposit in Gale Crater, Mars

*Jennifer L Eigenbrode[1], Roger E Summons[2], Andrew Steele[3], Caroline Freissinet[4], Maëva Millan[5], Rafael Navarro-González[6], Paul Mahaffy[1]

1. NASA Goddard Space Flight Center, 2. Massachusetts Institute of Technology, 3. Carnegie Institution of Washington, 4. Institut Pierre Simon Laplace, CNRS, 5. Georgetown University, 6. Universidad Nacional Autónoma de México

In situ analyses of lake-deposited mudstones of the Murray formation at Pahrump Hills, Gale crater, Mars show the presence of aliphatic, aromatic, and sulfur-bearing organic gases upon heating to 500-860˚C, as detected by the Sample Analysis at Mars (SAM) instrument suite on the Mars Science Laboratory's (MSL's) Curiosity rover. Organic-sulfur compounds, including thiophenes, dimethylsulfide and thiols were identified by gas chromatography-mass spectrometry (GCMS) and observed in evolved gas analyses (EGA). Other aromatic and aliphatic hydrocarbon components were also indicated by EGA. The distributions of organic molecules observed were specific to samples and cannot be from SAM's instrument background. The temperatures these organic volatiles were released is consistent with the pyrolytic cleavage of organic fragments from large molecules (macromolecules) indigenous to the mudstones. Some portion may also be derived from the thermal release of organics entrained within minerals.

The release of organic-sulfur compounds occurs at high temperatures in the SAM oven; thus, these compounds are most likely derived from sulfurized organics in the sediments and are not an artifact of sulfurization reactions in the oven. On Earth, sulfurization is a key process that facilitates organic matter preservation over geological time-scales by transforming individual organic molecules into recalcitrant macromolecules. Organic matter at the base of the Murray formation probably underwent sulfurization prior to deposition or during early diagenesis. Multiple factors likely contribute to the organic preservation in the Gale crater mudstones, however, sulfurization may be largely responsible for the greater abundance and the molecular diversity observed in the lower Murray formation.

Keywords: Mars, organic matter, lacustrine, Curiosity rover, Mars Science Laboratory (MSL) mission, Sample Analysis at Mars (SAM)

©2019. Japan Geoscience Union. All Right Reserved.

The third year sample return of Tanpopo: Capture and Exposure Experiment of Micrometeorite and Microbes on Exposure Facility of International Space Station

The third year sample return of Tanpopo: Capture and Exposure Experiment of Micrometeorite and Microbes on Exposure Facility of International Space Station

*山岸 明彦[1]、Hashimoto Hirofumi[2]、Yano Hajime[2]、Yokobori Shin-ichi[3]、Kobayashi Kensei[4]、Mita Hajime[5]、Yabuta Hikaru[6]、Higashide Masumi[7]、Tabata Makoto[8]、Kawai Hideyuki[8]、Imai Eiichi[9]

*Akihiko Yamagishi[1], Hirofumi Hashimoto[2], Hajime Yano[2], Shin-ichi Yokobori[3], Kensei Kobayashi[4], Hajime Mita[5], Hikaru Yabuta[6], Masumi Higashide[7], Makoto Tabata[8], Hideyuki Kawai[8], Eiichi Imai[9]

1. Tokyo University of Pharmacy and Life Science, Department of Molecular Biology、2. ISAS/JAXA, Sagamihara, Japan、3. Tokyo University of Pharmacy and Life Science, Tokyo, Japan、4. Yokohama National University, Yokohama, Japan、5. Fukuoka Institute of Technology, Fukuoka, Japan、6. Hiroshima University, Hirosima, Japan、7. Japan Aerospace Exploration Agency (JAXA), Tokyo, Japan、8. Chiba University, Chiba, Japan、9. Nagaoka University of Technology, Nagaoka, Japan

1. Tokyo University of Pharmacy and Life Science, Department of Molecular Biology, 2. ISAS/JAXA, Sagamihara, Japan, 3. Tokyo University of Pharmacy and Life Science, Tokyo, Japan, 4. Yokohama National University, Yokohama, Japan, 5. Fukuoka Institute of Technology, Fukuoka, Japan, 6. Hiroshima University, Hirosima, Japan, 7. Japan Aerospace Exploration Agency (JAXA), Tokyo, Japan, 8. Chiba University, Chiba, Japan, 9. Nagaoka University of Technology, Nagaoka, Japan

Purpose of Tanpopo mission

Tanpopo, a dandelion in Japanese, is a plant species whose seeds with floss are spread by wind. We proposed this mission to examine possible interplanetary migration of microbes, and organic compounds at the Exposure Facility of Japan Experimental Module (JEM: KIBO) of the International Space Station (ISS).

We are testing the panspermia hypothesis, which proposes the interplanetary transfer of life. We are also testing if the organic compound may be transferred from space before the origin of life on the earth.

The Tanpopo mission consists of six subthemes: Capture of microbes in space (Subtheme 1), exposure of microbes in space (Subtheme 2), analysis of organic compounds in interplanetary dust (Subtheme 3), exposure of organic compounds in space (Subtheme 4), measurement of space debris at the ISS orbit (Subtheme 5), and evaluation of ultra low-density aerogel developed for the Tanpopo mission (Subtheme 6).

Apparatus developed for Tanpopo mission

We have developed two types of apparatus used for Tanpopo mission: Capture Panels for aerogel to capture micro-particles and Exposure Panels for exposure of microbes and organic materials.

Each Capture Panel contains a silica aerogel block in an aluminum mesh container. Silica aerogel, which is the lowest density solid material, is used to capture micro particles, which may include, micrometeorite, artificial space debris and earth-originated natural particles. We are going to analyze if the particles contain terrestrial microbial cells or not, and if the micrometeorite contains organic

©2019. Japan Geoscience Union. All Right Reserved.

compounds or not.

Exposure Panels have been developed to expose microbes and organic compounds to the space environment. Several microbial species including, *Deinococcus radiodurans, Deinococcus aerius, Deinococcus aetherius, Nostoc sp., Schizosaccharomyces pombe,* have been exposed to the space environment. These species are expected to be resistant against space environment, vacuum, desiccation, temperature-cycle, UV and ionization radiation. We have tested the survival of these species after one-, two- and three-year exposure in space. Organic compound such as amino acids and the precursors have also been exposed.

Schedule of Tanpopo mission

Tanpopo apparatus was launched in April 2015. The Panels were placed on the Exposed Experiment Handrail Attachment Mechanism (ExHAM) in the ISS. The ExHAM with Panels were placed on the Exposure Facility of KIBO (JEM) with the Japanese robotic arms through the airlock of KIBO in May 2015.

The first set of Capture Panels and an Exposure Panel were retrieved in June 2016, contained in plastic bags, and stored in the pressurized area of the International Space Station. They have returned to the ground in the space capsule, and returned to JAXA in September 2016. The second set of Capture Panels and an Exposure Panel were detached in July 2017 and returned to JAXA in October 2017. The third set were detached in June 2018, the Exposure Panel and the Capture Panels were returned to JAXA in September 2018 and in February 2019, respectively.

Exposure Panel was separated into Exposure Units, each harboring either microbe or organic compound was handed over to the scientist in charge of each microbe or organic compound. Some of the Units are dedicated to the UV or radiation dose measurement.

Each aerogel block of each Capture Panel was examined for the particles captured and the tracks made upon the impact, which were extracted from the aerogel block and handed over to the scientists. The analysis includes, fluorescence microscopic inspection to test if there are microbial cells or not. Particles and tracks will be used for the mineral analysis as well as the analysis of organic compounds.

The first report has been published and the following results will be reported.

References: 1) A. Yamagishi, et al. “TANPOPO: astrobiology exposure and micrometeoroid capture experiments.” International Symposium on Space Technology and Science (ISTS) Web Paper Archives. 2008-k-05 , 2008. 2) Y. Kawaguchi, et a. “Investigation of the interplanetary transfer of microbes in the Tanpopo mission at the Exposed Facility of the International Space Station,” *Astrobiolgy* Vol. 16, pp. 1-14, 2016 .

3) A. Yamagishi, et al. Environmental data and survival data of *Deinococcus aetherius* from the Exposure Facility of the Japan Experimental Module of the International Space Station obtained by the Tanpopo Mission. *Astrobiology* Vol. 18, pp. 1369-1374., 2018.

キーワード：宇宙塵、微生物、有機物、デブリ、エアロゲル
Keywords: Micrometeotite, Microbes, Organics, Debris, Aerogel

©2019. Japan Geoscience Union. All Right Reserved.

低温度周りに適応可能な光合成色素の理論的探索：中心金属による物理化学的特性の調整

Theoretical search for photosynthetic pigments applicable around low temperature stars: Modulation of physical-chemical properties by central metals

*小松 勇[1,2]、滝澤 謙二[1,3]
*Yu Komatsu[1,2], Kenji Takizawa[1,3]

1. アストロバイオロジーセンター 、2. 国立天文台、3. 基礎生物学研究所
1. Astrobiology Center, 2. National Astronomical Observatory of Japan, 3. National Institute for Basic Biology

A lot of extrasolar planets have been discovered in the habitable zone, and the number of samples will be increasing in future. In order to discover planets which harbour lives, it will be a significant achievement to identify potential biosignatures, which are traces of life from planetary spectra. Gaseous molecules such as oxygen and ozone and spectral features in surface vegetation called as "vegetation red edge (VRE)" are considered as biosignatures. In current observations, planets around M dwarfs, lower temperature stars than the Sun, have been focused, and there are large uncertainties in how assumed photosynthetic organisms evolve in the planets and how they would exhibit spectral features. Recently, it has been shown that the Earth-type photosynthesis can be evolved even around M dwarfs, considered lighting conditions in shallow water and how phototrophs can adapt to it (Takizawa, K., et al.: 2017, *Scientific Reports*, **7**, 7561). Moreover, an interesting example has been discovered that a cyanobacteria, which are categorized into oxygenic photosynthetic bacteria, becomes to utilize longer wavelength radiation for photochemistry than previously known, after grown under near infrared light, 750 nm (Nürnberg, D. J. et al.: 2018, *Science*, **360**, 1210.). Accumulating such knowledges and benchmarks from various points of view would lead to implications for future observations.

We investigate thoroughly by quantum chemical calculations the properties of photosynthetic pigments like and artificial pigments which might form on early Earth or other planets to unravel the red limit of the pigment. Photosynthetic pigments play a central role to convert available light energies into chemical energies. Chlorophyll has a tetrapyrrole ring with a metal ion such as Mg in the center of the ring. The ring structure can encapsulate a variety of metals to have a modulation of physical-chemical properties. Starting with the tetrapyrrole, we search for the pigments which are applicable around M dwarfs by calculating their basic structures, functional groups, central metals and solvents to determine the absorption wavelength and other properties. At first, we focused on the role of the central metal. Metals *M={H2, Mg, Ca, Ni, Cu, Zn, Sr, Cd, Hg, Pb, ...}* are put in the center of rings and are evaluated. According to our calculations, the wavelength of the first excited state is slight long in *M=Ni* in chlorophylls *a* and *b* and bacteriochlorophylls *a* and *b*. Additionally, binding eneries for metals into the rings in solvent conditions, molecular orbitals and reactivities (ionization potential and electron affinity) are analyzed for each pigment.

キーワード：太陽系外惑星、バイオマーカー、光合成、量子化学
Keywords: Extrasolar planet, Biosignatures, Photosynthesis, Quantum Chemistry

©2019. Japan Geoscience Union. All Right Reserved.

地球類似惑星の気候安定性とハビタビリティにおける炭化水素エアロゾルの影響

Effects of the formation of hydrocarbon aerosols on the climate stability of Earth-like planets and their habitability

*渡辺 泰士[1]、田近 英一[1]、尾崎 和海[2]、洪 鵬[3]
*Yasuto Watanabe[1], Eiichi Tajika[1], Kazumi Ozaki[2], Peng Hong[3]

1. 東京大学、2. 東邦大学、3. 千葉工業大学
1. The University of Tokyo, 2. Toho University, 3. Chiba Institute of Technology

It is known that the haze particles composed of hydrocarbons can form in an anoxic atmosphere in which the CH_4/CO_2 ratio exceeds the critical level (~0.2), as observed in Titan's atmosphere. The haze particles have characteristic optical properties that could affect the planetary climate as discussed in the context of the anoxic early Earth before the rise of atmospheric oxygen owing to the activity of oxygen-producing photosynthetic bacteria. Under low pO_2 condition, CO_2 and CH_4 can be photochemically broken up to form CO, and the excess CO reacts with OH radical to form CO_2. If primitive anaerobic microbial ecosystem exists on the Earth-like planet as in the early Earth, it can also affect the balance between CO_2, CH_4, and CO. Primitive marine microbial ecosystem may produce CH_4 to the atmosphere-ocean system via methanogenesis. The primitive microbial ecosystem consumes CO_2 from the atmosphere-ocean system via anoxygenic photosynthesis, but it also provides CO_2 via decomposition of organic matters and methanogenesis, and/or other abiotic processes. This implies that the balance between CO_2, CH_4, and CO in the early Earth must have been significantly different from that at present. Photochemical reactions and biological processes in the ocean may affect the stability of the planetary climate through the formation of the haze particles.

Here we developed a coupled atmospheric photochemistry-marine microbial ecosystem-global carbon cycle model to explore how the atmospheric photochemistry and the primitive marine microbial ecosystem can affect the carbon cycle and CO_2 budget on the Earth-like planet. We found that when the primitive biosphere produces large CH_4 flux (~10^{11} cm^{-2} s^{-1}), OH radicals should be consumed in the lower atmosphere through the reaction with CH_4. As a result, the reaction between CO and OH, which produces CO_2, cannot compensate the photolysis of CO_2 in the upper atmosphere. This means that photochemical reactions may work as a net CO_2 consumption process in the atmosphere-ocean system. The excess CO in the atmosphere is considered to have been converted to CO_2 and CH_4 through the CO-using chemosynthesis and methanogenesis in the oceans on the early Earth. Therefore, marine microbial reactions can work as a net CO_2 production process in the atmosphere-ocean system. We also found that, when the CO_2 level is so low that the hydrocarbon haze can form, the photochemical net consumption of CO_2 exceeds the biospheric net production. In this case, CO_2 is removed from the atmosphere-ocean system as the haze particle. As a result, the climate with the hydrocarbon haze should be unstable, and the climate is expected to change to the snowball state with low pCO_2 or to the hot climate state (> ~310 K on the CO_2 degassing rate of the present Earth) with high pCO_2 and pCH_4 on the planets with anoxic environment and primitive microbial ecosystem in the ocean.

Our result would put a theoretical constraint on the existence of life on extrasolar Earth-like planets and their habitability.

©2019. Japan Geoscience Union. All Right Reserved.

キーワード：ハビタビリティ、気候安定性
Keywords: Habitability, Climate stability

©2019. Japan Geoscience Union. All Right Reserved.

[E] 口頭発表 | セッション記号 M (領域外・複数領域)：M-IS ジョイント

2019年5月30日(木) 10:45 ~ 12:15 | 201A 2F

[M-IS07] アストロバイオロジー

コンビーナ:薮田 ひかる(広島大学大学院理学研究科地球惑星システム学専攻)、杉田 精司(東京大学大学院理学系研究科地球惑星科学専攻)、深川 美里(国立天文台)、藤島 皓介(東京工業大学地球生命研究所)、座長:藤島 皓介(ELSI 地球生命研究所)、深川 美里(名古屋大学大学院 理学研究科)、杉田 精司(東京大学大学院 理学系研究科)、薮田 ひかる(広島大学大学院 理学研究科)

様々な分野を横断し、宇宙における生命の起源と進化、生命存在可能性の解明を目的とするアストロバイオロジーが発祥して20年。太陽系物質進化、惑星系形成、初期地球の前生物的化学、地球と生命の共進化、極限環境生物、ハビタブルな惑星環境、といった個々のテーマが複数分野の知見や手法で研究されるようになり、「我々はどこから来たか」を或る幾つかの形では示すことができるようになってきた。しかし、最終的には成し遂げるべき、挑戦的な領域が残っている。それは、地球惑星環境で生じた非生物的な物質は、どのように生命機能を獲得したのか？　生命の起源に至る、または、生命存在可能な条件を満たす、有機化学と生化学の接点には未だに隔たりが大きい。そこで、これからのJpGUアストロバイオロジーセッションでは、これまで以上の取り組みが重要と考えられる「天文学、地球科学、生化学の融合」を模索し、この未知領域の開拓に臨む。例えば系外惑星と分子進化など、試験管の中の知見を超えた、”場”と対応づけた生化学的・分子生物学的な事象を議論し「生命とはなにか」の理解に近づけ、将来の宇宙生命探査に必要な非生命と生命の識別法の議論や開発に繋げる。

10:45 ~ 11:05

[MIS07-11] the emergence of iron-sulfur protometabolism

★Invited Papers

*Sheref Mansy[1] (1.University of Trento)

11:05 ~ 11:25

[MIS07-12] Life-water-mineral interactions and their products

★Invited Papers

*白石 史人[1] (1.広島大学)

11:25 ~ 11:40

[MIS07-13] How much can we learn about ancient cells from sequence analysis? New metrics on an old problem.

*Shawn E McGlynn[1]、Sarah J Berkemer[2,3] (1.Earth-Life Science Institute, Tokyo Institute of Technology、2.Bioinformatics Group, Department of Computer Science, Interdisciplinary Center for Bioinformatics, University of Leipzig、3.Max Planck Institute for Mathematics in the Sciences, Leipzig, Germany)

11:40 ~ 11:55

[MIS07-14] Scientific significance of searching living cells on Mars surface by Life Detection Microscope (LDM)

*吉村 義隆[1]、山岸 明彦[2]、佐藤 毅彦[3]、宮川 厚夫[2]、今井 栄一[4]、佐々木 聰[5]、小林 憲正[6]、癸生川 陽子[6]、岡田 朋華[6]、塩谷 圭吾[3]、薮田 ひかる[7]、長沼 毅[7]、三田 肇[8]、藤田 和央[3]、臼井 寛裕[3] (1.玉川大学農学部、2.東京薬科大学、3.宇宙航空研究開発機構、4.長岡技術科学大学、5.東京工科大学、6.横浜国立大学、7.広島大学、8.福岡工業大学)

11:55 ~ 12:10

[MIS07-15] Civilization-bearing planets in the Milky-Way Galaxy; 50 necessary conditions must be satisfied in order

*丸山 茂徳[1] (1.東京工業大学地球生命研究所)

12:10 ~ 12:15

Discussion

the emergence of iron-sulfur protometabolism

*Sheref Mansy[1]

1. University of Trento

Iron-sulfur clusters are considered to be one of life's most ancient cofactors. Traditionally, the reliance of extant biology on iron-sulfur proteins has been interpreted to mean that iron-sulfur clusters of some type actively participated in the prebiotic chemistry that led to life. Since globular proteins were likely not present on the prebiotic Earth, most investigations into the early roles of iron-sulfur clusters have centered upon the potential activity of minerals, such as greigite and pyrite. Although minerals undoubtedly heavily impacted prebiotic chemistry and likely participated in the synthesis of molecules necessary for the emergence of life, it is unclear how minerals could have been later superseded by protein enzymes. Here we discuss our efforts in understanding the plausibility of synthesizing iron-sulfur clusters coordinated to prebiotically plausible peptides. We find that the solution conditions impact the type of iron-sulfur cluster formed, that UV light facilitates the synthesis of iron-sulfur clusters, and that iron-sulfur peptides can mediate the types of electron transfer reactions needed to sustain an early form of metabolism.

Keywords: iron-sulfur cluster, protocell, prebiotic chemistry, origins of life

©2019. Japan Geoscience Union. All Right Reserved.

Life-water-mineral interactions and their products

*白石 史人[1]
*Fumito Shiraishi[1]

1. 広島大学
1. Hiroshima University

Studies of modern and ancient microbial deposits on the Earth have demonstrated that the traces of microbial life are preserved as various kinds of minerals via life-water-mineral interactions. They include carbonates, phosphates, iron oxides, and manganese oxides, and their recent knowledge is introduced in the presentation.

For carbonates, cyanobacterial photosynthesis can produce $CaCO_3$ minerals to form deposits like stromatolites. However, their depositional fabrics are strongly influenced by the acidity of EPS (extracellular polymeric substances) secreted by cyanobacteria. In some cases, $CaCO_3$ minerals formed by cyanobacteria exhibit specific traces.

For phosphates, phosphorites are generally produced via degradation of organic matter during diagenesis. In the case of high phosphorus concentration in the euphotic zone, however, microbial photosynthesis potentially produces phosphate minerals to form phosphate stromatolites. Such process may occur after the snowball Earth glaciations in the Neoproterozoic as well as in the Paleoproterozoic.

For iron oxides, microbial Fe(II) oxidation is effective only when O_2 concentration is below ca. 50 μM, and inorganic process prevails above this level. The trace of iron-oxidizing bacteria is potentially preserved in the structure of iron oxide minerals.

For manganese oxides, substantial Mn(II) oxidation does not occur inorganically even under O_2 concentration equilibrated with the modern atmospheric level, and microbial processes are essential for it. In addition, manganese oxides adsorb various metals that potentially sustain metal-dependent microbial ecosystems in organic matter-deficient settings.

The knowledge about microbial traces on the Earth would provide valuable information for exploring extraterrestrial life.

©2019. Japan Geoscience Union. All Right Reserved.

How much can we learn about ancient cells from sequence analysis? New metrics on an old problem.

*Shawn E McGlynn[1], Sarah J Berkemer[2,3]

1. Earth-Life Science Institute, Tokyo Institute of Technology, 2. Bioinformatics Group, Department of Computer Science, Interdisciplinary Center for Bioinformatics, University of Leipzig, 3. Max Planck Institute for Mathematics in the Sciences, Leipzig, Germany

A longstanding goal is to apply molecular phylogenetics to understanding ancient physiological and evolutionary states (*e.g.* [1]). With the current explosion of molecular sequencing data (e.g. [2]), it is a good time to consider how far back we can peer with the comparative molecular lens, and ask if we can understand life in its nascent years. A standard test for inferring ancient genes is to look for conservation in microbial genomes, and to analyze phylogenetic branch positions and determine if a gene separates the archaea and the bacteria. However, many phylogenetic trees are cluttered by phenomena such as horizontal gene transfer and non-orthologous displacement [3], making inferences difficult.

In this presentation, we will give an overview of recent work in this area [4, 5], and also present new analyses which help identify ancient proteins. Using the COG database, we built phylogenetic trees for all protein families and analyzed the number of interdomain gene transfer events for each family. We find that proteins assigned to COGs exhibit widely variable amounts of interdomain gene transfer. By using distance matrices which relate *intra*-domain sequence similarity to *inter*-domain similarity, we find that protein families exhibiting numerous inter domain gene transfer events are also most self-similar between domains. Integrating this observation with previous analyses, ancient proteins appear to have large branch lengths separating the domains, but recent proteins are more bushy in tree shape. These findings will be discussed in the context of inferring the characteristics of the most ancient cells. Although this work provides new dimensions to analyze protein families with, more work is needed to definitively identify the proteins in the last common ancestor of the bacteria and archaea.

REFERENCES CITED

1. Woese, C.R.: Bacterial evolution. Microbiol. Rev. 51, 221–271 (1987)
2. Castelle, C.J., Banfield, J.F.: Major New Microbial Groups Expand Diversity and Alter our Understanding of the Tree of Life. Cell. 172, 1181–1197 (2018). doi:10.1016/j.cell.2018.02.016
3. Koonin, E.V.: Comparative genomics, minimal gene-sets and the last universal common ancestor. Nat. Rev. Microbiol. 1, 127–136 (2003). doi:10.1038/nrmicro751
4. Forterre, P.: The universal tree of life: an update. Front. Microbiol. 6, (2015). doi:10.3389/fmicb.2015.00717
5. Weiss, M.C., Sousa, F.L., Mrnjavac, N., Neukirchen, S., Roettger, M., Nelson-Sathi, S., Martin, W.F.: The physiology and habitat of the last universal common ancestor. Nat. Microbiol. 1, 16116 (2016). doi:10.1038/nmicrobiol.2016.116

Keywords: LUCA, Early life, Phylogenetics , Bioinformatics

©2019. Japan Geoscience Union. All Right Reserved.

Scientific significance of searching living cells on Mars surface by Life Detection Microscope (LDM)

*吉村 義隆[1]、山岸 明彦[2]、佐藤 毅彦[3]、宮川 厚夫[2]、今井 栄一[4]、佐々木 聰[5]、小林 憲正[6]、癸生川 陽子[6]、岡田 朋華[6]、塩谷 圭吾[3]、薮田 ひかる[7]、長沼 毅[7]、三田 肇[8]、藤田 和央[3]、臼井 寛裕[3]
*Yoshitaka Yoshimura[1], Akihiko Yamagishi[2], Takehiko Satoh[3], Atsuo Miyakawa[2], Eiichi Imai[4], Satoshi Sasaki[5], Kensei Kobayashi[6], Yoko Kebukawa[6], Tomoka Okada[6], Keigo Enya[3], Hikaru Yabuta[7], Takeshi Naganuma[7], Hajime Mita[8], Kazuhisa Fujita[3], Tomohiro Usui[3]

1. 玉川大学農学部、2. 東京薬科大学、3. 宇宙航空研究開発機構、4. 長岡技術科学大学、5. 東京工科大学、6. 横浜国立大学、7. 広島大学、8. 福岡工業大学
1. College of Agriculture, Tamagawa University, 2. Tokyo University of Pharmacy and Life Science, 3. Japan Aerospace Exploration Agency, 4. Nagaoka University of Technology, 5. Tokyo University of Technology, 6. Yokohama National University, 7. Hiroshima University, 8. Fukuoka Institute of Technology

Past trial of direct detection of life on Mars by 1970's Viking mission ended up with a negative conclusion [1]. Whereas, numbers of new finding provided by Mars exploration missions in the last decade indicate that there are good reasons to perform another life detection program. The sensitivity of the gas chromatograph mass spectrometer onboard the Viking mission was not very high, and was not able to detect the microbes 10^6 cells in 1 gram clay [2,3].

Recent findings on Mars tend to support the possible presence of living microbes near the surface of Mars. MSL Curiosity has found organic compounds [4], the temporal increase of methane concentration in Martian atmosphere [5] and reduced sulfur compounds such as pyrite in Martian soil [6]. Methane and reduced sulfur compounds can be energy sources to support the growth of chemoautotrophic microbes [7]. Possible presence of liquid water at Recurring Slope Lineae has been supported by the detection of hydrated salts [8]. These evidences tend to support the possible presence of living microbes near the surface of Mars and indicate that another life detection program is necessary.

The Life Detection Microscope (LDM) that we have proposed [7, 9] has the potential sensitivity much higher than the Viking instrument. Microscopes directly image life forms and identify their shapes, sizes, and other morphological structures and have the potential to detect a single cell in field of view. Therefore, the sensitivity can be as high as desired just by increasing the volume of sample to be scanned in a reasonable duration of experiment. LDM scans about 1 mm^3 and detects less than 10^4 cells in 1 gram soil at a spatial resolution of 1 μm [9]. LDM differentiates among organic compounds surrounded by membranes or with enzyme activity by staining the samples with fluorescent pigments. This technique is especially useful for the detection of living microorganisms.

The search for living microorganisms is important not only for scientific interest but for planetary protection. Before future human missions begin, surveys investigating the presence of living microorganisms should be conducted to mitigate the risk of human contact with Martian microorganisms, which may be harmful to human health. Scientific significance the development of LDM will be addressed in this report.

References

©2019. Japan Geoscience Union. All Right Reserved.

[1] Margulis, L. et al. *J. Mol. Evol.* 14 (1979)

[2] Glavin, et al, *Earth Planet. Sci. Let.*, 185 (2001)

[3] Navarro-González, et al., *Proc. Natl. Acad. Sci. USA.*, 103 (2006)

[4] Eigenbrode, J. L., et al., *Science*, 360 (2018).

[5] Webster, C. R., et al., *Science*, 360 (2018).

[6] Ming, D., et al., *Science*, 343 (2014)

[7] Yamagishi, A. et al. *Biol. Sci. Space*, 24 (2010)

[8] Ojha, L. et al. *Nature Geosci.*, 8 (2015)

[9] Yamagishi, A., et al., *Trans. JSASS, Aerospace Tech. Japan*, 16 (2018).

キーワード：蛍光顕微鏡、地球外生命
Keywords: fluorescent microscope, extraterrestrial life

©2019. Japan Geoscience Union. All Right Reserved.

Civilization-bearing planets in the Milky-Way Galaxy; 50 necessary conditions must be satisfied in order

*丸山 茂徳[1]
*Shigenori Maruyama[1]

1. 東京工業大学地球生命研究所
1. Earth-Life Science Institute, Tokyo Institute of Technology

<Purpose>

Is there any life in the Universe, or specifically civilization-bearing planets? Recent popular answer for this basic question is easy-going “Yes”, which was also trendy answer 100 years ago. They think there are so many stars in the Universe, e.g., 10^{11}, so it is reasonable to think the possibility of the presence of life in the Universe. However, is it right scientifically?

<Method>

If the number of necessary conditions to make civilization-bearing planet is 50, simple estimate of presence or absence is $(1/2)^{50}=1/(10^{11})$, indicating that it is only one in the Milky Way Galaxy. To discuss the presence of life in the Universe, the best example with the most detailed research information is the Earth and its history. Other examples are planets, asteroid and meteorites in the solar system. Applying those data to the Universe, we can lead to general aspects of necessary conditions to infer life in the Universe.

<Result>

Based on the data set inferred from the research of Earth and life, 48 requirements are listed up. Those necessary conditions are mainly categorized into the following four. First group has 11 planetary conditions to be a life-sustaining planet; for example, “Chemical composition of central star”, “Mass of central star”, and “Circular orbit”. Second Group has 14 conditions of rocky planets to prepare the cradle of life; such as “Formation of bimodal continental and oceanic lithospheres to initiate plate tectonics”, “Restricted amount of initial mass of ocean to supply of nutrients for life”. Third group has 9 conditions to emerge and evolve life; such as “continuous and strong outer energy by natural geyser”, and “well-balanced nutrients source of landmass”. Forth group has 10 conditions to evolve into civilization bearing planet; such as “Survival over 2 billion years until birth of Eukaryote”, “A way to Eukaryote from Prokaryotes”, “A way to metazoans and Plant”, “Acceleration of life evolution”. There are other important 4 conditions; such as “Galactic habitable Zone”

<Discussion>

If we simply calculate the probability of presence of life in the Universe, civilization-bearing planet is only one (Earth). It is also emphasized that the requirements mentioned above is treated as presence of absence for all requirements, but several requirements are definitely less than 50% probability, e.g., extremely strict constraint for the amount of ocean volume 3km±1km. Moreover, it is emphasized that the number 51 is combinations and not permutations. This strongly indicates that we are alone in the Universe, even including whole Universe beyond our Milky Way Galaxy.

©2019. Japan Geoscience Union. All Right Reserved.

キーワード：ハビタブルプラネット、文明を持つ惑星、条件
Keywords: habitable planet, civilization bearing planet, condition

©2019. Japan Geoscience Union. All Right Reserved.

[E] 口頭発表 | セッション記号 M (領域外・複数領域)：M-AG 応用地球科学

2019年5月30日(木) 13:45 ~ 15:15 | 302 3F

[M-AG38] Satellite Land Physical Processes Monitoring at Medium/High/Very High Resolution

コンビーナ:Jean-Claude Roger(University of Maryland College Park)、Shinichi Sobue(Japan Aerospace Exploration Agency)、Eric Vermote(NASA Goddard Space Flight Center)、座長:Jean-Claude Roger、Eric Vermote

We solicit papers on the land physical processes monitoring. In particular, it will include the inversion and use of land products from medium, high, and very high spatial resolution. For the last years, medium, high, and very high resolutions became a useful and a powerful toll for Earth studies. Topics of interest mainly include (not limited to):
- New developments for data processing, including atmospheric correction and cloud screening;
- Analysis and correction of directional effects in land surface reflectances;
- Use of time series of surface reflectances for land monitoring, including land cover classification and crop yield prediction (including data integration and data harmonization);
- Development and use of new vegetation indices (i.e. red edge) and other products for agriculture applications;
- Theoretical studies for sensors capabilities enhancements to future sensors at high/medium resolutions;
- Use of products in agricultural monitoring applications (such as crop area, crop type, crop growing, yield estimation and prediction, damage assessment);
- Agriculture monitoring algorithm description;
- Evaluation or validation of potential products with ground measurements, official statistics;
- International initiative to enhance Earth-Observing-based agricultural information.

Depending on outcome, we think about a special issue.

13:45 ~ 13:50

Introduction

13:50 ~ 14:05

[MAG38-01] 15-years of LSA-SAF/Eumetsat satellite-derived albedo products: method for retrieval validation, and recent advances using neural networks during spectral integration

*Florian Pinault[1]、Dominique Carrer[1]、Xavier Ceamanos[1]、Gabriel Lellouch[1]、Catherine Meurey[1]、Suman Moparthy[1]、Chloé Vincent[1]、Sandra Coelho[2]、Isabel Trigo[2] (1.Météo France, CNRM-GAME, UMR3589, Toulouse, France、2.IPMA, Lisbon, Portugal)

14:05 ~ 14:20

[MAG38-02] **Toward a Consistent Land Long Term Climate Data Records from Large Field of View Polar Orbiting Earth Observation Satellites**

*Eric Vermote[1]、Jean-Claude Roger[1,2]、Belen Franch[1,2]、Christopher Justice[2]、Ivan Csiszar[3]、Sadashiva Devadiga[1]、Edward Masuoka[1] (1.NASA Goddard Space Flight Center、2.University of Maryland, Dept. of Geographical Sciences、3.NOAA/NESDIS/STAR)

14:20 ~ 14:35

[MAG38-03] **LaSRC Cloud Detection Algorithm for Landsat 8 and Sentinel-2 Data**

*Sergii Skakun[1]、Eric Vermote[2]、Jean-Claude Roger[1] (1.University of Maryland College Park、2.NASA Goddard Space Flight Center)

14:35 ~ 14:50

[MAG38-04] **Aerosol models for the validation of Surface Reflectances for MODIS, VIIRS, Landsat-8, Sentinel-2 from LaSRC**

*Jean-Claude Roger[1,2]、Eric Vermote[2]、Sergii Skakun[1,2]、Belen Franch[1,2]、Georgia Doxani[4]、William Rountree[1,2]、Ferran Gascon[4]、chris justice[1]、oleg dubovik[3]、Brent holben[2] (1.University of Maryland, College Park, USA、2.NASA Goddard Space flight Center, Greenbelt, USA、3.LOA, University of Lille, Villeneuve d'Ascq, France、4.ESA, Frascati, Italy)

14:50 ~ 15:05

[MAG38-05] Quantity and spatial distribution of aboveground biomass carbon in Colombia's forest

*Pedro Rodriguez-Veiga[1,2]、Adriana Paola Barbosa-Herrera[3]、Edersson Cabrera[3]、Gustavo Galindo[3]、Valentin Louis[1]、Pilar Lozano[3]、Pacheco-Pascagaza Ana Maria[1]、Indira Pachon-Cendales[3]、Salinas Nelso Ricardo[3]、Heiko Balzter[1,2] (1.Centre for Landscape and Climate Research, University of Leicester, Leicester, UK、2.NERC National Centre for Earth Observation (NCEO), Leicester, UK、3.Institute of Hydrology, Meteorology and Environmental Studies (IDEAM), Bogota, Colombia)

15:05 ~ 15:15
Discussion

15-years of LSA-SAF/Eumetsat satellite-derived albedo products: method for retrieval validation, and recent advances using neural networks during spectral integration

*Florian Pinault[1], Dominique Carrer[1], Xavier Ceamanos[1], Gabriel Lellouch[1], Catherine Meurey[1], Suman Moparthy[1], Chloé Vincent[1], Sandra Coelho[2], Isabel Trigo[2]

1. Météo France, CNRM-GAME, UMR3589, Toulouse, France, 2. IPMA, Lisbon, Portugal

Using two sets of Eumetsat satellite sensors (geostationary MSG with SEVIRI sensor, polar orbiting Metop/EPS with AVHRR sensors), the Land Surface Analysis (LSA-SAF) team provides to the community several remote sensing products related to the land surface properties (http://lsa-saf.eumetsat.int/). The long-term continuity and consistency of these products is ensured from 2004 to at least 2022 thanks to the Eumetsat funding. In this contribution, we are focus on the various albedo products, presenting their properties, algorithms (from the L1 Top-Of-Atmosphere reflectance data to the L3 albedo), and validation results.

The main albedo retrieval algorithm is based on three steps. First, atmospheric correction is performed using a Smac approximation of a 6S off-line model. Second, the surface interaction is modeled by a kernel-based BRDF (Ross-thick-Li-sparse kernels), with an additional Kalman filter. Third, angular and spectral integrations are performed to compute spectral albedos (white-sky and black-sky) and broadband albedos (visible and NIR and total-shortwave).Validation results show a good match when comparing albedos with other sensors (MODIS) or with in-situ measurements. And performances are here analyzed in details with regards to the user requirements.

Finally we discuss the potential added value of using machine learning techniques in the scope of the launch of the next generation of European satellites which will provide observations in more spectral bands (as for instance MTG/FCI which characteristics are close to HIMAWARI 8/9: 5 visible bands and 3 NIR bands). In the third step of the albedo algorithm (spectral integration), non-convolutional neural networks seem to offer a promising way forward.

Keywords: brdf, albedo, satellite, remote sensing, neural network, machine learning

©2019. Japan Geoscience Union. All Right Reserved.

Toward a Consistent Land Long Term Climate Data Records from Large Field of View Polar Orbiting Earth Observation Satellites

*Eric Vermote[1], Jean-Claude Roger[1,2], Belen Franch[1,2], Christopher Justice[2], Ivan Csiszar[3], Sadashiva Devadiga[1], Edward Masuoka[1]

1. NASA Goddard Space Flight Center, 2. University of Maryland, Dept. of Geographical Sciences, 3. NOAA/NESDIS/STAR

Surface reflectance is one of the key products used in developing several higher-order land products, such as Vegetation Indices, Albedo and LAI/FPAR, it is therefore seminal to detecting trends in the biosphere and land surface and has been classed by NOAA as a “Fundamental Climate Data Record (FDCR) for Land”. Building a long-term surface reflectance data record of climate quality implies combining different instruments, sensors and satellites, accounting for different spatial resolutions and spectral characteristics, assuring consistent calibration, and correcting for atmospheric and directional effects. As the spatial resolution issue is addressed by aggregating the original data to a resolution still suitable for climate studies (e.g. 0.05 degree latitude, longitude), the instrument calibration becomes the first major hurdle one has to go through before being able to proceed any further.

In this work, we are using robust reflectance data records and inter-comparison methods that we have developed over the past several years (consisting of atmospheric correction, directional effect correction and spectral normalization) to establish and verify the inter-consistency of the reflectance products from the AVHRR sensors on-board NOAA 7, 9, 11, 14, 16, 17 and 18, the MODIS sensors on-board Aqua and Terra and the VIIRS sensors on-board Suomi-NPP and JPSS1. The resulting dataset being the 35+ years surface reflectance product and vegetation indices from 1981 to present.

Several other calibration techniques are also be applied that have been developed in the past by our team, in particular combining the cloud spectral band inter-calibration with BELMANIP cross sensor calibration in the near-infrared, using Landsat 5, 7 and 8 calibration to bridge between AVHRR and MODIS.

Keywords: surface reflectance, land climate data record, earth observations satellites

©2019. Japan Geoscience Union. All Right Reserved.

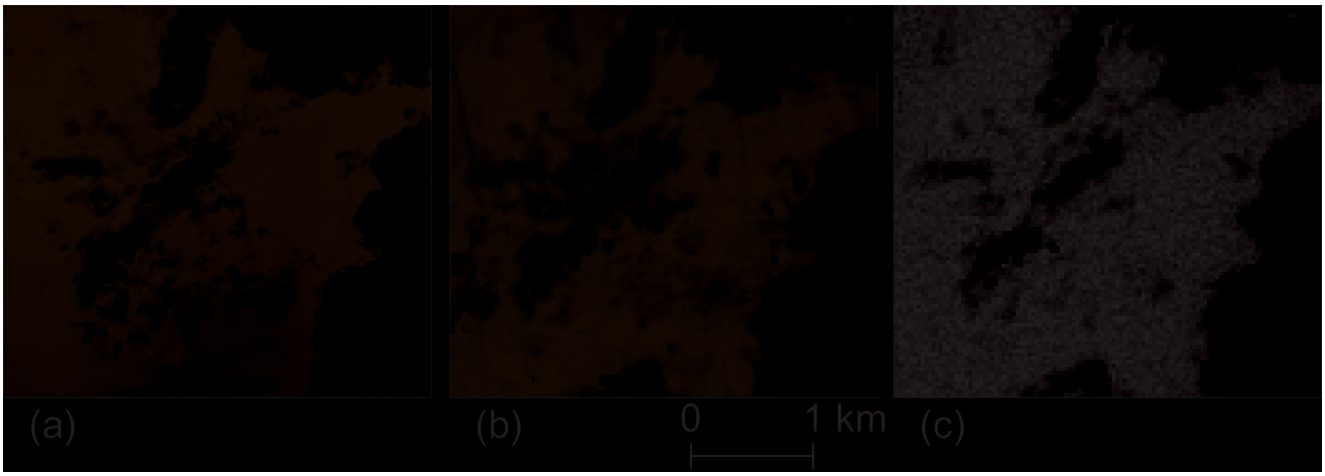
LaSRC Cloud Detection Algorithm for Landsat 8 and Sentinel-2 Data

*Sergii Skakun[1], Eric Vermote[2], Jean-Claude Roger[1]

1. University of Maryland College Park, 2. NASA Goddard Space Flight Center

This study aims at introducing and validating the cloud mask produced by the Land Surface Reflectance Code (LaSRC) for Landsat 8 and Sentinel-2 data. To detect clouds in optical satellite imagery, LaSRC uses quality assurance (QA) layers, which are produced during the atmospheric correction process. Validation is performed using two reference datasets. The former is the “L8 Biome” cloud validation dataset, which is produced by the US Geological Survey (USGS), and consists of 96 Landsat 8 scenes distributed globally over 12 different biomes. The latter is the dataset, which is produced over NASA GSFC assisted by ground photos of the sky and available for Landsat 8 and Sentinel-2A/B. We show that the LaSRC cloud detection algorithm reliably identifies thick clouds with commission and omission errors less than 4%. Large overdetection occurs for thin clouds. We conclude the study with recommendations on using the LaSRC QA layers, and provide an outlook on the need of acquiring objective reference cloud datasets.

Keywords: cloud, Landsat 8, Sentinel-2, LaSRC



©2019. Japan Geoscience Union. All Right Reserved.

Aerosol models for the validation of Surface Reflectances for MODIS, VIIRS, Landsat-8, Sentinel-2 from LaSRC

*Jean-Claude Roger[1,2], Eric Vermote[2], Sergii Skakun[1,2], Belen Franch[1,2], Georgia Doxani[4], William Rountree[1,2], Ferran Gascon[4], chris justice[1], oleg dubovik[3], Brent holben[2]

1. University of Maryland, College Park, USA, 2. NASA Goddard Space flight Center, Greenbelt, USA, 3. LOA, University of Lille, Villeneuve d'Ascq, France, 4. ESA, Frascati, Italy

The land surface reflectance is a fundamental climate data record at the basis of the derivation of other climate data records (Albedo, LAI/Fpar, Vegetation indices) and has been recognized as a key parameter in the understanding of the land-surface-climate processes.

This work relies on a generic approach developed to derive surface reflectance over land from a variety of sensors. The approach is based on the inversion of the radiative transfer equation in the Lambertian case, with no adjacency effects, that account for a simplified coupling of the absorption by atmospheric gases and scattering by molecules and aerosols as implemented in the 6SV radiative transfer code. The processing code relies on look-up tables generated by 6SV, for which the accuracy (~1%) has been well documented in several papers. The LaSRC code uses ancillary data such as pressure and gas concentrations but relies on a per pixel inversion of the aerosol properties to assure the best possible accuracy for the surface reflectance, as aerosols can be highly variable both in space and time. This new aerosol inversion builds on the extensive dataset acquired by the Terra platform, combining MODIS and MISR to derive an explicit and dynamic map of band ratio’ s between blue and red channels and is a refinement of the operational approach used for MODIS and LANDSAT over the past 15 years. The aerosol inversion is generic and applicable to a variety of sensors. We use this basic approach to derive Landsat 8 and Sentinel 2 surface reflectance products for medium, high and very high spatial resolution (MODIS, VIIRS, LANDSAT, SENTINEL-2, WORLD VIEW 3…). The validation scheme is based on using aerosol models developed for each AERONET sites. We will present here the methodology to get these models. We will also show comparison of surface reflectance products with field measurements done by an instrument developed by us.
Finally, we will presents performances of LaSRC inter-compared with other operational approaches in the framework of the CEOS-ACIX (Atmospheric Correction Intercomparison eXercise) Calibration Validation Task co-Lead by ESA and NASA.

Keywords: Aerosol model, Atmospheric correction, Validation, Medium and High spatial resolution

©2019. Japan Geoscience Union. All Right Reserved.

Quantity and spatial distribution of aboveground biomass carbon in Colombia’s forest

*Pedro Rodriguez-Veiga[1,2], Adriana Paola Barbosa-Herrera[3], Edersson Cabrera[3], Gustavo Galindo[3], Valentin Louis[1], Pilar Lozano[3], Pacheco-Pascagaza Ana Maria[1], Indira Pachon-Cendales[3], Salinas Nelso Ricardo[3], Heiko Balzter[1,2]

1. Centre for Landscape and Climate Research, University of Leicester, Leicester, UK, 2. NERC National Centre for Earth Observation (NCEO), Leicester, UK, 3. Institute of Hydrology, Meteorology and Environmental Studies (IDEAM), Bogota, Colombia

In-situ national forest inventory data - NFI (IDEAM, 2018) as well as multispectral optical and synthetic aperture radar (SAR) satellite imagery were used to characterize the spatial distribution of forest aboveground biomass carbon (AGBC) stocks in Colombia. ALOS-2 PALSAR-2 gamma-0 backscatter annual mosaics (2015-2017) provided by JAXA were normalised and corrected using previous ALOS PALSAR annual mosaics (2007-2010) as reference. A multi-temporal Landsat 7 & 8 composite over the whole of Colombia was used for the year 2016 ±1. The national forest inventory in-situ plots used to train our model consisted of 5-subplots each and were collected during the period 2015-2017 in the main biomes of the country. A sample of permanent 1ha plots (PPMs) were also measured. Pan-tropical allometries (Chave et al, 2014) using diameter, height and specific wood gravity (type I) and a biomass-to-carbon ratio of 0.5 were used to estimate AGBC. A non-parametric random forests (RF) algorithm was used within a k-fold framework to retrieve AGBC at 30m spatial resolution for the whole of Colombia. The algorithm was trained using forest inventory plots and validated at plot (0.35 ha) and PPM level (1 ha). The accuracy assessment found coefficients of determination (R^2) of 0.70 and 0.68, and root mean square errors (RMSE) of 29.93 t C ha^{-1} and 24.79 t C ha^{-1} at plot and at PPM level, respectively. The results were also compared to the NFI estimates, and to current pantropical and global aboveground biomass carbon maps.

Keywords: biomass, carbon, SAR, machine-learning, multispectral, forest inventory

©2019. Japan Geoscience Union. All Right Reserved.

[E] 口頭発表 | セッション記号 M (領域外・複数領域)：M-AG 応用地球科学

2019年5月30日(木) 15:30 ~ 17:00 | 201B 2F

[M-AG38] Satellite Land Physical Processes Monitoring at Medium/High/Very High Resolution

コンビーナ:Jean-Claude Roger(University of Maryland College Park)、Shinichi Sobue(Japan Aerospace Exploration Agency)、Eric Vermote(NASA Goddard Space Flight Center)、座長:Sergii Skakun(University of Mrayland, USA)、Eric Vermote

We solicit papers on the land physical processes monitoring. In particular, it will include the inversion and use of land products from medium, high, and very high spatial resolution. For the last years, medium, high, and very high resolutions became a useful and a powerful toll for Earth studies. Topics of interest mainly include (not limited to):
- New developments for data processing, including atmospheric correction and cloud screening;
- Analysis and correction of directional effects in land surface reflectances;
- Use of time series of surface reflectances for land monitoring, including land cover classification and crop yield prediction (including data integration and data harmonization);
- Development and use of new vegetation indices (i.e. red edge) and other products for agriculture applications;
- Theoretical studies for sensors capabilities enhancements to future sensors at high/medium resolutions;
- Use of products in agricultural monitoring applications (such as crop area, crop type, crop growing, yield estimation and prediction, damage assessment);
- Agriculture monitoring algorithm description;
- Evaluation or validation of potential products with ground measurements, official statistics;
- International initiative to enhance Earth-Observing-based agricultural information.
Depending on outcome, we think about a special issue.

15:30 ~ 15:35

Introduction

15:35 ~ 15:50

[MAG38-06] Introduction of GCOM-C/SGLI Leaf Area Index & Fraction of Absorbed Photosynthetically Active Radiation products

*小林 利行[1]、本多 嘉明[2]、小野 祐作[2]、小林 秀樹[3]、Wei Yang[2]、永井 信[3]、秋津 朋子[4]、奈佐原 顕郎[4]、宮崎 理紗[1]、堀 雅裕[1]、村上 浩[1] (1.国立研究開発法人　宇宙航空研究開発機構、2.千葉大学環境リモートセンシング研究センター、3.国立研究開発法人　海洋研究開発機構、4.筑波大学)

15:50 ~ 16:05

[MAG38-07] **35-years of Land Surface Albedo and 15-years of Down-Welling Short-Wave Radiation Retrievals from Satellites through the EUMETSAT/LSA-SAF and ECMWF/C3S projects**

*Dominique Carrer[1]、Florian Pinault[1]、Iskander Benhadj[2]、Xavier Ceamanos[1]、Sandra Coelho[3]、Gabriel Lellouch[1]、Catherine Meurey[1]、Suman Moparthy[1]、Else Swinnen[2]、Chloé Vincent[1]、Isabel Trigo[3] (1.Meteo France, CNRM, France、2.VITO, Belgium、3.IPMA, Portugal)

16:05 ~ 16:20

[MAG38-08] **Integrating the satellite-based biophysical model and environmental zonation scheme to estimate rice yield gap in Northeast China**

*Jiahua Zhang[1,3]、Jingwen Wang[1,2,3] (1.Institute of Remote Sensing and Digital Earth, Chinese Academy of Sciences、2.University of Chinese Academy of Sciences、3.Aerospace Information Research Institute, Chinese Academy of Sciences)

16:20 ~ 16:35

[MAG38-09] Landsat-based Phenological Classification Mapping in Japan

*堤田 成政[1]、永井 信[2]、Pedro Rodriguez-Veiga[3,4,1]、三浦 知昭[5] (1.京都大学大学院地球環境学堂、2.海洋研究開発機構地球環境観測研究センター、3.Centre for Landscape and Climate Research, University of Leicester、4. National Centre for Earth Observation, University of Leicester、5.Department of Natural Resources and Environmental Management University of Hawaii at Manoa)

16:35 ~ 16:50

[MAG38-10] **Incorporating satellite-retrieved canopy nitrogen content into the biophysical process model for estimating crop yield and N fertilizer recommendation**

*Jingwen Wang[1,2,3]、Jiahua Zhang[1,3] (1.Institute of Remote Sensing and Digital Earth, Chinese Academy of Sciences、2.University of Chinese Academy of Sciences、3.Aerospace Information Research Institute, Chinese Academy of Sciences)

16:50 ~ 17:00

Discussion

Introduction of GCOM-C/SGLI Leaf Area Index & Fraction of Absorbed Photosynthetically Active Radiation products

*小林 利行[1]、本多 嘉明[2]、小野 祐作[2]、小林 秀樹[3]、Wei Yang[2]、永井 信[3]、秋津 朋子[4]、奈佐原 顕郎[4]、宮崎 理紗[1]、堀 雅裕[1]、村上 浩[1]
*Toshiyuki Kobayashi[1], Yoshiaki HONDA[2], Yuhsaku Ono[2], Hideki Kobayashi[3], Wei Yang[2], Shin Nagai[3], Tomoko Akitsu[4], Kenlo Nasahara[4], Risa Miyazaki[1], Masahiro Hori[1], Hiroshi Murakami[1]

1. 国立研究開発法人　宇宙航空研究開発機構、2. 千葉大学環境リモートセンシング研究センター、3. 国立研究開発法人海洋研究開発機構、4. 筑波大学
1. Japan Aerospace Exploration Agency, 2. Center for Environmental Remote Sensing, Chiba University, 3. Japan Agency for Marine-Earth Science and Technology, 4. University of Tsukuba

The Japan Aerospace Exploration Agency (JAXA) launched the Global Change Observation Mission - Climate (GCOM-C) satellite on December 23rd, 2017. The Leaf Area Index (LAI) and the fraction of Absorbed Photosynthetically Active Radiation (fAPAR) product (Algorithm ID: T2B) is one of the GCOM-C standard land products. The dataset is being produced from Second Generation Global Imager (SGLI) at 250-m resolution on a daily basis. At the present time, there are several limitations on the product. In this research, we summarize the early results and limitations of the T2B products.

The LAI is defined as one half of the total green leaf area per unit ground surface area. In the GCOM-C product, LAI is estimated for overstory leaves. The information for understory vegetation is added as understory NDVI. The fAPAR is defined as the proportion of the effectively absorbed solar radiation by plants in the photosynthetically active wavelengths (the spectral region from 400 to 700 nm). LAI and fAPAR were estimated based on the Look-Up Tables (LUTs) showing the relationships between the multi-angle atmospherically-corrected land surface reflectance data and the LAI or fAPAR. The LUTs were produced to fit with the field-observed reference data collected from literatures using a radiative transfer simulator, the Forest Light Environmental Simulator (FLiES) [1]. It simulates radiative transfers in the forests and grasslands based on the Monte Carlo method.

The accuracy of the retrieved LAI and fAPAR was assessed using the in-situ observation data which was collected at several sites. The product has the tendency of overestimating LAI especially at the needle-leaved forests. One of the reasons is that the current algorithm cannot distinguish the difference between the overstory LAI and the understory vegetation well at the forested areas with sparse trees. The accuracy of the T2B product should be improved by revising the algorithm and the LUTs for retrieving LAI. We are planning to revise the land cover datasets which are the basis of retrieving LAI. The LUTs will be revised by fitting the vegetation parameters for FLiES with the SGLI data.

[1] H. Kobayashi *et al.*, A coupled 1-D atmosphere and 3-D canopy radiative transfer model for canopy reflectance, light environment, and photosynthesis simulation in a heterogeneous landscape, *Remote Sensing of Environment*, **112** (2008), 173-185.

キーワード：LAI、fAPAR、GCOM-C
Keywords: LAI, fAPAR, GCOM-C

©2019. Japan Geoscience Union. All Right Reserved.

35-years of Land Surface Albedo and 15-years of Down-Welling Short-Wave Radiation Retrievals from Satellites through the EUMETSAT/LSA-SAF and ECMWF/C3S projects

*Dominique Carrer[1], Florian Pinault[1], Iskander Benhadj[2], Xavier Ceamanos[1], Sandra Coelho[3], Gabriel Lellouch[1], Catherine Meurey[1], Suman Moparthy[1], Else Swinnen[2], Chloé Vincent[1], Isabel Trigo[3]

1. Meteo France, CNRM, France, 2. VITO, Belgium, 3. IPMA, Portugal

The space program of EUMETSAT (project CDOP3, LSA-SAF) and the Copernicus Climate Change program (managed by ECMWF) provide (or will provide) added-value satellite products for the meteorological and environmental science communities, especially in the fields of climate modelling, environmental management, natural hazards management, and climate change detection.

The EUMETSAT/LSA-SAF project started in 1999 with research and development activities. The delivered operational products include land surface albedos, temperature, short-wave and long-wave downwelling radiation fluxes, and many others. After twenty years (1999-2019) of research, development, and progressive operational activities, Meteo-France built on a strong expertise on satellite retrieval of the surface albedo and down-welling short-wave radiation variables. Based on that experience, we started in 2016 within the framework of the COPERNICUS/C3S_312 project to develop consistent surface albedo products from the 80’ s until now using multiple sensors from the past to the current generation of instrument. This will complete the EUMETSAT/LSA-SAF albedo archive for the past period. This work will lead in 2019 to more than 35 years of products characterizing the albedo properties of the surface and 15 years of short-wave downwelling radiation fluxes from different satellite sensors. First C3S collection will be available in autumn 2019 whereas more than 10 different albedos and short-wave downwelling radiation fluxes are already operational in EUMETSAT/LSA-SAF (http://lsa-saf.eumetsat.int/). Product characteristics, and performances are presented here. The next scientific challenges related to the next generation of European satellites and the emergence of artificial intelligence are also discussed.

Finally, it is important to emphasize that these programs provide a great opportunity to monitor human-induced climate change since consistent production of data sets is ensured until at least 2022. In this perspective, our effort will be in the development of open source scientific code in order to share our expertise in the remote sensing of the Earth.

Keywords: satellite, surface albedo, short-wave radiation

©2019. Japan Geoscience Union. All Right Reserved.

Integrating the satellite-based biophysical model and environmental zonation scheme to estimate rice yield gap in Northeast China

*Jiahua Zhang[1,3], Jingwen Wang[1,2,3]

1. Institute of Remote Sensing and Digital Earth, Chinese Academy of Sciences, 2. University of Chinese Academy of Sciences, 3. Aerospace Information Research Institute, Chinese Academy of Sciences

Yield gap analysis is a powerful method to reveal the difference between the actual crop yield and yield potential, and to understand the possible yield increase for fulfilling the growing food demand. It used to be restricted to small geographic areas in previous studies, and thus the scope of untapped yield often remains unclear at macro scale. To this end, we proposed an improved remote sensing approach to better assess the regional rice yield gap in northeast China. A biophysical model based on satellite-retrieved LAI and crop classification map was used to derive the actual yield and its spatial patterns. In addition, a machine-learning zonation scheme was developed to further evaluate the attainable potential yield for farmers within domains having similar climatic, geomorphic, and edaphic context. Results indicated that the satellite-based biophysical model can provide reliable estimates of rice yields, with RMSE all below 20 percent at the county level from 2006 to 2017; and the zonation scheme enabled better portrayal of the spatial variation in potential yield. To identify areas with the greatest potential for narrowing the yield gap, northeast China was divided into four parts with different priorities for future yield improvement. In general, south of northeast China possessed substantial yield gaps with the primary priority to be explored; whereas in the north, the actual yield already approximating yield potential, further yield increase was limited and challenging. Quantile regression model provided a complete view of relationships between natural factors and potential yield, and revealed the significant limiting effects of growing degree days, cumulative solar radiation and elevation. This study demonstrates the potential of remote sensing for agricultural decisions, and will aid planners to recognize the macro-scale food production capacity and security situation, to prioritize regions and needs for research and exploitation, and to evaluate the impact of future scenarios such as climate change.

Keywords: remote sensing, crop yield, yield gap, biophysical process model, environmental zonation scheme, Northeast China

©2019. Japan Geoscience Union. All Right Reserved.

Landsat-based Phenological Classification Mapping in Japan

*堤田 成政[1]、永井 信[2]、Pedro Rodriguez-Veiga[3,4,1]、三浦 知昭[5]
*Narumasa Tsutsumida[1], Shin Nagai[2], Pedro Rodriguez-Veiga[3,4,1], Tomoaki Miura[5]

1. 京都大学大学院地球環境学堂、2. 海洋研究開発機構地球環境観測研究センター、3. Centre for Landscape and Climate Research, University of Leicester、4. National Centre for Earth Observation, University of Leicester、5. Department of Natural Resources and Environmental Management University of Hawaii at Manoa
1. Graduate School of Global Environmental Studies, Kyoto Univeristy, 2. Research and Development Center for Global Change, Japan Agency for Marine-Earth Science and Technology, 3. Centre for Landscape and Climate Research, University of Leicester, 4. National Centre for Earth Observation, University of Leicester, 5. Department of Natural Resources and Environmental Management University of Hawaii at Manoa

Land surface phenology (LSP) is associated with climate and terrestrial conditions over space and time, and the monitoring of LSP helps understandings of the terrestrial environments. The LSP is often inferred by satellite observations, and long-term and regularly-composited satellite imagery is now freely available. Due to its complex interactions with geographical and environmental factors, it is often difficult to characterise phenological cycles by LSP. In order to understand the baseline of the phenological cycle which would be expected as the principal vegetation seasonal activity, we aim at classifying LSP temporal patterns over the entire territory of Japan. Normalised Vegetation Difference Index (NDVI) time series during the period of 2014 to 2017 with the spatial resolution of 30m calculated from Landsat 8 surface reflectance were decomposed into three harmonic terms by harmonic analysis with removing of the temporal trend. Then amplitudes and phases of these three harmonic terms were classified into 36 classes according to their orders. Considering tall vegetation (e.g., tree covers) and short vegetation (e.g., agricultural lands), while excluding other land covers, two types of phenological classification maps with 36 classes for each were produced. The phenological classification proposed in this study is a new terrestrial map which provides new important information for land cover studies regarding climate change, environmental degradation, and human impact assessment. This simple unsupervised classification approach can have diverse advantages such as i) only one specific variable (in this case NDVI) was used, yielding a consistent result compared to models with multivariate analysis, ii) complex temporal profiles can be considered, suggesting better descriptions of LSP than using phenological parameters such as start-of-season, peak-of-season, end-of-season, and length of greening period (In particular, our approach can classify temporal profiles with multiple peaks in the seasonal cycle), iii) the unsupervised classification approach do not need reference samples, which would require reliable observations of phenological events for a supervised classification scheme (such datasets are often limited), and iv) the non-thematic way of classification can avoid mislabelling problems. Interpretation of the classification map can be done by the users, making it easy to utilise towards further climate / environmental studies.

キーワード：フェノロジー、地球観測、ランドサット
Keywords: Phenology, Earth Observation, Landsat

©2019. Japan Geoscience Union. All Right Reserved.

Incorporating satellite-retrieved canopy nitrogen content into the biophysical process model for estimating crop yield and N fertilizer recommendation

*Jingwen Wang[1,2,3], Jiahua Zhang[1,3]

1. Institute of Remote Sensing and Digital Earth, Chinese Academy of Sciences, 2. University of Chinese Academy of Sciences, 3. Aerospace Information Research Institute, Chinese Academy of Sciences

Remote sensing-based biophysical process models (RSBPM) are powerful and indispensable tools for estimating crop productivity over field and landscape scales. However, due to the lack of regional fertilization data, nitrogen stress is often poorly parameterized in these models, which may lead to considerable biases in crop yield simulation. To address this issue, current study improves the representation of nitrogen constraints on photosynthetic capacity in the RSBPM. Canopy nitrogen content retrieved from the newly available high-resolution Sentinel-2 spectral bands is integrated into the model to constrain nitrogen availability in the vital photosynthetic enzyme. And a two-leaf upscaling scheme is used to account for the vertically varying nitrogen content inside canopies and the associated physiological differences between leaves. Measurement data was collected for 32 field-years that spans major crops including wheat, maize, soybean and rice from 2016 to 2017 in China. The satellite-retrieved canopy nitrogen content partially reflects the field fertilization, and identifies seasonality of Rubiso-limited photosynthetic capacity. The new representation of nitrogen constraints significantly reduces the bias of estimated crop yields, and improves the temporal correlations between the simulated and the measured biomass, relative to the commonly employed cases of using specified constant nitrogen stress factor, default fertilization schemes, and the big-leaf nitrogen-constrained model. The improved RSBPM also enables the remote estimation of nitrogen nutrient index, which indicates the status of actual N absorbed versus critical N requirement in the crop. This model improvement on nitrogen constraints has significant implications for better assessment and prediction of crop yield and nitrogen use efficiency and for studying human-environment interactions.

Keywords: canopy nitrogen content, crop yield, biophysical process model, Sentinel-2, fertilization, nitrogen nutrient index

©2019. Japan Geoscience Union. All Right Reserved.

[E] 口頭発表 | セッション記号 M (領域外・複数領域)：M-AG 応用地球科学

2019年5月30日(木) 9:00 ~ 10:30 | 202 2F

[M-AG40] CTBT IMS Technologies for Detecting Nuclear Explosion and Their Applications to Earth Science

コンビーナ:Nurcan Meral　Ozel(Comprehensive Nuclear-Test-Ban Treaty Organization)、松本 浩幸(国立研究開発法人海洋研究開発機構)、直井 洋介(国立研究開発法人日本原子力研究開発機構)、座長:Nurcan Meral Özel(Comprehensive Nuclear-Test-Ban Treaty Organization)、松本 浩幸(海洋研究開発機構)、鎌谷 紀子(東京大学地震研究所)

The Comprehensive Nuclear-Test-Ban Treaty Organization (CTBTO) was founded in 1996 in response to the adaption of the Treaty in 1996 by the United Nations General Assembly, which bans nuclear explosions on the Earth's surface, in the atmosphere, underwater and underground. The Treaty has a unique and comprehensive verification regime to make sure that no nuclear explosion goes undetected. The regime is supported by International Monitoring Systems (IMS) composed of the four state-of-art technologies; 1) Seismic, 2) Hydroacoustic, 3) Infrasound, and 4) Radionuclide, by the International Data Centre (IDC), and by the On-Site Inspections (OSI).
IMS will, when complete, consists of 337 facilities worldwide to monitor the planet for signs of nuclear explosion. Around 90 % of the facilities are in operation and sending the data to the IDC in Vienna, Austria.
The huge amount of data collected by the stations can be used for other purposes such as civil and scientific applications in addition to detecting nuclear explosions. They can provide Tsunami Warning centres with near real-time information about an underwater earthquake. During the Fukushima Daiichi Power Plant accident, in March 2011, the IMS network's radionuclide stations tracked the dispersion of radioactivity on a global scale. The data could also help better understand the oceans, volcanos, climate change, the movement of marine mammals, and many other issues.
This session will provide the overview of CTBTO and its IMS, the scientific discussion on each technology, and its outcomes. The session welcomes young scientists and engineers who are interested in four IMS technologies.

9:00 ~ 9:15

[MAG40-01] Japanese Contributions and Collaborations for IMS Technologies and the Verification Regime

*Nurcan Meral Ozel[1]、David Jepsen[1]、Naoko Nakashima[1]、Hideaki Komiyama[1]、Hiroyuki Matsumoto[1,2] (1.Comprehensive Nuclear-Test-Ban Treaty Organization (CTBTO)、2.Japan Agency for Marine-Earth Science and Technology (JAMSTEC))

9:15 ~ 9:30

[MAG40-02] 日本における地震波による核実験探知の研究

★招待講演

*鎌谷 紀子[1] (1.東京大学地震研究所)

9:30 ~ 9:45

[MAG40-03] Waveform Analysis on Induced Earthquakes after the 2017 Nuclear Test and Detected Mining Events in DPRK

*本橋 昌志[1]、藤井 孝成[1]、乙津 孝之[1] (1.一般財団法人日本気象協会)

9:45 ~ 10:00

[MAG40-04] Submarine volcanoes and where to find them: Harnessing IMS hydroacoustic data

★Invited Papers

*Dirk Metz[1] (1.Japan Agency for Marine-Earth Science and Technology)

10:00 ~ 10:15

[MAG40-05] CTBT検証技術における希ガス監視の重要性と高崎放射性核種監視観測所での観測結果

*山本 洋一[1]、木島 佑一[1]、冨田 豊[1] (1.国立研究開発法人日本原子力研究開発機構)

10:15 ~ 10:30

[MAG40-06] 日本で検出された放射性キセノンに関するATM解析結果

*木島 佑一[1]、山本 洋一[1]、冨田 豊[1] (1.国立研究開発法人　日本原子力研究開発機構)

Japanese Contributions and Collaborations for IMS Technologies and the Verification Regime

*Nurcan Meral Ozel[1], David Jepsen[1], Naoko Nakashima[1], Hideaki Komiyama[1], Hiroyuki Matsumoto[1,2]

1. Comprehensive Nuclear-Test-Ban Treaty Organization (CTBTO), 2. Japan Agency for Marine-Earth Science and Technology (JAMSTEC)

The CTBT verification regime is supported by the cooperation of member states who host monitoring stations and laboratories of the International Monitoring System (IMS) network. The proactive collaboration with state governments and research institutions hosting IMS facilities is crucial for improvement of the technologies for the verification regime.

Japan has contributed for many years in establishing and maintaining these facilities and in improving the verification technologies and regime, in a variety of aspects. Japan hosts stations for three of the technologies: seismic, infrasound and radionuclide. The technical contributions by Japan in projects for the improvement and enhancement of the radionuclide monitoring/detection capability are highlighted in this presentation.

In addition to the contributions through the operation of two IMS radionuclide monitoring stations in Japan, Okinawa, and Takasaki, two additional radionuclide measurement campaigns have been initiated at Horonobe and Mutsu, through financial support from the government of Japan (GoJ) in 2017. These campaigns started in early 2018, with the collaborations of Japan Atomic Energy Agency (JAEA). A new campaign in Fukuoka is being initiated, using another existing mobile system, aiming to configure a high dense measurement network for the evaluation and the calibration of the current noble gas system network of the IMS.

Another collaboration in the radionuclide sector is the air sampling for Ar-37 analysis and the new sampler testing at Takasaki station, in order to enhance the capability for On-site Inspection (OSI). Ar-37 is produced naturally by cosmic rays and exists in the atmosphere as background. Thus, it is also important to know its behavior in the environment. A 2-year sampling campaign was conducted at Takasaki in collaboration with JAEA in 2016-2018 utilizing their expertise.

The government of Japan (GoJ) has strongly supported to establish these collaborations, especially through voluntary contribution, in 2012, 2013 and 2017. They were used for enhancement of atmospheric transport modeling project, noble gas measurement campaign at Horonobe and Mutsu mentioned above, and sending Cost-free Experts (CFEs) of IMS HA Technology.

Keywords: Comprehensive Nuclear-Test-Ban Treaty (CTBT), International Monitoring System (IMS)

©2019. Japan Geoscience Union. All Right Reserved.

日本における地震波による核実験探知の研究
Review: Researches on detection of nuclear tests by seismic waves in Japan

*鎌谷 紀子[1]
*Noriko Kamaya[1]

1. 東京大学地震研究所
1. Earthquake Research Institute, the University of Tokyo

1　はじめに

日本では、北朝鮮付近を震源とする、自然地震ではない可能性がある地震波を気象庁が観測した場合は、気象庁は即座に首相官邸に連絡するとともに記者会見を開き、その事象のパラメーターを発表する。そして、過去に行われた北朝鮮の地下核実験や自然地震の波形と比較した資料を提示して、S波が不明瞭であるなどの地震波形の特徴を根拠として「自然地震ではない可能性がある」との説明を行う。これらの記者会見の資料は、気象庁ホームページで公開される。しかし、核実験の探知は気象庁の本来の業務ではないため、公に発表される解析結果はここまでである。また、CTBTO（包括的核実験禁止条約機構）のデータをもとに核実験を監視する機能を担うNDC1（国内データ・センター１）である気象協会は、核実験が行われた際には地震波形の解析を行うが、監視業務の委託元である日本国際問題研究所ホームページで公表されるのは、「爆発事象の特徴を有する波形であるので、この事象は核爆発を含む人工的な爆発事象である」といったシンプルな報告のみであることが多い。核実験の探知は日本の安全保障上重要な事柄であり、日本の研究者が核実験探知技術を研究することは重要である。今回は、これまでに日本語の文献で公表された、日本における地震波による核実験探知の研究についてレビューする。

2　事象を記録していた時代

現在入手できる最も古い文献は、久保寺・岡野（1960）であると考えられる。久保寺らは、1958年6月及び7月に米国がビキニ環礁で行った水爆の実験で、微気圧振動が到達するのと同じ時刻に、長周期地震計にも周期９分～１分程度の長周期の波動が記録されていたことを報告しており、それは、気圧変動によって地震計の振り子部分に浮力変化が生じたからであろうとしている。また、気象庁観測部（1972）は、1971年11月7日（日本時間）に米国によってアリューシャン列島アムチトカ島で行われた、TNT火薬約５メガトン級と言われる最大級の地下核実験による地震波形の記録を、ほぼ全国の観測点分掲載している。

3　自然地震との識別に関する研究

核実験を自然地震から識別するための研究は、主に松代地震観測所における地震波形を用いてなされている。山岸・他（1973）は、地下核実験のP波のスペクトルは短周期の波が卓越していることを述べた。また、大規模な地下核実験であれば、MsとmbをＢ較すれば識別は可能、と結論づけた。関・他（1980）は、地下核実験でも規模が大きくなるとS波や表面波が観測されることを指摘した。涌井・柿下（1986）は、MbとMSの比を使う識別方法は、大規模な地下核実験にしか適用できないことを指摘した。鎌谷（1998）は、複雑度、スペクトル比、周波数３次モーメントを使って、松代地震観測所の短周期上下動成分で観測された米国ネバダ州と中国シンチャンを震源とする地震波形を解析し、Mb5.3以上のイベントでは地下核実験の複雑度は全て1.00より小さいことを示し、自然地震からの識別には複雑度が最も有効であると述べた。岡本・神定（2007）は、2006年10月9日の北朝鮮による地下核実験について、松代の他、IRISの牡丹江と仁川の地震波形も解析し、PnやPgは自然地震のものと比較して高周波数に卓越していること、P波輻射は爆破震源に見られ

©2019. Japan Geoscience Union. All Right Reserved.

る等方輻射パターンであること等を示した。また、小山（2007）は、同じ実験について、松代の短周期地震計波形を使用して複雑度とスペクトル比を求め、複雑度よりもスペクトル比の方が識別しやすいとした。

菊池（1997）は、1995年～1996年の中国とフランスによる核実験について、IRIS観測点の波形を用いてモーメントテンソルを求め、３つの主値の組み合わせが自然地震とは明らかに異なることや、核実験の震源としては中国は針状、フランスは円盤状のものが推定されることを示した。菊池は、震源の深さが数キロ未満で、かつ、Msとmbの差が大きい地震についてモーメントテンソルを求めることにより効率的に核実験の監視ができるであろうと述べた。

これらの他、石川・他（1988）、森脇・石川（2007）、石川（2007）は、松代地震観測所における地下核実験の観測能力等について調査を行っている。また、吉澤（2008）は、IRISと防災科学技術研究所のF-netの地震波形を用いて各相の震幅や見かけ速度を求め、日本海の地震学的構造を論じた。

４　今後に向けて

日本における地震波による核実験探知の研究は、最近10年間はあまり進展していない。今後は、CTBTOとも連携しながら、核実験の識別技術について世界の研究成果を学ぶ努力が必要である。また、世界の地震波形を解析することにより、地下核実験の識別技術を高める研究を日本でも継続的に進めていくことが重要である。

キーワード：核実験、核爆発、地震波、複雑度、スペクトル比、モーメントテンソル
Keywords: Nuclear Test, Nuclear Explosion, Seismic waves, Complexity, Spectral Ratio, Moment Tensor

©2019. Japan Geoscience Union. All Right Reserved.

Waveform Analysis on Induced Earthquakes after the 2017 Nuclear Test and Detected Mining Events in DPRK

*本橋 昌志[1]、藤井 孝成[1]、乙津 孝之[1]
*Masashi Motohashi[1], Takanari Fujii[1], Takayuki Otsu[1]

1. 一般財団法人日本気象協会
1. Japan Weather Association

After the DPRK September 2017 nuclear test event, several earthquakes were occurred near the test site. The scale of these induced earthquake events was fairly very small, therefore there were a few CTBT IMS seismic stations (e.g. KSRS, USRK, KLR) which could detect earthquake signals. Japan NDC-1 (National Data Center-1) tried to locate and discriminate these events utilizing non-IMS data such as IRIS (Incorporated Research Institutions for Seismology).

Analyzing waveform data of these events, S-wave (Sn, Lg-Phase) amplitude of waveform at close stations is larger than that of P-wave (Pn, Pg-Phase) and the feature of these events is presumed to be natural earthquake rather than man-made explosion. Near the DPRK test site, there are two open-pit mines at Chung-gang city and Musan city which locates DPRK-China border. We also compared with past mining explosion event there and we discriminated events with the indexes such as regional P/S ratio, P/S Spectral Ratio.

It was quite difficult to make event discrimination using only IMS seismic waveform data. IMS seismic network is not designed for detecting small-scale nuclear test far less than 1kt. Therefore, local and non-IMS seismic network data could largely contribute to refine event location and event discrimination.

キーワード：Waveform Analysis、Event Discrimination、Nuclear Test、Induced Earthquake
Keywords: Waveform Analysis, Event Discrimination, Nuclear Test, Induced Earthquake

©2019. Japan Geoscience Union. All Right Reserved.

Submarine volcanoes and where to find them: Harnessing IMS hydroacoustic data

*Dirk Metz[1]

1. Japan Agency for Marine-Earth Science and Technology

Low-frequency underwater sound waves are a key feature of the hydroacoustic waveform component of the International Monitoring System (IMS), a global sensor network maintained by the Comprehensive Nuclear-Test-Ban Treaty Organization in an effort to detect clandestine nuclear explosions in the ocean, in the atmosphere, and underground. However, the potential of IMS data extends beyond test-ban monitoring, for instance, when studying sound phases generated by remote natural sources that otherwise would be difficult to detect, such as submarine earthquakes or volcanic eruptions. Here, we focus on IMS hydrophone recordings of Monowai, a volcanic center in the Kermadec Arc, and Ahyi volcano, located in the Northern Mariana Islands. Tripatite array data are processed using standard cross-correlation and time-difference-of-arrival techniques. Density-based clustering of arrivals at station H03, Juan Fernández Islands, reveals 82 discrete episodes of unrest at Monowai over the course of 3.5-years, making it one of the most active arc volcanoes currently known. IMS data suggests further volcanic activity at both known and unknown sites in the Tonga-Kermadec Arc region. Hydroacoustic recordings of the 2014 eruption at Ahyi show how data analysis can be advanced and streamlined, for example, to determine spectral parameters and acoustic energy release, which has implications for studying volcanic source processes and their respective impact on the ocean soundscape. IMS hydrophone arrays register volcanic seismicity as low as ~2.5 m_b even at megameter distances, thus exceeding the resolution of most regional, land-based networks by more than one order of magnitude. Detectability strongly depends on frequency, source depth, and ray path geometry, which is illustrated by 2D transmission loss modeling for a range of synthetic scenarios. The findings presented here highlight the capabilities of the IMS hydrophone network for remotely detecting and studying volcanic activity in the global ocean.

Keywords: CTBTO, IMS, Submarine volcanoes, Hydroacoustics

©2019. Japan Geoscience Union. All Right Reserved.

CTBT検証技術における希ガス監視の重要性と高崎放射性核種監視観測所での観測結果

Importance of noble gas monitoring in CTBT verification technology and observation results in Takasaki radionuclide monitoring station

*山本 洋一[1]、木島 佑一[1]、冨田 豊[1]
*Yoichi Yamamoto[1], Yuichi Kijima[1], Yutaka Tomita[1]

1. 国立研究開発法人日本原子力研究開発機構
1. Japan Atomic Energy Agency

CTBT検証において、放射性核種の監視は対象とする爆発事象が核実験であったかどうかを判断する唯一の手段である。地下核実験では、核爆発により生成された放射性核種の中でも希ガスは不活性で他の物質よりも地上に漏れ出てくる可能性が高いため、特に重要である。CTBTでは希ガスで監視対象としているのは4つの放射性キセノン同位体のみである。2006年10月の北朝鮮の一回目の核実験の後、希ガス観測装置が日本の高崎放射性核種監視観測所に設置され、2007年1月から放射性キセノンの観測を行っている。ここでは、高崎放射性核種監視観測所での放射性キセノンのこれまでの観測結果と放射性キセノンバックグラウンドの特徴について報告する。

キーワード：包括的核実験禁止条約、国際監視制度、希ガス、キセノン、高崎放射性核種監視観測所
Keywords: CTBT, international monitoring system, noble gas, xenon, Takasaki radionuclide monitoring station

©2019. Japan Geoscience Union. All Right Reserved.

日本で検出された放射性キセノンに関するATM解析結果
ATM analysis results on radioxenons detected in Japan

*木島 佑一[1]、山本 洋一[1]、冨田 豊[1]
*Yuichi Kijima[1], Yoichi Yamamoto[1], Yutaka Tomita[1]

1. 国立研究開発法人　日本原子力研究開発機構
1. Japan Atomic Energy Agency

日本原子力研究開発機構は、CTBT機関と共同して北海道幌延町及び青森県むつ市にそれぞれ移動型希ガス観測装置（TXL）を設置し、2018年から放射性キセノンの観測を行っている。これにより、現在日本ではCTBT高崎放射性核種監視観測所を加えた合計3つの観測点でCTBT検証のための放射性キセノンの観測を実施していることになる。これらの観測点で検出された放射性キセノンの放出源を調査するため、大気輸送モデル（ATM）による放出源推定解析を行った。ここでは3観測地点での放射性キセノンの観測結果及びATM解析結果について報告する。

©2019. Japan Geoscience Union. All Right Reserved.